CHEMICAL REVIEWS

Review

pubs.acs.org/CR

Supramolecular Hydrogelators and Hydrogels: From Soft Matter to Molecular Biomaterials

Xuewen Du, Jie Zhou, Junfeng Shi, and Bing Xu*

Department of Chemistry, Brandeis University, 415 South Street, Waltham, Massachusetts 02454, United States

Supporting Information

ABSTRACT: In this review we intend to provide a relatively comprehensive summary of the work of supramolecular hydrogelators after 2004 and to put emphasis particularly on the applications of supramolecular hydrogels/hydrogelators as molecular biomaterials. After a brief introduction of methods for generating supramolecular hydrogels, we discuss supramolecular hydrogelators on the basis of their categories, such as small organic molecules, coordination complexes, peptides, nucleobases, and saccharides. Following molecular design, we focus on various potential applications of supramolecular hydrogels as molecular biomaterials, classified by their applications in cell cultures, tissue engineering, cell behavior, imaging, and unique applications of hydrogelators. Particularly, we discuss the applications of supramolecular hydrogelators after they form supramolecular assemblies but prior to reaching the critical gelation concentration because this subject is less explored but may hold equally great promise for helping address fundamental questions about the mechanisms or the consequences of the self-assembly of molecules, including low molecular weight ones. Finally, we provide a perspective on supramolecular hydrogelators. We hope that this review will serve as an updated introduction and reference for researchers who are interested in exploring supramolecular hydrogelators as molecular biomaterials for addressing the societal needs at various frontiers.

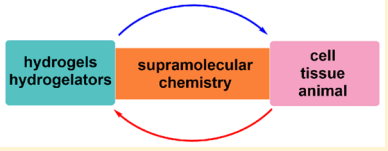

CONTENTS

Received: May 17, 2015
Published: December 8, 2015

DOI: 10.1021/acs.chemrev.5b00299
Chem. Rev. 2015, 115, 13165−13307

1. INTRODUCTION

1.1. Hydrogelators and Hydrogels

Molecular self-assembly is a ubiquitous process in nature, and is also believed to play an essential role in the emergence, maintenance, and advancement of life.[1−3] While the primary focus of the research on molecular self-assembly centers on the biomacromolecules (proteins, nucleic acids, and polysaccharides) or their mimics, the self-assembly of small molecules in water (or an organic solvent) also has profound implications from fundamental science to practical applications. Because one usual consequence of the self-assembly of the small molecules is the formation of a gel (or gelation), a subset of these small molecules is called gelators. Depending on the solvents in which they form gels, these small molecules are further classified as hydrogelators[4] (using water as the liquid phase) and organogelators[5] (using an organic "solvent" as the liquid phase). More precisely, hydrogelators (i.e., the molecules) self-assemble in water to form three-dimensional supramolecular networks that encapsulate a large amount of water to afford an aqueous mixture. The aqueous mixture is a supramolecular hydrogel because it exhibits viscoelastic behavior of a gel (e.g., unable to flow without shear force). Unlike the conventional polymeric hydrogels that are mainly based on covalently cross-linked networks of polymers (i.e., gellant), the networks in supramolecular hydrogels are formed due to noncovalent interactions between the hydrogelators (Figure 1A).[6] Considering that water is the unique solvent to maintain life forms on earth, it is important and necessary to distinguish water from organic solvents. Because supramolecular hydrogels are a type of relatively simple heterogeneous system that consists of a large amount of water, it is not surprising that the applications of hydrogels and hydrogelators in life science have advanced most significantly. Thus, in this review we mainly focus on the works that study the properties and explore the applications of supramolecular hydrogels and hydrogelators in biomedical science. Because of the rapid advancement of the field, it is unavoidable that some works are inadvertently absent from this review. Here we offer our sincere apology in advance and hope readers will let us know those deserving works so we can include them in future reviews.

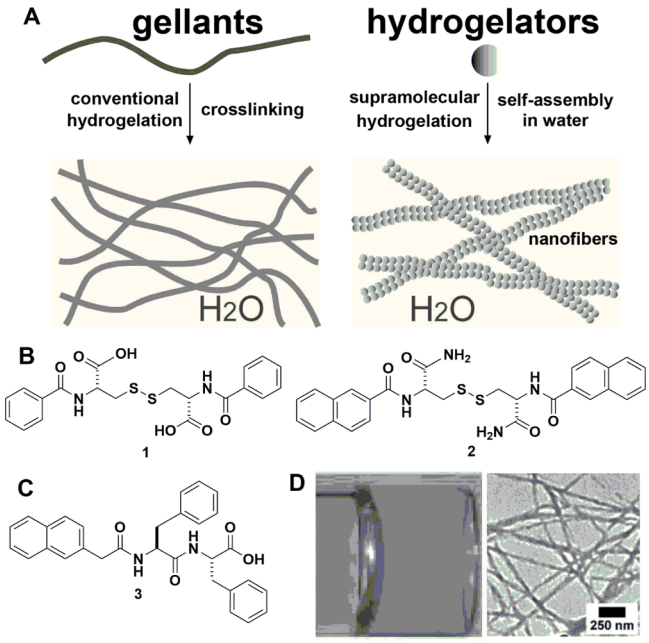

Figure 1. (A) Illustration of the process for creating polymeric hydrogels via cross-linking (left), or formation of supramolecular hydrogels via a chemical or physical perturbation initiated self-assembly (right). Adapted with permission from ref 6. Copyright 2006 Wiley-VCH Verlag GmbH & Co. KGaA. (B) Molecular structures of **1** and **2**. (C) Molecular structure of Nap-FF (**3**). (D) Optical image and negatively stained TEM image of the hydrogel of **3**. Adapted from ref 14. Copyright 2011 American Chemical Society.

DOI: 10.1021/acs.chemrev.5b00299
Chem. Rev. 2015, 115, 13165−13307

1.2. History and Serendipity

According to the report by Hoffman in 1921, the first small molecule hydrogelator was dibenzoyl-L-cystine (**1**) (Figure 1), which was able to form "a gel of 0.1% concentration [that] was rigid enough to hold its shape for a minute or more when the beaker containing the gel was inverted".[7] Interestingly, the same hydrogel was reported by Brenzinger almost 20 years earlier.[8] However, not until a century later did Menger et al. use modern physical methods in chemistry (e.g., X-ray crystallography, light and electron microscopy, rheology, and calorimetry) to examine the hydrogel of **1** again and provide invaluable molecular details that reveal many fundamental design principles for creating effective hydrogelators made of small molecules. Impressively, among the 14 aroyl-L-cystine derivatives studied by Menger in the seminal work in 2000,[9] the best hydrogelator (**2**) is able to self-assemble and to rigidify aqueous solutions at 0.25 mM, ca. 0.01 wt %, in less than 30 s, which probably still holds the record in terms of the lowest concentration of hydrogelators and the fastest rate for gelation.[10] One of the most revealing design principles in the study of **1** is that aromatic moieties are highly effective for enhancing intermolecular interactions in water. This principle is largely responsible for the successful use of aromatic−aromatic interactions to design hydrogelators of small peptides.[11,12] Not surprisingly, nature has already used aromatic−aromatic interactions to evolve proteins.[13] These facts imply that the use of aromatic−aromatic interactions is an effective and biomimetic way to enhance hydrogen bonds and other interactions in water for *molecular self-assembly in water* that usually lead to supramolecular hydrogels.[12] A notable example of this principle is that a small dipeptide derivative (**3**) is capable of enabling many other molecular motifs to self-assemble in water to form supramolecular hydrogels (Figure 1).[14]

Despite the above seemingly obvious general principle of supramolecular hydrogelation, one common theme mentioned by the researchers who study gelators, intriguingly, is that their work on gelators started from an accidental discovery of a particular molecule that forms a gel in a solvent. For example, the first small molecule hydrogelator reported by Hoffman unlikely was the intended goal. The research of organogelators also began with a surprise. In 1987, Weiss et al., while investigating the photochemistry of small organic molecules, serendipitously observed that small amounts (usually ca. 1% by weight) of cholesteryl 4-(2-anthryloxy)butyrate (CAB) are able to cause reversible gelation in a wide variety of organic liquids, the different types of functional groups of which in different positions can interact with CAB to affect gelation.[15] Similarly, Shinkai et al., in the process of developing a new synthetic route, have made a surprising finding that the recrystallization of a calix[8]arene derivative from certain solvents (e.g., *n*-hexane, 1-butanol, and carbon disulfide) results in gels, which is the first example of a gelator derived from macrocycles.[16] In fact, in the research of oligomeric peptides, it is rather common to obtain serendipitous hydrogels of the peptides even if the intended goals are something else.[17−21] It is quite intriguing that serendipity is a common occurrence throughout the encounter of small molecule gelators.[22] These fortuitous happenstances, paradoxically, imply that the formation of supramolecular hydrogels via the self-assembly of small molecules in water is, undeniably, a general phenomenon and a rather common process.[23] Therefore, the exploration of supramolecular hydrogels unlikely will be fruitless, and the applications of supramolecular hydrogelators will have a more profound impact than a mere serendipitous observation, as we intend to illustrate in this review.

1.3. Scope and Arrangement

The development of supramolecular hydrogels in the past two decades not only has underscored the above implication, but also has provided a fundamentally new approach for chemists to control the properties of soft materials via the molecular engineering of a diverse set of substrates for a wide range of applications.[4,24−35] To further realize the far-reaching impact of supramolecular hydrogels in many fields of science and technology, from chemistry to physics and to biology, and from materials to pharmacy to health, it would be helpful to review the progress made so far and to consider possible new directions.[36−44] To contribute to this objective, in this review we intend to provide a relatively comprehensive summary of the work of supramolecular hydrogelators after 2004 and to put emphasis particularly on the applications of supramolecular hydrogels/hydrogelators as molecular biomaterials. We make this rather arbitrary choice for several reasons: (i) The excellent review by Hamilton in 2004[4] has covered the works on hydrogelators prior to 2004. (ii) While the early research of gelators has made significant progress in the elucidation of the physiochemical properties of hydrogelators and the corresponding small molecule hydrogels,[4,45,46] the past decade has witnessed significant and exciting advances in the exploration of the applications of hydrogelators and hydrogels in biomedicine. (iii) The recent excellent reviews[25,36,47−55] on gelators (including hydrogelators) have already provided considerable insights into the structure−property relationships of supramolecular hydrogelators; thus, the emphasis on the use of supramolecular interactions and hydrogelators for various applications will complement other review papers and provide a broader perspective at the interface of chemistry and other fields of molecular science. We hope that, by summarizing the development of hydrogelators within 10 years or so and with the emphasis on the design of molecular biomaterials and the relevant applications, in this review we will provide a potential starting point not only for expanding the knowledge base of supramolecular hydrogels as soft molecular biomaterials, but also for attempting to address fundamental questions, perhaps providing a venue for chemists to address the holy grail question in chemistry, that is, the origin of life.[56]

We have arranged the review in the following order. After the brief introduction of the methods for generating supramolecular hydrogels, we discuss the supramolecular hydrogelators on the basis of their categories, such as small organic molecules, coordination complexes, peptides, nucleobases, and saccharides. After the introduction of the molecular building blocks for supramolecular hydrogels, we focus on the various potential applications of the supramolecular hydrogels as molecular biomaterials, classified by their applications in cell cultures, tissue engineering, cell behavior, imaging, immunology, and unique applications of hydrogelators. Particularly, we also discuss the applications of supramolecular hydrogelators after they form supramolecular assemblies but prior to reaching the critical gelation concentration (CGC) because this subject is less explored but may hold equally great promise for helping to address fundamental questions about the mechanisms or the consequences of the self-assembly of small molecules. Finally, we provide our (probably biased) perspectives on supramolecular hydrogelators. We hope that this review will serve as

DOI: 10.1021/acs.chemrev.5b00299
Chem. Rev. 2015, 115, 13165−13307

Scheme 1. Representative Molecular Structures of Hydrogelators To Form Hydrogels after Receiving Different Stimuli

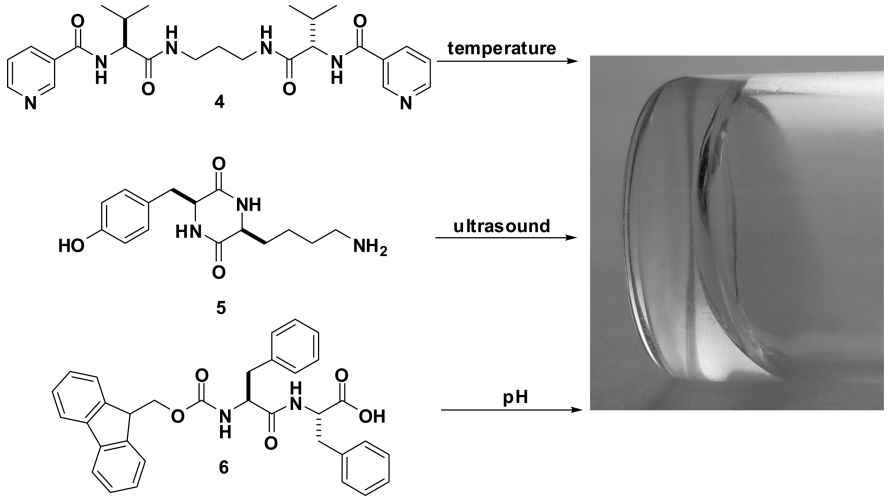

an updated introduction and reference for researchers who are interested in exploring the potentials of supramolecular hydrogelators for discovering, inventing, and creating innovative molecular assemblies, including soft matter and molecular biomaterials. We believe such molecular biomaterials will contribute to addressing the societal needs at various frontiers.

2. STIMULI FOR HYDROGELATION

Despite the fact that they share a prominent appearance and properties (e.g., soft and wet) with polymeric hydrogels, supramolecular hydrogels differ from polymeric hydrogels in many subtle ways. One essential difference is that supramolecular hydrogels, unlike the polymeric hydrogels that originate from a randomly cross-linked network made of strong covalent bonds, are the consequence of molecular self-assembly driven by weak, noncovalent interactions among hydrogelators in water. This subtle yet fundamental difference not only renders more ordered molecular arrangement in the supramolecular hydrogels, but also manifests itself in the process of hydrogelation. While simple swelling usually confers a polymeric hydrogel, a stimulus or a triggering force is necessary to bias thermodynamic equilibrium for initiating the self-assembly process or phase transition to obtain a supramolecular hydrogel. Therefore, there are many forms of stimuli or triggers for manipulating the weak interactions. For the transition from a nongel state to a hydrogel to occur, the free energy must be negative. Thus, the overall impact of the stimuli or triggers usually is negative ΔH or positive ΔS or both, which can be achieved by either physical methods (e.g., changing the temperature, applying ultrasound, or modulating the ionic strength) or chemical methods (e.g., pH change, chemical or photochemical reactions, redox, and catalysis). The following sections briefly introduce the commonly used methods for generating supramolecular hydrogels.

2.1. Temperature or Ultrasound

One of the key features of a supramolecular hydrogel, especially when compared to most cases of gels formed by polymers, is the apt thermal reversibility of the self-assembly process, during which the strengths of hydrophobic interactions and/or hydrogen bonding are temperature dependent. In this kind of hydrogel, the temperature of gelation (T_{gel}) is one most often reported parameter. Multiple methods are able to determine T_{gel}, including the "dropping ball" experiment, differential scanning calorimetry (DSC), and/or various rheological measurements.[57] The data collected via these methods are useful for comparing structurally diverse hydrogelators and evaluating the potential practical applications according to the thermodynamic features of given hydrogels. One notable point is that organogels and hydrogels may differ thermodynamically. For example, Miravet et al. found that the aggregation process is enthalpy driven in an organic solvent but entropy driven in water when studying the molecular hydrogels from bolaform amino acid derivatives **4** (Scheme 1) on the basis of the thermodynamics of gel solubilization.[58,59] This observation, also reported by others,[60−62] underscores the fundamental thermodynamic differences between supramolecular organogels and hydrogels, which deserve the attention of researchers.

Though cooling from an elevated temperature is a common approach for making supramolecular hydrogels, an increase of the temperature of a supramolecular hydrogel can give quite opposite consequences: the usual one is formation of a well-dissolved solution, but it is also possible that precipitation will occur at higher temperature. For example, Nandi et al. have applied a range of techniques to demonstrate the effects of temperature and elucidated the activation barriers for the assembly of riboflavin−melamine hydrogels,[63−65] the formation of which is triggered by cooling a homogeneous solution of the mixtures from 80 or 120 to 30 °C. Bhattacharya et al. reported another two-component hydrogel comprising fatty acids and amines, the spacer length of which in the di/oligomeric amine dictates the gel melting temperature.[55] However, Xu et al. observed that the increase of temperature induces a hydrogel, formed by a dipeptide derivative (Fmoc-D-Ala-D-Ala; Fmoc = (fluoren-9-ylmethoxy)carbonyl), starting syneresis and finally collapsing into a precipitate.[11] This behavior is similar to that of lower critical solution temperature (LCST) polymers,[66] indicating that the increase of the entropy drives the self-assembly of the hydrogelator to a kinetically stable state. A change of temperature also results in many other hydrogels explored for various kinds of applications.[67−72] During the past decade, many thermally reversible supramolecular hydrogels have emerged for potential applications in various fields,[73−77] such as drug delivery.[78,79] Regardless of a particular molecular system, gaining a more comprehensive understanding of the thermodynamic properties of supramolecular hydrogels by a

DOI: 10.1021/acs.chemrev.5b00299
Chem. Rev. 2015, 115, 13165−13307

change of temperature is always beneficial for the optimization and applications of supramolecular hydrogels.

In chemical laboratories or in industry, ultrasound commonly serves as a convenient physical stimulus to speed dissolution or dispersion or clean up the surface by disrupting weak intermolecular interactions. In fact, it is quite common to use ultrasound to assist the formation of supramolecular hydrogels, but the systematic study of ultrasound to control the properties of soft materials is a rather recent event. In essence, the force of ultrasound readily rearranges the aggregation of molecules by cleaving self-locked intramolecular hydrogen bonds or π stacking to form interlocked structures through intermolecular interactions, usually involving the participation of water molecules. The interest in using ultrasound for gelation has apparently received more attentions in generating organogels. Naota et al. reported an association-inert binuclear Pd complex which, being stabilized by intramolecular $\pi-\pi$ stacking interactions, can instantly form gels in a variety of organic solvents upon a brief irradiation with ultrasound.[80] Later, Naota et al. assumed that ultrasound could destroy intramolecular H-bonding of metal-containing peptides and consequently initiated polymerization under the intermolecular H-bonding in the semistable system.[81] Recently, Ratcliffe et al. found that ultrasound may reshape sheetlike dipeptide particles into elongated molecular assemblies, due to the sonocrystallization effect, as the origin of gelation.[82] Usually, with the treatment of ultrasound, it is easier for the gelators to induce fibril formation.[83] For example, Feng et al. reported that ultrasound can promote cyclo(L-Tyr-L-Lys) (**5**) to form a hydrogel when its aqueous solution is cooled (Scheme 1), although it normally precipitates in water and gels a number of polar organic solvents, including *N*,*N*-dimethylformamide (DMF) and dimethyl sulfoxide (DMSO).[84] In addition, Gu et al. concluded that ultrasound not only accelerates the gelation process and recovers the properties of an L-lysine-based hydrogelator, but also induces the self-assembly of fibrils to entangle and to form 3D networks.[85] However, ultrasound may also trigger precipitation instead of fibril formation. Nandi et al. reported a metastable bicomponent hydrogel of thymine and 6-methyl-1,3,5-triazine-2,4-diamine that slowly converts into a crystalline precipitate depending on the method of its preparation (e.g., sonication induced).[86] The similar rich phase behavior seems to be common when ultrasound, combined with a change of temperature, is applied to supramolecular hydrogels.[87]

2.2. pH

A change of pH probably is the most effective and the simplest chemical method to trigger supramolecular hydrogelation because a small amount of acid or base easily and rapidly can lead to a large pH shift via a diffusion-limited process. As an attractive chemical method, a change of pH is particularly useful for generating hydrogels since the pH of an aqueous solution not only is well-defined, but also can be determined easily by a pH paper and precisely by a pH meter. Although pH-triggered hydrogelation largely relies on reversible protonation/deprotonation of basic or acidic group(s) in a particular hydrogelator, a change of pH also may affect the intensity and strength of hydrogen bonding between the hydrogelator and water molecules. Moreover, pH may affect the conformation of molecules to favor hydrogelators to grow from a homogeneous solution to a fibrillar structure in water via noncovalent forces, including aromatic−aromatic interactions, hydrogen bonding, and hydrophobic interactions. Normally, the self-assembly of small molecules, especially molecules possessing acidic or basic groups, requires altering the pH to dissolve in the aqueous phase before adjusting the pH of the solution for screening the charge repulsion to result in hydrogels.

Among a variety of supramolecular hydrogelators, peptide-based hydrogelators are the most common ones that form supramolecular hydrogels on the basis of a change of pH. Specifically, according to the molecular structures of the peptides or peptide derivatives, a change of pH, by affecting the state of charges on the peptidic hydrogelators, usually results in three kinds of hydrogels. (i) Hydrogels that form at low pH: most of the N-terminal-blocked peptides or peptide derivatives result in this type of hydrogel.[88] (ii) Hydrogels that are stable at physiological pH: many small amphiphilic molecules self-assemble to form hydrogels of this category, and they usually are suitable for certain biological applications or share certain features with natural biomaterials.[89−92] (iii) Hydrogels that exist at a high pH: the hydrogelators serving as building blocks of this type of hydrogel likely have a very hydrophobic group or primary amine groups.[93−95] One intriguing and often overlooked fact of supramolecular hydrogelators is that the pK_a of the monomeric hydrogelator may differ from the pK_a of the assemblies of the hydrogelators. For example, Ulijn et al. recently reported that a decrease of the solution pH[96,97] of Fmoc-diphenylalanine (Fmoc-FF, **6**; Scheme 1) induces the self-assembly of **6** to form an entangled network of flexible fibrils or flat rigid ribbons, only the former of which results in a weak hydrogel. According to the authors, the self-assembly of **6** to form fibrils consisting of antiparallel β-sheets results in two apparent pK_a shifts, which are ∼6.4 and ∼2.2 pH units above the theoretical pK_a (3.5) of the monomeric **6**.[97]

Although protons or hydroxide anions diffuse fast, the self-assembly of the hydrogelators during hydrogelation introduces inhomogeneity. Thus, it is rather necessary and common to combine acid or base titration with mechanical mixing (including ultrasound) to achieve a homogeneous pH change. Recently, Adams and Donald et al. utilized the hydrolysis of glucono-δ-lactone (GdL) to gluconic acid as a means of adjusting the pH gradually in a solution of small molecule hydrogelators, which allows the specific targeting of a certain final pH. This method achieves a uniform pH change of the solution by slowing the release of protons, which appears to be particularly useful for the hydrogelation of the hydrogelators that are soluble at high pH and gel at a lower pH. One notable advantage of this approach is reproducibility of self-assembly and hydrogelation,[98−101] which may be particularly important in the study of the biological functions of the assemblies of small molecules. The same principle should be applicable to the slow release of hydroxide anion for the hydrogelation of amine-containing hydrogelators, which remains to be demonstrated. It is noteworthy that a change of pH usually influences other physiochemical properties of the hydrogelators (e.g., fluorescence[102,103] of the hydrogels or the morphology[104] of the matrixes of the hydrogels).

2.3. Chemical Reactions

Chemical reactions, which often yield products with properties different from the reactants, have become important tools in the production of soft materials, such as hydrogels. Particularly, the incorporation of chemical functional groups into biological molecules can create unique sites of addressable reactivity in even large and complex targets. Although many kinds of chemical reactions have found applications to generate

DOI: 10.1021/acs.chemrev.5b00299
Chem. Rev. 2015, 115, 13165−13307

Scheme 2. Representative Molecular Structures of Precursors and Hydrogelators To Form Hydrogels after Chemical Reactions

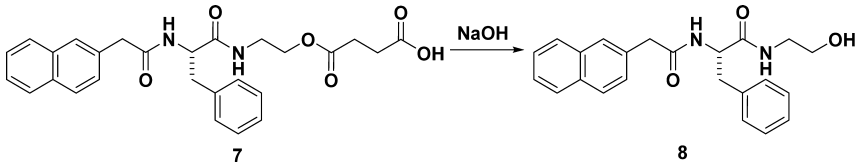

Scheme 3. Representative Molecular Structures of Hydrogelators

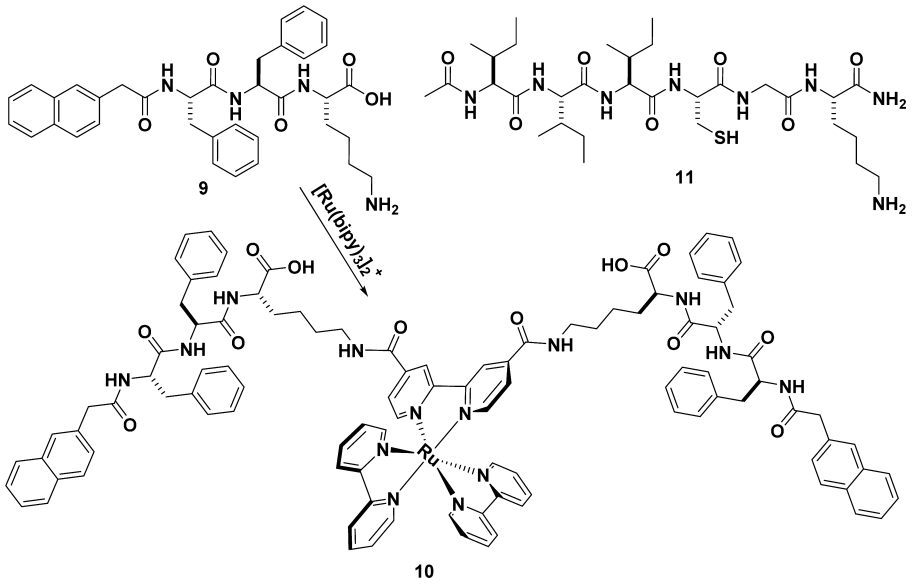

polymeric hydrogels,[105,106] such as click chemistry,[107] redox reactions,[108] Michael addition,[109] ligation reactions,[110] acid−base reactions,[111] and ring-opening metathesis polymerization (ROMP),[112,113] the use of similar approaches to produce supramolecular hydrogels has received much less attention. Recently, Xu et al. reported that a simple chemical modification of a small molecule (**8**) could generate another molecule (**7**) with excellent solubility at physiological pH. The solution of **7** turns into a hydrogel upon the addition of a strong base (NaOH) for the hydrolysis of the carboxylic ester bond of **7** to produce **8** (Scheme 2). The unusual property of the hydrogel of **8** is that it is kinetically stable over a wide pH range.[111] This result illustrates a simple method to produce supramolecular soft materials and may be particularly useful in designing a robust system of prodrugs that can maintain a constant release rate against abrupt changes in the environment. Moreover, Hamachi et al. demonstrated the use of a retro-Diels−Alder reaction to convert a bolaamphiphile to a hydrogelator. Simple heating triggers the reaction and results in a morphological transformation (from 2D nanosheets to a network of 1D nanofibers, as proved by means of transmission electron microscopy (TEM), atomic force microscopy (AFM), and small-angle X-ray scattering (SAXS)) to give a new heat-set supramolecular hydrogel.[43]

Besides hydrolysis, redox reaction[114,115] provides another useful method for controlling the self-assembly of small molecules. For example, Nilsson et al. demonstrated that reduction of a disulfide bond in a cyclic peptide is a viable strategy for controlling peptide self-assembly to form a hydrogel.[116] As shown in Scheme 3, Xu et al. reported that a tripeptide derivative (Nap-FFK, **9**), a versatile self-assembly motif, could be integrated with a ruthenium(II) tris(bipyridine) complex to afford the first supramolecular metallohydrogelator (**10**). As a hydrogelator, not only do the molecules of **10** self-assemble in water to form a hydrogel, but also the hydrogel exhibits a gel−sol transition upon oxidation of the metal center.[117] McNeil et al. developed a convenient and portable triacetone triperoxide (TATP) sensor by utilizing a thiol-to-disulfide oxidation to trigger a solution-to-gel phase transition.[118] Lu et al. introduced a cysteine-containing small peptide, Ac-I_3CGK-NH_2 (**11**). Under an oxidative environment, not only do the molecules of **11** form hydrogels at low concentrations, but also the hydrogels exhibit a tunable strength according to the degree of oxidation.[115] Recently, Das et al. used native ligation to generate a peptide that forms a dimer upon the oxidation of O_2 in air, and the dimer acts as a gelator in a mixed solvent of methanol/water.[119] These arbitrarily selected examples illustrate that there is hardly a limitation of using chemical reactions for generating supramolecular hydrogels. Although any aqueous chemical reaction potentially can generate hydrogels, it is likely that atom-economy reactions[120] will be particularly more suitable for creating supramolecular hydrogels.

2.4. Photochemical Reactions

For chemical reactions, light is a simple stimulus for activating the reactants and starting a chemical transformation. Particularly, the invention of coherent light sources (e.g., laser[121]) has greatly advanced photochemistry,[122,123] which has laid a perfect foundation for the application of photochemical reactions in the creation of materials. Besides being extensively used in the fabrication of a diverse array of materials that include industrial membranes and coatings, dental adhesives, and optical and electronic materials,[124−126] photochemical reactions have already found application in producing polymeric hydro-

DOI: 10.1021/acs.chemrev.5b00299
Chem. Rev. 2015, 115, 13165−13307

gels.[45,127,128] Because photochemical reactions allow the hydrogels to be defined with both temporal and spatial resolution, it is not surprising that light-derived hydrogels have received increasing attention for broad biomedical applications that include drug delivery, wound healing, tissue engineering, and construction of high-density cell arrays.[129−132] Recently, researchers have explored the use of light to initiate self-assembly for generating supramolecular hydrogels. For example, Yamamoto et al. described the formation and biodegradation of cross-linked natural and related polymer hydrogels, fibers, and capsules with photoinduced methods. The irradiation of the aqueous solutions of copoly[LysLys-(Cou)] containing 5−10 mol % ε-[(7-coumaryloxy)acetyl]-L-lysine [Lys(Cou)] residues causes a photo-cross-linking reaction between coumarin moieties in the side chains and turns the solutions to transparent hydrogels.[133] As shown in Scheme 4, Schneider et al. developed a photocaged peptide,

Scheme 4. Molecular Structures of a Photochemical Precursor of a Hydrogelator

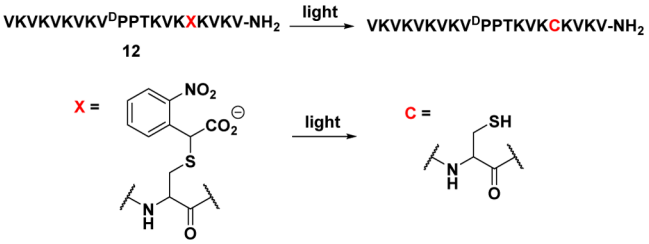

MAX7CNB (**12**), which remains unfolded and unable to self-assemble when being dissolved in an aqueous medium. The irradiation (260 nm < λ < 360 nm) of the solution releases the photocage, α-carboxy-2-nitrobenzyl protection, and triggers peptide folding to produce amphiphilic β-hairpins that self-assemble to generate viscoelastic hydrogels.[134] Besides initiating folding and self-assembly and regenerating rigid, nontoxic soft materials, this photocage chemical method is also used for other applications (e.g., photorelease of functional compounds) since light can be easily controlled in intensity, direction, and duration in both space and time, as illustrated by the widely used calcium photocages.[135,136] Wang et al. presents a photo-cross-linking strategy, based on the ruthenium-complex-catalyzed conversion of tyrosine to dityrosine upon light irradiation, to enhance the mechanical stability of a peptide-based hydrogel by 10^4-fold with a storage modulus of around 100 kPa, which, according to the authors, is one of the highest reported so far for hydrogels made of small peptide molecules at a concentration of 0.5 wt %.[137] Considering the well-established photochemistry of $[Ru(bpy)_3]^{2+}$, this method is convenient and versatile for enhancing the mechanical stability of tyrosine-containing peptide-based photo-cross-linked supramolecular hydrogels. Khan et al. used ultraviolet (UV) light to cross-link alginate hydrogels modified with methacrylate groups.[138] By using a rheometer to monitor the hydrogelation during UV exposure, they illustrated a potentially powerful tool to elucidate the dynamics of gelation and predict the mechanical properties of the hydrogels. Obviously, it is impossible to numerate all the cases of photochemically generated hydrogels in this section. While these examples illustrate the use of photochemical reactions for generating hydrogels, designing new hydrogelators, and predicting the properties of new molecules, we shall mention specific cases when we discuss the building blocks and applications of supramolecular hydrogels in the subsequent sections.

2.5. Catalysis and Enzymes

Catalysis, especially enzymatic reactions, undoubtedly is a prominent dynamic feature of life. Considering that self-assembly is the molecular foundation of life, and soft and wet are another two obvious characteristics of most types of cells, it is not surprising that catalysis and enzymes are attracting increased attention and are achieving many unexpected successes in the generation and applications of supramolecular hydrogelators and hydrogels.

To this day, the reports of catalytic control over self-assembly processes mostly deal with biocatalytic formation hydrogels (e.g., enzyme-instructed hydrogelation),[6,34,39,139−141] and much room remains for achieving directed self-assembly by catalytic action in fully synthetic systems. Recently, van Esch et al. reported the procedure for preparation of low-molecular-weight hydrogels in the presence of an acid or aniline, which acts as the catalyst for the in situ formation of a hydrogelator. The concentration of the catalyst controls the conjugation of two water-soluble precursors, an oligoethylene-functionalized benzaldehyde and a cyclohexane-derived trishydrazide, thus tuning the gelation time and mechanical properties of the final gels (also see Figure 3).[142,143] Recognizing catalyst-assisted self-assembly as a common process in nature to achieve spatial control over structure formation, they developed an ingenious way to generate a spatially controlled supramolecular hydrogel using a micropatterned catalyst on a surface.[144] According to their design, the precursors (cyclohexane-1,3,5-tricarbohydrazide and 3,4-bis[2-(2-methoxyethoxy)ethoxy]benzaldehyde, 3:1) of a gelator (trishydrazone derivative[144]) react on micropatterned catalytic sites on a surface to form building blocks of self-assembled nanofibers that act as the matrixes of the hydrogels. Unlike homogeneous catalysis, this method apparently can achieve multilevel organization among the nanofibers, which is uniquely promising for further development. Liu et al. introduced Cu^{2+} into a glutamic acid-based bolaamphiphilic lipid (*N*,*N*′-hexadecanedioyldi-L-glutamic acid, L-HDGA, **13**; Scheme 5) to form nanotubes with multilayer

Scheme 5. Representative Molecular Structure of Hydrogelators

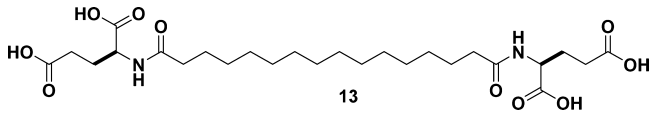

walls.[145] Providing a high density of catalytic sites (Cu^{2+}), such nanotubes showed enhanced-asymmetry catalytic behavior and accelerated the asymmetric Diels−Alder cycloaddition between cyclopentadiene and azachalcone. While any aqueous catalytic reaction may find applications for generating supramolecular hydrogels, the development of catalytic supramolecular hydrogelation for targeted applications likely will be most useful.

The pivotal importance of enzymes in a variety of cellular processes, including self-assembly and self-organization, justifies the exploration of enzymatic supramolecular hydrogelation. Although the application of enzymes to cross-link covalent polymers is an effective process for generating hydrogels,[146] the use of enzymes to prepare supramolecular hydrogels has several distinct advantages, such as the opportunity to achieve sophisticated secondary structure, adaptability to structural

DOI: 10.1021/acs.chemrev.5b00299
Chem. Rev. 2015, 115, 13165−13307

Scheme 6. Representative Molecular Structures of Precursors and Hydrogelators To Form Hydrogels on the Basis of Catalysis

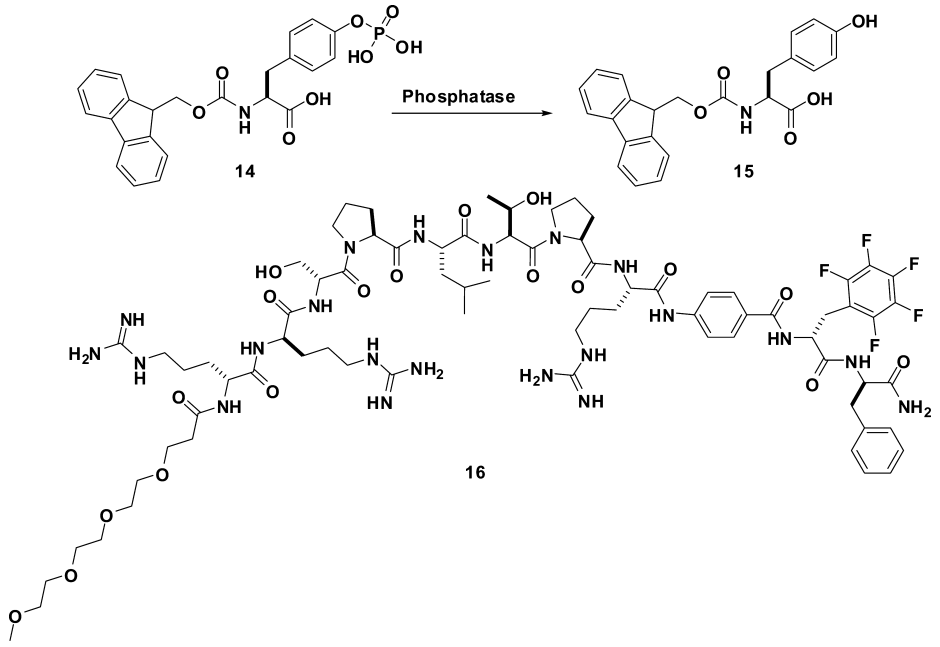

modification, and, most importantly, excellent accessibility to enzymes both in vitro and in vivo due to the fast diffusion of small molecules. Despite the huge diversity of enzymes, so far only a handful of enzymes have been explored for catalyzing hydrogelation. These enzymes are phosphatase,[147−158] β-lactamase,[159] esterase,[1289] matrix metalloproteinase-9 (MMP-9),[164,165] α-chymotrypsin,[166] thrombin,[167] chymotrypsin,[167] and β-galactosidase[168] (for catalyzing bond cleavage reaction), lipase,[169] microbial transglutaminase (MTGase),[170] and thermolysin[160−163,171] (for catalyzing bond-forming reactions), and some other enzymes such as glucose oxidase,[172] peroxidase,[173−175] and tyrosinase.[176] Regardless of the types of reactions or enzymes, the essential feature for enzymatic hydrogelation of small molecules involves the enzymatic conversion of a precursor into a hydrogelator (normally via bond cleavage or bond formation, but not limited to these two). The self-assembly of the hydrogelators to form supramolecular nanostructures (usually nanofibers), and the entanglement or alignment of the nanofibers, affords the matrixes of the hydrogel. The first case of enzymatic formation of supramolecular hydrogels is the use of an alkaline phosphatase[177] to dephosphorylate a precursor, Fmoc-tyrosine phosphate (**14**), under slightly basic conditions to form a hydrogelator (**15**), which self-assembles in water to form a supramolecular hydrogel (Scheme 6).[153] Besides promising a new methodology for the creation of hydrogels in situ, this process also builds up a platform for screening enzyme inhibitors[158,159] and detecting the presence of an enzyme.[159] Instead of catalytically breaking bonds for supramolecular hydrogelation, Ulijn et al. took a different approach by triggering the self-assembly of peptide hydrogels via reverse hydrolysis using thermolysin.[162] Utilizing the fact that certain proteases can thermodynamically favor the formation of peptide bonds, they used thermolysin to catalyze the coupling of two amino acid precursors to form a hydrogelator, which then self-assembled to form a hydrogel. A major advantage of employing reverse hydrolysis is that no byproducts except water are formed, although the use of hydrophobic precursors may be problematic in water. The demonstration of enzymatic supramolecular hydrogelation has sparked relatively active research of bioresponsive materials. For example, Yang et al. reported the use of an enzymatic dephosphorylation process to assist the formation of supramolecular hydrogels.[157] McNeil et al. recently developed a modular system for detecting protease activity.[167] They designed and developed a precursor (**16**; Scheme 6) which is unable to form a hydrogel under most conditions, but turned into a translucent gel upon the treatment of a protease (i.e., thrombin). The past decade has witnessed a considerable success in preparation of supramolecular hydrogels using enzymatic transformation. Certainly, the promises of enzymatic hydrogelation are far from fully realized. We hope that the more detailed discussion of the applications of the specific cases of enzymatic hydrogelation in the later sections will provide stimulation for further development.

3. CHARACTERIZATION OF SUPRAMOLECULAR HYDROGELS

The increased number of hydrogelators and the requirement of more information on supramolecular hydrogels at both the nanoscale and molecular levels require more accurate analysis and characterization of the hydrogels. In this review, we first give a brief introduction of various techniques generally used to characterize supramolecular hydrogels before discussing the classifications and potential applications of hydrogelators. Especially, we focus on the high-resolution techniques that elucidate the molecular self-assembly processes leading to gelation. Unavoidably, some sample preparation methods may affect the native nanostructures of the hydrogels. Thus, among all the characterization techniques, those methods that preserve the native properties of hydrogels should be preferred over the ones that need to dry or/and to stain the samples. Generally speaking, the analysis and characterization of supramolecular hydrogels aim to help scientists better understand how the small molecules are arranged and organized in the matrixes of hydrogels, which may lead to new approaches not only for

DOI: 10.1021/acs.chemrev.5b00299
Chem. Rev. 2015, 115, 13165−13307

rational design of supramolecular hydrogelators but also for the development of various functional molecular biomaterials.

3.1. Visual Inspection

The classic "inverting-vial" method is still the simplest way to initially assess a supramolecular hydrogel.[178,179] Visual inspection of the material just by flipping the vial upside down, which acts as a "zeroth-order" characterization technique, provides an intuitive impression for researchers on the shape and strength of the hydrogels. Thus, according to the visual inspection, one can easily classify the material as a solution, viscous liquid, half-gel, or solidlike gel, which may contribute to selection of more suitable techniques for further characterizing the hydrogels. Despite its simplicity, this assay by the "naked eye", in fact, provides important information—whether a small molecule self-assembles in water.

3.2. Microscopy

With the rapid development and easier operation of microscopic instruments, researchers rely more and more on the microscopy techniques to study the morphology of micro- and nanostructures that act as the matrixes of supramolecular hydrogels. Among all the microscopy techniques, atomic force microscopy (AFM) or scanning force microscopy (SFM), as high-resolution scanning probe microscopies, can achieve a resolution on the order of fractions of a nanometer, which is more than 1000 times better than the optical diffraction limit. Using AFM, one may analyze hydrated samples in situ under high humidity conditions or even without dehydration.[180,181] In addition, it is possible to measure the roughness of a sample surface at a high resolution, which helps classify a sample on the basis of its mechanical properties (e.g., hardness and roughness) and offers new capabilities for the microfabrication of a sample (e.g., an atomic manipulation). However, scanning force microscopy can be misleading due to multiple factors,[182] and it is imperative to use multiple techniques to verify uncommon observations obtained by AFM or SFM.

Electron microscopy techniques, including transmission (TEM)[183] and scanning (SEM)[184] microscopies, utilize a beam of accelerated electrons as a source of illumination. Since the wavelength of an electron is rather short, electron microscopy has the capacity to reveal the structures of small objects with resolution up to a nanometer. For example, TEM can achieve better than 50 pm resolution.[185] On the basis of these properties, electron microscopy can provide valuable information about the morphology of the molecular aggregates/nanofibrils leading to hydrogelation. However, the requirement of completely dried samples under the operating conditions (e.g., high vacuum) makes TEM and SEM less reliable for inferring the native molecular arrangement in the hydrogel state since the dehydration process may result in artifacts that are difficult to explain. Furthermore, staining agents (e.g., urnayl acetate, phosphotungstate, or osmium tetroxide), which are used to increase the electron density of TEM samples to improve the quality/contrast of the images, may interact with hydrogelators to change the self-assembly morphology and to induce artifacts. Cryogenic techniques have already been used in TEM for studying the self-assembled structures. For cryo-electron microscopy (cryo-EM) or electron cryomicroscopy, the samples are studied at cryogenic temperatures (generally liquid nitrogen temperatures) through creation of thin vitrified ice films.[186] Cryo-EM has the advantage of reducing or eliminating the artifacts by making nanometer resolution images of the native gel state feasible. Indeed, several research groups have already successfully determined the structures of supramolecular hydrogels and their related fibrous assemblies with cryo-EM.[187,188] Particularly, a seminal work of the use of cryo-EM to solve the structures of peptide nanofibers[189] has demonstrated the capability of EM for studying the self-assembly of small molecules in water, which is emerging as a new frontier of supramolecular chemistry at the intersection of chemistry and cell biology.[190] In addition, the development of another technique, environmental scanning electron microscopy (ESEM),[191] also provides a useful approach to characterize supramolecular hydrogels under a certain humidity.[192]

3.3. Oscillatory Rheometry and Differential Scanning Calorimetry

Oscillatory rheometry, as a comprehensive technique to characterize viscoelastic materials, is becoming a routine measurement of supramolecular hydrogels. Rheology, which studies the flow of supramolecular hydrogels, can provide tertiary structural information about the type, number, and strength of networks responsible for the observed hydrogelation.[193] Several types of setups, such as parallel plates, concentric cylinders, and cone-and-plate systems, are suitable for the measurement of the rheological properties of hydrogels. All the setups contribute to making a thin layer of supramolecular hydrogels between a stationary and a movable component. The basic principle of oscillatory rheometry is to measure the response of supramolecular hydrogels to an applied oscillatory stress, which is quantified by the elastic properties, such as G^* (complex modulus), G' (storage or elastic modulus), and G'' (loss modulus or viscosity). Meanwhile, the relationship between these variables and the oscillatory frequency, imposed stress, temperature, time, or hydrogelator concentration usually contributes to the studies of certain key characteristics (e.g., critical strains, thermodynamic nature of gelation) of hydrogels. The temperature of gelation (T_{gel}) is one of the most often studied characteristics of a gel, which is determined by the point that noncovalent cross-links or global molecular rearrangements are broken by thermal energy. Differential scanning calorimetry (DSC)[194] is a well-established characterization method for the test of T_{gel}, especially when there is a sharp phase transition associated with hydrogelation. Although the rheological, elastic, and thermodynamic properties of supramolecular hydrogels provide limited insight into the atomistic molecular arrangement and understanding of how small molecules self-assemble to form hydrogels, the combination of physical characterization with a systematic structural modification of the hydrogelators would contribute to establishing the structure−property relationships of supramolecular hydrogels. Clearly, this approach requires the synthesis of molecules, which is a core activity of chemistry. Moreover, the synthesis of new molecular entities provides opportunities for discovering new materials, especially supramolecular hydrogels. This kind of approach, together with additional techniques and greater correlation of various techniques, ultimately should help infer the nanostructures of supramolecular hydrogels in great molecular detail.

3.4. X-ray Diffraction

Small-angle X-ray scattering (SAXS) is another technique for characterizing supramolecular hydrogels with a resolution close to that of TEM.[195,196] Different from TEM, which focuses on the local morphology of gel matrixes, SAXS mainly provides averaged information on the matrixes of supramolecular

DOI: 10.1021/acs.chemrev.5b00299
Chem. Rev. 2015, 115, 13165−13307

Scheme 7. Representative Molecular Structures of Hydrogelators

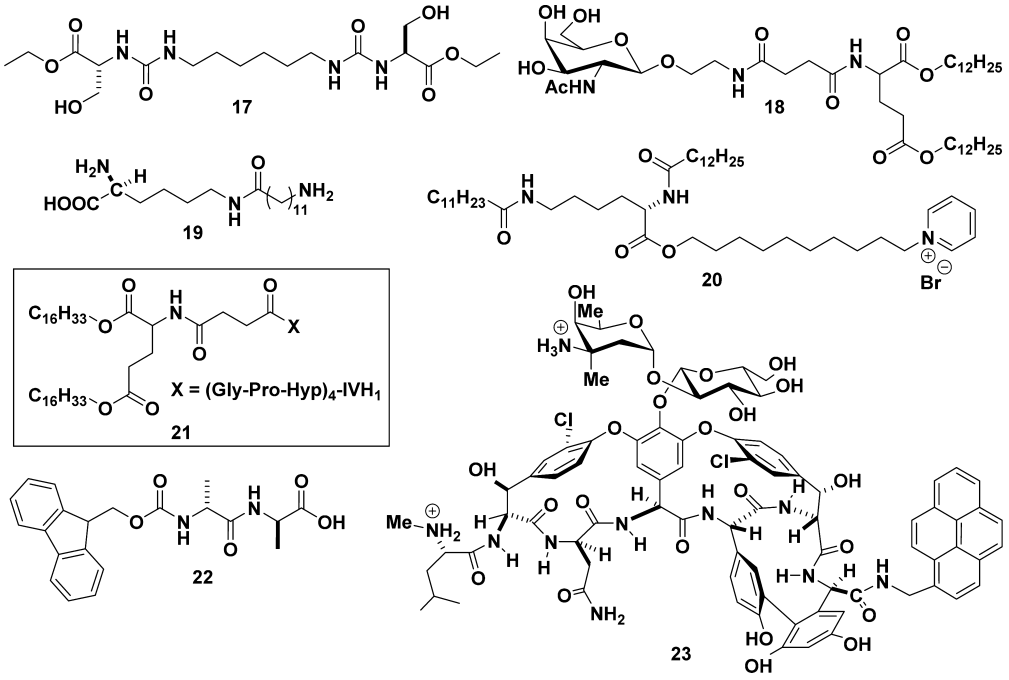

hydrogels by measuring the spatiality of the matrixes. In addition, wide-angle X-ray powder diffraction (XRD) contributes to the elucidation of the molecular organization and nanostructures of supramolecular hydrogels, especially when microcrystals are formed in the hydrogels.[197] The long *d* spacing obtained from XRD represents the longest repeat distance in the ordered structures by molecular self-assembly, which may provide insight into the packing of small molecules in either an extended or a bent conformation. A related technique for the characterization of gels is small-angle neutron scattering (SANS).[198,199] Although it is a rather specialized technique to which researchers have limited access, SANS is able to provide useful information about the average sizes and shapes of the nanostructures in a supramolecular hydrogel.[200−202]

3.5. Other Physical Methods

Besides the techniques referred to above, some other physical methods, such as circular dichroism (CD), UV/vis, infrared (IR) spectroscopy, fluorescence, or NMR, may also provide certain information about the molecular arrangement in supramolecular hydrogels through detection of the molecule−molecule or molecule−water interactions in primary or secondary structures. For instance, CD has a wide range of applications in many different fields, such as the study of the secondary structures of proteins, or the investigation of charge-transfer transitions. In the cases of soft materials such as hydrogels, CD is able to study the self-assembled superstructures in the gel phase or at the gel-to-sol transition.[203,204] However, it always remains a challenge to make any precise conclusion from the CD spectra alone, which means that it is better to combine CD with other techniques for studying secondary structures of supramolecular hydrogels. UV/vis is the technique used for investigating $\pi-\pi$ stacking (or aromatic−aromatic interactions) or metal coordination in the process of hydrogelation.[18,205−207] UV/vis, in combination with CD, may provide information for certain molecular arrangements in hydrogels. IR spectroscopy, dealing with the infrared region of the electromagnetic spectrum, is suitable for confirming the presence of hydrogen bonding and determining the protonation state of carboxylic acids.[208−211] Fluorescence is a useful tool for the investigation of the aggregation between aromatic groups and the formation of hydrophobic pockets inside hydrogels. In addition, the incorporation of fluorescent probes into supramolecular hydrogelators usually results in large, flat aromatic surfaces for self-assembly, thus providing a reliable approach for the design of an effective strategy to understand the gelation process and to discover more biological applications of supramolecular hydrogels.[212] Furthermore, solution-state NMR can identify the chemical shift changes in the aggregation process from the solution spectra to the gelled ones.[213] Solid-state magic angle spinning NMR (MAS NMR), being extensively used for characterizing structures of protein or peptide aggregates, may be useful for elucidating the structures of supramolecular hydrogels. Recent reports on the use of solid-state NMR to elucidate the packing of Aβ in Aβ amyloids[214] indicate solid-state NMR as a powerful method for elucidating the molecular arrangement of aggregates. However, the requirement of isotope labeling has limited the routine use of solid-state NMR for characterization of supramolecular hydrogels. In summary, it is always beneficial to analyze all the data collected via multiple methods for elucidating the nanostructures and potential applications of a given supramolecular hydrogel since data from various techniques are usually complementary to each other.

3.6. Modeling

On the basis of the molecular structural data collected from microscopy, XRD, SANS, or rheology, it is possible to use modeling for proposing a plausible arrangement of the molecular organization in supramolecular hydrogels.[215] Actually, researchers have already developed some relevant model systems from computer simulation about the gelation process of gelators in organic solvents.[216−220] However, few modeling approaches, currently, are reliable in describing the self-assembly of small molecules in water because of the inherent

DOI: 10.1021/acs.chemrev.5b00299
Chem. Rev. 2015, 115, 13165−13307

Scheme 8. Representative Molecular Structures of Urea-Containing Hydrogelators

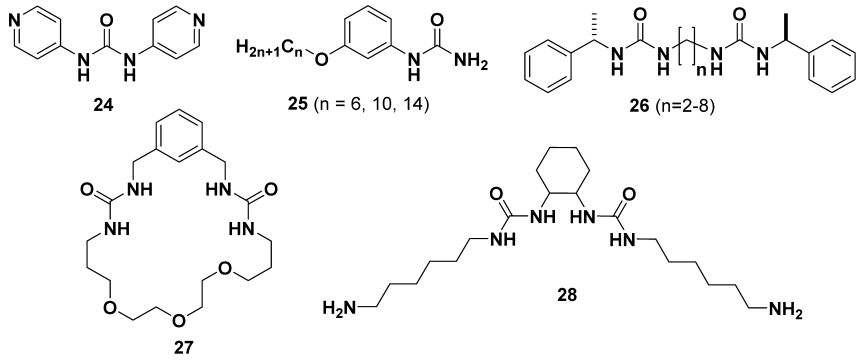

kinetic nature of hydrogels[221] and the lack of an accurate description of hydrophobic interactions, which, interestingly, are the major driving forces for small molecules self-assembling in water to form supramolecular hydrogels.

4. MOLECULAR DESIGN

While implying that the formation of supramolecular hydrogels via the self-assembly of small molecules in water is a common process, the serendipitous discoveries of many supramolecular hydrogelators also paradoxically indicate that, presently, it is still impossible to predict a hydrogelator a priori on the basis of its molecular structure. In fact, many designs of supramolecular hydrogelators only become possible after the serendipitous discovery of a particular hydrogelator. The inability of the prediction, in our opinion, mainly originates from the inaccurate evaluation of the interactions between water molecules and the hydrogelators (and their assemblies). Despite this currently unsolved problem, supramolecular hydrogelators, indeed, share common features despite their different molecular structures. Like certain proteins that self-assemble, supramolecular hydrogelators possess amphiphilicity and require noncovalent interactions ($\pi-\pi$ interactions, hydrogen bonding, and charge interactions among the molecules, among others) that allow effective building up of three-dimensional networks as the matrixes of hydrogels.

Scheme 7 shows a few classical examples of hydrogelators that certainly are the products of multiple weak interactions. Being derived from an existing family of low-molecular-weight organic gelators (urea derivatives),[222,223] **17**, an effective hydrogelator, maintains the intermolecular hydrogen bonds provided by its bisurea motif[224] and allows its free carboxylic acid groups for both solubility in water and pH control. Consisting of a saccharide (instead of using urea) for hydrogen bonding, **18** also relies on the long alkyl chain to enhance intermolecular hydrophobic interaction and to promote intermolecular hydrogen bonding among hydroxyl groups and amide bonds,[225,226] which results in a gelator that gels a diverse range of solvents (including water).[227] Incorporating L-lysine, which is easily made into an amphiphile, **19**[228] and **20**[37] not only act as hydrogelators, but also have inspired a wide range of other hydrogelators[76,211,229−232] based on L-lysine. Along the notion of synthetic amphiphiles,[233] **21** consists of two alkyl tails and self-assembles to form micelles, which result in hydrogelation.[234,235] Instead of relying on alkyl chain(s), **22**[11] utilizes aromatic−aromatic interactions of (fluoren-9-ylmethoxy)-carbonyl (Fmoc) to promote intermolecular hydrogen bonding for supramolecular hydrogelation. Because the Fmoc group is commonly used as a protection group for peptide synthesis, this convenience has led to many other Fmoc-based peptide hydrogelators.[236] These explorations and other related studies,[12,237,238] undoubtedly, establish aromatic−aromatic interaction as an effective hydrophobic force to enhance intermolecular hydrogen bonding for self-assembly of small molecules in water.[12,239] An intriguing and unexpected candidate as a hydrogelator is a vancomycin derivative (**23**).[18] Although a vancomycin analogue (ramoplanin) is able to form nanofibers upon binding to its receptor (a lipid I analogue),[240] it is still unusual for **23**[18] to act as a hydrogelator. This case, indeed, reflects the essential role and the diverse origins of multiple weak interactions for supramolecular hydrogelation. Despite the immense diversity of the hydrogelators, an essential requirement of a supramolecular hydrogelator is amphiphilicity. Although adequate intermolecular interactions among the hydrogelator are necessary for the self-assembly of the hydrogelators in water, one should avoid excessive intermolecular interactions that may result in the precipitation of the molecules in water. Since several excellent reviews[4,5,36] have already discussed molecular design in depth, interested readers are recommended to consult those reviews. Instead of prescribing a set of detailed rules of the design of a hydrogelator, we simply introduce the hydrogelators and hope the readers will formulate their own intuition on the aspect of the molecular design of supramolecular hydrogelators.

4.1. Hydrogels Based on Small Organic Molecules

Because the discovery of supramolecular hydrogels was made with small organic molecules,[4] we first discuss the small organic molecules that act as the molecular building blocks of supramolecular hydrogels (Table S1). The large and diverse pool of building blocks makes categorizing these small molecules rather subjective; thus, we arrange the hydrogelators according to their resemblance in molecular structure and start with the hydrogelator having the lowest molecular weight within each type. However, it is not necessarily that the hydrogelator having the lowest molecular weight would be the most effective hydrogelator. The most effective one should be the one that occupies the least volume fraction to form a hydrogel. Thus, highly effective hydrogelators should be able to gel water at a very low weight percentage. Another reason for this arrangement is that the structural similarity of the hydrogelator may offer a feasible starting point for the theoreticians who are interested in supramolecular hydrogels and strive to formulate principles for predicting supramolecular hydrogelation on the basis of molecular structures, which is still a challenge. In the following, we first discuss supramolecular hydrogels made of homotypic hydrogelators, and then introduce hydrogels consisting of a mixture of small molecules.

DOI: 10.1021/acs.chemrev.5b00299
Chem. Rev. 2015, 115, 13165−13307

Scheme 9. Representative Molecular Structures of Pyridine-Containing Hydrogelators

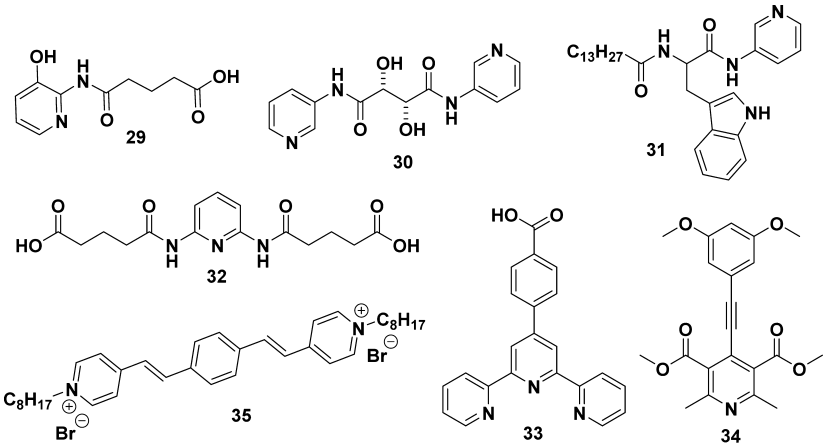

4.1.1. Urea-Containing Hydrogelators. By attaching a pyridyl group to the urea motif, Dastidar et al. synthesized a small hydrogelator (**24**; Scheme 8) that forms a hydrogel with the CGC of 0.8 wt %.[241,242] It was found that the urea group has to be at the para position of the pyridine to form the hydrogel. Because ethylene glycol molecules interact with both **24** and water, the authors were able to grow the crystals of **24** in a mixed solvent of water/ethylene glycol. The crystal structure contains both water and ethylene glycol and reveals valuable details about the intermolecular interactions that involve **24**, water, and ethylene glycol. Scanning electron microscopy (SEM) shows the fibrils formed by **24** in water are much thinner than the fibrils of this hydrogelator formed in water/ethylene glycol, suggesting the addition of ethylene glycol promotes the interfibrillar interactions. There are many other hydrogelators based on the urea motif developed during this decade.[243−256] For example, John et al. reported a urea-containing hydrogelator, 1-[3-(decyloxy)phenyl]urea (**25** (n = 10)) that not only forms a hydrogel in water at 0.1 wt %, but also serves as a matrix for preparing and stabilizing gold nanoparticles by in situ reduction.[257] Steed et al. reported the gelation ability of a series of chiral bisurea gelators (**26**).[258] When n is an even number in **26**, the molecules act as a gelator (1 wt %) in a mixed solvent (e.g., $CHCl_3$−MeCN−DMSO:H_2O = 7:1), but **26** fails to form a gel when n is an odd number. According to the crystal packing diagrams, the antiparallel urea tape motif appears to be necessary for the formation of hydrogels, which consist of matrixes made of microcrystals. Shimizu et al. designed second-generation self-assembling bisurea macrocycles (e.g., **27**), which consist of more flexible building blocks that form columnar structures in the solid state.[259] van Esch et al. reported a class of efficient hydrogelators based on a simple attachment of hydrophilic hydroxyl or amino functionalities to cyclohexane bisurea organogelators. They found that **28** in 1 N NaOH forms a hydrogel with a CGC of 0.5 wt %. Interestingly, after the formation of the hydrogel, the pH decreases to around 11.2. Further lowering the pH to 10.1 results in a gel−sol transition. While the pure enantiomer of **28** results in a more stable hydrogel than that made of racemic **28**, the hydrogel of racemic **28** melts, almost being independent of the concentration. The authors observed that the racemic hydrogel became turbid upon heating, a commonly observed phenomenon for an entropy-driven hydrogel.[260]

4.1.2. Pyridine-Containing Hydrogelators. As shown in Scheme 9, Tang et al. synthesized a small gelator, **29**, from 3-hydroxy-2-aminopyridine and glutaric anhydride. **29** forms a supramolecular hydrogel at a concentration of 1.5 wt %. The authors found that an increase of the power of the ultrasound from 200 to 500 W decreases the width of the self-assembled fibers from 8 to 2 μm, accompanied by an increasing network density in the hydrogels.[261] Dastidar et al. synthesized a series of bisamides derived from L-(+)-tartaric acid as potential hydrogelators. Among 14 bisamides synthesized, dipyrid-3-yltartaramide (**30**) displays an intriguing nanotubular morphology of its gel network in the gel made in DMF/water. Bearing a pyridyl group, **30** is able to coordinate with Cu(II)/Zn(II) salts under suitable conditions to afford metallogels. One unique aspect of this study is that the authors managed to obtain a considerable amount of single-crystal structures of those gelators. While polymorphism likely exists in the gel phase, these structural details have provided useful insights to understand the plausible intermolecular interactions among the gelators.[262]

While **30** fails to form a gel at pH below 7.0, another pyridine-containing amino acid-based gelator (**31**) forms gels in aqueous media in the presence of hydrochloric acid. Besides the fact that it forms a transparent gel in a water/ethanol mixture at a CGC of 0.2 wt %, the solution of the gelator successfully detects and traps hydrogen chloride gas, likely due to the sol−gel transition when the pH is lowered.[263] Tang et al. synthesized a hydrogelator, 2,6-bis[*N*-[(carboxypropyl)-carbonyl]amino]pyridine (**32**), from 2,6-diaminopyridine and glutaric anhydride by a one-step procedure. **32** forms a self-supporting hydrogel at a concentration of 4 wt %, which contains microcrystalline networks to immobilize water.[264] Sambri et al. reported a class of terpyridine derivatives (e.g., **33**), in their bisprotonated forms, to act as versatile hydrogelators upon ultrasound irradiation. Although the terpyridine ligand chelates with metal cations, resulting in stable gels with tunable emissive properties, the SEM images of the hydrogels exhibit only a slight change before and after the chelation.[265,266]

McNeil et al. designed an innovative class of pyridine-based gelators that formed gels in a mixed solvent of water and DMSO. For example, **34** forms a gel at 3 wt % in 1:1 DMSO/water. Besides investigating the relationship between molecular structure and gelation ability of these pyridine-based compounds,[267] the authors discovered that some of the gelators are

DOI: 10.1021/acs.chemrev.5b00299
Chem. Rev. 2015, 115, 13165−13307

Scheme 10. Alkyl-Chain-Containing Hydrogelators

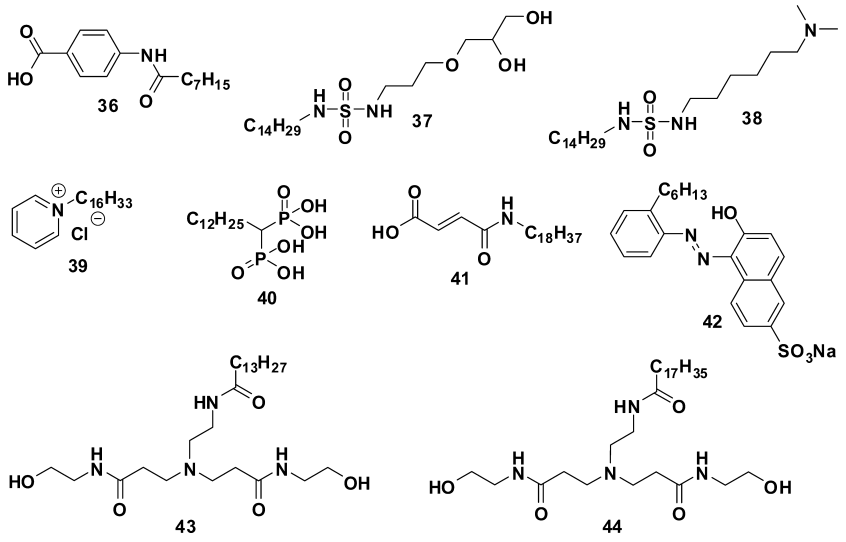

able to sense nitric oxide.[268] If this class of compounds can act as hydrogelators with a reduced use of DMSO, they likely will find broader applications. Bhattacharya et al. reported an effective hydrogelator (**35**) based on (phenylenedivinylene)-bispyridinium. With two *n*-octyl chains, **35** forms a hydrogel in water with a CGC of 0.12 wt %. This hydrogelator self-assembles to give a morphological transition from fiber to coil to tube, depending on the concentration of the gelator. Because the emission of the chromophore is sensitive to the environment, self-assembly of the gelator and a change of the ionic strength lead to the aggregates fluorescing in different colors.[274] This type of fluorescent colloid, recently rediscovered and termed "aggregation-induced emission" by Tang et al.,[269,270] was reported three decades ago or earlier.[271,272] In fact, the restriction of bond rotation to generate fluorescent colloids had already found applications in molecular imaging about two decades ago.[273] The generation of a white-light emission from a single chromophore in a single solvent (water),[274] indeed, agrees with the polymorphism of the assemblies of the hydrogelators, which illustrates the versatility of supramolecular hydrogels. The authors also observed a similar emission switch when the solvent was a mixture of ethanol and water and reported that the color of the emission depends on the temperature.[275]

4.1.3. Alkyl-Chain-Containing Hydrogelators. As shown in Scheme 10, Schmidt et al. designed and synthesized a series of derivatives of *N*-amidated 3- and 4-aminobenzoic acids with linear alkyl chains ranging between 3 and 13 methylene units long, among which the 4-(octanoylamino)benzoic acid sodium salt is able to form supramolecular hydrogels thermoreversibly in aqueous solutions of alkaline sodium salts at a concentration of 1 wt % **36** and 1 N NaOH. Moreover, a mold-casting/drying process can transfer the supramolecular assemblies to produce self-supporting, macroscopic, supramolecular, nanofiber mats, which are thermally and mechanically stable, and resistant to a large variety of organic solvents. On the basis of SEM, XRD, and cryo-TEM, the authors proposed the mechanism of the formation of the nanofibers of **36**, involving the transformation of spherical micelles into ribbons and platelets of multiple stacks of bilayers of the sodium salt of **36**.[276] Araki et al. reported an asymmetrically substituted sulfamide (**37**) that forms a hydrogel in water at a CGC of 1.0 wt %. SEM and XRD suggest the formation of lamellar superstructures via a hydrogen-bond-directed amphiphilic 2D sheet. **37** can also gel an organic solvent, such as benzene. One intriguing property is that the casted film of **37** and the xerogel of **37**, from benzene or water, result in almost identical XRD patterns. More interestingly, this gelator is able to form homogeneous and heterogeneous biphasic gels when the solvents are benzene and water. It would be useful to develop applications of the biphasic gels.[277] On the basis of a similar concept, Araki reported that **38** forms a hydrogel at a CGC of 0.5 wt % upon protonation of the tertiary amine groups. The authors also observed lamellar superstructures and suggested the formation of 2D sheetlike assemblies by the 2D hydrogen bond networks between sulfamide moieties. The authors also reported that, with an increase of the concentration of **38** to 2.0 wt %, the hydrogel exhibits relatively high mechanical stability.[278]

Patnaik et al. reported that cetylpyridinium chloride (CPC) (**39**) forms a gel with a CGC of 6 wt % in a mixed solvent of chloroform and water. On the basis of SAXS, the authors suggested that the packing of the molecules is polymorphic, which also leads to a lamellar organization.[279] The authors also reported a two-component gel resulting from **39** in the presence of a structure-forming bolaamphiphilic additive, 6-aminocaproic acid (6-ACA), and the CGC remains at 6 wt % for the mixture of **39** and 6-ACA. The authors used SAXS to infer that the gelators assemble as a lamellar organization of a loosely interdigitated bilayer structure of **39** and 6-ACA molecules predominantly due to charge transfer, hydrogen bonding, and hydrophobic interactions.[280] Alanne et al. recently reported a simple hydrogelator[281] based on bisphosphonates (BPs), a well-known class of compounds used for treating osteoporosis. Similar to the incorporation of bisphosphonates in both polymeric hydrogels[282] and supramolecular hydrogels,[283,284] **40** is a new supramolecular hydrogelator consisting of bisphosphonates which forms a transparent hydrogel (at 4 wt %) that contains lamellar structures.[281]

Baskar et al. reported that *N*-octadecylmaleamic acid (**41**) formed hydrogels with a CGC of 0.75 wt % in basic conditions. Small-angle X-ray diffraction indicates lamellar structures in the hydrogels. The hydrogels likely are lyotropic liquid crystals because they exhibit birefringence.[285] Tiller et al. reported that a simple azo dye gels water at 5 wt % upon cooling from hot

DOI: 10.1021/acs.chemrev.5b00299
Chem. Rev. 2015, 115, 13165−13307

Scheme 11. Representative Molecular Structures of Alkyl-Chain-Containing Hydrogelators

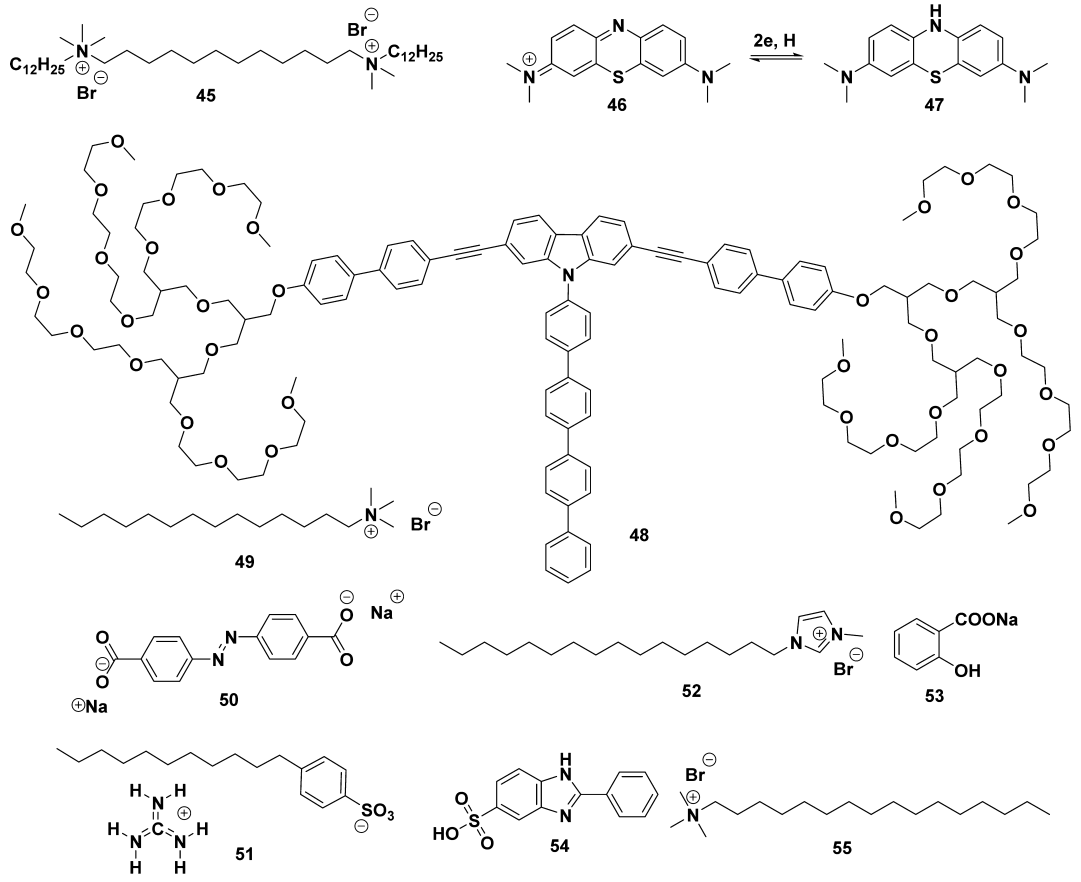

water. Using a glass slide coated with positive charge, the authors were able to induce hydrogelation on the surface when the solution concentration of **42** was as low as 0.10 wt %.[286] The authors suggested that this significant reduction of CGC might be a useful concept for the design of drugs. This concept,[287] indeed, is supported by the hydrogelators that inhibit bacteria[18] or cancer cells.[288] In a more detailed study, the authors found that the hydrogel prepared from **42** consisted of highly ordered and stable hierarchical structures. On the basis of nuclear magnetic resonance, rheology, X-ray scattering, birefringence, and microscopy, the authors suggested that **42** forms worm micelles as the matrixes of the hydrogel of **42**.[289] Kawai et al. reported hydrogelators **43** and **44**, which consist of three amide moieties and one alkyl chain. At pH 9.0, the CGC values for **43** and **44** are 1.2 and 0.3 wt %, respectively. A decrease of the pH of the gels leads to a gel−sol transition due to the protonation of the ternary amine. On the basis of X-ray diffraction and FT-IR analyses, the authors concluded that **43** and **44** form lamellar-like aggregates in the hydrogels, presumably because the amide moieties form strong intermolecular hydrogen bonds. Despite the fact that there is a suspension phase between the pH-induced gel−sol transitions, the hydrogel of **43** or **44** exhibits high sensitivity to the pH change, which is needed for the phase transition.[290]

While redox chemistry is a fundamental process in nature, there are only limited numbers of reports on the electrochemical characterization of supramolecular hydrogels.[291,292] Yang et al. has proposed an electrochemical strategy to characterize the hydrophobic microenvironment of micellar hybridized supramolecular gels.[293] As shown in Scheme 11, by using a gemini surfactant (**45**) and the classical gelator *N*,*N*-dibenzoyl-L-cystine (**1**) to form a micellar hybridized hydrogel, the authors quantitatively characterized the net positive shifts of the redox formal potential and the change of peak currents obtained from the cyclic voltammograms of methylene blue (**46**).[293] According to the authors, by comparing the apparent diffusion coefficients of **46** in these different systems, it is feasible to characterize the hydrophobicity change of the hybrid supramolecular hydrogel made of **1** and **45**.

Lee et al. demonstrated an ingenious way to combine a nonionic surfactant and an aromatic core to generate an innovative class of molecules that self-assemble in water.[294] For example, the authors reported that a T-shaped aromatic amphiphile, consisting of tetrabranched oligo(ethylene oxide) chains, self-assembles to form nanofibers in water, which result in hydrogelation at a concentration of 0.5 wt %.[295] Unlike most other hydrogelators, **48** forms a hydrogel when the temperature increases. This type of LCST, though being common for polymeric hydrogels, is less reported for supramolecular hydrogels.

Hao et al. investigated hydrogels formed by mixing alkyltrimethylammonium bromides **49** and sodium azobenzene-4,4′-dicarboxylic acid (**50**). In a typical example, **49** and **50** in a 2:1 ratio form a hydrogel at a concentration of about 4.0 wt %. The authors found that UV irradiation or the addition of a salt and an acid results in a gel−sol transition, while the addition of a base hardly changes the hydrogel, suggesting that it is important to maintain the ionic state of **50** for the hydrogelation.[296] Ward et al. reported that amphiphilic guanidinium alkylbenzenesulfonates **51** exhibit lyotropic

DOI: 10.1021/acs.chemrev.5b00299
Chem. Rev. 2015, 115, 13165−13307

Scheme 12. Hydrogelators Containing Multi/Polyhydroxyl Groups

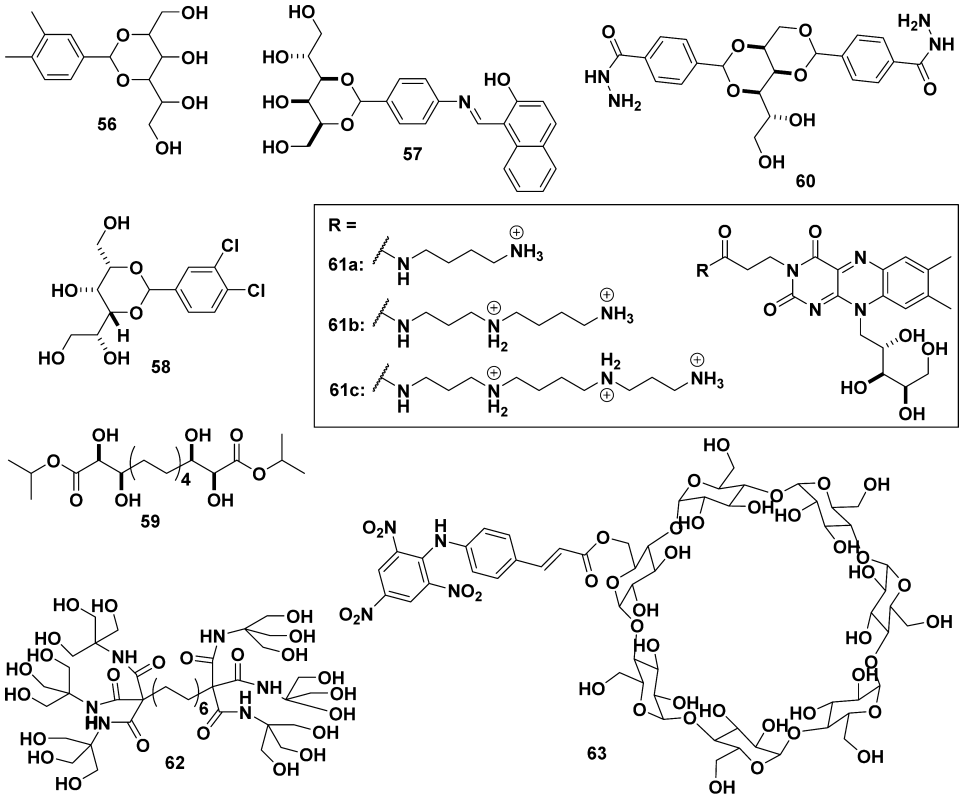

behavior in aqueous solvents. At a relatively high concentration, 10 wt %, **51** self-assembles to form a lamellar structure and results in hydrogels.[297] Huang et al. demonstrated that the mixture of an imidazole-type surfactant, 1-hexadecyl-3-methylimidazolium bromide (**52**), and a sodium salicylate (**53**) produces a thermoresponsive hydrogel at a CGC of 2 wt %. The authors reported that, above the critical temperature, the sample exhibits viscoelastic properties of wormlike micelles, and the viscoelastic solution transforms into an elastic hydrogel accompanied by a remarkable increase of the elastic modulus.[298] Hoffmann et al. studied the phase behavior and aggregation in the aqueous solutions of mixed 2-phenylbenzimidazole-5-sulfonic acid sodium (**54**), an anionic UV absorber, and cetyltrimethylammonium bromide (**55**), a cationic surfactant.[299] The authors found that the morphologies (i.e., vesicles, tubules, or ribbons) of the self-assembled structures depend on the ratio of the two components in the mixture. For example, a hydrogel forms at 0.6 wt % with a molar ratio of **54** and **55** of 8:2. The authors found that the formation of very long stiff tubules about 14 nm in diameter leads to hydrogelation, and suggested that the stiffness of the bilayer of the vesicles and the stiffness of the tubules originate from the rigidity of **54**.

4.1.4. Hydrogelators Containing Multi/Polyhydroxyl Groups. As shown in Scheme 12, Shan et al. reported an interesting small molecule (**56**) that self-assembles in 6 M KOH to form a hydrogel at a concentration as low as 0.3 wt %. When the concentration of **56** increases to 1.4 wt %, the gel−sol transition temperature almost reaches 100 °C. According to the authors, **56** is the first low-molecular-weight gel electrolyte having good electrochemical properties while solving the problem of solution leakage, which may find application in supercapacitors.[300] Also, using sorbitol, Niu et al. developed a smart functional gelator containing a salen moiety (**57**). **57** self-assembles in a mixed solvent of DMSO/H_2O to form a gel at a CGC of 3 mM (0.13 wt %). The gel turns to a solution upon the addition of copper(II), and the solution reverses back to the gel state upon the addition of EDTA to competitively coordinate away the copper(II).[301] Song et al. also reported a D-sorbitol-based hydrogelator and the effect of salt on the hydrogelation of 2,4-(3,4-dichlorobenzylidene)-D-sorbitol (DCBS, **58**), which forms a hydrogel at a concentration of 1 wt %. While SEM indicates that the hydrogels consist of globular aggregates, the addition of NaCl to the aqueous medium not only accelerates the gelation, but also results in networks of long fibers. Using UV/vis and fluorescence emission spectra to characterize the hydrogels, the authors concluded that extensive aggregation of the phenyl rings is responsible for the gelation. Variable-temperature ^{1}H NMR spectra further demonstrate that the addition of the salt NaCl enhances the $\pi-\pi$ interactions. Wide-angle X-ray diffraction shows that the hydrogels have a layered structure that is independent of the addition of NaCl. The authors also used density functional theory (DFT) calculations to support the proposed molecular packing of the gelator in the nanofibers.[302]

Griffiths et al. found that bis-α,β-dihydroxyl esters are able to gel thermoreversibly a wide range of solvents.[303] As a gelator, **59** forms a gel in a water-rich (75%) ethanol/water mixture at a concentration of 0.18 wt %. On the basis of SANS, Ohsedo et al. suggested that in the gelation mechanism the bis-α,β-dihydroxyl ester motif forms rodlike structures.[304,305] On the basis of a well-known organogelator, dibenzylidenesorbitol, Smith et al. developed a simple condensation between sorbitol and 2 equiv of a benzaldehyde derivative to form a hydrogelator (**60**) which is functionalized with hydrazide (as replacements for carboxylic acids). **60** not only self-assembles to form

DOI: 10.1021/acs.chemrev.5b00299
Chem. Rev. 2015, 115, 13165−13307

Scheme 13. Hydrogelators Having C_3 Symmetry

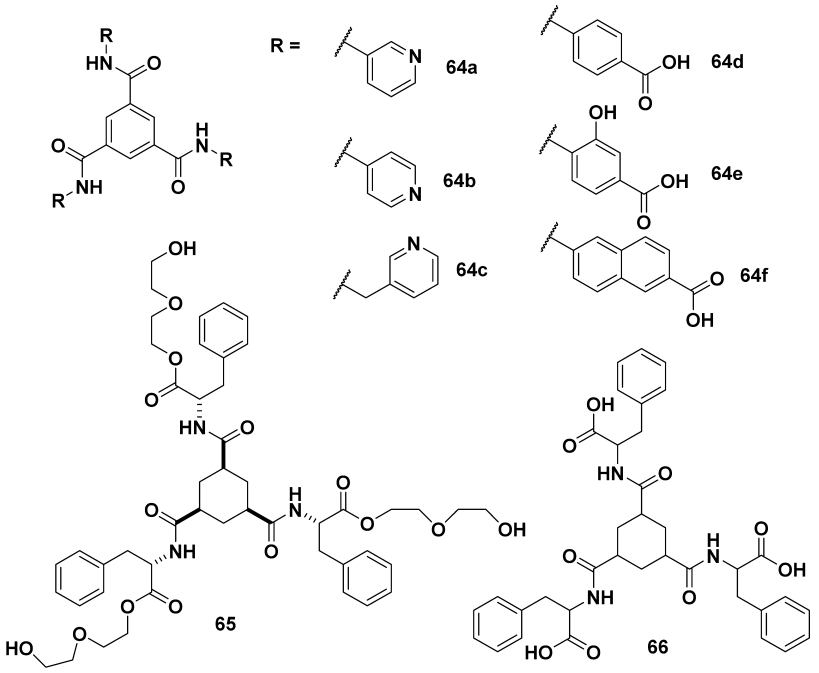

hydrogels, at a CGC of 0.8 wt % in water across a wide pH range, with a small amount of DMSO, but also exhibits pH-switchable dye adsorption−desorption depending on the protonation of the target dyes.[306] Kim et al. designed a hydrogelator (**61a**) derived from riboflavin (vitamin B_2).[307] The authors found that **61a** forms a hydrogel at a concentration of 1.6 wt %, but **61b** and **61c** are too soluble to form a hydrogel. One interesting observation reported by the authors is that the ability of hydrogelation apparently is beneficial for the delivery of vascular endothelial growth factor small interfering RNA (VEGF-siRNA) into human cells.[307] Russo et al. reported that arborols, a type of dumbbell-shaped molecules acting as bolaamphiphiles, are able to assemble spontaneously into long fibers and to lead to thermally reversible gels. On the basis of wide-angle X-ray scattering, the authors concluded that the self-assembly of **62** at 0.2 wt % results in fibrils in solution and the formation of bundles of fibrils at 2 wt % is responsible for the hydrogelation.[308] Harada et al. reported a chemical-responsive supramolecular hydrogel based on a derivative of β-cyclodextrin (**63**). After the hydrogelator **63** forms a hydrogel at a CGC of 2.9 wt %, the addition of 1-adamantanecarboxylic acid or a large amount of urea induced a gel-to-sol transition.[309] On the basis of a detailed NMR study, the authors suggested that the host−guest and hydrogen-bonding interactions of cyclodextrins lead to the formation of supramolecular fibrils, which explains the chemoresponsiveness of the hydrogels.[309] Instead of using β-cyclodextrin, Osakada et al. used α-cyclodextrin and an alkylpyridinium to generate a series of pseudorotaxanes that form hydrogels. According to the authors, the possible mechanism is that the host−guest interactions transform the micelles of an alkylpyridinium to nanofibers of the pseudorotaxanes and result in gelation at a concentration of about 12 wt %.[310]

4.1.5. Hydrogelators Having C_3 Symmetry. As shown in Scheme 13, Xu et al. developed a supramolecular gel in a mixture of ethanol and water (1:1) based on *N*,*N*′,*N*″-tris(3-pyridyl)trimesamide (**64a**).[311] The nitrogen and amide group in hydrogelator **64a** can bind with phosphate and carbonate ions via H-bonding and act as biomineralization active sites for growing biominerals. The authors found that the calcium phosphate grew into curved platelike nanostructures along the fibers. In another work, Dastidar and Das et al. reported hydrogelators **64a** and **64b** derived from the pyridyl amide of trimesic acid[312] and demonstrated that **64a** and **64b** are able to form gels in a mixed solvent of MeOH/H_2O at concentrations of 0.2 and 0.1 wt %, respectively. On the basis of the crystal structures of **64a** and **64b**, the authors also proposed intermolecular interactions among the gelators, which is reasonable if the matrixes of the gels are microcrystalline. Li and Xu et al. also studied the gel of **64a** (0.55 wt %) in a 1:1 mixture of ethanol and water at pH 7.0. They found that the macroscopic viscoelastic properties of the gel of **64a** depend on the microscopic hydrogen bonding between the amide N−H bond and the nitrogen on the pyridyl group (N−H···Py). One notable feature was the increase of the storage modulus of the gels upon a decrease of the pH to 5.0. The authors suggested that a partial break of the hydrogen bonds of N−H···Py leads to a highly branched and homogeneous fibrillar network in the gel, as revealed by XRD and field-emission scanning electron microscopy (FESEM) images.[313] Such highly branched fibrillar networks likely result from the reduction of the crystallinity of the fibrillar network, which is a useful insight for the design of supramolecular hydrogels. The same laboratory reported that another molecule of trimesic amide (**64c**) self-assembles to form hexagonal microtubes in a mixed solvent of H_2O/THF and is able to gel H_2O/THF at a concentration of 1.0 wt %.[314]

Replacing the pyridyl group in **64b** by a benzoic acid in the trisamide to produce **64d**, Schmidt et al. demonstrated that **64d** acts as a hydrogelator and forms a photoluminescent hydrogel in water at a CGC of 0.2 wt %. Having carried out DFT calculations, the authors suggested that the photoluminescence originates from the formation of a supramolecular chromophore.[103] On the basis of the structure of **64d**, researchers

DOI: 10.1021/acs.chemrev.5b00299
Chem. Rev. 2015, 115, 13165−13307

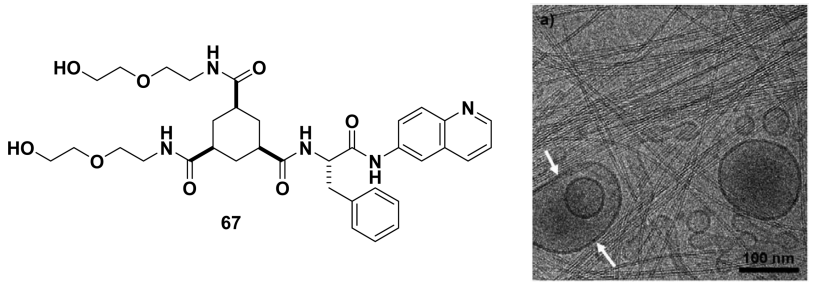

Figure 2. Cryo-TEM images of unilamellar dioleoylphosphocholine (DOPC) vesicles coexisting with a network of well-defined fibers of **67** with a high aspect ratio. Adapted with permission from ref 321. Copyright 2008 Wiley-VCH Verlag GmbH & Co. KGaA.

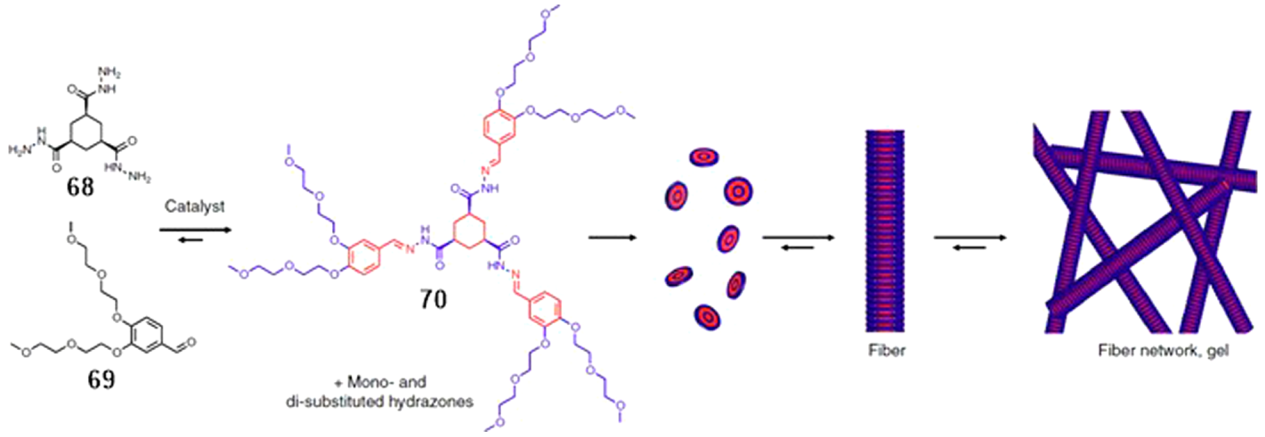

Figure 3. Catalytic formation of trishydrazone hydrogelator **70** from soluble building blocks **68** and **69** leads to supersaturation followed by formation of fibers that eventually cross-link to form a network that traps the surrounding solvent, leading to gelation: blue, hydrophilic functional groups; red, hydrophobic functional groups. Adapted with permission from ref 142. Copyright 2014 Nature America.

investigated a series of simple benzene-1,3,5-tricarboxamide (BTA)[315] aromatic carboxylic acid compounds. Lloyd et al.[316] found that the *N*-methylation of the amide bond in **64d** results in a compound to give a precipitate upon a decrease in pH, implying the critical role of hydrogen bonding between the amides for hydrogelation. The authors also introduced a hydroxyl group or a naphthyl moiety to generate the hydrogelators **64e** and **64f**, respectively. Both **64e** and **64f** have a CGC of 0.1 wt %. Compared to the hydrogel of **64d**, the hydrogel of **64e** exhibits a 10-fold higher yield stress, and the hydrogel of **64f** results in a 4-fold higher storage modulus. Nagarajan et al. reported that the replacement of carboxylic groups in **64d** by alkyl chains also leads to gelators which largely gel organic solvents such as DMSO.[317]

Bommel and van Esch et al. developed a class of effective hydrogelators based on cyclohexane-1,3,5-tricarboxylic acid. By capping the C-terminal phenylalanine with diethylene glycol, they obtained a hydrogelator (**65**) with a remarkably low CGC value (0.033 wt %).[318] The authors also obtained the crystal structure of an analogue (a nongelator) of **65** and provided useful insights for the molecular design of this type of hydrogelator.[318] In another illuminating study, Friggeri and van Esch et al. investigated the ability of several 1,3,5-cyclohexanetricarboxamide−phenylalanine derivatives **66** to form hydrogels. While they found that enantiomerically pure homochiral 1,3,5-cyclohexanetricarboxamide−L-phenylalanine crystallizes from water and fails to form gels, the heterochiral derivatives with either two L-phenylalanine moieties and one D-phenylalanine (LLD) or vice versa (DDL) are able to form hydrogels with a CGC value of 0.04 wt %. The authors also found that an increase of the concentration to 0.12 wt % LLD-**66** or DDL-**66** results in hydrogels with a remarkably high gel−sol transition temperature at 120 °C. The authors also demonstrated that the attachment of a second amino acid or a hydrophilic moiety to the C-terminal of the homochiral derivatives of **66** produces effective hydrogelators.[319] To align the amide bond in this type of 1,3,5-triamide cyclohexane derivatives, van Esch and Samori et al. used an electrical field to assist the alignment of the nanofibers and demonstrated that the application of a voltage bias, indeed, helps the directional orientation of the fibrils.[320]

Using the 1,3,5-triamide cyclohexane-based hydrogelators **67**, van Esch et al. demonstrated an elegant system that forms well-defined nanostructures by the orthogonal self-assembly of hydrogelators and surfactants.[321] Taking advantage of the thermoreversibility of the hydrogels made of the 1,3,5-triamide cyclohexane-based hydrogelators (e.g., **67**), the authors dissolved the hydrogelators in solutions of surfactants above the gel−sol transition temperature, followed by cooling the mixture and examining the hydrogelation. One of the most interesting results reported by the authors was that cryo-TEM studies revealed that, when lipids, DOPC, are used, the unilamellar DOPC vesicles encapsulate well-defined fibers with a diameter of 5 nm in the middle of their aqueous compartment (referred to as "gellosomes"[322]) (Figure 2). Another remarkable feature was that the membrane wall is able to restrict the growth of the fibers to a few hundred nanometers. These observations imply that one should be able to use the mutual interactions between both of the self-assembled structures to design sophisticated soft materials, as recently

DOI: 10.1021/acs.chemrev.5b00299
Chem. Rev. 2015, 115, 13165−13307

Scheme 14. Bile Acid-Derived Hydrogelators

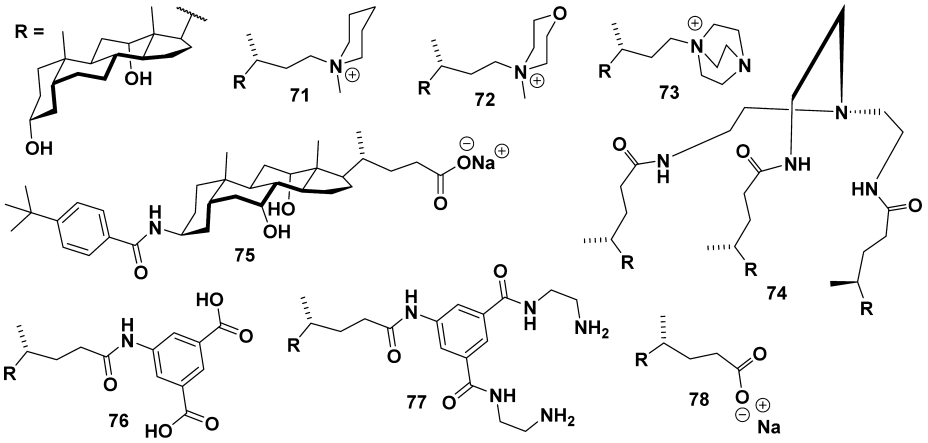

suggested and further demonstrated by van Esch et al.[323,324] van Esch et al. recently reported another seminal study on the catalytic formation of the triamide cyclohexane-based hydrogelators.[144] Specifically, either an acid or a base can catalyze the formation of a trihydrazone hydrogelator (**70**) from the soluble building blocks **68** and **69**. The authors demonstrated that the concentration of the catalyst used in the in situ formation of the hydrogelator controls the gelation time and mechanical stiffness of the final gel (Figure 3).[142,325] This work may lead to an elaborate way to form hydrogels via control of the reaction kinetics.[326]

4.1.6. Hydrogelators Derived from Rigid Aliphatics. As shown in Scheme 14, Terech et al. investigated hydrogels made of cationic bile acid derivatives (e.g., **71**). They found that **71** (I^- as the anion) forms a robust hydrogel at 2.0 wt % to exhibit a storage modulus of 0.3 MPa. On the basis of X-ray crystallography of the single crystals and X-ray scattering experiments, the authors concluded that the gel state consists of a morphology different from that of the solid, which is supported by EM investigations of the xerogels to reveal the fibrous nature of the gel networks. On the basis of the structural difference of the derivatives and the morphology of the networks in the hydrogels, the authors suggested an interesting notion that more compact structures would develop at low concentrations.[327] The same group of authors used SANS to study the self-assembled structures of the hydrogels formed by the hydrogelators **71**−**73**. They found that **71** forms thick cylindrical fibers (R = 68 Å), the aggregates of **72** are ribbons with a bimolecular thickness of t = 37 Å and an anisotropy of the section of $b/a \approx 0.1$, and **73** exhibits a remarkable transition from ribbons to thicker cylindrical fibers upon an increase of the concentration. The authors also suggested the existence of secondary aggregation mechanisms in the formation of bundles,[328] differing from the behaviors of the hydrogels formed by sodium lithocholate.[329,330] Terech et al. also extensively investigated the effect of the electrolyte and counterions on the gelation of **73**. They found that the addition of a monovalent salt (NaCl) favors the formation of gels. At larger salt concentrations, the gels become more heterogeneous with nodal zones on the micrometer scale.[331] These studies provide a rare case to compare the molecular arrangements of the gelators in water and in an organic solvent.[332]

To understand the remarkable ability of hydrogelators made of cationic derivatives of deoxycholic acid, Maitra et al. designed and synthesized a series of that class of hydrogelators and compared them with hydrogelators based on natural anionic bile salts.[333] According to the authors, these cationic hydrogelators are pH independent and start to aggregate in water at a concentration an order of magnitude lower than those at which natural anionic bile salts aggregate.[333] Recently, Maitra et al. reported tunable luminescent gels and xerogels formed by lanthanide(III) cholates, which, according to the authors, might find applications as luminescent coatings on a glass surface.[334] Another type of innovative bile acid derivative reported by Maitra et al. is the perfluoroalkyl bile esters, which are efficient gelators in organic and aqueous−organic media.[335] The requirement of an organic solvent as the cosolvent seems a quite common feature of the hydrogelators derived from bile acid, which occurs in several other bile acid derivatives reported.[336] Maitra et al. also reported a hydrogelator based on tripodal cholamide (**74**). As a supergelator, **74** forms a hydrogel with a CGC of 0.02 wt % in water containing 0.01% acetic acid. Using fluorescent probes, 8-anilinonaphthalene-1-sulfonic acid and pyrene, the authors found two critical aggregation concentrations and suggested a progressive increase in aggregate size and the microviscosity of the aqueous pool encompassed by the self-assembled fibrillar network during the gelation. One noteworthy result from this work is that the microviscosity of the aqueous phase around the network of nanofibers is far less than the bulk viscosity of the gel.[337] The authors also used the tripodal cholamide-based hydrogel to synthesize semiconducting nanostructures and obtained nanotubes and nanorods of CdS, ZnS, and CuS.[338]

Galantini and Tato et al. reported an interesting hydrogelator of a bile salt derivative that forms a hydrogel in bicarbonate buffer (pH 10) at a concentration of 0.18 wt %.[339] The authors used a range of techniques (static light scattering (SLS), CD, SAXS, TEM, and optical microscopies) to establish the details of the self-assembly of **75**, which occurs at 1.8 wt % in the buffer and forms supramolecular nanotubes. According to the authors, the tubule formation starts with the aggregation of the fibrils, followed by a slow transformation and ordering of the tubule walls in well-spaced layers. One interesting feature is that the final elongation of the tubules proceeds without a further aggregation of fibrils.[340,341] By introducing a diamine or a dicarboxylic aromatic residue on the lateral of a natural bile acid, Galantini et al. obtained compounds **76** and **77**. While **77** forms a hydrogel at a CGC of 0.16 wt %, a mixture of **76** and **77** results in a hydrogel at a CGC of 0.05 wt %. This work, thus,

DOI: 10.1021/acs.chemrev.5b00299
Chem. Rev. 2015, 115, 13165−13307

Scheme 15. Some Bile Acid- or Cholesterol-Derived Hydrogelators

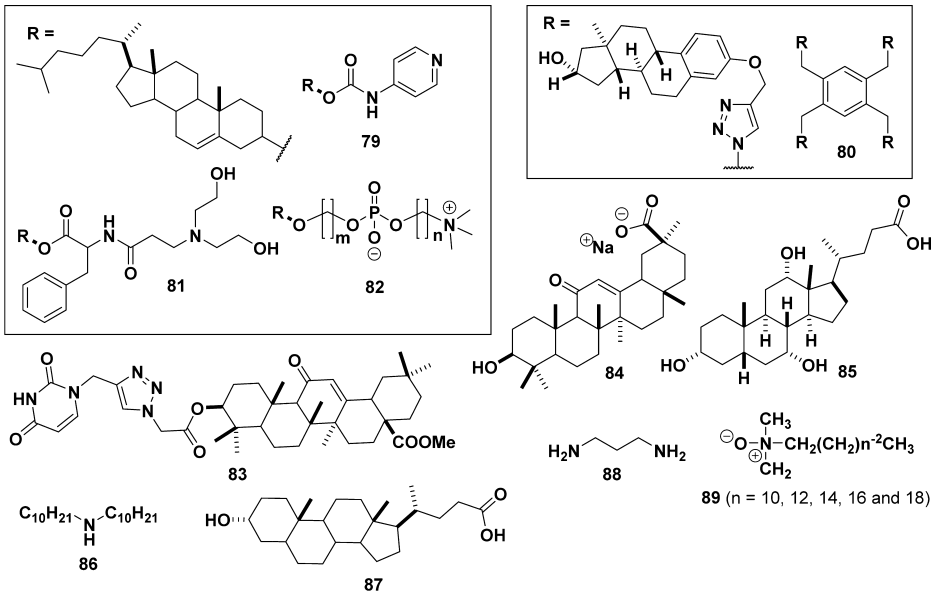

Scheme 16. Bolaamphiphiles as Hydrogelators

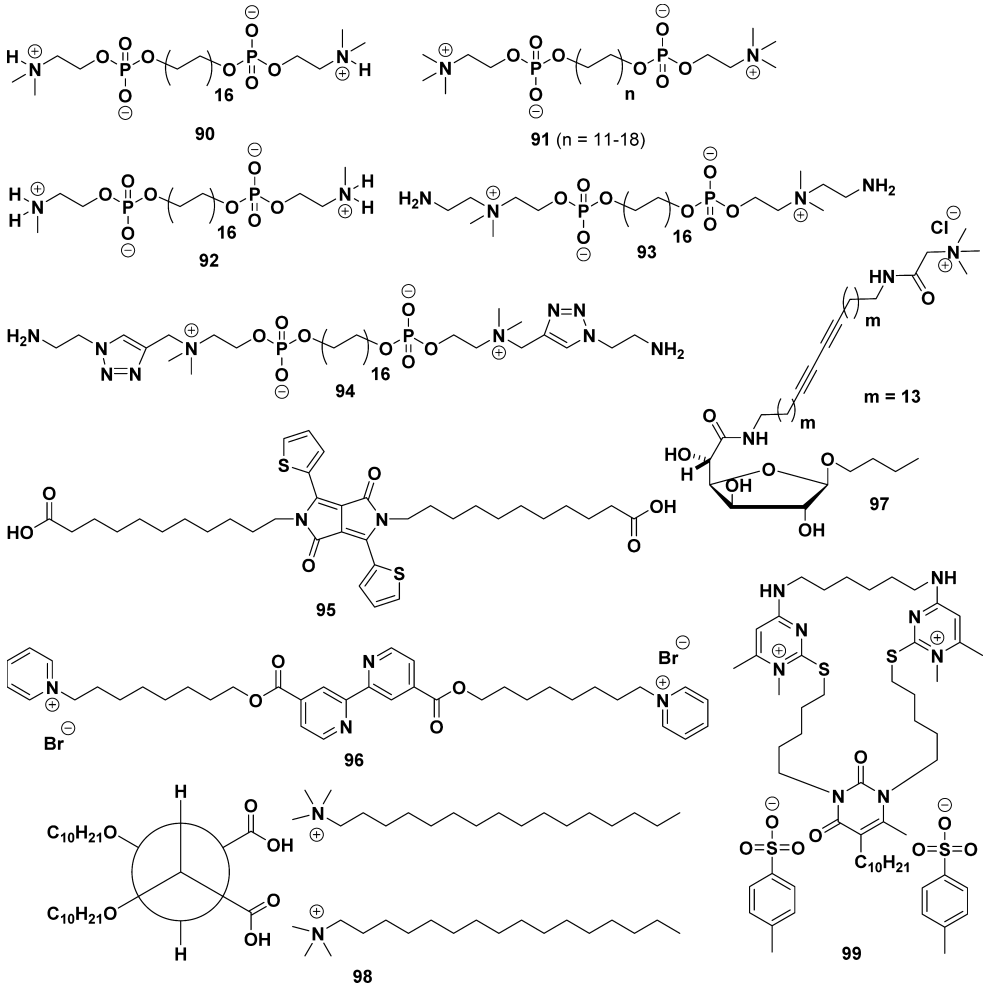

illustrates that the presence of the electrostatic interaction promotes the hydrogelation from more dilute samples, suggesting that cationic and anionic mixtures enhance the efficiency of the gelators.[342] Since there is greater understanding of the structures of the hydrogelators based on bile acids, the exploration of their applications is emerging as well. For example, Shen and Zhang et al. reported the use of the hydrogels of bile acid derivatives for creating gold and silver

DOI: 10.1021/acs.chemrev.5b00299
Chem. Rev. 2015, 115, 13165−13307

nanoparticles in situ.[343] Xin and Xu et al. reported that sodium deoxycholate (**78**) forms hydrogels at a concentration of 2 wt % in the presence of NaCl or NaBr.[344] They made an interesting observation that the addition of L-lysine or L-arginine turns the hydrogels to solutions. The authors suggested that the addition of amino acids competes with the hydrogen bonds needed for hydrogelation, thus causing a gel−sol transition.

As shown in Scheme 15, Shinkai et al. reported a versatile gelator (**79**) that is able to gel more than 10 different solvents.[345] Although **79** is unable to form a hydrogel, Sierra et al. used "click" chemistry to connect this type of estradiol-based gelator to form another effective gelator (**80**) that gels a DMSO and water mixture at concentrations as low as 0.04 wt %.[346] Using a cholesteryl derivative, Fang et al. developed another gelator (**81**) that gels a 1:1 mixture of acetone and water at 0.06 wt %.[347] Also employing a cholesteryl group, Ji et al. developed a series of phospholipid hydrogelators (**82**). Besides exhibiting polymorphism of the networks in the hydrogels, this type of hydrogelator forms hydrogels at CGC values as low as 0.05 wt % (**82**, m = 0, n = 2).[348] Ju et al. reported a conjugate of oleanolic acid with adenine (**83**) which forms a gel in mixed solvents of THF and water (2:3) at a CGC of 2 wt %. One feature of this gel is that the addition of uracil decreases the stability of the gel due to the disruption of hydrogen bonding between the hydrogelators.[54,349,350] Lu et al. recently reported that sodium glycyrrhetinate (**84**) is able to form a hydrogel with a CGC of 5.6 wt %, and the authors suggested the dipole−dipole interaction of sodium carboxylates as the main driving force for the hydrogelation of **84**.[351] Another related interesting work is the hydrolysis of succinated triamcinolone acetonide which forms triamcinolone acetonide and results in hydrogelation.[352]

Dastidar and Shibayama et al. took a combinatorial library approach to generate 60 organic salts by reacting 5 bile acids (e.g., **85**) with 12 secondary amines (e.g., **86**). After the gelation test with various aqueous and organic solvents, they found that 16 salts are supramolecular gelators, 6 of which are able to form gels in aqueous as well as organic solvents. The salt didodecylammonium cholate (**85** + **86**) is the most versatile gelator, forming a gel in a 1:1 mixed solvent of DMSO and H_2O at a CGC of 1 wt %. The authors used dynamic light scattering (DLS) and SANS to infer the fibrous network formed via flexible clusters of a few tens of nanometers in length, followed by the immobilization of the network in the gel.[68] Bhattacharya et al. demonstrated the formation of a supramolecular hydrogel by simply mixing lithocholic acid (**87**) with dimeric or oligomeric amines (e.g., **88**), at a total concentration of 5 wt %. However, the replacement of lithocholic acid (LCA) by cholic acid or deoxycholic acid results in no hydrogelation. On the basis of the single-crystal X-ray diffraction analysis with one of the amine−LCA complexes, the authors suggested that the electrostatic forces and hydrogen bonding between the amines and the carboxylate and hydroxyl moieties result in the formation of fibers as the matrixes of the hydrogels.[353] Song et al. used zwitterionic alkyldimethylamine oxide **89** to interact with litholic acid (**87**) to form hydrogels. When n = 12 in **89**, the two-component system exhibits a high gelation capability (CGC = 0.08 wt %). One notable feature is that an increase in the temperature results in a transition from helical fibrils to vesicles with an intermediate mesophase.[354] Tian et al. also reported an interesting photoswitchable cholesterol derivative as a gelator,[355] though it is too hydrophobic to act as a hydrogelator.

4.1.7. Bolaamphiphilic Hydrogelators. As shown in Scheme 16, Blume et al. reported a class of symmetric long-chain bolaamphiphiles that are efficient hydrogelators (**90** and **91**).[199,356−366] Among them, dotriacontane-1,19-diylbis[2-(dimethylammonio)ethyl phosphate] (**90**) forms a clear hydrogel at 0.1 wt % and pH 5. TEM reveals the hydrogelator to form a dense network of helically structured nanofibrils with a diameter of 3−4 nm. At pH 5, **90** self-assembles to form nanofibrils that are stable up to at least 75 °C. Although there is no gelation at pH 10, nanofibrils form, but they become fragmented at 75 °C.[358] The authors reported that SANS data support the significantly higher stability of the hydrogel of **90**.[199] While the formation of nanofibrils of **90** or **91** in the hydrogels agrees with these hydrogelators self-assembling to form worm micelles, the interfibrillar interactions depend on the kinetics of the self-assembly, thus resulting in rich polymorphism. For example, the cryo-TEM of the hydrogels of **91** (n = 17 or 18) reveals the formation of square lamellae.[361] Besides using the pH to control the morphology of the assemblies of those hydrogelators, the authors also demonstrated that the changes of the symmetry of the head groups are able to tune the self-assembly behavior of single-chain bolaamphiphiles in an aqueous suspension.[364]

Dobner et al. designed and synthesized a series of polymethylene-1,ω-bis(phosphocholine) (PC-C_n-PC) analogues,[367] and found that the even-numbered ones form nanofibers composed of stretched molecules with an *all-trans*-alkyl chain conformation.[367] Meanwhile, they synthesized the odd-numbered analogues to study a possible even−odd effect of these bolaamphiphiles during their aggregation in water. In addition to these bolaamphiphiles with phosphocholine head groups, they designed a series of polymethylene-1,ω-bis(phosphodimethylethanolamine)s (Me_2PE-C_n-Me_2PE) with smaller sizes of the head group. These bolaamphiphiles show an additional fiber−fiber transition when the alkyl chain length exceeds 26 carbon atoms. The behavior of the mixed bolaamphiphiles indicates that the fiber structure allows differences in the alkyl chains of up to six carbon atoms long. The mixing of two Me_2PE-C_n-Me_2PE- or PC-C_n-PC-type bolaamphiphiles with different alkyl chain lengths offers the possibility to adjust the temperature of the gel−sol transition, at which the cross-linking of the fibers breaks and the fibers dissociate. On the basis of this feature, the authors obtained thermally switchable hydrogels, which may allow fine-tuning for drug delivery applications. The comparison with dotriacontane-1,32-diylbis[2-(methylammonio)ethyl phosphate] (MePE-C_{32}-MePE, **92**), a bolaamphiphile with an even smaller phosphomonomethylammonium head group, illustrates the importance of the size of the head group for self-assembly. This bolaamphiphile self-assembles exclusively into lamellar structures, a type of assembly that persists in mixtures containing the fiber-forming molecules (**90**).[359]

Using different methods, researchers already have characterized the supramolecular behavior of the bolaamphiphilic hydrogelators dotriacontane-1,32-diylbis[2-(trimethylammonio)ethyl phosphate] (PC-C_{32}-PC, **91**) and the pH-sensitive dotriacontane-1,32-diylbis[2-(dimethylammonio)ethyl phosphate] (Me_2PE-C_{32}-Me_2PE, **90**).[357,359] Depending on the temperature, pH, and concentration, these bolaamphiphiles self-assemble into long nanofibers or other assemblies, such as short rods or micelles. To obtain information about the motional dynamics and microscopic order inside these assemblies, Blume et al. carried out a

DOI: 10.1021/acs.chemrev.5b00299
Chem. Rev. 2015, 115, 13165−13307

systematic electron spin resonance (ESR) spin probe study and reported that the spectra obtained with the spin probes 5-, 12-, and 16-doxylstearic acid (*n*-DSA) are highly sensitive to the changes in the bolaamphiphilic arrangement. The authors obtained rotational correlation times and order parameters from full ESR line shape simulations and found that the transition temperatures, determined by the maximum hyperfine splitting, agree with the differential scanning calorimetry (DSC) data. By comparimg 5-DSA and 12-DSA, which reside at different positions in the alkyl chain region of the assemblies, the authors found that trans−gauche isomerization predominantly occurs in the outer region of the assemblies. For Me_2PE-C_{32}-Me_2PE (**90**) at pH 10, the authors reported that ESR data indicate the micelles to be short rods rather than spherical in shape and that an increase of the concentration from 1 to 10 mg/mL leads only to a one-dimensional growth of these micelles.[360]

On the basis of the structure of **90**, Drescher and Meister et al. developed two unique bolalipids (**93** and **94**) which not only self-assemble at a concentration of 0.01 wt %, but also are able to modulate the viscoelastic properties of the hydrogel made of **90** or **91**.[368] Generally, these bolaamphiphiles are much more effective hydrogelators than the hydrogelators made of diacylphosphatidylcholine.[369] Zhang et al. developed a bolaamphiphile (**95**) that has two carboxylic acid ends and a diketopyrrolopyrrole chromophore in the center. On the basi of the color change associated with the self-assembly process, the authors concluded that the $\pi-\pi$ stacking of the central parts and the hydrogen bonding between the ends are responsible for the formation of the nanofibrils of **95** in water. Although **95** self-assembles at a concentration as low as 0.06 wt % in water, the formation of a hydrogel has not been reported by the authors.[370] Similarly, another bolaamphiphile (**96**) bearing a bipyridine moiety at the central part, though forming nanofibers at 0.15 wt % by self-assembly, was not reported to form a hydrogel by Zhang et al.[371] Benvegnu et al. reported unsymmetrical diacetylenic bolaamphiphiles **97**, which bear a carbohydrate residue and a cationic glycine betaine moiety. When m = 13, **97** forms a hydrogel at a CGC of 1.7 wt %. TEM studies by the authors revealed the polymorphism of these bolalipids and the dense filament of the hydrogelators in the hydrogels.[372] Patnaik et al. developed a series of two-component hydrogels based on cetyltrimethylammonium bromide (**55**) and bis(decyloxy)succinic acid (**98**) to study the effect of the chirality of the amphiphile on gelation. Besides finding that **55** and **98** form vesicles and hydrogels that are pH and temperature responsive, the authors concluded that molecular chirality is responsible for the formation of supertwisted fibrils in the hydrogels at a **98**:**55** molar ratio of 1:2 with 31% water.[71] Zakharova et al. reported a macrocyclic bolaamphiphile (**99**) consisting of thiocytosine fragments. **99** forms a gel in water−DMF (20 vol %) at a concentration of about 1 wt %. One interesting feature is the observation of two break points in the surface tension isotherms, which correspond to the critical micelle concentration (CMC) and critical gelation concentration. The authors also observed that the pH of the solution decreases with an increase of the concentration of the hydrogelators.[373]

4.1.8. Hydrogelators Bearing a Cavity. On the basis of cyclotriveratrylene (CTV), Jiang et al. developed a class of supramolecular hydrogelators having a cavity. By introducing deprotonable COOH or protonable NH_2 as the terminal groups into the rigid and hydrophobic CTV backbones, the authors successfully used **100** and **101** (Scheme 17) to form supramolecular hydrogels with CGCs of 1.0 and 1.5 wt %,

Scheme 17. Some Hydrogelators Containing a Cavity

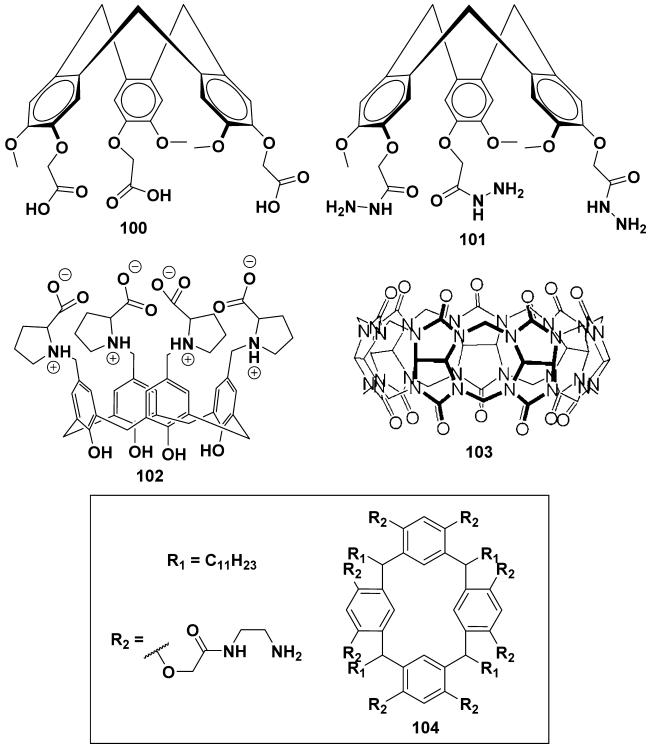

respectively. The obtained hydrogels of **100** and **101** are luminescent and exhibit pH-responsive, reversible gel−sol transitions. The work also illustrates that the skeleton of an organogelator is a promising starting point for designing a hydrogelator.[374] Mocerino and Ogden et al. reported a proline-functionalized calix[4]arene (**102**) that forms hydrogels in the presence of specific anions such as nitrate, bromide, iodide, and perchlorate. However, it requires a considerable amount of the hydrogelators (over 18 wt %) to form the hydrogels. Since acidic conditions and the presence of a lanthanide drastically reduce the amount of anions needed for hydrogelation, the hydrogelation likely depends on more than just the presence of the anions.[375] The later report by the same group, indeed, confirmed that the lanthanum cations connect two supramolecular helices to form a 2D network for hydrogelation.[376] Escuder, Miravet, and Ballester et al. developed an aryl-extended calix[4]pyrrole that acts as a receptor for tetramethylammonium. The authors found the formation of hydrogels in basic conditions and at neutral pH, thus suggesting that, as a guest molecule, tetramethylammonium interacts with the calix[4]pyrrole to form noncovalent polymers, resulting in hydrogelation.[377] Lee and Park also reported a similar structure−property relationship for another calix[4]arene-based hydrogelator, in which large alkali-metal cations (K^+ or Rb^+) trigger the hydrogelation.[378]

Marletta and Cunsolo et al. reported a type of pH-responsive hydrogelator based on calix[8]arene.[379] After capping the lower rim of calix[8]arene with an isopropyl group and attaching alkyl amino groups at the upper rim, the authors obtained a series of hydrogelators, the most effective one of which exhibits a CGC of 0.2 wt %. Kim et al. reported that cucurbit[7]uril (CB[7], **103**) is able to form a hydrogel in acidic conditions at a

DOI: 10.1021/acs.chemrev.5b00299
Chem. Rev. 2015, 115, 13165−13307

Scheme 18. Some Hydrogelators Containing a Polyaromatic Core

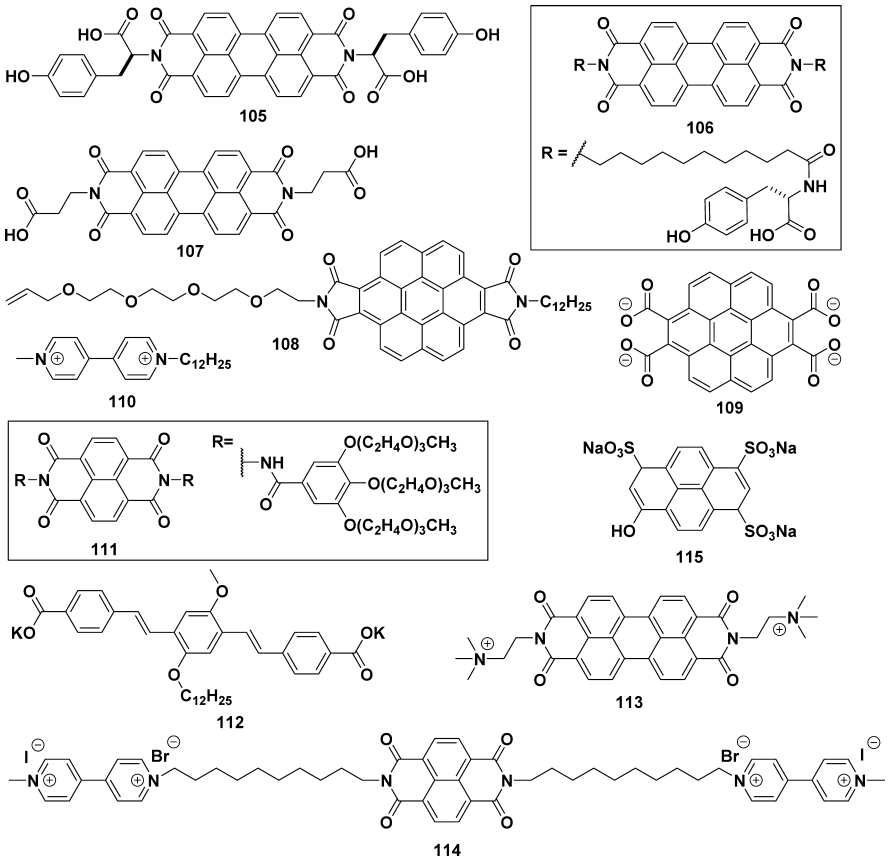

concentration of 3 wt %.[380] Although the optical appearance of the hydrogel is opaque, the authors demonstrated a unique guest-induced stimulus-responsive behavior of the gel of CB[7] by using 4,4′-diaminostilbene dihydrochoride as a guest. Besides the observation by Kim et al. that CB[7] forms a hydrogel,[380] Tan et al. reported a thermoresponsive supramolecular hydrogel consisting of cucurbit[6]uril (CB[6]) and butan-1-aminium 4-methylbenzenesulfonate (BAMB). However, the formation of the hydrogel requires relatively high concentrations of CB[6] (30 mM, 3 wt %) and BAMB (2.5 M).[381] Kazakova et al. reported an octaamino amide resorcin[4]arene (**104**)[382] acting as a hydrogelator that starts to aggregate at 0.1 wt % and forms a hydrogel at 1.2 wt %. SEM reveals a unique cell-like micrometer size feature when the concentration of **104** reaches 5%. The authors suggested that the fusion of aggregates (micelles) leads to the network for gelation, and found that the walls of the "cell-like" aggregates possess a multilayer structure consisting of 100−400 molecules of **104**.[383] Using surfactants (e.g., 10% *N*,*N*,*N*-trimethylhexadecan-1-ammonium bromide and 5% *N*-(3-((3-(3-((3-(3-(hexadecyldimethylammonio)-2-hydroxypropoxy)-3-oxopropanoyl)oxy)propoxy)-3-oxopropanoyl)oxy)-2-hydroxypropyl)-*N*,*N*-dimethylhexadecan-1-ammonium chloride) as the cogelators, Tian et al. reported the photoisomerization of two pseudorotaxanes (consisting of cucurbit[7]uril or being composed of α-cyclodextrin and cucurbit[7]uril) in the hydrogels.[384,385] Recently, the same laboratory and co-workers successfully achieved photoactivated sol−gel conversion using α-cyclodextrin[386,387] without using the surfactants. In addition, they also extended a similar interaction into polymeric hydrogels.[388]

4.1.9. Hydrogelators Containing a Polyaromatic Core.

As shown in Scheme 18, Banerjee et al. introduced L-tyrosine into the perylenebisimide core to generate a hydrogelator (**105**) that forms stable, semiconducting, photoresponsive, and pH-sensitive hydrogels. The authors found that the CGC value of **105** is about 0.27 wt % at pH 5. TEM indicates that the self-assembly of **105** starts at 8.8 μM (6.3 μg/mL), which is exceptionally low. On the basis of the impressive photoswitching behavior of this hydrogel, the authors suggested that such a high photoresponse value could lead to soft photodetectors.[389] Malik et al. reported an interesting case that perylene diimide derivatives with melamine form fluorescent hydrogels.[390] Employing the concept of bolaamphiphiles, Banerjee et al. reported another hydrogelator (**106**) based on perylenebisimide. They found that **106** self-assembles in water at physiological pH and forms a hydrogel at a CGC of about 1.3 wt %. The authors demonstrated that the incorporation of graphene oxide or reduced graphene oxide into the hydrogels enhances the photoresponsiveness of the hydrogel of **106**.[391] Zang et al. also reported that a perylenebisimide derivative (**107**) forms a hydrogel via pH triggering. The authors found that the addition of hydrochloric acid in the 4.4 mM (about 0.2 wt %) solution of **107** (in the presence of 26.4 mM triethylamine) results in a dark red hydrogel,[392] which agrees with the formation of a charge transfer complex.[393]

George et al. reported an amphiphile (**108**) that consists of coronenebisimide at the core of the molecule and self-assembles in THF/water through aromatic−aromatic interactions. Despite the observation of self-assembled nanotubes by TEM, hydrogelation was not reported.[394] However, the authors introduced the coronene motif to a donor−acceptor pair (**109**/

DOI: 10.1021/acs.chemrev.5b00299
Chem. Rev. 2015, 115, 13165−13307

Scheme 19. Some Hydrogelators of Homotypic Hydrogels

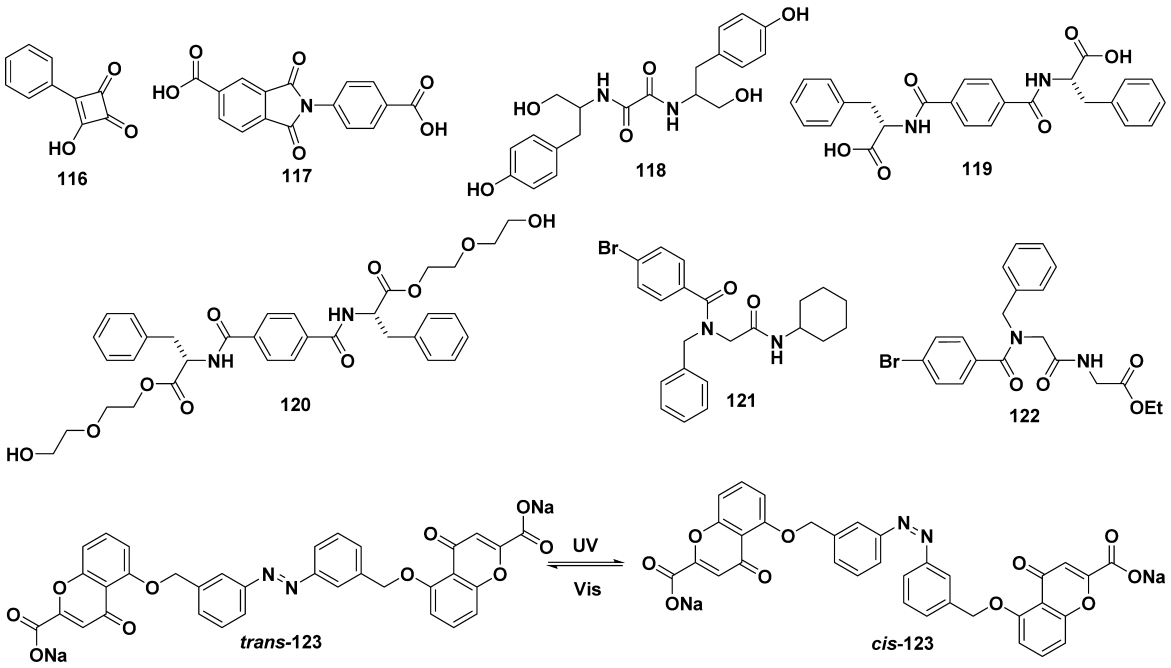

110), which is able to self-assemble to form a hydrogel with a CGC of 0.65 wt %. On the basis of UV−vis, NMR, and XRD, the authors suggested a molecular packing to explain the formation of the nanofibrils from cylindrical micelles.[395] Using a naphthalenediimide as the core and ethylene glycol as the side chains, Ghosh et al. developed a nonionic bolaamphiphile (**111**) that starts to aggregate at 0.05 wt % and forms vesicles. As an electron-deficient core-based bolaamphiphile, **111** forms donor−acceptor (DA) charge-transfer (CT) interactions with pyrene, a water-insoluble electron-rich donor. This interaction ruptures the membrane vesicles to form 1D fibers, thus producing CT-mediated hydrogels with a CGC of 0.3 wt %.[396] George et al. reported a two-component hydrogel that consists of an oligo(phenylenevinylene) derivative (**112**) and a perylenebisimide derivative (**113**). These two molecules form a strong donor and acceptor interaction in water to result in a hydrogel at a concentration of 0.4 wt %. TEM reveals that aggregation starts at much lower concentration (0.012 wt %). One impressive feature is the critical strain of the hydrogel is over 10%, which is unusual for a supramolecular hydrogel at such a low concentration.[397] Zhang et al. developed a bolaamphiphile (**114**) consisting of a naphthalenediimide as the rigid core and a viologen derivative as the hydrophilic head. The authors demonstrated that the addition of 8-hydroxypyrene-1,3,6-trisulfonic acid trisodium salt (**115**) turns the two-dimensional nanosheets of **114** into ultralong nanofibers. However, the hydrogelation of this interesting two-component system remains to be tested.[398]

4.1.10. Other Homotypic Hydrogelators. As shown in Scheme 19, the current record of the smallest hydrogelator likely is a squaric acid derivative containing a phenyl group (**116**) reported by Ohsedo et al.[399] According to the authors, the CGC of **116**, in 1 M HCl, is about 1 wt %. A slight increase of the pH (from 0 to 1.68) shifts the CGC to 10 wt %. SEM and XRD reveal that **116** forms microcrystals as the matrix of the hydrogel. This microcrystalline morphology explains that it requires 25 wt % **116** to obtain a reliable rheological measurement because the weak interactions between the microcrystals likely only offer a fragile hydrogel that fails to maintain integrity during oscillatory rheometry. The authors also proposed that, at a certain concentration, **116** forms fibrils with hydrophilic porous cavities which have diameters and lengths on the order of micrometers and submillimeters, respectively.[399] It would be very interesting to have more insight into the intermolecular interactions within these fibrils. Chi and Xu et al. reported an *N*-(4-carboxyphenyl)-trimellitimide (**117**) that forms a gel in a mixed solvent of DMF and water with a CGC of 0.4 wt %. Containing microcrystals as its matrix, this hydrogel exhibits a thermoirreversible property and precipitates upon heating, which indicates the hydrogelation likely is an entropy-driven process.[400]

On the basis of the earlier works of bis(amino acid) oxalamides,[401,402] Zinic reported gelators composed of bis(amino alcohol) oxalamides. For example, the authors found that 10 mg of (*S*,*S*)-bis(tyrosinol) oxalamide (**118**) forms a metastable hydrogel in 7.5 mL upon rapid cooling.[403] The structure−property relationship study carried out by Feng et al., in fact, suggests that the carbonyl groups in amino acids play a critical role in the formation of hydrogels. Feng et al. developed two C_2-symmetric benzene-based hydrogelators (**119** and **120**).[404] **119** forms a hydrogel at pH 2 with a CGC of 0.25 wt %. With ethylene glycol to cap the C-terminal of **119**, the authors obtained a more effective hydrogelator (**120**) which forms a hydrogel at 0.1 wt %. The authors found unique layered porous structures in the hydrogel of **119** and fibrous structures in the hydrogel of **120**. Wang et al. developed a one-pot Ugi reaction from simple starting materials for the synthesis of tripeptoids as hydrogelators, which lead to gelation in a mixed solvent of DMSO and H_2O (1:1) with CGCs of 0.5 wt % (**121**) and 0.2 wt % (**122**). This result also reflects that the sufficient unsubstituted amide moiety (−CONH−) is crucial for the formation of supramolecular hydrogels without a cosolvent.[405] Szymanski and Feringa reported the design of a dichromonyl compound (**123**) that bears an azobenzene photoswitch and forms a hydrogel in its trans conformation (with a CGC of 1.5 wt %). Compared to other reported photoswitchable hydro-

DOI: 10.1021/acs.chemrev.5b00299
Chem. Rev. 2015, 115, 13165−13307

Scheme 20. Some Hydrogelators Composed of Two Components

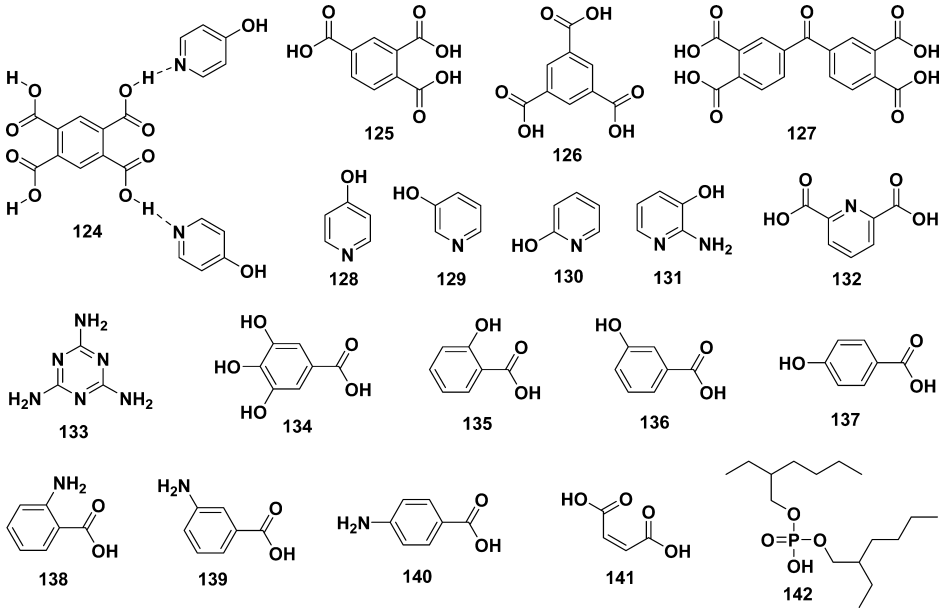

gelators,[406,408−410] **123** seems to exhibit much faster kinetics and is able to form a gel within 1 min upon the cis form of **123** being irradiated.[407]

4.1.11. Hydrogelators Composed of Two Components. A hydrogelator composed of two components usually means that the two constituents are nongelators by themselves, but together they can act as a gelator via intermolecular interactions. The two-component hydrogels have certain benefits over one-component small molecule hydrogels because the tunability of the individual components allows more versatile and dynamic reversibility, which may result in greater diversity in morphology and greater variation in mechanical and optical properties. Moreover, the gelation process and the properties of the gels can be easily tuned by changing the components or the compositions of the components or by functional modifications in one of the components, which should be beneficial for the applications of these hydrogels.

As shown in Scheme 20, Tang et al. reported a supramolecular hydrogel consisting of two types of building blocks, 1,2,4,5-benzenetetracarboxylic acid (**124**) and 4-hydroxypyridine (**128**), at a concentration of 2.5 wt %. On the basis of XRD of powders and other characterization methods, the authors derived the interactions of the building blocks. One interesting feature is that the hydrogen bonding between the carboxylic acid and pyridine units is strong enough to allow the fibers to be drawn from the melted building blocks.[411] The authors used *m*-hydroxypyridinium (**129**) to interact with **124** at a molar ratio of 1:2 to form hydrogels. One striking feature of these hydrogels is the rare gel-to-crystal transition, which agrees with microcrystalline particles constituting the networks of the hydrogels and the hydrogels being metastable. The solved crystal structure also provides confirmation that water mediates the hydrogen bonding between the pyromellitic acid and the 4-hydroxypyridine.[412] The authors used **126** to interact with **128**, **129**, or **130** to form hydrogels with a CGC of about 0.7 wt %.[413] Using a branched gelator consisting of 1,2,4-benzenetricarboxylic acid (**125**) and 4-hydroxypyridine (**128**), the same laboratory shows a two-component hydrogel with a CGC of 4 wt %. By analyzing the single-crystal structures of the complex formed from **128** and *o*-phthalic acid, and **125**, the authors suggested that the molecules assemble into branched fibers via different hydrogen bondings. Interestingly, the melting of the gelators also allows the supramolecular fibers to be pulled to a length of centimeters.[414] When the concentration of the gelator (i.e., the mixture of **125** and **128**) is 2.5 wt % and below the CGC, the authors found that the gelator self-assembles in water to form macrospheres with diameters of millimeters.[415]

Tang et al. developed another type of two-component hydrogelator by mixing 3,3′,4.4′-benzophenonetetracarboxylic acid (**127**) with **128** or **129** at molar ratios of 1:2 and 1:4, respectively. The authors reported that the self-assembled fibers act as the matrixes of the hydrogels.[416] Using 2-amino-3-hydroxypyridine (**131**) to interact with 1,2,4,5-benzenetetracarboxylic acid (**124**), the authors obtained a hydrogel that exhibits a higher T_{gel} than that of the hydrogel made of **124** and **129**, which likely originates from the formation of stronger hydrogen bonding enhanced by the *o*-amino group of **131**.[417] Tang et al. reported the use of ultrasound to promote the mixture of 1,3,5-benzenetricarboxylic acid (**126**) and 4-hydroxypyridine (**128**) to gel water at a concentration of 1.5 wt %. The authors observed that the width of the nanofibrils in the hydrogels depends on the power of the ultrasound,[418] and demonstrated that a higher power of the ultrasound results in nanofibrils with a smaller fiber width. On the basis of the works of Tang et al.,[412,419] Yang and Shen et al. employed microfluidics to generate microgels made of 1,2,4,5-benzenetetracarboxylic acid and 4-hydroxypyridine. On the basis of thermal analysis, the authors concluded that, due to the entangled three-dimensional network structures crowded in a small volume, the supramolecular hydrogel microspheres are more thermally stable and can immobilize more water molecules.[420]

Using a similar approach, Feng et al. reported a hydrogel made of 2,6-pyridinedicarboxylic acid (**132**) and 4-hydroxypyridine (**128**) at a concentration of 5 wt %. On the basis of a range of techniques of characterization, the authors suggested that the interaction between **132** and **128** is highly directional.[421] Nandi et al. reported a two-component hydrogel of

DOI: 10.1021/acs.chemrev.5b00299
Chem. Rev. 2015, 115, 13165−13307

Scheme 21. Some Representative Hydrogelators Composed of Two Components

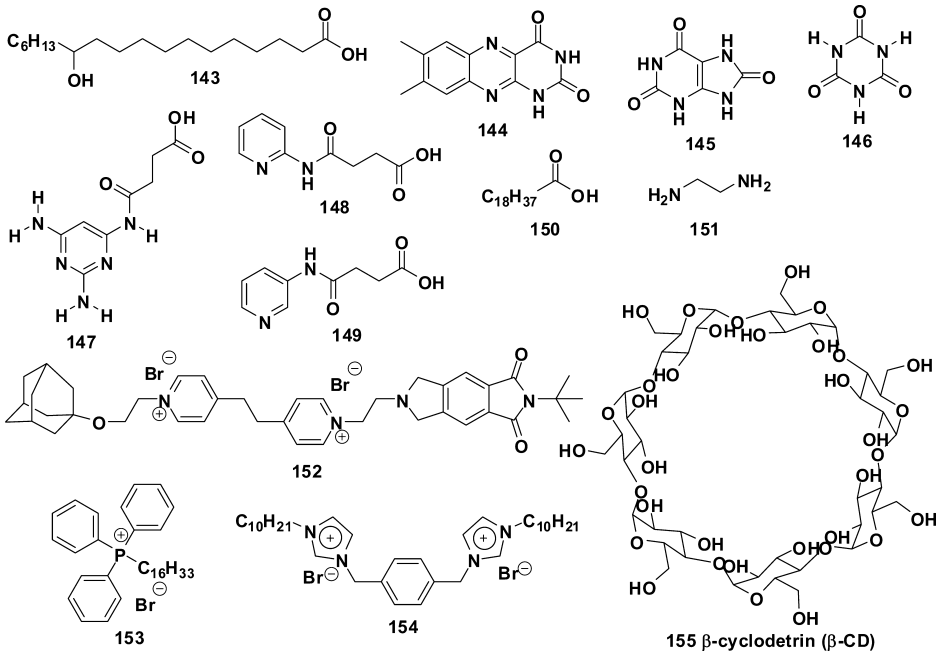

melamine (**133**) and gallic acid (**134**).[422] The authors mixed **133** and **134** in different ratios and demonstrated that hydrogels form at 2 wt %. The optical appearance of the hydrogel suggests the formation of microcrystalline networks or micrometer-sized fibrillar bundles, agreeing with SEM imaging. The authors also observed the enhancement of photoluminescence (PL) at the gel state, which is consistent with the enhanced fluorescence in the colloidal state.[64,423,424] Nandi et al. also used positional isomers of hydroxybenzoic acid (**135**−**137**) to interact with melamine (**133**) in a 1:1 molar ratio to form two-component hydrogels.[65] The CGC values are 0.5, 1.0, and 0.1 wt % for the hydrogels containing **135**, **136**, and **137**, respectively. On the basis of the upfield shift of the aromatic protons in the gels, the authors suggested that the $\pi-\pi$ stacking in the gels follows the order **137** (para) > **135** (ortho) ≈ **136** (meta). The authors found that the thermal stability, the storage moduli, and the critical strain of the two-component hydrogels follow the order **137** > **135** > **136**.

Tantishaiyakul et al. reported the thermoreversible gelling systems consisting of melamine (**133**) and three positional isomers of aminobenzoic acid (**138**−**140**) at a concentration of 3 wt %. The authors found that the gel strengths at lower temperatures follow the order **140** > **139** > **138**. It is interesting that the gel−sol transition temperatures follow the order **140** > **139** > **138**.[425] Ballabh et al. also used melamine to interact with maleic acid (**141**) to form a hydrogel at a CGC of 15 wt %, and applied this two-component hydrogel as a template for making silver nanoparticles.[426] Song et al. reported a hydrogel formed by mixing melamine and bis(2-ethylhexyl)phosphoric acid (**142**)[427] at a CGC of 6 wt %. One notable feature of this study is that the authors used a well-established polymer solubility theory (the Fedors method) to estimate Flory−Huggins interaction parameters for predicting the gelation behavior. Later, the same authors also calculated Hansen solubility parameters and Flory−Huggins parameters to estimate the gelator−solvent interaction in a mixed solvent of methanol and water.[428] Recently, Wang and Liu et al. reported a series of supramolecular nanotubes formed by combining melamine-based[429] and L-glutamic acid-based bolaamphiphiles.[430] The authors demonstrated that the ratio of the components dictates the final nanostructures formed by the self-assembly of the constituents. However, how these nanostructures influence hydrogelation remains to be determined.

As shown in Scheme 21, Douliez et al. reported that the ethanolamine salt of 12-hydroxystearic acid (**143**) forms tubes several tens of micrometers in length with a temperature-tunable diameter at a concentration of 1 wt %. Despite the observation of a gel−sol transition via DSC and SANS measurement, it is unknown whether these salts result in a hydrogel at 1 wt %.[431] To pair melamine (**133**) with more complicated molecules, such as lumichrome (**144**), Nandi et al. produced thermoreversible hydrogels that consist of **144** and **133** at a molar ratio of 3:1 or 1:1.[63] The hydrogels, formed at a concentration of 0.2 wt %, are thermoreversible and exhibit higher intensities of photoluminescence than that of pure **144**. On the basis of the red shift of the emission peak, the authors suggested a transformation from H-aggregates to J-aggregates.[63] Steed et al. reported hydrogelation by a mixed system comprising two entirely rigid, insoluble, mutually complementary small organic molecules, melamine (**133**) and uric acid (**145**), which act as a planar multifunctional hydrogen bond donor/acceptor and result in a hydrogel at a CGC of 0.8 wt %.[196] Combining molecular dynamic calculation and the data from ^{13}C MAS NMR spectroscopy and the powder XRD pattern of the xerogels, the authors proposed plausible intermolecular interactions to explain the hydrogelation of these two components.

Zhang et al. found that the addition of oxoanions (e.g., NO_3^-, PO_4^{3-}, ATP, and SO_4^{2-}) to a solution of melamine is able to trigger the formation of hydrogels. SEM reveals that microcrystals act as the matrixes of the hydrogels. The total amount of salts and melamine needed for gelation is from 3.1 to 10 wt %, apparently depending on the anions.[432] Nandi et al. reported a hydrogel of melamine (**133**) containing 6,7-dimethoxy[1*H*,3*H*]quinazoline-2,4-dione, riboflavin,[433] and rhodamine B in a proper proportion. The authors suggested

DOI: 10.1021/acs.chemrev.5b00299
Chem. Rev. 2015, 115, 13165−13307

that this type of gel might find application in generating white light.[434] Hud et al. reported an elegant design that uses cyanuric acid (**146**) and a modified triaminopyrimidine (**147**) to form noncovalent interactions that result in a hydrogel at pH 7 and a concentration of 5 mM (0.18 wt %). The authors suggested that the formation of a hexameric rosette can serve as a functional architecture to generate the hydrogels.[435,436] Tang et al. synthesized two isomeric building units, 4-oxo-4-(2-pyridinylamino)butanoic acid (**148**) and 4-oxo-4-(3-pyridinylamino)butanoic acid (**149**). While **148** and **149** form fiber- and treelike crystals in aqueous solutions, respectively, cooling the aqueous solutions of their mixtures over a wide range of molar ratios (7:1 to 1:3) yields a series of supramolecular hydrogels at a total concentration of 4 wt %.[72]

Bhattacharya et al. reported two-component hydrogels consisting of stearic acid (**150**) or eicosanoic acid with di- or oligomeric amines (**151**). The authors demonstrated that **150** and **151** at a molar ratio of 2:7, with a total concentration of 5 wt %, result in a hydrogel containing a three-dimensional network formed by the self-assembling nanofibers made of **150** and **151**. Since two of these hydrogelator salts are able to crystallize, the authors obtained very useful crystal structures which provide insights into the molecular packing in the condensed phase (Figure 4).[55] Taking advantage of the

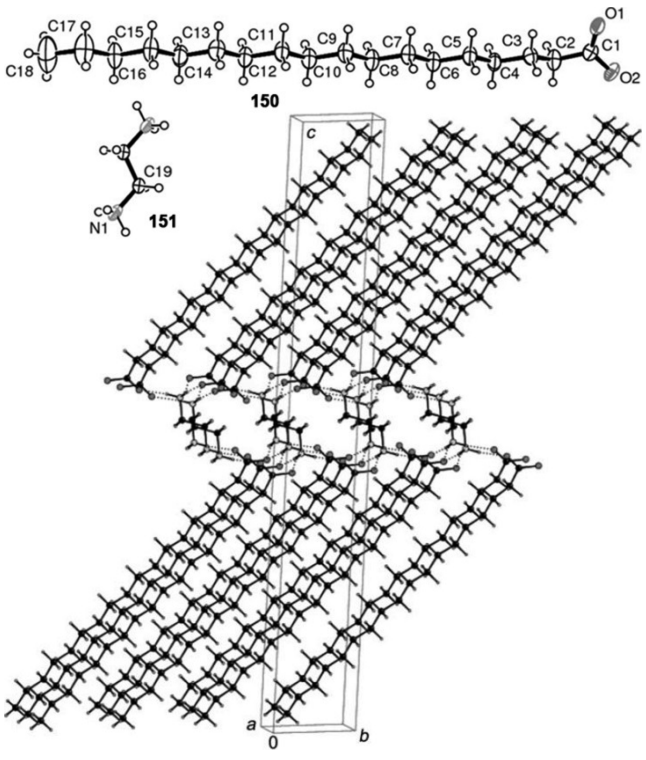

Figure 4. ORTEP diagrams of **150** and **151** with the atom numbering scheme for the asymmetric unit, and the molecular packing of **150** and **151** showing the columnar supramolecular architectures, characterized by a lipophilic exterior and a polar interior. Adapted with permission from ref 55. Copyright 2008 Wiley-VCH Verlag GmbH & Co. KGaA.

interaction of β-cyclodextrin (β-CD, **155**) with a ditopic molecule (**152**) having adamantane at one end and a pyromellitic diimide moiety, Gopidas reported a two-component hydrogel that is stable even with a 10^{-6} M concentration each of **155** and **152**. Considering that isothermal titration calorimetry (ITC) shows the association constant K between **155** and **152** is about 6×10^4 M^{-1}, it is unusual (and probably needs confirmation) that the hydrogel forms at such a surprisingly low CGC value (about 2 mg/L).[437] Harada used the interaction between **155** and adamantane to cross-link acrylamide to form self-healing hydrogels.[438] Hao et al. found that alkyltriphenylphosphonium bromide **153**, an ionic liquid-based surfactant, and **155** are able to form a supramolecular complex which further aggregates to result in vesicles in an aqueous solution. The authors found that the addition of inorganic salts (e.g., KCl, NaCl, CuCl, and K_2CO_3) induces the formation of sheetlike hydrogels.[439] Using diimidazolium salts with different alkyl chain lengths to interact with α-CD and **155**, D'Anna and Noto et al. developed another series of two-component hydrogels, with CGC values from 1.0 to 4.7 wt %, formed by host–guest interactions based on cyclodextrins and cationic imidazoliums **154**.[440] They demonstrated that the nature of the cyclodextrin, the salts, and the host:guest ratio are effective tools for tuning the properties of these two-component hydrogels.

4.2. Inorganic–Organic Hybrid Hydrogels

The incorporation of inorganic components into the hydrogels constitutes an irreplaceable way to introduce unique properties of the inorganic components or metal complexes, such as redox, catalytic, conductive, photoresponsive, photochemical, and other properties related to coordination complexes in soft materials. Similar to the development of hydrogels of small organic molecules, the development of metallogels[441,442] largely begins with organogels. Readers who are interested in organogels of metal complexes[443,444] are encouraged to consult several excellent reviews.[25,445] In this section we focus on the hydrogels of metal complexes (Table S2). Although the coordination between organic and metal ions is common in nature, the organic molecules used in these complexes for generating hydrogelators are largely centered on several functional groups that serve as the ligands for metal ions. Therefore, we arrange these relevant hydrogelators according to the following classifications: (i) carboxylic groups as the ligands, (ii) ligands containing nitrogen as electron donors to a metal ion, (iii) binding via phosphate groups, (iv) ligands comprised of thiol groups, and (v) others.

4.2.1. Hydrogelators Containing Carboxylic Groups as the Ligands. Although some amphiphiles with carboxylic groups themselves self-assemble in water to form nanostructures as the matrixes of hydrogels, organic–inorganic hybrid hydrogels still have attracted considerable interest due to the specific functions conferred by the metal ion or inorganic elements. As shown in Scheme 22, Kogiso et al.[446] reported that a dicarboxylic valylvaline bolaamphiphile (**156**) self-assembles in water to form nanofibers in the presence of divalent transition-metal cations (e.g., Cu^{2+} and Zn^{2+}) at a concentration of 1.6 wt %. The resulting nanofibers have widths of 15–20 nm and lengths of several micrometers. Suzuki et al.[447] designed molecules **157** and **158** containing a carboxylic group, which form a thermally sensitive hydrogel. The addition of the inorganic salts (e.g., K^+, Ca^{2+}) to the hydrogel affords improved mechanical strength at a CGC concentration of about 1.2 wt %. On the bsais of this result, they also developed an L-lysine derivative (**159**) and its alkali-metal salts. Compound **159** is insoluble in water, but **159** with an alkali metal is readily water soluble.[76] All these compounds alone fail to form a hydrogel. Surprisingly, the mixtures of these compounds (e.g., the mixture of **159** and its lithium salt) form hydrogels (at

DOI: 10.1021/acs.chemrev.5b00299
Chem. Rev. 2015, 115, 13165–13307

Scheme 22. Ligands That Bind Metal Ions via Carboxylic Group To Form Supramolecular Hydrogels

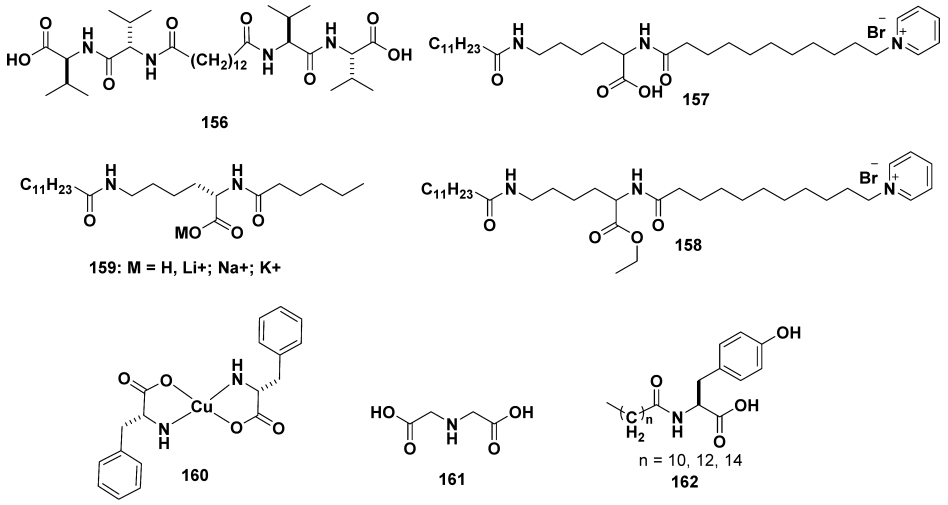

Scheme 23. Some of the Ligands That Bind Metal Ions via Nitrogen in the Supramolecular Hydrogels and Some Representative Complexes

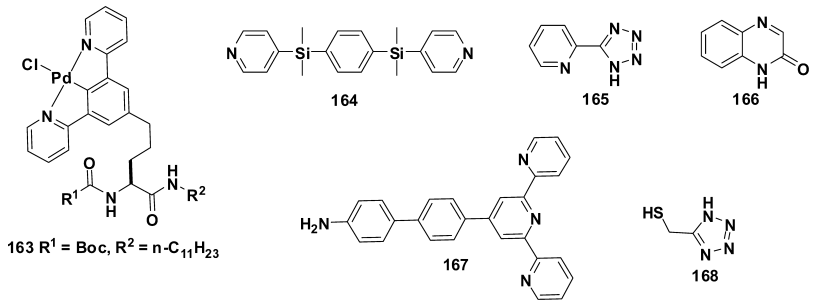

CGC values from 0.5 to 1.7 wt %) via hydrogen-bonding and van der Waals interactions. While **159** forms spherical micelles, the mixtures of the hydrogelators self-assemble to form nanofibers. Shen and Zhang et al.[448] reported an intriguing example in which the chirality of the ligand controls supramolecular hydrogelation via the coordination of phenylalanine (Phe, **160**) to Cu(II) at a CGC of 0.35 wt %. According to the authors, a decrease of the enantiomer excess of ligand L-Phe (or D-Phe) weakens the gelation ability of the Phe−Cu(II) complex. On the basis of this interesting observation, the authors suggested that this hydrogelator may open up a new window for developing promising chiral sensing and recognition platforms.

The photoluminescence of lanthanide ions has constantly attracted research interest[449] because of the long lifetimes, narrow-band emission, and robust photochemical stability. Maitra et al.[450] demonstrated a lanthanide-based luminescent hydrogel by mixing sodium cholate (**85**) and europium acetate, at a concentration of about 0.7 wt %, with the addition of pyrene at extremely low concentration (e.g., 10^{-6} M) as a sensitizer. In addition, the authors also synthesized nanoparticles (metal sulfides) in a calcium cholate hydrogel using the matrixes of the hydrogel as the template.[451] Huang et al.[452,453] used **85** as the ligand to bind lanthanide to generate a "superhydrogelator". At 0.04 wt %, **85** forms a hydrogel in which the hierarchical nanostructures are thermoresponsive (e.g., twisted nanohelices and nanotubes at low temperature (4 °C) and untwisted ribbons at a higher temperature (50 °C)). Huang et al. also found that the color of the emission of a lanthanide−cholate hydrogel depends on different lanthanide ions or codoping ions.[454] Utilizing the iminodiacetic acid (**161**) as a ligand to coordinate with lanthanides, Alves et al.[455] prepared a series of hydrogels with the lowest CGC value at 0.04 wt %. Banerjee et al.[456] designed a series of tyrosine-based amphiphiles (**162**) which bind with Ni^{2+} ion selectively and result in hydrogels at CGC values of 0.78, 0.75, and 0.63 wt % when the chain length is 10, 12, and 14, respectively. Yang et al.[457] reported a supramolecular hydrogel based on *N*,*N*-dibenzoyl-L-cystine (**1**) with a CGC of 0.2 wt %. Owing to the interaction between Eu(III) ions and the hydrogelators, immobilized Eu in the hydrogel exhibits enhanced luminescence.[457,458]

4.2.2. Hydrogelators Coordinating via Nitrogen(s). Due to its versatile catalytic properties, palladium is of great interest in synthetic chemistry.[459,460] It has also been explored in the context of supramolecular hydrogels. Escuder et al.[58] reported a supramolecular hydrogel (**4**) containing pyridine which forms a hydrogel at 0.5 wt %. Also acting as an organogelator, **4** binds with Pd(II) to create a functional material to catalyze the oxidation of benzyl alcohol, similar to the case reported by Xu et al.[441] As shown in Scheme 23, Takaya and Nakamura et al.[461] designed a supramolecular gel (**163**) containing Pd(II) for catalysis. The authors made the xerogel of **163** and used it to act as a highly efficient catalyst for the intramolecular addition−cyclization of alkynoic acid in water. Jung et al.[462] designed a molecule of 1,4-bis(dimethyl-4-pyridylsilyl)benzene (**164**), which binds with (tmeda)Pd-$(NO_3)_2$ (tmeda = *N*,*N*,*N*′,*N*′-tetramethylethylenediamine) to

DOI: 10.1021/acs.chemrev.5b00299
Chem. Rev. 2015, 115, 13165−13307

afford a hydrogel containing 98.5% water below 2 °C. According to the authors, one interesting feature of these hydrogels is the formation of dynamic catenated cyclotrimers in water. Andrew et al.[463] reported that the addition of water to the mixture of 1*H*-5-(2-pyridyl)tetrazole (**165**) with $LaCl_3$ results in a hydrogel. Surprised by this result, the authors also obtained the crystal structure of the complex, which appears to be consistent with the microcrystalline nature of the hydrogel.

Considering that the understanding of the relationship between molecular structure and gelation ability is still poor and the design of a gelator remains a significant challenge, McNeil et al.[464,465] proposed an approach that selects the molecules according to the intermolecular interaction revealed by the Cambridge Structural Database (CSD) for the development of hydrogels. On the basis of this principle, the authors selected **166**, which specifically binds with $Hg(OAc)_2$ to afford a gel in 90:10 MeOH/H_2O with a CGC value at 1.6 wt %. Mal and Rissanen et al.[466] also found that the ligand of 40-[4-(4-aminophenyl)phenyl]-2,2′:6′,2″-terpyridine (**167**) selectively binds with Hg^{2+} to afford a hydrogel. The interaction between benzo-18-crown-6 ether and the ammonium group on **167** is able to disrupt the hydrogelation, which can be partially recovered by the addition of K^+ to bind competitively with the crown ether. Employing the ligand 5-(mercaptomethyl)-tetrazole (**168**) as a surface coating to stabilize the CdTe nanocrystal, Voitekhovich and Eychmuller et al.[467] prepared a hybrid gel in the presence of Cd(II) cations. This work illustrated an interesting way to use colloids directly as part of 3D networks for generating hydrogels.

Utilizing *N*,*N*′-bis(3-pyridyl)butylenebisurea (**169**) to coordinate with Cu^{2+}, Dastidar et al.[468] made a gel in a DMSO/H_2O or DMF/H_2O mixture with CGCs of 8−10 wt %. EM reveals that the matrixes of these gels are largely microcrystalline. As shown in Scheme 24, MacGillivray et al.[469] reported a hydrogel

Scheme 24. Some of the Ligands That Bind Metal Ions via Nitrogen in the Supramolecular Hydrogels and Some Representative Complexes

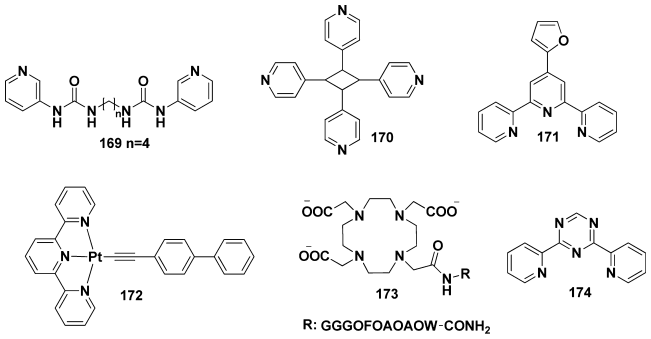

via coordination of copper with *rctt*-1,2-bis(3-pyridyl)-3,4-bis(4-pyridyl)cyclobutane (**170**). Being composed of nanoscale metal−organic particles, this hydrogel exhibits thixotropic properties with a yield value of 8.33 Pa. It is worth noting that Tu et al.[470,471] also prepared a thixotropic hydrogel via simple mixing of **171** and Cu(II) at a concentration of 0.25 wt %. Furthermore, they also developed a photoswitchable metallohydrogel by utilizing the photoresponsive 2,2′-azopyridine as the ligand.[472] In addition, Bhattacharya et al. also prepared a thixotropic hydrogel based on the interaction of pyridylenevinylene and copper(II).[473]

Being designed and reported by Che et al.,[474] a terpyridylplatinum(II) complex with biphenylacetylide ligands (**172**) self-assembles to form nanofibers with diameters of 20−40 nm and results in a hydrogel with a CGC of 3.7 wt %. Yu et al.[475] designed a pair of decapeptides, formyl-EFEAEAEAEW-carboxyl and formyl-OFOAOAOAOW-amide (O = ornithine), which are able to form a hydrogel at pH 7. Moreover, the peptide conjugated with a Gd(III) chelate (**173**) speeds the gelation process and increases the cross-sectional area of the peptide fibers. Further study found that the conjugates **173** are incorporated into the peptide fibers and aggregate toward the center of the peptide fibers. One notable feature of this study is that the authors correlated SAXS and T2-weight magnetic resonance imaging (MRI) to provide insights into the self-assembly process. Zhang and Ye et al.[476] prepared a metallogel in water by using 4,6-bis(2-pyridyl)-1,3,5-triazin-2-ol (**174**) to coordinate with copper acetate at a molar ratio of 4 (Cu:L, 5.6 wt %). It is interesting that the hydrogel is stable at room and high temperature (e.g., 60 °C), but flows upon cooling to 4 °C. This kind of LCST behavior is uncommon for supramolecular metallohydrogels.

Upon mixing melamine (**133**) with zinc(II) orotate at a 1:1 molar ratio, Nandi et al.[477] developed a bicomponent hydrogel at a CGC of 0.7 wt %. The authors demonstrated that this hydrogel is thixotropic and undergoes a gel−sol transition when being treated with formic acid or sodium borohydride. Employing a dendritic ligand (**175**) to coordinate diplatinum-(II), Yang et al.[478] developed a gel in a mixed solvent of acetone and water (5:3, v/v) with a CGC of 0.23 wt %. Moreover, the addition of bromide ions causes the gel−sol transition, which can be reversed by the addition of silver. Upon addition of α-cyclodextrin to the solution of the Pd(II) complex with a bipyridinium ligand (**176**), Osakada et al.[479] prepared a hydrogel with a T_{gel} of 47 °C. The authors suggested that the complex self-assembles to form polyrotaxane-like fibrous architectures and further aggregates to afford nanoparticles with a size around 20−40 nm to trap the water and to result in the hydrogel. Fernandez et al.[480] designed and synthesized a ligand (**177**) consisting of a pyridyl group, an oligo-(phenyleneethynylene) motif, and three ethylene glycol chains. **177** coordinates with Pt(II) metal ions to result in a hydrogel. On the basis of ROESY (rotating-frame Overhauser effect spectroscopy) NMR, the authors elucidated that $\pi-\pi$ interactions and unconventional C−H···X hydrogen bonding drive the complex to form a hydrogel at a concentration of 1.4 wt %. The most impressive result in this work is correlation of UV/vis spectroscopy, NMR spectroscopy, and X-ray crystal structure analysis to infer the molecular arrangement in the hydrogel. Diaz and Banerjee et al.[481] reported a complex of L-3-methyl-2-[(pyridin-4-ylmethyl)amino]butanoic acid (**178**) and Zn(II) to form a metallohydrogel with a CGC value of 8.4 wt % (Scheme 25). According to the authors, this hydrogel undergoes a gel−sol transition upon application of different stimuli (e.g., EDTA, ammonia solution, trifluoroacetic acid, sodium sulfide, shaking, or heating), which likely originates from the unique amphoteric property of zinc ions.

4.2.3. Hydrogelators Containing Thiol Groups as the Ligands. Ballabh et al.[482] designed 2-aminothiazole and its derivatives (**179**) that bind with mercury acetate to result in hydrogels with thixotropic behavior. One interesting feature of this work is the dependency of the thixotropic property on the substitution groups in the C-4 and C-5 positions of the aminothiazole. Jiang et al.[483] have demonstrated an intriguing

DOI: 10.1021/acs.chemrev.5b00299
Chem. Rev. 2015, 115, 13165−13307

Scheme 25. Some of the Ligands That Bind Metal Ions via Nitrogen in the Supramolecular Hydrogels and Some Representative Complexes

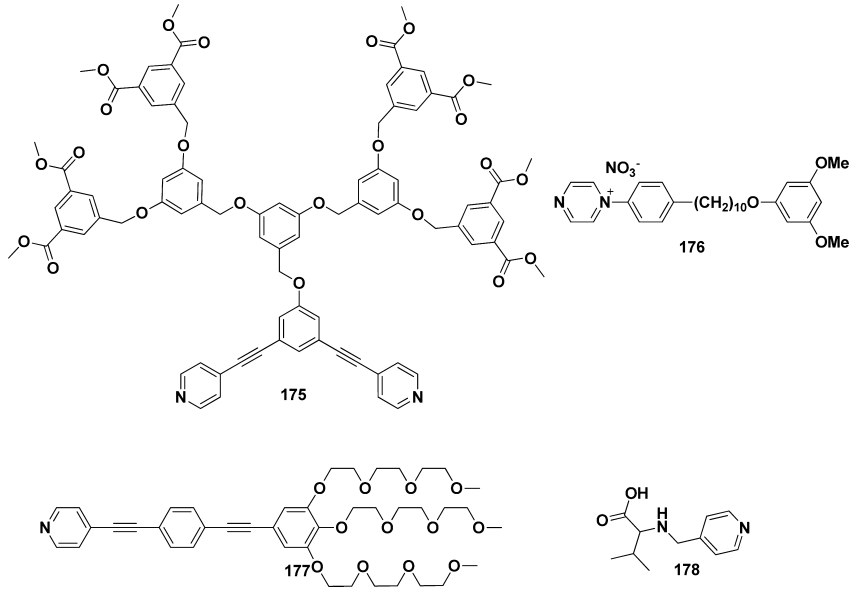

Scheme 26. Some of the Ligands Bearing Thiol Groups

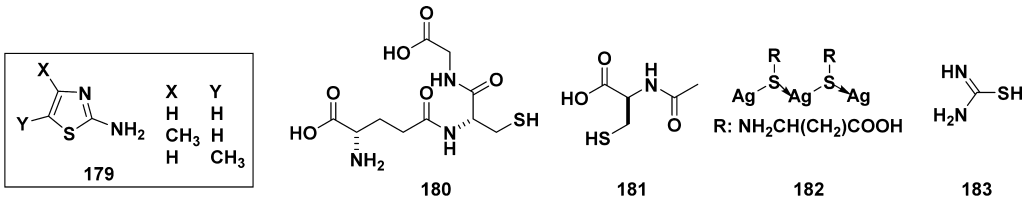

case of a highly selective anion-responsive supramolecular hydrogel, based on silver(I) glutathione (GSH) (**180**), with a CGC value of 0.20 wt %. Compared with other anions (F^-, Cl^-, Br^-, and $H_2PO_4^-$), I^- is capable of triggering the gel−sol transition, likely due to the higher affinity of iodide to silver ion than that of other halogen anions. Odriozola et al.[484] used a drug, *N*-acetyl-L-cysteine (NAC, **181**),[485] to generate the supramolecular hydrogel (0.82 wt %, 50 mM) in the presence of Au(III), Ag(I), and Cu(II) salts. Although the hydrogelation of these metal complexes occurs at a relatively low pH (<4), this work still provides new insights into creating supramolecular metallogels. Pakhomov et al.[486] reported a hybrid hydrogel based on the complex (**182**) of L-cysteine and silver nitrate (Scheme 26). Via sulfur−silver bonds, complex **182** self-assembles to form nanofibers and results in hydrogelation at a rather low concentration (0.01 wt %). Further studies found that the hydrogel exhibits antibacterial properties.[487] Odriozola et al. designed two N-terminal-capped tripeptides, Ac-RGC and Ac-RCG, which have an isoelectric point close to 7. Because these two peptides contain the cysteine residue, they form hydrogels upon the introduction of Au(I) to Ac-RGC and Ag(I) to Ac-RCG, at final peptide concentrations of about ∼3 wt %.[488] Arachchige et al.[489] reported a highly efficient method to prepare a monolithic Ag hydrogel by using a large amount of oxidant $C(NO_2)_4$ to remove the surface thiolate in Ag nanoshells. Moreover, the resulting aerogel exhibits extremely high surface areas (40−160 m^2/g) and interconnected mesoporous structures. Pal et al.[490,491] reported a Cu(I) metallogel at a concentration of 0.15 wt % via simple mixing of $CuCl_2$ and thiourea (**183**). The coordination of Cu(I)−thiourea and extensive hydrogen-bonding interactions result in a hydrogel which is redox responsive, and the oxidation of Cu(I) to Cu(II) by $FeCl_3$ leads to a gel−sol transition. Moreover, the metallogel shows high selectivity for picric acid, and the addition of picric acid causes a color change of the gel from white to yellow.

4.2.4. Hydrogelators Utilizing Phosphates as the Ligands. The phosphate group also has strong affinity with many kinds of metal ions.[44] Yeh et al.[492] developed a facile method to prepare hydrogel-like $GdPO_4·H_2O$ nanorods. The authors reported that the nanorods are cell compatible. On the basis of the high affinity between phosphate groups and certain metal ions, Takahara et al.[493] reported an imogolite-based hydrogel which is able to immobilize an enzyme containing phosphoric groups. The authors found the enzyme is easily recovered from the reaction system and reused. Patil and Mann et al.[494] reported that cerium oxide nanoparticles act as a catalyst to dephosphorylate Fmoc-Tyr-P (**14**), thus resulting in hybrid supramolecular hydrogels. The most interesting part of this study is the observation of Maltese cross-patterns (spherulites) or nematic birefringence of the hydrogels, which suggests directional orders. As shown in Scheme 27, Kasuga and co-workers[495−499] have prepared a metaphosphate hydrogel (**184**) via hydration of the metaphosphate glass powders. The authors have also performed extensive studies on the conductive properties of this viscous gel. The resulting hydrogel exhibits a low self-discharge rate and fast charge−discharge capability, and shows a high electrical conductivity of 5 mS cm^{-1} at room temperature because of proton hopping between

DOI: 10.1021/acs.chemrev.5b00299
Chem. Rev. 2015, 115, 13165−13307

Scheme 27. Chemical Structure of a Ligand Containing Phosphate Groups

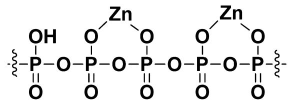

184

P−OH groups and water molecules. The authors suggested that this hydrogel promises an alternative electrolyte.

4.2.5. Others. Besides the electron donors discussed above, other types of nucleophiles may coordinate with metal centers to generate hydrogelators. As shown in Scheme 28, Kulkarni et al.[500] reported that copper(II) binds with inositol and 2,2′-bipyridine to form a trinuclear complex (**185**). The self-assembly of the complex affords a supramolecular hydrogel at pH 12.4 via inter- and intramolecular $\pi-\pi$ stacking between the bipyridyl groups. In addition, Rodriguez et al.[501] designed a discrete molecule [(PTA)Au(4-pyridylethynyl)] (PTA = 1,3,5-triaza-7-phosphaadamantane) (**186**); this complex forms a hydrogel immediately in water even at a concentration as low as 0.015 wt %. Che et al.[502] designed a dinuclear platinum(II) complex (**187**) having a [Pt(6-phenyl-2,2′-bipyridyl)((2,6-dimethylphenyl)isocyanide)] motif connected by an oligo(oxyethylene) chain which is able to form hydrogels driven by intra- and intermolecular Pt···Pt and $\pi-\pi$ interactions. Moreover, **187** acts as a supramolecular cross-linker to trigger the gelation of [Pt(6-phenyl-2,2′-bipyridyl)((2,6-dimethylphenyl)isocyanide)] at a molar ratio of 1:30. Wu et al.[503] designed a hydrogelator (**188**) based on hydrazide. **188** is able to afford a hydrogel with a CGC of 0.6 wt %. Upon the addition of Tb^{3+}, the resulting hydrogel exhibits enhanced green luminescence due to the coordination between the gelator and the metal ion. Lima and Rodriguez et al.[504] developed a hydrogelator of [Au{7-(prop-2-yn-1-yloxy)-1-benzopyran-2-one}(DAPTA)] (DAPTA = 3,7-diacetyl-1,3,7-triaza-5-phosphabicyclo[3.3.1]nonane) (**189**) which self-assembles to form long luminescent fibers and induces a hydrogel with a CGC of 0.01 wt %. Other cases in this category include the polyoxometalate (POM) reported by Bonchio et al.[505] as well as others,[506] which forms a gel at a specific condition (e.g., 90:10 MeOH/H_2O).

4.3. Hydrogels Based on Amino Acids and Peptides

Besides the small organic and inorganic hydrogelators, the hydrogelators derived from amino acids or peptides are of great importance due to their inherent biocompatibility and biological activities. The utilization of amino acids as the molecular building blocks of hydrogelators provides unique opportunities for generating supramolecular hydrogels that are not readily available from traditional organic/inorganic molecules. Peptide-based hydrogelators self-assemble via various noncovalent interactions, including hydrogen bonding, electrostatic interactions, aromatic−aromatic interactions, or hydrophobic interactions.[507] These intermolecular interactions lead to the formation of organized supramolecular structures that entrap water under appropriate stimuli. In addition, due to the well-established protocol of solid-phase peptide synthesis (SPPS),[508] it is easy to produce and to chemically and biologically modify peptides in large quantities and at a relatively fast turnaround. These merits have attracted considerable research activities focusing on the exploration of supramolecular hydrogels made of peptides. In this section we give a summary of different types of peptide-based hydrogelators in the past decade. We hope that the introduction of the recent progress will contribute to the understanding of the relationship between the peptide structures, the resulting conformation of the hydrogelators, and the morphologies of the matrixes of the supramolecular hydrogels. By presenting an updated report on peptidic hydrogelators, we intend to provide molecular information for researchers to uncover the hypotheses for the rational design of supramolecular hydrogelators.

We start with a brief description of the supramolecular hydrogels formed by amino acid derivatives. Strictly speaking, amino acid derivatives are not exactly "peptides", because the shortest peptides are dipeptides. However, because the building blocks of peptides are amino acids, amino acid-based hydrogelators share considerable similarities with peptide-based hydrogelators, making them relevant to be discussed in this section. We categorize the amino acid derivatives into three groups (i.e., those containing an alkyl chain, those that are salt-based, and those containing an aryl group (i.e., ferrocenyl, fluorenyl, naphthyl, pyrenyl, etc.)) and discuss several representative molecules in each group. Then we introduce

Scheme 28. Metal Complexes As Hydrogelators

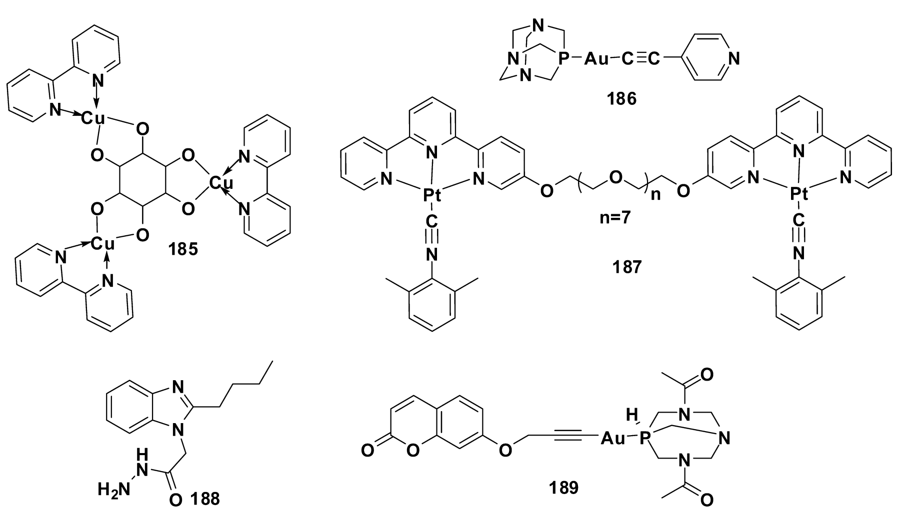

DOI: 10.1021/acs.chemrev.5b00299
Chem. Rev. 2015, 115, 13165−13307

Table 1. Peptide Sequences and Their Reported Hydrogelation Concentrations

peptide length (no. of amino acids)	peptide sequence	reported hydrogelation concn (wt %)	refs
2	FF (**208**)	0.1−10.0	555, 565−570
2	IF (**209**)	1.0−2.0	564
2	VF (**210**)	1.0−2.0	564
2	cyclic YK (**211**)	0.6−1.5	84
3	cyclic tripeptide (**212**)	0.5	577
3	cyclic tri-β-peptide (**213**)	0.006	578
3	^{D}VFF (**214**)	0.67	89, 579
3	^{D}FFV (**215**)	0.67	89, 579
3	^{D}LFF (**216**)	0.67	89
3	LFF (**217**)		89
3	FFY (**218**)	0.1	580
4	FEFK (**220**)	10	163, 582
4	PWWP (**221**)	0.25	583
4	RWDW (**222**)		584
5	KLVFF (**223**)	2.5	187
7	(2-Thi)(2-Thi)VLKAA (**224**)	2.0	585
8	FKFEFKFE (**225**)	0.1	588
8	AEAEAKAK (**226**)	0.8	591, 635
	AEAKAEAK (**227**)		
	FEFEFKFK (**228**)		
	FEFKFEFK (**229**)		
8	VKVKVEVK (**230**)	10.0	592
9	FEFEFKFKK (**231**)	2.0	594
10	GPGGDGPGGD (**232**)	1.0	595
11	QQRFEWEFEQQ (**233**)	0.016	597
	Ac-QQRFEWEFEQQ (**234**)		
12	RRRRGSWWWWSG (**235**)		599
	cyclic RRRRGSWWWWSG (**236**)		
13	PELELELELELEP (**237**)	3.6	600
13	PEFEFEFEFEFEP (**238**)	4.0	600
14	EIAQLEYEISQLEQ (**239**)	1.0	601
	KIAQLKYKISQLKQ (**240**)		
16	KKQLQLQLQLQLQLKK (**241**)	1.0	602
16	KKSLSLSLSLSLSLKK (**242**)	2.0	603
	EESLSLSLSLSLSLSLEE (**243**)		
	KKQLQLQLQLQLQLKK (**244**)		
16	LELELELELELELELE (**245**)	0.67	91
	VEVSVKVSVEVSVKVS (**246**)		
16	AAKAAAKAAAKAAAKA (**247**)	0.5	604, 605
16	RADARADARADARADA (**248a**)		181,606
	RADARADARADARADAKKKK (**248b**)		
	RADARADARADARADASSSSS (**248c**)		
16	FEFEFKFKFEFEFKFK (**249**)	0.007	607
20	VKVKVKVKV^{D}PPTKVKVKV (**250**)	0.5−2.0	134, 200, 610−625, 627, 636−638
	Max1: VKVKVKVKV^{D}PPTKVKVKVKV-NH_2 (**251**)		
	Max2: VKVKVKVKV^{D}PPTKVKTKVKV-NH_2 (**252**)		
	Max4: KVKVKVKVK^{D}PPSVKVKVKVK-NH_2 (**253**)		
	Max5: VKVKVKVKV^{D}PPSKVKVKVKV-NH_2 (**254**)		
	Max6: VKVKVKVKV^{D}PPTKVKEKVKV-NH_2 (**255**)		
	Max7: VKVKVKVKV^{D}PPTKVKCKVKV-NH_2 (**256**)		
	Max8: VKVKVKVKV^{D}PPTKVEVKVKV-NH_2 (**257**)		
	MLD: KVKVXVKVKV^{D}PPTKVKVXVKVK (**258**)		
	SSP1: VKVKVDPPTKVKVKVKVKVKV-NH_2 (**259**)		
	SSP2: VKVKVKV^{D}PPTKVKVKVKVKV-NH_2 (**260**)		
	SPP3: VKVKVKVKV^{D}PPTKVKVKVKV-NH_2 (**261**)		
	VKVKVKVKVPPTKVKVKVKV (**262**)		
	VKVKVKVKVPPTKVKVKV (**263**)		
20	VKVKVKVCGPKECVKVKVKV (**264**)	2.0	639
28	KIAALKQKIASLKQEIDALEYENDALEQ (**265**)		633

DOI: 10.1021/acs.chemrev.5b00299
Chem. Rev. 2015, 115, 13165−13307

Table 1. continued

peptide length (no. of amino acids)	peptide sequence	reported hydrogelation concn (wt %)	refs
	KIRRLKQKNARLKQEIAALEYEIAALEQ (**266**)		
30	CKQLEDKIEELLSKAACKQLEDKIEELLSK (**267**)		634

Scheme 29. Representative Molecular Structures of Amino Acid Derivative Hydrogelators Containing an Alkyl Chain

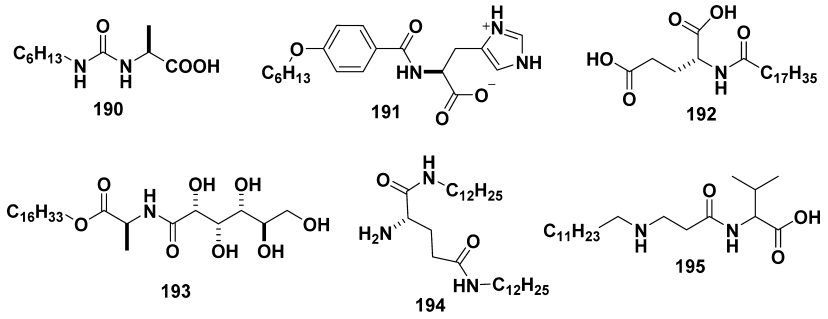

the hydrogels formed by native peptides (consisting of amino acids only and without any chemical modification). We summarize most of the peptidic hydrogelators according to their molecular size (Table 1). In such an arrangement, we give an overall review of the design strategies of peptide-based hydrogelators and highlight the notable advances made recently. After identifying key features of the native peptides, we discuss the chemically/biologically modified peptides (i.e., peptide derivatives) that are the representative hydrogelators from six subgroups. The six subgroups are the peptides with terminal acetylation (or formylation) and amidation, peptide derivatives containing an alkyl chain, peptide derivatives containing an aromatic group (e.g., fluorene-based, naphthalene-based, and pyrene-based peptide derivatives), peptide derivatives containing a photosensitive group, bolaamphiphiles, and dendritic peptides.

4.3.1. Amino Acid Derivatives. *4.3.1.1. Amino Acid Derivatives Containing Alkyl Chain(s).* Most amino acid derivatives containing alkyl chains are conventional amphiphiles, consisting of a polar head group and one or two hydrophobic tails.[509] The amino acids make the polar head, while the alkyl chains are the hydrophobic tails with many variations in the length and flexibility. These molecules are quite common in nature and are well-known to form a variety of nanostructures in water.[510−513] For example, Bhattacharya et al. reported the gelation of enantiomerically pure *N*-alkanoyl-L-alanine amphiphiles in a series of organic solvents.[514] Recently, Dey et al. designed and developed a series of amino acid-based gelators, *N*-(*n*-alkylcarbamoyl)-L-alanine (e.g., **190**) (Scheme 29), all of which form stable organogels in solvents in the presence of water at a concentration of 1% (w/v). The authors concluded that water-mediated intermolecular hydrogen bonds between amphiphiles result in the formation of supramolecular self-assemblies. The urea linkage of this hydrogelator, as the simplest motif that provides two hydrogen bond donors and one acceptor, is a common and useful hydrogen-bonding building block for supramolecular hydrogels.[515] Similarly, N^{α}-[4-(*n*-alkyloxy)benzoyl]-L-histidine (**191**) with a hydrocarbon chain, reported by the same group, affords thermoreversible hydrogels in a wide range of pH at room temperature. They also reported that the CGC value of **191** at different pH values varies from 2.5% to 5.0% (w/v).[516] Liu et al. reported a multiple-H-bonding amphiphile, *N*-stearoyl-L-glutaminc acid (C_{18}-Glu, **192**), which forms disk- and fiberlike nanostructures in both hydrophilic and hydrophobic environments, respectively, due to intra- and intermolecular hydrogen bonds.[517] Maruyama et al. reported that the attachment of a carbohydrate motif to the N-terminal of the alkyl chain−amino acid structure affords another hydrogelator, **193**, which is able to harden a broad range of solvents, in addition to gel water over a wide pH range at gelation concentrations of 0.1−2 wt %.[518] Using a similar synthetic strategy, Cai et al. produced zwitterionic supramolecular gel lubricants.[519] Interestingly, L-glutamic acid, through both α- and ω-aminoalkylation, affords a double-long-chain-terminated hydrogelator, **194**. This amphiphile disperses in various solvents ranging from water to hexane, and forms nanofibrils or aggregates. It also has a relatively good solubility, which results in a CGC value higher than 20 mM.[520] Dey et al. designed a zwitterionic hydrogelator of sodium *N*-(*n*-dodecyl-2-aminoethanoyl)-L-valinate (**195**) that is able to afford a supramolecular hydrogel with a CGC of 0.05 wt % in the presence of sodium dodecyl sulfate (SDS). In addition, the resulting hydrogel is thermoreversible and sensitive to a change of pH.[521]

4.3.1.2. Ionic Amino Acid Derivatives. While they augment the self-assembly ability of hydrogelators, long alkyl chains or aromatic rings are the hydrophobic segments that decrease the solubility of the hydrogelators in water. One of the simplest strategies to achieve relatively better solubility required for forming a hydrogel is to introduce charge(s) into the hydrogelators.[522−524] Suzuki et al. reported the synthesis and properties of L-lysine alkali-metal salt **159**. In water, **159** forms a supramolecular hydrogel, within which the self-assembled nanofibers entangle to result in a 3D network.[230] **158** is another L-lysine-based hydrogelator, with a pyridinium bromide salt, developed by Suzuki and Liu et al., independently.[525−527] It forms a hydrogel at a wide range of pH and has a CGC as low as 0.3 wt % at neutral pH. Yang et al. developed two chiral L-phenylalanine-based salts (**196**[528,529] and **197**[530]) as hydrogelators. As shown in Scheme 30, **196** has an ammonium salt, and **197** has a pyridinium salt. They both self-assemble in aqueous media at different pH values to form supramolecular hydrogels with CGC values of 1.2−2.0 wt % (for **196**) and <1.0 wt % (for **197**).

4.3.1.3. Amino Acid Derivatives Containing Aromatic Group(s). Although ionic force and the overlap between alkyl

DOI: 10.1021/acs.chemrev.5b00299
Chem. Rev. 2015, 115, 13165−13307

Scheme 30. Representative Hydrogelators of Ionic Amino Acid Derivatives

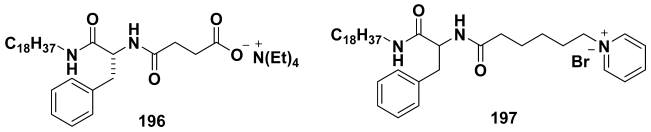

chains offer interfiber interactions, they are intrinsically weak and inefficient. Aromatic−aromatic interaction, extensively used by nature as a stabilizing force for generating ordered structures in proteins,[13] not only exceeds the Van der Waals interaction between the alkyl chains, but also leads to more predictable and efficient self-assembly of the molecules in the aqueous phase for the formation of mechanically strong and stable supramolecular hydrogels due to its compact volume. Thus, aryl motifs (e.g., ferrocenyl, fluorenyl, naphthyl, and pyrenyl)[531−533] and phenylalanine (or its derivatives) become prevalent and effective residues used in generating supramolecular hydrogels.

As shown in Scheme 31, Zhang et al. serendipitously discovered that ferrocenoylphenylalanine (**198**) aggregates in water via a rapid self-assembly to form a stable hydrogel which exhibits a sharp phase transition in response to multiple stimuli (i.e., oxidation−reduction reaction, guest−host interaction, and pH changes). Though being exceptionally simple and small, this hydrogelator is electrochemically active, which illustrates a remarkably facile approach to introduce an organometallic moiety into a supramolecular hydrogel.[114] Inspired by this work, He et al. also investigated the self-assembly properties of ferrocenoyldiphenylalanine.[534] Since the serendipitous observation of an effective hydrogelator made of [(fluorenylmethyl)-oxy]carbonyl (Fmoc)-protected dialanine,[11] Fmoc, widely used as the protecting group in SPPS, has become a popular N-terminal capping motif in peptidic hydrogelators because the Fmoc-protected amino acids or peptides are commercially available or relatively easy to make. The intensive use of Fmoc in making supramolecular hydrogelators also originates from its advantages, such as ease of being incorporated into peptide/amino acid derivatives (i.e., derived directly from SPPS), low cost, and excellent capacity to promote self-assembly. Changing the pH is a common way to make supramolecular hydrogels from Fmoc-protected amino acids. For example, Nilsson et al. reported supramolecular hydrogels generated by fluorinated Fmoc-phenylalanine derivatives.[535−537] Suspensions of Fmoc-pentafluorophenylalanine (**199**) in water undergo rapid self-assembly, which gives rise to rigid supramolecular hydrogels even at concentrations as low as 0.1 wt %. To better understand the electronic and steric contributions of the benzyl side chain to the hydrophobic and aromatic−aromatic interactions during self-assembly, the authors also changed the halogen substituents (i.e., F, Cl, Br) or the position of substitution (e.g., ortho, meta, or para) on the aromatic side chain of Fmoc-Phe (**200**). The authors reported that the position of the halogen and the size of the halogen atom significantly affect the rate of self-assembly and the bulk rheological properties of the resulting hydrogels. For example, the rate of self-assembly increases in the order ortho < meta < para, and the hydrogel rigidity increases in the order Br < Cl < F.[536,537]

Xu et al. also reported the first case of the use of Fmoc-amino acid derivatives to generate multicomponent supramolecular hydrogels.[153,538,539] Equal moles of **14** and **201** and 2 equiv of Na_2CO_3 afford a clear hydrogel after heating and addition of alkaline phosphatase.[153] Similarly, mixing and then heating 1 equiv of **200**, 1 equiv of **201**, and 2 equiv of Na_2CO_3 in water eventually leads to the formation of a clear solution, which turns into a hydrogel after being cooled back to room temperature. The subsequent hydrogel exhibits exceptionally high storage moduli and a rapid recovery of its original mechanical strength after removal of the external forces.[538,539] In another study, Xu et al. prepared a supramolecular hydrogel by mixing **200** and Fmoc-Lys (**202**). The resulting hydrogel acts as a reaction medium to mimick a bioluminescence environment with a more than 10-fold enhanced quantum yield of chemiluminescence.[540] Banerjee et al. also reported that

Scheme 31. Representative Molecular Structures of Hydrogelators Containing Aromatic Groups

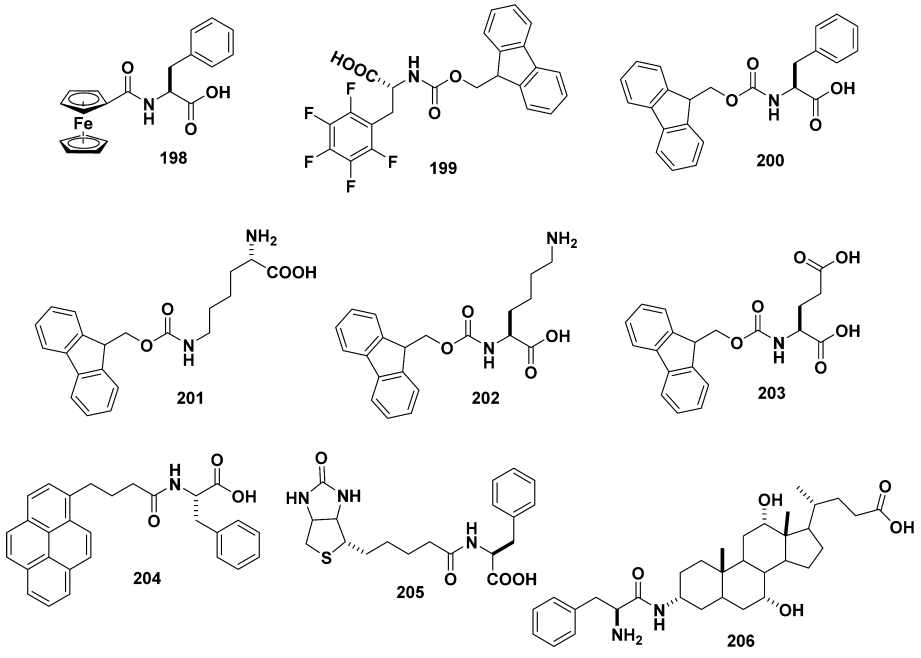

DOI: 10.1021/acs.chemrev.5b00299
Chem. Rev. 2015, 115, 13165−13307

supramolecular hydrogels were formed by coassembling two oppositely charged Fmoc-amino acids (i.e., **202** and Fmoc-Glu, **203**) with a CGC value of 50 mM (1.8 wt %).[541] The authors reported that molecular chirality is translated into the supramolecular helicity and the handedness of these fibers because the latter depends on the corresponding molecular chirality of the two-component system.

Fluorescent spectroscopy is a useful tool to study the interactions among the fluorophore-bearing hydrogelators in the gel state. Besides providing strong and efficient aromatic−aromatic interaction, pyrene is a suitable motif for fluorescent spectroscopy as its emission changes due to aromatic−aromatic interaction (e.g., the formation of an excimer[542]). Thus, pyrene has become a popular moiety to be incorporated into supramolecular hydrogelators.[18,543] Banerjee et al. designed and developed a hydrogelator (**204**) consisting of a single amino acid and a pyrene group. **204** forms hydrogels in a wide range of pH (7.5−14) in the aqueous phase. With an increase of the pH, a distinct morphological change of the nanofibers of the hydrogel occurs, and the morphology transforms from helical to tapelike.[104] Although the aromatic−aromatic interaction between two phenyl groups is weaker than that between two fluorenyl or two pyrenyl groups, phenylalanine is often incorporated into peptides for increasing their ability to self-assemble. Kim et al. reported a biotin-based small molecule (biotin-L-Phe, **205**) that displays remarkable gelation properties in aqueous media, including buffer solutions with different pH values.[546] Although biotin-based organogelators have been reported,[544] the study of supramolecular hydrogelators of biotin is rare.

Bile acids are among the most investigated rigid molecular motifs due to their ability to self-organize into many different supramolecular structures. Galantini et al. reported the synthesis and self-assembly behavior of cholic acid-connected amino acid derivatives[545] (e.g., **206**). The molecules of **206** aggregate in globular micelles at high pH, whereas they form tubular superstructures under acidic conditions and result in hydrogels at a concentration of 18 mM (1.2 wt %). These two representative cases imply that the conjugation of L-phenylalanine to natural products (i.e., biotin (**205**)[546] and cholic acid (**206**)[547]) likely will result in a rich class of supramolecular hydrogelators.

4.3.1.4. Amino Acid-Based Bolaamphiphiles. Bolaamphiphiles are a class of hydrogelators composed of two terminal hydrophilic groups linked by a hydrophobic backbone/chain. Variation of the structures of the "head group" and the linker of bolaamphiphiles has great influence on their ability to aggregate and the properties of the hydrogels. On the basis of L-valine- and L-proline-based peptide bolaamphiphiles, a class of efficient organogelators, Miravet et al. designed and developed one bolaform amino acid derivative (**4**) which self-assembles in water to form hydrogels.[59,549−551] The CGCs for these small molecules range from 4 to 26 mM (from 0.18 to 1.2 wt %).[59,548−551] As shown in Scheme 32, Liu et al. reported another series of bolaamphiphiles with head groups made of L-glutamic acid and a hybrid linker composed of two rigid benzene rings and a butyl segment (**207**). They controlled the hierarchical self-assemblies via changing the solution pH. For example, at pH 3, these molecules form a hydrogel in water at a concentration as low as 0.5 wt % (CGC); at pH 12, these hydrogelators then form vesicle-like aggregates.[552]

Scheme 32. Representative Molecular Structure of a Hydrogelator Based on a Bolaamphiphile

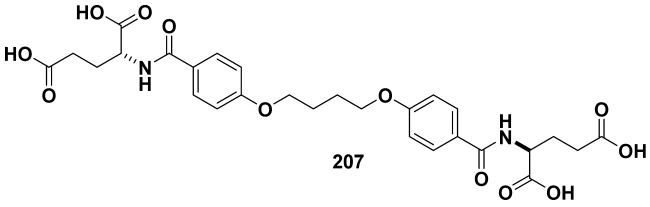

207

4.3.2. Peptides. As a consequence of evolution, proteins (e.g., insulin[19]) form hydrogels, implying that peptides, as the component of proteins, should be able to form supramolecular hydrogels. This notion turns out to be valid. For example, Namba et al. have demonstrated that the terminal regions of flagellin (consisting of 25 amino acids) form hydrogels at concentrations >15 mg/mL.[21] Surprisingly, much smaller peptides,[553,554] such as dipeptides, are able to self-assemble in water to generate supramolecular hydrogels. Besides the easy synthesis of peptides, several seminal works on peptide-based hydrogels[18,188,555−557] at the beginning of the century have stimulated the development of supramolecular hydrogels based on small peptides. In this section on supramolecular hydrogels formed by peptides, we put the emphasis on small peptides (20 or less amino acid residues) because there are already several excellent reviews on medium-sized oligopeptides and their derivatives.[558−563] We arrange the discussion of peptide-based hydrogelators according to the length of the peptides and start with the shortest one.

The report by Gazit et al. on the nanofibers formed by the self-assembly of diphenylalanine (FF, **208**)[555,565−568] has stimulated intensive investigations of the self-assembly of small peptides, including dipeptides.[569−572] Ventura et al. examined the dipeptides Ile-Phe (IF, **209**) and Val-Phe (VF, **210**) and found that **209**, at 1.5 wt %, forms a hydrogel consisting of persistent nanofibers with a diameter of about 55 nm. The nanofibers appear to be crystalline and melt upon heating. Unlike **209**, **210** cannot self-assemble. Besides the fact that **209** is probably the smallest hydrogelator, it is worth noting that the difference of one methyl group between **210** and **209** has a profound impact on their capabilities to self-assemble.[564] The authors also proposed the self-assembled structure of **209** (Figure 5), which is quite similar to the recent structure of $A\beta_{1-40}$ determined by solid-state NMR.[214] Since the report of Gazit et al. on diphenylalanine, several other groups have explored the properties of **208** in great detail. Park et al. have demonstrated that **208** self-assembles to form nanowires and nanotubes with high thermal, chemical, and proteolytic stability. An XRD study of these nanowires and nanotubes reveals their crystallinity.[569] Qi et al. reasoned the use of hexafluoroisopropyl alcohol (HFIP) to dissolve **208** would introduce a solvent effect, so they used CH_3CN/H_2O as the solvent to process **208**. They found that cooling the solution of **208** results in microtubes and the evaporation of the solution of **208** on a glass surface affords nanofibers. The higher content of CH_3CN leads to bigger diameters of the nanofibers.[570] Krishnan et al. also investigated the effect of HFIP and found that the amount of HFIP significantly affects the morphologies of the nanotubes formed by the self-assembly of **208**.[571] Considering the morphology of nanoscale assemblies dictates their interactions with proteins,[573,884] this work, indeed, provided a useful insight for understanding the discrepancy[574] in the reports on the cytotoxicities of $A\beta$

DOI: 10.1021/acs.chemrev.5b00299
Chem. Rev. 2015, 115, 13165−13307

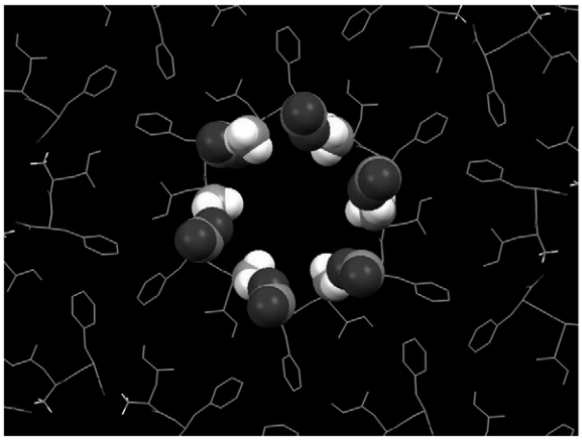

Figure 5. Molecular model of **209** self-assembled structures. The model is based on the crystal X-ray structure of the diphenylalanine peptide. The dipeptide backbone and hydrophobic side chains are shown as stick representations. Adapted with permission from ref 564. Copyright 2007 Biophysical Society.

because HFIP is the most common solvent used to dissolve commercially available Aβ.

As shown in Scheme 33, Feng et al. reported that an innovative cyclodipeptide (**211**), made of tyrosine and lysine, acts as a hydrogelator and forms a hydrogel at a CGC of 0.6 wt %. The hydrogel, having a relatively low mechanical strength, only forms during cooling with the assistance of ultrasound for breaking up the intermolecular interactions. Interestingly, after the attachment of an alkyl chain at the ε-amino group of **211**, the CGC in water becomes 1.5 wt %. Due to the difficulty of synthesis, reports on the self-assembly of cyclic peptides are rather scarce.[575,576] Zhao and Dory et al. reported a cyclic tripeptide (**212**) forming micrometer-sized tubes by self-assembly in a liquid crystal. On the basis of molecular dynamics, the authors suggested a hierarchical hexagonal assembly to generate the observed hollow macrotubes of **212**.[577] In a similar study, Kimura et al. reported the self-assembly of a unique tri-β-peptide (**213**) that consists of two β-glucosamino acids and one *trans*-2-aminocyclohexanecarboxylic acid. **213** self-assembles in a mixture of formic acid and water to form nanofibers at a concentration of about 0.006 wt %.[578] It would be interesting to obtain more information about the biological properties of **213**.

Marchesan et al. systematically investigated tripeptides containing one D-amino acid residue at the N-terminal and found that chirality plays a critical role in the morphology of the nanofiber networks of the resulting hydrogels. The authors observed a very interesting and unexpected result by modulating the chirality of the tripeptides: while the tripeptides VFF and FFV fail to self-assemble at physiological pH, ^{D}VFF (**214**) and ^{D}FFV (**215**) are able to self-assemble at a concentration of about 0.67 wt %. Both **214** and **215** self-assemble to form distinct nanostructures: the former results in nanotapes and the latter twisted nanofibers.[579] The authors also observed similar behavior for ^{D}LFF (**216**), which forms a hydrogel at 0.67 wt %. While the self-assembly of **216** results in mainly nanofiber networks, the self-assembly of LFF (**217**) is rather polymorphic and fails to form a self-supporting hydrogel.[89] Cao et al. examined the self-assembly of FFY (**218**) and Fmoc-FFY (**219**) for photo-cross-linking after the self-assembly. They found **218** self-assembles to form nanoparticles which turn into nanorods after photo-cross-linking tyrosine residues. **219** forms a weak hydrogel at 0.1 wt % which consists of nanofibers that turn into nanoparticles after photo-cross-linking. This result provides a useful insight into the effect of cross-linking to the self-assembled nanostructures.[580] Moreover, Ulijn and Tuttle et al. have presented a coarse-grain molecular dynamics (MD) protocol for screening tripeptides for their aggregation behavior and applied this to a set of 8000 gene-encoded tripeptides.[581] It would be highly valuable to verify if these self-assembly tripeptides exist endogenously and at concentrations high enough to self-assemble.

Miller et al. designed a tetrapeptide (FEFK, **220**) consisting of two hydrophobic residues, one positive residue, and one negative residue. While **220** itself hardly forms a hydrogel, **220** can serve as a substrate for thermolysin to undergo reverse hydrolysis for enzymatic hydrogelation by the formation of octapeptides as the final products. Although the hydrogelation concentration of the tetrapeptide concentration is 10 wt %, this unique reversible hydrolysis of the amide bond represents an evolutionary approach to screen hydrogelators from a dynamic library of peptides.[163] Saiani et al. further studied this tetrapeptide for enzymatic hydrogelation and reported that the initial concentration of the tetrapeptide dictates the morphology of the peptide nanofiber network, and the concentration of the enzyme has little effect on the final morphology of the nanostructures formed by the self-assembly of the peptides.[582] Verma et al. reported the self-assembly of a tetrapeptide, PWWP (**221**), which forms vesicular microstructures. The author reported that the vesicles can entrap dye molecules and the addition of KCl (0.25 mM) disrupts the vesicles.[583] Tine et al. examined the effect of temperature on the self-assembly of RWDW (**222**) and found that an increase of temperature produces nanofibers with smaller diameters.[584] According to the AFM experiment, the authors also found that **222** self-assembles to form a dense network of entangled nanofibers at 15 °C, but assembles into sparse globular and fibrillar structures at 35 °C.

Hamley et al. used an array of techniques to investigate the self-assembly of the pentapeptide KLVFF (**223**), which is the core motif of β-amyloid peptide. The authors reported that **223** forms a hydrogel at 2.5 wt % in water, but at 3.0 wt % in

Scheme 33. Representative Molecular Structures of Cyclopeptide Hydrogelators

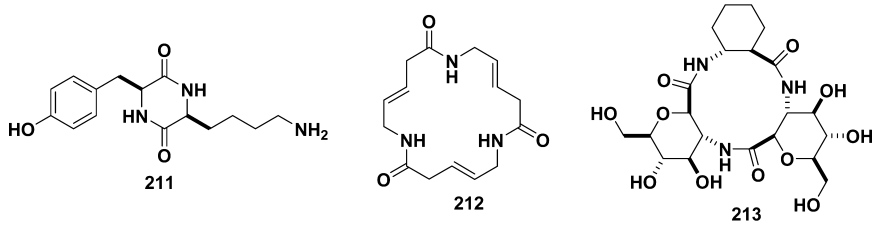

DOI: 10.1021/acs.chemrev.5b00299
Chem. Rev. 2015, 115, 13165−13307

phophate-buffered saline (PBS). The nanofiber dimensions determined by cryo-TEM and SAXS confirm that fibrils (10 nm in diameter) are formed in aqueous solution, which helps to address some contradictions in the literature, as the authors pointed out.[187] On the basis of the motif AAKLVFF, Hamley et al. replaced phenylalanine with β-2-thienylalanine (2-Thi) to generate (2-Thi)(2-Thi)VLKAA (**224**). **224** starts to self-assemble at a concentration of 0.03 wt % and forms a hydrogel in water at 2.0 wt %. Although the self-assembly of **224** occurs as designed, the conductivity of the nanofibrils has yet to be demonstrated.[585]

Doyle et al. studied the kinetics of the hydrogelation of an octapeptide (FKFEFKFE, **225**) and found that **225** forms a hydrogel at about 0.1 wt %. One notable feature of the hydrogelation of **225** is that an increase of the pH from 3.5 to 4.0 speeds the formation of the nanofiber networks by almost 2 orders of magnitude, from hours to minutes, but the gelation follows the same mechanism. The authors proposed a simple model of self-assembly based on Derjaguin−Landau−Verwey−Overbeek (DLVO) theory.[586,587] This detail kinetic study offers a useful insight for the design of fast responsive hydrogelators.[588] Saiani et al. investigated a set of four octapeptides, AEAEAKAK (**226**), AEAKAEAK (**227**), FEFEFKFK (**228**),[589,590] and FEFKFEFK (**229**), which consist of oppositely charged residues and hydrophobic residues with slightly different positionings. The authors found the phenylalanine in the octapeptides to promote β-sheet conformations in solution and the alanine to favor α-helices. According to the authors, **227** is unable to self-assemble in solution, but **226** self-assembles to form thick, rigid nanofibers (6 nm in diameter). However, **226** fails to form a hydrogel at concentrations up to 10 wt %. On the contrary, both phenylalanine-based peptides **228** and **229** self-assemble in solution and form hydrogels at a CGC of 0.8 wt %. Both hydrogels contain a dense network of semiflexible nanofibers 4 nm in diameter. Besides further confirming the importance of aromatic−aromatic interactions for the self-assembly of peptides in water, the detailed SANS measurement in this work has provided invaluable information on the morphologies of the nanofibers in solutions and in hydrogels.[591] Miller et al. developed an innovative way to stabilize enzymes by covalently attaching a self-assembling peptide (**230**) to pentaerythritol tetranitrate reductase, which co-self-assemble to form hydrogels. The stability of the entrapped enzyme increases significantly, and the activity of the enzyme is retained even after exposure to a high temperature (90 °C) and 12 months of storage,[592] which is quite remarkable.

Cavalli et al. synthesized a nonapeptide, FEFEFKFKK (**231**), which forms a hydrogel at 2.0 wt %. On the basis of this result, the authors conjugated **231** with a DNA-recognizing protein (Tus) by a sortase A methodology.[593] The authors demonstrated that the hydrogel containing Tus binds to DNAs.[594] Sun et al. designed and synthesized a decapeptide, GPGGDGPGGD (**232**) based on the spider flagelliform silk protein and the Ca^{2+} binding domain of lipase Lip A. The authors suggested that such a design can avoid redundancy and preserve the properties of both sequences. At 1.0 wt %, **232** largely forms nanospheres which become nanofibers upon the addition of Ca^{2+}. On the basis of CD data, the authors suggested a β-spiral structure as the secondary structure of the peptide.[595] McPherson et al. reported a new method to synthesize peptide QQRFEWEFEQQ (**233**) based on the protein expression in *Escherichia coli*.[596] The recombinant peptide self-assembles to form nanofibers and results in a hydrogel at a concentration of 1.5 wt % and pH 2.0.

McPherson et al. used a SUMO (small ubiquitin-related modifier)−peptide fusion approach for efficient production and purification of β-structured recombinant self-assembling peptides with native N- and C-terminals (**233**) to compare with the chemically synthesized peptide that has an acetylated N-terminal (**234**). The authors reported that the chemically synthesized peptide **234** forms a hydrogel at 1.0 wt % and pH 2.0,[597] which are essentially the same conditions as those needed for SUMO−**233**.[598] Intending to investigate the effect of the topology of the peptides on self-assembly, Lim et al. designed and synthesized two dodecapeptides that have the same sequence (RRRRGSWWWWSG) but different topologies: one (**235**) is linear, and the other (**236**) is cyclic. Their study revealed that the cyclic and linear peptides exhibit significantly different self-assembled nanostructures and thermal stabilities, but share similar critical aggregation concentrations and cytotoxicity profiles.[599] This study offers an important topological approach to tailor the nanostructures formed by the self-assembling peptides. Rapaport et al. reported four tridecapeptides (e.g., PELELELELELEP (**237**) and PEFEFEFEFEFEP (**238**)) consisting of negatively charged residues and hydrophobic residues. As an amphiphilic and acidic peptide, **237** self-assembles to form β-sheet structures and results in a hydrogel at pH 7 and a concentration of 4 wt %. The addition of calcium ion can increase the storage modulus of the hydrogel by almost 10-fold. Furthermore, the authors also demonstrated that the hydrogel of **238** could provide scaffolds for cell adhesion and spreading of Saos-2 cells.[600] Hartgerink et al. reported a tetradecapeptide (EIAQLEYEISQLEQ, **239**) consisting of two heptads for adopting coiled-coil structures. At a concentration of 1 wt %, the mixture of **239** with another tetradecapeptide (KIAQLKYKISQLKQ, **240**) containing a positively charged residue results in the formation of nanofibers having β-sheet features. The authors suggested that these short peptides illustrate the minimum requirements necessary to form dimeric coiled coils.[601]

Hartgerink et al. developed a hexadecapeptide (KKQLQLQLQLQLQLKK, **241**) which fits into an ABA triblock motif (termed "multidomain peptides" (MDPs) by the authors). The authors reported that **241**, at 1 wt % and with 10 mM Tris at pH 7, self-assembles to form nanofibers and results in a hydrogel. One impressive result in this work is the control of the length of the nanofibers, as demonstrated by the fact that the aging of the solution of **241** hardly changes the maximal length of the nanofibers.[602] On the basis of the same principle, the authors also developed several other MDPs (KKSLSLSLSLSLSLKK (**242**), EESLSLSLSLSLSLSLEE (**243**), KKQLQLQLQLQLQLKK (**244**)) and used them to form hydrogels at 2 wt %. Moreover, they demonstrated the use of lysyl oxidase or plasma amine oxidase to oxidize primary amines to aldehydes so the reactive aldehydes react further to cross-link the nanofibers in the hydrogels. However, the efficiency of the oxidation process remains to be improved.[603] Kinoshita et al. designed two kinds of β-peptide, $(LE)_8$ (**245**) and $(VEVSVKVS)_2$ (**246**). Both peptides self-assembled to form nanofibers and afford hydrogels upon addition of calcium ion. Owing to the interaction between the carboxylic acid in the peptide and the calcium ions, the resulting hydrogel exhibited enhanced mechanical properties with an increase of the concentration of the calcium ions. The authors suggested that

DOI: 10.1021/acs.chemrev.5b00299
Chem. Rev. 2015, 115, 13165−13307

this mineralization approach provides a new way to prepare bone-filling materials.[91]

After Schweitzer-Stenner et al. observed that the hexadecapeptide AAKAAAKAAAKAAAKA (**247**) forms a hydrogel at low concentration (0.5 wt %),[604] Li et al. analyzed the initial phase of the aggregation process by molecular dynamics. They reported that the peptide aggregates into stable antiparallel β-sheets. In addition, the authors suggested that the formation of trimers is very sensitive to the concentration of the peptides,[605] which provides a useful insight to explain the conformation transition of **247** from an α-helix to a β-sheet.[604] After Zhang et al. reported the hydrogels of RADARADARADARADA (**248a**), Unsworth et al. carried out a detailed study to provide a mechanistic understanding of the self-assembly process by designing and synthesizing two peptides (RADARADARADARADAKKKK (**248b**) and RADARADARADARADASSSSS (**248c**)) that are related to **248a**. The authors observed that **248b** is unable to self-assemble, suggesting the role of the charged residues. The authors also found that self-assembly of **248a** and **248c** is entropy driven, with hydrophobic force as the main factor for **248a** and hydrogen bonding as the main factor for **248c**.[606] The authors also confirmed that counterions contribute little to self-assembly, which differs from the current conceptual understanding of the self-assembly of **248a**. Muller et al. designed a library of peptides having alternating hydrophobic and polar amino acids by substituting phenylalanine in FEFEFKFKFEFEFKFK (**249**) with glycine, alanine, valine, leucine, or isoleucine. The authors found that an increase of the number of glycines eventually prevents the hydrogelation of the peptide, and concluded that the sequence and steric size of the nonpolar residues dictate the secondary structure and morphology of the nanofibers of the self-assembled peptides.[607] As supramolecular hydrogelators, one of the most impressive classes of oligopeptides made of 20 amino acids is the de novo β-hairpin peptides (**250**−**264**) pioneered by Schneider and Pochan et al.[188,608] These synthetic peptides undergo intramolecular folding at a proper condition, and the subsequent intermolecular self-assembly generates β-sheets in water to result in hydrogels.[609] The authors ingeniously used D-Pro-L-Pro to define a type II′ β turn. At physiological pH, the peptides exist as random coils and exhibit excellent solubility in water, but a stimulus (e.g., ionic strength, pH, temperature, light, or shear forces) switches the peptide to a β-hairpin conformation so these β-hairpin peptides self-assemble into a highly cross-linked, but semiflexible, network of nanofibers[610] to afford mechanically rigid hydrogels. A notable application of these peptides is that they act as antibacterial hydrogels. Since there are several excellent reviews on the β-hairpin hydrogelators and their applications, we only list some representative sequences[134,200,610−627] in Table 1, and interested readers are encouraged to read the excellent reviews written by Schneider et al.[28,628−630]

When the peptides get longer, the intermolecular interactions certainly can increase and favor self-assembly and physical cross-linking to form a hydrogel.[631] However, the synthesis of long peptides becomes more difficult or more expensive so the peptides should have unique functions or aims to address important and general problems to justify the high cost. After reporting the first example of peptide hydrogels consisting of purely helical structures,[632] Woolfson et al. recently designed a self-assembling fiber system consisting of a dimeric coiled-coil peptide (e.g., KIAALKQKIASLKQEIDALEYENDALEQ (**265**) and KIRRLKQKNARLKQEIAALEYEIAALEQ (**266**)) that assemble in a controlled manner. The self-assembly of **265** and **266** results in fibers that are tens of nanometers wide and tens of micrometers long. Using cryo-TEM, the authors also obtained an ultrastructure for interpreting the packing of individual α-helices within the fibers. On the basis of the electron density map, the authors derived a model for elucidating how these α-helical fibrils pack into larger fibers.[633] To understand how to use local interactions between proteins for creating materials that have well-determined microstructures, Fairman et al. designed and synthesized an oligopeptide (CKQLEDKIEELLSKAACKQLEDKIEELLSK, **267**) that relies on hydrophobic interactions to drive self-assembly. As pointed out by the authors, the hydrophobic effect between **267** molecules favors axial assembly and their electrostatic forces modulate lateral assembly. At a concentration of 0.05 wt %, the peptide self-assembles to form a filament consisting of about 120 molecules of **267**. The authors also reported that various environmental factors (e.g., pH, salt, molecular crowding reagents, and "'capping'" peptides) can regulate the self-assembled filaments in an assembly of predictable manner,[634] which provides useful insights for developing coiled coils as peptide-based materials. It would be interesting to know the proteolytic stability of these self-assembled filaments.

4.3.3. Peptide Derivatives. *4.3.3.1. Peptides with Capped N- and C-Terminals.* Besides native peptides acting as hydrogelators, peptide derivatives can also self-assemble in water to form hydrogels. The most common way to modify a peptide is to cap the N-terminal by an acetyl or the C-terminal by an amide or to cap both ends.[640−642] As shown in Scheme 34, Solaro et al. reported a capped tetrapeptide, Ac-RWDW-

Scheme 34. Representative Molecular Structure of a Peptidic Hydrogelator with Capped N- and C-Terminals

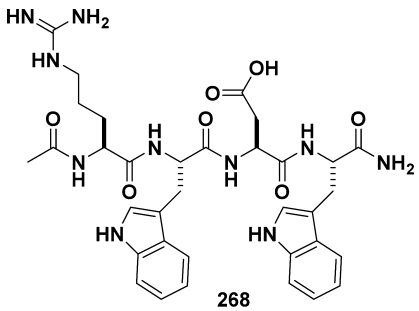

268

NH_2 (**268**), containing oppositely charged residues and hydrophobic residues, to form a soft hydrogel at 0.026 wt % in PBS buffer. They also observed an increase of the concentration of **268** and the addition of $CaCl_2$ to result in a thick and transparent hydrogel. Moreover, the authors demonstrated the use of the hydrogels for culturing cells (mouse embryo fibroblasts balb/3T3 clone A31 and human hepatoblastoma HepG2).[643] Xu and Lu et al. reported a capped hexapeptide, Ac-IIICGK-NH_2 (**269**, Table 2), which self-assembles in water to form long nanofibers and results in a hydrogel at 0.53 wt %. It is worth noting that oxidation of the Cys residue in **269** greatly increases the storage modulus of the hydrogels (from 200 to ∼10000 Pa). Moreover, the authors found that oxidation reduces the CGC to as low as 0.034 wt %. Replacing the Cys by a Met residue allows the formation of nanofibers at 1.7 mM, but fails to generate any hydrogels.[115] Nilsson et al. synthesized a series of capped octapeptides (Ac-

DOI: 10.1021/acs.chemrev.5b00299
Chem. Rev. 2015, 115, 13165−13307

Table 2. Peptide Sequences and Their Reported Hydrogelation Concentrations

peptide length (no. of amino acids)	peptide sequence	reported hydrogelation concn (wt %)	refs
4	Ac-RWDW-NH_2 (**268**)	0.026	643
6	Ac-IIICGK-NH_2 (**269**)	0.53	115
8	Ac-VKVKVKVK-NH_2 (**270a**)	∼0.8	644
	Ac-IKIKIKIK-NH_2 (**270b**)		
	Ac-FKFKFKFK-NH_2 (**270c**)		
	Ac-XKXKXKXK-NH_2, X = F5Phe (**270d**)		
	Ac-XKXKXKXK-NH_2, X = cyclohexylalanine (**270e**)		
8	Ac-FKFEFKFE-NH_2 (**271a**)	∼0.4	646, 647
	Ac-AKAEAKAE-NH_2 (**271b**)		
	Ac-VKVEVKVE-NH_2 (**271c**)		
	Ac-LKLELKLE-NH_2 (**271d**)		
	Ac-FKFKFEFE-NH_2 (**271e**)		
	Ac-KEFFFFKE-NH_2 (**271f**)		
	Ac-KFFEKFFE-NH_2 (**271g**)		
	Ac-FFKEKEFF-NH_2 (**271h**)		
8	Ac-LIVTQTMK (**272a**)	1.0	648
	LIVTQTMK-NH_2 (**272b**)		
9	Ac-PSFNFKFEP-NH_2 (**273**)	1.0	650
11	Ac-KWKAKAKAKWK-NH_2 (**274**)	2.3	651
	Ac-EWEAEAEAEWE-NH_2 (**275**)		
11	Ac-QQRFQWQFEQQ-NH_2 (**276a**)	0.01−0.1	652−654
	Ac-QQRFQWQFQQQ-NH_2 (**276b**)		
	Ac-SSRFSWSFESS-NH_2 (**276c**)		
	Ac-QQRFOWOFEQQ-NH_2 (**276d**)		
	Ac-SSRFEWEFESS-NH_2 (**276e**)		
	Ac-SSRFOWOFESS -NH_2, O = ornithine (**276f**)		
11	Ac-CFKFEFKFECG-NH_2 (with S−S bond) (**277**)	0.9	116
11	Ac-QQKFQFQFEQQ-NH_2 (**278a**)	0.76	656
	Cys-QQKFQFQFFEQQ-Gly-thioester (**278b**)		
21	Ac-GGRGDSGGGQQKFQFQFFEQQ-NH_2 (**279**)		656
16	Ac-AAKAAAKAAAKAAAKA-NH_2 (**280**)	0.5	657
16	Ac-RADARADARADARADA-NH_2 (**281**)	0.5	181, 648, 659, 660
	Ac- RASARADARADARADA-NH_2 (**282**)		
	Ac- RASARASARASARADA-NH_2 (**283**)		
16	Ac-KKQLQLQLQLQLQLKK-NH_2 (**284a**)	1.0	661, 662
	Ac-EQLQLQLQLQLQLE-NH_2 (**284b**)		
	Ac-KKSLSLSLSLSLSLKK-NH_2 (**284c**)		
	Ac-ECLSLCLSLCLSLE-NH_2 (**284d**)		
	Ac-KKQFQLQFQLQFQLKK-NH_2 (**284e**)		
	Ac-KKQFQFQFQFQFQFKK-NH_2 (**284f**)		
	Ac-KKQWQWQWQWQWQWKK-NH_2 (**284g**)		
	KKQYQYQYQYQYQYKK-NH_2 (**284h**)		
13	Ac-GTAGLIGQERGDS (**285**)	1.0	663
21	Ac-LKELAKVLHELAKLVSEALHA-NH_2 (**286**)	0.1	93
10	Ac-WKVKVKVKVK-NH_2 (**287a**)	0.25	664, 666
	Ac-EWEVEVEVEV-NH_2 (**287b**)		
	formyl-WOAOAOAOAO-NH_2 (**287c**)		
	formyl-WEAEAEAEAE-NH_2 (**287d**)		
	formyl-WOAOAO-NH_2 (**287e**)		
	formyl-WEAEAE-NH_2 (**287f**)		
	formyl-WOAOAOAOAOAOAO-NH_2 (**287g**)		
	formyl-WEAEAEAEAEAEAE-NH_2 (**287h**)		
16	SASLSASLSASLSASL-NH_2 (**288**)	1.0	667

XKXKXKXK-NH_2; X = Val (**270a**), Ile (**270b**), Phe (**270c**), ^{F5}Phe (**270d**), and cyclohexylalanine (Cha) (**270e**)) that are composed of alternating hydrophobic residues (Val) and positively charged residues (Lys). At 8 mM, **270a** is too hydrophilic to form a hydrogel, but **270b**, **270c**, **270d**, or **270e** self-assembles in water to form a hydrogel. On the basis of CD, the authors concluded that these peptides adopt β-sheet structures in the nanofibers formed by self-assembly. The authors also found that **270c** and **270d**, containing aromatic residues, form rigid hydrogels, but **270b** and **270e** form weak gels. One notable feature is that the self-assembly of **270b**−**270e** requires the addition of NaCl to the solution.[644]

DOI: 10.1021/acs.chemrev.5b00299
Chem. Rev. 2015, 115, 13165−13307

To understand the relative contributions of different hydrophobic groups (e.g., aromatic vs nonaromatic hydrophobic groups), Nilsson et al. designed another series of octapeptides (Ac-FKFEFKFE-NH_2 (**271a**),[645] Ac-AKAEAKAE-NH_2 (**271b**), Ac-VKVEVKVE-NH_2 (**271c**), and Ac-LKLE-LKLE-NH_2 (**271d**)). They found that only **271a** formed a hydrogel at a concentration of 0.46 wt % in a NaCl (40 mM) solution, suggesting that aromatic−aromatic interactions, though less essential for the self-assembly of this type of peptide (Ac-XKXEXKXE-NH_2), are necessary for hydrogelation. Moreover, the authors also reported that the cosolvent HFIP exerts a significant influence on the stabilization of the helical morphology of the self-assembled nanofibers.[646] The authors also varied the sequence of **271a** to Ac-FKFKFEFE-NH_2 (**271e**), Ac-KEFFFFKE-NH_2 (**271f**), Ac-KFFEKFFE-NH_2 (**271g**), and Ac-FFKEKEFF-NH_2 (**271h**). The authors found that the self-assembly of these peptides is pH dependent. At pH 3−4, **271e** self-assembles to form β-sheet nanoribbons and **271f** forms distinct nanotapes with a width of ∼20 nm, but **271g** and **271h** fail to self-assemble to form fibrils/tapes; however, **271h** does form micelle-like aggregates. At neutral pH, **271h** forms 20 nm nanotapes and the other peptides behave similarly to the way they do at pH 3−4.[647] These results underscore that the amino acid sequence plays a key role in the self-assembly of the oligopeptides, which is quite reasonable. Voyer et al. designed a series of octapeptides based on milk proteins (lactoglobulin). They found that both the N-terminal-capped octapeptide Ac-LIVTQTMK (**272a**) and the C-terminal-capped octapeptide LIVTQTMK-NH_2 (**272b**) adopt a β-sheet conformation and self-assemble to form hydrogels at a concentration of 0.1 wt %. However, **272a** forms hydrogels instantly at neutral pH and acidic pH, and **272b** forms hydrogels only at basic pH. This study also provided useful insight into the transition from a random coil to a β-sheet conformation upon a change of the pH.[648]

By introducing four phenylalanine residues into a capped nonapeptide (Ac-Pro-Ser-Phe-Asn-Phe-Lys-Phe-GIu-Pro-NH_2, **273**), Zhao et al., found that **273** forms a hydrogel at 1 wt %. The authors reported that the β-turn and β-sheet structures result in a concentration-dependent self-assembly to afford hierarchically arranged nanostructures.[649,650] Yu et al. investigated the effect of the ionic strength on the mechanical, structural, and transport properties of the hydrogels made of two capped undecapeptides, Ac-KWKAKAKAKWK-NH_2 (**274**) and Ac-EWEAEAEAEWE-NH_2 (**275**). At a peptide concentration of about 2.3 wt %, the authors changed the ionic strength of the solution and found that an increase of the ionic strength results in higher final storage moduli, slows the rate of hydrogelation, decreases the cross-section of the nanofibers in the hydrogels, and reduces the diffusion coefficients of water in the hydrogels.[651] Waigh et al. used photon correlation spectroscopy to study the internal dynamics of self-assembled fibrils of charged peptides, such as Ac-QQRFQWQFEQQ-NH_2 (**276a**), Ac-QQRFQWQFQQQ-NH_2 (**276b**), Ac-QQRFEW-EFEQQ-NH_2 (**234**), and Ac-SSRFSWSFESS-NH_2 (**276c**). The authors found that these peptides form hydrogels at 0.1 wt %, but they have different critical concentrations for self-assembly, which are 0.05, 0.03, 0.01, and 0.1 mM for **276a, 276b**, **234**, and **276c**, respectively.[652] Aggeli et al. studied the effect of the ionic strength on the self-assembly, morphology, and gelation of charged peptides, such as **234**, Ac-QQRFOWOFEQQ-NH_2 (**276d**), Ac-SSRFEWEFESS-NH_2 (**276e**), and Ac-SSRFOW-OFESS-NH_2 (**276f**) (O = ornithine). According to their study, at a concentration of 0.7 wt %, **234** and **276e**, in water, exhibit a sharp transition from antipaprallel β-sheets at pH < 6.5 to random coils at pH > 8. This transition results in a change of the properties of the solutions from a nematic solution (pH < 8) to an isotropic fluid (pH > 8). Bearing charges opposite those of **234** and **276e**, **276d** and **276f** undergo a transition from antiparallel β-sheets (pH > 10) to random coils (pH < 8) at 8 < pH < 10. The most insightful observation is that, in the presence of NaCl (130 mM), **234**, **276d**, **276e**, and **276f** all form nematic hydrogels at physiological pH.[653] Nelson et al. used electrochemical impedance spectroscopy to examine the interaction of this class of peptides with phospholipid monolayers. They found that peptides with side chains of serine and threonine interact with DOPC layers more strongly compared to peptides with side chains of glutamine and asparagine.[654] These insights should be useful for designing the hydrogels to interact with cells.

By introducing cysteine residues into **271a**, Nilsson et al. designed a novel cyclic peptide, Ac-CFKFEFKFECG-NH_2 (**277**). Upon reduction by DTT, *cyclic*-**277** becomes a linear peptide, *linear*-**277**, which forms a hydrogel at 0.9 wt %.[116] This excellent strategy also has been applied by Yang et al. to design redox-trigged hydrogelation of small peptides.[655] To improve the mechanical properties of the self-assembled peptide hydrogels, Collier et al. devised an innovative approach to perform native chemical ligation (NCL) of the peptides after the self-assembly. On the basis of the self-assembling peptide Ac-QQKFQFQFEQQ-NH_2 (**278a**), they designed and synthesized the sequence Cys-QQKFQFQFFEQQ-Gly-thioester (**278b**). The self-assembling **278b** forms a hydrogel at 0.76 wt %, and NCL of the hydrogel results in a 6-fold increase of the storage modulus. The authors reported that ligation also leads to a significant enhancement of HUVEC cell proliferation on the surface of the hydrogel. Moreover, they demonstrated that NCL is orthogonal to the inclusion of an RGD-functionalized peptide (e.g., Ac-GGRGDSGGGQQKFQF-QFFEQQ-NH_2, **279**), which further increases the cell proliferation.[656] Schweitzer-Stenner et al. investigated the self-assembly of a hexadecapeptide (Ac-AAKAAAKAAAKAAAKA-NH_2, **280**) and found that the presence of a salt can stabilize the self-assembly of **280** to result in a hydrogel at a CGC of 0.5 wt %. It was found that **280** starts self-assembling at about 0.001 wt % and forms a network of filaments at 1 wt %, and the filaments turn into a nanoweb after the addition of 1.0 M NaCl. The authors also showed that the hydrogel can encapsulate and slowly release proteins.[657]

Yokoi, Arosio, and Zhang et al. further evaluated the Ac-RADARADARADARADA-NH_2 peptide (**281**)[181] by reassembling the peptides after disassembling the hydrogel of **281** by sonication or by changing the ionic strength.[658] After examining the kinetics of the reassembly, the authors proposed a sliding diffusion model for the reassembly of **281**.[181] Zhao et al. further investigated the temperature and pH effects on the self-assembly of **281** and found that the extent of β-sheet conformation decreases at low or high pH and an increase of the temperature to 70 °C results in smaller globular aggregates.[659] Later, Yokoi et al. mutated **281** to change the number and position of the net charges on the peptide. For example, they found that, at a concentration of 0.5 wt % and pH of 1.0, while Ac-RASARADARADARADA-NH_2 (**282**) fails to form a hydrogel, Ac-RASARASARASARADA-NH_2 (**283**) does form a hydrogel. Their results confirm that the number of charges and the sequence are critical for the formation of the

DOI: 10.1021/acs.chemrev.5b00299
Chem. Rev. 2015, 115, 13165−13307

Scheme 35. Representative Molecular Structures of Hydrogelators Containing Alkyl/Lipid Chains

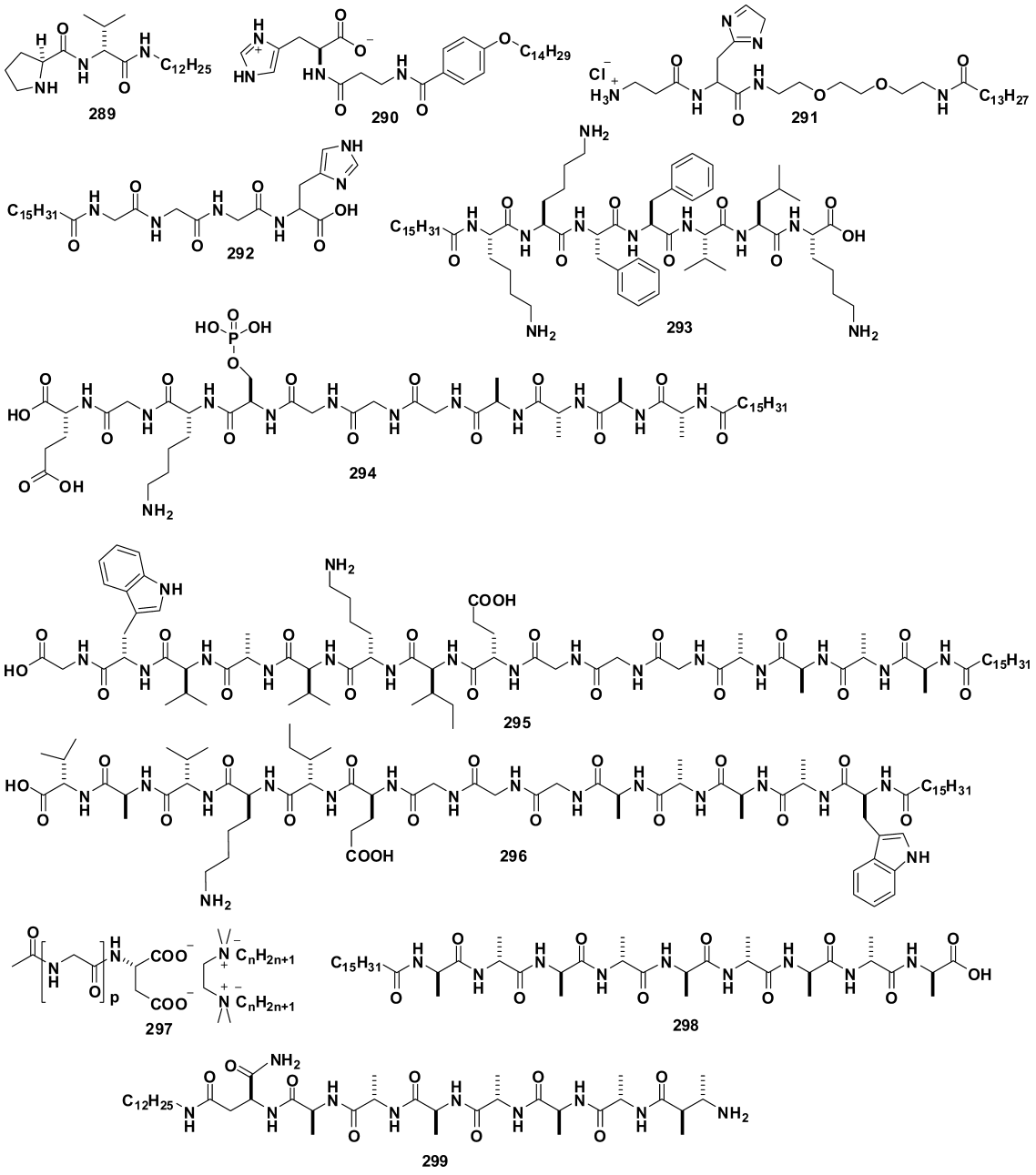

antiparallel β-sheets for self-assembly.[660] On the basis of their design of MDPs, Hartgerink et al. varied the sequence of the MDP motif to generate a series of hexadecapeptides (Ac-KKQLQLQLQLQLQLKK-NH_2 (**284a**), Ac-EQLQLQLQLQ-LQLE-NH_2 (**284b**), Ac-KKSLSLSLSLSLSLKK-NH_2 (**284c**), and Ac-ECLSLCLSLCLSLE-NH_2 (**284d**)) for enhancing the viscoelasticity of the hydrogels formed by these peptides at 1 wt %. The authors found that **284a**−**284d** all self-assemble to form nanofibers with diameters of 6 nm and lengths on the order of hundreds of nanometers. The addition of Mg^{2+} to the solutions of **284b** and **284d** and PO_4^{3-} to the solution of **284c** increases the length of the nanofibers to result in entangled networks and hydrogelation. The authors also demonstrated that the addition of Mg^{2+} to the hydrogels of **284b** and **284d** and PO_4^{3-} to the hydrogels of **284a** and **284c** or the oxidation of the hydrogel of **284d** significantly increase the storage moduli of the hydrogels, by up to about 60-fold.[661] In another study, Hartgerink et al. introduced aromatic residues into the MDP peptides to obtain Ac-KKQFQLQFQLQFQLKK-NH_2 (**284e**), Ac-KKQFQ-FQFQFQFQFKK-NH_2 (**284f**), Ac-KKQWQWQWQW-QWQWKK-NH_2 (**284g**), and KKQYQYQYQYQYQYKK-NH_2 (**284h**).[662] The authors reported that the peptides **284e**−**284h** self-assemble to form nanofibers with intertape spaces larger than that of **284a**. At 1 wt %, **284e**−**284h** all form hydrogels at pH 7.4, and **284e** and **284f** exhibit higher storage moduli than those of **284g** and **284h**.[662] In addition, Hartgerink et al. designed a peptide amphiphile containing a tridecapeptide (Ac-GTAGLIGQERGDS, **285**). While the sequence RGDS promotes cell adhesion, Ac-GTAGLIGQ serves as a substrate of MMP-2. The authors demonstrated the enzymatic degradation (by type IV collagenase) of the hydrogels made of the peptide amphiphile, and suggested that the degradation

DOI: 10.1021/acs.chemrev.5b00299
Chem. Rev. 2015, 115, 13165−13307

Scheme 36. Representative Molecular Structures of Hydrogelators Containing Aromatic Groups

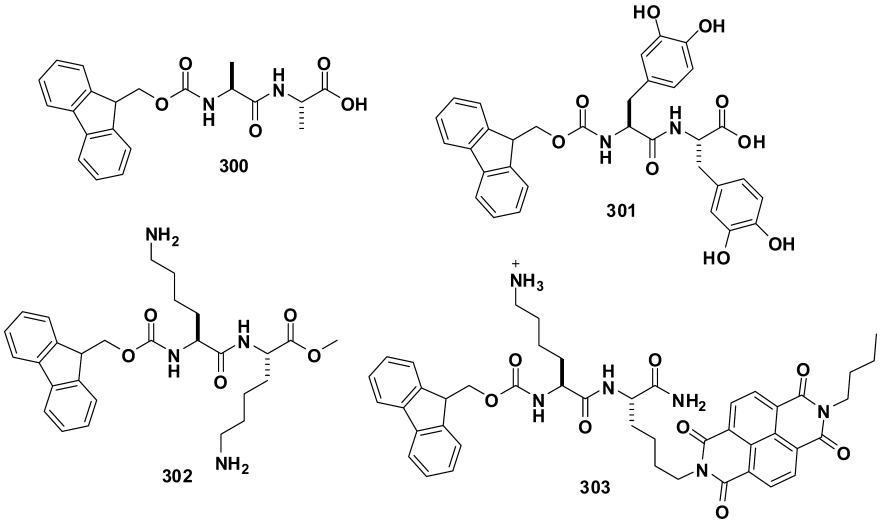

of the nanofiber networks mimics a key property of the natural extracellular matrix (ECM).[663]

Dexter et al. developed a 21-residue peptide (Ac-LKELA-KVLHELAKLVSEALHA-NH_2, (**286**)) that forms a hydrogel at 0.1 wt % upon a change of the pH. On the basis of TEM, DLS, and electronic circular dichroism (ECD) studies, the authors reported that **286**, due to hydrophobic interactions, self-assembles to form hexameric coiled coils, which promote vertical alignment for rearrangement to fibril networks for hydrogelation.[93] Tseng and Yu et al. designed a pair of self-repulsive peptides (Ac-WKVKVKVKVK-NH_2 (**287a**) and Ac-EWEVEVEVEV-NH_2 (**287b**)) consisting of alternating charged/neutral amino acid sequences. The authors reported that the simple mixing of the two peptides, at a total concentration of 0.25 wt %, affords a hydrogel. It was found that the coassembled hydrogel exhibits rapid recoveries from repeated shear-induced breakdowns. The authors also found that the hydrophobicity of the neutral amino acids dictates the viscoelastic properties of the hydrogels.[664] By designing two similar peptides, formyl-WOAOAOAOAO-NH_2 (**287c**) and formyl-WEAEAEAEAE-NH_2 (**287d**), Yu et al. found that the temperature significantly affects the structure and mechanical properties of hydrogels formed by mixing **287c** and **287d** at a total concentration of 1 wt %. The authors found that the peptide nanofibers assemble faster to result in mechanically stronger hydrogels at 25 °C than at 5 °C,[665] suggesting entropy-driven self-assembly. Later, Yu et al. compared **287c** and **287d** with other similar peptides that have the same alternative amino acid sequences but different lengths of the peptides (i.e., formyl-WOAOAO-NH_2 (**287e**), formyl-WEAEAE-NH_2 (**287f**), formyl-WOAOAOAOAOAOAO-NH_2 (**287g**), and formyl-WEAEAEAEAEAEAE-NH_2 (**287h**)). They found that, upon mixing, **287c** + **287d** and **287g** + **287h** form hydrogels at 1 wt %, but the mixture of **287d** + **287e** does not. In addition, the hydrogel formed by **287g** + **287h** is mechanically weaker than that of **287c** + **287d**, likely due to the tighter packing of the amino acid side chains in the nanofibers formed by **287c** + **287d**.[666] Kinoshita et al. designed a C-terminal-capped hexadecapeptide, SASLSASLSASLSASL-NH_2 (**288**). They found that **288** adopts a β-sheet structure and forms a hydrogel at 1 wt %. One interesting feature of **288** is that it also forms organgels in polar organic solvents (e.g, DMF, DMSO, *N*-methyl-2-pyrrolidone (NMP), and 2,2,2-rifluoroethanol (TFE)).[667]

4.3.3.2. Peptide Derivatives Containing Alkyl/Lipid Chain(s). Alkyl-chain-containing peptide derivatives,[668−672] sometimes termed "surfactant-like peptides",[673] essentially consisting of hydrophilic and hydrophobic domains,[674−679] are some of the most representative peptide amphiphiles.[680] The alkyl or lipid chains, usually attaching to the N-terminal or the C-terminal of peptides, not only drive self-assembly through van der Waals force, but also allow the functional peptides to be presented on the surface of nanofibrils at an exceedingly high density.[681] Moreover, the modular nature of peptide chemistry facilitates the variation of the amino acids or chain length, thus easily tuning both the mechanical properties and biological activities of the subsequent self-assembled nanofibrils or hydrogels.[682] As shown in Scheme 35, Miravet and Escuder et al. reported an L-proline-based supramolecular hydrogelator (**289**) which affords a supramolecular hydrogel at a concentration of 0.25 wt %. This L-proline-based supramolecular hydrogel has a remarkable efficiency as a heterogeneous organocatalyst for a direct aldol reaction.[683,684] Another dipeptide derivative (**290**), consisting of two amino acids (i.e., L-histidine and β-alanine) and a lipid chain, is able to form a hydrogel in a variety of conditions (e.g., at both alkaline and acidic conditions and in the presence of additives, such as NaCl or alcohol) with a CGC value of 3.4−6.8 wt %.[685] **291** (β-Ala-His-$(EO)_2$-alkyl chain), with one more ethylene glycol group compared with **290**, can also self-assemble to form a hydrogel at a concentration of 2.0 wt %.[686] Goto et al. reported a tetrapeptide amphiphile (**292**) which has a simple molecular structure but results in a hydrogel at a remarkably low concentration (0.03 wt %).[687] Hamley et al. designed and developed an enzymatically cleavable peptide amphiphile (C_{16}-KKFFVLK, **293**)). The peptide part of this small molecule is cleaved by α-chymotrypsin at two sites, leading to several products: C_{16}-KKF, FVLK, C_{16}-KKFF, and VLK. **293** molecules form nanotubes and helical ribbons at room temperature, and both C_{16}-KKF and C_{16}-KKFF self-assemble to form spherical micelles. FVLK and VLK are unable to adopt well-defined aggregated structures. In this way, the enzyme can modulate the self-assembly of the systems and tune the resulting nanostructure.[688] It would be more interesting to determine the

DOI: 10.1021/acs.chemrev.5b00299
Chem. Rev. 2015, 115, 13165−13307

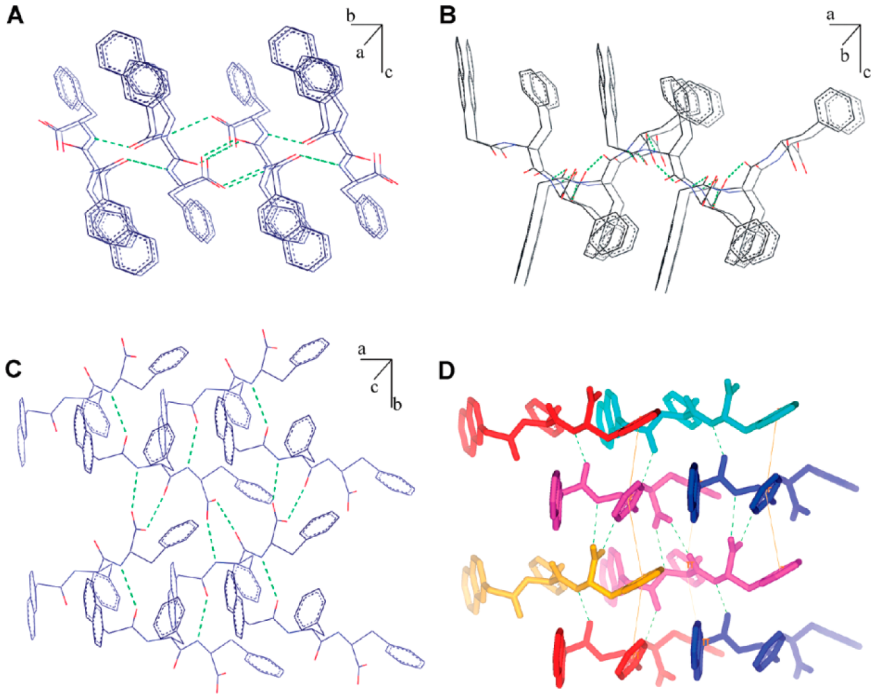

Figure 6. Molecular packing and hydrogen bonds in the crystal of **3** (recrystallized from ethanol): views from the (A) *a*, (B) *b*, and (C) *c* axes and (D) view from the *c* axis to show the hydrogen bonding (green dotted lines) of one molecule with four other molecules and some aromatic−aromatic interactions (yellow lines). Adapted from ref 14. Copyright 2011 American Chemical Society.

biological activities of **293** in a cellular environment. Stupp et al. reported a peptide amphiphile (**294**) with more than 10 amino acids. The addition of soluble metal ions or an adjustment of the pH triggers the hydrogelation of this molecule at a concentration of 20 mM (2.4 wt %), indicating the self-assembly is mediated by a screening counterion and stabilized by van der Waals and hydrophobic forces, ionic bridging, and hydrogen bonding.[689] To elucidate the self-assembly behavior of the peptide amphiphiles, which tend to form cylindrical nanostructures that imply worm micelles, the same group used a pair of compounds (**295** and **296**), containing chromophores (i.e., tryptophan), to study the aqueous solvation within the self-assembled structures. Self-assembly constrains the chromophores to a defined location within the aggregate, which leads to different fluorescence changes of the chormophores after the addition of aqueous acrylamide (a quencher of fluorescence). The authors found that, at lower pH, **295** and **296** have a tendency to form a cylindrical structure with the alkyl chain inside the nanostructure as a hydrophobic core.[690] **297** represents a class of peptide derivatives, called gemini peptides, formed by the complexation of cationic gemini surfactants and anionic oligoglycine-aspartate. By studying the aggregation behaviors of these molecules (the hydrophobic chain length (C_{10} to C_{22}) and the length of the oligoglycine (0−4)), Oda et al. found that the hydrogels of **297** only form below a certain temperature (e.g., the Krafft temperature[691,692]) when either the hydrophobic chains or the peptides are long enough.[693] Besides one-component hydrogels, Stupp et al. developed hydrogels formed by coassembly of amphiphiles with opposite peptide polarities (i.e., peptide amphiphiles with free N-terminals or C-terminals), for example, **298** and **299**. The mixture of these molecules with complementary polarities results in coassembled structures which show unusual thermal stability compared to the assemblies composed by only one of the constituents.[694]

4.3.3.3. Peptide Derivatives Containing Aromatic Group(s). Peptides functionalized at the N-terminal with large aromatic groups have recently emerged as an exciting class of small molecular hydrogelators.[695−698] The most used aromatic group is Fmoc.[699−701] As shown in Scheme 36, shortly after the report of an unexpected small peptidic hydrogelator made of Fmoc-L-Ala-L-Ala (**300**) and Fmoc-D-Ala-D-Ala (**22**),[11] Ulijn et al. reported the development of Fmoc-diphenylalanine (Fmoc-FF or Fmoc-Phe-Phe (**6**)), one of the most investigated low molecular weight hydrogelators.[703−705] The molecules of **6** form hydrogels by adjusting the pH of the aqueous solution of **6**,[97,703] by applying **6** to a silica wafer surface,[706] or by the addition of water to a DMSO solution of **6**.[707,708] Despite considerable studies on **6**,[566,709−715] it was unclear why the mechanical properties reported for the hydrogels of **6** vary significantly, up to 4 orders of magnitude. To address this inconsistency, Adams et al. have systematically studied the mechanical properties of hydrogels of **6** prepared using different protocols. They demonstrated that, independently of the method of gel formation, the final pH of the hydrogels is the principal determinant of the mechanical properties, which is quite reasonable due to the C-terminal carboxylic group in **6**. Besides, additional variability arises from experimental factors such as the fraction of DMSO or the nature of the buffers used in the selected systems.[716] In addition to Fmoc-FF (**6**), a variety of Fmoc-dipeptide derivatives have been reported in the past several decades.[717−731] Adams and Firth et al. investigated the influence of the molecular structure on the gelation behaviors of a range of Fmoc-dipeptides. In general, they found that the overall hydrophobicity of the Fmoc-dipeptide determines the ability to form a stable hydrogel.[718] Interestingly, Gazit et al. designed a 3,4-dihydroxy-L-phenylalanine (DOPA)-containing Fmoc-dipeptide (**301**) by using DOPA to

DOI: 10.1021/acs.chemrev.5b00299
Chem. Rev. 2015, 115, 13165−13307

Scheme 37. Representative Molecular Structures of Hydrogelators Containing Naphthalenyl Groups

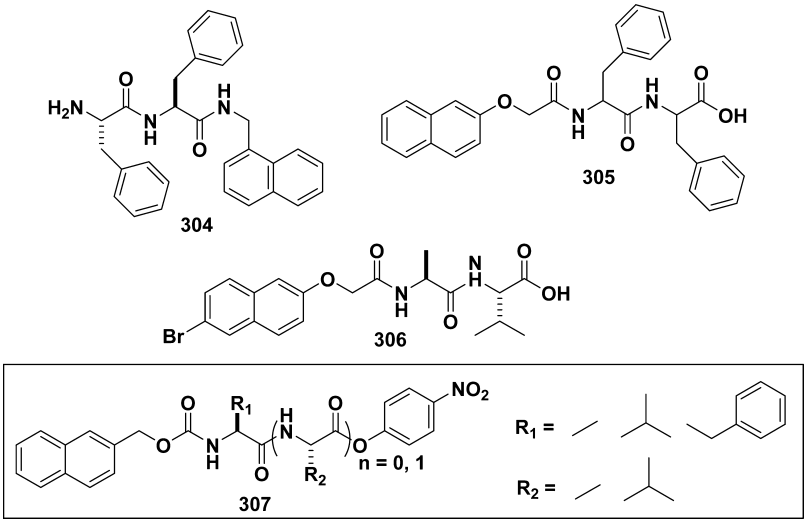

Scheme 38. Representative Molecular Structures of Hydrogelators Containing Pyrene Groups

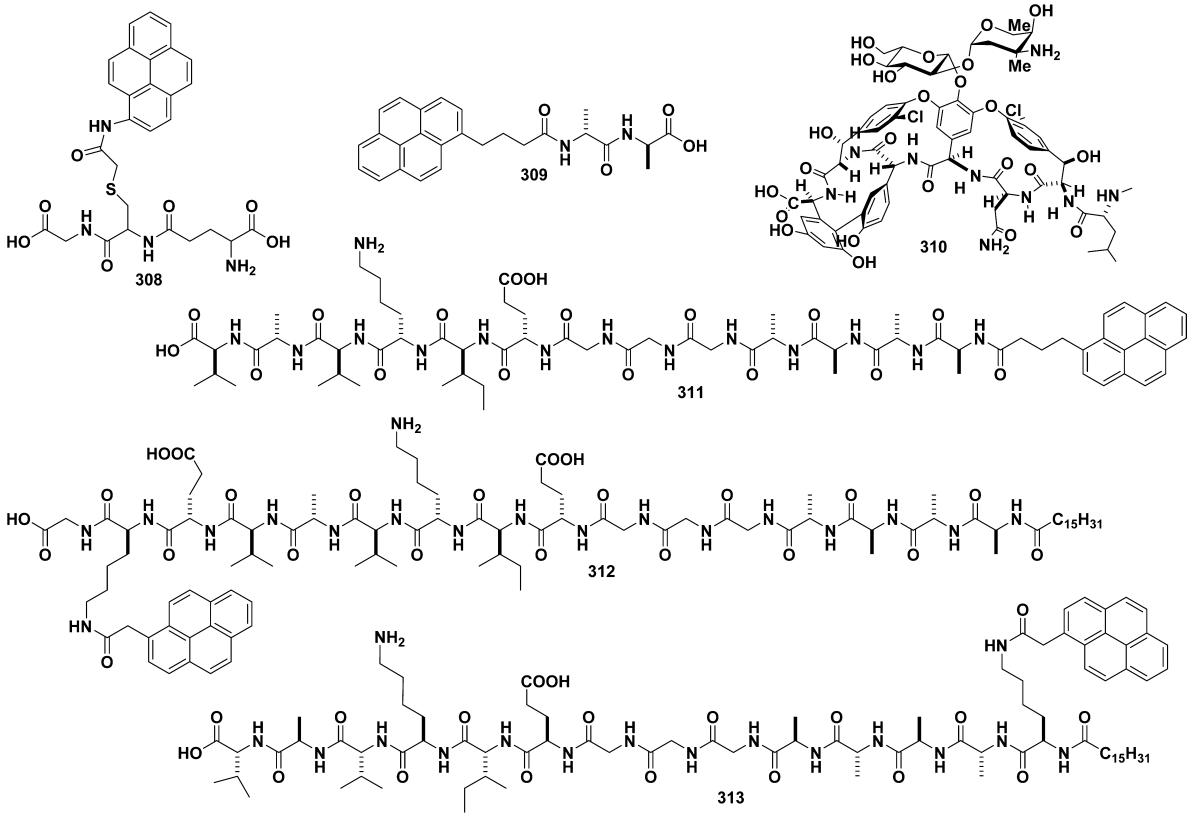

substitute for the phenylalanines in **6**. The resulting hydrogelator self-assembles at a concentration of 0.5 wt % and forms supramolecular nanostructures, which can be used as multifunctional platforms for various technological applications, such as glass glue.[732] In addition to Fmoc-dipeptide, Fmoc-peptide derivatives with more than two amino acids are also excellent candidates for self-assembly to form hydrogels.[733,734] These small molecules are obtained by both chemical approaches[674,735−737] and enzymatic reactions.[161,162,738−741] Parquette et al. further functionalized Fmoc-dipeptide Fmoc-KK (**302**) at the ϵ-amino position with a naphthalenediimide (NDI) chromophore to afford Fmoc-KK(NDI) (**303**). The resulting molecule forms a self-supporting hydrogel at a concentration as low as 1.5 wt % which exhibits high thermal stability up to 75 °C.[742]

Like Fmoc, naphthalene[743,744] is another aromatic group frequently used in peptide derivatives to achieve strong intermolecular interaction for self-assembly.[745] Among them, 2-(naphthalen-2-yl)acetic acid is a convenient motif for constructing naphthalene-based peptide derivatives because of its ease of being directly used in SPPS.[169,238,655,746−759] For example, compound **3**, reported by Xu et al., is a dipeptide derivative made by conjugating 2-(naphthalen-2-yl)acetic acid with Phe-Phe. In the molecule of **3**, the naphthalenyl group

DOI: 10.1021/acs.chemrev.5b00299
Chem. Rev. 2015, 115, 13165−13307

Scheme 39. Representative Molecular Structures of Hydrogelators Containing Aromatic Groups

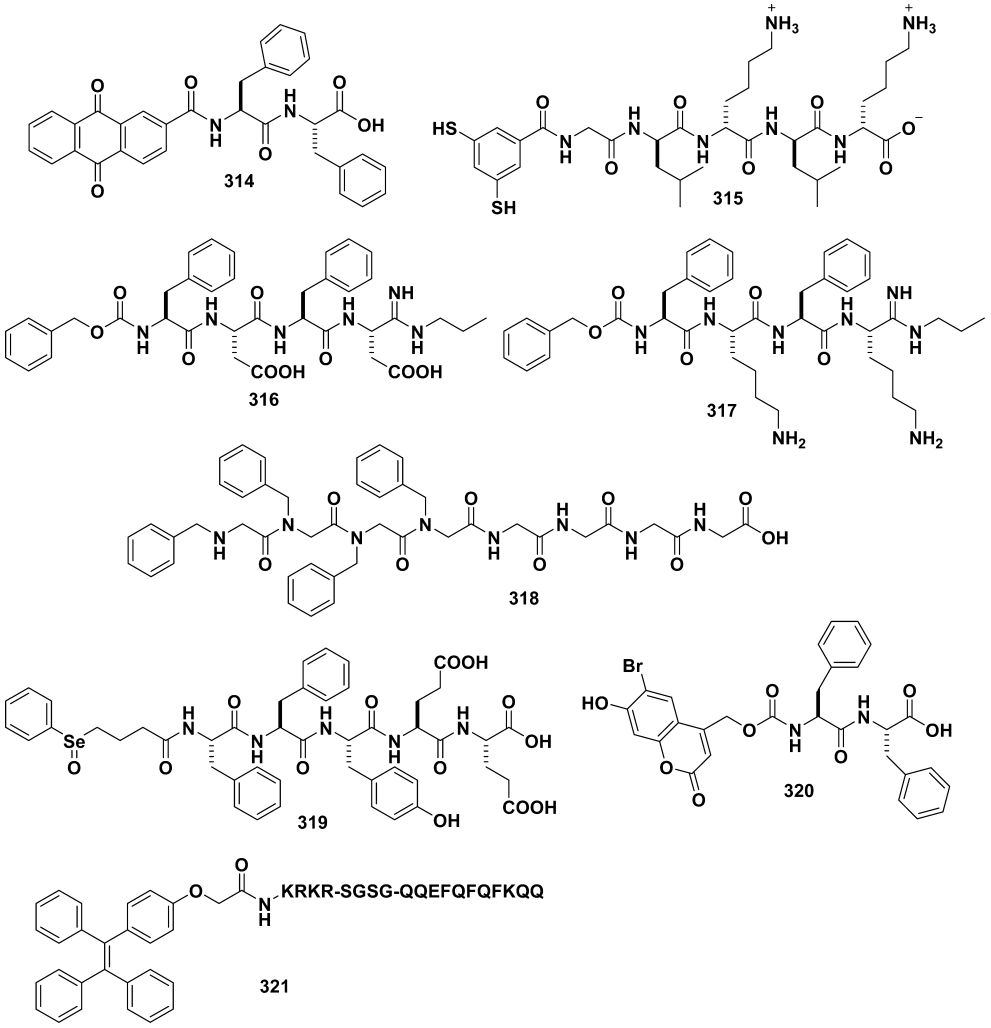

provides the hydrophobic force to enhance self-assembly in an aqueous environment, while the dipeptide backbone acts as both hydrogen bond acceptors and hydrogen bond donors. Xu et al. demonstrated **3** as an effective hydrogelator that forms a hydrogel at a concentration of 0.8 wt %, with the gel−sol transition temperature at about 323 K.[760] The crystal structure of **3** (Figure 6),[14] though obtained from single crystals grown from a mixed solvent of ethanol and water, reveals that the aromatic−aromatic and hydrogen-bonding interactions apparently reinforce each other. Moreover, **3** has found applications in enabling other molecules to be hydrogelators.[761,762] Xu et al. also designed and synthesized a similar small molecule (**304**) with an exposed N-terminal and a naphthalene-blocked C-terminal. This N-terminated hydrogelator affords a stable hydrogel even below a concentration of 0.8 wt %, but unlike its C-terminal analogues **3**, **304** forms hydrogels only within a narrow pH range (5−6) (Scheme 37).[763] Adams et al. used 2-naphthol to construct naphthalene-based dipeptide derivatives[764,765] with an ether bond,[88,99,100,205,766−770] such as **305**[101] and **306**.[767] They reported that the hydrogelation of **305** and **306** could be controlled by reducing the pH value with the hydrolysis of GdL at a concentration of 2.2 mM. They chose GdL for pH control because its hydrolysis to gluconic acid allows a slow, uniform pH change. Das et al. also developed a series of hydrogelators (e.g., **307**) with 2-naphthol as a terminal, but with an ester bond.[119,771]

As mentioned before, the pyrene motif not only enhances intermolecular interaction to promote self-assembly, but also exhibits fluorescence that acts as a useful tool for studying the aggregation behaviors of the hydrogelators.[772,773] Atkins et al. replaced the disulfide bond in the oxidized disulfide form of glutathione (γ-glutamylcysteinylglycine (GSH)) (GSSG) to increase the self-assembly ability of GSSG in aqueous solution, which otherwise only self-assembles to generate fibrillar aggregates and gels in organic solvents. The resulting GSH−pyrene (**308**; Scheme 38) then forms a gel in a mixed solvent (95% H_2O and 5% DMSO) at a concentration of 1 mM (0.056 wt %).[774] Xu et al. developed a pyrene-terminated dipeptide (**309**) which affords a weak hydrogel at a concentration of 30 mM (1.3 wt %). However, the addition of vancomycin (**310**) at a 1:1 ratio remolds the self-assembly of hydrogelators and drastically increases the elasticity of the hydrogel by 10^6-fold due to the ligand−receptor interaction between vancomycin and **309**. A spectroscopic analysis confirms the aromatic−aromatic interactions between the pyrene groups in the hydrogel.[237] EM also reveals the formation of highly cross-linked networks in the hydrogels, likely contributing to the significant increase of the storage modulus. Stupp et al. developed several molecules (**311**, **312**, and **313**) with pyrene

DOI: 10.1021/acs.chemrev.5b00299
Chem. Rev. 2015, 115, 13165−13307

Scheme 40. Representative Molecular Structures of Hydrogelators Containing a Photoresponsive Group

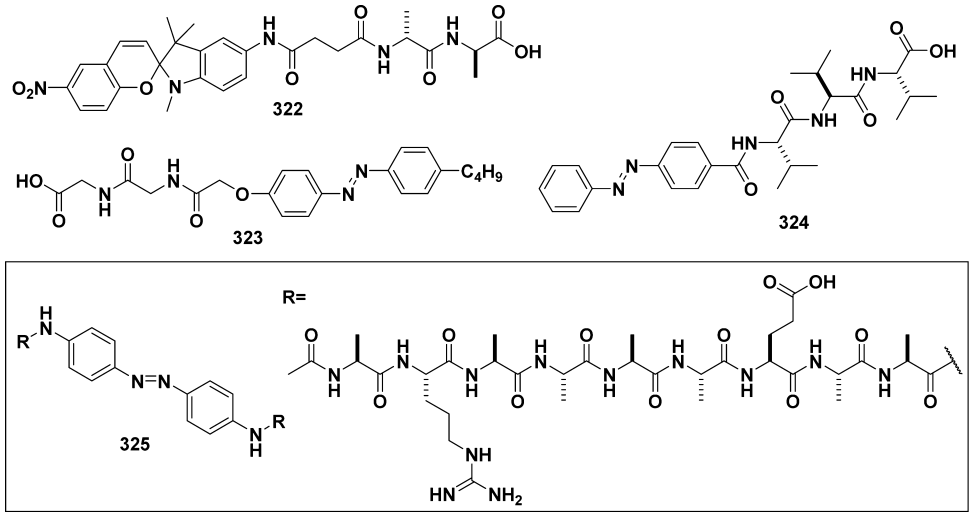

chromophores in the backbone to investigate the aqueous solvation within the self-assembled structure formed by these peptide amphiphiles. They found that, as the chromophore is placed closer to the exterior of the aggregates, the Stern–Volmer quenching constants and the fractional accessibility of covalently bound pyrene progressively increase. Their study also demonstrated that covalently bound fluorophores within an aggregate can interact with the external environment.[690]

In addition to the exploration of Fmoc, naphthalene, and pyrene, Ladouceur et al. have synthesized novel self-assembling hydrogelators that contain an electroactive aromatic group, anthraquinone. As shown in Scheme 39, they used the well-known redox couple of anthraquinone/anthrahydroquinone as the hydrophobic component for a series of hydrogelators, such as **314**. The molecules of **314** undergo two separate processes: a reversible redox reaction and a reversible self-assembly at ta concentration of 4 wt %.[772] Dynamic combinatorial chemistry was originally a method for developing synthetic receptors and ligands for biomolecules by linking building blocks together using a reversible reaction, resulting in a thermodynamically controlled product distribution. The studies of Otto et al. proved that dynamic covalent disulfide linkages are not only instrumental in dynamic combinatorial discovery of self-assembling materials, but also further stabilize the consequent self-assembly. They designed a building block (**315**) equipped with a short peptide sequence capped by a dithiol terminal and reasoned that self-assembly would become feasible for a macrocycle ($\mathbf{315}_6$) that reached a critical size. They discovered that photoirradiation of the solution containing $\mathbf{315}_6$ (0.6 mM) results in the formation of a hydrogel.[775] Miravet and Escuder et al. prepared a pH-sensitive complex molecular hydrogel from oppositely charged tetrapeptide components (e.g., **316** and **317**). They have shown that small peptides bearing alternating phenylalanine and aspartic acid residues such as **316** are able to form hydrogels at low concentration, and **317**, designed as a charge complementary analogue bearing alternating phenylalanine and lysine, is also able to aggregate at low concentration. Then they obtained a pH-sensitive coassembled network from these two oppositely charged small self-assembling peptides. By changing the pH of this system, they were able to switch between two-component networks at neutral pH and one-component networks at either basic or acidic pH.[776] Wang et al. described the design and synthesis of molecular hydrogelators composed of peptides and peptoids (i.e., one type of unnatural peptide with the side chain attached to the amide nitrogen as well), such as **318**. They tested the hydrogelation ability of **318** by the inverted-tube method and found that **318** and its analogues afford hydrogels with CGC values of 0.5–0.8 wt %.[777] Yang et al. developed a reversible hydrogelation system using a redox system with selenium-containing peptides (**319** and its reduced version). They achieved the reversible transformation between the solution and hydrogel of the peptide derivative **319** at a concentration of 1 wt %, which is accompanied by the reversible transformation between selenide and selenoxide, by triggering with vitamin C and H_2O_2 (0.1 wt %).[778] Hamachi et al. reported a series of dipeptide derivatives, for example, Bhcmoc-FF (**320**), in which FF is tethered with [(6-bromo-7-hydroxycoumarin-4-yl)-methoxy]carbonyl (Bhcmoc). They found that compound **320** forms a hydrogel above 0.35 wt % and the resulting hydrogel collapses upon application of stimuli such as UV irradiation.[779] Liang et al. developed a salt-responsive peptide (**321**) as a luminescent hydrogelator with a CGC of 0.3 wt %. They found that only the presence of salt rather than the temperature, pH, or solvent caused the dispersed hydrogelators to self-assemble to form a hydrogel network to turn on bright emission.[780]

4.3.3.4. Peptide Derivatives Containing a Photoresponsive Group. In addition to enzyme-responsive hydrogelation,[781−783] supramolecular hydrogelators containing a photoresponsive group are of great interest since light can act as an external stimulus to modulate the properties of the hydrogels.[784] For example, upon photoirradiation, a solution can transform into a hydrogel, and vice versa. A variety of photoresponsive groups have served as the photochemical module in peptides for the design of photoresponsive hydrogelators. UV and visible light can regulate the geometry of spiropyran (between the nonplanar spiropyran form and the planar merocyanine) to control the hydrogelation process because the planar merocyanine isomer favors the formation of aggregates (due to stronger intermolecular $\pi-\pi$ stacking) while the nonplanar spiropyran form disfavors $\pi-\pi$ interaction. As shown in Scheme 40, Zhang et al. reported that the spiropyran-conjugated dipeptide **322** forms a hydrogel upon photoisomerization to a merocyanine form. Besides responding light, this hydrogel undergoes a gel–sol transition upon the addition

DOI: 10.1021/acs.chemrev.5b00299
Chem. Rev. 2015, 115, 13165–13307

Scheme 41. Representative Molecular Structures of Hydrogelators Based on Bolaamphiphiles

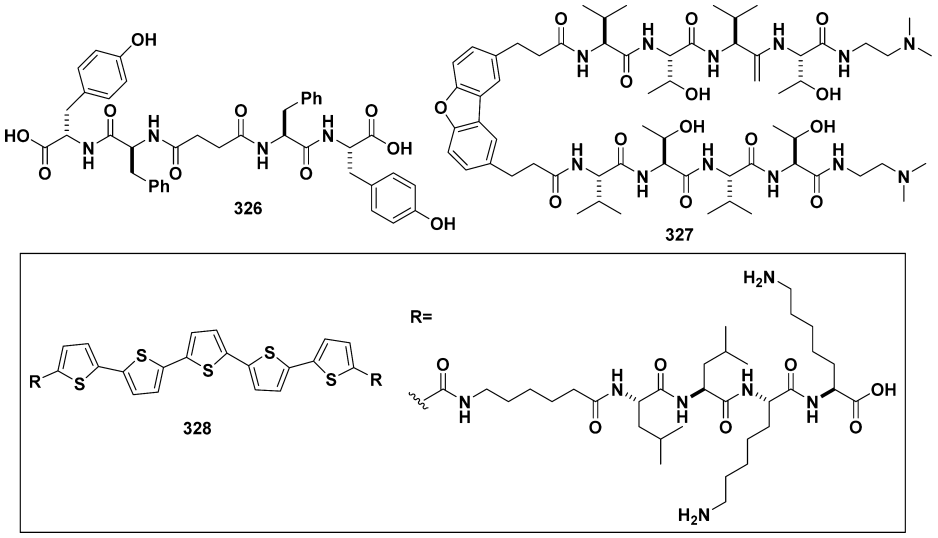

of vancomycin because of the strong interaction of vancomycin with the peptide unit D-Ala-D-Ala.[785] Azobenzene-group-containing peptides are another typical class of photoresponsive hydrogelators.[786−789] The reversible photoregulated trans to cis isomerization of azobenzene significantly influences the intermolecular interaction among the hydrogelators, thus changing the morphologies of the aggregates or controlling the gel−sol transition. Huang et al. reported a dipeptide amphiphile incorporated with an azobenzene moiety (**323**) which self-assembles to form well-defined nanoribbons that result in a macroscopic hydrogel. After UV irradiation, the authors found a dramatic decrease of the viscosity of the sample, accompanied by a transition from laminated ribbons to short fibers, as revealed by EM.[790] Tamaoki et al. studied the mechanism by which azobenzene isomerization induces the breaking and reorganization of the assemblies of *N*-(L-valyl-L-valyl-L-valyl)azobenzene-4-carboxamide (azo(L-Val)$_3$, **324**). As a hydrogelator, **324** forms photoresponsive nanofibrils, and undergoes dispersion/reorganization upon trans to cis photoisomerization that breaks and re-forms the hydrogen bonds to induce reversible gel−sol transitions.[791] Zhang et al. reported an azobenzene-linked symmetrical gemini α-helical peptide (**325**) that undergoes light-switched self-assembly. With the reversible molecular structure transition between trans and cis (U-shape), the morphology of the self-assembled gemini α-helical peptide can reversibly change between nanofibers and nanospheres in acidic conditions, and between nanospheres and vesicles in basic conditions.[792]

4.3.3.5. Peptide Bolaamphiphiles. Many different types of amphiphilic molecules are able to form organogels or hydrogels, but they usually gel either water or an organic solvent. In other words, few of them have the ability to form gels in both water and an organic solvent, except certain peptide-based bolaamphiphiles.[793] Because of the versatile functional groups on peptides, such as carboxyl, amine, thiol, hydroxyl, and other hydrophobic groups, peptide-based bolaamphiphiles exhibit diverse self-assembly behaviors in responding to different environments.[794] As shown in Scheme 41, Das et al. developed a library of bolaamphiphiles by varying the amino acids (e.g., Phe, Tyr, Leu, or Gly) as the head groups, and reported that sequential pH changes trigger the hydrogelation of these peptide bolaamphiphiles (e.g., **326** with a gelation concentration of 0.003 wt %). One interesting observation reported by them is that the addition of dimethyl sulfate, a reagent used for the methylation of phenols and esterification of acids via an S_N2 reaction, can dramatically change the morphologies of the hydrogels.[795] Zinic et al. systematically studied the gelation properties, self-assembly motifs, chirality effects, and morphological characteristics of the gels formed by retro-dipeptidic bolaamphiphiles similar to **326**, and the dimethyl ester and dicarboxamide derivatives of these bolaamphiphiles.[796] **327**, comprising a dibenzofuran template and two peptide strands made up of alternating hydrophilic and hydrophobic residues and a blocked carboxyl terminal, represents another class of bolaamphiphiles that have a collapsed U-shaped structure. In the bolaamphiphiles **327**, the dibenzofuran template positions the strands about 10 Å apart. These molecules afford wide nanofibers, having a cross-β-sheet structure, in water via intermolecular hydrogen-bonding and hydrophobic interactions.[797] Self-assembly of π-conjugated small molecules has attracted a lot of attention for potential use in organic electronic devices, such as photovoltaic cells. Recently, several laboratories have introduced π-conjugated nanostructures into peptide-based bolaamphiphiles to replace the lipid chain in the linker segment.[798,799] For example, Stupp et al. designed a peptide-based bolaamphiphile (**328**) that has three segments (e.g., polar amino acids for solubility, β-sheet-forming amino acids for self-assembly, and an oligothiophene core for conductivity). The self-assembly of this molecule results in a self-supporting hydrogel at low concentrations (1 wt %). The authors envisioned that, in combination with biological epitopes, the 1D nanostructure formed in the hydrogelation process may be used to simultaneously signal cells with electrical currents and epitope−receptor interactions.[800]

4.3.3.6. Dendrimers or Dendrons Made of Peptides. In the early 1990s, Newkome et al. pioneered the development of dendritic bolaamphiphiles as effective hydrogelators.[801] Since then, there has been considerable interest in exploring the dendritic hydrogelators for self-assembly to form hydrogels due to their highly controllable sizes, topologies, and surface properties. One particular appealing attribute of peptide-based dendrons or dendrimers is their extremely broad structural diversities by varying the α-amino acids used in their construction. As shown in Scheme 42, Woolfson et al.

DOI: 10.1021/acs.chemrev.5b00299
Chem. Rev. 2015, 115, 13165−13307

Scheme 42. Representative Molecular Structures of Hydrogelators Based on Dendrimers or Dendrons

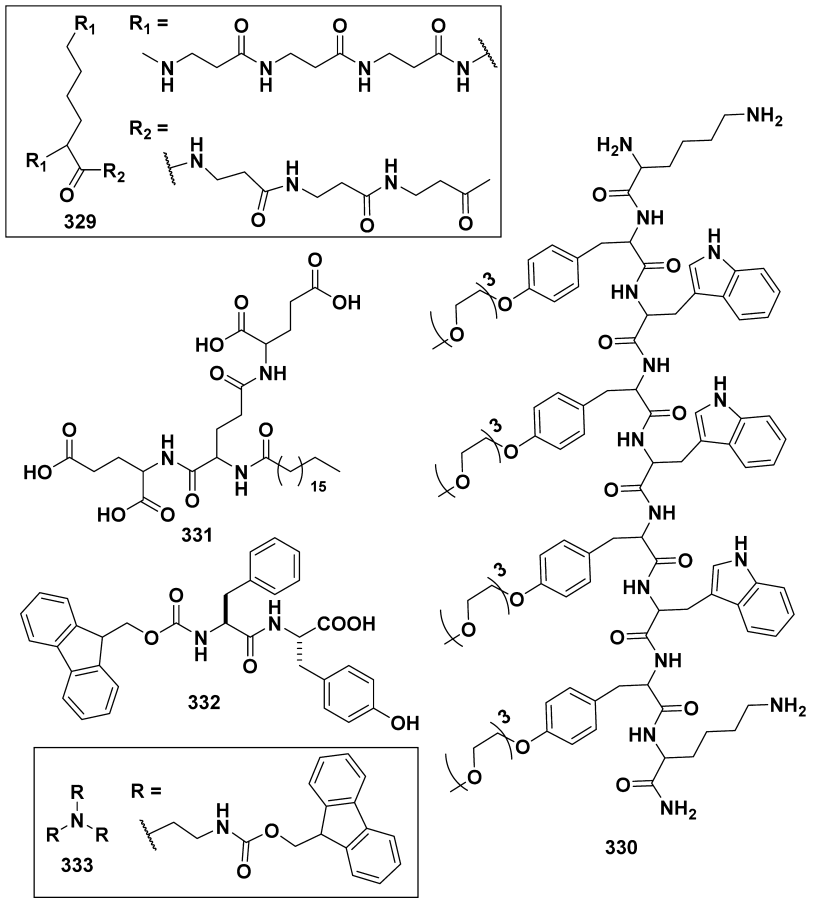

Scheme 43. Representative Molecular Structures of Hydrogelators

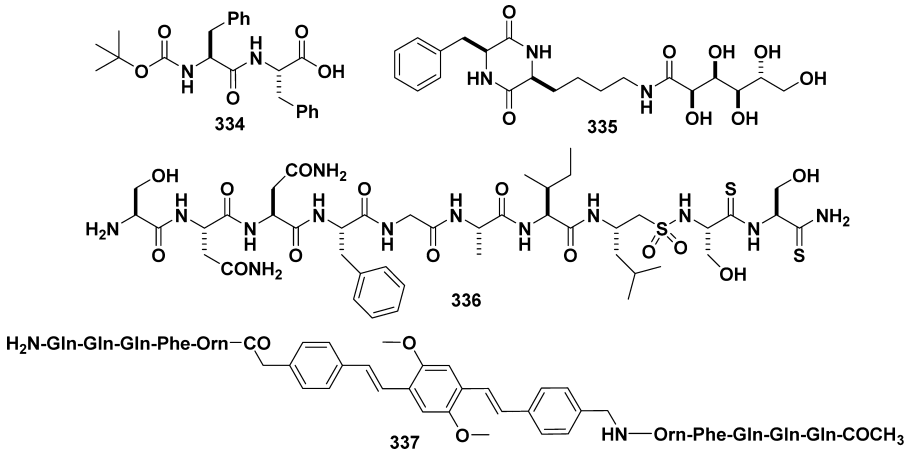

described an approach that utilizes nonlinear or dendritic peptides, such as **329**, to direct the self-assembly of two complementary linear peptides. The two peptides, which combine to form exclusively linear fibers, coassemble with **329** (at 100 μM) to form specific structures, such as hyperbranched networks, polygonal matrixes, and regularly segmented and terminated fibers.[803] Dendritic peptide **330**, with repeating hydrophobic and hydrophilic residues as well as lysine terminals, self-assembles to give a uniform toroid structure. Lee et al., who developed this small molecule, also found that removing the electrostatic repulsions or increasing the hydrophobic interactions of this peptide drives the β-sheet peptides to form 1D nanostrucutres.[804] Liu et al. reported an amphiphilic dendron containing three dendrite L-glutamic acid units and a long alkyl chain (**331**). The dendron can form hydrogels over a wide pH range (from 2 to 13). The lowest CGC is 2.2 mM at pH 2, and when the pH value is increased, the CGC also increases. At pH 13, nearly 10 mM **331** is needed to form a hydrogel.[805] Chau et al. developed a two-component self-assembling system (**332** and **333**) using the interaction of aromatic groups (Fmoc) to construct nanoparticles. The triskelion Fmoc conjugate **333** can quickly self-assemble to form spherical particles around 70 nm in diameter at physiological pH and at a concentration of 100 μM. The

DOI: 10.1021/acs.chemrev.5b00299
Chem. Rev. 2015, 115, 13165−13307

Scheme 44. Hydrogelators Containing Nucleobases

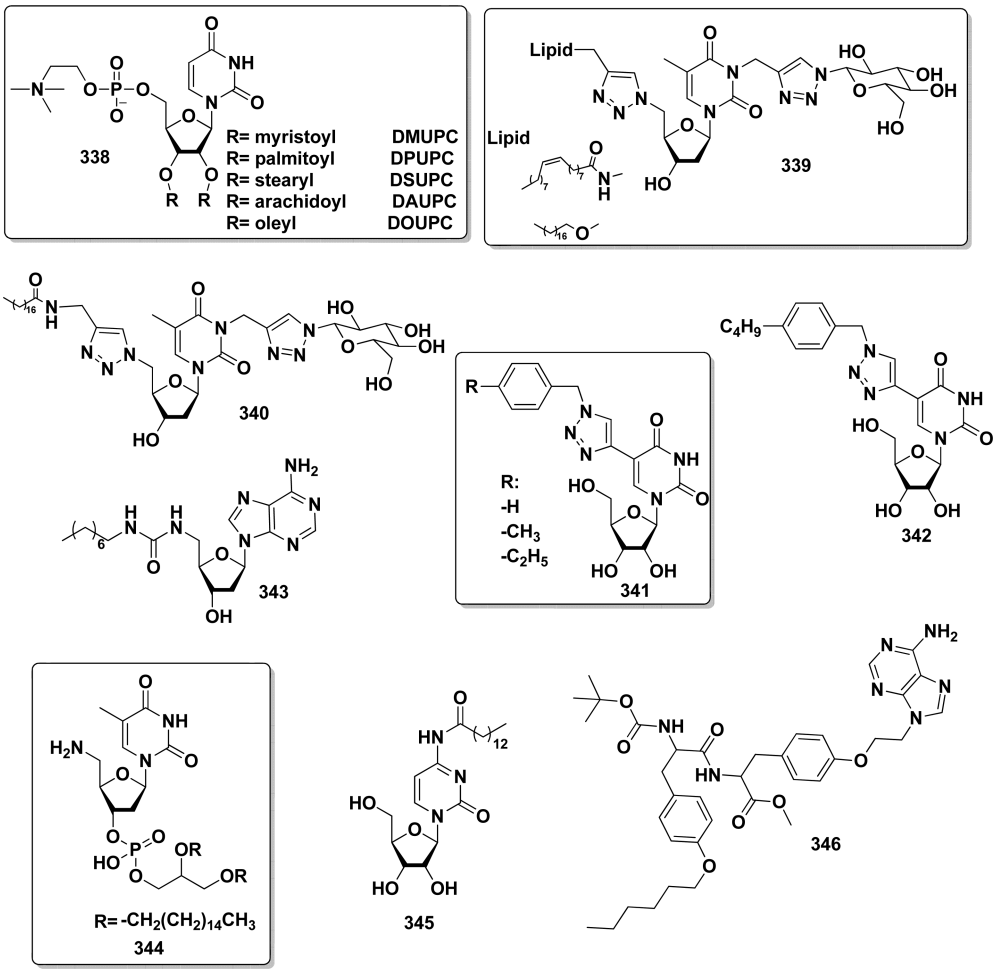

Fmoc-dipeptide **332** can wrap up the resulting nanoparticles and stabilize them.[806]

4.3.3.7. Others. Some self-assembling peptides have a (*tert*-butyloxy)carbonyl (Boc) group on their N-terminal.[807−811] As shown in Scheme 43, Reches et al. describe the formation of complex nanostructures by the coassembly of two simple peptides, Boc-FF (**334**) and FF (**208**). They found that **334** itself self-assembles to form nanospheres and **208** self-assembles to give tubular structures, but being combined together, the two peptides coassemble into a construction of beaded strings at concentrations of each higher than 0.3 wt %.[812] Feng et al. developed cyclic dipeptide **335**, conjugated with a carbohydrate, and found that the solution of **335** transforms into a transparent hydrogel with the assistance of shear force at a concentration of 5.0 wt %.[813] According to the authors, cyclic dipeptides are a group of special peptides with unique properties, and most of them afford hydrogels after shearing.[813−815] Liskamp et al. studied the incorporation of a single β-aminoethane sulfonyl amide moiety in highly amyloidogenic peptide sequences (e.g., **336**) and observed that this incorporation results in a complete loss of amyloid fibril formation. Instead, they found **336** affords supramolecular nanofibers at a concentration of 0.1 wt %.[816] Similarly, Maggini et al. inserted an oligo(*p*-phenylenevinylene) into a peptide to afford **337**. They found that pH changes trigger a reversible self-assembly of **337**, which has a CGC of 13 mM (2.3 wt %).[817] Tian et al. recently reviewed the complexion between metal ions and a series of interesting peptides,[818] which can also lead to hydrogelation.

4.4. Hydrogels Based on Nucleobase Derivatives

Since the discovery of the DNA double helix structure over 60 years ago, the interactions between base pairs have been a subject of interest in the fields of cell biology and supramolecular chemistry. Because of their exceptional abilities for forming intermolecular interactions in water, nucleobases are able to serve as the building blocks of hydrogelators and have received considerable research attention. Because Araki et al.[26] reviewed the development of nucleobase-containing gelators in 2005, in this section we mainly focus on supramolecular hydrogelators made of nucleobases over the past decade (Table S3). Considering that the most attractive feature of nucleobases is the intermolecular interactions between base pairs, we arrange these nucleobase hydrogelators according to the classification of homotypic and multicomponent hydrogels.

4.4.1. Homotypic Hydrogels Based on Nucleobases. As shown in Scheme 44, Barthelemy et al.[195] prepared a family of new uridine phosphocholine hydrogelators (**338**) which self-assemble in water to form DNA-like helical nanofibers and result in hydrogels at a concentration around 6 wt %. One interesting feature of this hydrogel is that the hydrogelators, below the phase transition temperature (T_m), self-assemble to form helical fibers which are transformed to compact bilayers above the T_m. In addition, they also designed and synthesized a series of glycosyl nucleoside lipids (GNLs; **339**, **340**) by using a

DOI: 10.1021/acs.chemrev.5b00299
Chem. Rev. 2015, 115, 13165−13307

convenient "double-click" chemistry. **339** and **340** are able to form nanofibers and result in hydrogels. Particularly, **340** self-assembles to form circular nanofibers (Figure 7) that afford a

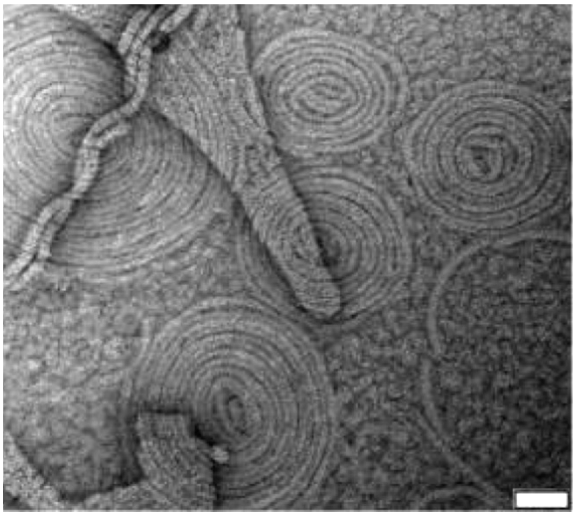

Figure 7. TEM images of gel **340** (scale bar 50 nm). Adapted from ref 819. Copyright 2009 American Chemical Society.

hydrogel with a CGC of 0.1 wt %.[819] It would be interesting to determine the mechanism of the formation of those circular nanostructures. In another study, Barthelemy et al. prepared a hydrogel of the GNLs for trapping nanoparticles or nanomaterial from an aqueous suspension, and suggested the use of hydrogelators as an additive for decontamination.[820]

To compare the effect of hydrophilic/hydrophobic balance on hydrogelation, Kim et al.[821] designed and synthesized four nucleosides (**341**, **342**) by modifying the 5-position of the uracil base with an (alkylbenzyl)triazole unit. Unlike **341**, which forms metastable partial gels in water when the concentrations are higher than 2.5 wt %, **342** affords a stable hydrogel with a CGC of 1.0 wt %, likely due to the hydrophobicity of the butylbenzyl group. Kim et al.[822] reported an intriguing example in which a 2′-deoxyladenosine derivative (**343**) forms aggregates in the process of heating to cooling, but only forms a hydrogel under ultrasonic radiation. The authors suggested a very interesting explanation: that the production of oxidized species of 2′-deoxyladenosine during sonication might contribute to tuning the hydrophilic/hydrophobic balance to result in a hydrogel. Yang et al.[823] developed an aminonucleoside phospholipid (**344**) which self-assembles to form superhelical strands and results in a hydrogel at a concentration of 6 wt %. They found that **344** binds with double-stranded DNA on the basis of $\pi-\pi$ stacking and H-bonding, so they suggested that this work has potential application in gene delivery. Marlow et al.[824] designed and synthesized a new cytidine-derived gelator (**345**) that forms a gel in a mixture of methanol and water (MeOH:H_2O = 1:1) at a concentration of 0.5 wt %. Sleiman et al.[825] prepared a series of nucleobase peptide amphiphiles in which **346** self-assembles to form nanofibers and results in a hydrogel in water (5% DMSO) with a CGC of 0.5 wt %. On the basis of the base pair interaction, the authors suggested this work provides new avenues for nucleobase-specific electrophoresis and oligonucleotide delivery.

4.4.2. Multicomponent Hydrogels Based on Nucleobases. As shown in Scheme 45, Lehn et al.[826] reported an interesting example in which guanosine hydrazide (**347**) affords a stable hydrogel (0.46 wt %) on the basis of the formation of a guanine quartet (G-quartet) in the presence of various metal cations (e.g., Na^+, K^+). The authors used various spectroscopies (electronic and vibrational circular dichroism) to reveal that **347** forms long-range chiral aggregates consisting of G-quartets which result in columns due to the binding of metal cations between G-quartet species.[827] In addition, the supramolecular structure is sensitive to the cations. Further studies by the authors prove that **347** in solution confers a pseudo-four-stranded helix with guanine−guanine hydrogen bonding to form a continuous helical strand rather than the usually planar G-quartet.[828] Moreover, **347** is capable of forming reversible acylhydrazone bonds with various aldehydes so that the nature of the aldehyde can tailor the macroscopic properties of the resulting materials. For example, **347** reacts with pyridoxal monophosphate to afford **348**, which forms a hydrogel (0.8 wt %) in the presence of K^+. This seminal work illustrates a dynamic combinatorial library, based on the proper aldehyde, for the selection of the strongest hydrogel within a pool of certain building blocks. Using DFT calculations, Urbanova et al.[829] predicted and elucidated the molecular arrangement of **347** in the gel state, and reported that the predictions are in good agreement with the experimental data.

Using nucleotides **349** and **350** as counterions to interact with cationic gemini surfactants, Oda and co-workers[830] designed and synthesized nucleobase−gemini hybrids which are able to form hydrogels with a proper hydrophobic chain length (e.g., **349** forms a hydrogel at a CGC of 0.64 wt %). Intriguingly, the addition of complementary nucleosides to the solution of **349** affords a stable hydrogel at an even lower CGC (e.g., the addition of adenosine to **349** reduces the CGC to 0.32 wt %). By simply mixing a nongelator, 2′,3′,5′-tri-*O*-acetylguanosine (**351**), with a guanosine gelator (**352**), Rowan et al.[831] prepared a hydrogel in the presence of potassium. The resulting hydrogel exhibits an extended lifetime and enhanced thermal stability compared with that of **352** alone, likely due to the incorporation of the more hydrophobic **351** into G-quartets. Besides demonstrating the ratio of the two components as a tool to tune the mechanical and thermal properties of the hydrogels, the authors used a combination of light scattering, small-angle neutron and X-ray scattering, and viscometric experiments to study the mechanism of hydrogelation and found that an increase in the volume fraction of microgel domains ultimately leads to macroscopic gelation.[832] By mixing guanosine (**352**) with 0.5 equiv of $KB(OH)_4$, Davis et al.[833] developed a guanosine−borate hydrogel. Further studies found that the resulting hydrogel is able to selectively absorb a cationic dye and nucleosides via electrostatic interaction and hydrogen bonding. Employing Ag^+ as the metal ion to coordinate with 5′-guanosine monophosphate (**353**), Mann et al.[834] prepared a hydrogel based on the Ag−GMP (guanosine monophosphate) nanofilaments in water. This hydrogel binds a cationic dye and protein (e.g., cytochrome *c*) without the loss of biological activity, suggesting possible use in controlled drug release and molecular recognition. In another experiment, Kumar et al.[835] reported a porous hydrogel based on a mixture of **350** and β-FeOOH. The freeze-dried gel shows a high swelling ratio of 326% and loading capacity for methylene blue, suggesting that this hydrogel has potential applications in drug delivery and other biological applications. Li et al.[836] reported a new two-component hydrogel based on thymidine (**354**) and melamine at a CGC of 0.1 wt %. Using FT-IR and X-ray diffraction, the

DOI: 10.1021/acs.chemrev.5b00299
Chem. Rev. 2015, 115, 13165−13307

Scheme 45. Nucleobase Derivatives for Multicomponent Hydrogels

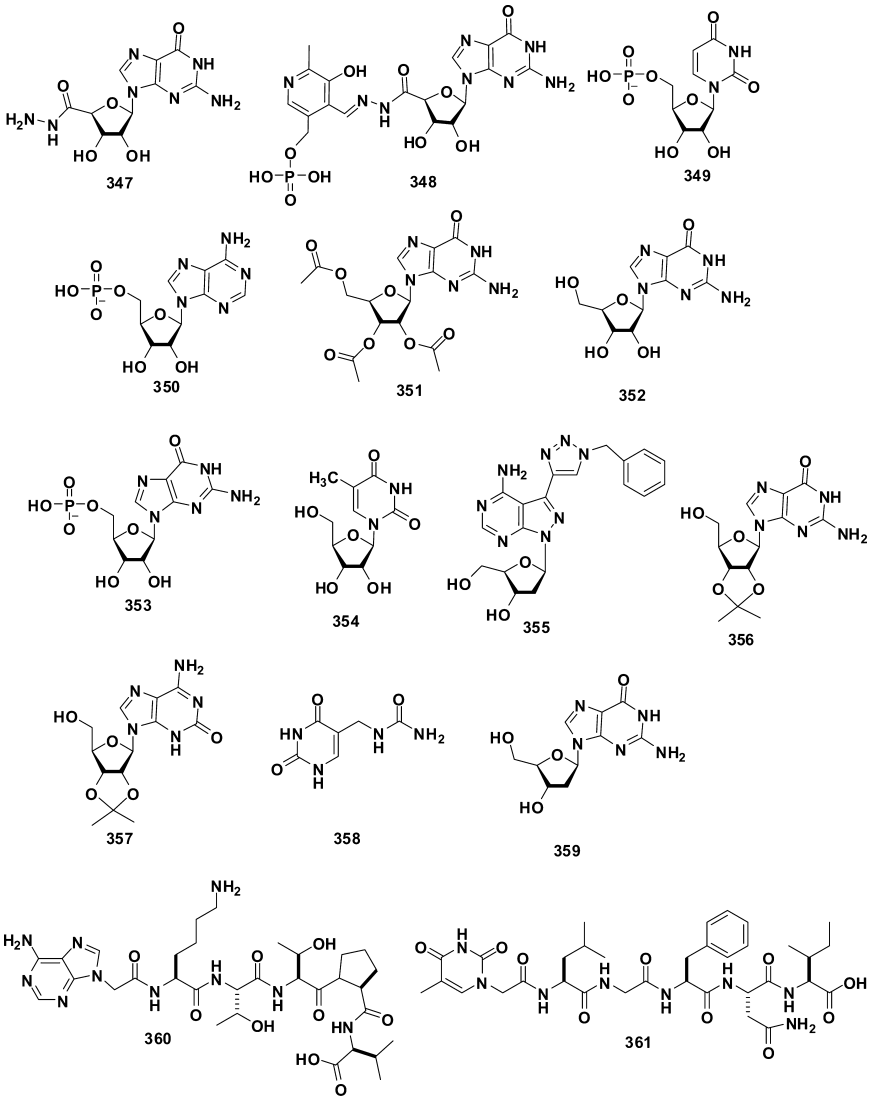

authors confirmed that the thymidine and melamine, via intermolecular hydrogen bonding, form supramolecular complexes. Utilizing click chemistry to connect benzyl azide and 8-aza-7-deaza-2′-deoxyadenosine, Seela et al. prepared a nucleoside hydrogel of **355** at a concentration of 0.3 wt % in water. SEM reveals that **355** self-assembles to form nanotubes.[837] Abet et al. recently reviewed guanosine and isoguanosine derivatives (**356** and **357**) that self-assemble in water.[838] This review provides useful information on different self-assembled architectures generated by guanosine and isoguanosine scaffolds, including recent examples of their use in the preparation of functional devices. In another work, Nachtsheim et al. reported *N*-(uracil-5-ylmethyl)urea (**358**) as a minimalistic hydrogelator which undergoes phosphate-induced self-assembly, as evidenced by IR, UV/vis, and NMR spectroscopy, electron microscopy, and rheological experiments. According to the authors, it is a rare example of an anion-triggered self-assembly in aqueous solution without additional aromatic or lipophilic groups. The macroscopic appearance of the hydrogels implies the formation of microcrystals as the gel matrixes.[256] Adhikari and Kraatz et al. designed and synthesized a hydrogelator of deoxylguanosine (**359**) that affords a hydrogel with a CGC of 0.57 wt % in the presence of Ag^+. One interesting feature of this work is that the cogel of **352** and **359**, being injectable, exhibits enhanced stability, an extended lifetime, and self-healing properties.[839] Xu et al. designed two nucleopeptides (**360** and **361**) that alone fail to form hydrogels, while the mixture of the two nucleopeptides self-assembles to form nanofibers and result in a hydrogel. One intriguing feature of this work is that the resulting heterodimer dramatically enhances the proteolytic stability of these nucleopeptides.[840]

4.5. Hydrogels Based on Saccharides

Bearing multiple hydroxyl groups, saccharides provide hydrogen bond donors and acceptors for intermolecular interactions that are critical for molecular self-assembly in water to result in hydrogelation. Moreover, the inherent hydrophilicity of saccharides allows the easy dissolution of the hydrogelators prior to the triggering of the hydrogelation by changing the pH, temperature, or ionic strength. In this section, we categorize the saccharide-based hydrogelators into monosaccharide-based and oligosaccharide-based hydrogelators (Table S4).

4.5.1. Monosaccharide-Based Hydrogelators. As shown in Scheme 46, Lu et al. designed and synthesized a hydrogelator (**362**) containing a phenyl β-D-glucopyranoside which self-assembles to form a tubular structure and results in a hydrogel

DOI: 10.1021/acs.chemrev.5b00299
Chem. Rev. 2015, 115, 13165−13307

Scheme 46. Some Monosaccharide-Based Hydrogelators

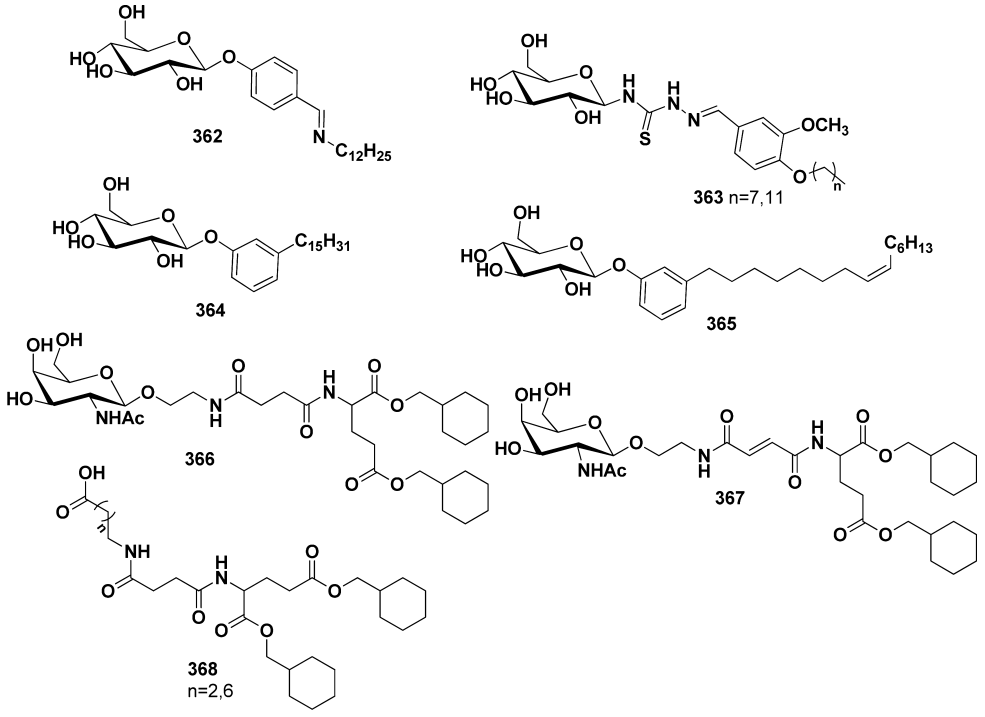

Scheme 47. Some Monosaccharide-Based Hydrogelators

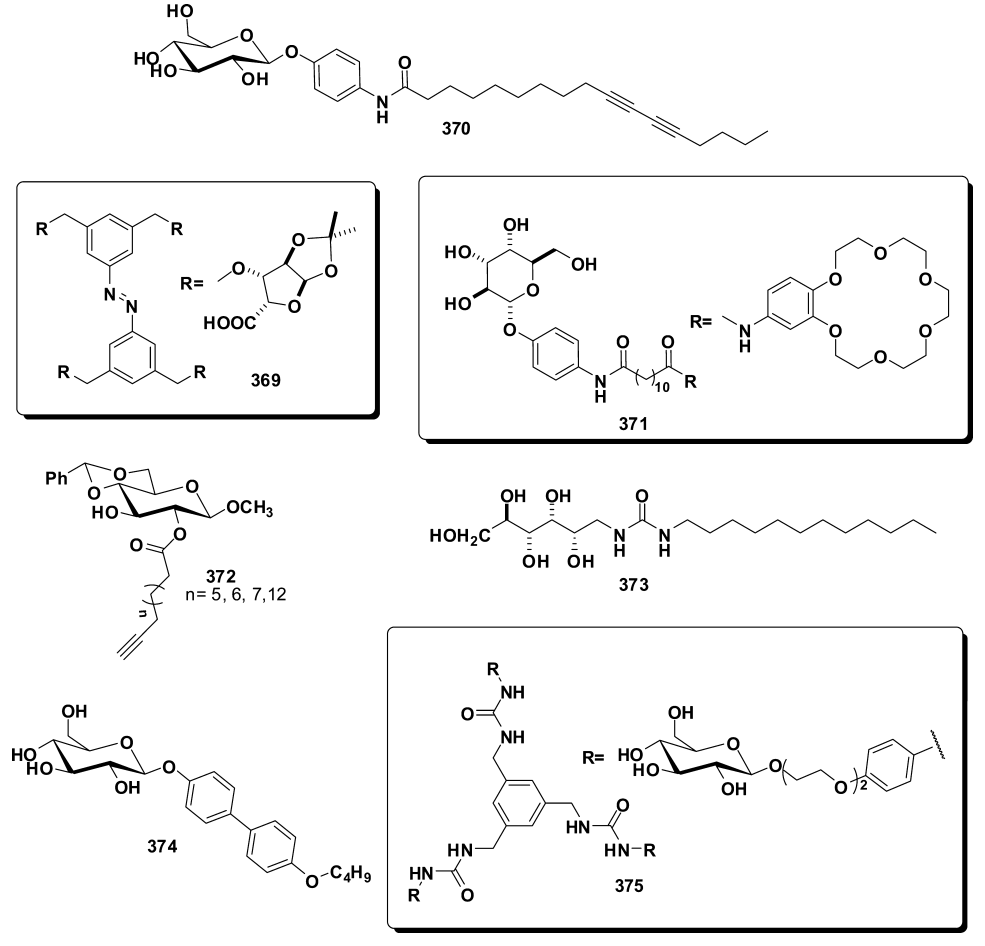

DOI: 10.1021/acs.chemrev.5b00299
Chem. Rev. 2015, 115, 13165−13307

Scheme 48. Monosaccharide-Based Hydrogelators

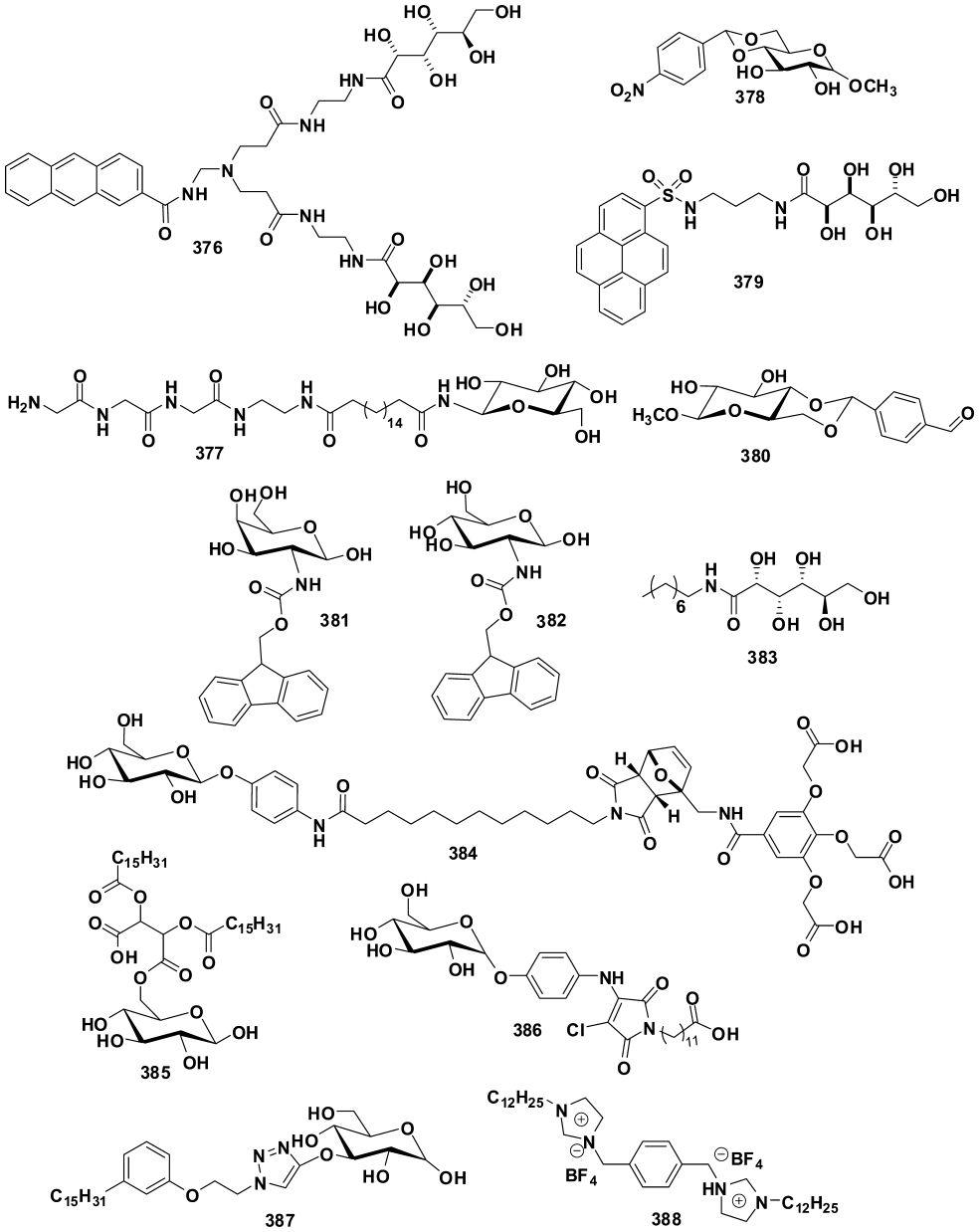

at a concentration of 0.2 wt %.[841] They also prepared hydrogels based on β-D-glucopyranoside substituent thiosemicarbazide derivatives **363**,[842,843] and used the hydrogels as templates for fabricating netlike CdS nanofibers. John and Shimizu et al. reported a series of low molecular weight gelators (**364**, **365**) based on simple glycolipids which are capable of forming gels in a water/alcohol mixture at a concentration of 0.15 wt %. They found that the T_{gel} of **364** is higher than that of **365**.[844] Hamachi et al. developed a supramolecular hydrogelator (**366**) composed of *N*-acetyl-D-glucosamine which self-assembles to form nanofibers and results in a hydrogel with a CGC of 0.1 wt %.[845] This work pioneered the use of a supramolecular hydrogel array to monitor enzymatic reactions. According to the authors, this work has potential applications in pharmaceutical research and diagnosis. Meanwhile, Hamachi et al. also developed a photoresponsive gel droplet based on the hydrogelator **367** and demonstrated the use of light to trigger mass transport in gels. The authors suggested this type of hydrogel as an intelligent delivery system.[846] Moreover, their further studies found that **366**, mixed with an appropriate amount of **368** (e.g., **366**:**368** = 1:1), affords a pH-responsive shrinkage/swelling supramolecular hydrogel at a concentration of 0.5 wt %.[847] Particularly, the authors envisioned that this approach is useful for triggering the release of hydrophilic drugs.

Bhattacharya et al. reported an intriguing example in which a tetrameric D-xylofuranuronic acid derivative containing an azobenzene core (**369**), assisted by initial dissolution in a small amount of DMSO, exhibits pronounced hydrogelation at 0.1 wt %. Since the hydrophobic azobenzene group is packed inside the gel state, the resulting hydrogel displays a remarkable photostability under UV irradiation. Moreover, the addition of a salt (e.g., $CaCl_2$) to the hydrogel changes the morphology of the networks in the hydrogel from globular spongy to "rodlike" fibers.[848] Jung et al.[849] reported a D-glucopyranoside-based hydrogelator (**370**) by incorporation of an unsaturated

DOI: 10.1021/acs.chemrev.5b00299
Chem. Rev. 2015, 115, 13165−13307

Scheme 49. Some Oligosaccharide-Based Hydrogelators

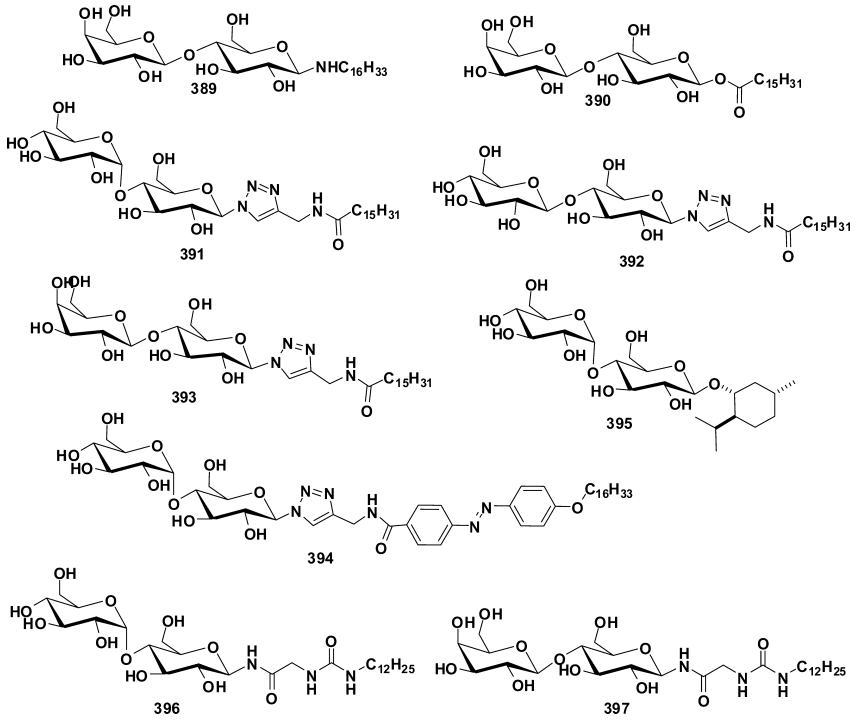

diacetylene unit as the hydrophobic group. After its self-assembly in water, **370** forms well-defined helical ribbons with diameters of 20−150 nm, which results in a hydrogel with a CGC of 0.5 wt %. Upon UV irradiation at 254 nm, **370** forms typical nanofibers. On the basis of CD spectra and other measurements, the authors suggested that photopolymerization turns the well-ordered bilayer structure into disordered molecular packing. Jung et al.[850] also designed other hydrogelators (e.g., **371**) which self-assemble to form fibrils with diameters of 10−38 nm. Meanwhile, the hydrogel based on **371** with crown ether can serve as a template to prepare various structures of silica nanomaterials.[851]

By functionalization of a commercially available glucose derivative, Wang et al.[852,853] designed and prepared a series of D-glucose-based hydrogelators (**372**) (Scheme 47). Among them, **372** (n = 5, 12) exhibits an excellent gelation ability and affords a hydrogel at a concentration of 0.4 wt %. Further studies[854] found that the conjugates containing a terminal acetylene and an aryl group exhibit an enhanced ability of gelation. One interesting feature of this work is that these gelators form birefringent fibers[855] and tubules. By connecting the D-glucamine derivatives and hydrophobic unit via ureido or bis(ureido) moieties, Cintas et al.[856] prepared a family of carbohydrate amphiphiles and bolaamphiphiles. The resulting molecules form hydrogels upon application of thermal or ultrasound stimuli. For example, **373** molecules afford a gel at room temperature under sonication. Wan et al.[857] reported a new saccharide-appended hydrogelator of 4-(4′-butoxyphenyl)-phenyl β-*O*-D-glucoside (**374**) which self-assembles to form planar ribbons with widths ranging from tens to thousands of nanometers and results in a hydrogel in water with a CGC of 0.5 wt %. Yamanaka et al.[858] designed and synthesized a D-glucose-based hydrogelator (**375**) which self-assembles to form a hydrogel with a CGC of 0.25 wt % in the presence of Tris−glycine buffer. The intriguing feature of this work is that the hydrogel can serve as an electrophoresis matrix to separate the native protein. This underexplored application appears to have much potential.

As shown in Scheme 48, Takaguchi et al.[859] reported a unique example of an anthracene-based photoresponsive hydrogelator (**376**) which self-assembles in water to afford a hydrogel with a CGC of 2.9 wt % and a T_{gel} of 46 °C. Upon photoirradiation, the hydrogel is transformed to a solution due to the dimerization of the anthryl moieties. Kameta and Shimizu et al.[860] reported an intriguing example in which *N*-(β-D-glucopyranosyl)-*N*′-[2-(glycylglycylglycinamido)ethyl]-octadecanediamide (**377**) self-assembles to form nanotubes with a 9 nm inner diameter and results in a hydrogel at a concentration of 0.5 wt % and pH 8.0. Notably, the fixed green fluorescent protein (GFP) and myoglobin (Mb) in the hollow cylinders of the nanotubes exhibit remarkable resistance to denaturants such as guanidinium chloride and urea at high concentration. Furthermore, Kameta et al.[861] also found that the nanotubes of this hydrogelator (**377**) are able to act as artificial chaperones to assist the transformation of encapsulated proteins into their refolded states via simply changing the pH values. The authors suggested that the modification of the diameter and inner surface of the nanotubes enhances the efficiency of encapsulation and refolding of the proteins.

Tritt-Goc et al.[862] prepared an α-D-glucopyranoside-based hydrogel (**378**) at a concentration of 1.5 wt %. The authors measured the thermal properties of the resulting hydrogel and determined the gel−sol transition enthalpy as 43 kJ/mol. By conjugating pyrene and a glucose derivative, Fang et al.[863] reported a superhydrogelator (**379**) which affords a hydrogel in water with a CGC of 0.07 wt %. Interestingly, **379** also gels many of the organic solvents tested. Zhang et al.[864] designed and synthesized an α-D-glucopyranoside-based hydrogelator (**380**) containing an aldehyde group which forms a hydrogel with a CGC of 0.8 wt %. Due to the existence of aldehyde and acetal groups, the resulting hydrogel not only responds to the pH, but also reacts with cysteine, which may lead to a new

DOI: 10.1021/acs.chemrev.5b00299
Chem. Rev. 2015, 115, 13165−13307

approach to design smart delivery systems. Birchall and Edward et al.[865] reported a class of supramolecular hydrogels (**381** and **382**) derived from glucosamine and Fmoc. Notably, the authors suggested that CH−π interaction, rather than π−π stacking and H-bonding, drives the self-assembly and subsequently hydrogelation. Pfannemuller and Welte et al. reported that *N*-octyl-D-gluconamide (**383**) is able to form a hydrogel which is converted to crystallites over a few hours.[866] By adding a nonionic surfactant (e.g., polyethylene glycol (PEG)), Rowan et al.[867] elucidated not only that the resulting hydrogel is stable for more than one year, but also that changing the ratios of the components in the gel allows systematic tuning of the thermomechanical properties of the hydrogels. One notable result is that hydrogelator **383** exhibits potent activity to inhibit ice crystal formation at a concentration of 0.5 mM.[868]

Ikeda and Hamachi et al.[43,869] reported an intriguing example in which a well-designed bolaamphiphile (**384**) forms a hydrogel via "retro-Diels−Alder" reaction induced by heat. The authors used TEM to show the morphology transition from a twisted ribbon to a helical ribbon, and suggested that this simple and versatile molecular design should produce smart materials for various applications. Altenbach et al.[870] designed and synthesized a D-glucose-based hydrogelator (**385**) via two simple steps. The resulting hydrogelator, acting as a surfactant and emulsifier, affords a hydrogel with a CGC of 2.5 wt %. Hamachi et al.[871] prepared a glycolipid-based supramolecular hydrogelator (**386**) that forms a hydrogel with a CGC of 0.1 wt %. The most interesting feature of this work is that the resulting hydrogel exhibits a color change when heated or upon the addition of relevant glycosidases to induce a gel−sol transition. Employing click chemistry, Mishra and Rao et al.[872] reported a glucose-based lipid (**387**) that forms a hydrogel with a CGC of 0.03 wt % in a mixture of water and methanol (50:50). Noto et al.[440] designed and synthesized a molecule (**388**) which affords a hydrogel with a CGC of 1.0 wt % in the presence of α-cyclodextrin. Meanwhile, simply changing the ratio of cyclodextrin and **388** can easily tune the gelation properties.

4.5.2. Oligosaccharide-Based Hydrogelators. As shown in Scheme 49, Britt et al. prepared the conjugates **389** and **390** of lactose and fatty amine or fatty acid, which act as gelators and afford gels in a mixture of water and propanol (50:50).[873] Thompson et al.[874] designed and synthesized a series of α-cyclodextrin−aldonamide conjugates. Upon the addition of glucose, the solution of hexaaldonamide-substituted α-cyclodextrin turns into a hydrogel. It was suggested to be useful in developing glucose sensors and glucose-sensitive drug delivery systems.

Oriol et al.[875,876] designed and synthesized a class of maltose-based supramolecular hydrogelators (**391**−**393**) via click chemistry. **391** and **393** self-assemble in water to form typical ribbons with a left-handed twist and result in hydrogels with a CGC of 1.0 wt %, while **392** forms ribbons with a right-handed twist and affords a hydrogel with a CGG of 0.5 wt %. By incorporating azobenzene into the gelator **391**, Oriol et al.[877] also prepared another hydrogelator (**394**) that forms a stable hydrogel with a CGC of 5.0 wt %. Interestingly, CD reveals that UV irradiation is unable to induce cis−trans isomerization of azobenzene. The authors suggested that the dense packing of azobenzene in the gel state hinders the photoisomerization, which may serve as a useful caution for designing photomechanical actuators based on gels. Kirimura et al. synthesized a maltoside-based hydrogelator (**395**) via an enzymatic reaction.[878] The resulting hydrogelator is able to gel water at a concentration of 3.0 wt % and 12 °C. It is worth noting that its stereoisomers fail to form a hydrogel. Mathiselvam et al. prepared a family of urea−glycolipid-based hydrogelators (**396** and **397**) and found that **396** forms a hydrogel at a concentration of 0.5 wt %, while its stereoisomer **397** fails to form a hydrogel.[879] This observation underscores that the orientation of the hydroxyl group in the saccharide has a profound influence on the self-assembly of this class of hydrogelators.

5. APPLICATIONS

In recent years, on the basis of the increased understanding of protein functions from cell biology and structural biology, considerable efforts have focused on the incorporation of peptide epitopes as the functional motifs on supramolecular hydrogelators for a wider range of biological applications.[880−882] These endevors also stimulated the determination of the protein targets of supramolecular hydrogels.[883,884] In this section, we mainly focus on the recent advances in the design and development of supramolecular hydrogels for biological and biomedical applications. We discuss the different types of hydrogels and highlight some representative applications. Since most of the biomedical applications demand multiple functionalities of the hydrogel network and dynamic interactions between the surrounding matrixes and cells, we first discuss hydrogelators for cell-related applications, followed by fluorescent hydrogelators used for imaging, and then hydrogels for tissue engineering, drug delivery, immunomodulation, and wound healing. We finally describe the unique applications of supramolecular hydrogels and hydrogelators in a cell environment.

5.1. Cell-Related Applications

Because the most obvious features of hydrogels are soft and wet, which resemble the cellular environment, it is not surprising that the most attempted applications of the hydrogels are to mimic the ECM for cell culture (or tissue engineering), and the necessary initial test for a hydrogelator is its cell compatibility.[29,885] Since SPPS allows oligomeric peptides to be made quickly, most of the hydrogelators examined for cell-related applications are self-assembling peptides or peptide derivatives. In the following subsections, we discuss various hydrogelators that have been evaluated for the applications related to cells,[886−888] such as hydrogelators for cell culture,[889,890] cell-compatible hydrogelators,[891,892] cytotoxic hydrogelators,[893,894] and hydrogels for cell adhesion.

5.1.1. Three-Dimensional Cell Culture. Ulijn et al. reported the first case of cell culture using Fmoc-dipeptides. As first reported by Xu et al., the hydrogel of Fmoc-Gly-Gly-OH (**398**; Scheme 50) consists of nanofibers with average diameters of 33 nm and exhibits a CGC of 0.15 wt % at pH < 4.[11] Later, Ulijn used the hydrogel of a mixture of **398** and Fmoc-Phe-Phe-OH (**6**) for the 2D or 3D cell culture.[96] In addition, at pH 7, **6** itself forms hydrogels with a concentration between 0.22 and 2.14 wt % which contain polydispersed nanofibers with average diameters of 56 nm. On the basi sof the fact that the Fmoc-dipeptide building blocks are approximately 2 nm in length, the authors suggested that the nanofibers consist of bundles of supramolecular stacks. Although the results of cell viability indicate that **6** shows a relatively high cytotoxicity to bovine chondrocyte cells or Caco-2 and HGF-1 cells[705] after 7 days, Ulijn et al. demonstrated that **6** can still be

DOI: 10.1021/acs.chemrev.5b00299
Chem. Rev. 2015, 115, 13165−13307

Scheme 50. Representative Molecular Structures of Hydrogelators for 3D Cell Culture

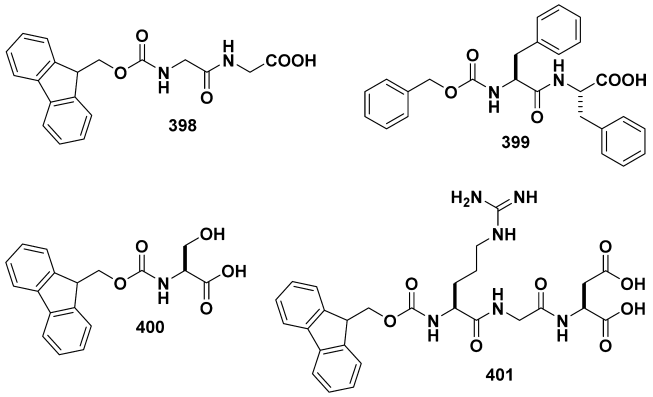

RGDA16: Ac-RADARGDARADARGDA-CONH$_2$ 402

GRGDSP-RADA16: Ac-GRGDSP-GG-RADARADARADARADA-CONH$_2$ 403

YIGSR-RADA16: Ac-YIGSR-GG-RADARADARADARADA-CONH$_2$ 404

RLN: Ac–RADARADARADARADAGG DHLSDNYTLDHDRAIH–CONH$_2$ 405

RAD16: Ac-RARADADARARADADACONH$_2$ 406

Q11: Ac-QQKFQFQFEQQ-CONH$_2$ 407

RGDS-Q11: Ac-GGRGDSGGG-QQKFQFQFEQQ-CONH$_2$ 408

IKVAV-Q11: Ac-GGIKVAVGGG-QQKFQFQFEQQ-CONH$_2$ 409

RGD-Q11: Ac-GGRGDGGG-QQKFQFQFEQQ-CONH$_2$ 410

applied to 2D and 3D cell culture. According to the authors, the hydrogel is stable under cell culture conditions and consists of nanofibers that have dimensions similar to those of the fibrous components of the ECM.[96] Besides **6**, Ulijn et al. also studied two other diphenylalanine analogues, Nap (naphthalene)-Phe-Phe-OH (**3**)[14] and Cbz ((benzyloxy)carbonyl)-Phe-Phe-OH (**399**), and compared their self-assembly properties and cell culture applications with those of **6**. After demonstrating that all three hydrogelators form hydrogels consisting of nanofibers with β-sheet arrangements and varying fibril dimensions, the authors used LDH (lactate dehydrogenase) assays to prove that all three structures can support cell proliferation and cell culture of chondrocytes in both two and three dimensions for up to 10 days.[895] On the basis of the early work of Ulijn et al., Liebmann et al. evaluated the hydrogel of **6** as 3D cultures of COS-7 and MDCK cells for 7 days.[896] However, **6** still has limitations, especially in terms of long-term gel performance, stability, and cytotoxicity when being used for culturing other cell types (e.g., skin cells such as human dermal fibroblasts and mouse 3T3 cells). Thus, Ulijn et al. mixed **6** with positively charged Fmoc-Lys-OH (**202**), uncharged/polar Fmoc-Ser-OH (**400**), and negatively charged Fmoc-Glu-OH (**203**) in the same hydrogel for examining the proliferation of chondrocytes, 3T3, and human dermal fibroblast (HDF) cells.[897] Besides confirming that these heterotypic hydrogelators undergo self-assembly to form fibrous scaffolds by mainly adopting an antiparallel β-sheet arrangement, the authors used the LIVE/DEAD staining assay to show that these three types of mixed hydrogels maintain the viability of bovine chondrocytes. The hydrogel of **6** + **400** (Fmoc-FF/Fmoc-S) and the hydrogel of **6** + **203** (Fmoc-FF/Fmoc-E) are compatible with HDF cells, and only the hydrogel of **6** + **400** (Fmoc-FF/Fmoc-S) supports the proliferation of 3T3 fibroblast cells.[898,899]

Besides the above three Fmoc-peptide mixtures, Ulijn et al. designed another hydrogel, a mixture of **6** and Fmoc-Arg-Gly-Asp-OH (Fmoc-RGD, **401**), as a 3D scaffold for HDF cells. They found that this mixed hydrogel provides a highly hydrated, stiff nanofiber network with β-sheets interlocked by $\pi-\pi$ stacking of the Fmoc groups. The authors suggested that the RGD motif plays a dual role: as a structural component that locates at the surface of the unique, interwoven cylindrical nanofiber structure and as a biological ligand that forms the specific RGD−integrin binding to promote adhesion, spreading, and proliferation of cells.[900] Using a similar design principle, Hamley et al. found that **401** itself forms a self-supporting hydrogel consisting of well-defined amyloid fibrils with β-sheet features at a concentration of 2 wt %. In addition, the preliminary cell culture experiments showed that **401** can be used to culture bovine fibroblasts.[901]

On the basis of the earlier report of a hydrogel made of a hexadecapeptide (RADA16,[181,902] **248a**), Hirose et al. used the **248a** self-assembling peptide solution (PuraMatrix)[903−906] to evaluate the osteogenic differentiation of mesenchymal stem cells (MSCs) that are derived from rat bone marrow. The authors reported that over 80% of the MSCs in the hydrogel are alive and have spread within the hydrogel of **248a**, and suggested that **248a** acts as a scaffold for three-dimensional culture of MSCs. The authors observed a significantly higher expression of alkaline phosphatase (ALP) activity and osteocalcin (OC) contents at both the protein and mRNA levels for 3 or 4 weeks, and thus concluded that MSCs in the **248a** hydrogel differentiate into mature osteoblasts, followed by the growth of a mineralized extracellular matrix. Although it is suggested that the biodegradable/biocompatible hydrogel **248a** may become an attractive option in bone tissue engineering,[907] the complexity of the bone remolding and growth process likely requires more than one component in the hydrogel.[908] The commercial availability of **248a** allows many research laboratories to evaluate the use of the hydrogel of **248a** for 3D cell culture.[909−911] For example, Zhao et al. studied the cellular behavior of human lung cancer cells A549 within a **248a** nanofiber scaffold. They found that the cells show morphologies in a 3D scaffold different from those on a 2D Petri dish, an observation that is consistent with RADA being a cell adhesion motif.[912] Xie et al. mixed **248a** and RGDA16 (Ac-RADARGDARADARGDA-CONH$_2$, **402**) solutions at a concentration of 10 mg/mL (1%, w/v) and found that the mixture scaffold can significantly promote the cell attachment and proliferation of MC3T3-E1 cells compared with the **248a** scaffold.[913] Semino et al. used the hydrogel of **248a** functionalized with biologically active motifs (e.g., GRGDSP, **403**, or YIGSR, **404**) to replace the use of collagen I in the traditional culture sandwich technique for maintaining functional hepatocytes in vitro.[914] Moreover, Wang et al. used the mixture of the peptide solutions of RLN (**405**) and **248a** to guide rabbit nucleus pulposus cells (NPCs), and demonstrated that NPCs migrate from the surface into the hydrogel in the 3D cell culture experiments and exhibit stimulated synthesis of the ECM.[915] Narmoneva et al. used RAD16 (**406**) peptide nanofibers for vascular tissue engineering. They reported enhanced angiogenesis in vitro and in vivo, and suggested that the observation results from low-affinity integrin-dependent interactions of microvascular endothelial cells (MVECs) with the RAD motifs.[916] These results imply that the development of multicomponent hydrogels may address several limitations of single-component hydrogels. Using **406** to form a

DOI: 10.1021/acs.chemrev.5b00299
Chem. Rev. 2015, 115, 13165−13307

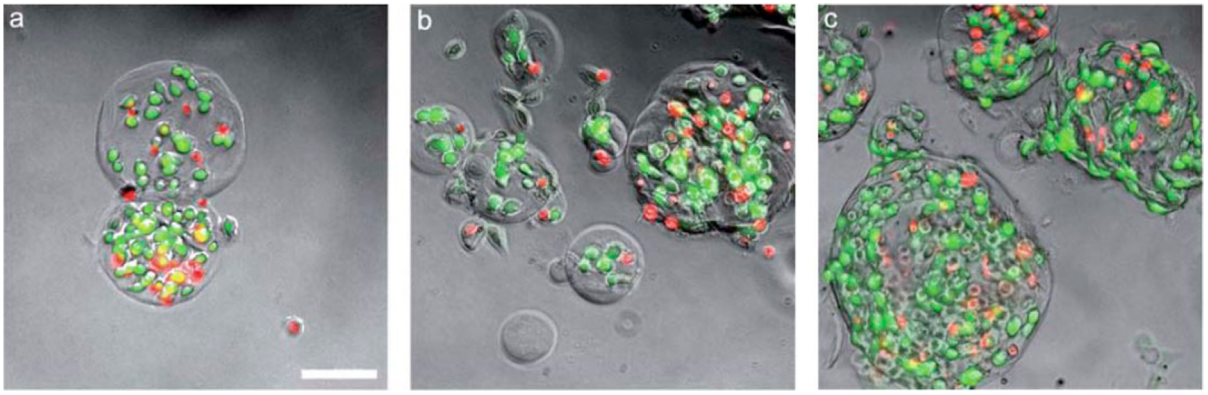

Figure 8. The viability of NIH/3T3 cells encapsulated in 30 mM **407** microgels was quantified with calcein/ethidium homodimer staining. The assay was conducted 2 h after the incubation of (a) 1 day, (b) 2 days, and (c) 3 days. The scale bar in (a) represents 100 mm. The magnification is the same in (a)−(c). Adapted with permission from ref 918. Copyright 2011 Royal Society of Chemistry.

Scheme 51. Representative Molecular Structures of Hydrogelators for 3D Cell Culture

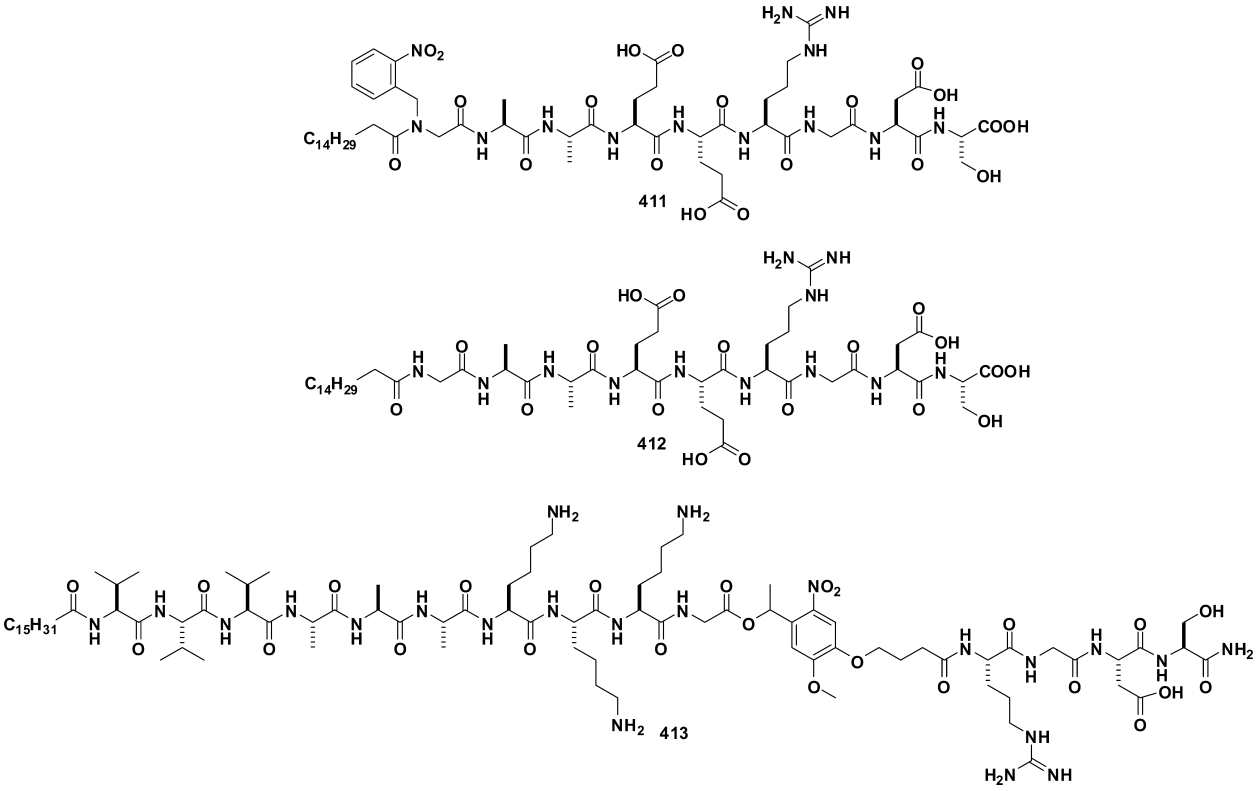

hydrogel, Urtti et al. established 3D hepatic cell cultures in the hydrogel to improve the 3D phenotype of Hep G2 cells, a human liver carcinoma cell. The authors reported that Hep G2 cells formed multicellular spheroids which consist of filamentous actin accumulation and large tubular bile canalicular structures to indicate apicobasal cell polarity.[917]

Realizing the merits of multicomponent hydrogels, Collier et al. designed and examined multipeptide coassembling hydrogels based on peptides RGDS-Q11 (**408**) and IKVAV-Q11 (**409**) consisting of two segments: a nanofiber-forming peptide, Q11 (**407**), which self-assembles to form a β-sheet, at the C-terminal and a ligand of integrins, RGDS or IKVAV, at the N-terminal. The authors suggested that such a design allows the ligands to be presented on the surface of the nanofibers. In coassemblies of the ligand-bearing peptides containing **407**, the amount of the incorporated ligands is able to influence the attachment, spreading, morphology, and growth of human umbilical vein endothelial cells (HUVECs) without significantly altering the materials' properties, such as fibrillization, β-turn secondary structure, or stiffness. The authors reported that while **408**, being coassembled into the gels of **407**, specifically increases HUVEC attachment, spreading, and growth, **409** exerts a more subtle influence on the attachment and morphology of the cells. Additionally, they reported that **407** and **408** are minimally immunogenic in mice, making the **407**-based biomaterials attractive candidates for applications in vivo.[919] However, the proteolytic stability of these peptides remains to be established. Recently, on the basis of the sensitivity of **407** to the ionic strength, Collier et al. developed a microgel made of RGD-Q11 (**410**) by triggering peptide self-assembly within the aqueous phase of water-in-oil emulsions. According to the authors, one of the advantages of microgels is that they can be embedded

DOI: 10.1021/acs.chemrev.5b00299
Chem. Rev. 2015, 115, 13165−13307

Scheme 52. Representative Molecular Structures of Hydrogelators for 3D Cell Culture

TSS1: VKVKVKVKV^{D}PPTKVKVKVKDPPTKVKVKVKV-NH_2 414 $C_{16}H_{31}O$-AAAGGGGDD 415

$C_{16}H_{31}O$-AAAGGGGDDIKVAV 416 KLD-12: Ac-KLDLKLDLKLDL-$CONH_2$ 417

$K_2(SL)_6K_2$GRGDS 418 $K(SL)_3RG(SL)_3K$ 419 $K(SL)_3RG(SL)_3K$GRGDS 420

$E_2(SL)_6E_2$GRGDS 421 $K(TL)_2SLRG(TL)_3K$GRGDS 422

P_{11}-8: Ac-QQRFOWOFEQQ-NH_2 423 P_{11}-12: Ac-SSRFOWOFESS-NH_2 424

P_{11}-13: Ac-EQEFEWEFEQE-NH_2 425 P_{11}-14: Ac-QQOFOWOFOQQ-NH_2 426

P_{11}-16: Ac-NNRFOWOFENN-NH_2 427 P_{11}-18: Ac-TTRFOWOFETT-NH_2 428

within other self-assembled peptide matrixes for generating composites of different peptide formulations. The authors, indeed, demonstrated an example of microgels that are cytocompatible and encapsulate NIH/3T3 fibroblasts (Figure 8) and C3H10T-1/2 mouse pluripotent stem cells with good viability.[918]

On the basis of their seminal works of the applications of peptide amphiphiles for cell cultures,[557,920−922] Stupp et al. designed and synthesized a peptide amphiphile molecule, **411** (Scheme 51), containing both the photocleavable 2-nitrobenzyl group as well as the bioactive epitope Arg-Gly-Asp-Ser (RGDS). The 2-nitrobenzyl group of **411** can be photocleaved to afford **412**, which self-assembles to form high-aspect-ratio nanofibers in the presence of charge-screening salts. In vitro experiments with NIH/3T3 mouse fibroblasts indicate that **412** and the byproducts of the photoreaction at a concentration of 7.9×10^{-3} M are not toxic to the cells and that cell proliferation is normal after the irradiation.[923] In another case, Stupp et al. reported a photoresponsive, synthetic ECM mimic through linking peptide amphiphiles **413** to the ECM-derived cell adhesion epitope RGDS by a photocleavable nitrobenzyl ester group. This derivative self-assembles to form cylindrical nanofibers, and light irradiation on the photolabile group in the peptide backbone efficiently removes the RGDS epitopes without affecting the nanofibers. The authors demonstrated that the adhesion of mouse NIH/3T3 fibroblast cells on the surface of peptide amphiphile (PA) hydrogels can be dynamically controlled by rapid photolytic removal of the RGDS peptide from the supramolecular nanofibers.[924]

As shown in Scheme 52, Schneider and Pochan et al. reported a hydrogel based on TSS1 (**414**), a de novo designed three-stranded β-sheet. **414**, containing 29 amino acids with 12 lysine residues and 12 valine residues, undergoes thermally triggered folding and self-assembly to afford a network of well-ordered β-sheet-rich fibrils that constitute a mechanically rigid hydrogel. A gelation test indicated that **414** remains unfolded at lower temperatures but folds and self-assembles into rigid hydrogels upon raising the temperature of the aqueous solutions (pH 9.0 or 7.4 (150 mM NaCl)) of **414**. TEM images and SANS show that **414** self-assembles into monodispersed fibrils with a width of around 3 nm, which corresponds to the width of the peptide in its folded state. The authors demonstrated the in vitro culture of C3H10t1/2 mesenchymal stem cells on the gel surface for 24 h, and suggested that the surface of the hydrogel supports cell adhesion and allows cell migration.[925] Schneider and Pochan et al. developed a class of self-assembling β-hairpin peptides[188,608,926] to create physical hydrogels as injectable therapeutic delivery vehicles. On the basis of their works on peptide hydrogels, the authors studied the behavior of β-hairpin peptide-based hydrogels Max1 (**251**) and Max8 (**257**) during and after flow. Importantly, the authors verified that the observed shear-thinning and rehealing, after flow, represent the authentic bulk gel properties. In another experiment, the author utilized the hydrogel of **257** (at a concentration of 0.5 wt %) to encapsulate MG63 cells, a progenitor osteoblast cell line from rat. However, 3 h after injection, some cells were already dead in the 3D gel−cell construct.[927] A scaffold with biocompatibity and in vivo stability needs to be designed in the future.

Conjugating peptide epitope IKVAV from laminin to a peptide amphiphile, $C_{16}H_{31}O$-$A_3G_4D_2$ (**415**), Song et al. generated peptide amphiphile $C_{16}H_{31}O$-$A_3G_4D_2$IKVAV, **416**,[928] which is similar to the IKVAV peptide amphiphiles reported by Stupp et al.[557] After observing that a 1 wt % concentration of the peptide amphiphile self-assembles to form a hydrogel in cell media, the authors investigated 2D[929] and 3D[930] culture of neural stem cells (NSCs) using the hydrogel, and found that mice NSCs proliferate and differentiate into neurofilament (NF)-positive neurons and glial fibrillary acidic protein (GFAP)-positive astrocytes on the surface of the hydrogel. Zheng et al. synthesized a peptide with the sequence of KLD-12 (**417**) and found that **417**, at 0.5 wt %, self-assembles to produce a hydrogel consisting of nanofibers (diameters of 30−40 nm). The authors reported that rabbit MSCs, being encapsulated within the hydrogel of **417** for 3D culture for 2 weeks, grow well and proliferate with the culture time.[931] Kim et al. reported that MSCs encapsulated in the hydrogel of **417** decelerate the progression of cartilage destruction in osteoarthritis in a rat knee model. The authors suggested that the beneficial effect may result from the prevention of chondrocyte apoptosis, the alteration of the subchondral bone mineral density, a reduction of inflammation, and a potential chondrogenic mechanism.[932] Gelain et al. developed a co-assembly of peptides, which are analogs of **417**, for culturing neuronal cells.[933]

Hartgerink et al. designed and synthesized a series of amphiphilic multidomain peptides (MDPs; **418**, **419**, and **420**) with an innovative modular ABA block motif in which the amphiphilic B block drives self-assembly and the flanking A blocks bear charges for controlling the conditions of self-assembly. In their peptide design, the authors created four different variants with a matrix metalloprotease 2 (MMP-2)-specific cleavage motif, an RGDS adhesion sequence, and either one or two lysine residues in the flanking regions. The lyophilized peptides self-assemble to form hydrogels after being dissolved in a sucrose solution. With a final peptide concentration of 1.0 wt %, the hydrogels consist of β-sheet fibrils formed by the cross-linking of lysine-containing peptides

DOI: 10.1021/acs.chemrev.5b00299
Chem. Rev. 2015, 115, 13165−13307

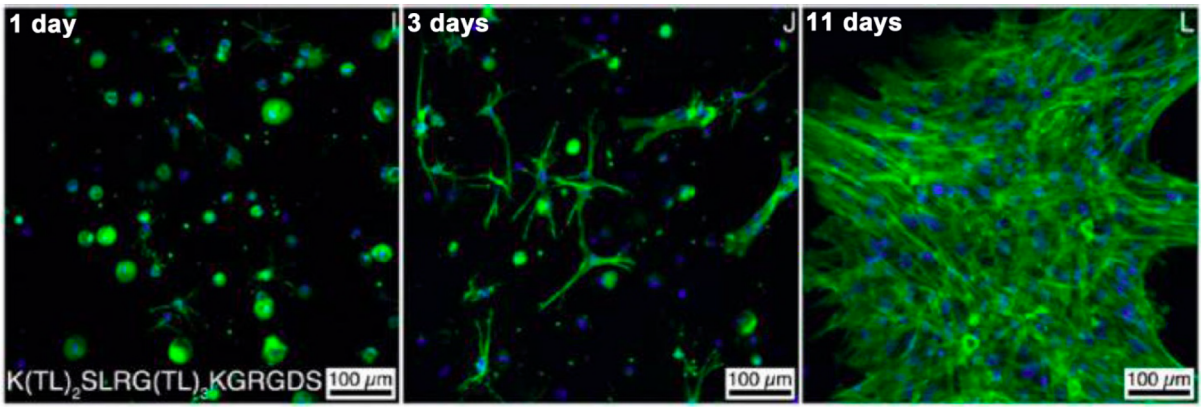

Figure 9. Confocal microscopy of SHED cells 1, 3, or 11 days after 3D encapsulation in **422** hydrogels. Adapted from ref 934. Copyright 2014 American Chemical Society.

Scheme 53. Representative Molecular Structures of Hydrogelators for 3D Cell Culture

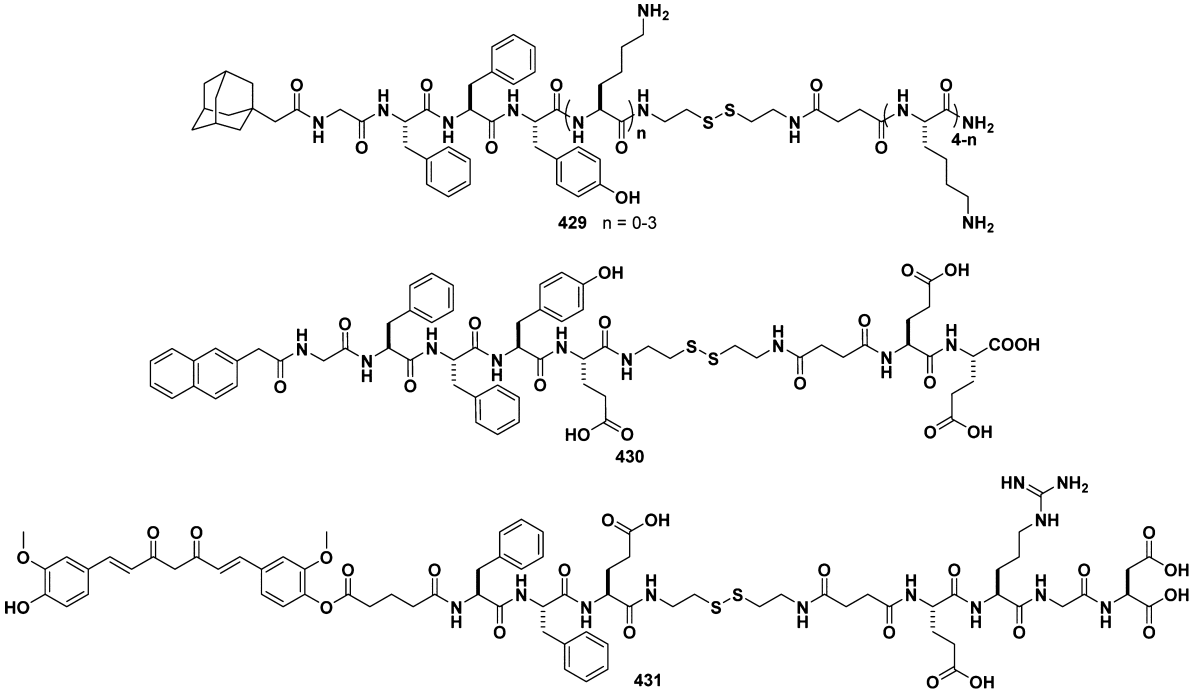

due to the presence of negatively charged phosphate ions in the buffer. The authors illustrated that the structures of the peptides control the lengths and diameters of self-assembled nanofibers, the gelation conditions, and the viscoelastic properties of the formed hydrogels, which highlights the promises of this approach for materials and biological applications. More interestingly, in an in vitro experiment with mesenchymal stem cells from human exfoliated deciduous teeth (SHED), the authors demonstrated that the incorporation of an MMP-2-specific cleavage site and a cell adhesion motif increases the cell viability, cell spreading, and cell migration into the hydrogel matrix.[935] Later, the authors designed another MDP, $E_2(SL)_6E_2GRGDS$ (**421**), which self-assembles to form β-sheet nanofibers approximately 8 nm wide, 2 nm high, and micrometers in length in the presence of Mg^{2+}. The corresponding hydrogel undergoes shear thinning and recovers nearly 100% of its elastic modulus after shearing, making it ideal for being used as an injectable material. Interestingly, in the in vitro experiments with human embryonic stem cells (ESCs), the hydrogel acts like a sponge, soaking up most of the growth factors and cytokines released by the ESCs. Using in vivo experiments, the authors demonstrated a promising application of the hydrogel—as a depot to release stem cell secretome gradually over time.[936] By changing the serine residues in the amphiphilic region to threonine, Hartgerink et al. also designed another MDP, $K(TL)_2SLRG(TL)_3KGRGDS$ (**422**), which forms porous hydrogels with antiparallel β-sheet nanofibers. The authors also used this hydrogel to encapsulate the SHED cells (Figure 9), and observed more fibroblast-shaped cells after 7 days in culture.[934] Recently, they also demonstrated the angiogenic properties of the MDP hydrogels.[937]

Aggeli et al. reported a class of positively charged tape-forming and gel-forming amphiphilic peptides in physiological solutions, all of which bear 2 positive charges and 11 amino acid residues. By changing the peptides to be amphiphilic or completely polar, they systematically synthesized several derived peptides. Each of them has a different polar uncharged

DOI: 10.1021/acs.chemrev.5b00299
Chem. Rev. 2015, 115, 13165−13307

Scheme 54. Representative Molecular Structures of Hydrogelators for 3D Cell Culture

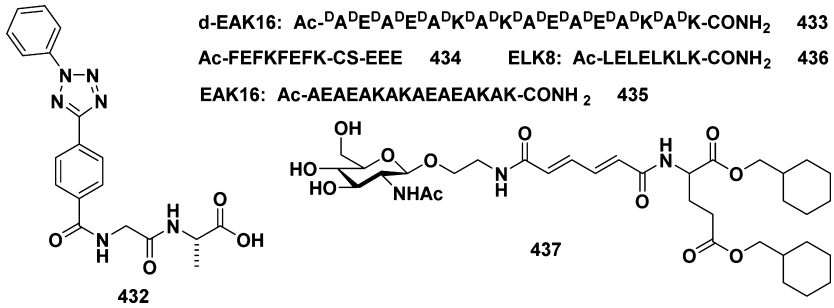

group: P_{11}-8 (**423**, based on glutamine Q, sequence Ac-QQRFOWOFEQQ-NH_2; O represents ornithine), P_{11}-12 (**424**, based on serine S, sequence Ac-SSRFOWOFESS-NH_2), P_{11}-16 (**427**, based on asparagine N, sequence Ac-NNRFOWOFENN- NH_2), and P_{11}-18 (**428**, based on threonine T, sequence Ac-TTRFOWOFETT- NH_2). They found that all of these amphiphilic peptides carrying a +2 charge at neutral pH form self-supporting gels at concentrations above 25 mg/mL (ca. 1.8%, w/v) in physiological solutions. All these hydrogels contain a network of semiflexible, micrometer long nanofibers. In addition, all of these self-assembling peptide hydrogels show biocompatibility with L929 murine fibroblast cells, on the basis of the contact cytotoxicity test. However, only **423** supports L929 cell growth in 3D cell cultures inside 2% (w/v) gels for 14 days without observation of macroscopic degradation of the peptide gel matrix during the experiment, while the other peptides are unable to support cell growth.[938] Later, Aggeli and Ingham et al. designed complementary self-assembling peptides comprising the unimers P_{11}-13 (**425**) and P_{11}-14 (**426**), which exhibit negative and positive charges, respectively, under physiological conditions. Being mixed in equal quantities, they instantaneously form a self-supporting hydrogel that consists of long fibrils with widths ranging from 10 to 20 nm. Although the hydrogels of **425** + **426** appear to be cytocompatible with primary human dermal fibroblasts, they fail to support the proliferation of this cell type, and the cell numbers began to decline after 7 days.[939]

As shown in Scheme 53, Yang et al. reported several supramolecular hydrogels based on adamantane-derivatized peptides that respond to the presence of β-cyclodextrin (β-CD, **155**) motifs. The authors used dithiothreitol (DTT) or GSH to reduce the disulfide bond in the precursors (**429**) to convert the solutions to hydrogels for encapsulations of cells and drugs. Since the hydrogel is transparent and stable over months and undergoes a gel−sol transition upon the addition of **155**-containing molecules, the authors applied them for cell culture and postculture cell recovery in an in vitro experiment of mouse fibroblast 3T3 cells.[940] Later, Yang et al. designed several other hydrogels formed via GSH reduction, and demonstrated the use of the concentrations and structures of the hydrogelators to regulate the mechanical properties and ζ potential of the hydrogels. Among these hydrogels, **430**, having a storage modulus (G') of hundreds of pascals, is suitable for 3T3 cell spreading and proliferation.[941] In addition, the authors also reported the formation of **431**, a curcumin-based hydrogelator, after disulfide bond reduction, to inhibit cancer cells and tumor growth in vitro and in vivo.[942] Taking advantage of the self-assembling ability of Phe-Phe, Yang et al. have developed useful hydrogels made of D-peptides as potential adjuvants for HIV vaccine[943] or for self-assembling on cell surface.[944]

As shown in Scheme 54, Zhang et al. reported an intriguing example tin which a hydrogel of dipeptide Tet-GA[945] (**432**) serves two functions: as the medium for 3D cell culture and as the carrier for the delivery of miRNA into live cells. The authors found that **432** is able to form a transparent and stable hydrogel at concentrations higher than 0.15 wt % in PBS buffer. After confirming the cell compatibility of the hydrogelator, the authors used repressed target gene expression in an in vitro experiment to indicate the delivery of the miRNA, encapsulated together with cells in the hydrogel matrix, into the encapsulated cells. It would be important to elucidate the mechanism of the observed delivery. Luo et al. reported a hydrogel made of a D-form peptide, d-EAK16 (**433**), for 3D cell cultures. After confirming the proteolytic resistance of the D-peptide, the authors used the hydrogel of **433** for 3D cell culture and reported the human hepatoma cell SMMC-7721 to show a high cell viability and low-level cell apoptosis for weeks in the hydrogel.[946] Later, Li and Ding et al. reported an EFK8-based small peptide, Ac-FEFKFEFK-CS-EEE (**434**), that self-assembles to form a hydrogel via disulfide bond reduction with a concentration of 0.5 wt % at physiological pH. Using the LIVE/DEAD assay, the authors demonstrated that the hydrogel of **434** is suitable for the 3D cell culture of NIH/3T3 cells.[947] Furthermore, Saiani et al. reported the use of thermolysin, a protease, to trigger the gelation of FEFEFKFK octapeptide (**228**), which is able to encapsulate human dermal fibroblast cells for 3D cell culture for 5 days.[948] By replacing the alanine residue in EAK16 (**435**) with a more hydrophobic residue, leucine, Lu et al. designed a new peptide, ELK8 (**436**), and directly attached three kinds of functional motifs (e.g., an osteogenic growth peptide, an osteopontin cell adhesion motif, and a two-unit RGD binding sequence) to the C-terminal of **436**. Using in vitro experiments, several labs illustrated that the mixtures of these peptides (**228**, **435**, and **436**) are suitable for the 3D cell culture of mouse preosteoblast MC3T3-E1 cells and promote the attachment, proliferation, and osteogenic differentiation of those cells.[949,950]

Hamachi et al. designed a series of glycolipid mimics with muconic amide as the spacer and found that **437**, consisting of *N*-acetylglucosamine as its hydrophilic head and methylcyclohexyl groups as hydrophobic tails, forms a stable hydrogel with a CGC of 0.05 wt %. Besides using TEM to elucidate that hydrogelator **437** self-assembles into a helical, bilayer-type nanofiber with a well-defined network of nanofibers of a high aspect ratio, the authors unexpectedly found that polystyrene nanobeads (100−500 nm in diameter) greatly facilitate the homogeneous 3D dispersion of the supramolecular nanofiber networks. Since **437** also forms a stable hydrogel in cell culture media, such as RPMI1641 or Dulbecco's modified Eagle's medium (DMEM), the resultant hybrid supramolecular matrix

DOI: 10.1021/acs.chemrev.5b00299
Chem. Rev. 2015, 115, 13165−13307

Scheme 55. Representative Molecular Structures of Cell-Compatible Hydrogelators

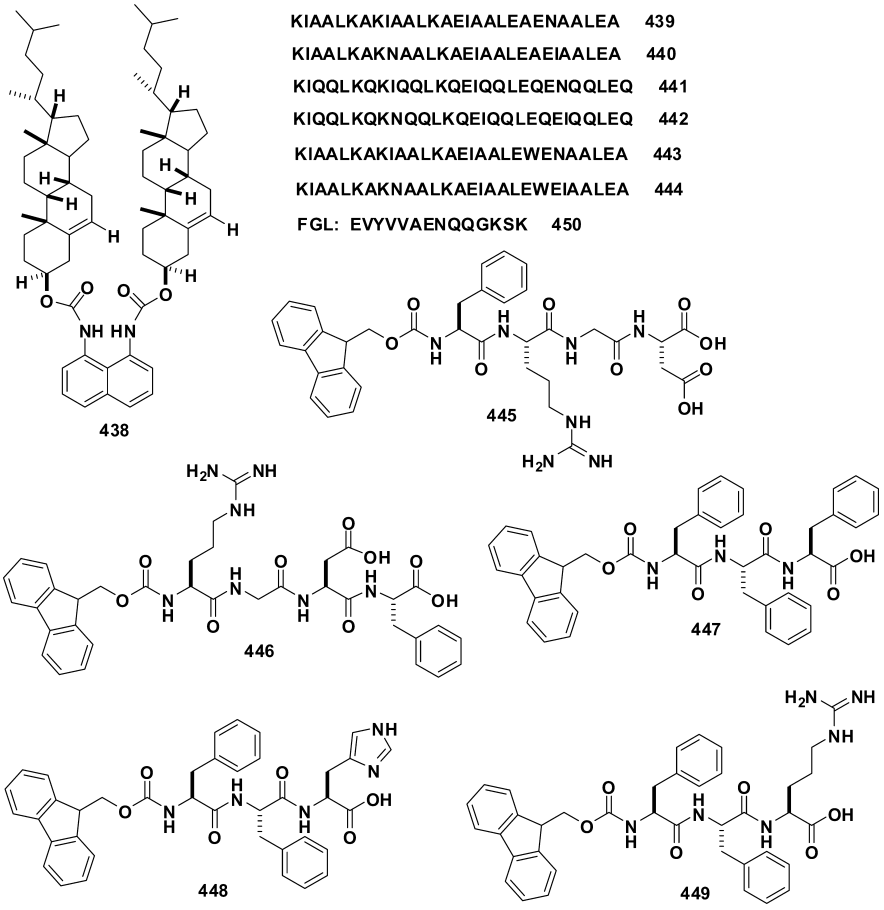

efficiently encapsulates and distributes live Jurkat cells (a human T cell lymphoblast-like cell line) in 3D cell culture under physiological conditions.[951] Recently, Hamachi et al. also reported photoresponsive hydrogels for controlling cell motions[952] and chemically responsive hydrogels for enhancing analyte sensitivity.[953]

5.1.2. Cell-Compatible Hydrogelators. Chou et al. proposed a simple and economical methodology to synthesize dimeric cholesterol derivatives (DCDs) with high yields. The dynamic light scattering analysis and TEM images showed that in aqueous solution most DCD dispersions are irregularly angular shaped with two peaks in the size distribution centered at 204 and 837 nm. In addition, an MTT (3-(4,5-dimethylthiazol-2-yl)-2,5-diphenyltetrazolium bromide)-based cell viability assay indicated that **438** (Scheme 55) is innocuous to human keratinocyte (HaCaT) and squamous cell carcinoma (SCC25) cells at a concentration of 0.05 mM after 24 h incubation with **438**.[954] As a representative example of the de novo β-hairpin peptides, **251** folds as a β-hairpin peptide upon the addition of saline solution, and the β-hairpin peptide self-assembles to form a hydrogel at 2 wt %. Thus, DMEM cell culture media initiate the folding and consequent self-assembly of **251** to afford a hydrogel which is cytocompatible with NIH/3T3 cells.[955,956]

Woolfson et al. reported supramolecular hydrogels formed by rationally designed standard linear peptides (**439**−**444**). Consisting of two 28-residue peptides designed to coassemble, the pair of peptides results in an offset α-helical dimer with complementary sticky ends which promote longitudinal assembly into α-helical coiled-coil fibrils bundling to form nanofibers. On the basis of the coiled-coil heptad repeat that is rich in alanine (for hydrophobic interaction) and glutamine (for hydrogen bonding) residues, the authors demonstrated that the glutamine-rich peptide (**441** + **442**) forms a gel at low temperature which melts on warming, whereas the alanine-rich peptide (**439** + **440**) forms a weak gel at low temperature that strengthens on warming. By replacing one of the surface-exposed alanine residues with the more hydrophobic tryptophan, the authors obtained **443** and **444**, which form hydrogels that support the proliferation and differentiation of rat adrenal pheochromocytoma (PC12) cells.[632,957] Gazit et al. also extended the family of the aromatic Fmoc-dipeptides with a series of new Fmoc-peptides which consist of natural and synthetic amino acids with an aromatic nature for making supramolecular hydrogels. With the assistance of DMSO as the cosolvent, the authors produced the hydrogels at a final peptide concentration of 0.5 wt %. TEM and SEM analysis indicated that the self-assembly of these Fmoc-peptides results in various structures and distinctive molecular and physical properties. A pair of notable peptides in their work are Fmoc-FRGD (**445**) and Fmoc-RGDF (**446**), which self-assemble to form β-sheet-based nanofibers. Using the MTT assay, the authors demonstrated that Chinese hamster ovary (CHO) cells on the hydrogels of **445** and **446** show a high viability after 24 h. However, the cell viability decreases significantly at 72 h.[958]

Palocci et al. used a lipase to trigger the self-assembly of peptide hydrogels of Fmoc-FFF (**447**) via reverse hydrolysis to control or modulate the functions and responses of the

DOI: 10.1021/acs.chemrev.5b00299
Chem. Rev. 2015, 115, 13165−13307

Scheme 56. Representative Molecular Structures of Cell-Compatible Hydrogelators

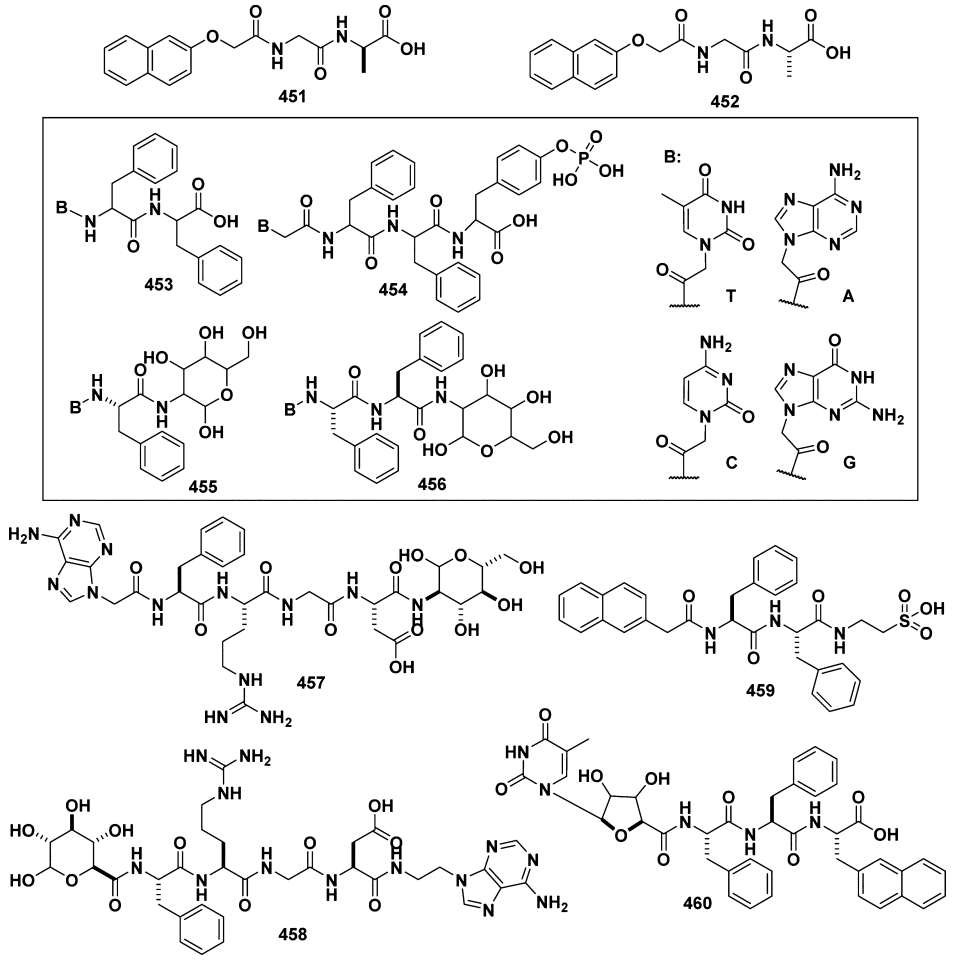

hydrogels according to their preparation conditions. Under physiological conditions, the authors obtained amphiphilic building blocks consisting of tripeptides (Phe-Phe-Phe) linked to Fmoc. SEM and AFM images indicated that the hydrogels of **447** consist of a nanofiber network at 0.14 wt %.[169] On the basis of the cell viability of rat microglial cells incubated with **447** at concentrations up to 300 μg/mL, the authors suggested that the hydrogelator is biocompatible. Later, the authors reported that the hydrogelator also stimulates the production of neurotrophic factor NGF (nerve growth factor) from the microglial cells.[959] Liu et al. reported a hydrolase model based on the nanotubes formed by the self-assembly of a synthetic Fmoc amphiphilic short peptide (Fmoc-FFH, **448**). According to the authors, the imdazolyl groups on the surface of the nanotubes act as the catalytic centers for the hydrolysis of *p*-nitrophenyl acetate (PNPA). Replacing the histidine of **448** with arginine, the authors produced a structurally similar peptide, Fmoc-FFR (**449**), the guanidyl groups of which reside in the nanotubes through the coassembly of these two molecules to stabilize the transition state of the hydrolysis. The authors also reported that this model of peptide hydrolase is compatible with HeLa cells and suggested the applications of these peptides as a substitute for natural hydrolases.[960] Liu et al. synthesized an FGL pepitide amphiphile (**450**) that self-assembles to form nanofibers (10−20 nm) as the scaffold for NSCs. Besides self-assembling to form a hydrogel at a CGC of 1 wt %, **450** at a concentration of 50, 100, or 200 mg/L promotes the proliferation of NSCs, which agrees with the NCAM mimietic properties of the FGL peptide.[961,962] Meanwhile, the authors found that the nanofibers of **450** increase the rate of neuron differentiation from NSCs and concluded that the self-assembled nanofibers of **450** have good biocompatibility with NSCs.[963]

As shown in Scheme 56, Xu et al. designed a series of hydrogelators based on the conjugates of a dipeptide and (naphthalen-2-yloxy)acetic acid. Among these hydrogelators, Nap-Gly-D-Ala (**451**) and Nap-Gly-Ala (**452**) form hydrogels efficiently with CGCs of 0.07 wt %. The hydrogen bonding between dipeptides and aromatic−aromatic interactions of the naphthyl groups cooperatively result in the excellent hydrogelation ability of these hydrogelators. Besides demonstrating that the handedness of the helical fibril structures in the hydrogels correlates with the chirality of the hydrogelators, the authors also found that these molecular hydrogelators are compatible with HeLa cells when the concentration of the hydrogelators is 200 μM and the incubation time is 24 h.[964] Recently, Xu et al. reported a new class of hydrogelator (**453** and **454**) based on conjugates of nucleobases (e.g., thymine, adenine, cytosine, and guanine) and ultrashort peptides which self-assemble in water upon application of a pH or enzymatic stimulus to afford a new class of supramolecular hydrogels that are biocompatible (Figure 10). The studies on the gelation properties indicate that all these nucleopeptides self-assemble to generate β-sheet nanostructures at a concentration of 2 wt %. In addition, the hydrogelators also exhibit significant resistance to proteinase K, which makes them attractive materials for

DOI: 10.1021/acs.chemrev.5b00299
Chem. Rev. 2015, 115, 13165−13307

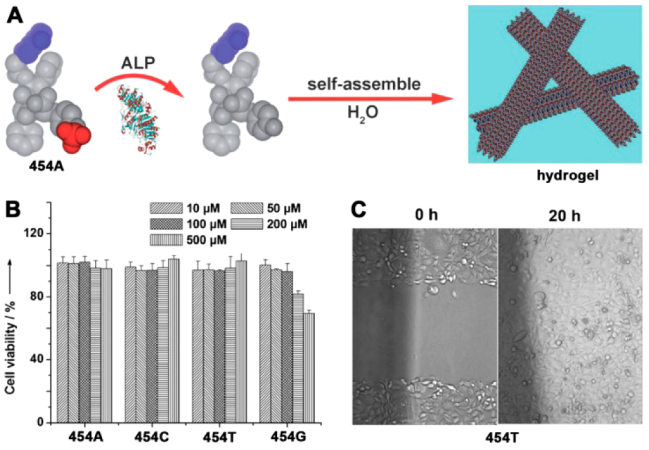

Figure 10. (A) Dephosphorylation process catalyzed by ALP with **454A** to result in nanofibers and a hydrogel. (B) Cell viability test for 72 h of **454**. (C) Optical images of HeLa cells on the surface 0 and 20 h after creation of scratchs in the presence of hydrogel **454T** (by adding 27.7 mM **454T** to the media). Adapted with permission from ref 965. Copyright 2011 Wiley-VCH Verlag GmbH & Co. KGaA.

applications in vivo. Besides illustrating the first example of nucleopeptides as hydrogelators made by an enzymatic reaction, the approaches illustrated by the authors provide a facile way to explore the potential applications of nucleopeptides as soft biomaterials.[965] One possible application may be kinase detection, as shown by Yang et al.[966] Meanwhile, Xu et al. also developed simple conjugates of a nucleobase, amino acids, and a glycoside as a new class of supramolecular hydrogelators (**455** and **456**). Consisting of the three unified building blocks of life,[967] these hydrogelators self-assemble in water to yield ordered nanostructures and supramolecular hydrogels at a concentration of 3 wt %. The conjugates not only exhibit exceptional biocompatibility and biostability, but also facilitate the entry of nucleic acids into the cytosol and nuclei of cells through interbase interactions with nucleic acids. In addition, the integration of a saccharide at the C-terminal into the hydrogelators significantly enhances their resistance to proteinase K,[968] which greatly expands the use of this kind of hydrogel in vivo. As a facile way to generate a fundamentally new molecular architecture from the unified building blocks of life,[967] this approach promises the development of sophisticated soft biomaterials from a rather simple pool of building blocks.

Encouraged by the self-assembly of the conjugates of a nucleobase, amino acids, and a glycoside, Xu et al. explored the biological functions of the self-assembly of this kind of conjugate. They engineered a multifunctional small molecule that consists of adenine (as an assembly domain), an Arg-Gly-Asp sequence (RGD, as a binding domain), and glycosamine (as a glycogen), and found that the assemblies of the conjugates (**457**) promote the proliferation of mES cells and the development of zygotes into blastocysts of mouse.[969] In addition, they found that each module (i.e., nucleobase, RGD, and glycosamine) in the conjugate is indispensable for the observed functions according to the cell proliferation test of the "structural mutants" of **457**. On the basis of this work, the authors suggested that the self-assembly of this kind of de novo glycoconjugate (**457**) promises a potential approach to use supramolecular assemblies as multifunctional mimics of glycoconjugates,[969] including glycoproteins. Furthermore, Xu et al.[970,971] replaced the adenine of **457** with thymine, generating an analogue of **457** which belongs to an unprecedented type of small molecules that consist of unified building blocks of life.[967] This analogue self-assembles in water to form nanofibrils and results in a hydrogel at a concentration of 3.0 wt %. One important observation of this work is that the glycoside at the C-terminal of the peptide greatly enhances the proteolytic resistance of RGD in the hydrogelator (**457**).

Later, Xu et al. synthesized another glycoconjugate, **458**, and its analogues based on the three fundamental biological building blocks (i.e., saccharides, amino acids, and nucleobases) by SPPS. They found that all these conjugates were compatible

Scheme 57. Representative Molecular Structures of Cell-Compatible Hydrogelators

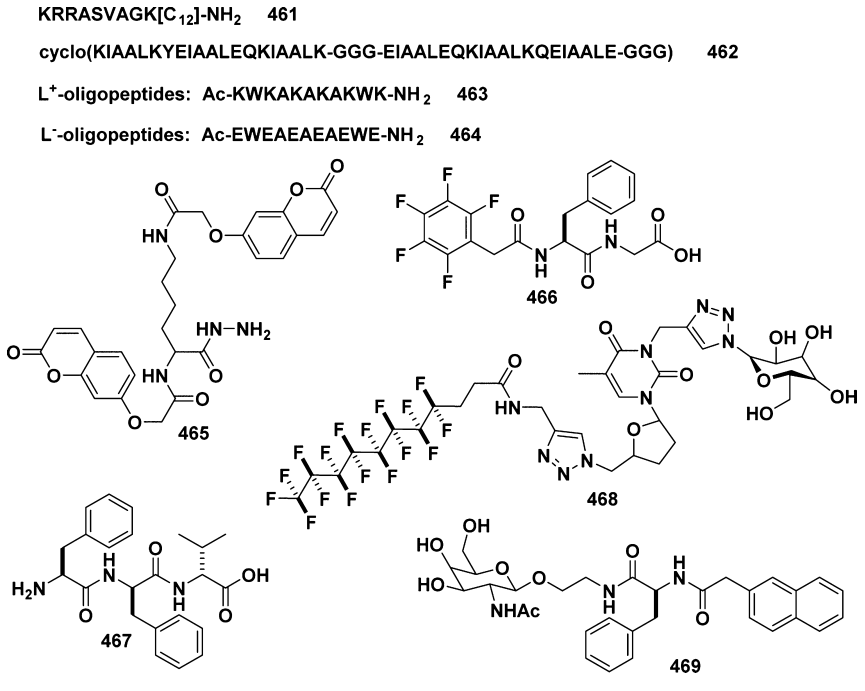

DOI: 10.1021/acs.chemrev.5b00299
Chem. Rev. 2015, 115, 13165−13307

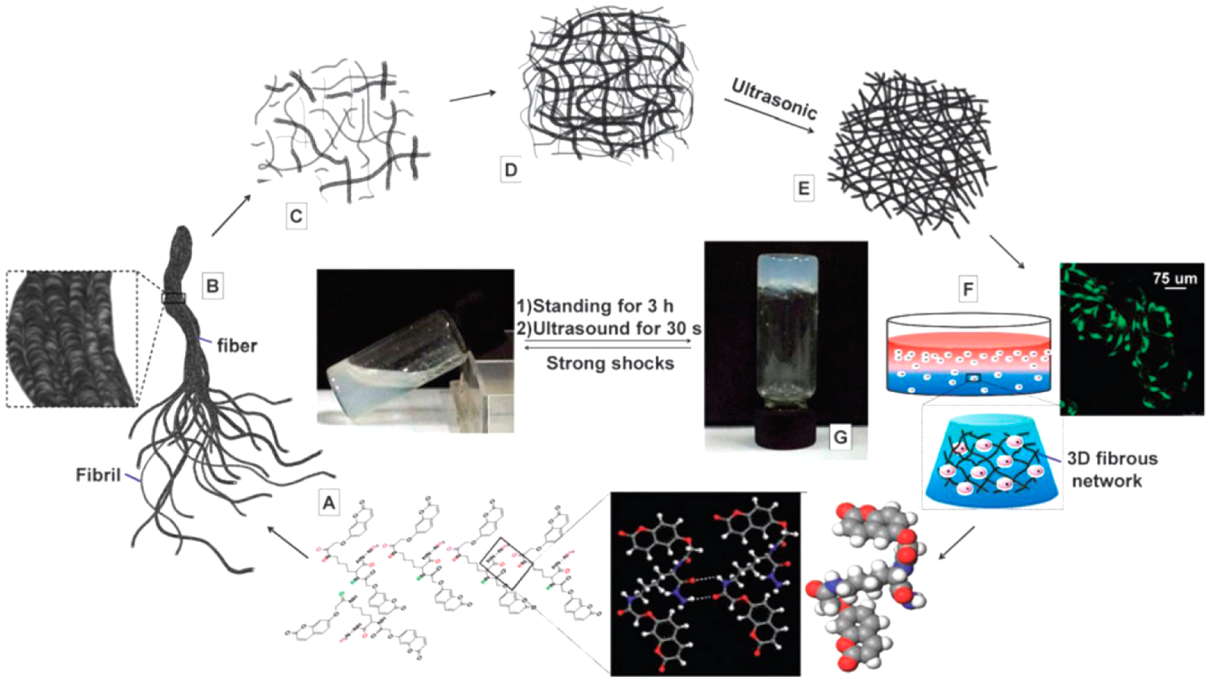

Figure 11. Formation mechanism of hydrogel **465**: (A) hydrogen-bond-driven self-assembly, (B) self-assembled fibrils, (C) fibrils with a hydrogelator concentration lower than the minimum gelation concentration (MGC), (D) entangled fibrils with a hydrogelator concentration higher than the MGC, (D) well-organized 3D hierarchical nanoarchitectures with ultrasound treatment, (F) cells seeded in hydrogels, (G) optical image of the hydrogel (the transition from solution to hydrogel was reversible). Adapted with permission from ref 85. Copyright 2013 Royal Society of Chemistry.

with HeLa cells even at a concentration of 415 μg/mL.[972] Xu et al. reported the first hydrogelator (**459**) consisting of both proteinogenic amino acids (e.g., phenylalanine) and a non-proteinogenic amino acid (e.g., taurine) by attaching taurine at the C-terminal of a well-established self-assembly motif (**3**). The authors found that, besides the pH, the temperature and ultrasound affect the gelation behavior of **459** to result in different morphologies of the nanostructures. In addition, the MTT-based cell viability assay indicated that **459** is biocompatible with HeLa cells for 3 days at a concentration of 500 μM.[87] On the basis of the study of the nucleobase−amino acid−saccharide conjugates, Xu et al. also designed another kind of hydrogelator which is a nucleobase−saccharide−amino acid conjugate.[973] Among all the hydrogelators, **460** forms a typical hydrogel (with a CGC of 0.8 wt % at pH 7.0) which turns into a solution at 59 °C or at pH above 9.0. This study illustrates the incorporation of L-3-(2-naphthyl)alanine as an effective strategy to promote molecular self-assembly in water. Furthermore, the addition of T_{10} appears to result in a mechanically stronger hydrogel which consists of nanofibers with widths increasing from 7 ± 2 to 17 ± 2 nm. The in vitro experiments indicate that **460** is compatible with HeLa cells at concentrations up to 500 μM for 3 days.[974]

As shown in Scheme 57, Stupp et al. reported a peptide amphiphile (**461**) with its sequence (KRRASVAGK[C_{12}]-NH_2) containing the specific consensus substrate (RRXSO; X = any residue; O = hydrophobic) for protein kinase A (PKA), a ubiquitous kinase in intracellular signaling and metabolism that has also been demonstrated to be an extracellular cancer biomarker. **461** is able to form a hydrogel with a β-sheet secondary structure in the nanofibers, and its assembly and disassembly can be reversibly controlled by PKA. In addition, the authors suggested that the disassembly of the nanofibers of **461** by using PKA might contribute to an enzyme-triggered release of an encapsulated cancer drug. The authors also reported an in vitro experiment to show the peptides themselves to be compatible with cells while the drug-loaded nanofibers of **461** induce preferential cytotoxicity in a cancer cell line that is known to secrete high levels of PKA, such as the MDA-MB-231 human breast cancer cell line.[975] Ryadnov et al. designed a self-assembling peptide (**462**) which contains two domains that oligomerize by forming a parallel coiled-coil heterodimer. In this arrangement, each domain pairs with its complementary partner from another copy of the same peptide, connected through two short linkers and cyclized antiparallel to each other such that interactions occur between different peptides. One unusual feature of **462** is that it forms hyperbranched fibrillar networks spanning from nano- to micrometer dimensions. Although this elaborately designed peptide is less effective than collagen for promoting the proliferation of human dermal fibroblast cells, the decoration of a cell attachment motif (e.g, a mimic of YIGSR) results in a 20% increase of cell proliferation compared with the bare scaffold.[976]

Yu et al. designed four oligopeptides; the two positive sequences (L^+ (**463**) and D^+ (**463**)) contain alternating neutral (W and A) and positively charged (K) residues, while the two negative sequences (L^- (**464**) and D^- (**464**)) replace lysine by negatively charged glutamic acid (E). The oppositely charged oligopeptide modules can interact with each other electrostatically, coassemble, and form a hydrogel. According to the in vitro experiments reported by the authors, the L-homochiral hydrogels of **463** are the most cell compatible, leading to the highest human mesenchymal stem cell (hMSC) viability and proliferation, but the peptides are susceptible to proteases. However, the D-oligopeptide hydrogels of **463**, which resist

DOI: 10.1021/acs.chemrev.5b00299
Chem. Rev. 2015, 115, 13165−13307

proteases, are unable to support cell hMSC proliferation. The authors found that negative charges significantly improve hMSC growth in the D-oligopeptide hydrogels of **464** but have little effect on their interactions with the L-oligopeptide hydrogels of **464**. This interesting observation indicates that negative charges can compensate for the disadvantage of the D-homochiral hydrogels.[977] Gu et al. reported a hydrogelator connecting 7-(carboxylmethoxy)coumarin molecules and hydrazine linked by L-lysine (DCOU-Lys-CONH-NH_2, **465**) to act as lipophilic and water-soluble moieties. **465** self-assembles to form hydrogels in distilled water with a CGC of 1 wt %. **465** starts to self-assemble into short fibrils even at concentrations lower than the CGC. In addition, ultrasound accelerates the gelation and induces homogeneous self-assembly to form nanofibers with average diameters between 30 and 40 nm (Figure 11). On the basis of a LIVE/DEAD assay, the authors reported that the hydrogel is preferable for the migration and proliferation of NIH/3T3 fibroblast cells.[85]

Lin et al. have reported the detailed study of a new series of small molecular hydrogelators, among which the intramolecular alternative packing of the phenyl/perfluorophenyl pair promotes the formation of supramolecular nanofibers and hydrogels at pH 5 with a CGC of 1.0 wt %. The authors also reported that **466** is compatible with the CTX TNA2 cells in a concentration range of 10−500 μM for 48 h.[978] The same lab recently reported a co-assembled hydrogel based on naphthalene diimide for treating MCF-7 cells.[979] Marchesan et al. designed a series of uncapped hydrophobic heterochiral tripeptides with all combinations of D- and L-amino acids to minimize the disadvantages of L- or D-peptides. Rheology and XRD results indicated that, among all the heterochiral tripeptides, **467** forms a hydrogel with a β-sheet amyloid structure. According to the LIVE/DEAD assay, the authors showed that **467** maintains the viability and proliferation of L929 mouse fibroblast cells in vitro for 3 days.[980] Taking advantage of click chemistry, Barthélémy et al. designed and synthesized two glycosyl-nucleoside fluorinated amphiphiles (GNFs, **468**) which feature either β-D-glucopyranosyl or β-D-lactopyranosyl moieties linked to a thymine nucleobase. On the basis of the air−solution surface tension (γ) measurements, the authors reported that the critical aggregation concentrations (CACs) are 5.9 and 3.7 μM, respectively. Gelation tests indicate that both of the GNFs self-assemble to form entangled nanofibers roughly 10−20 nm in diameter and the β-D-glucopyranosyl-based GNF shows a CGC of 0.1% (w/w). The authors also reported that β-D-glucopyranosyl is compatible with a human cell line (Huh-7, human hepatocarcinoma cell line).[981] The same lab also reported the hydrogels made of glycosyl-nucleoside bola-amphiphiles (GNBAs) for culturing human mesenchymal stem cells isolated from adipose tissues.[982] Wang et al. designed and synthesized three amino acid derivative−saccharide conjugates, among which **469** self-assembles to form stable hydrogels containing nanofibers with diameters of 80−300 nm at a concentration of 0.2 wt %. The authors found that the extensive hydrogen bonds between sugar rings contributed to the formation of $\pi-\pi$ stacking between aromatic naphthalene groups, which results in the formation of stable hydrogels in aqueous solutions. Using an MTT-based cell viability assay, the authors verified that these kinds of saccharide-based hydrogels are compatible with NIH3T3, HepG2, AD293, and HeLa cells. In addition, these cells show a good adhesion and proliferation rate on the surface of hydrogels in a 2D environment.[983] It would be interesting to know how the hydrogelators affect the morphological properties of these cells.

5.1.3. Cytotoxic Hydrogelators. While most of the research activities are centered on the use of supramolecular hydrogels for promoting cell proliferation, Xu et al. have been working on the design of supramolecular hydrogelators to inhibit cell selectively. For example, as shown in Scheme 58, Xu

Scheme 58. Representative Molecular Structures of Cytotoxic Hydrogelators

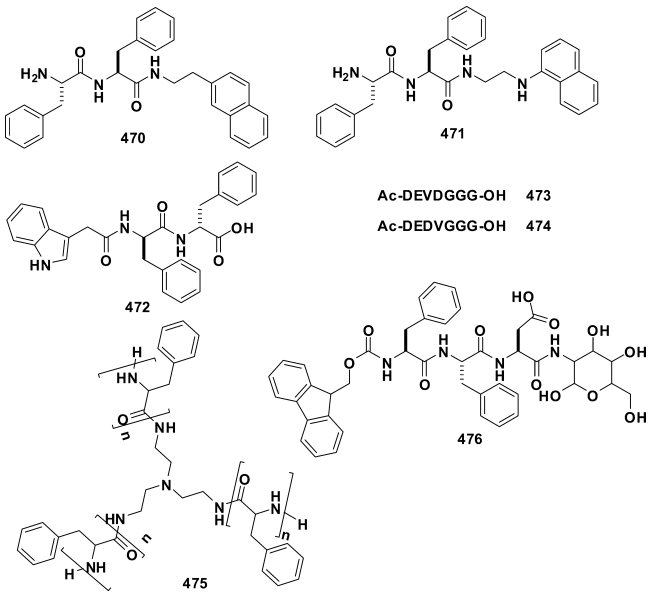

et al. designed and synthesized a new class of supramolecular hydrogelators (**304**, **470**, and **471**) consisting of N-terminated diphenylalanine and naphthalene motifs. They found that the hydrogelators self-assemble to result in nanofibers and hydrogels at a concentration of less than 0.8 wt %, but within a relatively narrow pH range (5.0−6.0). Interestingly, the authors found that these hydrogelators exhibited significantly higher cytotoxicity to HeLa cells than to Ect1/E6E7 cells, which proves that hydrogelators selectively inhibit cancer cells.[763] Thordarson et al. reported the synthesis of a new hydrogelator (**472**) with an indole capping group which forms exceptionally strong hydrogels in a variety of environments with a CGC of 0.4 wt %. Cell viability studies of HeLa cells indicate that **472** exhibits compatibility with cells at lower concentrations while being cytotoxic at concentrations up to 0.1 wt %.[984] Liang et al. reported heptapeptide hydrogelators **473** based on the DEVD peptide sequence, which is a specific substrate for caspase-3. The cryo-TEM photograph indicates that **473** self-assembles to form a hydrogel containing flexible and long nanofibers with an average width of 6.1 ± 1.2 nm. The MTT cell viability assay shows that **473** is slightly more compatible with Hep G2 cells than its isomeric control hydrogelator (**474**) at 400 μM for 3 days. Western blot analysis indicated that the isomer **474**, which is not a substrate of caspase-3, at 400 μM, obviously is able to activate caspase-3 to induce cell death via apoptosis.[985]

Numata et al. reported the high-yield chemoenzymatic synthesis of linear oligo(L-phenylalanine) by proteinase K from *Tritirachium album*. By connecting the synthesized linear oligo(L-phenylalanine) with tris(2-aminoethyl)amine, they obtained a star oligo(L-phenylalanine) (**475**) that self-assembles

DOI: 10.1021/acs.chemrev.5b00299
Chem. Rev. 2015, 115, 13165−13307

into fluorescent fibers with various branching ratios. The authors reported that the oligo(L-phenylalanine) analogues exhibit slight cytotoxicity to human embryonic kidney 293 cells (HEK293) at a concentration above 25 mM after 8 h.[986] Zhang et al. designed and synthesized a glycopeptide (**476**) consisting of the Fmoc-Phe-Phe-Asp sequence and a therapeutic glucosamine moiety. **476** dissolves well to form a homogeneous solution at an elevated temperature and a concentration of 1 wt % and forms a stable hydrogel at pH 7.4 upon being cooled to room temperature. An MTT-based cell viability assay indicated that the glycopeptide slightly inhibits the NIH/3T3 fibroblast cells on the surface of the hydrogel. Most importantly, the authors reported that the hydrogel of **476** is able to inhibit postoperative fibrosis in eye surgery (Figure 12), as evidenced

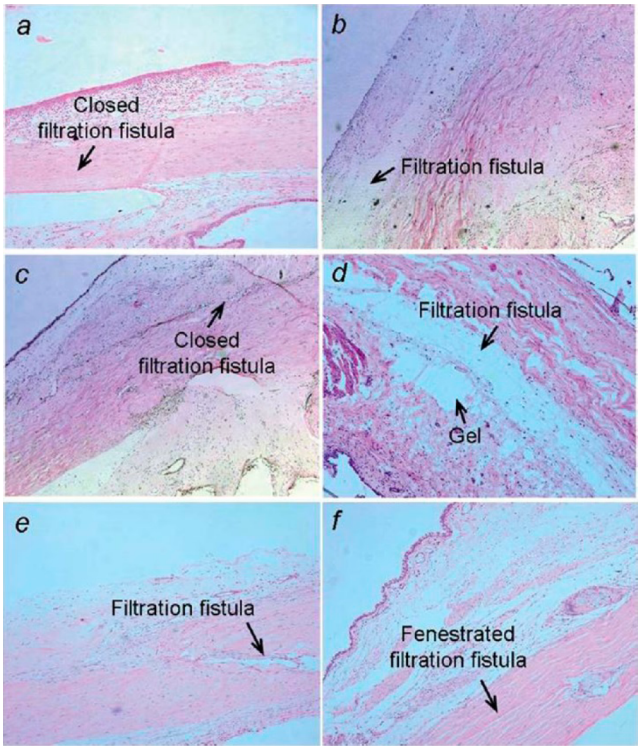

Figure 12. Histological section of rabbit eyes which underwent filtration surgery (a) alone at 14 days postsurgery, received the Fmoc-FF (**6**) hydrogel at (b) 7 and (c) 14 days postsurgery, and received the glycopeptide hydrogel (**476**) at (d) 7, (e) 14, and (f) 21 days postsurgery. Hematoxylin−eosin; magnification 100×. Adapted with permission from ref 92. Copyright 2012 Royal Society of Chemistry.

by the fact that the filtration fistula is constantly smooth and the mean intraocular pressure is significantly lower within 21 days postsurgery compared with the results from conventional antiproliferative drug injections.[92]

5.1.4. Cell Adhesion. As shown in Scheme 59, Stupp et al. linked a cyclic RGD motif at the side chain of a peptide amphiphile to construct a branched architecture in the monomer **477**, which self-assembles to form cylindrical nanofibers having a very high aspect ratio and therefore mimicks the soft fibrous environment in the ECM. By changing the local dynamics either through the architecture of the molecules or dilution of the epitopes, the authors were able to tailor the density of RGD epitopes on the nanofibers to an extremely high level. In addition, the authors found that branched architectures of the monomers and additional space for epitope motion improve signaling for cell adhesion, spreading, and migration of NIH/3T3 fibroblast cells in 2D and MDA 231 cells in 3D cell migration.[987] In a related study, Zhou and Zhang et al. reported cyclic RGD exhibiting synergistic effect with a BMP-7 derived peptide in the differentiation of mesenchymal stem cells.[988] Besides the branched architecture with the cyclic RGD epitope reported by Stupp et al., Hamley et al. investigated the Fmoc-tetrapeptide Fmoc-RGDS (**478**) consisting of the RGDS cell adhesion motif from fibronectin. Circular dichroism and fiber X-ray diffraction indicated that the self-supporting hydrogel formed by sonication and heating/cooling at a concentration of 1 wt % is comprised of parallel β-sheet nanofibers with a diameter of approximately 10 nm. The authors suggested that **478** may be used to produce collagen-based gels for growing corneal fibroblasts.[989]

Yang et al. reported an intriguing example in which the peptide **479** self-assembles to form nanofibers and results in a hydrogel with a CGC of 0.3 wt %. The resulting hydrogel is able to selectively form a thin layer of hydrogel at the surface of platelets, thus preventing human platelet aggregation induced by various agonists such as collagen.[990] Yang et al. also designed and synthesized a class of supramolecular hydrogelators consisting of the tripeptide sequence glycine-Xaa-4(*R*)-hydroxyproline (GXO; Xaa is any one of the natural amino acids) from collagen. Among all these hydrogelators, **480** self-assembles in aqueous solution to form nanofibers with a diameter of 20−30 nm and with a CGC of 0.06 wt %. Furthermore, **480** promotes the cell adhesion of NIH/3T3 fibroblasts, a property similar to that of collagen, which makes it suitable for 2D cell culture.[991] They reported another collagen mimic hydrogelator, **481**, that self-assembles to form a thixotropic hydrogel, consisting of flexible nanofibers of about 9 nm, at a concentration of 2 wt %. Importantly, the authors found that the hydrogel of **481** selectively enhances Flk1 expression in differentiated murine embryonic stem (mES) cells.[992] Mihara et al. designed a glutamic acid residue-conjugated β-sheet peptide, E1Y9 (**482**), which, at a concentration of 2 wt %, undergoes hydrogelation in the presence of Ca^{2+}. The hydrogel contains disentangled and wider nanofibers than the original Y9 nanofibers. The hydrogel maintains its shape well to allow it to be molded to a short string. The authors conjugated the RGDS sequence to the C-terminals of **482** peptides and obtained a new peptide, E1Y9-RGDS (**483**), which can be mixed with **482** to form hydrogel strings. One impressive result is that PC12 adheres to the hydrogel string and differentiates in 6 days (Figure 13), suggesting that the surface of the hydrogels resembles that of fibronectin surfaces.[993]

As shown in Scheme 60, Feng et al. reported a series of PEG-containing hydrogelators by coupling ethylene glycol (EG) monomers and the RGD motif onto C_2-benzene cores to resist protein adsorption and promote cell adhesion. TEM images indicated that **484** self-assembles to form entangled fibrous gel networks with fiber diameters of 68.9 ± 4.3 nm at a CGC of 0.07 wt %. The incorporation of the RGD sequence into **484** not only influenced the supramolecular structure and viscoelasticity of the fibers, but also contributed to overcoming nonspecific protein adsorption and promoting adhesion of encapsulated cells, which makes **484** suitable for 2D and 3D culture of human hepatoma cells and normal human skin fibroblasts.[994] Furthermore, it is feasible to vary the supramolecular self-assembly of **484** for controlling the cell adhesion

DOI: 10.1021/acs.chemrev.5b00299
Chem. Rev. 2015, 115, 13165−13307

Scheme 59. Representative Molecular Structures of Hydrogelators for Cell Adhesion

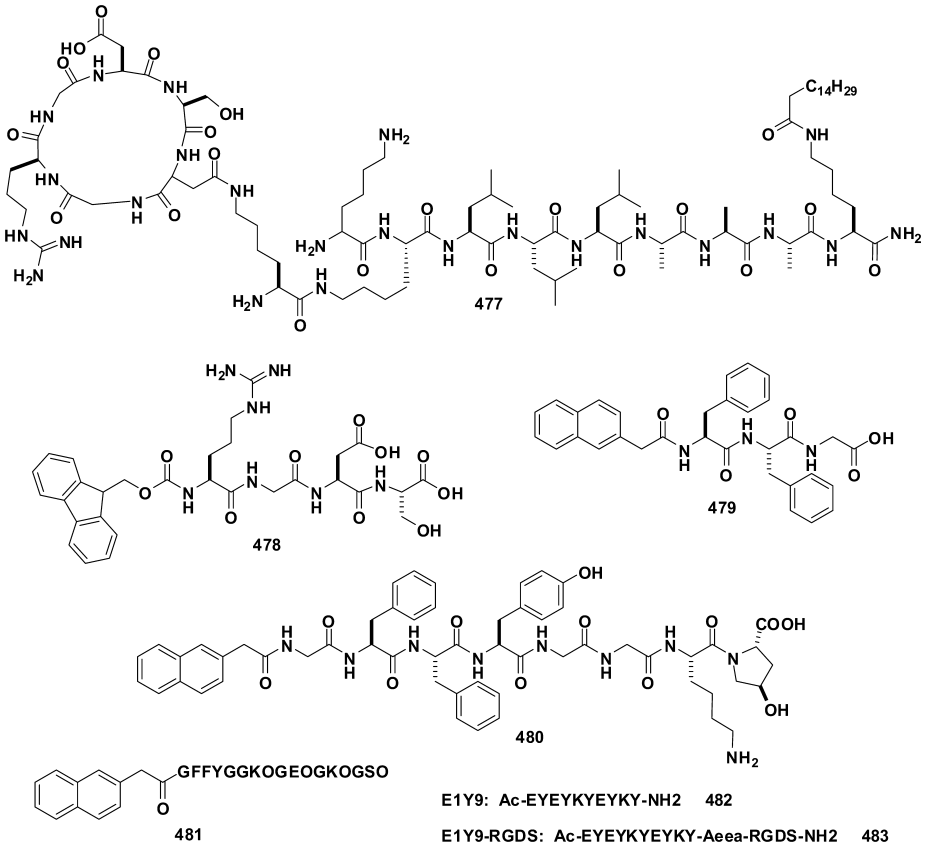

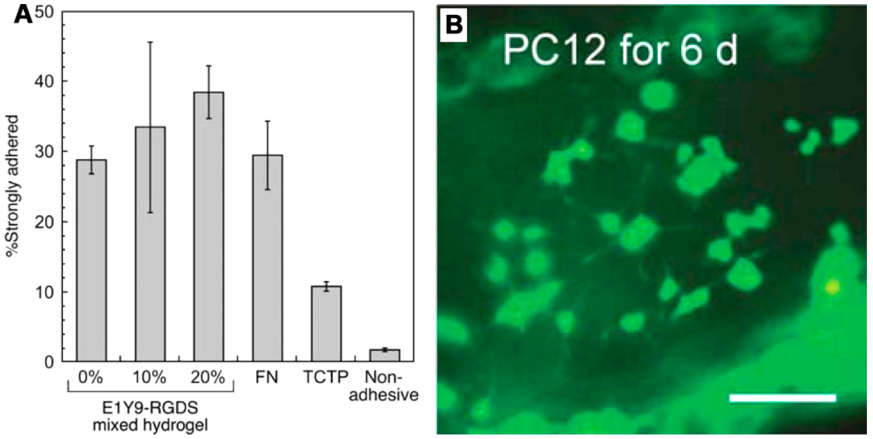

Figure 13. (A) Percentages of strongly attached 3T3-L1 cells. 3T3-L1 cells were incubated on the flat hydrogels composed of **482** containing 0%, 10%, or 20% **483**, fibronectin (FN), tissue-culture-treated plates (TCTPs), or nonadhesive plate surfaces in Dulbecco's modified Eagle's medium containing 5 mM Ca^{2+}. (B) Fluorescence microscopic images of cell-adhered peptide gel strings. PC12 cells were cultured in Dulbecco's modified Eagle's medium containing 5 mM Ca^{2+} for 6 days. The scale bar represents 100 μm. Adapted with permission from ref 993. Copyright 2012 The Society of Polymer Science, Japan (SPSJ).

and proliferation in 2D and 3D microenvironments.[995,996] Meanwhile, Feng et al. also reported a new kind of hydrogel derived from the combination of a C_2-phenyl-derived gelator and a polysaccharide (alginate). After addition of Ca^{2+}, the conjugate self-assembles to form flexible nanofibers with branches and twists. The LIVE/DEAD cell viability assay indicates that the hydrogel exhibits no cytotoxicity to normal human skin fibroblasts (NHSFs) and promotes cell adhesion and spreading in vitro.[997] The hydrogels formed by the coassembly of C_2-phenyl-based hydrogelators and sodium hyaluronate showed a high swelling property to ensure cell migration and proliferation inside the bulk of the hydrogels.[998] The authors also investigated the influence of the chirality of the nanofibers on cell adhesion and proliferation by using two enantiomers of C_2-phenyl-derived hydrogelators. They found that left-handed helical nanofibers (containing an L-phenylalanine derivative) can increase cell adhesion and proliferation, whereas right-handed nanofibers (containing a D-phenylalanine derivative) have the opposite effect.[999] It would be more

DOI: 10.1021/acs.chemrev.5b00299
Chem. Rev. 2015, 115, 13165−13307

Scheme 60. Representative Molecular Structures of Hydrogelators for Cell Adhesion

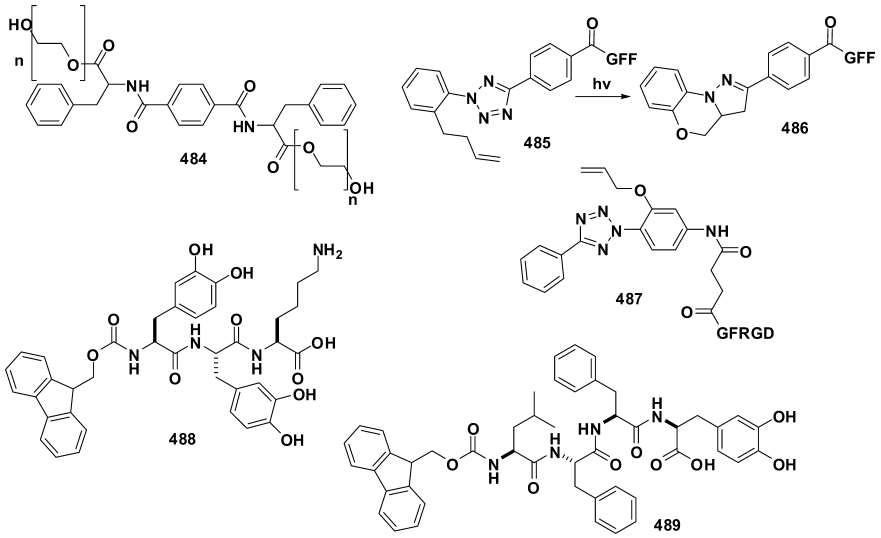

informative if the authors had examined the biostability of the hydrogelators.

Zhang et al. reported a class of photoresponsive small molecular hydrogels (Tet(I)-GFF (**485**) and Tet(II)-GFRGD (**487**)) formed by the self-assembly of short peptides linked with a biaryl-substituted tetrazole-moiety-based phototrigger. At pH 7, **485** forms a clear and stable hydrogel with a CGC of 0.08 wt %. Upon mild light irradiation, **485** undergoes fast intramolecular photo click ligation, and the complete transformation from **485** to **486** takes <2 min. This photoreaction disturbs the self-assembled hydrogel matrixes and induces the photodegradation of the hydrogel, which modulates the cellular microenvironments when the hydrogel of **485** serves as the scaffolds for cell cultures. The authors demonstrated that the irradiation of the hydrogel causes the cell to express much higher levels of differentiation markers. The authors also demonstrated that the hydrogel of **487** at a concentration of 0.9 mg/mL can mimic the 3D microenvironment for the hMSCs.[1000] On the basis of the Fmoc-FF (**6**) hydrogelator, Gazit et al. designed the DOPA-containing DOPA-DOPA and Fmoc-DOPA-DOPA peptides **301** that self-assemble to form a hydrogel at 0.25 wt %. The authors reported that the hydrogels of these DOPA-containing peptides reduce ionic silver into silver nanoparticles. In addition, the conjugation of lysine (Lys) with **301** generates **488**, which self-assembles to form ordered nanostructures in the presence of dimethyl sulfoxide (DMSO) and water. The authors envision that it may serve as a multifunctional platform for various biotechnological applications.[732] He et al. reported an Fmoc-protected tetrapeptide amphiphile for fabricating a bioadhesive hydrogel with DOPA groups as affinity fusion tags (Fmoc-LFF-DOPA, **489**). A 2000 U/mL concentration of of metalloprotease can trigger **489** to form a transparent yellow molecular hydrogel. On the basis of a LIVE/DEAD assay, the authors inferred that the hydrogel of **489**, containing the catechol groups, could successfully promote the adhesion and proliferation of adult human dermal fibroblast cells in vitro.[1001] It would be useful to know the mechanism behind this adhesion.

5.1.5. Others. As shown in Scheme 61, Liang et al. designed a radioactive probe (**490**) that intracellularly forms radioactive nanoparticles under the action of furin in living tumor cells. They found that, upon 160 min of cellular efflux, the

Scheme 61. Representative Molecular Structures of Hydrogelators

Acetyl-Arg-Val-Arg-Arg-Cys(StBu)-Tyr(I-125)-CBT **490**

FEFKFEFKGRGD **491** ^{D}FEFK^{D}FEFKYRGD **492**

radioactivity retained in MDA-MB-468 cells incubated with **490** remains at a high level.[1002] Wang and Long et al. intended to design the peptide sequence FEFKFEFKGRGD (**491**) by adding a hydrophilic peptide (RGD) to the EFK8 peptide to decrease the strong aggregation properties of EFK8, therefore allowing hydrogels to form in neutral pH conditions. However, the results proved that this strategy was unsuccessful. Interestingly, they found that the hydrogel of **491** specfically supports and stimulates the growth of *Delftia XD*, a bacterium.[1003] Chen and Yang et al. reported another strategy to form hydrogels of EFK8 peptide derivatives at neutral conditions by the replacement of F with ^{D}F and the introduction of a hydrophilic RGD tripeptide (^{D}FEFK^{D}F-EFKYRGD, **492**). They found that **492** self-assembles to form hydrogels in PBS buffer with a CGC of 0.15 wt %. In addition, the LIVE/DEAD assay showed that the hydrogel of **492**, at a concentration of 2 wt %, is suitable for cell proliferation and produces a colony of HeLa cells in vitro.[1004] This ingenious doping of D-amino acid residues for controlling the self-assembly behaviors of the hydrogelator may be general and applicable for other peptide sequences.

5.2. Chemo/Biosensors

Chemo/biosensors for visual detection are a class of increasingly attractive tools for the analysis of many targets (e.g., biological markers, enzymes, ions, gases, etc.).[562] They are extremely useful for rapid and high-throughput diagnostics or detection in situations where low cost, speed, and ease are required. "Stimulus-responsive" or "smart" supramolecular hydrogels, thus, attract tremendous attention as a platform[1005] for chemosensors because they have the following properties/advantages: (i) A variety of biological, chemical, or physical triggers (e.g., temperature, pH, ionic strength, electric field, enzyme, etc.) instruct the formation of supramolecular hydrogels which report the presence of the targets.[1006,1007] For example, hydrogel formation triggered by enzymes can serve as an indicator of certain enzymes.[1008,1009] (ii) Supra-

DOI: 10.1021/acs.chemrev.5b00299
Chem. Rev. 2015, 115, 13165−13307

Scheme 62. Representative Molecular Structures of Hydrogelators

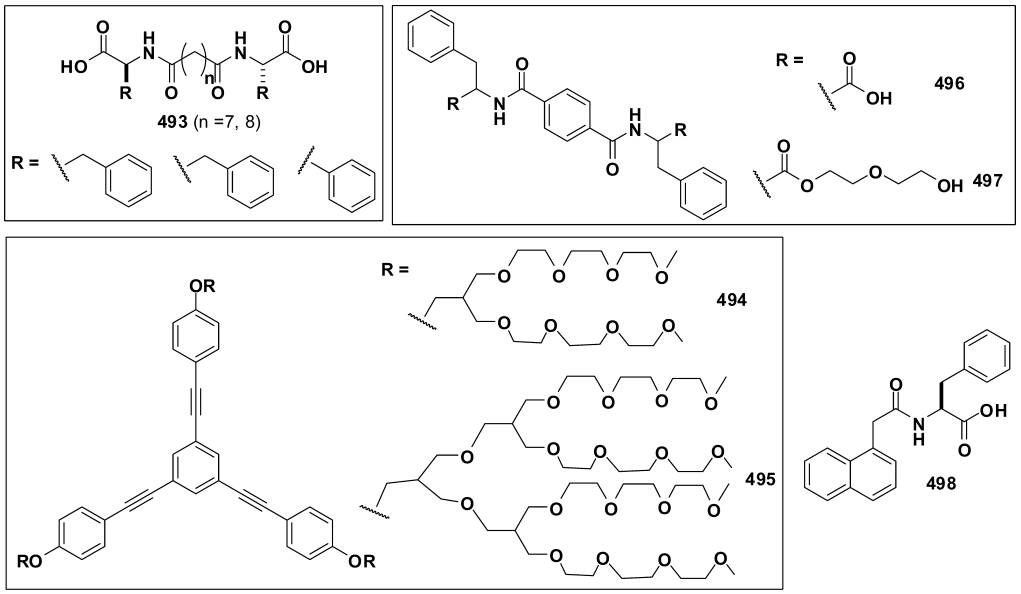

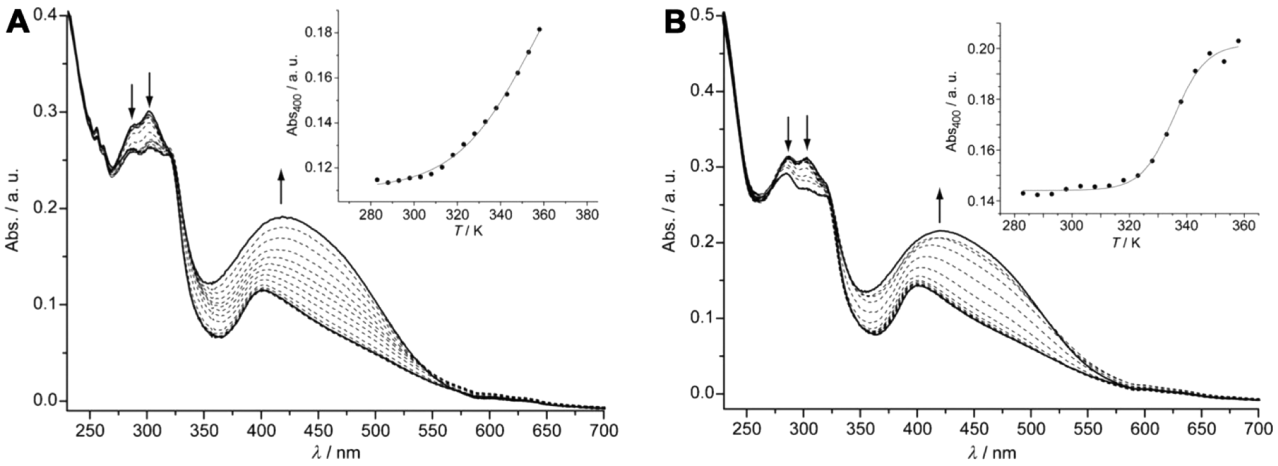

Figure 14. Temperature-dependent UV/vis spectra of aqueous solutions (~10^{-5} M) of (A) **494** and (B) **495** containing 1 equiv of disperse orange 3. Arrows indicate the spectroscopic changes with increasing temperature. The insets depict the changes in the absorbance at 400 nm as a function of temperature. Adapted with permission from ref 1021. Copyright 2010 Wiley-VCH Verlag GmbH & Co. KGaA.

molecular hydrogels are able to incorporate/immobilize a variety of colorimetric reagents, such as visible dyes, both covalently and noncovalently.[1010] A range of diverse yet selective molecular interactions can lead to a color change of the hydrogel, for example, stimulus-induced release or absorbance of dye molecules and color changes of the hydrogels initiated by target binding. (iii) Supramolecular-hydrogel-based chemosensors can work in aqueous conditions, which is of extreme importance because most biological substances (e.g., enzymes, biomarkers, etc.) remain active only in physiological conditions (i.e., in aqueous solution).[1011] In the following subsections, we briefly describe these applications.

5.2.1. Dye/Molecule Absorption. Supramolecular hydrogels show solidlike, yet soft, properties and contain three-dimensional networks, formed by hydrogelators, to not only imbibe water, but also immobilize other components, such as small molecules, enzymes, and ions, especially when the hydrogels serve as chemo/biosensors. Before discussing supramolecular-hydrogel-based chemo/biosensors, we first highlight some recent works on hydrogels used as efficient absorbents of dyes, metal ions, and other molecules.[1012−1015] Due to the use of a wide range of dyes in several industries (e.g., paper, plastics, textiles, and cosmetics), it is necessary to remove the dyes from industrial discharge to prevent pollution. Among all kinds of methods, absorption is more preferred due to its low cost, high efficiency, and easy handling. Supramolecular hydrogels which contain both hydrophilic and hydrophobic groups can absorb a variety of dyes[1016−1018] and may have superiority in the recycle and adsorption rate compared with some traditional methods. As shown in Scheme 62, Banerjee and co-workers report a phenylalanine-based bolaamphiphile, **493**, containing a centrally located oligomethylene group, which affords a hydrogel at pH 6.5−7.2 in the presence of divalent metal salts (e.g., $MnCl_2$, $CoCl_2$, $CuSO_4$, and $NiCl_2$). By studying the hydrogelation behaviors of these molecules, Banerjee et al. concluded that these hydrogels not only can entrap and release a biological substance, but also can efficiently adsorb various toxic dyes, such as crystal violet and naphthol blue black from water.[1019] The same group reported

DOI: 10.1021/acs.chemrev.5b00299
Chem. Rev. 2015, 115, 13165−13307

Scheme 63. Representative Molecular Structures of Hydrogelators for Chemosensing

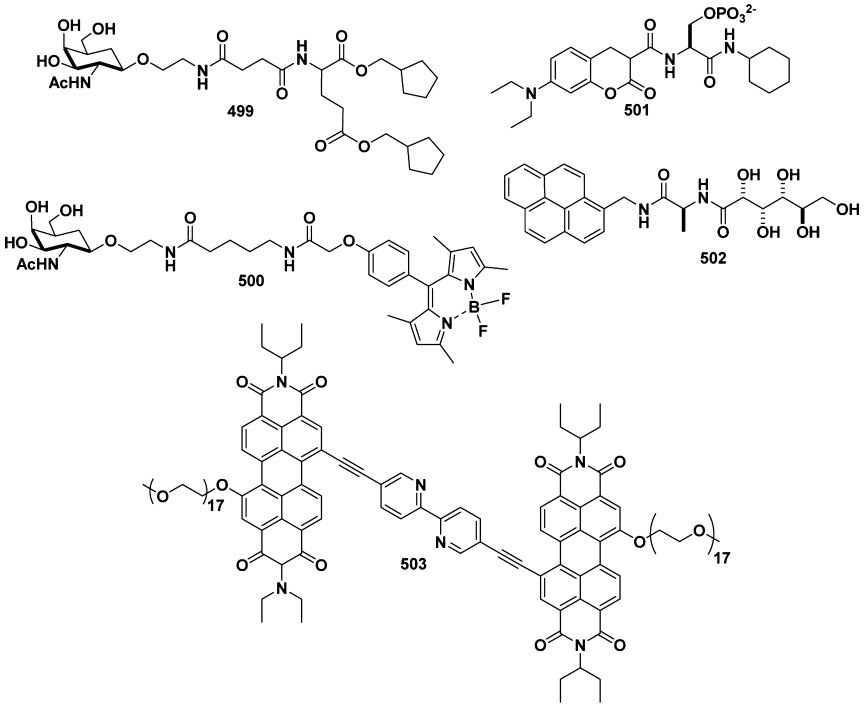

several tripeptide-based hydrogels and their use in removal of dyes from wastewater.[1020] Sanchez et al. used a supramolecular hydrogel formed by triangular-shaped dendronized oligo(phenyleneethynylene) amiphiphiles **494** and **495** for dye encapsulation, such as disperse orange 3, a hydrophobic dye (Figure 14).[1021]

Feng et al. recently developed two C_2-symmetric benzene-based hydrogelators, **496** and **497**. They easily obtained hydrogels by changing the pH of the solution of **496**, or by heating and then cooling the solution of **497**. Both of the hydrogels exhibit a unique layered structure of activated carbon and are capable of the controllable adsorption of 97−99% of certain organic dyes, such as methylene blue and methyl violet 2B, within 2 min.[404] Srivastava et al. used Nap-F (**498**), which gels water even at a concentration 0.025 wt %, as a network for dye entrapment. Besides, they demonstrated that the addition of chaotropic reagents, as well as increasing the pH value, disassembles the gel and promotes the release of the entrapped molecules.[1022] Song et al. studied the hydrogenation behavior of lithocholate (**87**) by introducing alkali-metal ions and NH_4^+ into the aqueous solution of **87**. This hydrogelator shows a CGC varying from 75 to 130 mM (from 2.8 to 4.9 wt %), depending on the ions added. The authors demonstrated that these hydrogels show high efficiency and the capability of absorption of cationic dyes, and thus may be a promising candidate for the removal of toxic substances.[1023,1024]

5.2.2. Chemosensors. The networks of supramolecular hydrogels can reversibly entrap a variety of probe molecules, which allows the development of various readout systems, such as fluorescence enhancement or quenching, color changes, or fluorescence resonance transfer (FRET), based on the hydrogels. Acting as a class of chemosensor, hydrogels help monitor the signal changes associated with molecular recognition.[1025,1026] As a pioneer in the applications of hydrogels for chemosensing, Hamachi et al. developed a supramolecular hydrogel formed by **499** molecules (Scheme 63) as a platform for a semiwet sensor chip.[845] They created a hydrogel-based array on a glass plate by incorporating artificial receptors into the heated solution of the hydrogelator **499** and spotting them on a glass plate. They found that this semiwet sensor chip not only recognizes a variety of cations by simply changing the incorporated artificial receptors/probes, but also can work as a pH probe. They also demonstrated that the integrated supramolecular sensor chip can accept mixtures without tedious isolation steps.[1027] Hamachi et al. also used the same supramolecular hydrogel to construct a fluorescent lectin array for detecting saccharides. By noncovalently fixing the fluorescent lectins into the hydrogel matrix to act as a molecular probe for various glycoconjugates, they demonstrated that one can read a series of saccharides on the basis of the selectivity and affinity of the immobilized lectins.[1028] Using similar molecules, **367** and **500**, Hamachi et al. designed a novel polyanion-selective fluorescence sensing system composed of a hybrid material of supramolecular hydrogels, enzymes, and aminoethyl-modified MCM41-type mesoporous silica particles with cationic nanopores encapsulating anionic fluorescent dyes (e.g., **501**). This system efficiently coordinates (i) the release of an anion-selective probe (e.g., **501**) from MCM41 and (ii) the translocation of the probe facilitated by enzymatic reaction (e.g., dephosphorylation catalyzed by phosphatases) with (iii) FRET sensing in the hydrogel form by **367** and **500**.[1029] On the basis of similar strategies, Hamachi et al. also developed several fluorescent sensors for rapid and convenient detection of chemicals, such as phosphate derivatives,[1030] polyamines,[1031] and polyols.[1032] Kim et al. prepared a library of amphiphiles, each comprising a pyrene group and a polar carbohydrate head group. They found that all of the amphiphiles form robust hydrogels with CGC values ranging from 0.07 to 0.30 wt %, but only amphiphile **502** (a derivative of D-gluconolactone) affords a fluorescent hydrogel which is sensitive to the presence of insulin in aqueous media. They suggested that this supramolecular hydrogel can serve as an efficient probe for

DOI: 10.1021/acs.chemrev.5b00299
Chem. Rev. 2015, 115, 13165−13307

insulin.[1033] Rybtchinski et al. demonstrated that molecule **503**, based on a perylenediimide chromophore decorated with polyethylene glycol, self-assembles in aqueous media to form extended supramolecular fibers which afford a stable hydrogel. As reported by the authors, the hydrogel of **503** can respond to multiple stimuli, such as temperature changes and chemical reductions. The authors suggested that the dual sensitivity toward chemical reduction and temperature with a distinct and interrelated response to each of these stimuli is especially useful to applications in the area of adaptive functional materials, such as chemosensors.[77]

As shown in Scheme 64, Kim et al. reported the design of an anisotropic supramolecular hydrogel of γ-CD (**504**) and an azo

Scheme 64. Representative Molecular Structures of Hydrogelators for Chemosensors

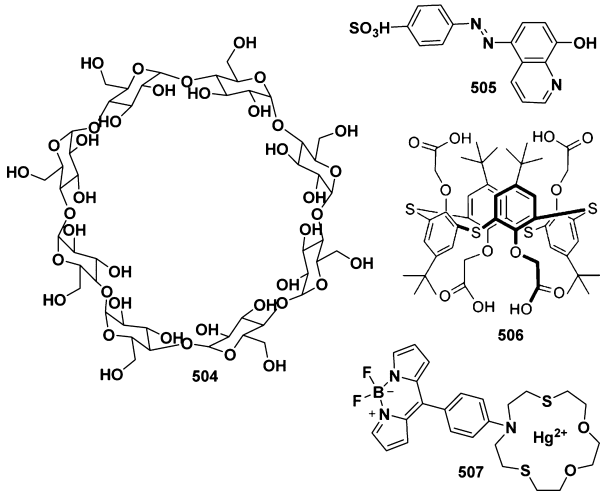

dye (**505**) in which the host–guest interaction between the two molecules leads to hydrogelation. They tested the obtained hydrogel for identifying different classes of metal ions and demonstrated visual detection of lead ions by the naked eye.[1034] In addition to sensing ions in aqueous solution, hydrogel-based chemosensors can serve as probes for gases. For example, Jung et al. designed tetracarboxylic acid-appended thiacalix[4]arene (**506**), which is able to self-assemble in the presence of Co^{2+}. They unexpectedly found that the red color of the filter paper coated with the resulting hydrogel selectively changed to a blue color by exposure to a toxic VGCl (volatile gas containing a chlorine atom), such as HCl, $SOCl_2$, $(COCl)_2$, and $COCl_2$, which hydrolyzed to yield HCl. They concluded that the strategy may lead to useful applications in sensing other chemical vapors.[1035] Singh et al. developed a Hg^{2+} coordinate complex of a 1,4-dioxa-7,13-dithia-10-azacyclopentadecane–BODIPY dyad (**507**) which selectively recognizes L-cysteine over other amino acids via a reversible complexation/decomplexation. As reported by them, the detection relies on the switch of fluorescence upon sequential addition of Hg^{2+} and a cysteine solution.[1330]

5.2.3. Biosensors. The most attractive feature of supramolecular hydrogels is that the 3D, semiwet nanofiber network can entrap biological substances without a detrimental effect on the activities or functions of the entrapped substances.[1037−1039] For certain hydrogels formed by enzyme instruction, the state changing from a solution to a hydrogel itself can serve as a signal for reporting the existence of certain enzymes.[149,966,1040,1041] For example, Xu et al. developed a simple assay based on the hydrogelation of small molecules Fmoc-Y_p (**14**) for the rapid detection of the inhibitors of enzymes (i.e., acid phosphatase). On the basis of the fact that phosphatase catalytically transforms the solution of **14** into a solid hydrogel within 30 min, Xu et al. demonstrated that the sol–gel transition can serve as a visual assay for screening the inhibitor of the enzymes.[158] Similarly, Wang et al. developed a strategy that utilized an aptamer-functionalized hydrogel to detect human thrombin through a diffraction measurement (**508**; Figure 15). Being a serine protease, thrombin acts as a model

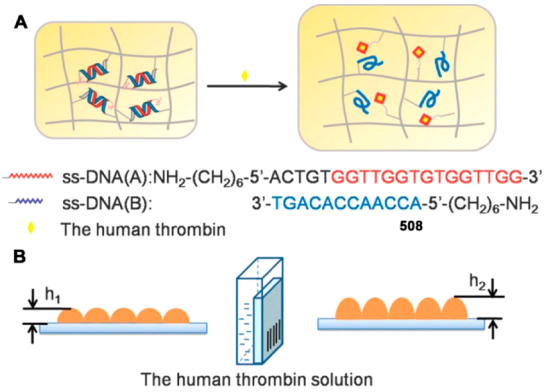

Figure 15. Schematic illustration of the sensing strategy of diffraction grating for human thrombin detection. (A) The hydrogel **508** contains an aptamer and its complementary sequence as the supermolecular cross-linking points and swells when exposed to the human thrombin. (B) Response of the hydrogel grating to human thrombin in the solution. Adapted with permission from ref 1036. Copyright 2013 Royal Society of Chemistry.

protein to test its binding with an aptamer. Wang et al. constructed the thrombin-responsive hydrogel by functionalizing the hydrogelator with both the aptamer and its complementary sequence as the physical cross-linking points. When exposed to human thrombin solution, the aptamer tends to bind with thrombin rather than its complementary sequence, which causes the hydrogel to swell due to the decrease of cross-linking and the change in the diffraction efficiency.[1036] Park et al. employed a self-assembled peptide hydrogel consisting of Fmoc-FF (**6**) as a biosensing platform. By encapsulating enzymes (e.g., glucose oxidase or horseradish peroxidase) and fluorescent reporters (e.g., CdTe, and CdSe quantum dots) physically within the hydrogel matrix via simply mixing them in a peptide solution, they successfully applied the system to detect analytes (e.g., glucose or phenolic compounds) on the basis of a photoluminescence quenching of the hybridized quantum dots.[1042] Shimizu reported that an unsymmetrical bolaamphiphile, **509** (Scheme 65), with glucose and triglycine groups at both ends, exclusively self-assemblies into nanotubes. The nanotubes allow the doping of a compound (**510**) containing a chromophore. They demonstrated that the self-assembled nanotubes with an interior recognition probe on the inner surface not only detect the encapsulation, transportation, and release behavior of GFP in real time, but also report the stability of GFP in the hollow cylinder.[1043]

Recently, Yang et al. reported a self-assembling vacomycin derivative (**511**) for bacterial detection and inhibition. They demonstrated that the conjugation of vancomycin to the side chain of the peptide derivatives increases its antimicrobial

DOI: 10.1021/acs.chemrev.5b00299
Chem. Rev. 2015, 115, 13165−13307

Scheme 65. Representative Molecular Structures of Hydrogelators for Biosensors

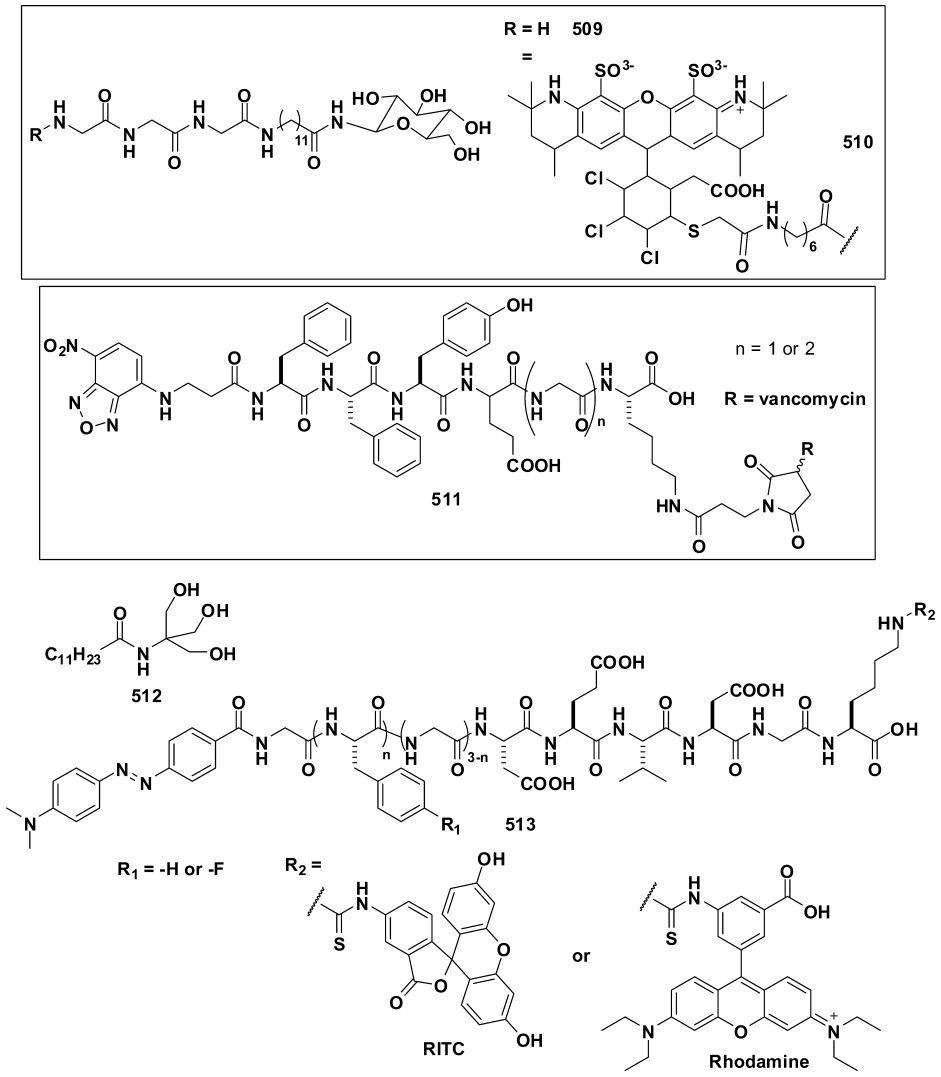

activity by 7-fold. By monitoring the fluorescence response of the solution of **511** to the bacteria, they found that the fluorescence of **511** increases gradually with increasing concentration of the bacteria. Similar to the bacterial surface-induced self-assembly of **23**, this specific peptide−antibiotic interaction initiates the self-assembly of an environment-sensitive conjugate (**511**), which may find applications for simultaneous detection and inhibition of bacteria.[1044] Vemula et al. recently developed a self-assembled nanofibrous hydrogel using a biologically inert amphiphile (**512**) which possesses unique physical/mechanical properties and easily carries a diverse range of payloads. The authors found that **512** exhibits excellent self-assembly ability in multiple solvents, including aqueous and organic solvents, typically at a concentration of 1−4 wt %. By noncovalently encapsulating a pH dye (pHrodo) into the self-assembled hydrogel/fibers of **512**, they obtained a pH sensor which can be internalized into macrophages at both physiological and subphysiological temperatures through an energy-dependent, passive process and report the pH in both the cytoplasm and phagosomes as well as the nucleus.[1045] Yang et al. synthesized compounds of dabcyl-GF$_n$G$_{3-n}$DEVDGK-(FITC/rhodamine) (**513**) (n = 0−3) with and without F-substitution on the 4-position of the benzyl ring of phenylalanine as the self-assembling probes for caspase-3. They demonstrated that the incorporation of one or two amino acids of phenylalanine (F), especially 4-fluorophenylalanine (^{F}F), would greatly lower the background fluorescence intensities of conventional quenched probes with quenchers (dabcyl) by the synergistic effect of FRET and aggregation-caused quenching (ACQ). By varying the amount of ^{F}F, they optimized the properties of the resulting probes, such as self-assembly ability, fluorescence recovery, and kinetics of enzyme cleavage. They found that these probes can detect caspase-3 in complex environments such as that in apoptotic cells, which offers a simple strategy to design fluorescent molecular probes with better signal-to-noise ratios.[1046]

5.3. Fluorescence/Imaging

Due to the promising applications of hydrogels in drug delivery, biosensors, tissue engineering, immunology, and other biomedicine, it is necessary to gain a comprehensive understanding of the self-assembly behavior of small molecules in the biological environment, aiming for optimal molecular design. Such being the case, imaging would be one of the most direct and revealing methods to distinguish, depict, and record the supramolecular self-assembly during the biological events or cellular processes. Compared to other imaging modalities (e.g., positron emission tomography (PET), MRI, etc.), the use of

DOI: 10.1021/acs.chemrev.5b00299
Chem. Rev. 2015, 115, 13165−13307

Scheme 66. Representative Molecular Structures of Fluorescent Hydrogelators

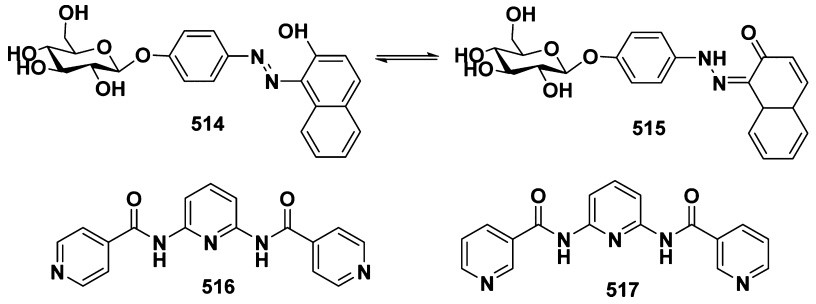

fluorescence has many advantages, such as easy access, low damage, and ready adaptability to specific molecular events despite poor depth penetration. Most importantly, fluorescent imaging provides the highest spatial resolution for imaging the molecular process at the cellular level. Various successful examples have been established to use specific fluorophores noncovalently staining supramolecular self-assemblies to reveal their existence, formation, and degradation, such as using Congo red to stain amyloids. In contrast, the covalent incorporation of a suitable fluorophore into a self-assembling small molecule (e.g., a hydrogelator) not only allows the self-assembly process to align the hydrogelators into nanofibers or other ordered structures, but also forces the appended fluorophore to comply with the ordered organization. In this subsection, we focus on the applications of fluorescent hydrogelators for imaging in a cellular environment, and introduce it as a powerful and facile method to reveal the emergent properties of supramolecular self-assemblies because it couples fluorescence with the self-assembly process.

5.3.1. Fluorescent Hydrogels. Before describing imaging of molecular self-assembly in a cellular environment, we present several typical examples of fluorescent hydrogels formed by small molecules. There are two kinds of fluorescent hydrogels: one consists of fluorescent hydrogelators,[117,1047−1055] and the other forms by fluorescent dyes diffusing into the matrix of the hydrogel.[197,1056−1062] For example, Shinkai et al. developed a supramolecular hydrogelator (β-D-glucopyranoside−azonaphthol conjugate, **514** or **515**; Scheme 66) which affords a fluorescent hydrogel in a mixture of water and ethanol (80:20, v/v). The azonaphthol moiety serves not only as an aggregative functional group but also as a probe for microscopic solvent polarity. On the basis of a UV−vis spectral change induced by the azo−hydrazone tautomerism, it is possible to estimate the microenvironmental polarity in the fibrous aggregates of the hydrogelators.[1047] Jung et al. reported two fluorescent hydrogels formed by amide-linked tripyridine derivatives **516** and **517**, with para or meta substituents. They demonstrated that both molecules gel water or water−DMSO and the hydrogelation ability depends mainly on CH−π and π−π stacking or strong intermolecular hydrogen bonding between the amide groups.[1049] Another interesting example is the ruthenium(II) tris(bipyridine) complex (**10**), developed by Xu et al. The integration of a tripeptide derivative, a versatile self-assembly motif, with a ruthenium complex affords the first supramolecular metallohydrogelator that not only self-assembles in water to form a hydrogel but also exhibits a gel−sol transition upon oxidation of the metal center (Figure 16). They found that this hydrogel formed by **10** exhibits strong fluorescence upon the irradiation of UV light.[117] It is also noteworthy that

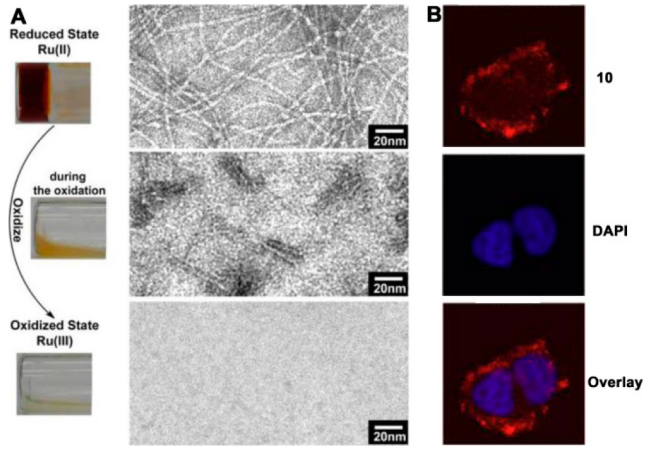

Figure 16. (A) Optical images of the oxidation-induced gel−sol transition and the TEM images corresponding to the samples at different states of transition. The hydrogel (reduced state) is formed by 0.8% (w/v) **10** in water at pH 1. The scale bar represents 10 nm. (B) Fluorescent images of a HeLa cell incubated with **3** (200 μM, 24 h). Adapted from ref 117. Copyright 2013 American Chemical Society.

the long lifetime and photostability of $[Ru(bipy)_3]^{2+}$ will likely find applications in molecular imaging in cells.[117]

5.3.2. Imaging Self-Assembly in a Biological Environment. Supramolecular hydrogelators serve as an excellent system for exploring the properties of molecular nanofibrils in a cellular environment. One of the successful cases is imaging of phosphatases inside living cells. Xu et al. developed a method to image enzyme-instructed self-assembly of small molecules inside live cells (see section 5.9.2).[156,1063] In a different study, Tomasini et al. found that a physical hydrogel prepared with small molecules of $CH_2(C_3H_6CO$-L-Phe-D-Oxd-$OH)_2$ (**518**; Scheme 67) is a potential "Trojan horse" carrier into cells. To check the internalization process by confocal microscopy, they prepared a fluorescent hydrogelator, introducing the fluorescent dansyl moiety into the molecules (**519**).[1064] Yang and coworkers conjugated the environment-sensitive fluorophore NBD to the peptide FFYEEGGH at its N-terminal and found that the resulting peptide derivatives **520** yield supramolecular nanofibers with enhanced cellular uptake, brighter fluorescence, and a significant fluorescence response to external stimuli (Figure 17).[1065]

5.4. Antibacterial Hydrogelators/Hydrogels

Infectious disease remains a major threat to public health, and there is an urgent need for novel antimicrobial agents with activities against multi-drug-resistant bacteria. The discovery of antimicrobial peptides has stimulated the use of self-assembly of peptide amphiphiles to develop antibacterial hydrogels.

DOI: 10.1021/acs.chemrev.5b00299
Chem. Rev. 2015, 115, 13165−13307

Scheme 67. Representative Molecular Structures of Hydrogelators

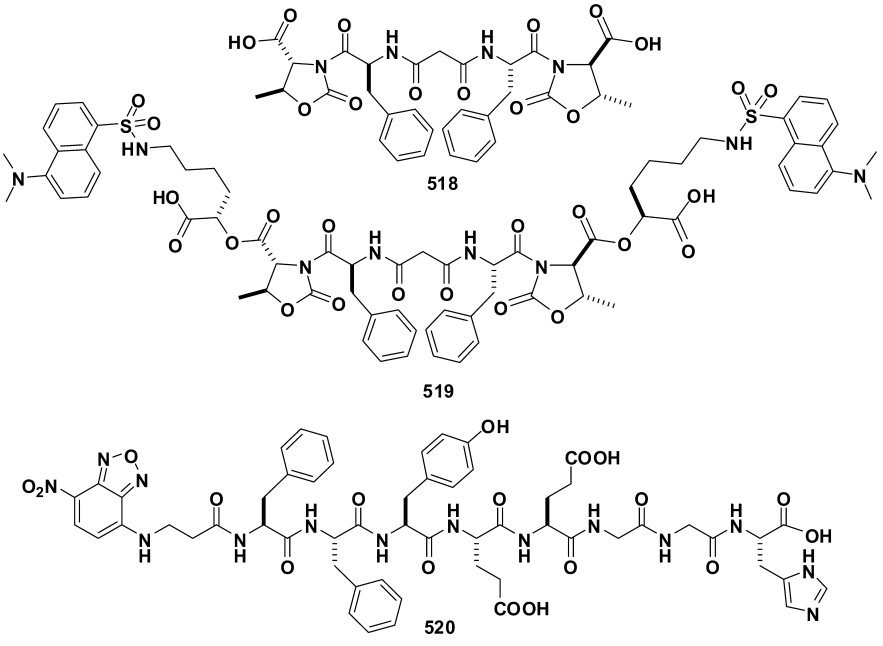

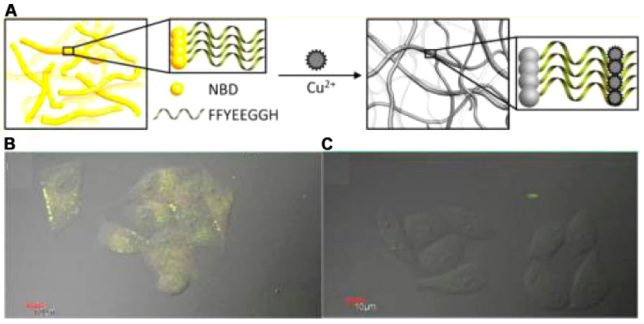

Figure 17. (A) The nanofibers of **520** could specifically bind to Cu^{2+}, leading to the formation of fluorescence-quenched elongated nanofibers. Confocal images (bright field + fluorescence) of (B) HeLa cells treated with **520** (0.05 wt %) at a 2 h time point and (C) HeLa cells pretreated with 100 μM Cu^{2+} and then treated with **520** (0.05 wt %) at a 6 h time point. Adapted from ref 1065. Copyright 2014 American Chemical Society.

Particularly, the pioneering work by Schneider et al. on antibacterial hydrogels has provided useful insights into the development of hydrogelators for antibacterial applications. Several comprehensive reviews have focused on this subject.[1066,1067] In the following section, we only give a brief discussion of the works on antibacterial hydrogelators reported over the past decade.

Schneider and Pochan et al. reported a series of β-sheet peptide-based hydrogels,[1069] among which the surface of **251** is inherently antibacterial and exhibits broad-spectrum activity against both Gram-negative (*Klebsiella pneumoniae* and *E. coli*) and Gram-positive (*Staphylococcus epidermidis*, *Staphylococcus aureus*, and *Streptococcus pyogenes*) bacteria without incorporating exogenous antimicrobial agents. Using the LIVE/DEAD assays by laser scanning confocal microscopy (LSCM), they found that the surface of the hydrogel of 2 wt % **251** displays broad-spectrum antibacterial activity when incubated with bacterial solutions ranging in concentration from 2×10^3 to 2×10^9 colony-forming units (CFUs)/dm^2 (Figure 18). On the basis of the β-galactosidase leakage experiments, they suggested that the surface of the **251** hydrogel likely causes inner and outer membrane disruption and controls the release of β-galactosidase from the cytoplasm of lactose permease-deficient *E. coli* ML-35, resulting in cell death upon cellular contact with the surface of the hydrogel. Furthermore, coculture experiments showed that, when NIH3T3 fibroblasts and a mixture of *Achromobacter xylosoxidans* and *Stenotrophomonas maltophilia* are introduced onto the hydrogel, the surface of the hydrogel inhibits bacterial proliferation yet allows mammalian cell adhesion and proliferation, indicating that the surfaces are selective against bacteria.[1068] Later, they switched two lysine residues of **251** to two arginines, generating another β-hairpin peptide, MARG1 (**521**; Scheme 68). They found that the surface of the hydrogel of 2 wt % **521** imparts potent antibacterial activity against methicillin-resistant *S. aureus* (MRSA) while it is noncytotoxic toward mammalian cells (murine C3H10t1/2 mesenchymal stem cells).[1070] On the basis of this result, Schneider et al. designed another arginine-rich β-hairpin peptide, PEP6R (**522**),[1071] which self-assembles to form hydrogels at 1.5 wt % or higher concentration containing NaCl. They found that the hydrogel surfaces of **522** exhibit potent activity for killing both Gram-positive and Gram-negative bacteria, including multi-drug-resistant *Pseudomonas aeruginosa*, while they exhibit cytocompatibility toward human erythrocytes as well as mammalian mesenchymal stem cells.[1072]

Recently, Laverty et al. reported a series of cationic, naphthalene-derivatized self-assembling ultrashort peptides, among which **523** self-assembles to form hydrogels with a β-sheet structure at a concentration of 1 wt % and pH of 7.4 in water. The authors found that the hydrogel of 2 wt % **523** significantly reduces the viable *S. epidermidis* biofilm by 94% while exhibiting little hemolytic side effect toward human red blood cells (hRBCs). On the basis of the cytotoxicity assays against murine fibroblast (NCTC 929) cell lines and hemolysis assays using equine erythrocytes, the authors concluded that the hydrogels are compatible with mammalian cells.[1073] Yang and Wang et al. reported self-assembled vancomycin derivatives **511** based on FF or FFY with aromatic capping groups that

DOI: 10.1021/acs.chemrev.5b00299
Chem. Rev. 2015, 115, 13165−13307

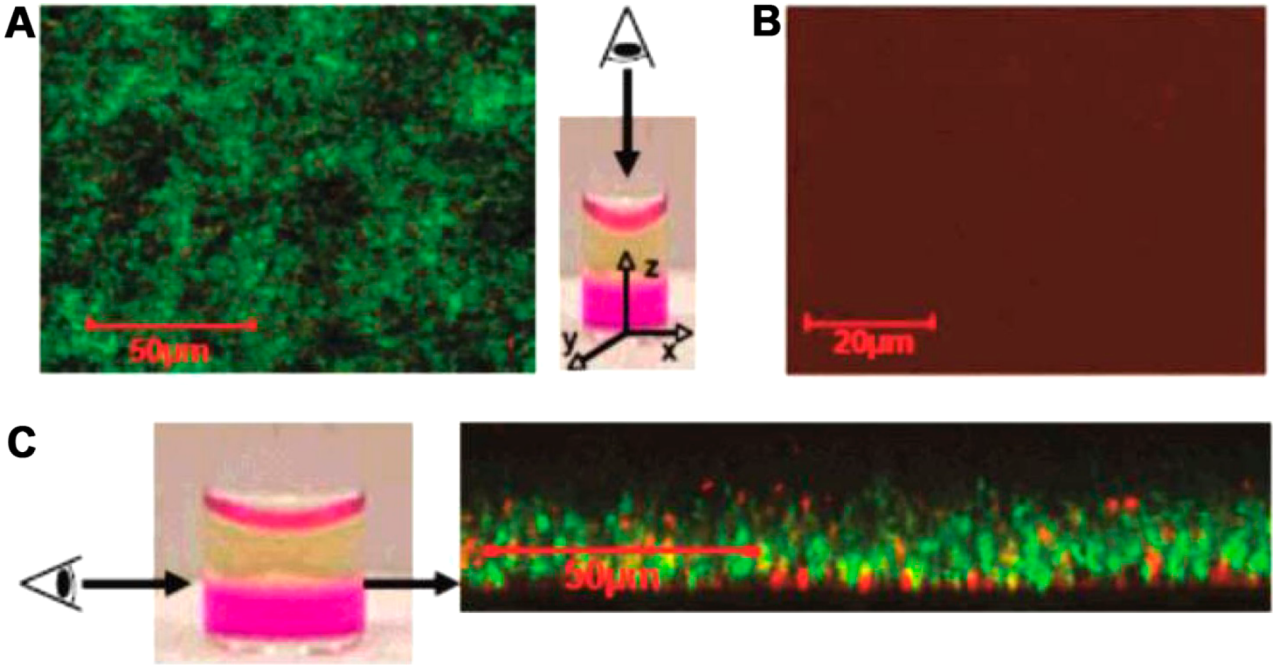

Figure 18. LSCM *xy* projections taken of 2.5×10^3 CFUs/dm^2 *E. coli* incubated on (A) a borosilicate control surface and (B) the hydrogel of 2 wt % **251** after 24 h. The gel is viewed parallel to the *z*-axis. Green fluorescence denotes live cells, and red fluorescence denotes dead cells with compromised membranes. (C) LSCM *xy* projections taken of 2.5×10^9 CFUs/dm^2 *E. coli* incubated on the surface of the hydrogel of 2 wt % **251** viewed perpendicular to the *z*-axis. Arrows denote the gel−bacterial interface. Adapted from ref 1068. Copyright 2007 American Chemical Society.

Scheme 68. Representative Molecular Structures of Antibacterial Hydrogelators

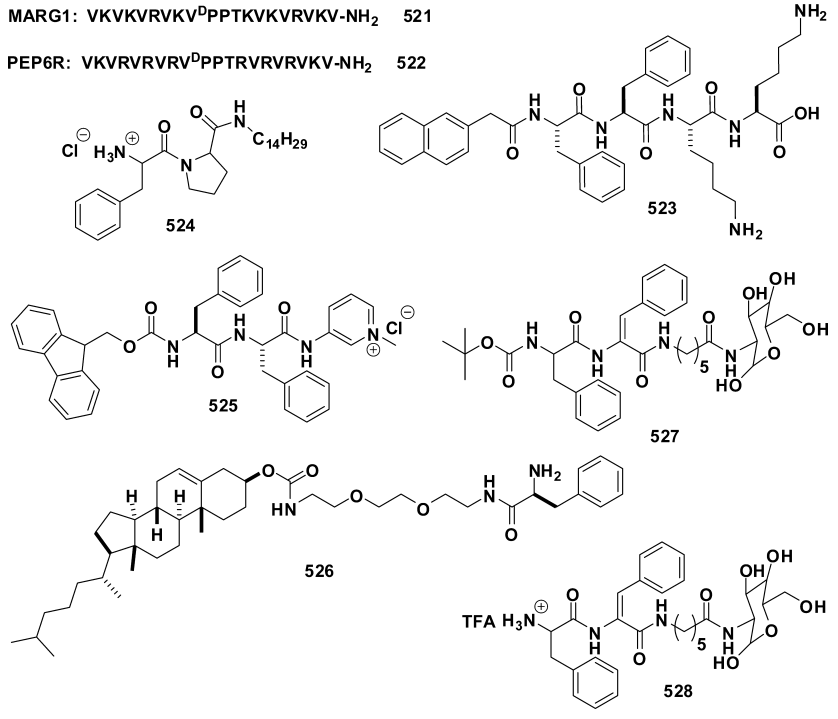

showed great self-assembly ability in PBS buffer with a critical micelle concentration (CMC) of 75 μg/mL. Using the standard broth microdilution assay, the authors studied the bacterial inhibition capacity of **511** and found that the minimum inhibitory concentration (MIC) of **511** is about 4.5 μM, which was similar to that of the parent Van molecule (1.3 μM).[1044] Meanwhile, Wang and Chen et al. reported a selenium-containing vancomycin derivative with a redox-controllable self-assembly property and antibacterial activity.[1074]

Das et al. designed and synthesized several dipeptide-based cationic amphiphiles with different head group structures by varying the combinations of L-amino acid residues. Among all the dipeptide derivatives, although **524** requires a relatively high concentration (MGC), 22 wt %, to form a hydrogel, the authors reported that **524** inhibits the growth of several Gram-

DOI: 10.1021/acs.chemrev.5b00299
Chem. Rev. 2015, 115, 13165−13307

Scheme 69. Representative Molecular Structures of Antibacterial Hydrogelators

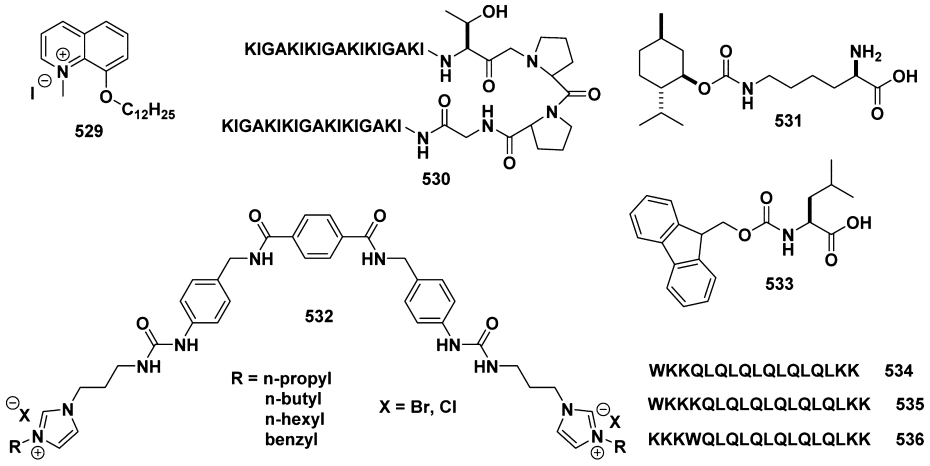

positive (MIC = 0.1−0.5 μg/mL) and Gram-negative (MIC = 5−10 μg/mL) bacteria as well as fungi (MIC = 1−5 μg/mL). Moreover, the authors reported that **524** is compatible with different mammalian cell lines such as Hep G2, HeLa, and SiHa.[1075] Later, the authors reported a new class of antibacterial hydrogelators based on anti-inflammatory Fmoc-amino acid/peptide-functionalized cationic amphiphiles (**525**). By the incorporation of a pyridinium moiety at the C-terminal of Fmoc-amino acid/peptides, the positively charged hydrogelators self-assemble to form an antiparallel β-sheet arrangement of the peptide backbone and exhibit efficient antibacterial activity against both Gram-positive and Gram-negative bacteria.[1076] Das et al. also designed and synthesized several cholesterol-based amino acid-containing hydrogelators (**526**) that exhibit a high gelation efficiency (MGC of 0.9−3.1 wt %) and biocompatibility with human hepatic cancer-derived Hep G2 cells. After the incorporation of silver nanoparticles (AgNPs), the soft nanocomposite of the amphiphile and AgNPs exhibits a notable bactericidal property against both Gram-positive and Gram-negative bacteria.[1077] Sharma et al. designed and synthesized two self-assembled amphiphilic α,β-dehydrophenylalanine-containing small glyco-dehydropeptides, **527** and **528**, with glucosamine attached at the C-terminal through a 6-aminocaproic acid linker. The authors found that **527** and **528** self-assemble to form gels in a mixture of methanol and water at a concentration of 0.1 wt %, with the sizes of the nanostructures being ∼197 and ∼235 nm, respectively. In addition, the authors used a disk diffusion assay to test the antimicrobial activity of the peptides **527** and **528**, and they found that the peptides display antimicrobial activity against *Micrococcus flavus*, *Bacillus subtilis*, and *P. aeruginosa*.[1078]

Das and Ramesh et al. reported several structurally diverse quinoline-based amphiphiles containing a fluorescent head group and hydrophobic chain of different lengths. Among these amphiphiles, **529** (Scheme 69) is the most potent antibacterial amphiphile to exhibit a dose-dependent bactericidal activity on target pathogens and even inhibits the growth of a presumptive MRSA strain. The authors found that this bactericidal activity may result from the electrostatic binding of **529** to bacteria. Most importantly, **529** has high antimicrobial selectivity, but hardly decreases the viability of human HT-29 cells.[1079] Zhao et al. designed a peptide (**530**) by connecting two Gram-positive antibacterial peptide sequences $(KIGAKI)_3$-NH_2 with a central tetrapeptide linker. They found that the electrostatic repulsion of the charged lysine residues balances the hydrophobic collapse of the isoleucine and alanine residues and backbone β-sheet hydrogen bonding to favor the self-assembly of **530**, which forms individually dispersed nanofibers with a β-hairpin conformation. Furthermore, after 36 h of incubation, the hydrogel of **530** effectively inhibits *E. coli* proliferation when the concentrations of the initially introduced *E. coli* resuspensions are in the range of 10^3−10^6 CFUs/mL. However, when the bacteria reach a density of 10^7 CFUs/mL, the hydrogel starts to lose its inhibitory capacity.[95] Yang and Yi et al. designed and synthesized a unique hydrogelator (**531**) based on (−)-menthol and a lysine. **531** self-assembles to form an opaque hydrogel at a concentration of 0.83 wt %. Interestingly, the hydrogelators form the 3D multiporous networks through acid−base interactions and strong double hydrogen bonding between amino acids for encapsulating some known antibacterial agents such as Zn^{2+} and a series of water-soluble organic antibiotic medicines such as lincomycin, amoxicillin, etc. Using the Oxford cup method, the authors found that the antimicrobial susceptibility of the hydrogels loaded with Zn^{2+} or lincomycin was much more effective than that of the corresponding aqueous solution when they were incubated with *E. coli* and *S. epidermidis*. In addition, the hydrogel of **531** is innocuous to mammalian cells such as HeLa cells.[1080] Yang and Hedrick et al. reported the synthesis, self-assembly, and antimicrobial activity of a series of oligomeric cationic compounds (**532**). Containing a rigid hydrophobic terephthalamide−bisurea core flanked by hydrophilic imidazolium groups with short alkyl (C_nH_{2n+1}, $n < 6$) or simple aryl tails, all the hydrogelators self-assemble to form nanostructures in aqueous solutions. These cationic hydrogelators exhibit potent, broad-spectrum antimicrobial activity and high selectivity toward Gram-positive bacteria (including clinically isolated MRSA), killing the microbes via the membrane-lytic mechanism. Notably, the bacteria tested fail to develop resistance even after multiple exposures to sublethal doses of the compounds, which is remarkably encouraging.[1081]

Chen and Li et al. reported the preparation of biocompatible hydrogels with antimicrobial activity against Gram-positive bacteria by taking advantage of the intermolecular aromatic−aromatic interactions of Fmoc and the phenyl group. They generated a hydrogel based on the coassembly of Fmoc-Phe (**200**) and Fmoc-Leu (**533**), and found that the coassembled

DOI: 10.1021/acs.chemrev.5b00299
Chem. Rev. 2015, 115, 13165−13307

(**200** + **533**) supramolecular hydrogel is bactericidal against Gram-positive bacteria via a mechanism involving cell wall and membrane disruption (Figure 19). Being biocompatible with normal mammalian cells, this type of antibacterial hydrogel may potentially serve as an antimicrobial coating in clinical devices and wound dressings or a topical agent for the treatment of clinical skin and wound infections mainly caused by Gram-positive bacteria such as *S. aureus*, as suggested by Li and Chen.[1082] On the basis of the concept of multidomain peptides (MDPs),[602,661,662] Dong et al. synthesized three hydrogelators, **534**, **535**, and **536**, that self-assemble above critical assembly concentrations (CACs) of 0.87, 1.24, and 1.37 μM, respectively. In addition, they found that the position of tryptophan (W) determines the molecular secondary structure, supramolecular nanostructure, stability, and antimicrobial activity. After incubation with Gram-negative bacteria (*E. coli* and *P. aeruginosa*) or Gram-positive bacteria (*S. epidermidis* and *S. aureus*), a bacterial killing efficiency study shows that 99% of Gram-negative bacteria are killed by **535** and **536**, while less than 40% are killed by **534**. A surprising observation is the reverse dose-dependent relationships between the concentration of the peptides and their cytotoxicity toward primary mouse bone-marrow-derived monocytes (BMDMs),[1083] a result that is consistent with the formation of aggregates.[884,1084−1088]

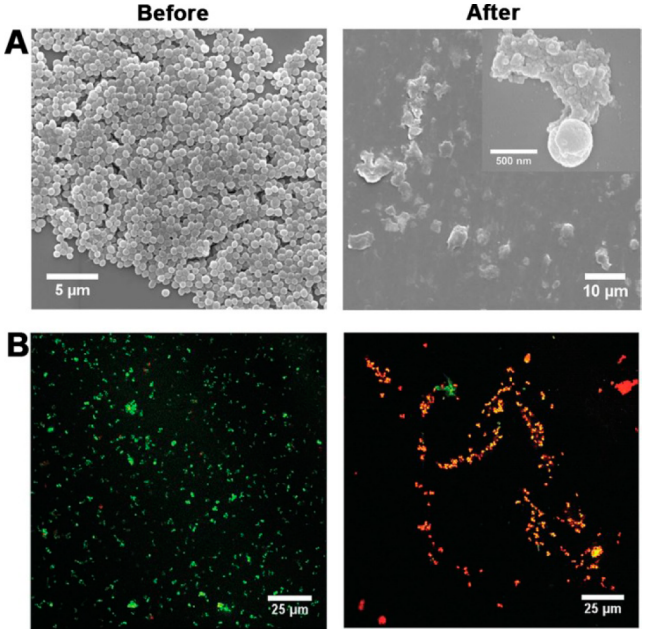

Figure 19. (A) Representative SEM images and (B) overlapping fluorescence images for the LIVE/DEAD bacterial staining assay of *S. aureus* before and after contact with the coassembled (**200** + **533**) hydrogel for 2 h. Two fluorescent dyes were used in LIVE/DEAD staining in which SYTO 9 with green color labeled both live and dead bacteria while propidium iodide with red color stained only dead bacteria. Adapted with permission from ref 1082. Copyright 2015 Wiley-VCH Verlag GmbH & Co. KGaA.

5.5. Tissue Engineering

If one looks into a mirror, it is not difficult to realize that we are largely made of soft tissues. Because of the striking resemblance between hydrogels and soft tissues, the most attractive and sought-after biomedical application of supramolecular hydrogels is tissue engineering.[1089−1094] However, most of the demonstrations, so far, center on the culture of certain cells in vitro, which is still far away from the repair processes needed for regenerating damaged tissues or diseased organs.[1095−1097] There are several reasons for such a slow progress. First, the complexity and dynamics of biological processes at the tissue level are just beginning to be understood,[1098] and the understanding is far from complete. Thus, it remains difficult to devise working engineering principles for tissue engineering without adequate insights into the process. Second, most of supramolecular hydrogels consist of only one or two molecular species, which limits their roles to be only complementary or supplementary to the inherent or endogenous processes. Third,

Scheme 70. Representative Molecular Structures of Hydrogelators for Tissue Engineering

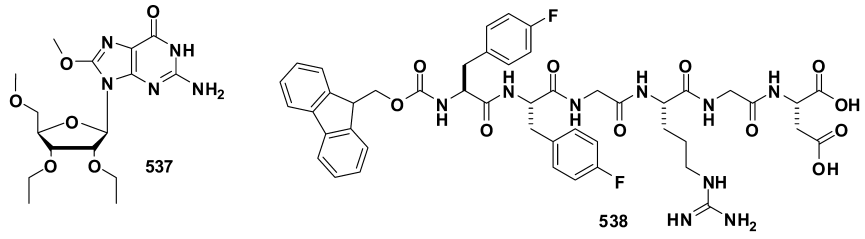

NH_2-FAQRVPP-GGG-LDLKLDLKLDLK-$CONH_2$ **539**

NH_2-QHLPRDH-GGG-LDLKLDLKLDLK-$CONH_2$ **540**

NH_2-KLPGWSGGGGLDLKLDLKLDLK-$CONH_2$ **541**

Biot-GGGAFASTKT-$CONH_2$ **542**

PDFDFDFDFDFDP **543**

Ac-RADARADARADARADAIKVAV-$CONH_2$ **545**

Ac-RADARADARADARADAGRGDS-$CONH_2$ **546**

Ac-RADARADARADARADAYIGSR-$CONH_2$ **547**

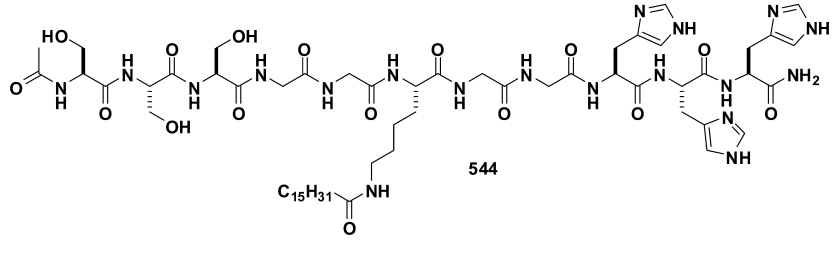

DOI: 10.1021/acs.chemrev.5b00299
Chem. Rev. 2015, 115, 13165−13307

currently, supramolecular hydrogels still lack the sophistication or context-dependent features required for the regeneration of tissues, which usually consist of a myriad of transient biological processes.[1099,1100] Despite these enormous challenges, it is still worthwhile to review the progress made to date in "tissue engineering" by supramolecular hydrogels so that further development can be made to meet the challenges ahead.

In the hope of developing an approach for repairing the degenerated nucleus pulposus (NP) of intervertebral disks, Ulijn et al. tested the growth of bovine nucleus pulposus cells on the hydrogel made of [(fluorenylmethoxy)carbonyl]-diphenylalanine (Fmoc-FF, **6**)/Fmoc-diglycine (Fmoc-GG, **398**) in 1:0 and 1:1 ratios.[1101] Using cryo-SEM, the authors verified that the hydrogels of **6** (1.0 wt %) consist of a dense network of nanofibers, whereas the hydrogels of **6**/**398** (1:1, 0.7 wt %) contain an overlapping mesh of flat ribbons.[895] In addition, the authors found that the majority of the NP cells remain in a rounded morphology within both the hydrogels of **6** and the hydrogels of **6**/**398** after 5 days of culture. On the basis of that observation, the authors suggested that the morphology of the network has a limited effect on the NP cells. Although the authors reported the deposition of collagen and sulfate−glycosaminoglycan by the NP cells cultured within both the hydrogels of **6** and the hydrogels of **6**/**398** over 3 weeks, it is still too preliminary to establish the application of the hydrogel of **6** for intervertebral disk tissue repair. Recently, Thordarson et al. examined the degradation of the hydrogels of **6** and observed that **6** or its degraded products result in the necrosis of cells in vitro.[705] This result, indeed, suggests that the fate of **6** in vivo remains to be firmly established.

As shown in Scheme 70, Rowan et al. reported the studies of the hydrogel of a guanosine-based hydrogelator, 8-methoxy-2′,3′,5′-tri-*O*-acetylguanosine (**537**), for the cell culture of a murine endothelial cell line (C166). **537** forms hydrogels at as low as 0.5 wt % in 100 mM NaCl. This hydrogelator forms helical assemblies, rather than the macrocyclic quartet assemblies commonly found in guanosine hydrogels. Contrary to the claim of the authors that there is little-to-no cytotoxicity of the hydrogels, the cell viability of the C166 cells, in the presence of hydrogels containing 2 wt % **537**, is only about 50% of the control.[1102] It would be more interesting to elucidate the cell mechanism of cell death caused by the self-assembly of this hydrogelator. Li et al. developed a short peptide derivative containing halogenated phenylalanine and reported that the partially halogenated peptide exhibits better gelation properties than Fmoc-Phe (**200**) in aqueous solutions.[1103] They found that Fmoc-4-fluorophenylalanine is the most efficient gelator (among the molecules derived by them) that gels PBS buffer solution at a minimum gelation concentration of 0.15 wt %. On the basis of this observation, the authors designed and synthesized an Fmoc-peptide (Fmoc-$^{F}F^{F}$FGRGD, **538**) and used the peptidic hydrogel to culture NIH/3T3 cells. Although **538** only formed a clear hydrogel in PBS buffer containing 20% DMSO, the authors reported that the hydrogel could efficiently promote the adhesion and proliferation of NIH/3T3 cells.[1103] In a related study, Parish and Nisbet et al. reported that Fmoc-self-assembling peptides (i.e., Fmoc-DIKVAV, Fmoc-FRGDF, Fmoc-DYIGSRF) have been used as a vehicle for the delivery and support of cell transplants in vivo.[1104]

On the basis of self-assembling P11-family of peptides reported by Boden,[1105] McPherson et al. reported the production of self-assembling peptides (QQRFEWEFEQQ, **233**)[597] in a relatively high yield using an *E. coli* expression system. Being triggered by various physicochemical cues, **233** self-assembles to generate self-supporting isotropic or liquid crystalline hydrogels at peptide concentrations of 10−30 mg/mL (1−3 wt %). Using human dermal fibroblasts, the authors demonstrated that the hydrogels formed by the recombinant peptides display excellent cytocompatibility.[1106] Zheng et al. synthesized KLD-12 peptide (**417**) and studied its biocompatibility with the host rabbit and MSCs, also, in the hope for repairing the degenerated nucleus pulposus of intervertebral disks. On the basis of the histological examination, the authors concluded that the **417** peptide hydrogel has a good biocompatibility with the host rabbit and MSCs so that the **417** peptide hydrogel could serve as a good scaffold material for tissue engineering of intervertebral disks.[1107]

Gelain et al. used phage display to identify the peptide sequences (e.g., FAQRVPP (**539**), QHLPRDH (**540**)[1108]) preferably interacting with murine NSCs and connected those peptide sequences to LDLK12 peptides[802] for generating functional self-assembling peptides. Confirmed by rheology, these synthesized self-assembling peptide sequences behave as classic hydrogelators to form hydrogels at a concentration of 1 wt % which consist of nanofibers of ∼12 nm width and ∼1.6 nm height. The authors found that the new functional peptide sequences, being linked to the LDLK12 peptide, have the capacity to bind to NSC-derived neural precursor cells (NPCs) and promote the proliferation and differentiation of the cells in vitro. On the basis of the high stem cell viability and neural differentiation achieved by the **539** peptide in vitro, the authors tested that peptide in acute contusive spinal cord injury in rats, and reported that the peptides foster nervous tissue regrowth and improve locomotor recovery. On the basis of these results, the authors concluded that phage-display-derived functional motifs need further investigation to elucidate their relevant molecular targets and cellular pathways. According to the authors, in vitro experiments are essential but still poorly informative for in vivo experiments. In another phage display panning, the same laboratory identified KLPGWSG (**541**)[1109] as the NSC binding peptide and linked it to LDLK12 peptides for the differentiation of NSCs. The authors concluded that the enhancement provided by the peptide conjugate still required the presence of the growth factors (e.g., epidermal growth factor (EGF) and basic fibroblast growth factor (bFGF)) and differentiative substrates. Again, this emphasizes the need to understand the molecular mechanisms linked to the observed neuronal phenotype. On the basis of their works on BMHP1, Gelain et al. derived a series of self-assembling peptides by connecting biotin to various mutated BMHP1 peptides. After identifying that one of the peptides (biotin-GGGAFASTKT-$CONH_2$, **542**) is particularly effective at fostering adhesion, differentiation, and proliferation of human NSCs in vitro, the authors conducted in vivo experiments and reported that **542** causes a negligible immune response in the host nervous tissue in the short term, though its performance on nerve fibers is similar to that of saline.[1110]

Using a β-sheet-forming peptide, PDFDFDFDFDFDP (denoted as P_{FD}-5, **543**), to form hydrogels as the depot of tricalcium phosphate (β-TCP), Rapaport et al. tested the proliferation of human fetal osteoblasts in vitro and evaluated the performance of the hydrogels of **543** in rat bone defect models. The authors found that the hydrogels of **543** (at a concentration of 5%, w/v) are able to absorb calcium ions and to induce osteoblast differentiation in vitro. Although the TCP-loaded hydrogels exhibit an efficacy of bone generation similar

DOI: 10.1021/acs.chemrev.5b00299
Chem. Rev. 2015, 115, 13165−13307

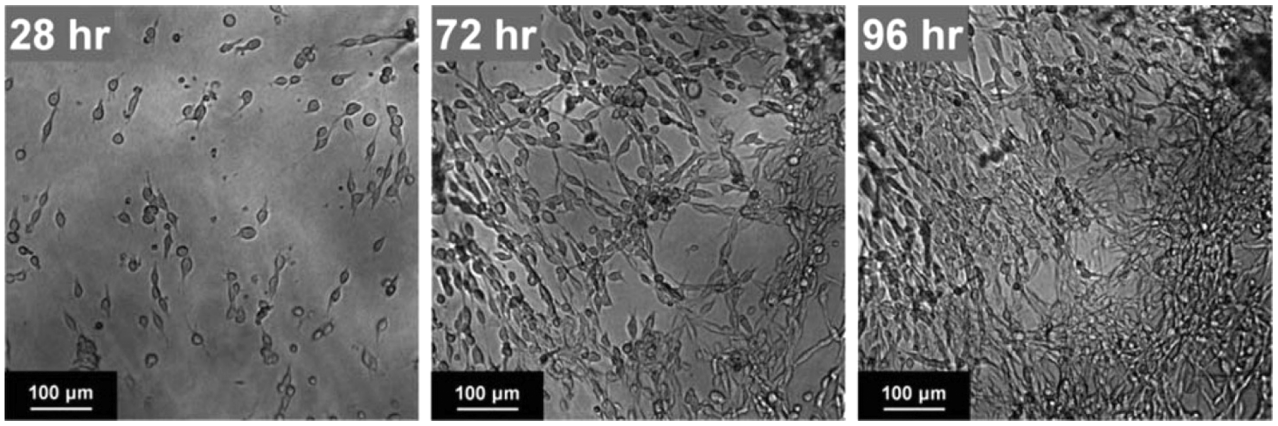

Figure 20. Nanofibrous hydrogels are reported to be compatible with NIH/3T3 fibroblasts. In the presence of serum, fibroblasts spread by 28 h. At 72 h, spreading appeared to be spindle-like, resembling the natural morphology of the cell type. The fibroblasts proliferated for a minimum of 96 h. These images are from a single hydrogel of **544**. Adapted with permission from ref 1117. Copyright 2012 Royal Society of Chemistry.

to that of nonporous TCP, the in vivo results of bone defect healing in rat demonstrate that the peptide hydrogel alone induces better bone regeneration in comparison to the control (nontreated defects). This result, indeed, agrees with the observation of calcium absorption by the hydrogels due to the presence of a high density of aspartic acids in the peptides, and the hydrogels and the mineral act synergistically to enhance bone regeneration. The authors concluded that the hydrogels of **543** might act as biocompatible and biodegradable matrixes to support cellular osteogenic activity and to promote the turnover of calcium minerals, through cellular processes, into bone tissue.[1111]

Banta et al. have evaluated a series of peptides[1112] consisting of β-roll peptide derivatives as the calcium-responsive motif and an α-helical leucine zipper domain (LZ) for intermolecular interactions. One of the most valuable features of these peptides is that the β-roll domain of the peptides is intrinsically disordered in the absence of calcium, while upon the addition of calcium, the peptide forms a β-roll secondary structure.[1113] The authors reported that these peptides form hydrogels only in calcium-rich environments. Recently, the same laboratory reported another class of β-roll peptides,[1114] but the application of these specific peptides in tissue engineering has yet to be reported. Recently, George et al. reported the use of LZ-based self-assembling peptides to form hydrogels for tissue engineering. The authors performed a quite comprehensive study of these hydrogels, from in vitro culture of human marrow stem cells (HMSCs) to in vivo evaluation of the hydrogels. Besides demonstrating that the concentration of the LZ peptide is able to tune the pore size of LZ hydrogels by altering the peptide concentration from 7 to 12 wt %, the authors functionalized the LZ polypeptide by the incorporation of the RGD domain for creating a suitable microenvironment for cell adhesion. According to the results reported by the authors, the incorporation of the canonical RGD domain has drastically improved the performance of the LZ hydrogels in many aspects. For example, an increase of the percentage of RGD in the hydrogels not only improves the proliferation of the HMSCs, but also allows the HMSCs to travel long distances within the LZ-RGDS hydrogels. The in vivo implantation of the LZ-RGDS scaffolds in a mouse model also significantly reduces the foreign body reaction to the scaffold. In vivo experiments with HMSCs also show that LZ-RGDS hydrogels have a better ability to support neovascularization than the LZ hydrogels do. On the basis of these results, the authors concluded that it should be possible to generate a functional and stable LZ scaffold for tissue engineering applications in vivo.[1115]

Galler and D'Souza et al. reported the use of the hydrogel of a self-assembling, multidomain peptide for dental pulp tissue engineering.[1116] The authors used a peptide with a sequence of $K(SL)_3RG(SL)_3KGRGDS$ (**420**; with a final peptide concentration of 1 wt %) to interact with heparin (with a final concentration of 0.1 wt %) to form a hydrogel for incorporating growth factors (e.g., vascular endothelial growth factor (VEGF), fibroblast growth factor (FGF), and transforming growth factor β 1 (TGFβ1)) and then tested the use of the hydrogels for encapsulating dental pulp stem cells in vitro and in vivo. The authors observed that the proliferation of the cells increases in the FGF-containing hydrogel, but decreases in the TGFβ1-containing hydrogel and that the dental pulp stem cells spread and form a collagenous matrix in the peptide hydrogel. One important observation is the formation of a vascularized soft connective tissue similar to dental pulp subcutaneously after transplantation of the hydrogel within dentin cylinders into immunocompromised mice. Although the authors concluded that the multidomain peptide is a highly promising candidate for regenerative endodontics, the requirement of dental pulp stem cells, various growth factors, and dentin highlights the complexity of this regenerative process and underscores the importance of mechanistic understanding. Tirrell et al. reported an innovative branched peptide amphiphile (**544**) that forms a hydrogel upon changing the pH from acidic to neutral. In addition, at 1% (w/v) **544**, the hydrogel is capable of achieving a storage modulus of 10 kPa. By modulating the concentration of **544**, the authors were able to regulate the viscoelastic properties of the hydrogels, thus broadening their versatility for complying with the mechanical requirement of a wide range of tissues. The authors tested the culture of NIH/3T3 fibroblast cells on the hydrogel of **544** for evaluating the biocompatibility of the hydrogel (Figure 20). After seeding the fibroblasts in the absence of serum to ensure the cells attach to the hydrogels through nonspecific interactions, the authors observed that these previously attached cells spread when serum was added. On the bais of LIVE/DEAD staining, the authors determined that the fibroblasts are predominately alive and suggested that the hydrogel is a viable biocompatible nanofiber-based tissue scaffold for supporting 3D cell growth.[1117]

DOI: 10.1021/acs.chemrev.5b00299
Chem. Rev. 2015, 115, 13165−13307

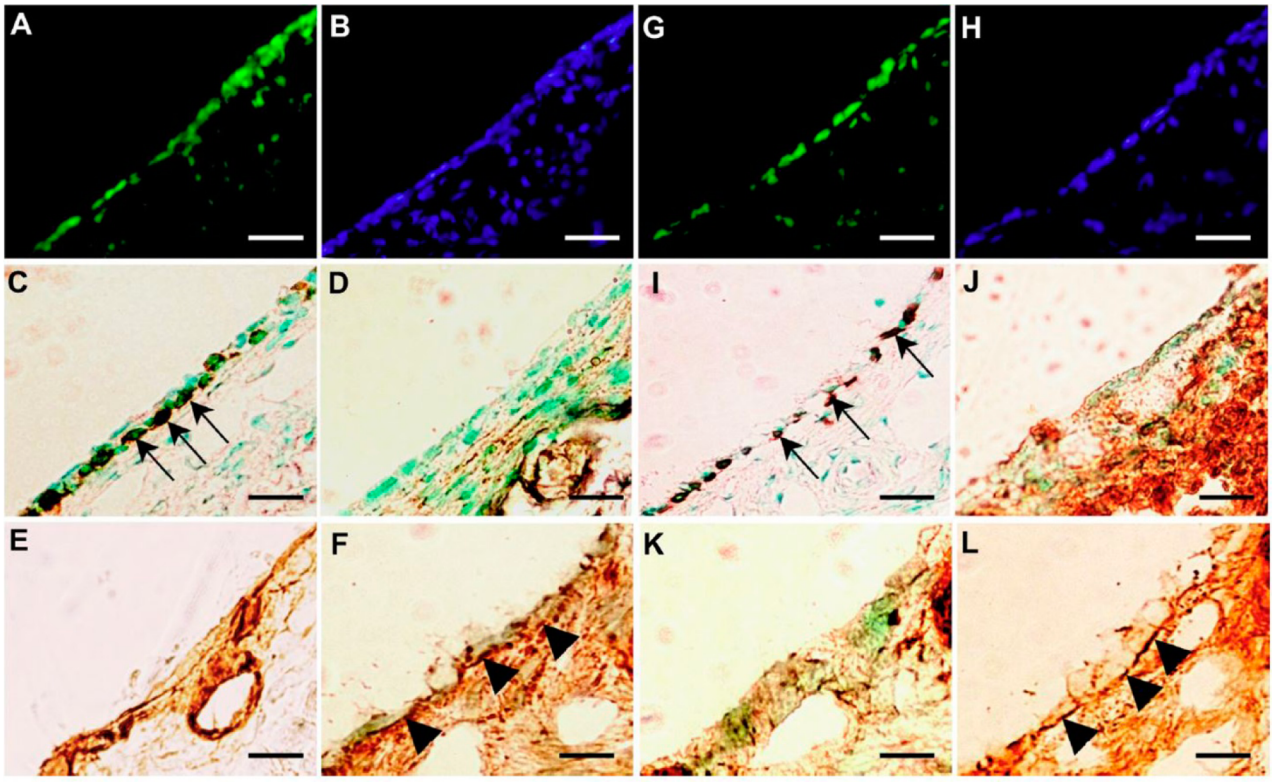

Figure 21. (A–L) Analysis of transplanted mucosal epithelial cells in recipient tissues at postoperative days 14 and 28. Serial frozen sections of middle-ear bullae after transplantation (0.5×10^6 cells/mL) at (A–F) postoperative day 14 and (G–L) postoperative day 28. (A, B, G, H) Fluorescence images at several time points. Enhanced green fluorescent protein (EGFP)-expressing cells were detected on the internal surface of recipient middle-ear bullae (green, EGFP; blue, 4′,6-diamidino-2-phenylindole) (A, G). Results of immunostaining with (C, I) antipancytokeratin, (D, J) antivimentin, (E, K) anticollagen III, and (F, L) anticollagen IV antibody. EGFP-expressing cells were positive for pancytokeratin (C, I, arrows), but not for vimentin (D, J). Collagen III-positive regions were detected mainly in the subepithelium (E, K). Collagen IV-positive regions were detected under the monolayer structure of donor cells at 14 and 28 days after transplantation (F, L, arrowheads). The scale bars represent 50 μm. Adapted with permission from ref 1121. Copyright 2013 Dove Medical Press Ltd.

Akiyama et al. have designed a synthetic peptide hydrogel which consists of a 16-amino acid peptide (**281**)[1118] and is called PuraMatrix.[1119,1120] The authors used **281** to assess the feasibility of transplantation of isolated mucosal cells to repair a damaged middle ear. The authors collected middle-ear bullae with mucosa from rats, transfected the cells with enhanced green fluorescent protein (EGFP), encapsulated the cultured middle-ear mucosal epithelial cells into PuraMatrix hydrogels (1%, w/v), and then transplanted the cells into the immunosuppressed rats (Figure 21). Besides validating that primary cultured cells retain the character of middle-ear epithelial cells, the authors found that a high proportion of EGFP-expressing cells reside in the recipient middle ear after the transplantation using the hydrogel, but not without the hydrogel. These extensive studies demonstrated the feasibility of transplantation of cultured middle-ear mucosal epithelial cells encapsulated within **281** for regeneration of surgically eliminated mucosa of the middle ear in Sprague Dawley (SD) rats.[1121] However, the authors also observed that the proliferation rate depends on the seeding density and suggested that it might be due to contact inhibition or the limitation of the nutrient supply. In another related study, PuraMatrix served as the carrier for recombinant human bone morphogenetic protein-2, which significantly enhances bone regeneration in a bone augmentation rabbit model.[1122]

Wang et al. tested the hydrogels made of the self-assembling peptide **281**[1118] or **281** containing the laminin epitope IKVAV (**545**) at the C-terminal to act as a functional peptide-based scaffold to repair injured brain tissue. They found that **545** self-assembles to form nanofibers with a bilayer β-sheet structure and affords a hydrogel with mechanical stiffness similar to that of brain tissue, which makes the hydrogel suitable for encapsulating NSCs in an animal model study. The authors reported that the in vitro results showed that **545** serves as a guiding cue to promote the adhesion of the encapsulated NSCs and to bias the neuronal differentiation of these cells. Using the injected peptide solution to form the 3D hydrogel immediately in situ for filling up the cavity and bridging the gaps in the wound created in the brain, the authors demonstrated that the hydrogel of **545** enhances the survival of the encapsulated NSCs and reduces the formation of astrocytes. Although the authors reported enhanced neuronal differentiation and an improvement in brain tissue regeneration after 6 weeks post-transplantation,[1123] the functional recovery of the damaged brain remained to be evaluated. In addition, the authors also linked other functional groups derived from fibronectin and laminin (e.g., GRGDS (**546**) or YIGSR (**547**)) to the **281** motif to evaluate the capability of these functionalized self-assembling peptides for the purpose of maintaining hemostasis and liver tissue regeneration.[1124] After developing responsive α-helical peptide hydrogels,[632] Woolfson et al. tested these hydrogels for cell culture.[1125] They reported that the cell viability is high and the α-helical gel network is stable in tissue culture conditions over 14 days.

DOI: 10.1021/acs.chemrev.5b00299
Chem. Rev. 2015, 115, 13165–13307

Scheme 71. Representative Molecular Structures of Hydrogelators Encapsulating Drugs

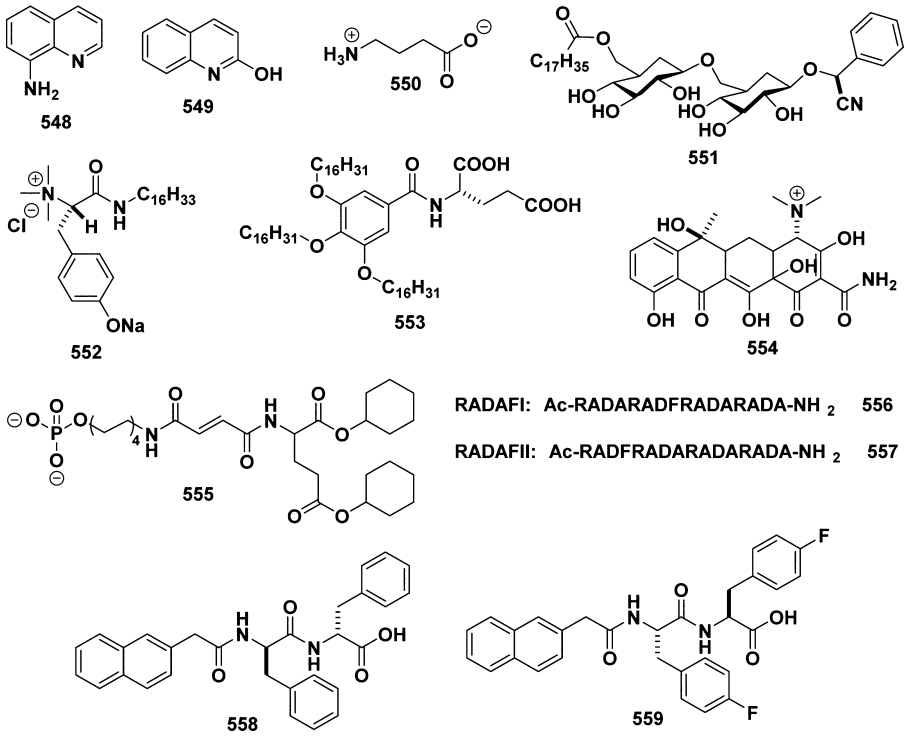

5.6. Drug Delivery

Besides macroscopic properties, such as soft and wet, the majority of the volume of supramolecular hydrogels is micropores filled with water. These interstices allow the hydrogels to serve as a carrier or medium of other bioactive molecules[1126−1128] for a relatively straightforward application, such as drug delivery.[28,60,890,1091,1093,1129−1139] To describe the applications of supramolecular hydrogels for drug delivery, we arrange the following section in two parts: first, we mainly describe various hydrogelators used for encapsulating drugs;[1140−1146] second, we focus on hydrogelators covalently conjugated with therapeutics.[1147−1153]

5.6.1. Hydrogels Encapsulating Drugs. As shown in Scheme 71, van Esch et al. reported the use of the classical small molecular hydrogelator *N*,*N*′-dibenzoyl-L-cystine (DBC, **1**) for the release of small molecules 8-aminoquinoline (AQ, **548**) and 2-hydroxyquinoline (HQ, **549**) as model molecules of drugs. Using self-assembly of **1** to form stable, clear hydrogels in 150 mM NaCl solution and PBS buffer, the authors tested this kind of hydrogel for the release of certain small molecules. The authors concluded that the release profiles depend on the interactions of the hydrogelator with the entrapped molecules because they observed that the release of **549** from the gels of **1** was 7 times faster than that of **548** due to acid−base interactions between **548** and **1**. As suggested by the authors, the judiciary combinations of the hydrogelator and the drug molecules should be able to control the release of the drugs.[78] Xu et al. reported the combination of two simple Fmoc-amino acids (**533** and **201**) to form semitransparent hydrogels at pH 9.1 with a minimum concentration of **533** or **201** of 10 mM. After the addition of 2 molar equiv of Na_2CO_3, the mixture of **533** or **201** forms a clear hydrogel consisting of entangled irregular fibers with widths of 120−500 nm. Besides the inclusion of **201**, an anti-inflammatory drug candidate,[1154] the hydrogels act as carriers for other bioactive agents, such as 5-fluoro-2A-deoxyuridine (5-FU), an antineoplastic agent, or pamidronate, an osteoporosis drug,[282] by the simple mixing of the drugs in the solution of **533** or **201** prior to hydrogelation.[1155] Haldar et al. reported that the addition of γ-aminobutyric acid (**550**) to the solution of Fmoc-lysine (**202**) leads to the formation of a hydrogel at pH 6.9 without any heating−cooling cycle at a concentration of 2 wt %. The authors suggested that this hydrogel could be used for the recognition and release of the anti-inflammatory agent **202**.[1156]

John et al. synthesized a hydrogelator made of amygdalin−fatty acid conjugates (**551**). In this type of hydrogelator, the sugar moiety facilitates intermolecular hydrogen bonding, the phenyl ring enhances intermolecular aromatic−aromatic interactions, and the hydrophobic hydrocarbon chain decreases the solubility in water and increases the molecular association through the van der Waals interactions. The authors used the networks made of helical ribbons and fibers (∼50 nm) in the hydrogel of **551** for encapsulating curcumin, a chemopreventive hydrophobic drug, to demonstrate the potential application of the hydrogel of **551** in drug release.[1157] On the basis of L-phenylalanine and L-tyrosine with subtle variation in the structure of the head group, Das et al. designed and synthesized 10 structurally correlated amino acid-based amphiphiles for screening hydrogelators, and found 3 of them to confer pH-responsive hydrogels at room temperature. Forming at a CGC of 4 wt %, the hydrogel of **552** exhibits remarkable sensitivity to pH, which makes the hydrogels suitable for the release of vitamin B_{12} and cytochrome *c*. The authors found that, at pH 7.4, all three hydrogelators form suitable hydrogels to release the entrapped biomolecules via diffusion. At endosomal pH (∼5.5) or a further lower pH, the release rate of biomolecules from the hydrogel of **552** increases by about 10-fold compared to that observed at pH 7.4, largely due to the dissociation of the gels.[74]

DOI: 10.1021/acs.chemrev.5b00299
Chem. Rev. 2015, 115, 13165−13307

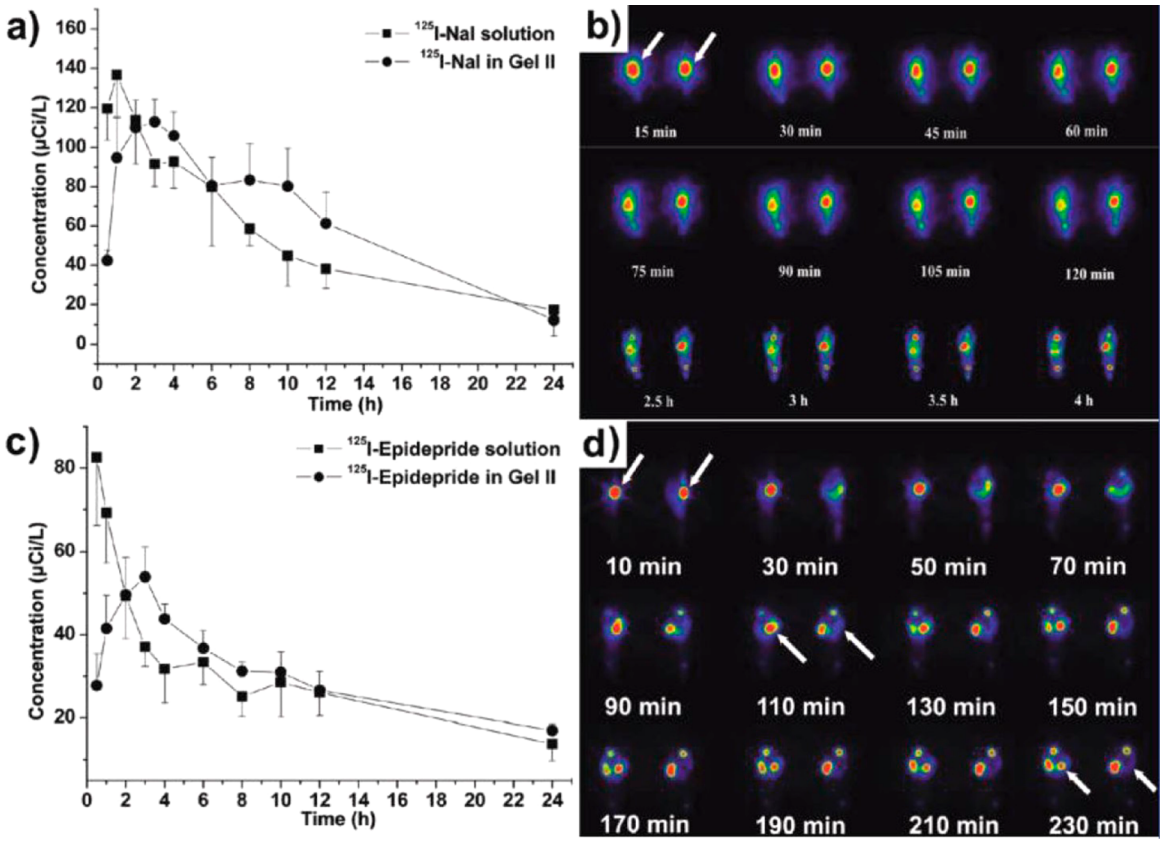

Figure 22. (a) Profiles of the mean blood concentration of ^{125}I-NaI vs time after subcutaneous (sc) administration to rats (160 μCi/kg) (■, control, ^{125}I-NaI solution, AUC (area under the curve) = 1213.3 μCi·h/L; ●, experimental, ^{125}I-NaI in gel II, AUC = 1453.5 μCi·h/L). (b) Dynamic (upper two lines) and static (lower line) single-photon emission computed tomography (SPECT) images of rats with ^{131}I-NaI (500 μCi/rat; left, in solution; right, in gel II) administered sc. (c) Profiles of the mean blood concentration of ^{125}I-epidepride vs time after sc administration to rats (160 μCi/kg) (■, control, ^{125}I-epidepride solution, AUC = 645.5 μCi·h/L; ●, experimental, ^{125}I-epidepride in gel II, AUC = 693.6 μCi·h/L). (d) Dynamic SPECT images of rats with ^{131}I-epidepride (500 μCi/rat; left, in gel II; right, in solution) administered sc. Adapted from ref 1176. Copyright 2009 American Chemical Society.

Lehn et al. reported a guanosine derivative, guanosine-5′-hydrazide (**347**), that forms tetramers (i.e., G-quartet (G4)[1158,1159]) in the presence of cations such as Na^+, K^+, and NH_4^+. The authors used the hydrogel of **347** to entrap acyclovir, vitamin C, or vancomycin for controlled release.[1160] Besides the physical trap and release of biological molecules, Lehn et al. later reported that the G-quartet structure of **347** acts as a delivery system for the slow release of bioactive carbonyl derivatives since aldehydes or ketones can reversibly react with the free hydrazide functions at the periphery of the G-quartet to form acylhydrazones.[1161] Barthelemy et al. reported the first example of the use of a glycosyl-nucleoside lipid for the delivery of oligonucleotides into cells (human Huh7 cells). They linked a simple monosaccaride, a lipidic chain, and a nucleoside together by 1,2,3-triazole bridges to obtain **339**, which self-assembles to form nanofibers roughly 20−30 nm in diameter and results in hydrogels at a concentration above 2.5 wt %. They reported that **339** is compatible with Huh7 cells after 5 days of incubation and the nucleic acid−**339** complex enhances the cellular uptake of the nucleic acids in the presence of serum.[1162] Yi et al. designed and synthesized three amphiphilic 3,4,5-trihydroxybenzoic derivatives with alkyl chains of different lengths, among which **553** and **554** gel aqueous ethanol in the presence of the water-soluble drug tetracycline hydrochloride. They found that a small amount of small molecules (10 mg/mL **554** or 3.3 mg/mL **553**) are able to entrap a large amount of tetracycline, up to 91.5%. In addition, the release studies of tetracycline in various solutions indicate that the release rate of tetracycline for a bovine serum albumin (BSA) solution (10 mg/mL) is faster than that with the other solutions because of the strong interaction between tetracycline and BSA.[1163]

Schneider and Pochan have designed a class of self-assembling peptides that undergo triggered hydrogelation in response to physiological pH and in salt conditions (pH 7.4, 150 mM NaCl) to form mechanically rigid, viscoelastic hydrogels.[28] Among the β-hairpin peptides, **251** and **257** are two peptide sequences with different charge states for directly encapsulating and controllably releasing model fluorescein isothiocyanate (FITC)−dextran macromolecules of varying size and hydrodynamic diameters.[1164] Using fluorescence recovery after photobleaching (FRAP), the authors studied the self-dissociation of the hydrogels and bulk release of model FITC−dextran macromolecules. The authors reported that the mobility of the macromolecules or the probes within and release of these hydrogels depended on the sizes of the probes, the peptide sequences, and the mesh size of the hydrogel.[1165,1166] Later, the authors also found that the self-assembling **257** peptide hydrogel is an effective vehicle for the local delivery of curcumin.[1167] Hamachi et al. reported a single-component, multiple-stimulus responsive hydrogelator, **555**, containing a phosphate group that displays a macroscopic

DOI: 10.1021/acs.chemrev.5b00299
Chem. Rev. 2015, 115, 13165−13307

Scheme 72. Representative Molecular Structures of Hydrogelators Encapsulating Drugs

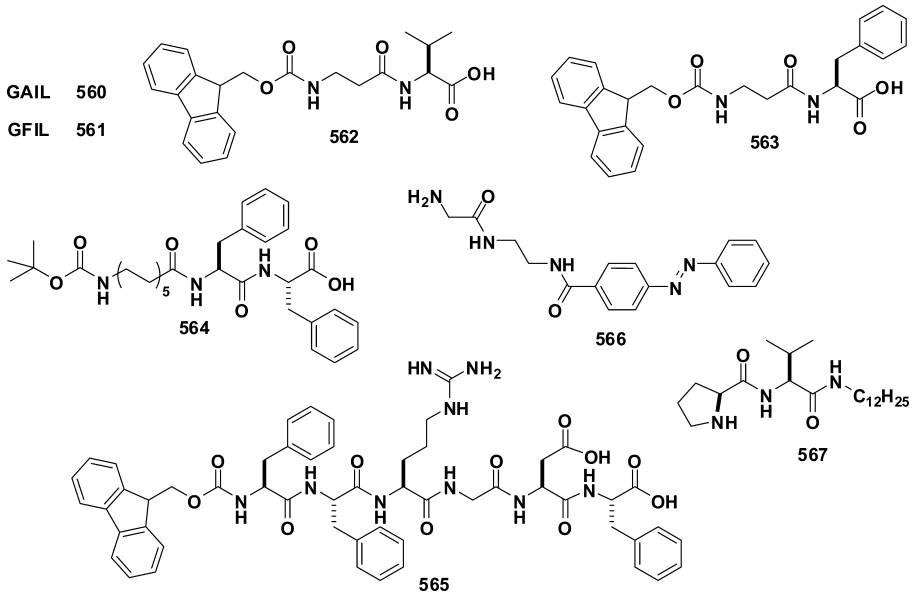

gel−sol response toward four distinct input stimuli (temperature, pH, Ca^{2+}, and light). The authors suggested that the hydrogelator confers gel-based supramolecular logic gates displaying AND, OR, NAND, and NOR functions. By using these logic-gate-like functions, they found that the hydrogel is able to hold and release bioactive substances (e.g., vitamin B_{12} or the protein Rh-Con A) in response to various input triggers.[1168]

Several labs evaluated the Ac-$(RADA)_4$-$CONH_2$ (**281**) peptide hydrogel to act as an efficient slow release carrier of a variety of proteins,[1169,1170] such as lysozyme, trypsin inhibitor, BSA, and immunoglobulin G (IgG), which differ in physicochemical properties and morphologies. The results of the fluorescence correlation spectroscopy (FCS) analysis indicated that the peptide hydrogel of **281**, at a concentration of 1 wt %, can encapsulate the proteins and release the proteins when the hydrogel disintegrates due to the degradation of the peptides by proteolytic enzymes in vivo. Furthermore, Zhang et al. found that the protein diffusion through the hydrogel of **281** depends primarily on the size of the proteins and the encapsulation and release barely affect the protein conformations and functions.[1171] Later, Zhang et al. reported the use of the peptide hydrogels for facilitating slow and sustained release of active cytokines related to many areas of regenerative medicine. However, the release of negatively charged VEGF from the hydrogel of **281** is slower compared to that of cytokines of somewhat similar molecular weight but opposite charge, suggesting that the positive guanidinium interacts with VEGF and hinders the diffusion of VEGF. The authors also found that the release of functional human βFGF and VEGF occurs over 2−3 weeks within the hydrogel of **281** and two other hydrogels formed by peptides with net positive or negative charges located at the C-terminal.[1172] Shibata et al. have recently found that the aqueous solution of **281** and insulin form a hydrogel, in vitro and in vivo, with an increase of the ionic strength by phosphate ion and an increase of the pH. The in vitro experiments indicated that the release rate of insulin depends on the concentration of **281** and the controlled release of insulin occurs at final concentrations of **281** between 0.1 and 2.0 wt %. Furthermore, the authors found that **281** forms a hydrogel in vivo for a sustained-release insulin, which also depends on the concentration of **281**.[1173] Tan and Kinoshita modified the **281** peptide scaffolds by positioning a phenylalanine residue at the C-terminal to generate **556** and **557** and studied the entrapment and the release of certain enantiomers (e.g., D-, and D-phenylalanine) of amino acids. They found that the amount and chirality of the guests tailor the network nanostructures, thus affecting the release of the enantiomers. In addition, the release rate of the enantiomers from the hydrogels containing one phenyl group (**556** and **557**) is much slower than from the hydrogels without a phenyl group (**281**), agreeing with the aromatic interactions between the hosts and the guests. The concentration of the trapped enantiomers after the diffusion[1174] matches with the release kinetics controlled by Fickian diffusion, which depends on both the rational design of the peptides used for making the hydrogels and the choice of the size and lipophilicity of the entrapped molecules.[1175]

Xu et al. reported the first in vivo imaging for investigating the drug release properties of the supramolecular hydrogel formed by hydrogelators **558** and **559** consisting of naphthalene (Nap) and a D-peptide of diphenylalanine (Figure 22). TEM images show that the hydrogels consist of nanofibers with a length of over tens of micrometers, a width of about 50 nm, and an average mesh size of about 200 nm. Since the hydrogels resist hydrolysis catalyzed by proteinase K and offer long-term biostability, the hydrogel of **559** is suitable for the controlled release of drugs in vivo.[1176]

As shown in Scheme 72, Banerjee et al. reported two synthetic self-assembling tetrapeptides, GAIL (**560**) and GFIL (**561**), that form thermoreversible and pH-sensitive hydrogels which consist of long, interconnected nanofibrillar network structures with diameters of 15−30 and 10−25 nm, respectively. These hydrogels entrap doxorubicin to allow its slow release at physiological pH, and achieve almost 85% (for peptide gel **560**) and 90% (for peptide gel **561**) release of the drug molecules after 45 h.[1177] Adams et al. reported the hydrogels of Fmoc-Phe (**200**) and Fmoc-Tyr (**15**) formed by careful adjustment of the pH of the solution using GdL. They found that the hydrogels of **200** and **15** entrap and release

DOI: 10.1021/acs.chemrev.5b00299
Chem. Rev. 2015, 115, 13165−13307

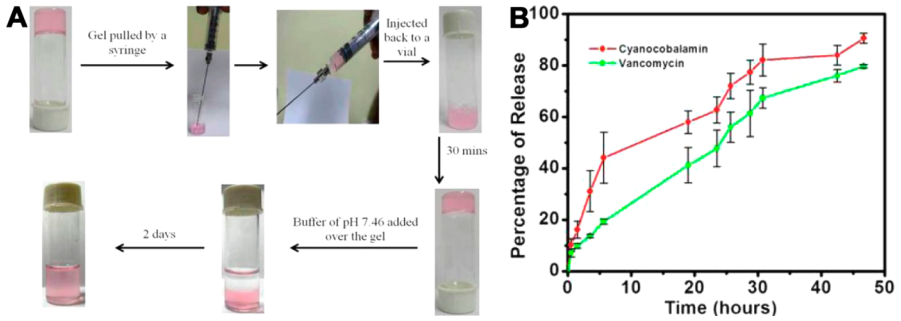

Figure 23. (A) Illustration of the injectable nature of the hydrogel and its vitamin release phenomenon with vitamin B_{12}. (B) Percentage release plot of some important biomolecules from hydrogel **564** at physiological pH (7.46) and temperature (37 °C), where the concentration of the drugs loaded into the hydrogel was 1.14 mg/mL for cyanocobalamin (vitamin B_{12}) and 0.24 mg/mL for vancomycin. Adapted from ref 1179. Copyright 2014 American Chemical Society.

Scheme 73. Representative Molecular Structures of Hydrogelators Encapsulating Drugs

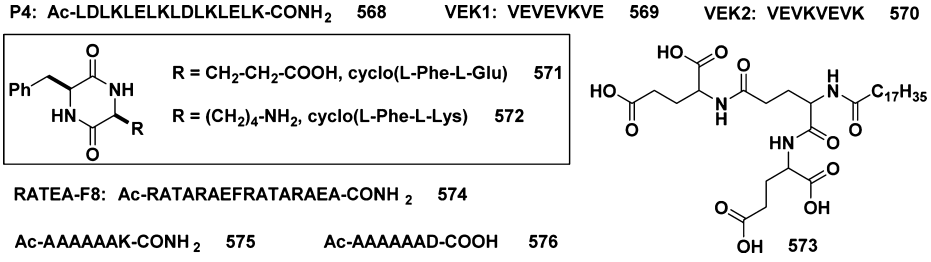

certain dye molecules under the control of Fickian diffusion. On the basis of the similar diffusion coefficients of the dyes of different radii from the hydrogel of **200**, the authors concluded that the networks in the hydrogel of **200** only restrict molecules larger than 5 nm.[1178] Banerjee et al. reported two N-terminally protected dipeptides (**562** and **563**) with a β-amino acid residue that form hydrogels at physiological pH (7.46) and temperature (37 °C). Having different CGCs (0.85 wt % for **562** and 1.21 wt % for **563**), the hydrogels consist of nanofibers of different widths (45−130 nm for **562** and 30−60 nm for **563**). In addition, these two hydrogels can encapsulate and sustainably release two vitamins (vitamin B_2 and vitamin B_{12}) over 3 days.[90] Banerjee et al. reported that a designed tripeptide-based hydrogelator (**564**) having both 11-amino-undecanoic acid and Phe-Phe residues forms hydrogels that entrap vancomycin and vitamin B_{12} for sustained release at physiological pH and temperature for about 2 days (Figure 23). According to an MTT-based cell viability assay at 24 h, the authors suggested that this peptide gelator, **564**, is innocuous to cells.[1179]

Zhang and Jiang et al. reported a new peptide comprised of a peptide backbone containing an Arg-Gly-Asp (RGD) sequence and a hydrophobic Fmoc tail. The peptide derivative **565** self-assembles to form a transparent hydrogel and exhibits biocompatibility in rabbit eyes. The authors found that this peptide hydrogel, acting as an implanted carrier, delivers an antiproliferative model drug (5-fluorouracil, 5-FU) in rabbit eyes and inhibits postoperative scarring formation. According to the in vivo experiments reported by the authors, the 5-FU-loaded peptide hydrogel releases 5-FU to inhibit scleral flap fibrosis efficiently after the surgery.[1180] Later, Castelletto et al. reported another functionalized peptide, **401**, which also contains RGD. They found that **401**, at a concentration of 10 wt %, formed homogeneous hydrogel monoliths that are stable in water for nearly 40 days. Consisting of a rigid porous structure made of the peptide fibers, the hydrogel monoliths are able to encapsulate and release various molecules, including model hydrophilic dyes and drug compounds (e.g., bioactive riboflavin and hydrophilic pseudodrug salicylic acid).[1181]

Diaz et al. reported the supramolecular coassembly of complementary structures followed by controlled thiol−ene coupling as a new strategy for fine-tuning the drug release kinetics of self-assembled hydrogels made of small molecules **1**. TEM and SEM images indicate that **1** self-assembles into fibers 30−150 nm in diameter at a concentration of 0.2 wt %. Using in vitro experiments, the authors showed that the hydrogel of **1** entraps and releases small drugs, such as 2-hydroxyquinoline (**549**), a model of water-soluble and UV-active drugs.[1182] Jung and John et al. reported the formation of a coordination polymeric hydrogel made of a simple pyridine derivative (**516**) and Cu^{2+} ions. Consisting of a fibrillar network of fibers several micrometers in length and 45−65 nm in width, the hydrogel of **3** can encapsulate curcumin. Being pH-triggered at physiological temperature, the hydrogel dissociates and releases the encapsulated curcumin.[1183] Shimizu et al. designed and synthesized a simple amphiphile, **566**, consisting of a photoresponsive azobenzene and a hydrogen-bonding glycine to construct self-assembled nanotubes. TEM showed that the self-assembled morphologies strongly depend on the pH conditions; that is, the self-assembly of **566** at pH 6.1 gives fibers, but at pH 9.2 gives sheets. Upon UV-light irradiation, the trans−cis photoisomerization of the azobenzene within the tubular wall results in a morphological change from nanotubes to cylindrical nanofibers to release the pre-encapsulated guests (e.g., carboxyfluorescein (CF)) in the hollow cylinder of the nanotubes.[1184] Miravet and Escuder et al. reported a hydrogelator bearing a nucleophilic reactive site that reacts with aldehydes to cause the disassembly of the hydrogel network. **567** forms stable hydrogels at a concentration above 2 mM. The authors found that the hydrogels of **567** entrap and release

DOI: 10.1021/acs.chemrev.5b00299
Chem. Rev. 2015, 115, 13165−13307

Scheme 74. Representative Molecular Structures of Hydrogelators Conjugated with Drugs

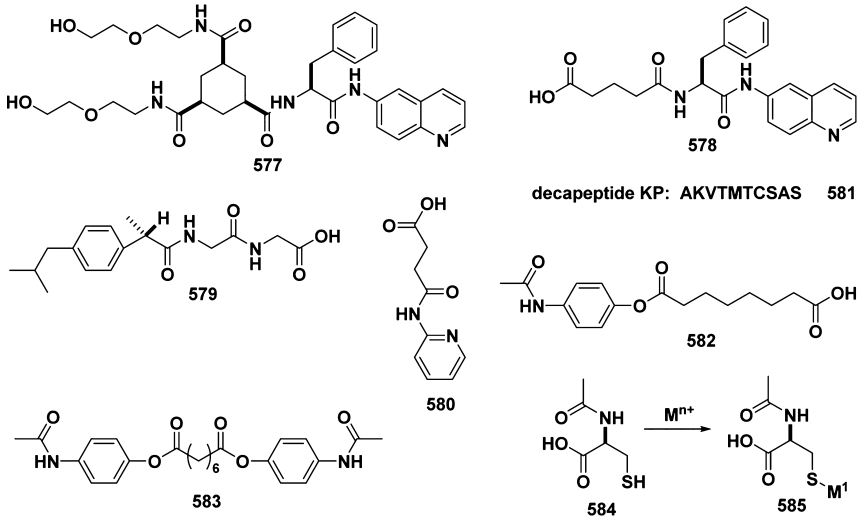

dyes or drugs (e.g., methylene blue or ketoprofen) in response to the presence of specific aldehydes. In addition, **567** is highly biocompatible, which may present a protective effect against toxic aldehydes.[1185] Rapaport et al. have developed amphiphilic β-sheet peptides P_{FD}-5 (**543**) decorated by acidic amino acids. **543** self-assembles to form ordered monolayers at the interfaces as well as hydrogels near physiological pH. The authors found that the mildly amphiphilic doxorubicin can be entrapped within the amphiphilic matrix of the peptide hydrogel, due to electrostatic forces and hydrophobic interactions. The peptide−doxorubicin interactions may affect the release of doxorubicin from the peptide hydrogels as less doxorubicin was released from the hydrogels with a higher loading of doxorubicin.[1186]

As shown in Scheme 73, Zhao et al. designed a self-assembling peptide, P4 (**568**), containing 16 amino acids that forms stable β-sheet nanofibers with a diameter of 25 nm and a length of micrometers. The authors found that the hydrogel of **568** is capable of stabilizing hydrophobic anticancer agents, such as ellipticine, a natural plant alkaloid. SEM images showed that the state of ellipticine in the complexes relies on the concentration of **568**, which also affects the size and morphology of the complex. It was found that the complexes of ellipticine and the peptide significantly reduce the viability of two cancer cell lines (SMMC7721 and EC9706 cells).[1187] Miller et al. reported three octapeptides, VEVEVKVE (VEK1, **569**), VEVKVEVK (VEK2, **570**), VKVKVEVK (VEK3, **230**), which carry a net charge of −2, 0, and +2 at neutral pH, respectively. The author found that all three peptides form transparent and self-supporting hydrogels. The hydrogels of **570** and **230** encapsulate two hydrophilic model drug molecules (naphthol yellow and martius yellow) and release them following Fickian diffusion and depending on the fibrillar network and the overall charges of the complex molecules.[1188]

Nachtsheim et al. reported the simple and remarkable small molecular hydrogelators of phenylalanine-containing cyclic dipeptides (diketopiperazines, DKPs, **571** and **572**), which only contain proteinogenic amino acids (serine, cysteine, glutamate, histidine, or lysine) as building blocks. **571** and **572** form stable and self-healing hydrogels with a porous network or dense lamellar sheets with bundled nanofiber connections between the sheets, respectively. Furthermore, the authors found that the mixture of **571** and **572** forms heterotypic hydrogels and demonstrated their use for the release of BSA and tetracycline.[1189] Liu et al. designed a supramolecular hydrogel based on a peptide dendron (**573**) and found that metal ions can trigger a continuous shrinkage after the gels have been annealed for several hours. It is reported that the metal ions (e.g., Mg^{2+}, Cu^{2+}) significantly promote the gelation capacity, and decrease the CGC from 0.3 to 0.08 wt % or below. In addition, the reversible shrinkage property of the hydrogels allows the controlled release of small molecules such as vitamin B_1 after addition of divalent metal ions (such as Mg^{2+}) into the gel.[1190,1191] Saiani et al. focused on an octapeptide, FEFEFKFK (**228**), which self-assembles into antiparallel β-sheet-rich fibers and forms hydrogels at concentrations above 2 wt % in water. The authors used the hydrogel of **228** for the delivery of two commercial drugs, lidocaine and flurbiprofen. They found that the addition of lidocaine to the hydrogel stiffens the samples without affecting the overall peptide release, while the hydrogel encapsulating flurbiprofen exhibits improved resistance erosion and enhances drug retention.[1192]

Kumar et al. reported the use of a class of phenylalanine (Phe)-containing self-assembling peptide nanofibrous material (RATEA-F8, **574**) for the delivery of 5-fluorouracil (5-FU) and leucovorin (LV), which shows synergistic action against colon cancer cells. The study of the gelation properties indicated that **574** self-assembles to form nanofibers in water and Tris−HCl buffer at a concentration of 0.78 wt % with a diameter of 5−20 nm and a length of 60−80 nm. The in vitro experiments indicated that the hydrogel of **574** slowly releases 5-FU, LV, and Phe.[1193] Koutsopoulos et al. designed a class of lipid-like peptides with an aspartic acid or lysine hydrophilic head and a hydrophobic tail composed of six alanines ($Ac\text{-}A_6K\text{-}CONH_2$ (**575**) or $Ac\text{-}A_6D\text{-}COOH$ (**576**)). The authors found that the addition of this kind of lipid-like peptide into water or an electrolyte solution results in formation of a turbid suspension due to self-assembly of the peptide monomers to minimize the interaction between the hydrophobic domains and polar environment. In addition, it was found that **576** is more suitable for the encapsulation and release of carboxyfluorescein and Nile red.[1194] In a related study, Qiu et al. reported the use of **575** to transfer pyrene into living HepG2 cells.[1195]

5.6.2. Hydrogelators Conjugated with Drugs. As shown in Scheme 74, van Esch et al. reported the gelation properties of a class of cyclohexanetrisamide-based hydrogelators with an L-

DOI: 10.1021/acs.chemrev.5b00299
Chem. Rev. 2015, 115, 13165−13307

phenylalanylamidoquinoline (L-Phe-AQ, **577**) moiety as well as two ethylene glycol chains.[1196] According to this design, α-chymotrypsin (α-chy) can enzymatically cleave the **577** moiety to release the fluorogenic model "drug" 6-aminoquinoline (6-AQ, **578**). Moreover, the cleavage of the two ethylene glycol chains increases the hydrophobicity of the overall structure to improve the gelation properties. The hydrogelator forms fibers with identical diameters of 4.2 nm and a thermoreversible hydrogel with a CGC of 0.03 wt % at room temperature. The authors envisioned that the hydrogel might act as a two-stage enzyme-mediated drug release system. That is, AQ (**548**), in the gel fibers, is initially protected from enzymatic cleavage; after the temperature is increased, more hydrogelators become available for enzymatic cleavage to result in a dramatic increase in the rate of release of **548**.[1197] Kim et al. synthesized a class of (*S*)-(+)-ibuprofen-based hydrogelators, among which **579** forms hydrogels consisting of entangled irregular fibers with widths of 60−100 nm and with a CGC of 0.9% (w/w). Two hours after the addition of an enzyme (carboxypeptidase Y), the hydrogel is able to release the drug (*S*)-(+)-ibuprofen.[1198]

Wang et al. reported a simple drug candidate, 4-oxo-4-(2-pyridinylamino)butanoic acid (**580**), which self-assembles to form hydrogels at a 4 wt % concentration under various conditions. They found that this hydrogel with different backbone structures releases drug molecules at different speeds.[1199] Polonelli et al. reported a synthetic decapeptide KP (**581**) derived from the variable region of the light chain of a recombinant antibody. They found that, in nonreducing conditions, the solubilized **581** molecules easily dimerize due to the formation of disulfide bridges and spontaneously and reversibly self-assemble to generate an organized network of fibril-like structures. Furthermore, this self-assembled network, likely being resistant to proteolysis, slowly releases the active dimeric form of **581**, which acts as a microbicide in vitro against a number of pathogenic microorganisms, such as *Candida albicans*.[1200] John et al. reported the synthesis of small hydrogelators **582** and **583** containing amphiphilic prodrugs, such as acetaminophen. The prodrugs self-assemble to form branched or entangled fibrous/sheetlike gel networks with a fiber thickness of 50−400 nm and fiber lengths of several micrometers. The hydrogels are able to encapsulate a second drug such as curcumin. Using the in vitro experiments with MSCs, the authors showed that the hydrogels of **582** and **583** release single or multiple drugs under physiological conditions and upon enzyme catalysis, and retain certain features of the MSCs.[1201] Odriozola et al. reported the use of coordination for converting *N*-acetyl-L-cysteine (**584**), a mucolitic agent or an antidote in paracetamol intoxication, into a hydrogelator. **585** is a metal−thiolate that self-assembles to form metallophilic hydrogels in the presence of Au(III), Ag(I), and Cu(II) salts with a microporous structure in the form of flakes. Although these specific hydrogels only form at pH < 4 to be able to act as drug delivery systems,[484] the concept demonstrated by Odriozola et al. should be applicable to other systems that form metallophilic hydrogels at physiological pH.

On the basis of the serendipitous discovery of a supramolecular hydrogelator made of vancomycin,[18] Xu et al. reported the first example of a hydrogelator (**586**) derived from an aminoglycoside antibiotic (e.g., kanamycin) and the resultant hydrogel for sequestering 16S rRNA selectively via divalent interaction (Figure 24, Scheme 75). **586** self-assembles to form a transparent hydrogel containing small fibrils with diameters from 50 to 60 nm at neutral pH with a CGC of 0.3 wt %. Kanamycin A in the hydrogel of **586** likely binds to the A-site of 16S rRNA. The association constant between **586** and 16S rRNA is much higher than the binding constant of kanamycin A with 16S rRNA, suggesting cooperative binding.[1202] Xu et al. designed and synthesized another hydrogelator (**587**) by using a tripeptide derivative that consists of a naphthyl group, two phenylalanines, and one modified lysine residue carrying an olsalazine moiety (a clinically used anti-inflammatory prodrug) in the side chain of the lysine residue. They found that **587** self-assembles to form supramolecular hydrogels under mildly acidic conditions with a CGC of 0.8 wt %. In addition, the reduction of olsalazine not only leads to a gel-to-sol phase transition but also controls the release of 5-aminosalicylic acid as the anti-inflammatory agent, which potentially provides a way to encapsulate the prodrug and release the active ingredients upon biological cues.[1203]

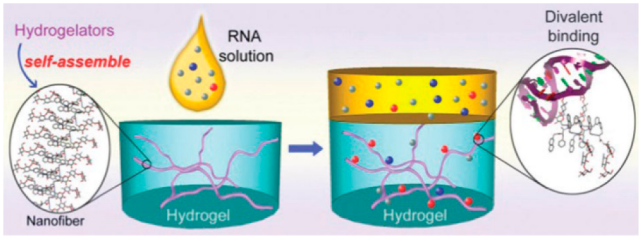

Figure 24. Supramolecular nanofibers sequester the potential targets (e.g., 16S rRNA (in red)) in the gel phase. Adapted with permission from ref 1202. Copyright 2012 Royal Society of Chemistry.

Xu et al. designed another hydrogel precursor (**588**) based on paclitaxel, a well-established antineoplastic agent that binds specifically to the β-tubulin subunit of microtubules to arrest mitosis and result in apoptosis. Upon the action of alkaline phosphatase, **588** turns into a hydrogelator (**589**) that self-assembles to form nanofibers with a uniform width of 29 nm and affords a supramolecular hydrogel of the paclitaxel derivative. The MTT cell viability assay indicated that, after 48 h of incubation with HeLa cells, **588** exhibited an IC_{50} value of 25 nM, which is comparable to that of paclitaxel (13.5 ± 2.2 nM). In addition, **589** itself also exhibited an IC_{50} of 25 nM, which is also comparable to that of paclitaxel and **588**.[155] Miravet et al. reported a class of innovative hydrogelators (**590**) by connecting a gel-forming lysine moiety with model drugs (e.g., benzylamine and phenethylamine) through a self-immolating spacer (*p*-aminobenzyloxycarbonyl). TEM images showed that **590** self-assembles to form hydrogels containing fibers with dimensions ranging from hundreds of nanometers in width and several micrometers in length. The authors found that trypsin catalyzes the hydrolysis of the amide linkage between the gelator moiety and the spacer of **590**, thus releasing the model drug.[1204]

As shown in Scheme 76, Yang et al. designed and synthesized the first example of a folic acid (FA)−paclitaxel conjugate,[1205] FA-G_pYK-paclitaxel (**591**). This innovative precursor contains paclitaxel, an effective, clinically used anticancer drug, folic acid, a ligand targeting cancer cells, and tyrosine phosphate, an enzymatic trigger for self-assembly.[1206] Upon dephosphorylation catalyzed by phosphatases, **591** forms a transparent hydrogel in PBS buffer at a concentration of 0.2 wt % with a nanosphere morphology. In addition, **591** also acts as a prodrug for releasing paclitaxel upon ester cleavage.[1207] Later, Yang et al. designed and synthesized another precursor (**592**) that contains two complementary anticancer drugs, dexamethasone

DOI: 10.1021/acs.chemrev.5b00299
Chem. Rev. 2015, 115, 13165−13307

Scheme 75. Representative Molecular Structures of Hydrogelators Conjugated with Drugs

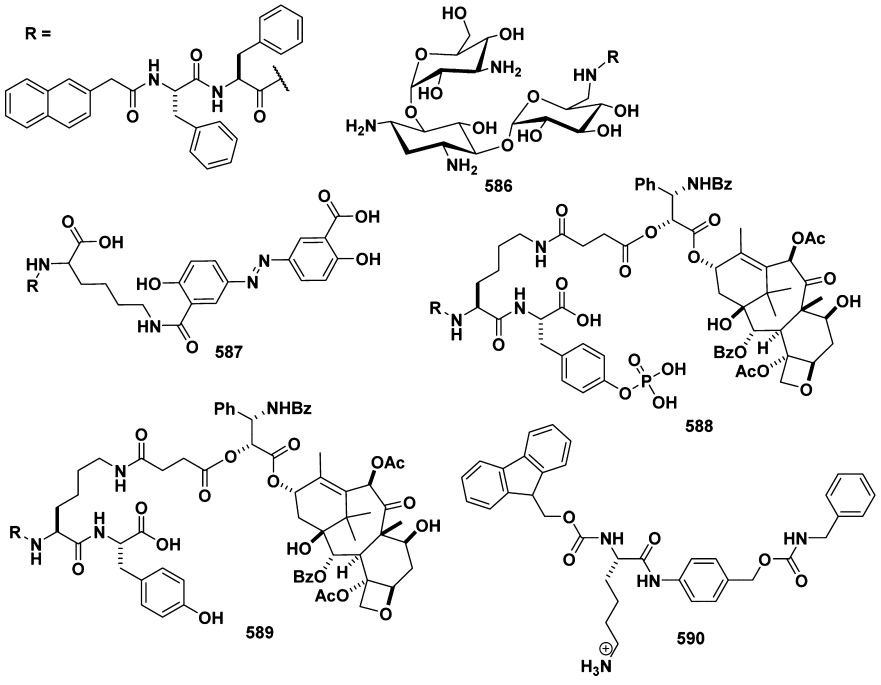

Scheme 76. Representative Molecular Structures of Hydrogelators Conjugated with Drugs

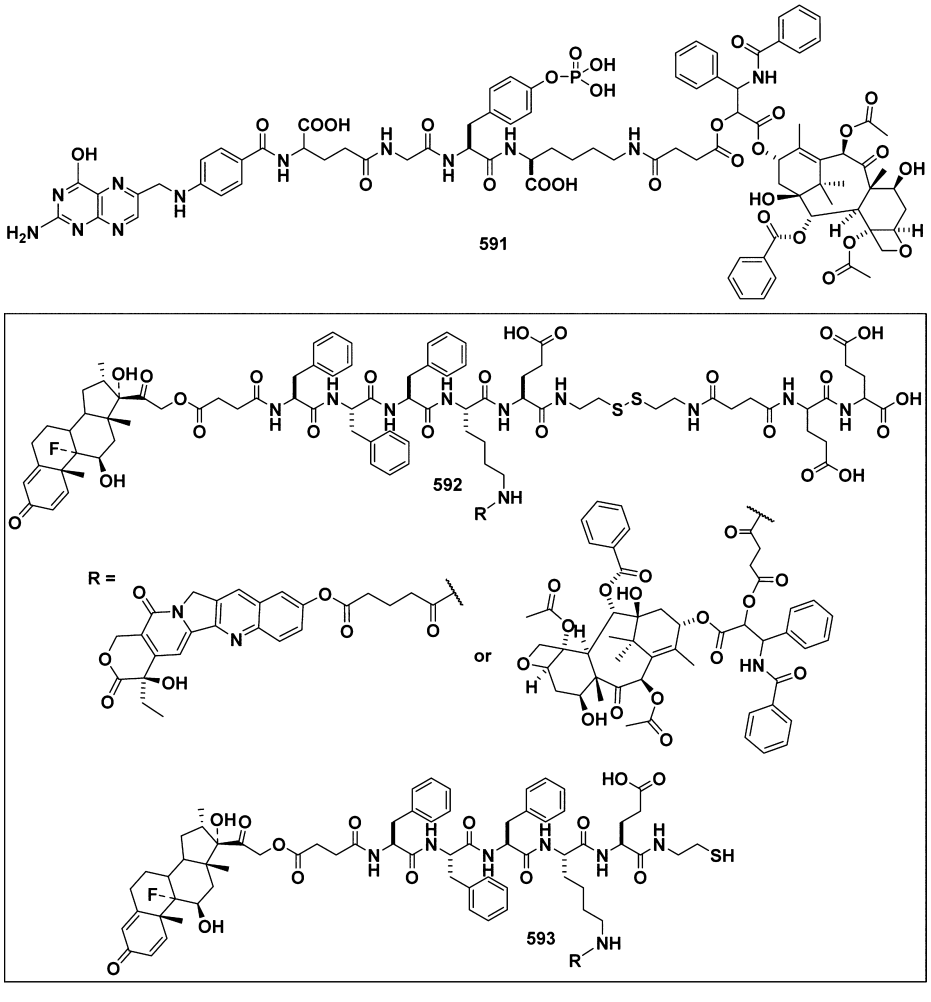

DOI: 10.1021/acs.chemrev.5b00299
Chem. Rev. 2015, 115, 13165−13307

Scheme 77. Representative Molecular Structures of Hydrogelators Conjugated with Drugs

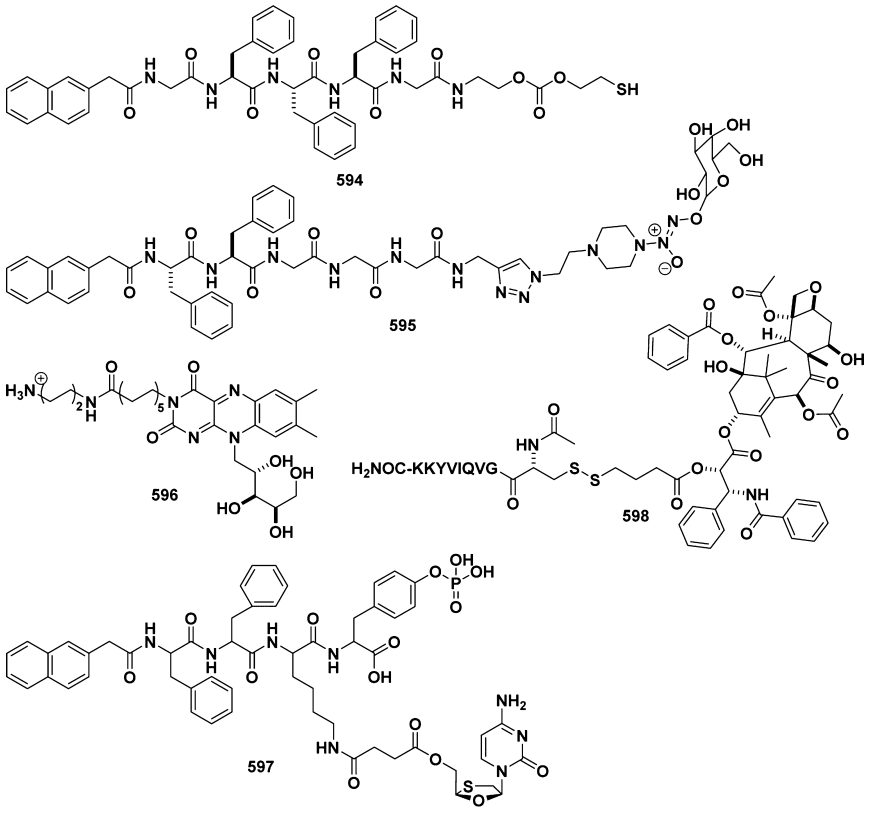

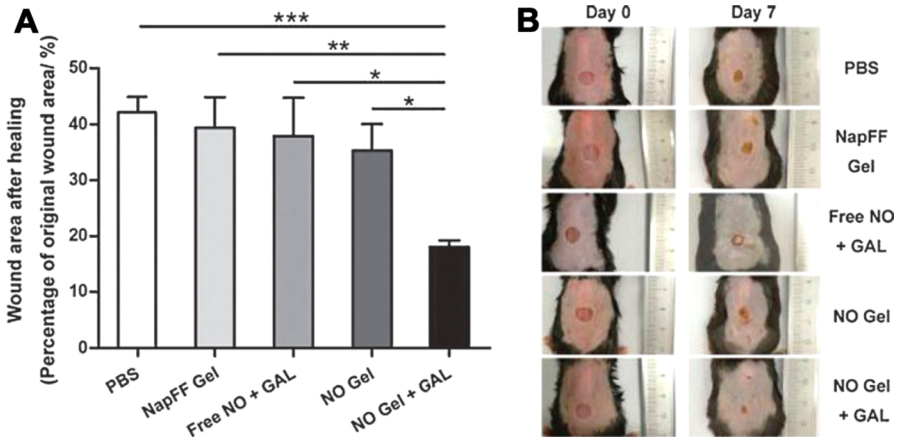

Figure 25. (A) Percentage of wound area left in different groups at day 7 compared to the original wound area (mean ± SEM) at day 0. (B) Photographs of wounds in animals treated with PBS buffer, **3** (hydrogel containing 1.0 wt % **3**), free NO + GAL (solution containing 0.2 wt % NO donor with daily addition of 1.5×10^{-4} U of β-galactosidase), NO gel (hydrogel containing 1.0 wt % **3** and 0.6 wt % **595** without the addition of β-galactosidase), and NO gel + GAL (hydrogel containing 1.0 wt % **3** and 0.6 wt % **595** with the addition of 1.5×10^{-4} U of β-galactosidase each day). Adapted with permission from ref 1211. Copyright 2013 Royal Society of Chemistry.

(Dex), an anti-inflammatory and immunosuppressant, and paclitaxel or hydroxycamptothecin (HCPT). Upon the reduction by GSH and DTT, **592** turns to **593**, which self-assembles to form hydrogels with CGCs of about 0.25 and 0.75 wt %, respectively, in PBS buffer. Four hours after the formation of the hydrogels, the authors added an equal volume of fresh PBS buffer solution and observed the original drug molecules of Dex, paclitaxel, and HCPT releasing from the gels due to the hydrolysis of the ester bond.[1208] They also developed a series of hydrogelators based on paclitaxel and short peptides/amino acids with simple synthetic strategies and high yields that could be used for the release of paclitaxel without any burst releases.[1209]

As shown in Scheme 77, Yang et al. also designed a precursor (**594**) by using a releasable disulfide carbonate linker to form stable molecular hydrogels. Although **594** is unable to be completely converted from the gelator terminated by a free thiol group to the gelator terminated by a hydroxyl group, the authors succeeded in generating a stable molecular hydrogel mainly formed by the hydrogelator terminated with a hydroxyl group. In addition, upon the endosomal reduction of the disulfide bond, a self-cyclization process results in the

DOI: 10.1021/acs.chemrev.5b00299
Chem. Rev. 2015, 115, 13165−13307

Scheme 78. Representative Molecular Structures of Hydrogelators for Immunological Modulation

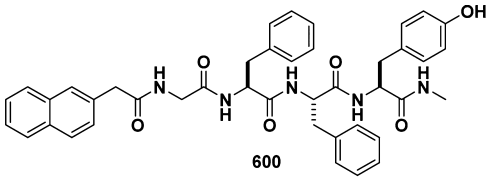

600

FLIVIGSIIGPGGDGPGGD 599

Aβ1–42 Wild type (PWT): DAEFRHDSGYEVHHQKLVFFAEDVGSNKGAIIGLMVGGVVIA 601

Aβ1–42 with Flemish mutation (PFM): DAEFRHDSGYEVHHQKLVFFGEDVGSNKGAIIGLMVGGVVIA 602

Aβ1–42 with Dutch mutation (PDM): DAEFRHDSGYEVHHQKLVFFAQDVGSNKGAIIGLMVGGVVIA 603

Aβ1–42 with Flemish and Dutch mutation (PFDM): DAEFRHDSGYEVHHQKLVFFGQDVGSNKGAIIGLMVGGVVIA 604

Aβ1–42 with novel mutation (P24M): DAEFRHDSGYEVHHQKLVFFAEDGGSNKGAIIGLMVGGVVIA 605

Aβ1–42 with novel mutation (P22W): DAEFRHDSGYEVHHQKLVFFAMDVGSNKGAIIGLMVGGVVIA 606

HGVTSAPDTRPAPGSTAPPASGSGQQKFQFQFEQQ 607

HGVTSAPDTRPAPGST(R_1)APPASGSGQQKFQFQFEQQ 608

HGVTSAPDT(R_1)RPAPGSTAPPASGSGQQKFQFQFEQQ 609

HGVTSAPDT(R_1)RPAPGST(R_1)APPASGSGQQKFQFQFEQQ 610

R_1 =

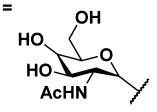

OVA-Q11: NH_2-ISQAVHAAHAEINEAGR-SGSG-QQKFQFQFEQQ-NH_2 611

OVA-KEF8: NH_2-ISQAVHAAHAEINEAGR-SGSG-FKFEFKFE-NH_2 612

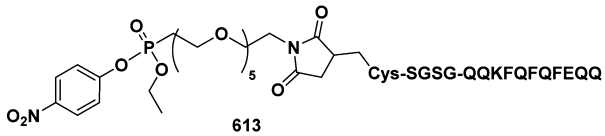

613

unmodified drug.[1210] Yang and Zhao et al. combined a galactose-caged nitric oxide (NO) donor and a short peptide of Nap-FFGGG to generate a hydrogelator (**595**) that forms hydrogels in PBS buffer at a concentration of 0.5 wt %. Using the β-galactosidase to remove the protective galactose from the NO donor, the authors demonstrated enzyme-triggered release of NO from the hydrogel of **595**. Furthermore, the in vivo experiments showed that the two-component hydrogels of **595** improve wound healing of mice (Figure 25).[943,1211−1214]

Kim et al. designed and synthesized an amphiphile (**596**) containing riboflavin, an essential biomolecule (vitamin B_2) that is involved in various biochemical processes. **596** forms hydrogels at a concentration of 1.6 wt % in acidic (pH 5) and neutral (pH 7.4) buffer solution with mild heating. The authors found that the hydrogel of **596**, being cell compatible, helps deliver VEGF-siRNA efficiently into human cells.[307,1215] Xu et al. conjugated anti-HIV reverse transcriptase inhibitor 2′,3′-dideoxy-3′-thiacytidine (3TC) or azidothymidine (AZT) to a versatile self-assembly motif of hydrogelators **597** to form supramolecular nanofibers as the matrixes of hydrogels in weak acidic conditions. In the presence of prostatic acid phosphatase (PAP), the hydrogels exhibit drastically enhanced elasticity, which should help to match the change of the physiological environment. In addition, the hydrogelators are biocompatible, and are able to release the HIV inhibitors under physiological conditions.[1216] Cui et al. reported the synthesis and assembly of a type of innovative amphiphile (**598**) containing a very bulky anticancer drug, paclitaxel, and a short peptide. With a relatively high loading (41%) of paclitaxel, **598** self-assembles to form nanofibers typically a few micrometers in length and with a diameter of 11.8 ± 1.3 nm in PBS buffer. The addition of GSH induces the release of paclitaxel, and the release depends on the concentration of **598**. In addition, the in vitro cytotoxicity of **598** showed that the amphiphile inhibited the growth of cancer cells (e.g., MCF-7, A549, and PC3-flu).[1217]

5.7. Immunological Modulation

As adjuvants are crucial components of vaccines, safer and more potent adjuvants are gaining increasing interest and attention. As injectable biomaterials for drug delivery and tissue engineering, supramolecular hydrogels made of peptides or peptide derivatives are excellent candidates as adjuvants because of their low cost of production, ease of being produced in large quantities, and relatively high activity and stability. These merits of peptides or peptide derivatives promise their applications in cancer immunotherapies and vaccination against infectious diseases, particularly for enhancing the potency of vaccines or for delivery of vaccines. For example, Sun et al. reported a self-assembling peptide, FLIVIGSIIGPGGDG-PGGD (**599**) (Scheme 78), consisting of two native sequences from an elastic segment of spider silk and a transmembrane segment of the human muscle L-type calcium channel. They prepared supramolecular hydrogels with **599** either by changing the pH of its solution or by adding the cation Ca^{2+} at a concentration of 0.5 wt % and found that the two resulting hydrogels formed by **599** through different approaches have distinct physical properties. They also found that the shear-thinning, rapid-strength-recovering hydrogel made of **599** and Ca^{2+} can be used as an H1N1 influenza vaccine adjuvant which is biologically safe and improves the immune response by 70% compared with an oil-based commercial adjuvant.[1218] They also evaluated the potential of **599** to act as an adjuvant for the porcine reproductive and respiratory syndrome virus (PRRSV) attenuated live virus (MLV) vaccine. Their studies suggest that the supramolecular hydrogel of **599**, when combined with the

DOI: 10.1021/acs.chemrev.5b00299
Chem. Rev. 2015, 115, 13165−13307

PRRSV MLV vaccine, can enhance the vaccine efficacy against two different PRRSV strains by modulating both the host humoral and the host cellular immune responses.[1219] Jiang and Yang et al. also reported a nanovector composed of a peptide-based nanofibrous hydrogel formed by NapGFFY-NMe (**600**) with a CGC value of 0.01%. According to their report, **600** can condense DNA to lead to a strong immune response against HIV by activating both humoral and cellular immune responses in mice. Their results indicate that the peptide-based nanovector promises biocompatibility and may provide a safe, straightforward, and effective approach for HIV DNA vaccines[943] if HIV DNA vaccines are effective in humans (Figure 26).[1220] Moreover, the impressive potency of **600** indicates its applications in other immunotherapies such as its use as an adjuvant in cancer immunotherapy.

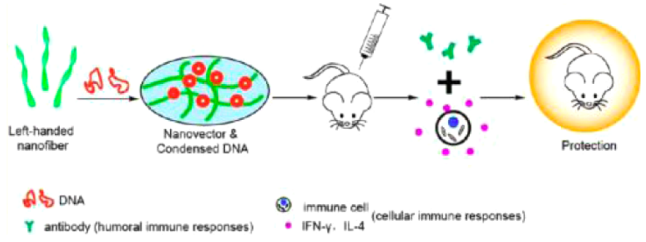

Figure 26. Process of a peptide-based nanofibrous hydrogel enhancing the immune responses of HIV DNA vaccines. Adapted from ref 943. Copyright 2014 American Chemical Society.

Besides being immunomodulating adjuvants, synthetic peptides or peptide derivatives are excellent candidates as antigens due to their precise chemical definitions, which allow one to specify the exact epitopes against an immune response. However, most peptides, despite being antigenic, are poorly immunogenic by themselves, thus requiring the assistance of strong adjuvants. Thus, the unique properties of self-assembling peptides motivate the pursuit of self-adjuvanting or adjuvant-free systems derived from peptides. Cao et al. developed a vaccine with mutant Aβ peptides **601**−**606** that avoid the use of an adjuvant. They demonstrated that these adjuvant-free vaccines with different Aβ peptides are able to induce a good antibody response without stimulating an unwanted inflammation reaction, thus acting as a safe vaccination approach against Alzhheimer's disease.[1221] Another example of a self-adjuvanting vaccine is derived from the understanding of MUC1 (mucin 1, cell surface associated). MUC1 proteins are key targets of the vaccines for epithelial tumors, which have a variable number of tandem repeats bearing tumor−tumor-associated carbohydrate antigens. However, short MUC1 peptides usually exhibit low immunogenicity, which remains a major obstacle in cancer vaccine development. To overcome this problem, Li et al. synthesized and evaluated a class of synthetic self-adjuvanting vaccine candidates (**607**−**610**) comprising a B-cell epitope with different glycosylation patterns and a nonimmunogenic self-assembling domain. They found that all of the peptide derivatives self-assemble into fibers over 200 nm long in aqueous solution at a concentration of 400 μM and display B-cell epitopes on the fiber surfaces. They demonstrated that the vaccine with Tn glycosylation in the PDTRP domain (**610**) after intraperitoneal injection elicits a significant immune response in mice.[1222]

Collier and Rudra et al. investigated the molecular determinants and immunological mechanisms leading to the significant immunogenicity of the self-assembling peptide OVA-Q11 (**611**), which elicits strong antibody responses in mice.[1223−1226] Their results showed that the deletion of amino acid regions in the peptide recognized by T cells or the mutation of the key residues in the self-assembling domain to prevent fibrillization could diminish or attenuate the immunogenicity of the peptides. Using a different self-

Scheme 79. Representative Molecular Structures of Hydrogelators for Immunological Modulation

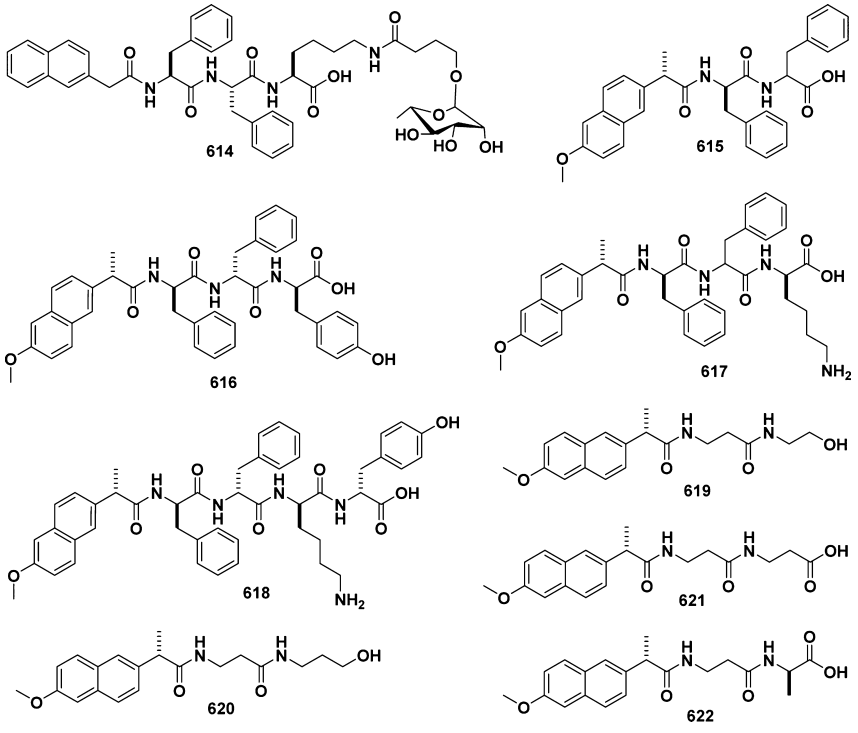

DOI: 10.1021/acs.chemrev.5b00299
Chem. Rev. 2015, 115, 13165−13307

assembling sequence to make OVA-KFE8 (**612**), which also self-assembles to form nanofibers and elicits a strong immune response, they demonstrated that **407** and KFE8 themselves are unrelated to immumogenicity while it is the peptide assembly that matters. Collier et al. concluded that a key strategy for modulating the immunogenicity appears to center on the effective T cell epitope, and this appears to be broadly applicable to fibrillar peptide assemblies.[1227] Collier et al. also utilized the same self-assembling domain **407** to design and develop another self-adjuvanting supramolecular vaccine which carries a folded protein antigen. They first synthesized pNP-Q11 (**613**), having a pNP (*p*-nitrophenyl phosphonate) ligand[919] on the N-terminal of the **407** domain. In parallel they designed and expressed a fusion protein (cut-GFP) containing cutinase and GFP domains separated by a flexible linker of glycine and serine residues. They found that **613** self-assembles to form nanofibers, with a morphology similar to that of the nanofibers of **407**, and the resulting nanostructure remains unchanged after reaction with cutinase fusion proteins. The cutinase−pNP interaction allows antigens to be conjugated without destroying their tertiary structures. Their results demonstrate that the nanofibers bearing GFP elicit robust anti-GFP antibodies, which indicates that the supramolecular assemblies can act as self-adjuvanting vaccines for whole-protein antigens.[1228]

In addition to boosting the immune response, supramolecular hydrogels formed by peptide or peptide derivatives also suppress immunity. Xu et al. designed and synthesized a conjugate, **614**, of a self-assembling motif and L-rhamnose to examine its immunomodulatory properties (Scheme 79). They found that **614** self-assembles in water to form a weak hydrogel (0.4 wt %) which allows the encapsulation of a fluorescent model antigen, (*R*)-phycoerythrin (PE). Surprisingly, they found that the resulting hydrogel, in contrast to the properties of monomeric L-rhamnose, suppresses the antibody response of mice to PE.[1229] Several laboratories also explored supramolecular hydrogels as anti-inflammatory agents. Xu et al. demonstrated that the covalent conjugation of D-amino acids to naproxen (i.e., a nonsteroidal anti-inflammatory drug (NSAID)) not only affords supramolecular hydrogelators (e.g., **615**, **616**, **617**, and **618**) for potential topical anti-inflammatory gels but also significantly raises the selectivity toward COX-2 about 20-fold at little expense of the activity of naproxen.[1230] Similarly, Dastidar et al. conjugated naproxen with *β*-amino acid to generate a variety of supramolecular conjugates such as **619**, **620**, **621**, and **622**, all of which are able to gel pure water, NaCl solution, or PBS buffer with CGC values of 0.80−2.0 wt %. They found that all of the hydrogelators display an anti-inflammatory response comparable to that of the parent drug.[1231]

5.8. Wound Healing

Although many wound dressings have entered clinical use, these wound dressings still are unable to fully satisfy the requirement of wound healing. An ideal wound-healing therapeutic should offer an optimal microenvironment to achieve a rapid wound closure, a functionally satisfactory recovery, and minimal scar formation.[1232,1233] Hydrogels are of great interest as wound dressing or its component because hydrogels preserve the gaseous permeability, provide a hydration environment, absorb wound exudate, and serve as the matrixes for drug delivery.[1234] However, current wound-healing hydrogels have only limited functions and are still unable to adequately match the complexity of wound-healing processes. Despite the enormous challenges in the development of hydrogels for wound healing, the exploratory works described in the following have provided useful insights for further development of supramolecular hydrogels for wound healing.

On the basis of the biological functions of glucosamine in the wound-healing process,[1236] Xu et al. designed a hydrogelator (**623**) containing glucosamine. **623** is able to form a hydrogel at a concentration of 0.2 wt %. The preliminary animal model study found that the application of the hydrogel of **623** to the mice with a skin wound promotes wound healing and reduces the formation of scars, compared to the results for the control mice without the treatment (Figure 27).[1235] One intriguing

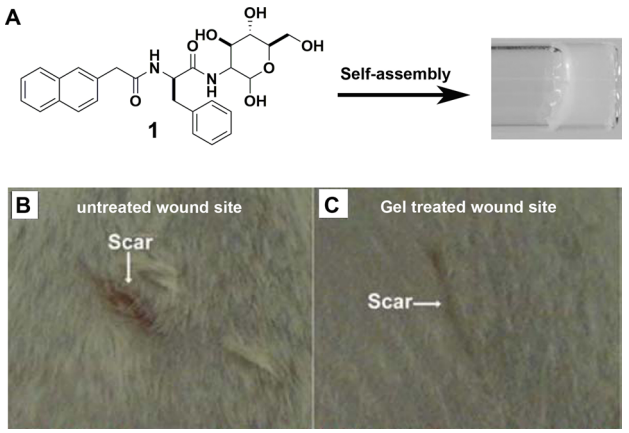

Figure 27. (A) Molecule **623** self-assembles to form a hydrogel. Gross appearance of the wound site treated without (B) or with (C) the gel on day 6. Adapted with permission from ref 1235. Copyright 2007 Royal Society of Chemisty.

observation is that the use of L-Phe in **623** fails to afford a wound-healing hydrogel, which indicates that the subtle structure change in the glycopeptide may have profound impacts on both hydrogelation and their biological functions. It would valuable to understand the underlying mechanisms of this kind of observation. In another experiment on wound healing, Xu et al. used disodium pamidronate (**624**) (Scheme 80), a clinically used drug that binds with UO_2^{2+}, to generate a supramolecular hydrogel with Fmoc-Leu (**533**) and Fmoc-Lys (**201**). Four equivalents of **624** plus **533** and **201** yields a transparent hydrogel at pH 10.4. The resulting hydrogel is able to reduce the uranyl ion poisoning in the wound on mice because the pamidronate remains active in the form of a hydrogel.[139,283] Later, the authors conjugated pamidronate with the motif of naphthelene-L-Phe-L-Phe to generate hydrogelator **625**, which self-assembles to form nanofibrils and induces hydrogelation. The hydrogel of **625** significantly reduces the amount of uranyl nitrate in the kidney and enhances the survival rate of the wounded mice.[284]

The synthetic self-assembling peptide **248a**, initially discovered by Zhang et al.,[181] is able to form nanofibers under physiological conditions and results in a hydrogel with a CGC of 0.1 wt %. Serving as a wound dressing, the hydrogel of peptide **248a** can reduce the edema of burn wound, advance the beginning and disappearance of eschar, and speed wound contraction. Zhao et al. suggested that the hydrogel of **248a** provides an optimal hydration microenvironment and simulates various cytokines and growth factors in the extracellular matrix

DOI: 10.1021/acs.chemrev.5b00299
Chem. Rev. 2015, 115, 13165−13307

Scheme 80. Some Supramolecular Hydrogelators for Wound Healing

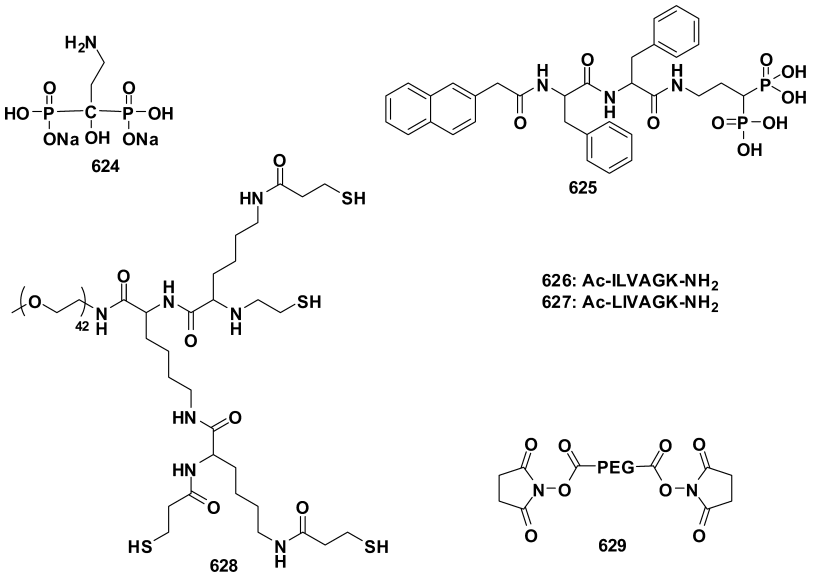

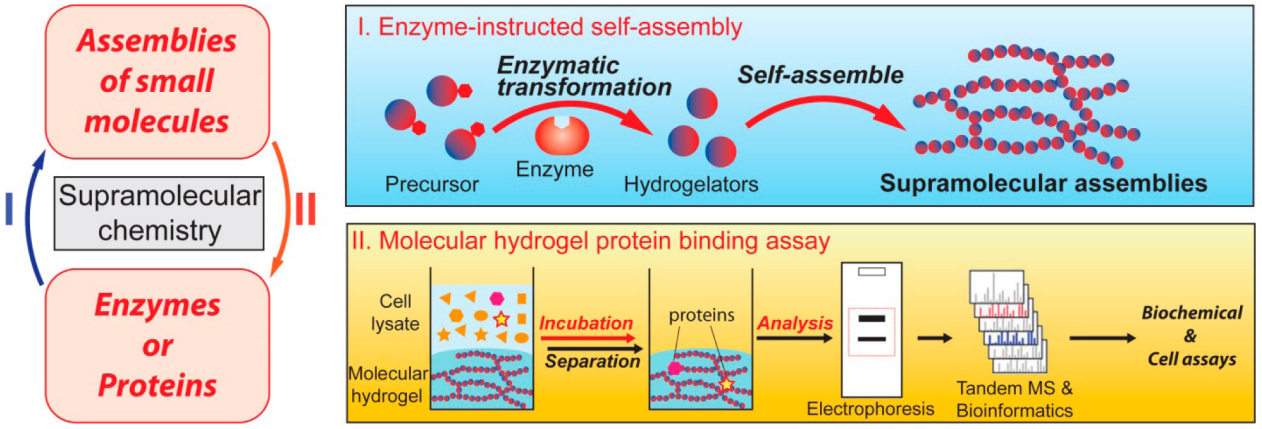

Figure 28. Interplay between supramolecular assemblies and proteins. (I) Enzyme-instructed self-assembly (EISA): the enzyme transforms a precursor to the self-assembling small molecules (i.e., hydrogelator) to form the supramolecular assemblies (in the form of nanofibers/hydrogel). (II) Molecular hydrogel protein binding (MHPB) assay: the hydrogels formed by the supramolecular assemblies bind proteins for proteomic analysis and identification of the protein targets of the assemblies.

to confer a beneficial effect.[1237] In another experiment, Ellis-Behnke and So et al. found that **248a** is able to immediately stop bleeding of a wound in the brain, spinal cord, femoral artery, liver, or skin of mammals.[1238,1240] Zhao et al. reported a molecular mechanism for such an observation.[1239] Zhang et al. designed another peptide, EAK16, for rapid homeostasis.[1241] On the basis of a similar principle, Hauser et al. developed two supramolecular hydrogels based on the short peptides Ac-ILVAGK-NH_2 (**626**) and Ac-LIVAGK-NH_2 (**627**). **626** and **627** form rigid and transparent hydrogels in PBS buffer at the concentrations of 0.5 and 0.75 wt %, respectively. Compared to the standard-of-care wound dressing Mepitel,[1242] the authors reported that the hydrogels of these two peptides, in a rat model, result in earlier onset and completion of autolytic debridement, and promote epithelial and dermal regeneration without the exogenous growth factor.[1243] It would be important to correlate the in vivo stability of these peptides with this exciting result. After mixing a dendron, **628**, and the polymer **629** in PBS buffer, Grinstaff et al.[1244] prepared a thioester hydrogel within several seconds at a concentration of 30 wt %. This resulting hydrogel is transparent, adhesive, and cell compatible, and exhibits strong mechanical properties even after swelling 4-fold in PBS buffer. As a hydrogel sealant for wound closure, this hydrogel could be washed away from the skin by simply using a thiolate solution during surgical care.

5.9. Unique Biological Functions of Supramolecular Hydrogelators

Compared to the conventional polymeric hydrogels,[1245,1246] self-assembly is a ubiquitous feature of supramolecular hydrogels. Considering self-assembly of proteins to generate assemblies that are crucial for cellular functions (e.g., actins and tubulins to form cytoskeletons[1247]), the biological functions of supramolecular assemblies of small molecules are scientifically intriguing and increasingly significant in biology and medicine. The development of supramolecular hydrogelators, thus, provides a new frontier for scientists to explore molecular self-assemblies at the intersection of supramolecular chemistry and cell biology.[190] In the following section, we discuss how the development of supramolecular hydrogelators and hydrogels leads to the interplay between supramolecular assemblies of small molecules and proteins (Figure 28) as a new paradigm in

DOI: 10.1021/acs.chemrev.5b00299
Chem. Rev. 2015, 115, 13165−13307

chemistry and in biology. We first introduce enzyme-instructed self-assembly (EISA),[34] a process that allows the control of the formation and the location (extra- or intracellular) of the supramolecular assemblies and hydrogels. Second, we highlight several examples of enzyme-instructed self-assembly in a cellular environment. Third, we illustrate the use of the hydrogels formed by the assemblies of small molecules to bind proteins, including the molecular hydrogel protein binding (MHPB) assay[883,884,1248] and the assemblies of small molecules promiscuously interacting with proteins inside cells to control the cell fate.

5.9.1. Enzyme-Instructed Self-Assembly To Form Supramolecular Hydrogels. To investigate the biological functions of the supramolecular assemblies of small molecules, one has to generate supramolecular assemblies in a cellular environment. Enzyme-instructed self-assembly (EISA)—the integration of enzymatic transformation and self-assembly—of small molecules, which usually results in the formation of supramolecular hydrogels, has provided a facile approach to examine and to create supramolecular assemblies in a cellular environment. In general, there are two strategies of enzyme-instructed self-assembly for generating supramolecular nanofibers—making or breaking bonds. Both routes allow the enzyme to convert a precursor to a hydrogelator which self-assembles in the aqueous phase to form nanofibers and results in hydrogelation (Figure 29). Such a relatively simple design

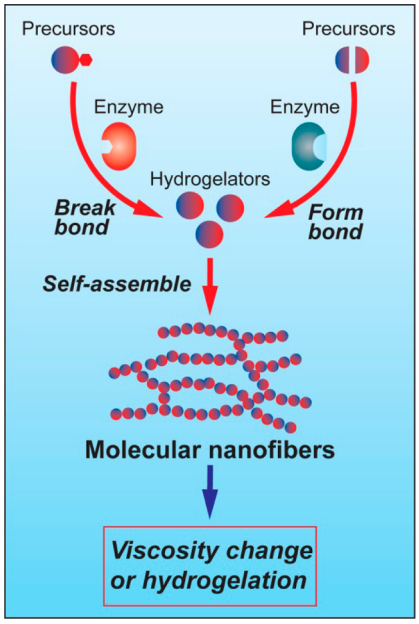

Figure 29. Illustration of EISA to form supramolecular nanofibers via bond formation or bond cleavage and the macroscopic outcomes (i.e., viscosity change or hydrogelation).

permits enzymatic formation of supramolecular nanofibers to be applicable on (almost) any gelators[9,226,1157,1249−1253] because the attachment of a hydrophilic segment to a hydrogelator easily generates a precursor that is soluble in the aqueous phase. The removal of the hydrophilic segment by the enzyme-catalyzed bond cleavage converts the precursor back to the hydrogelator, which self-assembles into nanoscale assemblies (e.g., nanofibers) and affords the hydrogel.[34,153] Similarly, an enzyme can catalyze bond formation to link two precursors together to create a hydrogelator that self-assembles into nanofibers.[162] One obvious advantage is the self-assembly of the hydrogelator to exhibit a selective response to the biological environments because the expression of enzymes in a living organism usually is highly specific in a spatiotemporal manner.

As discussed earlier (Scheme 6[153]), Xu et al. demonstrated enzyme-instructed self-assembly of small molecules based on an alkaline phosphatase and an amino acid derivative.[153] Catalyzing the removal of phosphate groups from a variety of substrates containing the phosphate group, phosphatase can control the balance between hydrophilicity and hydrophobicity, thus converting a precursor to a hydrogelator which self-assembles in water to form supramolecular nanofibers. As shown in Figure 30, the commercially available Fmoc-tyrosine phosphate (**14**) dissolves in a weak alkaline aqueous solution. The addition of alkaline phosphatase to the solution converts **14** to a hydrogelator, **15**, which self-assembles into a three-dimensional network of nanofibers and affords a hydrogel.[153] Because phosphatases, prevailingly existing in the cellular environment and constituting a large family of enzymes, act as the integral component of the canonical phosphatase/kinase enzyme switch that dictates cellular signaling, this seemingly simple process promises many possibilities and has opened a new paradigm of molecular biomaterials, as evidenced by the subsequent research.[30,34,140,152−154,156,288,883,888,1254−1259]

Unlike phosphatases that catalyze hydrolysis to trigger molecular self-assembly, thermolysin catalyzes the formation of a covalent bond via reverse hydrolysis. Ulijn et al.[162] reported the use of thermolysin to couple two peptide derivatives (**200** and **208**) to make a hydrogelator (**447**) which self-assembles to form a three-dimensional network of nanofibers and affords a hydrogel (Figure 31). Since thermolysin catalyzes the reverse hydrolysis of many substrates, especially hydrophobic amino acids and peptides, it greatly expands the scope of enzyme-instructed self-assembly and the formation of supramolecular nanofibers/hydrogels. Although bond formation may serve as a useful route to produce hydrogels as scaffolds for tissue engineering,[96] the low solubility of the hydrophobic precursors in the aqueous phase likely limits their application (especially in vivo).

Many advances have taken place in the development of enzyme-instructed self-assembly.[14,890,922,1260−1263] On the basis of the enzyme switch in the cellular process,[177] Xu et al. designed a substrate that undergoes phosphorylation and dephosphorylation catalyzed by an alkaline phosphatase and a tyrosine kinase, and examined the use of the kinase/phosphatase switch to regulate the formation of nanofibers/hydrogels.[1254] As shown in Figure 32A, a pentapeptide derivative, Nap-FFGEY (**630**; Nap = 2-(naphthalen-2-yl)acetic acid; F = phenylalanine (Phe); G = glycine (Gly); E = glutamic acid (Glu); Y = tyrosine (Tyr)), self-assembles into nanofibers and results in a hydrogel at 0.6 wt %. The addition of a kinase to the hydrogel in the presence of adenosine triphosphates (ATPs) phosphorylates **630** to give the corresponding precursor **631**, thus disrupting the self-assembly to induce a gel−sol phase transition and produce a solution; treating the resulting solution with a phosphatase converts the precursor **631** to the hydrogelator **630**, again, thus repeating the self-assembly of the hydrogelator to form the network of nanofibers and afford the hydrogel. Besides illustrating a general way of using enzymes to instruct the formation or disassembly of supramolecular nanofibers, this work demonstrates that enzyme-instructed self-assembly generates more ordered self-

DOI: 10.1021/acs.chemrev.5b00299
Chem. Rev. 2015, 115, 13165−13307

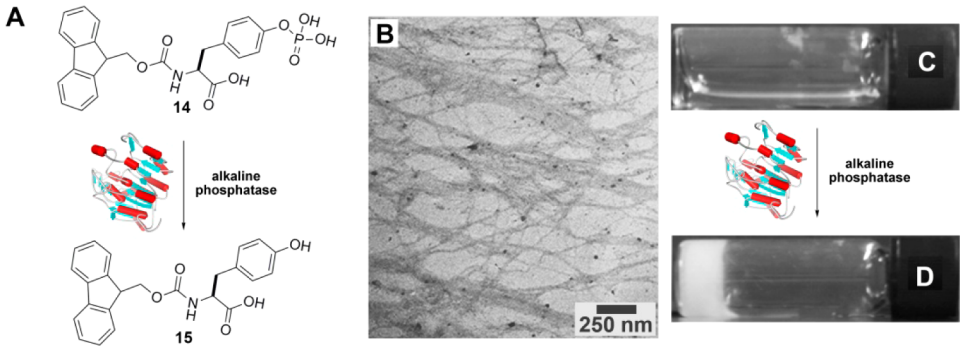

Figure 30. (A) Molecular structures of the precursor **14** and its corresponding hydrogelator **15** and the enzymatic transformation. (B) Transmission electron microscopy (TEM) image of the nanofibers made by the self-assembly of **15**. Optical images of (C) the solution of **14** in alkali buffer (pH 9.8) and (D) the hydrogel formed by adding the phosphatase to the solution of **14** to produce the nanofibers of **15**. Adapted with permission from ref 153. Copyright 2004 Wiley-VCH Verlag GmbH & Co. KGaA.

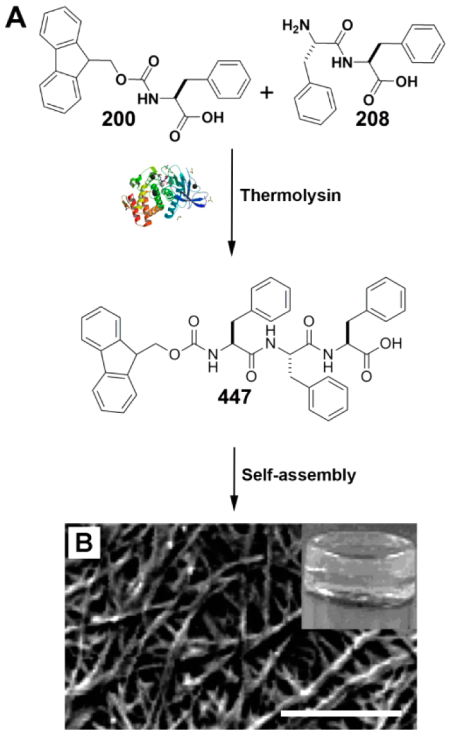

Figure 31. (A) Structures of the precursors **200** and **208** and the hydrogelator **447** and the enzymatic transformation. (B) SEM image of the corresponding nanofibers (scale bar 500 nm). Inset: optical image of the hydrogel. Adapted from ref 162. Copyright 2006 American Chemical Society.

assembling nanostructures than a simple adjustment of the pH does (Figure 32B).[1254]

To serve as therapeutic agents, the supramolecular nanofibers have to be innocuous to normal tissues. Therefore, it is essential to evaluate the biochemical properties (e.g., biocompatibility, biodurability, and toxicity) of enzyme-instructed supramolecular nanofibers in vivo. After confirming that **630** is biocompatible, Xu et al. injected the solution of **631** into mice to evaluate enzymatic formation of the nanofibers and the hydrogel of **630** in vivo. They observed that the hydrogel forms at the location of subcutaneous injection (Figure 33A). HPLC analysis of the hydrogel reveals that 80% of precursor **631** turns into hydrogelator **630**. On the basis of the weight change of the mice after being injected with **631** (Figure 33B), subcutaneous administration of **631** at the experimental dosage results in little acute toxicity to the mice. Moreover, because the enzyme-catalyzed reaction quickly converts **631** to the biocompatible molecule **630**, there is hardly long-term in vivo toxicity of **631**.[1254]

To generate supramolecular nanofibers that resist hydrolytic enzymes (e.g., proteases) in challenging biological conditions (e.g., biological fluids), Xu et al. designed a precursor based on a β-amino acid.[1255] As shown in Figure 34, tyrosine phosphate attaches at the C-terminal of a β-amino acid derivative to afford a precursor (**632**) which serves as a substrate of phosphatase. After being treated with a phosphatase, **632** hydrolyzes to give a hydrogelator (**633**) which self-assembles to afford nanofibers. Moreover, this enzymatic formation of nanofibers proceeds in complex and challenging biofluids (e.g., blood and cytoplasm) that contain a variety of proteases and results in the hydrogelation of these fluids (Figure 34C,D).[1255] The β-peptide-based nanofibers exhibit a longer half-life than the α-peptide nanofibers do.[1255] The excellent biostability renders β-amino acids and other non-natural amino acids as potential candidates for creating supramolecular hydrogels for long-term biomedical applications.

β-Lactamases are an important family of bacterial enzymes that catalyze the hydrolysis of β-lactam antibiotics and have caused widely spread antimicrobial drug resistance.[1264,1265] Xu et al. explored enzyme-instructed self-assembly by β-lactamases.[159] As shown in Figure 35, the precursor **634**, consisting of a cephem nucleus as the linker coupling a hydrophilic group and a proper hydrogelator, is too soluble to self-assemble in water and bacteria cell lysates. Upon the action of a β-lactamase, the lactam ring opens to release the hydrogelator **635**, which self-assembles to form nanofibers and to afford a hydrogel. This facile process allows the detection of β-lactamase in the lysates of bacteria. Specifically, β-lactamase in a bacterial lysate could convert the precursor **634** to its corresponding hydrogelator **635**, resulting in the formation of supramolecular nanofibers (Figure 35C–F). Without β-lactamase, no nanofiber was observed. This result not only confirms the stability of the nanofibers of **635** in bacteria lysates consisting of a wide range of enzymes, but also suggests that one may use β-lactamase to control the self-assembly of small molecules as a general platform to target antimicrobial-drug-resistant Gram-negative bacteria since only bacteria express β-lactamases.

Xu et al. also reported the use of β-galactosidase to remove galactose from precursor **637** in water to trigger the self-assembly of the corresponding hydrogelator and to result in a hydrogel at a concentration of 0.1 wt % at pH 7.5.[168] The

DOI: 10.1021/acs.chemrev.5b00299
Chem. Rev. 2015, 115, 13165–13307

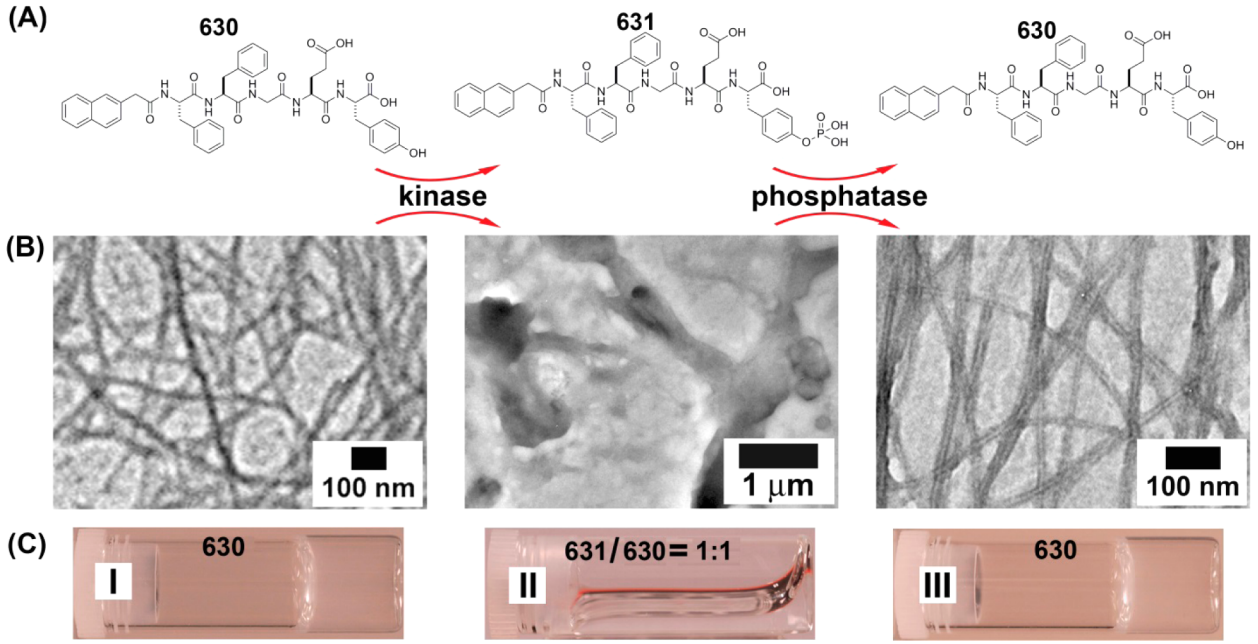

Figure 32. (A) Structures of the precursor **630** and the hydrogelator **631** and the corresponding transformations catalyzed by phosphatase and kinase. (B) TEM images showing (I, left) the nanofibers of **630** formed by adjusting the pH, (II, middle) the absence of nanofibers due to enzymatic phosphorylation of **630**, and (III, right) the restored nanofibers of **630** by enzymatic dephosphorylation of **631**. (C) Optical images of (I) the hydrogel of **630** formed by changing the pH, (II) the solution obtained by treating the hydrogel with a kinase and ATP (at 50% conversion), and (III) the hydrogel of **630** restored by adding phosphatase. Adapted from ref 1254. Copyright 2006 American Chemical Society.

synthetic difficulty of saccharides is apparently the limiting factor for the exploration of enzymatic hydrogelation using glycolytic hydrolases. In another experiment, Xu et al. designed and synthesized a short peptide with a sequence of FFFFC-GLDD (**638**) as a substrate of matrix metalloprotease-9 (MMP-9). After successfully cleaving the hydrophilic residue of LDD off **638**, the resulting hydrogelator (FFFFCG) self-assembles to form nanofibrils and affords a hydrogel at a concentration of 0.4 wt %. Since MMP-9 is an important enzyme related to the invasiveness and metastatic potency of human malignant tumors, this work may lead to a new strategy for making biomaterials or therapeutics for cancer therapy or other diseases.[164] Later, Xu et al.[111] reported an esterase-based approach to generate supramolecular hydrogels. By using esterase to hydrolyze the precursor **7**, the resulting hydrogelator **8** self-assembles to form a hydrogel at a concentration of 0.8 wt % and pH 7.4. One intriguing feature of this work is that the hydrogel of **8** is stable over a wide pH range, likely due to the presence of the alcohol group instead of a carboxylic group at the C-terminal. Moreover, breaking the ester-bond apparently is the only path to make hydrogel of **8**. Relying on both aromatic−aromatic interactions and enzyme catalysis, Xu et al. reported that enzymatic dephosphorylation of the precursor **639** generates a hydrogel consisting of spontaneously aligned supramolecular nanofibers as the matrix of the gel.[152] As shown in Scheme 81, Xu et al. also designed a new class of conjugates (**640**) containing a nucleobase, amino acids, and a saccharide which afford a supramolecular hydrogel (0.5 wt %) upon addition of phosphatase. Furthermore, **640** is able to inhibit the proliferation of HeLa cells.[1257] In another experiment, Xu et al. reported that **641** affords a supramolecular hydrogel at a concentration of 0.5 wt % in the presence of acid phosphatase (AP). The immobilized AP in the hydrogel shows higher activity and stability compared with free AP in the same solvent.[154] Integrating enzymatic catalysis and self-assembly, Xu et al.[702] reported a feasible way to prepare the supramolecular hydrogel of an adenosine derivative (**642**). This exploration may lead to a new type of biomaterial because of the ubiquitous importance of adenosine 5′-monophosphate (AMP) in bioenergetics, metabolism, and transfer of genetic information. Meanwhile, Xu et al. also prepared a series of nucleopeptides by connecting a nucleobase with Phe-Phe which self-assemble to form nanofibers and trigger hydrogelation at a concentration of 2.0 wt % and pH 5.0.[965] It is worth noting that the nucleopeptides exhibit better proteolytic resistance than their corresponding peptides.

Ulijn et al. further explored the use of thermolysin to catalyze the bond formation of a series of peptides for self-assembly and hydrogelation.[1266,1267] In one case, they reported that thermolysin catalyzes the condensation of Fmoc-Ser and phenylalanine to form **643** (Scheme 82). The favorable product **643** of the condensation self-assembles to form nanosheets that result in an opaque hydrogel.[1268] Later, they used subtilisin to hydrolyze Fmoc-peptide methyl esters (e.g., **644**) to obtain the corresponding hydrogelator **645**,[1269] which self-assembles to form nanotubes and affords a hydrogel.[160] They also reported a case in which enzyme-catalyzed dephosphorylation of precursor **646** affords a hydrogel at a concentration of 0.55 wt %. This work provides useful insights into the mechanism of **646** transforming from micelles to nanofibers.[1270] By incorporating a metalloproteinase substrate of PVGLIG into self-assembling peptides, Langer et al. prepared an enzyme-sensitive hydrogel of **647** at a concentration of 1.0 wt % for eliciting cell and tissue remodeling activities. Further studies found that enzyme-mediated degradation occurred on the gel surface.[1271] While Schneider et al. reported the use of MMP-13 to degrade β-hairpin self-assembled hydrogels by proteolysis,[1272] Collier et al. designed a series of depsipeptides containing ester bonds within the peptide backbone which are able to self-assemble into β-sheet

DOI: 10.1021/acs.chemrev.5b00299
Chem. Rev. 2015, 115, 13165−13307

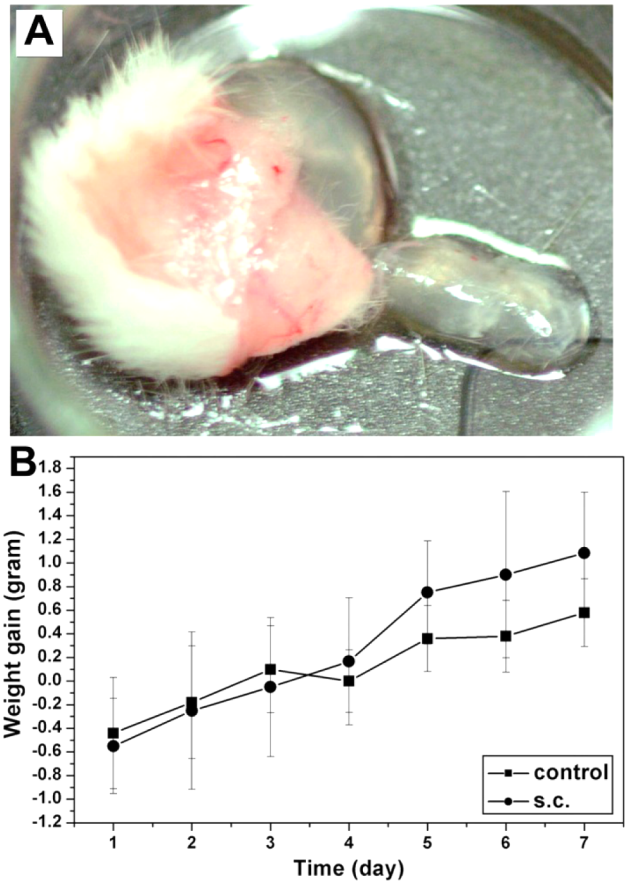

Figure 33. (A) Optical image of the hydrogel formed 1 h after subcutaneously injecting the solution of the precursor **631** into the mice. (B) Weight gain of the mice (n = 6, initial body weight 20 ± 2 g) after subcutaneously injecting 0.5 mL of **631** at 0.8 wt % concentration. A saline solution (0.5 mL) served as the control. Adapted from ref 1254. Copyright 2006 American Chemical Society.

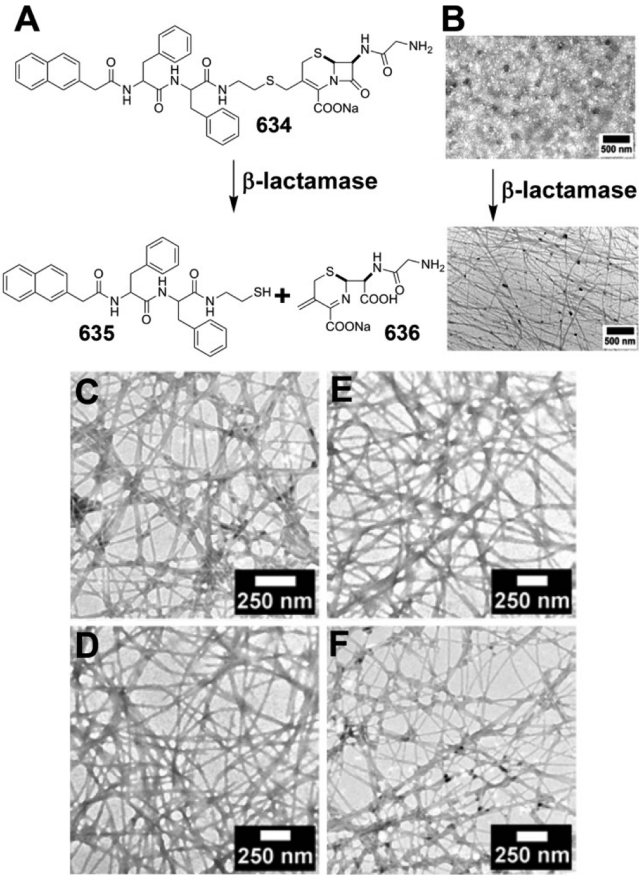

Figure 35. (A) Structures of the precursor **634** and the hydrogelator **635** and the β-lactamase-catalyzed transformation. (B) TEM images showing the enzymatic formation of nanofibers of **635**: top, the solution, bottom, the gel. (C–F) Images showing formation of nanofibers of **635** in the lysates of *E. coli* that express different β-lactamases (C, CTX-M13; D, CTX-M14; E, SHV-1; F, TEM-1). Adapted from ref 159. Copyright 2007 American Chemical Society.

fibrillar materials and degrade via ester hydrolysis with rates controllable by the amino acid proximal to the ester bonds.[1273] Among them, **648** forms a very stiff hydrogel ($G' > 10^5$ Pa) which becomes soft and dissociates over time. Unexpectedly,

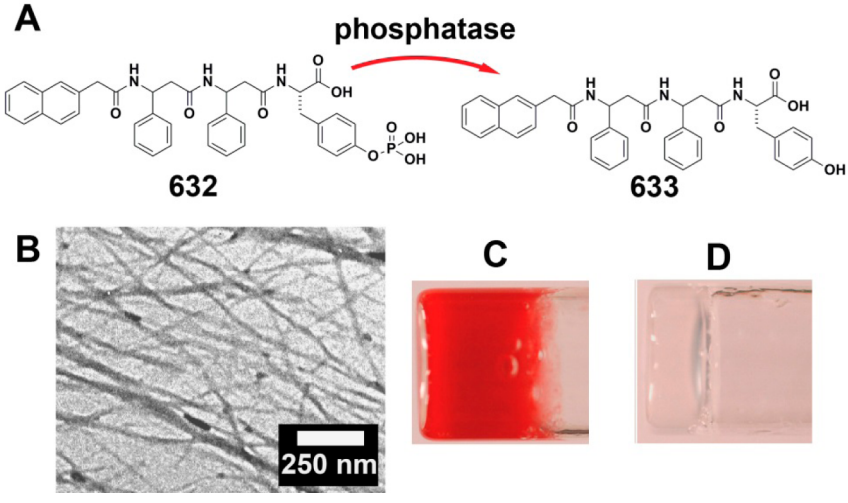

Figure 34. (A) Structures of the precursor **632** and the hydrogelator **633** and the enzyme-catalyzed transformation. (B) TEM image of the nanofibers of **633**. (C) Hydrogel formed by mixing blood, PBS buffer, and alkaline phosphatase. (D) Gel formed by mixing the solution of **632** (1.0 wt % in PBS buffer, pH 7.4), alkaline phosphatase, and the cytoplasm collected from 1.0 × 10^6 broken HeLa cells. Adapted with permission from ref 1255. Copyright 2007 Wiley-VCH Verlag GmbH & Co. KGaA.

DOI: 10.1021/acs.chemrev.5b00299
Chem. Rev. 2015, 115, 13165–13307

Scheme 81. Molecular Structures of Representative Hydrogelators Formed via Enzymatic Transformation

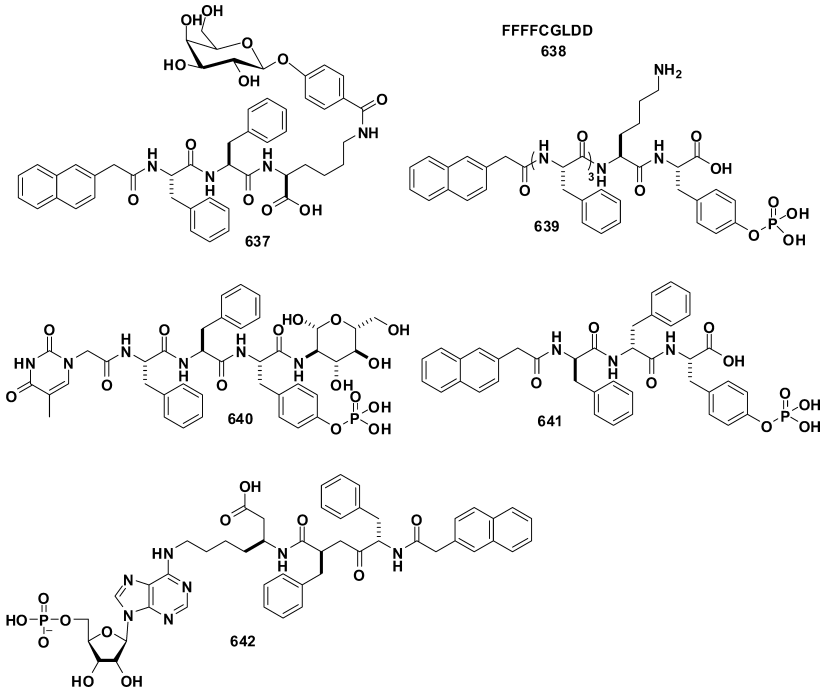

Scheme 82. Molecular Structures of Small Representative Hydrogelators Formed via Enzymatic Transformation

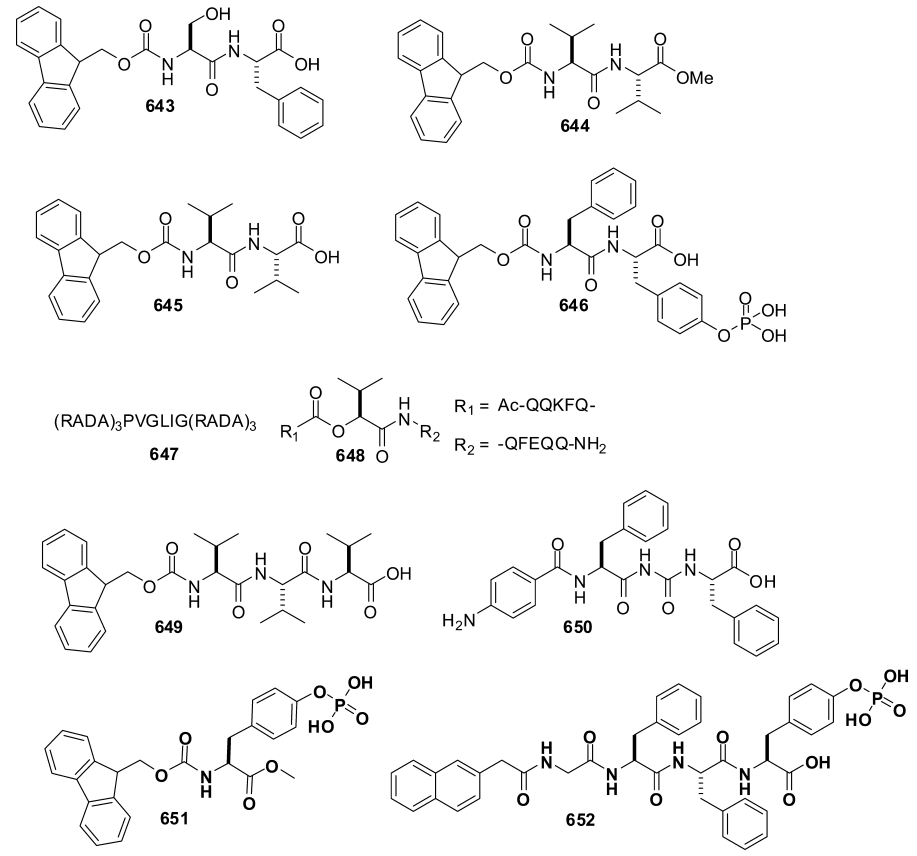

C3H10T1/2 cells were encapsulated in the hydrogel of **648** and exhibit better spreading and proliferation than the peptide without an ester bond. Williams et al. reported a new approach in which thermolysin catalyzes the reverse hydrolysis to produce Fmoc-Leu-Leu-Leu (**649**) efficiently in the presence of laminin. Hydrogelator **649** self-assembles to form nanofibrils that interact with laminin to result in a hydrogel. The authors reported that the immobilized laminin is more stable after being microinjected into a disease site of zebrafish.[1274]

DOI: 10.1021/acs.chemrev.5b00299
Chem. Rev. 2015, 115, 13165−13307

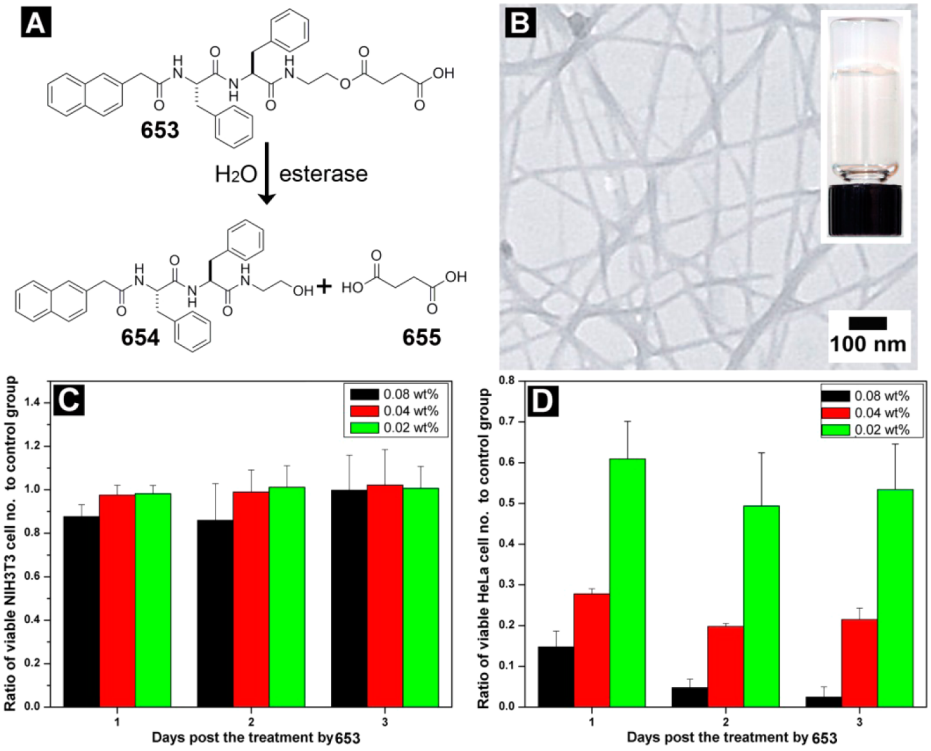

Figure 36. (A) An esterase to convert the precursor **653** to the hydrogelator **654**. (B) TEM image of the nanofiber formed by **654** (inset: optical image of the hydrogel). MTT assays of (C) NIH/3T3 cells and (D) HeLa cells treated with **653** at concentrations of 0.08, 0.04, and 0.02 wt %. Adapted with permission from ref 1289. Copyright 2007 Wiley-VCH Verlag GmbH & Co. KGaA.

McNeil and Soellner et al.[165] reported a generalizable method to detect protease activity via hydrogelation. They designed a recognition sequence for targeting the protease of interest (e.g., MMP-9 and prostate-specific antigen (PSA)); meanwhile an aminopeptidase removes the residues to release the hydrogelator **650** at physiological conditions. Assuming that the MMP-9 and PSA are potential biomarkers for cancer, the authors suggested that this simple visual assay might be useful for early cancer detection. This innovative two-enzyme approach may find broader applications than the detection of a specific hydrolase. In addition, Ulijn et al. examined the effect of the concentration of alkaline phosphatase on the gelation time, mechanical properties, and molecular arrangement of the enzymatic hydrogelation of **15**, and reported that an increase of the enzyme concentration enhances the elastic modulus and the apparent order of the resulting hydrogel.[148] Recently, employing enzymatic dephosphorylation of Fmoc-tyrosine-phosphate (**14**),[153] Mann et al. prepared a supramolecular hydrogel to act as a matrix for calcium phosphate mineralization.[1275] SEM suggested that the mineralization occurred along the smooth fiber surface of **15**. The authors suggested that this approach may produce biomaterials for tissue engineering, wound treatment, and drug release. Meanwhile, Yang et al. reported the methylation of **14** to afford a slightly more hydrophobic precursor, **651**. Although **651** is more hydrophobic than **14**, phosphatase still dephosphorylates **651** to result in a supramolecular hydrogel.[157] Yang and co-workers reported a short peptide (Nap-GFFY$_p$, **652**) that results in a hydrogel of Nap-GFFY[1276] at a minimum gelation concentration of 0.08 wt % after dephosphorylation, and its methylation form Nap-GFFY$_p$-OMe has a minimum gelation concentration of 0.01 wt % after enzymatic conversion, which is one of the most efficient small molecular hydrogelators.[1277,1278] As a group pioneering the study of the Nap-GFFY motif, Yang et al. also extensively explored the properties and applications of the supramolecular hydrogels based on Nap-GFFY derivatives.[1279]

5.9.2. Enzyme-Instructed Self-Assembly in a Cellular Environment. *5.9.2.1. Intracellular Formation of Supramolecular Nanofibers To Control the Cell Fate.* Enzyme-instructed self-assembly allows the exploration of molecular self-assembly in a wide range of biological processes involving enzymes, thus providing abundant opportunities to evaluate intracellular molecular self-assembly of small molecules, a previously unexplored subject. The ability to form supramolecular assemblies inside cells offers a new way to examine the emergent properties of small molecules at a new level of complexity—supramolecular and intracellular, thus providing a multiple-step process to control the fate of cells. As shown in the following sections, these studies have confirmed (at least) two aspects of enzyme-instructed intracellular supramolecular nanofibers: (i) the supramolecular nanofibers change the viscosity of the cytosol and result in selective cell death and (ii) intracellular enzyme catalysis plays the key role.

To form supramolecular nanofibers within a cell, an intracellular enzyme should convert a soluble precursor, which does not self-assemble outside cells, into a hydrogelator that self-assembles to generate the nanofibers inside the cells. To meet this requirement, Xu et al. designed and synthesized precursor **653** as an esterase substrate.[1289] Mammalian cells uptake **653**; the endogenous esterases in the cells convert **653** to a hydrogelator, **654**. The molecules of **654** self-assemble to form nanofibers, resulting in hydrogelation when a threshold concentration is reached, and thus changing the viscosity of the cytoplasm to cause cell death. As shown in Figure 36, most HeLa cells died at day 3 after the addition of **653** to the culture medium, while most of the NIH/3T3 cells remained alive and

DOI: 10.1021/acs.chemrev.5b00299
Chem. Rev. 2015, 115, 13165−13307

dividing. According to the esterase activity assays,[1289] the levels of expression of esterase between these two cell lines are different. With higher esterase activities, HeLa cells likely convert more **653** to **654** than NIH/3T3 cells do. More nanofibers form in HeLa cells than in NIH/3T3 cells, and the resulting nanofibers/hydrogel in HeLa cells cause the cell death. The kinetics of the formation of intercellular nanofibers of **654** is specific to different types of cells, which opens a new paradigm for controlling the fate of cells by enzyme-instructed self-assembly of small molecules.

To further demonstrate intracellular enzyme-instructed self-assembly to control the cell fate, Xu et al. used two types of *E. coli* strains: the wild-type BL21 (as the control) and a BL21 strain (BL21(P+)) that overexpresses human tyrosine phosphatase (hPTP). Since the only difference between the two strains is the expression of the phosphatase, any discrepancy in the uptake of the precursor is minimized. After the precursor **656** diffuses into the *E. coli*, the phosphatase converts the precursor **656** into the hydrogelator **657**. **657** self-assembles to form nanofibers and results in hydrogelation. The BL21(P+) bacteria stopped growing upon the addition of **656** (IC_{50} = 20 μg/mL), but the wild-type BL21 bacteria grew normally (IC_{50} > 2000 μg/mL) under the same conditions (Figure 37).[1259] On the basis of on HPLC analysis, the authors found significant accumulation of **657** inside BL21(P+) cells. TEM analysis on the broken BL21(P+) cells suggests the formation of nanofibers of **657** inside BL21(P+) cells.[1259] These results confirm that enzymatic formation of the nanofibers and the subsequent hydrogelation inside the bacteria inhibit their growth. This work illustrates that intracellular enzyme-instructed self-assembly allows enzymatic transformation rather than tight ligand–receptor binding[1264] to control the cell fate. Ulijn et al. reported the self-assembly of several Fmoc-protected dipeptide (e.g., Fmoc-Phe-Tyr, and Fmoc-Tyr-Asn) amphiphiles and the design of their corresponding phosphorylated precursors. All the precursors could be dephosphorylated by alkaline phosphatases, generating hydrogelators that self-assemble to form nanofibers. In addition, the peptide amphiphiles showed a similar antimicrobial response when incubated with the phosphatase-overexpressed *E. coli*.[1280]

Xu et al. reported a straightforward method for studying the enzyme-instructed self-assembly of small molecules inside cells. As shown in Scheme 83, they designed a new precursor, **658a**, containing a fluorophore which exhibits low fluorescence. After dephosphorylation catalyzed by phosphatases, the resulting hydrogelator **658b** self-assembles to form nanofibers that display bright fluorescence. On the basis of this principle, they found that **658a** is easily accumulated inside cells to form nanofibers/hydrogel, and thus exhibits a bright spot near the nucleus (Figure 38). Further experiments show that most of the self-assembly of **658b** occurs in the endoplasmic reticulum (ER) due to the dephosphorylation catalyzed by a tyrosine phosphatase (PTP1B).[156] This work illustrates a facile approach for studying enzyme-instructed self-assembly of small molecules by other enzymes inside live cells.

To address the undesired issues in the fluorescence labeling technique (e.g., toxicity and alternation of macromolecular interaction), Xu et al. reported a facile method to image enzyme-instructed self-assembly of small molecules without a high concentration of fluorescent labels inside mammalian cells via a doping method. Specifically, after incorporating a dansyl (DNS)-labeled molecule of **660a** into the self-assembly of the native molecule **659a** as the fluorescent dopant, they

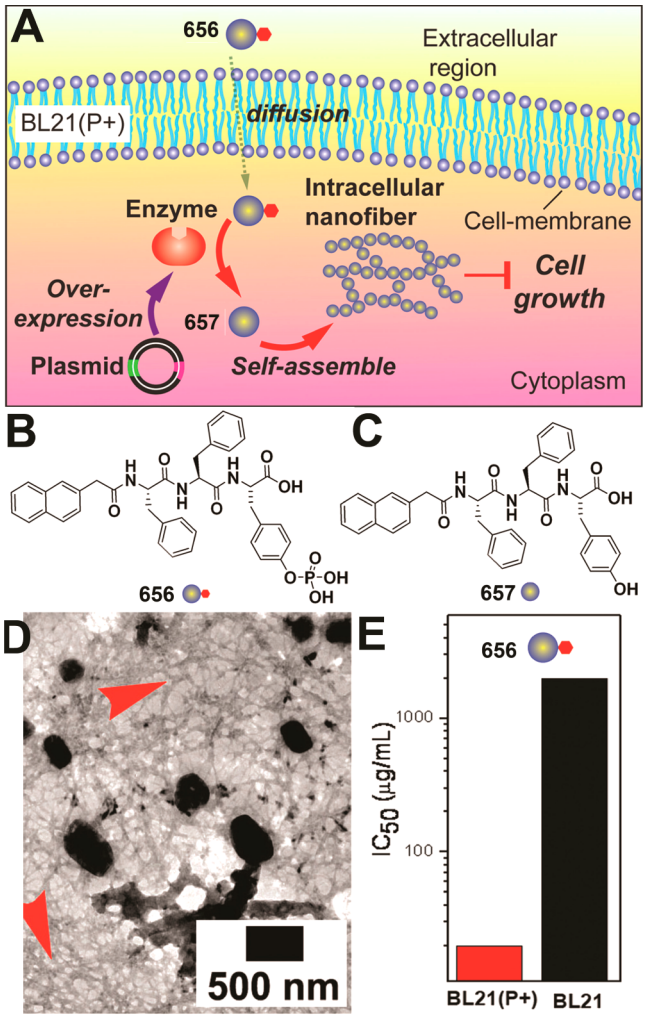

Figure 37. (A) A schematic representation of intracellular nanofiber formation and the inhibition of bacterial growth. (B, C) Structures and graphic representations of the precursor **656** and the corresponding hydrogelator **657**. (D) TEM image of the nanofibers of **657** (indicated by arrows) formed inside the bacteria after culturing with **656**. (E) Concentration of **656** needed to inhibit BL21(P+) and BL21 by forming nanofibers of **657** inside the bacteria. Adapted with permission from ref 1259. Copyright 2007 Wiley-VCH Verlag GmbH & Co. KGaA.

determined the formation, localization, and progression of molecular assemblies generated from the nonfluorescent small molecular hydrogelator by enzyme-instructed self-assembly. After using the cell fraction experiment to confirm that self-assembly occurs in the endoplasmic reticulum (ER), they used correlative light and electron microscopy (CLEM) to further prove that molecular assemblies localized near or inside the ER and are likely processed via the cellular secretory pathway (e.g., ER–Golgi–lysosomes/secretion) by the cells. As shown in Figure 39, CLEM directly correlates the fluorescence signal of **659b**/**660b** molecular assemblies imaged in live cells (Figure 39B–E) with ultrastructural changes of the treated cell in EM (Figure 39F–I). In the fluorescence region, the authors observed a high accumulation of vesicles with low-electron-density material in the cytoplasmic area.[212] Therefore, this work establishes a general strategy that may reveal the spatiotemporal profile of the assemblies of small molecules inside cells.

DOI: 10.1021/acs.chemrev.5b00299
Chem. Rev. 2015, 115, 13165–13307

Scheme 83. Some Precursors and Hydrogelators for Intracellular Self-Assembly

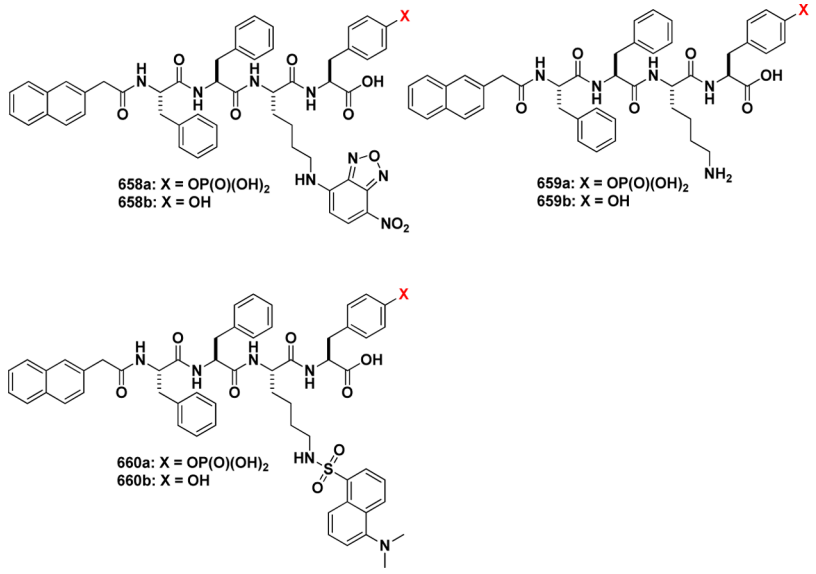

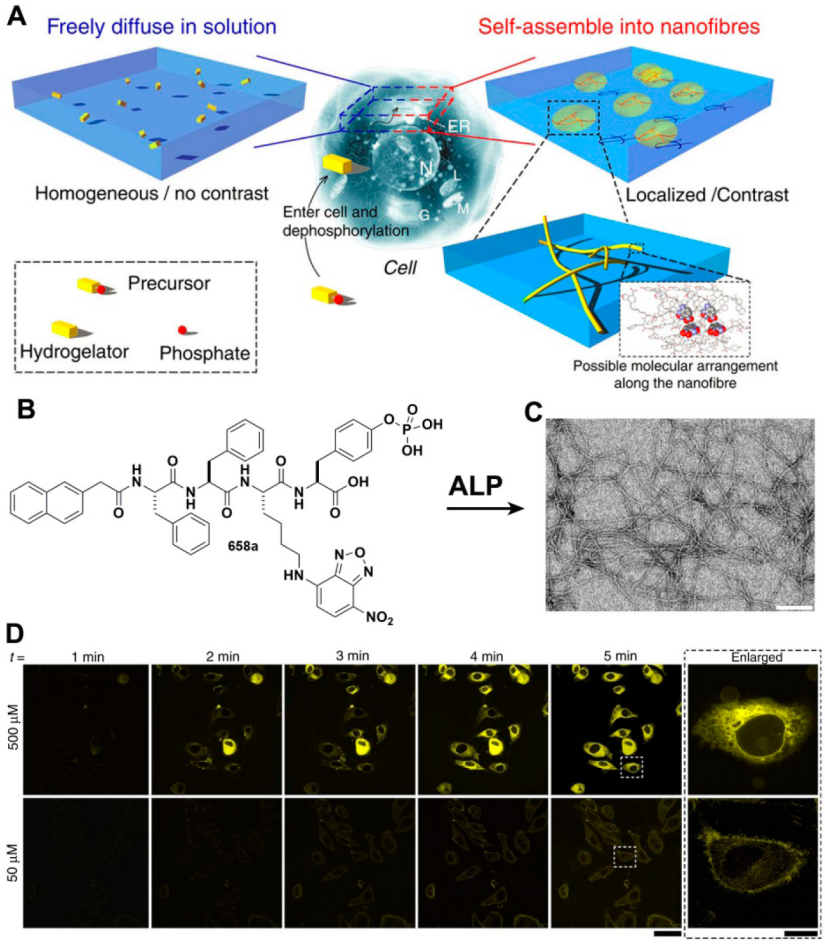

Figure 38. (A) Principle of imaging enzyme-instructed self-assembly inside cells. (B) Chemical structures of **658a**. (C) TEM image of the hydrogel made of **658b**. (D) Fluorescent confocal microscopy images showing the time course of fluorescence emission inside the HeLa cells incubated with 500 or 50 μM **658a** in PBS buffer. Adapted with permission from ref 156. Copyright 2012 Nature Publish Group.

5.9.2.2. Pericellular Formation of Supramolecular Nanofibers To Control the Cell Fate. Unlike intracellular enzymes and the cytosolic catalytic domains of membrane enzymes, ectoenzymes (i.e., an enzyme that locates on the cell surface with catalytic domains outside the plasma membrane) are less explored. However, emerging evidence indicates the important role of ectoenzymes in cellular processes.[1281−1284] Coincidentally, several laboratories are exploring ectoenzyme-instructed

DOI: 10.1021/acs.chemrev.5b00299
Chem. Rev. 2015, 115, 13165−13307

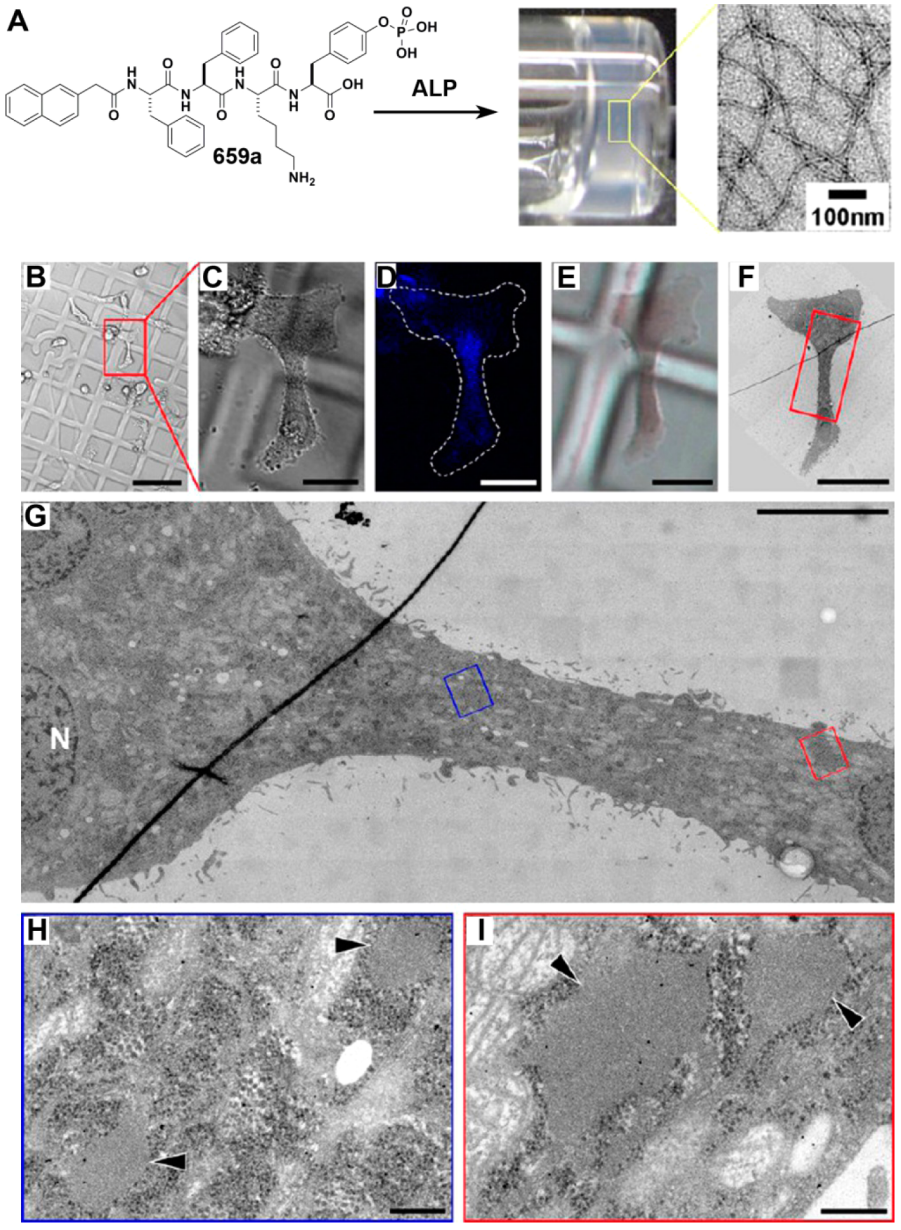

Figure 39. (A) Precursor **659a** self-assembles to form nanofibers/hydrogels upon the addition of ALP. (B–I) Correlative light and electron microscopy (CLEM) images of HeLa cells incubated for 48 h with 500 μM **659a** and 200 nM **660a**. (B–E) Differential interference contrast (DIC) and fluorescence light microscopy images of treated HeLa cells growing on an Aclar plastic film. (F–I) TEM images of the cell of interest shown in (B)–(E). Adapted from ref 212. Copyright 2013 American Chemical Society.

self-assembly to form nanofibers on and near the cell surface (i.e., pericellular space).[288,886,888,894,1256,1258,1285] These studies suggest that one of the promising applications of the pericellular nanofibers is selective inhibition of targeted cells (e.g., cancer cells) without harming normal cells.

Xu et al. reported the first example of enzyme-instructed self-assembly to form hydrogel/nanonets in pericellular space,[288,1256] which selectively inhibits cancer cells, including certain drug-resistant cell lines.[288] Specifically, the ectophosphatases (e.g., placental alkaline phosphatases (ALPP)[1286]) dephosphorylate the precursor **661a** made of a small D-peptide to a hydrogelator, **661b**, which self-assembles to form nanofibrils at a concentration of 280 μM and results in pericellular nanofibers/hydrogel (Scheme 84). The resulting hydrogel can prevent the diffusion of a nucleus dye (4′,6-diamidino-2-phenylindole, DAPI) into the cells. A further

Scheme 84. Structures of Precursors That Are the Substrates of Ectophosphatases and the Corresponding Hydrogelators

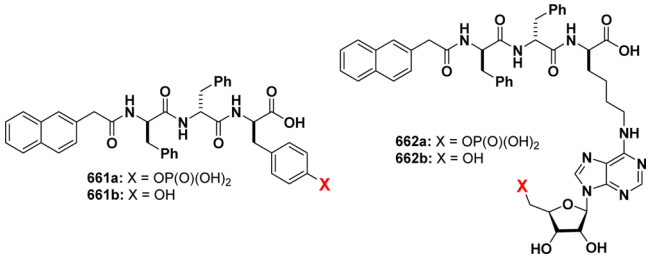

experiment proves that the pericellular hydrogel is able to block secretary protein/enzyme in the culture medium. Therefore, such blocking of cellular mass exchange has a profound negative

DOI: 10.1021/acs.chemrev.5b00299
Chem. Rev. 2015, 115, 13165–13307

effect on the critical cellular activities. An enzyme-linked immunosorbent assay (ELISA) shows that active caspase-3 and active PARP increase significantly with an increase of the incubation time, suggesting that the cells undergo caspase-dependent apoptosis (Figure 40). The authors also found that

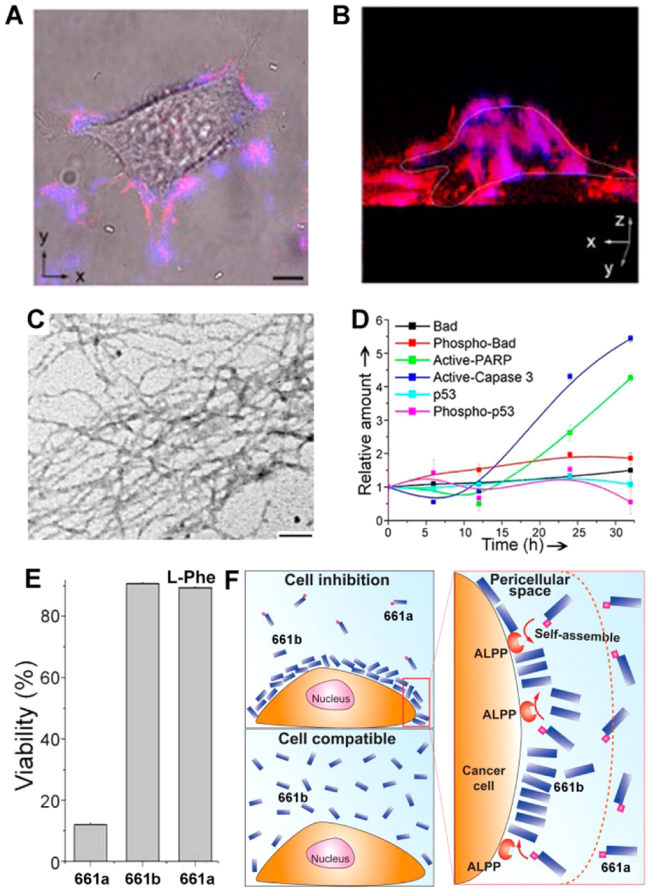

Figure 40. (A) Overlaid images and (B) 3D stacked *z*-scan image of Congo red- and DAPI-stained HeLa cells after the incubation of the HeLa cell with **661a** for 12 h. (C) TEM image of the pericellular hydrogels on the HeLa cells treated by **661a** (280 μM). (D) Change of the relative amount of apoptosis signal molecules over time in HeLa cells treated by **661a** (280 μM). (E) Cell viability of HeLa cells incubated with **661a** (280 μM), **661b** (280 μM), and **661a** (280 μM) plus L-Phe (1.0 mM). (F) Illustration of enzyme-instructed self-assembly to form pericellular nanofibers/hydrogel and selectively induce cell death. Adapted with permission from ref 288. Copyright 2014 John Wiley and Sons. Adapted from ref 1256. Copyright 2014 American Chemical Society.

the enantiomer of **656**, an L-peptide derivative, is unable to inhibit HeLa cells due to proteolysis. On the basis of this observation, they investigated how a D-amino acid affects the cellular response to the enzyme-instructed nanofibers by systematically using D-amino acid residue(s) to replace the L-amino acid residue(s) in tripeptidic precursor **656** or its hydrogelator **657**. Further studies found that the enantiomeric precursors exhibit dramatically different cellular responses, while enantiomeric hydrogelators show similar cellular responses (Figure 41).[1256] The use of the uncompetitive inhibitor of ALPP abrogates the inhibitory effects of **661a**, suggesting that the overexpressed ALPP on HeLa cells is the major enzyme responsible for enzyme-instructed self-assembly and cell inhibition.

The most revealing result is that the hydrogelator itself, **661b**, at 280 μM, is innocuous to the HeLa cells. This result indicates that ALPP, as the enzyme on the cell membrane, catalytically generates hydrogelators to achieve a high local concentration on the cell surface to form pericellular nanofibers/hydrogel to inhibit the cancer cells. These results further establish enzyme-instructed self-assembly as a multiple-step process to control cell fates. In another experiment, Xu et al. developed a nucleopeptide (**662a**) as the substrate of CD73, an ectoenzyme. The resulting hydrogelator **662b** self-assembles to form nanofibrils and induces a hydrogel at a concentration of 2.0 wt %. One interesting feature of this work is that **662a** inhibits HepG2 cells, likely resulting from CD73-instructed self-assembly to form nanofibers of **662b**.[1258]

In a related study, Ulijn and Pires et al. reported a novel carbohydrate amphiphile (**663**) that is able to self-assemble into nanofibers upon enzymatic dephosphorylation. More importantly, the authors also confirmed that the membrane-bound alkaline phosphatase expressed by the osteosarcoma cell line (Saos-2) is responsible for triggering the hydrogelation of **382** in the pericellular environment (Figure 42). The resulting pericellular hydrogel reduced the metabolic activity of the cells, which induced cancer cell death.[1285] An important observation by the authors is that the membrane-bound alkaline phosphatase (i.e., an ectoenzyme) is responsible for the selective inhibition of the Saos-2 cells over the ATDC5 cells.[1285] This work, together with the results reported by Xu et al.,[288,1256] further validates the use of enzyme-instructed self-assembly, rather than an enzyme inhibitor, for selectively inhibiting cancer cells without harming normal cells. These results, together with the earlier studies,[1259,1289] are remarkable because they firmly establish the use of *a process* (i.e., EISA), not simply *a molecule* (e.g., **661b**), for targeting cancer cells.

Since it is a challenge to know how the assemblies of small molecules behave in cellular environments to affect the cells, Xu et al. developed a facile and reliable method for evaluating the spatiotemporal profiles of the assemblies of small molecules. In this work, they incorporated a series of fluorophores (e.g., NBD) into a precursor (e.g., **658a**) which is transformed to a hydrogelator (**658b**) upon the addition of phosphatase. Except **666b**, all other dephosphorylated molecules form hydrogels at a concentration of 0.6 wt % and physiological conditions.[1063] Cell imaging experiments show that the molecules with different self-assembly properties exhibit a distinct spatial distribution and result in different cellular responses. As shown in Figure 43, **658a** enters the cells to form intracellular nanofibers and is able to curtail the effect of an F-actin toxin. Self-assemblies of **664b** mainly were localized in the cell membrane, resulting in considerable cytotoxicity. The resulting **665b** hardly accumulated in the cell, but self-assembles to form nanofibers outside the cells and exhibits little effect on the cell adhesion. This work not only illustrates a useful approach to visualize and modulate the spatiotemporal profiles of small molecules in a cellular environment, but also serves as a caution to the indiscriminate use of fluorescent aggregates as imaging probes because the interactions between the aggregates and endogenous proteins may interfere with the goal of molecular imaging.

Recently, Maruyama et al. reported that MMP-7 generates hydrogelators made of peptide lipids to result in intracellular self-assembly of the hydrogelator, which leads to the selective inhibition of cancer cells. As shown in Figure 44, they designed a precursor (**667**, *N*-palmitoyl-GGHGPLGLAAK-$CONH_2$) which turns into a hydrogelator (**668**, *N*-palmitoyl-GGHG-

DOI: 10.1021/acs.chemrev.5b00299
Chem. Rev. 2015, 115, 13165−13307

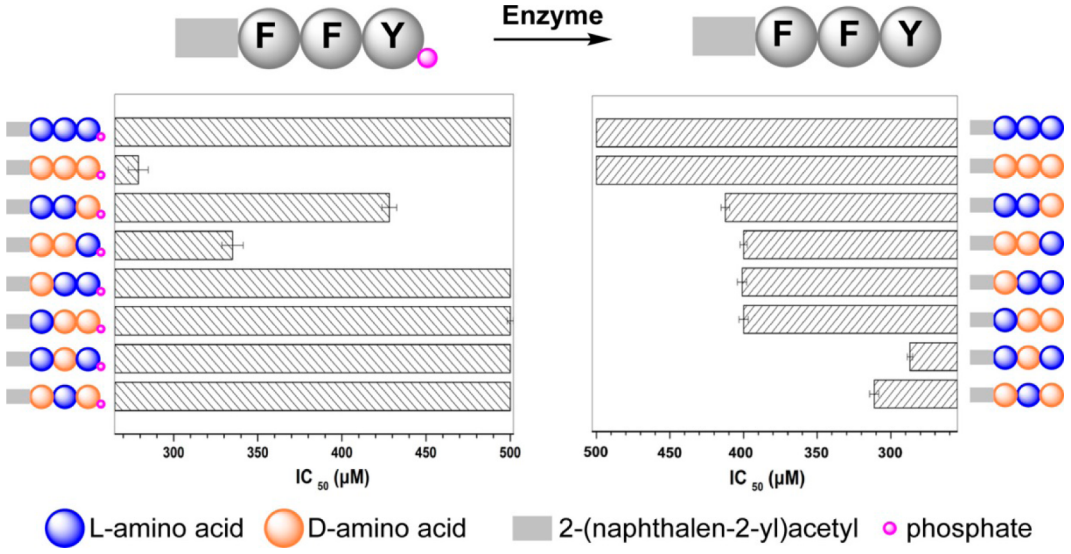

Figure 41. IC_{50} values of precursors and their hydrogelators on HeLa cells. F and Y indicate phenylalanine and tyrosine. Adapted from ref 1256. Copyright 2014 American Chemical Society.

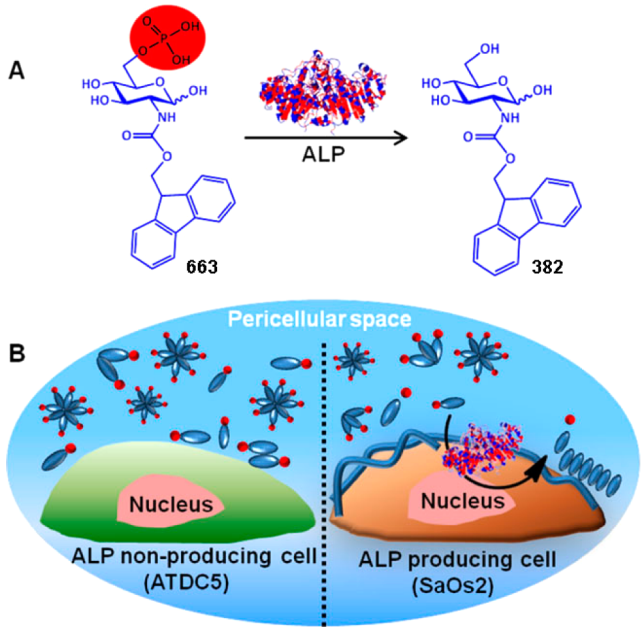

Figure 42. (A) Chemical structures of precursors and hydrogelators made of a carbohydrate amphiphile. (B) Enzyme-instructed self-assembly for pericellular nanofiber formation/hydrogelation on Saos-2 cells. Adapted from ref 1285. Copyright 2015 American Chemical Society.

PLGL) after enzymatic hydrolysis by MMP-7. The resulting hydrogelators enter the cells and are accumulated to form nanofibers which result in cancer cell death. The likely key design is the incorporation of a lipid into the peptide because the palmitoyl chain favors the localization of the precursors on the cell surface for the cleavage catalyzed by MMP-7.[894] Interestingly, the inhibition concentration is around 250 μg/mL, which also falls into the average cytotoxicity of the molecular aggregates.[894,1287] This work illustrates a promising approach that combines extracellular and intracellular self-assembly to control the cell fate.

5.9.3. Assemblies of Hydrogelators Promiscuously Interact with Proteins. The above results[288,894,1256,1259,1285] are remarkable because they firmly establish the use of *a process* (i.e., EISA), not simply *a molecule* (e.g., **661b**), for targeting cancer cells. To further understand the details and improve the efficiency of this fundamentally new process, one also needs to elucidate how the supramolecular assemblies of the small molecules promiscuously interact with the endogenous proteins of cells. In the following, we discuss the approaches for helping address the fundamental questions about the mechanisms or the consequences of the self-assembly of small molecules.

5.9.3.1. Molecular Hydrogel Protein Binding (MHPB) Assay. Xu et al. reported the use of a supramolecular hydrogel to discover the interaction between proteins and supramolecular assemblies of small molecules. In this study, Xu et al. designed a supramolecular hydrogelator (**669**) containing a photoreactive motif. **669** is able to form a transparent hydrogel at a concentration of 0.6 wt % and pH 7.4. Upon UV irradiation, the resulting hydrogel can retain the proteins that bind to the nanofibers in the hydrogels. The bound proteins in the hydrogel are separated on sodium dodecyl sulfate–polyacrylamide gel electrophoresis (SDS–PAGE) and evaluated by silver staining. Tandem MS analysis suggested that the supramolecular nanofibers interact with tubulins, actins, and several other proteins. On the basis of this observation, the authors eliminated the step of photofixation, and directly used the supramolecular hydrogel for discovering the interaction of proteins and assemblies of small molecules.[883] Using this hydrogel protein binding assay to evaluate the interaction of cytosol protein with different morphological molecular aggregates formed by the same molecule (Nap-FF, **3**), Xu et al. found that the nanofibers of **3** in the hydrogel are able to bind proteins, but the precipitates of **3** bind with few proteins. Moreover, the authors found that two types of nanofibers formed by WFF show similar morphologies and bind with a similar set of proteins. These results indicate that MHPB offers a simple and reproducible method for identifying the protein targets of the supramolecular assemblies of the small molecules.[884]

5.9.3.2. Promiscuous Interactions with Proteins. Xu et al. studied the gelation properties and bioactivities of hydrogelator Nap-FF (**3**), which contains a naphthyl group and two phenylalanine residues.[884] They found that **3** is able to self-

DOI: 10.1021/acs.chemrev.5b00299
Chem. Rev. 2015, 115, 13165–13307

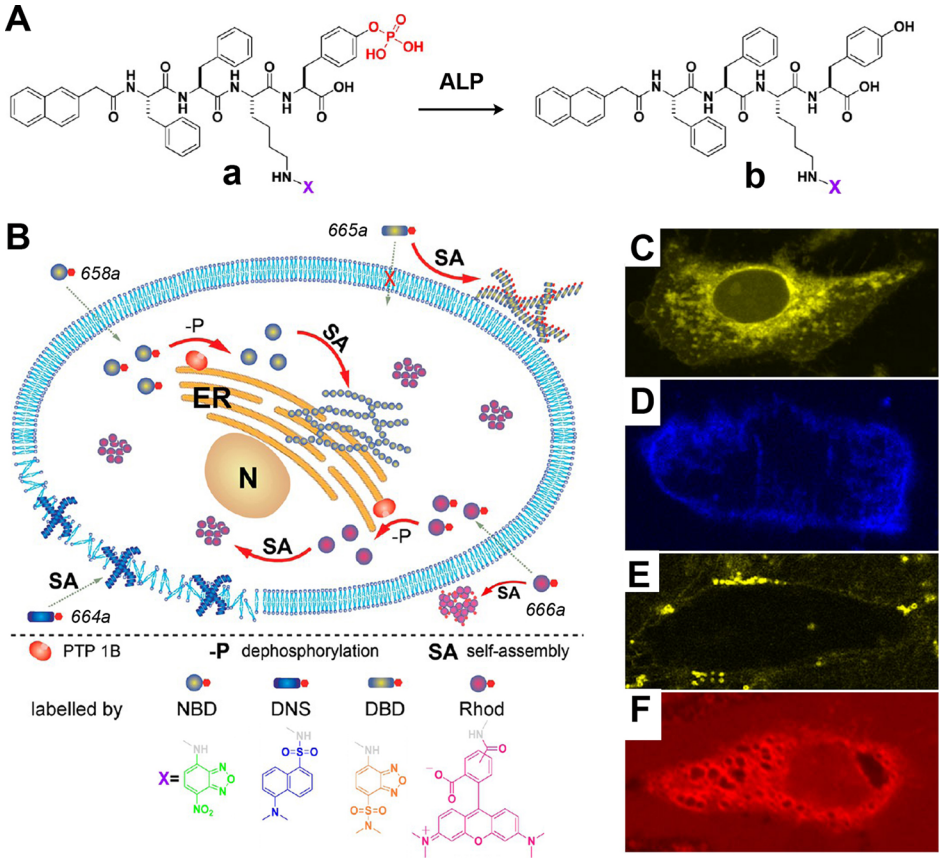

Figure 43. (A) Molecular structures of the precursors and the hydrogelators containing different fluorophores. (B) Illustration of the distinct spatial distribution of the small molecules in a cellular environment. Fluorescent confocal images of the HeLa cells incubated with 500 μM (C) **658a**, (D) **664a**, (E) **665a**, and (F) **666a** for 30 min. Adapted from ref 1063. Copyright 2013 American Chemical Society.

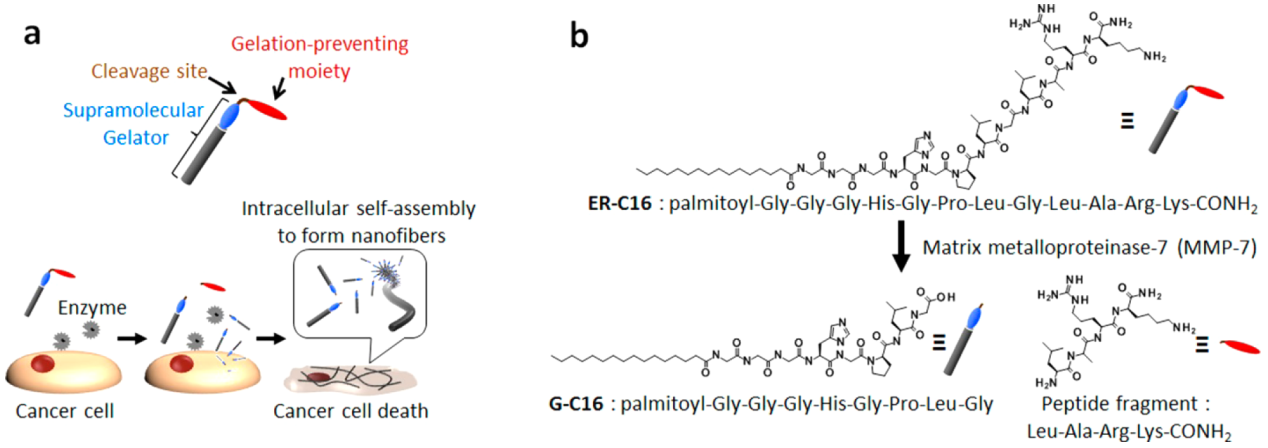

Figure 44. (a) Illustration of how enzyme-instructed molecular self-assembly induces cancer cell death. (b) Chemical structures of precursor ER-C16 (**667**) and hydrogelators G-C16 (**668**). Adapted from ref 894. Copyright 2015 American Chemical Society.

assemble in PBS buffer to form β-strand-like nanofibers with a uniform width of 24 nm below a CGC of 0.4 wt %. Furthermore, the MTT cell viability assay indicates that the nanofibers of **3** significantly inhibit the proliferation of HeLa and T98G cells at a concentration of 400 μM while showing little toxicity toward PC12 cells. Besides confirming that the nanofibers of **3** disrupt the dynamics of microtubules and consequently induce apoptosis of glioblastoma cells,[1290] the authors also demonstrated that the nanofibers of **3** inhibit tumor growth in the xenograft mice model.[573] These results support the approach that uses the supramolecular nanofibrils as de novo molecular amyloids for inhibiting the growth of cancer cells.

Encouraged by the emerging results that show that the assemblies of small molecules play an important role in biology,[1259,1288−1290] Xu et al. examined the mechanism of how the assemblies of **3** inhibit the proliferation of cells. Using the MHPB assay (Figure 45)[883,884] to investigate the interaction between nanofibers of **3** and cytosol proteins (upper panel of Figure 46a), they found that nanofibers of **3** promiscuously interact with different proteins, particularly with tubulins, vimentin, and actins, as confirmed by Western blot analysis

DOI: 10.1021/acs.chemrev.5b00299
Chem. Rev. 2015, 115, 13165−13307

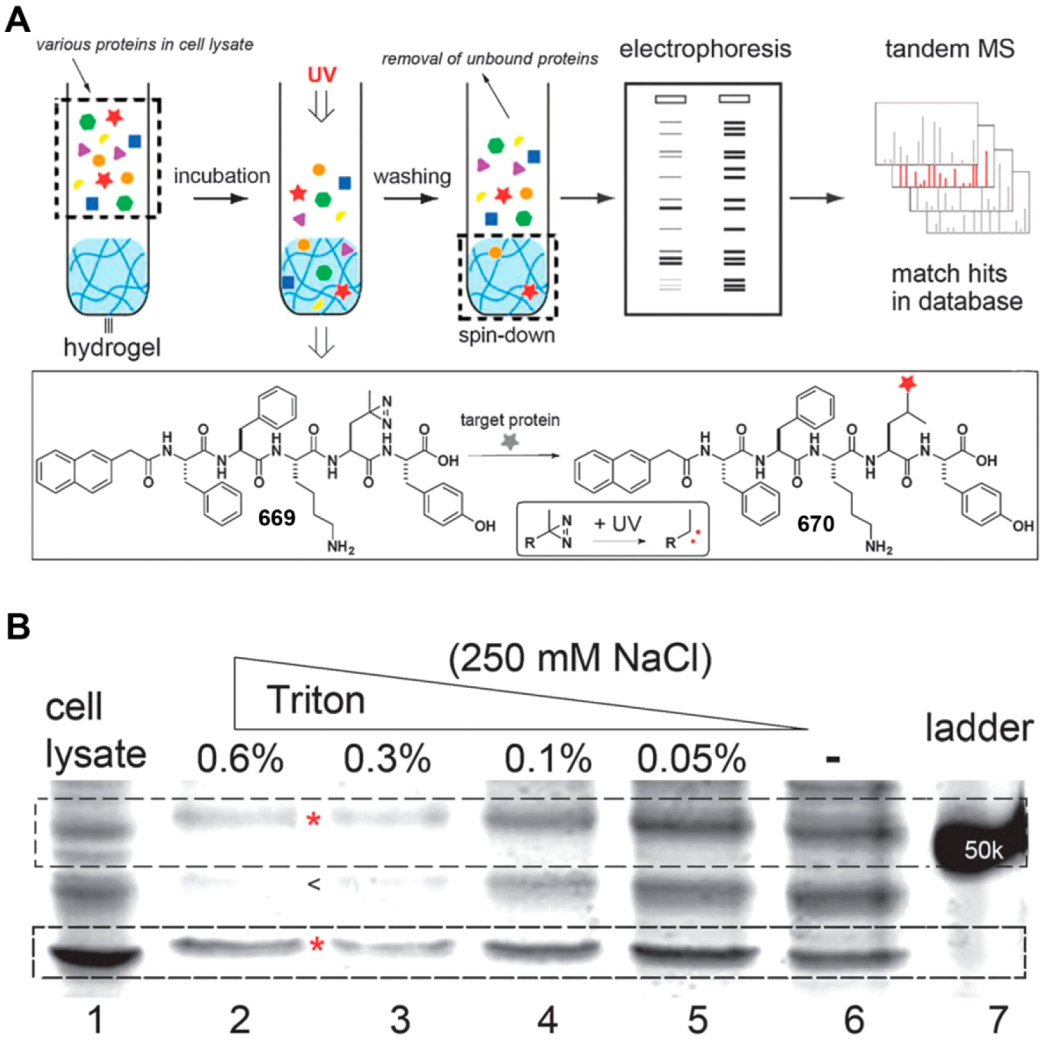

Figure 45. Illustration of the MHPB assay and hydrogel protein pull-down coupled with electrophoresis and tandem mass spectrometry for identifying cytosolic proteins that bind to supramolecular nanofibers. (A) Photoreaction of the hydrogelator and supramolecular nanofibers that bind with proteins. (B) Silver staining of the SDS−PAGE gel shows that different conditions alter the protein binding on the supramolecular hydrogel. Adapted with permission from ref 883. Copyright 2012 Royal Society of Chemistry.

(lane B, lower panel of Figure 46a). Specifically, the absence of glyceraldehyde 3-phosphate dehydrogenase (GAPDH) in lane B (lower panel of Figure 46a) indicates that the nanofibers of **3**, indeed, bind to proteins in a rather specific manner, despite the promiscuity. Furthermore, the tubulin polymerization assay (Figure 46b) shows that assemblies of **3** significantly reduce the polymerization rate. This result, together with TEM and confocal images (Figure 46c), confirmed that nanofibers of **3** impede the polymerization of microtubules.[1291] In addition, confocal fluorescent imaging (Figure 46d,e), together with the MHBP assay, implies that assemblies of **3** also disrupt the dynamics of actin filaments and intermediate filaments of vimentins in cells. By selectively inhibiting the endocytosis processes and measuring the intracellular concentration of **3** (Figure 46f), they determined that both the assemblies of **3** and the monomers of **3** enter the cell via micropinocytosis. Using PathScan apoptosis multitarget sandwich ELISA[1292] to monitor the change of several key signaling molecules in the intrinsic pathway of apoptosis, they found that the assemblies of **3** initiate the activation of Bad and p53, which later activate the caspase cascade and downstream PARP to induce apoptosis in HeLa cells (Figure 46g). On the basis of these results, the authors proposed a partial mechanism for the biological functions of the nanoscale assemblies of **3**. As summarized in Figure 46h, the assemblies of **3** enter the cell via macropinocytosis, promiscuously interact with cytoskeleton proteins, and eventually induce apoptosis via the intrinsic pathway of apoptosis. As the first case of nanoscale, supramolecular assemblies of small molecules to impede the dynamics of multiple cytoskeletal proteins, this work not only provides a mechanism for inherent cytotoxicity of hydrophobic molecular assemblies, but also illustrates a facile approach for developing nanoscale assemblies of small molecules to perform a diverse range of biological functions, including serving as a new type of anticancer agent via enzyme-instructed self-assembly.

6. FUNDAMENTAL QUESTIONS RELATED TO SUPRAMOLECULAR HYDROGELATORS

The active research and development of supramolecular hydrogels over the past 20 years have revealed a simple fact; that is, one can (almost) make any small molecule a supramolecular hydrogelator, providing proper derivatization.[14] This is remarkable because it implies that self-assembly of small molecules in water is beyond the scope of lipids. Such a basic

DOI: 10.1021/acs.chemrev.5b00299
Chem. Rev. 2015, 115, 13165−13307

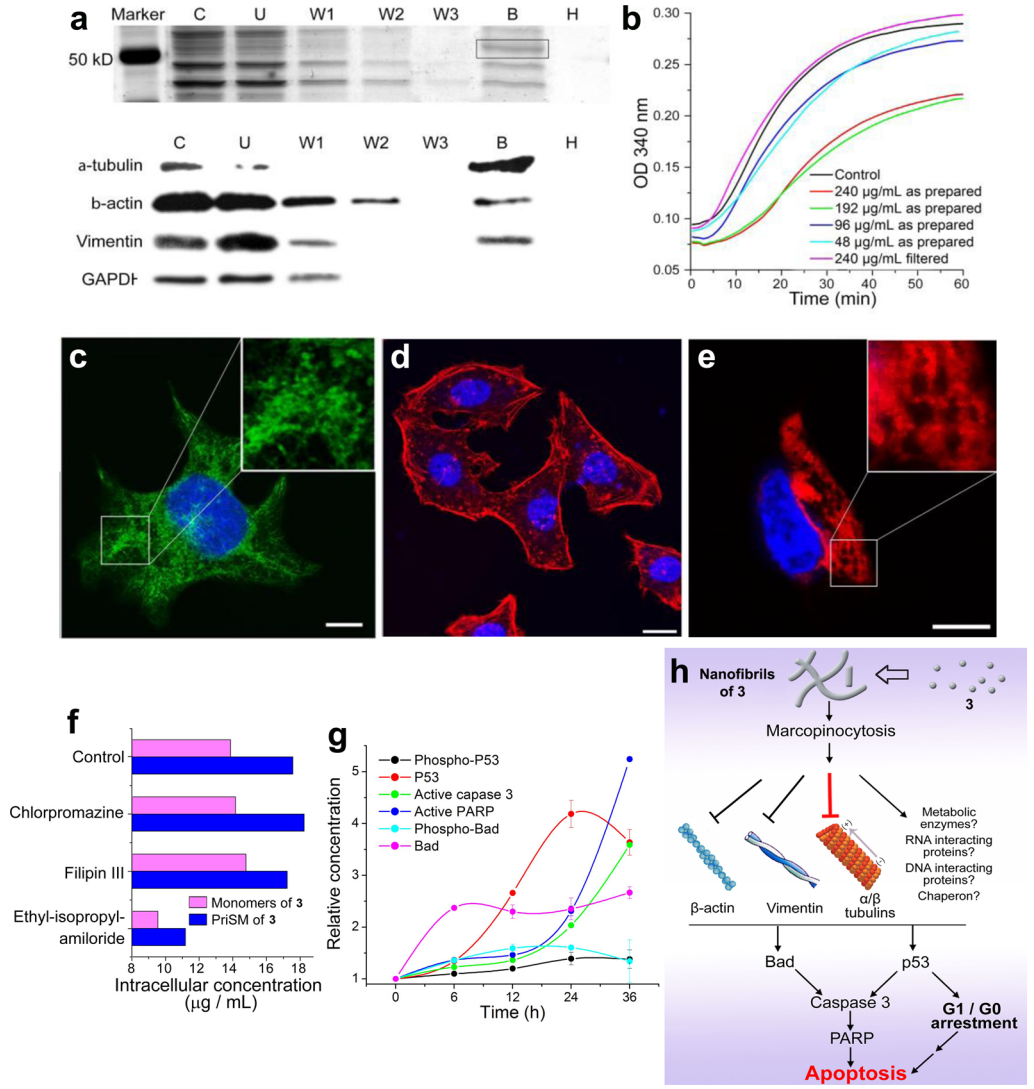

Figure 46. (a) Molecular hydrogel protein binding (MHPB) assay: upper panel, silver staining of SDS−PAGE reveals a major protein band at ∼55 kDa in lane B; lower panel, Western blot confirms the cytoskeletal proteins as the primary protein targets. (b) Tubulin polymerization assays with **3**. (c−e) Confocal images showing the assemblies of **3** impede the dynamics of cytoskeletal proteins. (f) Cellular uptake of **3** in HeLa cells treated by endocytosis inhibitors. (g) Time-dependent activation of the apoptotic proteins of HeLa cells treated with **3**. (h) Mechanism of the selective cytotoxicity of **3** toward cancer cells. Adapted with permission from ref 1248. Copyright 2014 American Society for Biochemistry and Molecular Biology. Adapted with permission from ref 1290. Copyright 2013 John Wiley and Sons.

phenomenon, like the formation of liposomes, also raises many fundamental questions. We arbitrarily and briefly discuss three of them for the purpose of stimulating possible discussion rather than providing answers.

6.1. Molecular Arrangements in the Hydrogels

Like many other fields in science, the promises always bring challenges. There is no exception for supramolecular hydrogels. One persistent and still unmet challenge is how to obtain the atomistic details of intermolecular interactions in the hydrogels or in the assemblies of the hydrogelators. Since the hydrogelators self-assemble to form nanofibers, this problem is analogous to the structural elucidation of the molecular arrangement of Aβ peptide (1−42) in the amyloid fibrils. Recent studies reveal the polymorphism of β-amyloid fibrils,[1293,1294] which implies the polymorphic nature of the nanofibers of supramolecular hydrogelators. Although the current methodologies still fall short of addressing this challenge, the rapid advancements in cryo-TEM[1295,1296] and X-ray lasers[1297] may lead to the solution of this problem in the near future. In other words, the lack of structural details of the aggregates of the hydrogelators should not be the deterrent to the exploration of the functions and applications of the assemblies of the hydrogelators or supramolecular hydrogels, as long as the functions are important and reproducible. In fact, the successful demonstration of important applications of supramolecular hydrogels is probably the prerequisite for the initiation of the endeavor of structural elucidation.[189,1298]

6.2. Self-Assembly vs Self-Organization of the Hydrogelators

The majority of the research activities on supramolecular hydrogels have largely focused on molecular self-assembly under thermodynamic equilibrium conditions.[4] Realizing a living system is at far from equilibrium and taking advantage of the self-assembly of hydrogelators, an increased number of researchers are beginning to explore the self-assembly of hydrogelators in the context of a dynamic library[739,826,1299−1302]

DOI: 10.1021/acs.chemrev.5b00299
Chem. Rev. 2015, 115, 13165−13307

or with energy input.[216,217,326] The reaction diffusion features of these cases, however, remain to be examined rigorously. Arguably, one can consider enzymatic hydrogelation accompanied by energy input, but the unanswered question in enzyme-instructed self-assembly is the role of the energy generated during bond breaking[153] or bond formation.[162] Does the dissipation of the energy promote or disfavor the self-assembly or simply raise the temperature? Does the energy input in enzyme-instructed self-assembly actually result in highly ordered nanostructures (e.g., Figure 32B[1254])? Although this question remains to be answered, nature already provides an insightful hint by evolving the energy-dissipating self-organization that is ubiquitous in cellular processes, such as the self-organization of microtubules or actin filaments. However, none of the currently reported hydrogelators are able to mimic the unique feature of actin or tubulin proteins, such as unidirectional elongation of the filaments, but the continuing exploration of the sophisticated supramolecular hydrogelators[1303] offers an opportunity to examine the fundamental differences between self-assembly and self-organization, which ultimately may lead to a man-made molecular system that self-organizes.

6.3. Origin of Life

The origin of life remains one of the most perplexing and challenging mysteries in all of science.[56] Currently, there are three main theories on the origin of life: "RNA world first" suggests that early forms of life arise from RNA,[1304,1305] "metabolism first" argues that life began from primordial metabolism networks created by existing energy sources and nonequilibrium environments, such as found in hydrothermal vents,[1306] and "lipid first" proposes that life started via the compartmentalization provided by liposomes.[1307] While each theory has its own validity and captures certain features of modern life, they all have a crucial missing link. That is, how do molecules evolve from simple ones to greater complexity? For example, what are the molecular processes that result in RNA from simple prebiotic building blocks, produce protoenzymes for the metabolic cycles, and generate the sophisticated contents to be encapsulated by the liposomes? Since one of the undeniable facts of life is that cells are largely made of molecules noncovalently packed in a highly viscous setting, it is tempting to suggest supramolecular hydrogels may provide clues for the origin of life, as hypothesized by Pollack.[1308] Interestingly, Luo et al. recently reported that a clay hydrogel enhances transcription and translation.[1309] While it remains unknown whether the primordial soup[1310] contains supramolecular hydrogels, we speculate that a series of serendipitous events in the exploration of more sophisticated supramolecular hydrogels or hydrogelators[1303] may offer more revealing clues about hydrogels in the context of the origin of life.

7. CONCLUSION AND OUTLOOK

Over the past decade, the research on supramolecular hydrogels and hydrogelators has experienced rapid growth, as evidenced by the fact that the numbers of published works on the supramolecular hydrogels in 2014 was about 10 times that in 2004, according to the Web of Science. As illustrated by the supramolecular hydrogels and hydrogelators in this review, the research focuses of hydrogelators are expanding from the curiosity for an intriguing type of soft matter to the rational development of molecular biomaterials. This trend coincides with the tremendous successes and explosive generation of data in the biological sciences. Particularly, the successful completion of the human genome project and maturation of a variety of omics projects have laid the knowledge foundations to support the molecular engineering of supramolecular hydrogels and hydrogelators for potential biomedical applications. For example, the knowledge on protein−protein interactions may provide a useful guide for developing heterotypic supramolecular hydrogels.[840,1311] On the other hand, the rapid increase of the exploration of supramolecular hydrogels for developing biomaterials itself attests to the fact that self-assembly of small molecules in water offers a facile, promising, and powerful approach for scientists and engineers to develop supramolecular hydrogelators or hydrogels that aim to improve human health. However, the current supramolecular hydrogelators or hydrogels, due to insufficient molecular engineering, are still too primitive to serve as sophisticated functional molecular biomaterials.

After billions of years of evolution, a fundamental fact is that living organisms are largely made of molecules. These molecules usually self-assemble or self-organize to perform necessary cellular functions. For example, the most common form of protein assemblies is dimers (e.g., 38% of proteins in *E. coli* exist as dimers[1312]), and the most abundant proteins in cells self-organize (i.e., actins for formation of the cytoskeleton) for many functions. Therefore, it is reasonable to take nature as the inspiration to develop supramolecular hydrogelators for generating sophisticated molecular self-assembly or self-organization in water for functions. By preserving the essence of the functions, not just the appearance of the structures, of biology systems in supramolecular hydrogelators or hydrogels, one may ultimately discover or create molecular biomaterials as a new kind of biomedicine that has prescribed functions. To achieve this goal, it is necessary to identify the problems from diseases, to define the objectives from functions, and to engineer the materials from molecules. Needless to say, this endeavor requires interdisciplinary collaborations among scientists and engineers from different disciplines of the biological, physical, and medical sciences, but it needs more than just assembling an interdisciplinary team. Since the building blocks of supramolecular hydrogels are molecules, the successful development of supramolecular hydrogelators or hydrogels as molecular biomaterials demands bioengineers or medical doctors to have a deep understanding of molecular interactions, and chemists to acquire knowledge of molecular and cell biology. For example, the completion of the synthesis of molecules and the characterization of molecular structures or supramolecular structures becomes the starting point of the research for chemists, not the ending point. If the goal of the research on the supramolecular hydrogelators is to develop molecular biomaterials, it would be beneficial to have a chemist who has the knowledge of molecular biology and cell biology and clinical medicine, is able to communicate with the language of biochemistry, and possesses the skills of bioinformatics. While these capabilities seemed to be quite demanding two decades ago, the impressive development of information technology, digitalized knowledge, and the new generation of young scientists make these prerequisites increasingly easy to meet. On the other hand, having more insights into the molecular structures and intermolecular interactions, bioengineers and medical doctors will likely more accurately and effectively identify the problems, define the objective, and devise the plan. It is our conviction that the creative exploration of supramolecular hydrogelators and hydrogels not only will

DOI: 10.1021/acs.chemrev.5b00299
Chem. Rev. 2015, 115, 13165−13307

bring innovative molecular biomaterials, but also may lead to new frontiers of science.

On the basis of the above rationale and optimism, we propose several prejudiced possible directions of supramolecular hydrogels and hydrogelators, including controlled drug release (e.g., autogel-like[33,1313,1314] systems), tissue engineering (e.g., organoids[1315,1316] of human immune systems), intracellular delivery,[1317] regenerative medicine (e.g., control of stem cell[1318−1320] differentiation), immunomoduation (e.g., molecular adjuvants of vaccines or even panflu vaccines[1321,1322]), wound healing (e.g., treatment of diabetic ulcers[1323,1324]), and cell signaling (e.g., biomimetics of autocrines, paracrines, or juxtacrines). Considering the complexity of biological systems, it is unlikely that one type of hydrogelator would meet all needs in biomedical applications. Having said that, our biased view is that hydrogelators, which consist of basic biological building blocks or are able to mimic a particular biological process, are excellent starting points for exploring the biomedical applications aforementioned. The applications of supramolecular hydrogels and hydrogelators certainly go beyond biomedicine; they already have found applications in the catalysis,[31] food, cosmetic, and art industries. We have witnessed the exciting development of supramolecular hydrogelators and hydrogels in the past decade. This astonishing versatility of supramolecular hydrogelators and hydrogels has offered scientists a fruitful playground to reinvent chemistry[1325] in the context of molecular biomaterials. By shifting the research focus from molecules to processes,[34,1326] from thermodynamics to kinetics,[1327−1329] and from molecules to cells, the research on supramolecular hydrogels and hydrogelators will lead to the integration of molecular science and bioinformatics, and contribute to the use of molecules for better human life.

ASSOCIATED CONTENT

Supporting Information

The Supporting Information is available free of charge on the ACS Publications website at DOI: 10.1021/acs.chemrev.5b00299.

Tables giving the hydrogelation concentrations of the compounds described in the molecular design session (PDF)

Special Issue Paper

This paper is an additional review for *Chem. Rev.* **2015**, *115*, issue 15, "Supramolecular Chemistry".

AUTHOR INFORMATION

Corresponding Author

*E-mail: bxu@brandeis.edu.

Notes

The authors declare no competing financial interest.

Biographies

Xuewen Du obtained his B.S. degree in the Department for Intensive Instruction (DII) of Kuang Yaming Honors School from Nanjing University in 2010. He is currently in his fifth year as a graduate student in chemistry with Professor Bing Xu at Brandeis University. His current work focuses on nanomaterials for controlling cell fates.

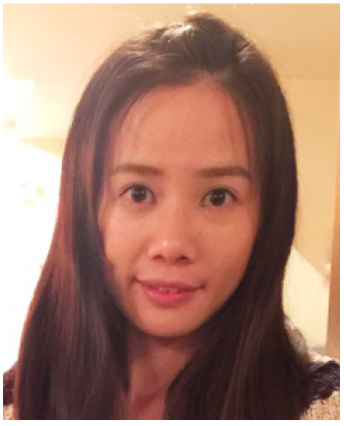

Jie Zhou obtained her B.S. degree in the Department of Chemistry & Chemical Engineering at Nanjing University in 2012. During her undergraduate study, she investigated the applications of photochemistry. She is currently in her fourth year as a graduate student in chemistry with Professor Bing Xu at Brandeis University. As a Howard Hughes Medical Institute (HHMI) International Graduate Fellow, her research interest lies in designing self-assembling bioactive materials.

Junfeng Shi obtained his B.S. degree in the Department of Chemistry from Xiangtan University in 2007, followed by an M.S. degree under the supervision of Prof. Liming Zhang from Sun Yat-sen University in 2009. He recently obtained his Ph.D. degree in Bing Xu's laboratory at Brandeis University, and will start postdoctoral research at the

DOI: 10.1021/acs.chemrev.5b00299
Chem. Rev. 2015, 115, 13165−13307

National Institutes of Health. His current work focuses on ligand−receptor interactions and their biological applications.

After receiving his B.S. and M.S. degrees from Nanjing University in 1987 and 1990, Bing Xu obtained his Ph.D. in 1996 from the University of Pennsylvania. Before starting his independent research at the Hong Kong University of Science and Technology (HKUST) in August 2000, he was a National Institutes of Health (NIH) postdoctoral fellow at Harvard University. He was tenured as an associate professor in January 2006 and became a full professor in July 2008 at HKUST. On the basis of his work at HKUST and Brandeis, Bing Xu is identified on the Thomson Reuters 2014 and 2015 Highly-Cited Researchers lists in chemistry. He is currently a professor in the Department of Chemistry, Brandeis University. His research focuses on the applications of molecular engineering in materials, biology, and medicine.

ACKNOWLEDGMENTS

This work was partially supported by the National Institutes of Health (NIH) (Grant R01CA142746), W.M. Keck Foundation, National Science Foundation (NSF) (Grant DMR-1420382), Human Frontier Science Program (HFSP) (Grant RGP0056/2008), and Kenneth Ranin Foundation. J.Z. is a Howard Hughes Medical Institute (HHMI) International Research Fellow.

ABBREVIATIONS

2D	two-dimensional
3D	three-dimensional
5-FU	5-fluoro-2A-deoxyuridine
6-ACA	6-aminocaproic acid
ACQ	aggregation-caused quenching
AgNPs	silver nanoparticles
ALP	alkaline phosphatase
ALPPs	placental alkaline phosphatases
AQ	8-aminoquinoline
BAMB	butan-1-aminium 4-methylbenzenesulfonate
β-CD	β-cyclodextrin
β-TCP	tricalcium phosphate
Bhcmoc	[(6-bromo-7-hydroxycoumarin-4-yl)methoxy]-carbonyl
BMDMs	bone-marrow-derived monocytes
Boc	(*tert*-butyloxy)carbonyl
BPs	bisphosphonates
BSA	bovine serum albumin
BTA	benzene-1,3,5-tricarboxamide
CAB	cholesteryl 4-(2-anthryloxy)butyrate
CAC	critical assembly concentration
CGC	critical concentration of gelation
CHO	Chinese hamster ovary
CLEM	correlative light and electron microscopy
CMC	critical micelle concentration
CPC	cetylpyridinium chloride
CSD	Cambridge Structural Database
CT	charge transfer
CTV	cyclotriveratrylene
DA	donor−acceptor
DCDs	dimeric cholesterol derivatives
Dex	dexamethasone
DFT	density functional theory
DLVO	Derjaguin−Landau−Verwey−Overbeek
DMSO	dimethyl sulfoxide
DOPA	3,4-dihydroxy-L-phenylalanine
DOPC	dioleoylphosphocholine
DSA	doxylstearic acid
DSC	differential scanning calorimetry
DTT	dithiothreitol
ECD	electronic circular dichroism
ECM	extracellular matrix
EG	ethylene glycol
EISA	enzyme-instructed self-assembly
ESCs	embryonic stem cells
FA	folic acid
FCS	fluorescence correlation spectroscopy
FESEM	field-emission scanning electron microscopy
Fmoc	(fluoren-9-ylmethoxy)carbonyl
FRAP	fluorescence recovery after photobleaching
FRET	fluorescence resonance transfer
GdL	glucono-δ-lactone
GFP	green fluorescent protein
GNFs	glycosyl-nucleoside-fluorinated amphiphiles
GNLs	glycosyl-nucleoside lipids
GSH	glutathione
GSSG	glutathione (γ-glutamylcysteinylglycine (GSH))
HaCaT's	human keratinocytes
HCPT	hydroxycamptothecin
HDFs	human dermal fibroblasts
HEK293 cells	human embryonic kidney 293 cells
HFIP	hexafluoroisopropyl alcohol
HMSCs	human marrow stem cells
HQ	2-hydroxyquinoline
hRBCs	human red blood cells
HUVECs	human umbilical vein endothelial cells
ITC	isothermal titration calorimetry
LCA	lithocholic acid
LCST	lower critical solution temperature
LDH	lactate dehydrogenase
LSCM	laser scanning confocal microscopy
LZ	leucine zipper domain
Mb	myoglobin
MDPs	multidomain peptides
MHPB	molecular hydrogel protein binding
MIC	minimum inhibitory concentration
MMP-2	matrix metalloprotease 2
MRSA	methicillin-resistant *Staphylococcus aureus*
MSCs	mesenchymal stem cells
MTT	3-(4,5-dimethylthiazol-2-yl)-2,5-diphenyltetrazolium bromide
MVECs	microvascular endothelial cells
NCL	native chemical ligation
NHSF	normal human skin fibroblast

DOI: 10.1021/acs.chemrev.5b00299
Chem. Rev. 2015, 115, 13165−13307

NO	nitric oxide
NPCs	nucleus pulposus cells
NSAID	nonsteroidal anti-inflammatory drug
NSCs	neural stem cells
OC	osteocalcin
Pa	pascal
PA	peptide amphiphile
PAP	prostatic acid phosphatase
PC12 cells	pheochromocytoma cells
PKA	protein kinase A
PL	photoluminescence
PNPA	*p*-nitrophenyl acetate
POM	polyoxometalate
PRRSV	porcine reproductive and respiratory syndrome virus
PSA	prostate-specific antigen
PTA	1,3,5-triaza-7-phosphaadamantane
ROMP	ring-opening metathesis polymerization
SCC25	squamous cell carcinomas
SDS	sodium dodecyl sulfate
SEM	scanning electron microscopy
SHED	human exfoliated deciduous teeth
SPPS	solid-phase peptide synthesis
SUMO	small ubiquitin-related modifier
T_{gel}	temperature of gelation
T_m	phase transition temperature
TATP	triacetone triperoxide
UV	ultraviolet

REFERENCES

(1) Lehn, J. M. Perspectives in Supramolecular Chemistry - from Molecular Recognition Towards Molecular Information-Processing and Self-Organization. *Angew. Chem., Int. Ed. Engl.* **1990**, *29*, 1304−1319.

(2) Whitesides, G. M.; Mathias, J. P.; Seto, C. T. Molecular Self-Assembly and Nanochemistry - a Chemical Strategy for the Synthesis of Nanostructures. *Science* **1991**, *254*, 1312−1319.

(3) Luisi, P. L. Chemistry Constraints on The Origin of Life. *Isr. J. Chem.* **2015**, *55*, 906−918.

(4) Estroff, L. A.; Hamilton, A. D. Water Gelation by Small Organic Molecules. *Chem. Rev.* **2004**, *104*, 1201−1217.

(5) Terech, P.; Weiss, R. G. Low Molecular Mass Gelators of Organic Liquids and the Properties of Their Gels. *Chem. Rev.* **1997**, *97*, 3133−3159.

(6) Yang, Z.; Xu, B. Using Enzymes to Control Molecular Hydrogelation. *Adv. Mater.* **2006**, *18*, 3043−3046.

(7) Cortner, R. A.; Hoffman, W. F. An Interesting Colloid Gel. *J. Am. Chem. Soc.* **1921**, *43*, 2199−2202.

(8) Brenzinger. *Z. Physiol. Chem.* **1892**, *16*, 537.

(9) Menger, F. M.; Caran, K. L. Anatomy of a Gel. Amino Acid Derivatives That Rigidify Water at Submillimolar Concentrations. *J. Am. Chem. Soc.* **2000**, *122*, 11679−11691.

(10) Shi, J.; Gao, Y.; Yang, Z.; Xu, B. Exceptionally Small Supramolecular Hydrogelators Based on Aromatic-Aromatic Interactions. *Beilstein J. Org. Chem.* **2011**, *7*, 167−172.

(11) Zhang, Y.; Gu, H. W.; Yang, Z. M.; Xu, B. Supramolecular Hydrogels Respond to Ligand-Receptor Interaction. *J. Am. Chem. Soc.* **2003**, *125*, 13680−13681.

(12) Ma, M.; Kuang, Y.; Gao, Y.; Zhang, Y.; Gao, P.; Xu, B. Aromatic-Aromatic Interactions Induce the Self-Assembly of Pentapeptidic Derivatives in Water to Form Nanofibers and Supramolecular Hydrogels. *J. Am. Chem. Soc.* **2010**, *132*, 2719−2728.

(13) Burley, S. K.; Petsko, G. A. Aromatic-Aromatic Interaction - a Mechanism of Protein-Structure Stabilization. *Science* **1985**, *229*, 23−28.

(14) Zhang, Y.; Kuang, Y.; Gao, Y.; Xu, B. Versatile Small-Molecule Motifs for Self-Assembly in Water and the Formation of Biofunctional Supramolecular Hydrogels. *Langmuir* **2011**, *27*, 529−537.

(15) Lin, Y. C.; Weiss, R. G. A Novel Gelator of Organic Liquids and the Properties of Its Gels. *Macromolecules* **1987**, *20*, 414−417.

(16) Aoki, M.; Murata, K.; Shinkai, S. Calixarene-Based Gelators of Organic Fluids. *Chem. Lett.* **1991**, 1715−1718.

(17) Zhang, S. G.; Holmes, T.; Lockshin, C.; Rich, A. Spontaneous Assembly of a Self-Complementary Oligopeptide to Form a Stable Macroscopic Membrane. *Proc. Natl. Acad. Sci. U. S. A.* **1993**, *90*, 3334−3338.

(18) Xing, B. G.; Yu, C. W.; Chow, K. H.; Ho, P. L.; Fu, D. G.; Xu, B. Hydrophobic Interaction and Hydrogen Bonding Cooperatively Confer a Vancomycin Hydrogel: A Potential Candidate for Biomaterials. *J. Am. Chem. Soc.* **2002**, *124*, 14846−14847.

(19) Hutchison, K. G. Assessment of Gelling in Insulin Solutions for Infusion Pumps. *J. Pharm. Pharmacol.* **1985**, *37*, 528−531.

(20) Jimenez, J. L.; Nettleton, E. J.; Bouchard, M.; Robinson, C. V.; Dobson, C. M.; Saibil, H. R. The Protofilament Structure of Insulin Amyloid Fibrils. *Proc. Natl. Acad. Sci. U. S. A.* **2002**, *99*, 9196−9201.

(21) Vonderviszt, F.; Sonoyama, M.; Tasumi, M.; Namba, K. Conformational Adaptability of the Terminal Regions of Flagellin. *Biophys. J.* **1992**, *63*, 1672−1677.

(22) Kato, M.; Han, T. W.; Xie, S.; Shi, K.; Du, X.; Wu, L. C.; Mirzaei, H.; Goldsmith, E. J.; Longgood, J.; Pei, J.; et al. Cell-Free Formation of Rna Granules: Low Complexity Sequence Domains Form Dynamic Fibers within Hydrogels. *Cell* **2012**, *149*, 753−767.

(23) Doak, A. K.; Wille, H.; Prusiner, S. B.; Shoichet, B. K. Colloid Formation by Drugs in Simulated Intestinal Fluid. *J. Med. Chem.* **2010**, *53*, 4259−4265.

(24) Ulijn, R. V.; Bibi, N.; Jayawarna, V.; Thornton, P. D.; Todd, S. J.; Mart, R. J.; Smith, A. M.; Gough, J. E. Bioresponsive Hydrogels. *Mater. Today* **2007**, *10*, 40−48.

(25) Sangeetha, N. M.; Maitra, U. Supramolecular Gels: Functions and Uses. *Chem. Soc. Rev.* **2005**, *34*, 821−836.

(26) Araki, K.; Yoshikawa, I. In *Low Molecular Mass Gelators: Design, Self-Assembly, Function*; Fages, F., Ed.; Topics in Current Chemistry, Vol. *256*; Springer: Berlin, 2005.

(27) Shimizu, T. Bottom-up Synthesis and Morphological Control of High-Axial-Ratio Nanostructures through Molecular Self-Assembly. *Polym. J.* **2003**, *35*, 1−22.

(28) Branco, M. C.; Schneider, J. P. Self-Assembling Materials for Therapeutic Delivery. *Acta Biomater.* **2009**, *5*, 817−831.

(29) Du, X.; Zhou, J.; Xu, B. Supramolecular Hydrogels Made of Basic Biological Building Blocks. *Chem. - Asian J.* **2014**, *9*, 1446−1472.

(30) Li, X. M.; Kuang, Y.; Xu, B. "Molecular Trinity" for Soft Nanomaterials: Integrating Nucleobases, Amino Acids, and Glycosides to Construct Multifunctional Hydrogelators. *Soft Matter* **2012**, *8*, 2801−2806.

(31) Gao, Y.; Zhao, F.; Wang, Q.; Zhang, Y.; Xu, B. Small Peptide Nanofibers as the Matrices of Molecular Hydrogels for Mimicking Enzymes and Enhancing the Activity of Enzymes. *Chem. Soc. Rev.* **2010**, *39*, 3425−3433.

(32) Xu, B. Gels as Functional Nanomaterials for Biology and Medicine. *Langmuir* **2009**, *25*, 8375−8377.

(33) Zhao, F.; Ma, M. L.; Xu, B. Molecular Hydrogels of Therapeutic Agents. *Chem. Soc. Rev.* **2009**, *38*, 883−891.

(34) Yang, Z.; Liang, G.; Xu, B. Enzymatic Hydrogelation of Small Molecules. *Acc. Chem. Res.* **2008**, *41*, 315−326.

(35) Foster, J. A.; Steed, J. W. Exploiting Cavities in Supramolecular Gels. *Angew. Chem., Int. Ed.* **2010**, *49*, 6718−6724.

(36) Babu, S. S.; Praveen, V. K.; Ajayaghosh, A. Functional Pi-Gelators and Their Applications. *Chem. Rev.* **2014**, *114*, 1973−2129.

(37) Suzuki, M.; Hanabusa, K. L-Lysine-Based Low-Molecular-Weight Gelators. *Chem. Soc. Rev.* **2009**, *38*, 967−975.

(38) Tomatsu, I.; Peng, K.; Kros, A. Photoresponsive Hydrogels for Biomedical Applications. *Adv. Drug Delivery Rev.* **2011**, *63*, 1257−1266.

DOI: 10.1021/acs.chemrev.5b00299
Chem. Rev. 2015, 115, 13165−13307

(39) Ulijn, R. V. Enzyme-Responsive Materials: A New Class of Smart Biomaterials. *J. Mater. Chem.* **2006**, *16*, 2217−2225.
(40) Wu, Z. L.; Gong, J. P. Hydrogels with Self-Assembling Ordered Structures and Their Functions. *NPG Asia Mater.* **2011**, *3*, 57−64.
(41) Lin, Y.; Kachar, B.; Weiss, R. G. Novel Family of Gelators of Organic Fluids and the Structure of Their Gels. *J. Am. Chem. Soc.* **1989**, *111*, 5542−5551.
(42) Weiss, R. G. The Past, Present, and Future of Molecular Gels. What Is the Status of the Field, and Where Is It Going? *J. Am. Chem. Soc.* **2014**, *136*, 7519−7530.
(43) Ikeda, M.; Ochi, R.; Kurita, Y. S.; Pochan, D. J.; Hamachi, I. Heat-Induced Morphological Transformation of Supramolecular Nanostructures by Retro-Diels-Alder Reaction. *Chem. - Eur. J.* **2012**, *18*, 13091−13096.
(44) Tamaru, S.; Hamachi, I. *Recognition of Anions*; Structure and Bonding, Vol. *129*; Springer: Berlin, 2008.
(45) Qiu, Y.; Park, K. Environment-Sensitive Hydrogels for Drug Delivery. *Adv. Drug Delivery Rev.* **2001**, *53*, 321−339.
(46) Rubinstein, A. Approaches and Opportunities in Colon-Specific Drug-Delivery. *Crit. Rev. Ther. Drug Carrier Syst.* **1995**, *12*, 101−149.
(47) Brizard, A.; Oda, R.; Huc, I. In *Low Molecular Mass Gelators: Design, Self-Assembly, Function*; Fages, F., Ed.; Topics in Current Chemistry, Vol. *256*; Springer: Berlin, 2005.
(48) Dastidar, P. Supramolecular Gelling Agents: Can They Be Designed? *Chem. Soc. Rev.* **2008**, *37*, 2699−2715.
(49) Hirst, A. R.; Escuder, B.; Miravet, J. F.; Smith, D. K. High-Tech Applications of Self-Assembling Supramolecular Nanostructured Gel-Phase Materials: From Regenerative Medicine to Electronic Devices. *Angew. Chem., Int. Ed.* **2008**, *47*, 8002−8018.
(50) Le Bideau, J.; Viau, L.; Vioux, A. Ionogels, Ionic Liquid Based Hybrid Materials. *Chem. Soc. Rev.* **2011**, *40*, 907−925.
(51) Lu, J.; Yan, F.; Texter, J. Advanced Applications of Ionic Liquids in Polymer Science. *Prog. Polym. Sci.* **2009**, *34*, 431−448.
(52) Smith, D. K. Lost in Translation? Chirality Effects in the Self-Assembly of Nanostructured Gel-Phase Materials. *Chem. Soc. Rev.* **2009**, *38*, 684−694.
(53) Vintiloiu, A.; Leroux, J.-C. Organogels and Their Use in Drug Delivery - a Review. *J. Controlled Release* **2008**, *125*, 179−192.
(54) Zinic, M.; Vogtle, F.; Fages, F. In *Low Molecular Mass Gelators: Design, Self-Assembly, Function*; Fages, F., Ed.; Topics in Current Chemistry, Vol. *256*; Springer: Berlin, 2005.
(55) Basit, H.; Pal, A.; Sen, S.; Bhattacharya, S. Two-Component Hydrogels Comprising Fatty Acids and Amines: Structure, Properties, and Application as a Template for the Synthesis of Metal Nanoparticles. *Chem. - Eur. J.* **2008**, *14*, 6534−6545.
(56) Mann, S. The Origins of Life: Old Problems, New Chemistries. *Angew. Chem., Int. Ed.* **2013**, *52*, 155−162.
(57) Terech, P.; Rossat, C.; Volino, F. On the Measurement of Phase Transition Temperatures in Physical Molecular Organogels. *J. Colloid Interface Sci.* **2000**, *227*, 363−370.
(58) Miravet, J. F.; Escuder, B. Pyridine-Functionalised Ambidextrous Gelators: Towards Catalytic Gels. *Chem. Commun.* **2005**, 5796−5798.
(59) Nebot, V. J.; Armengol, J.; Smets, J.; Prieto, S. F.; Escuder, B.; Miravet, J. F. Molecular Hydrogels from Bolaform Amino Acid Derivatives: A Structure-Properties Study Based on the Thermodynamics of Gel Solubilization. *Chem. - Eur. J.* **2012**, *18*, 4063−4072.
(60) de Loos, M.; Feringa, B. L.; van Esch, J. H. Design and Application of Self-Assembled Low Molecular Weight Hydrogels. *Eur. J. Org. Chem.* **2005**, *2005*, 3615−3631.
(61) Ghosh, A.; Dey, J. Ph-Responsive and Thermoreversible Hydrogels of N-(2-Hydroxyalkyl)-L-Valine Amphiphiles. *Langmuir* **2009**, *25*, 8466−8472.
(62) Johnson, E. K.; Adams, D. J.; Cameron, P. J. Peptide Based Low Molecular Weight Gelators. *J. Mater. Chem.* **2011**, *21*, 2024−2027.
(63) Bairi, P.; Roy, B.; Nandi, A. K. Bicomponent Hydrogels of Lumichrome and Melamine: Photoluminescence Property and Its Dependency on Ph and Temperature. *J. Phys. Chem. B* **2010**, *114*, 11454−11461.
(64) Roy, B.; Saha, A.; Esterrani, A.; Nandi, A. K. Time Sensitive, Temperature and Ph Responsive Photoluminescence Behaviour of a Melamine Containing Bicomponent Hydrogel. *Soft Matter* **2010**, *6*, 3337−3345.
(65) Roy, B.; Bairi, P.; Saha, A.; Nandi, A. K. Variation of Physical and Mechanical Properties in the Bicomponent Hydrogels of Melamine with Positional Isomers of Hydroxybenzoic Acid. *Soft Matter* **2011**, *7*, 8067−8076.
(66) Barker, J. A.; Fock, W. Theory of Upper and Lower Critical Solution Temperatures. *Discuss. Faraday Soc.* **1953**, *15*, 188−195.
(67) Bhattacharjee, S.; Datta, S.; Bhattacharya, S. Remarkable Regioisomer Control in the Hydrogel Formation from a Two-Component Mixture of Pyridine-End Oligo(P-Phenylenevinylene)S and N-Decanoyl-L-Alanine. *Chem. - Eur. J.* **2013**, *19*, 16672−16681.
(68) Dastidar, P.; Okabe, S.; Nakano, K.; Iida, K.; Miyata, M.; Tohnai, N.; Shibayama, M. Facile Syntheses of a Class of Supramolecular Gelator Following a Combinatorial Library Approach: Dynamic Light Scattering and Small-Angle Neutron Scattering Studies. *Chem. Mater.* **2005**, *17*, 741−748.
(69) Kawano, S.; Kobayashi, D.; Taguchi, S.; Kunitake, M.; Nishimi, T. Construction of Continuous Porous Organogels, Hydrogels, and Bicontinuous Organo/Hydro Hybrid Gels from Bicontinuous Microemulsions. *Macromolecules* **2010**, *43*, 473−479.
(70) Krishnan, A. S.; Vargantwar, P. H.; Spontak, R. J. Thermorheological Behavior of Coexisting Physical Networks: Combining Safin and Samin Organogels. *Soft Matter* **2012**, *8*, 12025−12033.
(71) Shankar, B. V.; Patnaik, A. A New Ph and Thermo-Responsive Chiral Hydrogel for Stimulated Release. *J. Phys. Chem. B* **2007**, *111*, 9294−9300.
(72) Wu, J. W.; Tang, L. M.; Chen, K.; Yan, L.; Li, F.; Wang, Y. J. Formation of Supramolecular Hydrogels with Controlled Microstructures and Stability Via Molecular Assembling in a Two-Component System. *J. Colloid Interface Sci.* **2007**, *307*, 280−287.
(73) Trivedi, D. R.; Ballabh, A.; Dastidar, P.; Ganguly, B. Structure-Property Correlation of a New Family of Organogelators Based on Organic Salts and Their Selective Gelation of Oil from Oil/Water Mixtures. *Chem. - Eur. J.* **2004**, *10*, 5311−5322.
(74) Shome, A.; Debnath, S.; Das, P. K. Head Group Modulated Ph-Responsive Hydrogel of Amino Acid-Based Amphiphiles: Entrapment and Release of Cytochrome C and Vitamin B-12. *Langmuir* **2008**, *24*, 4280−4288.
(75) Das, D.; Dasgupta, A.; Roy, S.; Mitra, R. N.; Debnath, S.; Das, P. K. Water Gelation of an Amino Acid-Based Amphiphile. *Chem. - Eur. J.* **2006**, *12*, 5068−5074.
(76) Suzuki, M.; Yumoto, M.; Shirai, H.; Hanabusa, K. Supramolecular Gels Formed by Amphiphilic Low-Molecular-Weight Gelators of N-Alpha,N-Epsilon-Diacyl-L-Lysine Derivatives. *Chem. - Eur. J.* **2008**, *14*, 2133−2144.
(77) Krieg, E.; Shirman, E.; Weissman, H.; Shimoni, E.; Wolf, S. G.; Pinkas, I.; Rybtchinski, B. Supramolecular Gel Based on a Perylene Diimide Dye: Multiple Stimuli Responsiveness, Robustness, and Photofunction. *J. Am. Chem. Soc.* **2009**, *131*, 14365−14373.
(78) Friggeri, A.; Feringa, B. L.; van Esch, J. Entrapment and Release of Quinoline Derivatives Using a Hydrogel of a Low Molecular Weight Gelator. *J. Controlled Release* **2004**, *97*, 241−248.
(79) Wang, H.; Zhang, W.; Dong, X.; Yang, Y. Thermo-Reversibility of the Fluorescence Enhancement of Acridine Orange Induced by Supramolecular Self-Assembly. *Talanta* **2009**, *77*, 1864−1868.
(80) Naota, T.; Koori, H. Molecules That Assemble by Sound: An Application to the Instant Gelation of Stable Organic Fluids. *J. Am. Chem. Soc.* **2005**, *127*, 9324−9325.
(81) Isozaki, K.; Takaya, H.; Naota, T. Ultrasound-Induced Gelation of Organic Fluids with Metalated Peptides. *Angew. Chem., Int. Ed.* **2007**, *46*, 2855−2857.
(82) Bardelang, D.; Camerel, F.; Margeson, J. C.; Leek, D. M.; Schmutz, M.; Zaman, M. B.; Yu, K.; Soldatov, D. V.; Ziessel, R.; Ratcliffe, C. I.; et al. Unusual Sculpting of Dipeptide Particles by

DOI: 10.1021/acs.chemrev.5b00299
Chem. Rev. 2015, 115, 13165−13307

Ultrasound Induces Gelation. *J. Am. Chem. Soc.* **2008**, *130*, 3313−3315.
(83) Garvin, K. A.; VanderBurgh, J.; Hocking, D. C.; Dalecki, D. Controlling Collagen Fiber Microstructure in Three-Dimensional Hydrogels Using Ultrasound. *J. Acoust. Soc. Am.* **2013**, *134*, 1491−1502.
(84) Xie, Z. G.; Zhang, A. Y.; Ye, L.; Feng, Z. G. Organo- and Hydrogels Derived from Cyclo(L-Tyr-L-Lys) and Its Epsilon-Amino Derivatives. *Soft Matter* **2009**, *5*, 1474−1482.
(85) Pan, S. F.; Luo, S.; Li, S.; Lai, Y. S.; Geng, Y. Y.; He, B.; Gu, Z. W. Ultrasound Accelerated Gelation of Novel L-Lysine Based Hydrogelators. *Chem. Commun.* **2013**, *49*, 8045−8047.
(86) Roy, B.; Bairi, P.; Nandi, A. K. Metastability in a Bi-Component Hydrogel of Thymine and 6-Methyl-1,3,5-Triazine-2,4-Diamine: Ultrasound Induced Vs. Thermo Gelation. *Soft Matter* **2012**, *8*, 2366−2369.
(87) Kuang, Y.; Gao, Y.; Shi, J. F.; Li, J.; Xu, B. The First Supramolecular Peptidic Hydrogelator Containing Taurine. *Chem. Commun.* **2014**, *50*, 2772−2774.
(88) Grigoriou, S.; Johnson, E. K.; Chen, L.; Adams, D. J.; James, T. D.; Cameron, P. J. Dipeptide Hydrogel Formation Triggered by Boronic Acid-Sugar Recognition. *Soft Matter* **2012**, *8*, 6788−6791.
(89) Marchesan, S.; Waddington, L.; Easton, C. D.; Winkler, D. A.; Goodall, L.; Forsythe, J.; Hartley, P. G. Unzipping the Role of Chirality in Nanoscale Self-Assembly of Tripeptide Hydrogels. *Nanoscale* **2012**, *4*, 6752−6760.
(90) Nanda, J.; Banerjee, A. Beta-Amino Acid Containing Proteolitically Stable Dipeptide Based Hydrogels: Encapsulation and Sustained Release of Some Important Biomolecules at Physiological Ph and Temperature. *Soft Matter* **2012**, *8*, 3380−3386.
(91) Nonoyama, T.; Ogasawara, H.; Tanaka, M.; Higuchi, M.; Kinoshita, T. Calcium Phosphate Biomineralization in Peptide Hydrogels for Injectable Bone-Filling Materials. *Soft Matter* **2012**, *8*, 11531−11536.
(92) Xu, X. D.; Liang, L.; Cheng, H.; Wang, X. H.; Jiang, F. G.; Zhuo, R. X.; Zhang, X. Z. Construction of Therapeutic Glycopeptide Hydrogel as a New Substitute for Antiproliferative Drugs to Inhibit Postoperative Scarring Formation. *J. Mater. Chem.* **2012**, *22*, 18164−18171.
(93) Fletcher, N. L.; Lockett, C. V.; Dexter, A. F. A Ph-Responsive Coiled-Coil Peptide Hydrogel. *Soft Matter* **2011**, *7*, 10210−10218.
(94) Imura, Y.; Matsue, K.; Sugimoto, H.; Ito, R.; Kondo, T.; Kawai, T. Ambidextrous Gel Property and Ph-Responsive Sol-Gel Transition of Low Molecular Mass Gelator Based on a Long-Chain Amide Derivative. *Chem. Lett.* **2009**, *38*, 778−779.
(95) Liu, Y. F.; Yang, Y. L.; Wang, C.; Zhao, X. J. Stimuli-Responsive Self-Assembling Peptides Made from Antibacterial Peptides. *Nanoscale* **2013**, *5*, 6413−6421.
(96) Jayawarna, V.; Ali, M.; Jowitt, T. A.; Miller, A. E.; Saiani, A.; Gough, J. E.; Ulijn, R. V. Nanostructured Hydrogels for Three-Dimensional Cell Culture through Self-Assembly of Fluorenylmethoxycarbonyl-Dipeptides. *Adv. Mater.* **2006**, *18*, 611−614.
(97) Tang, C.; Smith, A. M.; Collins, R. F.; Ulijn, R. V.; Saiani, A. Fmoc-Diphenylalanine Self-Assembly Mechanism Induces Apparent Pk(a) Shifts. *Langmuir* **2009**, *25*, 9447−9453.
(98) Aufderhorst-Roberts, A.; Frith, W. J.; Kirkland, M.; Donald, A. M. Microrheology and Microstructure of Fmoc-Derivative Hydrogels. *Langmuir* **2014**, *30*, 4483−4492.
(99) Chen, L.; Morris, K.; Laybourn, A.; Elias, D.; Hicks, M. R.; Rodger, A.; Serpell, L.; Adams, D. J. Self-Assembly Mechanism for a Naphthalene-Dipeptide Leading to Hydrogelation. *Langmuir* **2010**, *26*, 5232−5242.
(100) Chen, L.; Pont, G.; Morris, K.; Lotze, G.; Squires, A.; Serpell, L. C.; Adams, D. J. Salt-Induced Hydrogelation of Functionalised-Dipeptides at High Ph. *Chem. Commun.* **2011**, *47*, 12071−12073.
(101) Chen, L.; Revel, S.; Morris, K.; Adams, D. J. Energy Transfer in Self-Assembled Dipeptide Hydrogels. *Chem. Commun.* **2010**, *46*, 4267−4269.
(102) Pal, A.; Dey, J. Rheology and Thermal Stability of Ph-Dependent Hydrogels of N-Acyl-L-Carnosine Amphiphiles: Effect of the Alkoxy Tail Length. *Soft Matter* **2011**, *7*, 10369−10376.
(103) Bernet, A.; Albuquerque, R. Q.; Behr, M.; Hoffmann, S. T.; Schmidt, H. W. Formation of a Supramolecular Chromophore: A Spectroscopic and Theoretical Study. *Soft Matter* **2012**, *8*, 66−69.
(104) Nanda, J.; Biswas, A.; Banerjee, A. Single Amino Acid Based Thixotropic Hydrogel Formation and Ph-Dependent Morphological Change of Gel Nanofibers. *Soft Matter* **2013**, *9*, 4198−4208.
(105) Hennink, W. E.; van Nostrum, C. F. Novel Crosslinking Methods to Design Hydrogels. *Adv. Drug Delivery Rev.* **2002**, *54*, 13−36.
(106) Winter, H. H.; Chambon, F. Analysis of Linear Viscoelasticity of a Cross-Linking Polymer at the Gel Point. *J. Rheol.* **1986**, *30*, 367−382.
(107) Malkoch, M.; Vestberg, R.; Gupta, N.; Mespouille, L.; Dubois, P.; Mason, A. F.; Hedrick, J. L.; Liao, Q.; Frank, C. W.; Kingsbury, K.; et al. Synthesis of Well-Defined Hydrogel Networks Using Click Chemistry. *Chem. Commun.* **2006**, 2774−2776.
(108) Mao, F.; Mano, N.; Heller, A. Long Tethers Binding Redox Centers to Polymer Backbones Enhance Electron Transport in Enzyme "Wiring" Hydrogels. *J. Am. Chem. Soc.* **2003**, *125*, 4951−4957.
(109) Elbert, D. L.; Pratt, A. B.; Lutolf, M. P.; Halstenberg, S.; Hubbell, J. A. Protein Delivery from Materials Formed by Self-Selective Conjugate Addition Reactions. *J. Controlled Release* **2001**, *76*, 11−25.
(110) Wathier, M.; Johnson, C. S.; Kim, T.; Grinstaff, M. W. Hydrogels Formed by Multiple Peptide Ligation Reactions to Fasten Corneal Transplants. *Bioconjugate Chem.* **2006**, *17*, 873−876.
(111) Zhao, F.; Gao, Y.; Shi, J.; Browdy, H. M.; Xu, B. Novel Anisotropic Supramolecular Hydrogel with High Stability over a Wide Ph Range. *Langmuir* **2011**, *27*, 1510−1512.
(112) Hu, X. R.; Shi, J. F.; Thomas, S. W., III Photolabile ROMP Gels Using Ortho-nitrobenzyl Functionalized Crosslinkers. *Poly. Chem.* **2015**, *6*, 4966−4971.
(113) Patel, P. R.; Kiser, R. C.; Lu, Y. Y.; Fong, E.; Ho, W. C.; Tirrell, D. A.; Grubbs, R. H. Synthesis and Cell Adhesive Properties of Linear and Cyclic Rgd Functionalized Polynorbornene Thin Films. *Biomacromolecules* **2012**, *13*, 2546−2553.
(114) Sun, Z. F.; Li, Z. Y.; He, Y. H.; Shen, R. J.; Deng, L.; Yang, M. H.; Liang, Y. Z.; Zhang, Y. Ferrocenoyl Phenylalanine: A New Strategy toward Supramolecular Hydrogels with Multistimuli Responsive Properties. *J. Am. Chem. Soc.* **2013**, *135*, 13379−13386.
(115) Cao, C. H.; Cao, M. W.; Fan, H. M.; Xia, D. H.; Xu, H.; Lu, J. R. Redox Modulated Hydrogelation of a Self-Assembling Short Peptide Amphiphile. *Chin. Sci. Bull.* **2012**, *57*, 4296−4303.
(116) Bowerman, C. J.; Nilsson, B. L. A Reductive Trigger for Peptide Self-Assembly and Hydrogelation. *J. Am. Chem. Soc.* **2010**, *132*, 9526−9527.
(117) Zhang, Y.; Zhang, B.; Kuang, Y.; Gao, Y.; Shi, J. F.; Zhang, X. X.; Xu, B. A Redox Responsive, Fluorescent Supramolecular Metallohydrogel Consists of Nanofibers with Single-Molecule Width. *J. Am. Chem. Soc.* **2013**, *135*, 5008−5011.
(118) Chen, J.; Wu, W.; McNeil, A. J. Detecting a Peroxide-Based Explosive Via Molecular Gelation. *Chem. Commun.* **2012**, *48*, 7310−7312.
(119) Rasale, D. B.; Maity, I.; Konda, M.; Das, A. K. Peptide Self-Assembly Driven by Oxo-Ester Mediated Native Chemical Ligation. *Chem. Commun.* **2013**, *49*, 4815−4817.
(120) Trost, B. M. Atom Economy - a Challenge for Organic-Synthesis - Homogeneous Catalysis Leads the Way. *Angew. Chem., Int. Ed. Engl.* **1995**, *34*, 259−281.
(121) Maiman, T. H. Stimulated Optical Radiation in Ruby. *Nature* **1960**, *187*, 493−494.
(122) Denk, W.; Strickler, J. H.; Webb, W. W. 2-Photon Laser Scanning Fluorescence Microscopy. *Science* **1990**, *248*, 73−76.
(123) Kamat, P. V. Photochemistry on Nonreactive and Reactive (Semiconductor) Surfaces. *Chem. Rev.* **1993**, *93*, 267−300.

DOI: 10.1021/acs.chemrev.5b00299
Chem. Rev. 2015, 115, 13165−13307

(124) Moszner, N.; Salz, U. New Developments of Polymeric Dental Composites. *Prog. Polym. Sci.* **2001**, *26*, 535−576.
(125) Frechet, J. M. J. The Photogeneration of Acid and Base within Polymer-Coatings - Approaches to Polymer Curing and Imaging. *Pure Appl. Chem.* **1992**, *64*, 1239−1248.
(126) Yu, P. G.; Wilson, G. S. An Independently Addressable Microbiosensor Array: What Are the Limits of Sensing Element Density? *Faraday Discuss.* **2000**, *116*, 305−317.
(127) Holtz, J. H.; Asher, S. A. Polymerized Colloidal Crystal Hydrogel Films as Intelligent Chemical Sensing Materials. *Nature* **1997**, *389*, 829−832.
(128) Jeong, B.; Bae, Y. H.; Lee, D. S.; Kim, S. W. Biodegradable Block Copolymers as Injectable Drug-Delivery Systems. *Nature* **1997**, *388*, 860−862.
(129) HillWest, J. L.; Dunn, R. C.; Hubbell, J. A. Local Release of Fibrinolytic Agents for Adhesion Prevention. *J. Surg. Res.* **1995**, *59*, 759−763.
(130) West, J. L.; Hubbell, J. A. Separation of the Arterial Wall from Blood Contact Using Hydrogel Barriers Reduces Intimal Thickening after Balloon Injury in the Rat: The Roles of Medial and Luminal Factors in Arterial Healing. *Proc. Natl. Acad. Sci. U. S. A.* **1996**, *93*, 13188−13193.
(131) Elisseeff, J.; McIntosh, W.; Anseth, K.; Riley, S.; Ragan, P.; Langer, R. Photoencapsulation of Chondrocytes in Poly(Ethylene Oxide)-Based Semi-Interpenetrating Networks. *J. Biomed. Mater. Res.* **2000**, *51*, 164−171.
(132) Revzin, A.; Tompkins, R. G.; Toner, M. Surface Engineering with Poly(Ethylene Glycol) Photolithography to Create High-Density Cell Arrays on Glass. *Langmuir* **2003**, *19*, 9855−9862.
(133) Yamamoto, H.; Kitsuki, T.; Nishida, A.; Asada, K.; Ohkawa, K. Photoresponsive Peptide and Polypeptide Systems. 13. Photoinduced Cross-Linked Gel and Biodegradation Properties of Copoly(L-Lysine) Containing Epsilon-7-Coumaryloxyacetyl-L-Lysine Residues. *Macromolecules* **1999**, *32*, 1055−1061.
(134) Haines, L. A.; Rajagopal, K.; Ozbas, B.; Salick, D. A.; Pochan, D. J.; Schneider, J. P. Light-Activated Hydrogel Formation Via the Triggered Folding and Self-Assembly of a Designed Peptide. *J. Am. Chem. Soc.* **2005**, *127*, 17025−17029.
(135) Brown, E. B.; Shear, J. B.; Adams, S. R.; Tsien, R. Y.; Webb, W. W. Photolysis of Caged Calcium in Femtoliter Volumes Using Two-Photon Excitation. *Biophys. J.* **1999**, *76*, 489−499.
(136) Kao, J. P. Y.; Harootunian, A. T.; Tsien, R. Y. Photochemically Generated Cytosolic Calcium Pulses and Their Detection by Fluo-3. *J. Biol. Chem.* **1989**, *264*, 8179−8184.
(137) Ding, Y.; Li, Y.; Qin, M.; Cao, Y.; Wang, W. Photo-Cross-Linking Approach to Engineering Small Tyrosine-Containing Peptide Hydrogels with Enhanced Mechanical Stability. *Langmuir* **2013**, *29*, 13299−13306.
(138) Bonino, C. A.; Samorezov, J. E.; Jeon, O.; Alsberg, E.; Khan, S. A. Real-Time in Situ Rheology of Alginate Hydrogel Photocrosslinking. *Soft Matter* **2011**, *7*, 11510−11517.
(139) Yang, Z.; Xu, B. Supramolecular Hydrogels Based on Biofunctional Nanofibers of Self-Assembled Small Molecules. *J. Mater. Chem.* **2007**, *17*, 2385−2393.
(140) Yang, Z.; Liang, G.; Xu, B. Enzymatic Control of the Self-Assembly of Small Molecules: A New Way to Generate Supramolecular Hydrogels. *Soft Matter* **2007**, *3*, 515−520.
(141) Hahn, M. E.; Gianneschi, N. C. Enzyme-Directed Assembly and Manipulation of Organic Nanomaterials. *Chem. Commun.* **2011**, *47*, 11814−11821.
(142) Poolman, J. M.; Boekhoven, J.; Besselink, A.; Olive, A. G. L.; van Esch, J. H.; Eelkema, R. Variable Gelation Time and Stiffness of Low-Molecular-Weight Hydrogels through Catalytic Control over Self-Assembly. *Nat. Protoc.* **2014**, *9*, 977−988.
(143) Boekhoven, J.; Poolman, J. M.; Maity, C.; Li, F.; van der Mee, L.; Minkenberg, C. B.; Mendes, E.; van Esch, J. H.; Eelkema, R. Catalytic Control over Supramolecular Gel Formation. *Nat. Chem.* **2013**, *5*, 433−437.
(144) Olive, A. G. L.; Abdullah, N. H.; Ziemecka, I.; Mendes, E.; Eelkema, R.; van Esch, J. H. Spatial and Directional Control over Self-Assembly Using Catalytic Micropatterned Surfaces. *Angew. Chem., Int. Ed.* **2014**, *53*, 4132−4136.
(145) Jin, Q.; Zhang, L.; Cao, H.; Wang, T.; Zhu, X.; Jiang, J.; Liu, M. Self-Assembly of Copper(Ii) Ion-Mediated Nanotube and Its Supramolecular Chiral Catalytic Behavior. *Langmuir* **2011**, *27*, 13847−13853.
(146) Hu, B.-H.; Messersmith, P. B. Rational Design of Transglutaminase Substrate Peptides for Rapid Enzymatic Formation of Hydrogels. *J. Am. Chem. Soc.* **2003**, *125*, 14298−14299.
(147) Gao, J.; Zheng, W.; Kong, D.; Yang, Z. Dual Enzymes Regulate the Molecular Self-Assembly of Tetra-Peptide Derivatives. *Soft Matter* **2011**, *7*, 10443−10448.
(148) Thornton, K.; Smith, A. M.; Merry, C. L. R.; Ulijn, R. V. Controlling Stiffness in Nanostructured Hydrogels Produced by Enzymatic Dephosphorylation. *Biochem. Soc. Trans.* **2009**, *37*, 660−664.
(149) Wang, W.; Qian, J.; Tang, A.; An, L.; Zhong, K.; Liang, G. Using Magnetic Resonance Imaging to Study Enzymatic Hydrogelation. *Anal. Chem.* **2014**, *86*, 5955−5961.
(150) Li, J.; Gao, Y.; Kuang, Y.; Shi, J.; Du, X.; Zhou, J.; Wang, H.; Yang, Z.; Xu, B. Dephosphorylation of D-Peptide Derivatives to Form Biofunctional, Supramolecular Nanofibers/Hydrogels and Their Potential Applications for Intracellular Imaging and Intratumoral Chemotherapy. *J. Am. Chem. Soc.* **2013**, *135*, 9907−9914.
(151) Li, J.; Kuang, Y.; Shi, J.; Gao, Y.; Zhou, J.; Xu, B. The Conjugation of Nonsteroidal Anti-Inflammatory Drugs (Nsaid) to Small Peptides for Generating Multifunctional Supramolecular Nanofibers/Hydrogels. *Beilstein J. Org. Chem.* **2013**, *9*, 908−917.
(152) Zhou, J.; Du, X.; Gao, Y.; Shi, J.; Xu, B. Aromatic-Aromatic Interactions Enhance Interfiber Contacts for Enzymatic Formation of a Spontaneously Aligned Supramolecular Hydrogel. *J. Am. Chem. Soc.* **2014**, *136*, 2970−2973.
(153) Yang, Z. M.; Gu, H. W.; Fu, D. G.; Gao, P.; Lam, J. K.; Xu, B. Enzymatic Formation of Supramolecular Hydrogels. *Adv. Mater.* **2004**, *16*, 1440−1444.
(154) Wang, Q. G.; Yang, Z. M.; Gao, Y.; Ge, W. W.; Wang, L.; Xu, B. Enzymatic Hydrogelation to Immobilize an Enzyme for High Activity and Stability. *Soft Matter* **2008**, *4*, 550−553.
(155) Gao, Y.; Kuang, Y.; Guo, Z. F.; Guo, Z. H.; Krauss, I. J.; Xu, B. Enzyme-Instructed Molecular Self-Assembly Confers Nanofibers and a Supramolecular Hydrogel of Taxol Derivative. *J. Am. Chem. Soc.* **2009**, *131*, 13576−13577.
(156) Gao, Y.; Shi, J. F.; Yuan, D.; Xu, B. Imaging Enzyme-Triggered Self-Assembly of Small Molecules inside Live Cells. *Nat. Commun.* **2012**, *3*, 1033.
(157) Gao, J.; Wang, H. M.; Wang, L.; Wang, J. Y.; Kong, D. L.; Yang, Z. M. Enzyme Promotes the Hydrogelation from a Hydrophobic Small Molecule. *J. Am. Chem. Soc.* **2009**, *131*, 11286−11287.
(158) Yang, Z. M.; Xu, B. A Simple Visual Assay Based on Small Molecule Hydrogels for Detecting Inhibitors of Enzymes. *Chem. Commun.* **2004**, 2424−2425.
(159) Yang, Z. M.; Ho, P. L.; Liang, G. L.; Chow, K. H.; Wang, Q. G.; Cao, Y.; Guo, Z. H.; Xu, B. Using Beta-Lactamase to Trigger Supramolecular Hydrogelation. *J. Am. Chem. Soc.* **2007**, *129*, 266−267.
(160) Das, A. K.; Collins, R.; Ulijn, R. V. Exploiting Enzymatic (Reversed) Hydrolysis in Directed Self-Assembly of Peptide Nanostructures. *Small* **2008**, *4*, 279−287.
(161) Williams, R. J.; Gardiner, J.; Sorensen, A. B.; Marchesan, S.; Mulder, R. J.; McLean, K. M.; Hartley, P. G. Monitoring the Early Stage Self-Assembly of Enzyme-Assisted Peptide Hydrogels. *Aust. J. Chem.* **2013**, *66*, 572−578.
(162) Toledano, S.; Williams, R. J.; Jayawarna, V.; Ulijn, R. V. Enzyme-Triggered Self-Assembly of Peptide Hydrogels Via Reversed Hydrolysis. *J. Am. Chem. Soc.* **2006**, *128*, 1070−1071.
(163) Guilbaud, J. B.; Vey, E.; Boothroyd, S.; Smith, A. M.; Ulijn, R. V.; Saiani, A.; Miller, A. F. Enzymatic Catalyzed Synthesis and

DOI: 10.1021/acs.chemrev.5b00299
Chem. Rev. 2015, 115, 13165−13307

Triggered Gelation of Ionic Peptides. *Langmuir* **2010**, *26*, 11297−11303.
(164) Yang, Z.; Ma, M.; Xu, B. Using Matrix Metalloprotease-9 (Mmp-9) to Trigger Supramolecular Hydrogelation. *Soft Matter* **2009**, *5*, 2546−2548.
(165) Bremmer, S. C.; McNeil, A. J.; Soellner, M. B. Enzyme-Triggered Gelation: Targeting Proteases with Internal Cleavage Sites. *Chem. Commun.* **2014**, *50*, 1691−1693.
(166) Qin, X.; Xie, W.; Tian, S.; Cai, J.; Yuan, H.; Yu, Z.; Butterfoss, G. L.; Khuong, A. C.; Gross, R. A. Enzyme-Triggered Hydrogelation Via Self-Assembly of Alternating Peptides. *Chem. Commun.* **2013**, *49*, 4839−4841.
(167) Bremmer, S. C.; Chen, J.; McNeil, A. J.; Soellner, M. B. A General Method for Detecting Protease Activity Via Gelation and Its Application to Artificial Clotting. *Chem. Commun. (Cambridge, U. K.)* **2012**, *48*, 5482−5484.
(168) Zhao, F.; Weitzel, C. S.; Gao, Y.; Browdy, H. M.; Shi, J. F.; Lin, H. C.; Lovett, S. T.; Xu, B. Beta-Galactosidase-Instructed Formation of Molecular Nanofibers and a Hydrogel. *Nanoscale* **2011**, *3*, 2859−2861.
(169) Chronopoulou, L.; Lorenzoni, S.; Masci, G.; Dentini, M.; Togna, A. R.; Togna, G.; Bordi, F.; Palocci, C. Lipase-Supported Synthesis of Peptidic Hydrogels. *Soft Matter* **2010**, *6*, 2525−2532.
(170) Song, F.; Zhang, L.-M. Enzyme-Catalyzed Formation and Structure Characteristics of a Protein- Based Hydrogel. *J. Phys. Chem. B* **2008**, *112*, 13749−13755.
(171) Guilbaud, J.-B.; Vey, E.; Boothroyd, S.; Smith, A. M.; Ulijn, R. V.; Saiani, A.; Miller, A. F. Enzymatic Catalyzed Synthesis and Triggered Gelation of Ionic Peptides. *Langmuir* **2010**, *26*, 11297−11303.
(172) Liu, Y.; Javvaji, V.; Raghavan, S. R.; Bentley, W. E.; Payne, G. F. Glucose Oxidase-Mediated Gelation: A Simple Test to Detect Glucose in Food Products. *J. Agric. Food Chem.* **2012**, *60*, 8963−8967.
(173) Sakai, S.; Komatani, K.; Taya, M. Glucose-Triggered Co-Enzymatic Hydrogelation of Aqueous Polymer Solutions. *RSC Adv.* **2012**, *2*, 1502−1507.
(174) Ogushi, Y.; Sakai, S.; Kawakami, K. Synthesis of Enzymatically-Gellable Carboxymethylcellulose for Biomedical Applications. *J. Biosci. Bioeng.* **2007**, *104*, 30−33.
(175) Sakai, S.; Ogushi, Y.; Kawakami, K. Enzymatically Crosslinked Carboxymethylcellulose-Tyramine Conjugate Hydrogel: Cellular Adhesiveness and Feasibility for Cell Sheet Technology. *Acta Biomater.* **2009**, *5*, 554−559.
(176) Choi, Y. C.; Choi, J. S.; Jung, Y. J.; Cho, Y. W. Human Gelatin Tissue-Adhesive Hydrogels Prepared by Enzyme-Mediated Biosynthesis of Dopa and Fe3+ Ion Crosslinking. *J. Mater. Chem. B* **2014**, *2*, 201−209.
(177) Lodish, H.; Berk, A.; Kaiser, C.; Krieger, M.; Bretscher, A.; Ploegh, H.; Amon, A.; Scott, M. *Molecular Cell Biology*, 7th ed.; W. H. Freeman: New York, 2013.
(178) Chung, Y. I.; Lee, S. Y.; Tae, G. The Effect of Heparin on the Gellation of Pluronic F-127 Hydrogel. *Colloids Surf., A* **2006**, *284-285*, 480−484.
(179) Kurisawa, M.; Chung, J. E.; Yang, Y. Y.; Gao, S. J.; Uyama, H. Injectable Biodegradable Hydrogels Composed of Hyaluronic Acid-Tyramine Conjugates for Drug Delivery and Tissue Engineering. *Chem. Commun.* **2005**, *94*, 4312−4314.
(180) Wang, S. F.; Chen, T.; Zhang, Z. L.; Shen, X. C.; Lu, Z. X.; Pang, D. W.; Wong, K. Y. Direct Electrochemistry and Electrocatalysis of Heme Proteins Entrapped in Agarose Hydrogel Films in Room-Temperature Ionic Liquids. *Langmuir* **2005**, *21*, 9260−9266.
(181) Yokoi, H.; Kinoshita, T.; Zhang, S. G. Dynamic Reassembly of Peptide Rada16 Nanofiber Scaffold. *Proc. Natl. Acad. Sci. U. S. A.* **2005**, *102*, 8414−8419.
(182) Stirling, J.; Lekkas, I.; Sweetman, A.; Djuranovic, P.; Guo, Q.; Pauw, B.; Granwehr, J.; Levy, R.; Moriarty, P. Critical Assessment of the Evidence for Striped Nanoparticles. *PLoS One* **2014**, *9*, e108482.
(183) Willcox, P. J.; Howie, D. W.; Schmidt-Rohr, K.; Hoagland, D. A.; Gido, S. P.; Pudjijanto, S.; Kleiner, L. W.; Venkatraman, S. Microstructure of Poly(Vinyl Alcohol) Hydrogels Produced by Freeze/Thaw Cycling. *J. Polym. Sci., Part B: Polym. Phys.* **1999**, *37*, 3438−3454.
(184) Chen, J.; Park, H.; Park, K. Synthesis of Superporous Hydrogels: Hydrogels with Fast Swelling and Superabsorbent Properties. *J. Biomed. Mater. Res.* **1999**, *44*, 53−62.
(185) Erni, R.; Rossell, M. D.; Kisielowski, C.; Dahmen, U. Atomic-Resolution Imaging with a Sub-50-Pm Electron Probe. *Phys. Rev. Lett.* **2009**, *102*, 1−4.
(186) Kuehlbrandt, W. Cryo-Em Enters a New Era. *eLife* **2014**, *3*, e03678.
(187) Krysmann, M. J.; Castelletto, V.; Kelarakis, A.; Hamley, I. W.; Hule, R. A.; Pochan, D. J. Self-Assembly and Hydrogelation of an Amyloid Peptide Fragment. *Biochemistry* **2008**, *47*, 4597−4605.
(188) Schneider, J. P.; Pochan, D. J.; Ozbas, B.; Rajagopal, K.; Pakstis, L.; Kretsinger, J. Responsive Hydrogels from the Intramolecular Folding and Self-Assembly of a Designed Peptide. *J. Am. Chem. Soc.* **2002**, *124*, 15030−15037.
(189) Egelman, E. H.; Xu, C.; DiMaio, F.; Magnotti, E.; Modlin, C.; Yu, X.; Wright, E.; Baker, D.; Conticello, V. P. Structural Plasticity of Helical Nanotubes Based on Coiled-Coil Assemblies. *Structure* **2015**, *23*, 280−289.
(190) Zhou, J.; Du, X. W.; Xu, B. Prion-Like Nanofibrils of Small Molecules (Prism): A New Frontier at the Intersection of Supramolecular Chemistry and Cell Biology. *Prion* **2015**, *9*, 110−118.
(191) Gibson, P.; Schreuder-Gibson, H.; Rivin, D. Transport Properties of Porous Membranes Based on Electrospun Nanofibers. *Colloids Surf., A* **2001**, *187-188*, 469−481.
(192) Xia, Y. Q.; Guo, T. Y.; Song, M. D.; Zhang, B. H.; Zhang, B. L. Hemoglobin Recognition by Imprinting in Semi-Interpenetrating Polymer Network Hydrogel Based on Polyacrylamide and Chitosan. *Biomacromolecules* **2005**, *6*, 2601−2606.
(193) Nowak, A. P.; Breedveld, V.; Pakstis, L.; Ozbas, B.; Pine, D. J.; Pochan, D.; Deming, T. J. Rapidly Recovering Hydrogel Scaffolds from Self-Assembling Diblock Copolypeptide Amphiphiles. *Nature* **2002**, *417*, 424−428.
(194) Siepmann, J.; Peppas, N. A. Modeling of Drug Release from Delivery Systems Based on Hydroxypropyl Methylcellulose (Hpmc). *Adv. Drug Delivery Rev.* **2001**, *48*, 139−157.
(195) Moreau, L.; Barthelemy, P.; El Maataoui, M.; Grinstaff, M. W. Supramolecular Assemblies of Nucleoside Phosphocholine Amphiphiles. *J. Am. Chem. Soc.* **2004**, *126*, 7533−7539.
(196) Anderson, K. M.; Day, G. M.; Paterson, M. J.; Byrne, P.; Clarke, N.; Steed, J. W. Structure Calculation of an Elastic Hydrogel from Sonication of Rigid Small Molecule Components. *Angew. Chem., Int. Ed.* **2008**, *47*, 1058−1062.
(197) Roy, S.; Banerjee, A. Amino Acid Based Smart Hydrogel: Formation, Characterization and Fluorescence Properties of Silver Nanoclusters within the Hydrogel Matrix. *Soft Matter* **2011**, *7*, 5300−5308.
(198) Iton, L. E.; Trouw, F.; Brun, T. O.; Epperson, J. E.; White, J. W.; Henderson, S. J. Small-Angle Neutron-Scattering Studies of the Template-Mediated Crystallization of Zsm-5-Type Zeolite. *Langmuir* **1992**, *8*, 1045−1048.
(199) Meister, A.; Bastrop, M.; Koschoreck, S.; Garamus, V. M.; Sinemus, T.; Hempel, G.; Drescher, S.; Dobner, B.; Richtering, W.; Huber, K.; et al. Structure-Property Relationship in Stimulus-Responsive Bolaamphiphile Hydrogels. *Langmuir* **2007**, *23*, 7715−7723.
(200) Hule, R. A.; Nagarkar, R. P.; Hammouda, B.; Schneider, J. P.; Pochan, D. J. Dependence of Self-Assembled Peptide Hydrogel Network Structure on Local Fibril Nanostructure. *Macromolecules* **2009**, *42*, 7137−7145.
(201) Verma, G.; Aswal, V. K.; Hassan, P. Ph-Responsive Self-Assembly in an Aqueous Mixture of Surfactant and Hydrophobic Amino Acid Mimic. *Soft Matter* **2009**, *5*, 2919−2927.
(202) Ryan, A. J.; Crook, C. J.; Howse, J. R.; Topham, P.; Geoghegan, M.; Martin, S. J.; Parnell, A. J.; Ruiz-Perez, L.; Jones, R. A. L. Mechanical Actuation by Responsive Polyelectrolyte Brushes and Triblock Gels. *J. Macromol. Sci., Part B: Phys.* **2005**, *B44*, 1103−1121.

DOI: 10.1021/acs.chemrev.5b00299
Chem. Rev. 2015, 115, 13165−13307

(203) Pan, K. M.; Baldwin, M.; Nguyen, J.; Gasset, M.; Serban, A.; Groth, D.; Mehlhorn, I.; Huang, Z. W.; Fletterick, R. J.; Cohen, F. E.; et al. Conversion of Alpha-Helices into Beta-Sheets Features in the Formation of the Scrapie Prion Proteins. *Proc. Natl. Acad. Sci. U. S. A.* **1993**, *90*, 10962−10966.
(204) Zhao, Y. L.; Stoddart, J. F. Azobenzene-Based Light-Responsive Hydrogel System. *Langmuir* **2009**, *25*, 8442−8446.
(205) Raeburn, J.; McDonald, T. O.; Adams, D. J. Dipeptide Hydrogelation Triggered Via Ultraviolet Light. *Chem. Commun.* **2012**, *48*, 9355−9357.
(206) Nakayama, Y.; Takatsuka, M.; Matsuda, T. Surface Hydrogelation Using Photolysis of Dithiocarbamate or Xanthate: Hydrogelation, Surface Fixation, and Bioactive Substance Immobilization. *Langmuir* **1999**, *15*, 1667−1672.
(207) Rabindranath, A. R.; Maier, A.; Schafer, M. Luminescent and Ionochromic Polyiminofluorene with Conjugated Terpyridine Substituent Groups. *Macromol. Chem. Phys.* **2009**, *210*, 659−666.
(208) Makarevic, J.; Jokic, M.; Peric, B.; Tomisic, V.; Kojic-Prodic, B.; Zinic, M. Bis(Amino Acid) Oxalyl Amides as Ambidextrous Gelators of Water and Organic Solvents: Supramolecular Gels with Temperature Dependent Assembly/Dissolution Equilibrium. *Chem. - Eur. J.* **2001**, *7*, 3328−3341.
(209) Iwaura, R.; Yoshida, K.; Masuda, M.; Ohnishi-Kameyama, M.; Yoshida, M.; Shimizu, T. Oligonucleotide-Templated Self-Assembly of Nucleotide Bolaamphiphiles: DNA-Like Nanofibers Edged by a Double-Helical Arrangement of a-T Base Pairs. *Angew. Chem., Int. Ed.* **2003**, *42*, 1009−1012.
(210) Shimizu, T.; Masuda, M. Stereochemical Effect of Even-Odd Connecting Links on Supramolecular Assemblies Made of 1-Glucosamide Bolaamphiphiles. *J. Am. Chem. Soc.* **1997**, *119*, 2812−2818.
(211) Suzuki, M.; Yumoto, M.; Kimura, M.; Shirai, H.; Hanabusa, K. A Family of Low-Molecular-Weight Hydrogelators Based on L-Lysine Derivatives with a Positively Charged Terminal Group. *Chem. - Eur. J.* **2003**, *9*, 348−354.
(212) Gao, Y.; Berciu, C.; Kuang, Y.; Shi, J.; Nicastro, D.; Xu, B. Probing Nanoscale Self-Assembly of Nonfluorescent Small Molecules inside Live Mammalian Cells. *ACS Nano* **2013**, *7*, 9055−9063.
(213) Kim, H.; Ralph, J. Solution-State 2d Nmr of Ball-Milled Plant Cell Wall Gels in Dmso-D(6)/Pyridine-D(5). *Org. Biomol. Chem.* **2010**, *8*, 576−591.
(214) Schuetz, A. K.; Vagt, T.; Huber, M.; Ovchinnikova, O. Y.; Cadalbert, R.; Wall, J.; Guentert, P.; Boeckmann, A.; Glockshuber, R.; Meier, B. H. Atomic-Resolution Three-Dimensional Structure of Amyloid Beta Fibrils Bearing the Osaka Mutation. *Angew. Chem., Int. Ed.* **2015**, *54*, 331−335.
(215) Estroff, L. A.; Leiserowitz, L.; Addadi, L.; Weiner, S.; Hamilton, A. D. Characterization of an Organic Hydrogel: A Cryo-Transmission Electron Microscopy and X-Ray Diffraction Study. *Adv. Mater.* **2003**, *15*, 38−42.
(216) van Esch, J.; Schoonbeek, F.; de Loos, M.; Kooijman, H.; Spek, A. L.; Kellogg, R. M.; Feringa, B. L. Cyclic Bis-Urea Compounds as Gelators for Organic Solvents. *Chem. - Eur. J.* **1999**, *5*, 937−950.
(217) Schoonbeek, F. S.; van Esch, J. H.; Hulst, R.; Kellogg, R. M.; Feringa, B. L. Geminal Bis-Ureas as Gelators for Organic Solvents: Gelation Properties and Structural Studies in Solution and in the Gel State. *Chem. - Eur. J.* **2000**, *6*, 2633−2643.
(218) vanEsch, J.; DeFeyter, S.; Kellogg, R. M.; DeSchryver, F.; Feringa, B. L. Self-Assembly of Bisurea Compounds in Organic Solvents and on Solid Substrates. *Chem. - Eur. J.* **1997**, *3*, 1238−1243.
(219) Malik, S.; Maji, S. K.; Banerjee, A.; Nandi, A. K. A Synthetic Tripeptide as Organogelator: Elucidation of Gelation Mechanism. *J. Chem. Soc. Perk. T. 2* **2002**, 1177−1186.
(220) Bhattacharya, S.; Acharya, S. N. G. Impressive Gelation in Organic Solvents by Synthetic, Low Molecular Mass, Self-Organizing Urethane Amides of L-Phenylalanine. *Chem. Mater.* **1999**, *11*, 3121−3132.
(221) Mikami, M.; Matsuzaki, T.; Masuda, M.; Shimizu, T.; Tanabe, K. Molecular Dynamics Simulation for the Crystal Structure of Synthetic Sugar-Based Bolaamphiphiles. *Comput. Mater. Sci.* **1999**, *14*, 267−276.
(222) Carr, A. J.; Melendez, R.; Geib, S. J.; Hamilton, A. D. The Design of Organic Gelators: Solution and Solid State Properties of a Family of Bis-Ureas. *Tetrahedron Lett.* **1998**, *39*, 7447−7450.
(223) Shi, C.; Huang, Z.; Kilic, S.; Xu, J.; Enick, R. M.; Beckman, E. J.; Carr, A. J.; Melendez, R. E.; Hamilton, A. D. The Gelation of Co2: A Sustainable Route to the Creation of Microcellular Materials. *Science* **1999**, *286*, 1540−1543.
(224) Wang, G. J.; Hamilton, A. D. Low Molecular Weight Organogelators for Water. *Chem. Commun.* **2003**, 310−311.
(225) Kiyonaka, S.; Shinkai, S.; Hamachi, I. Combinatorial Library of Low Molecular-Weight Organo- and Hydrogelators Based on Glycosylated Amino Acid Derivatives by Solid-Phase Synthesis. *Chem. - Eur. J.* **2003**, *9*, 976−983.
(226) Kiyonaka, S.; Sugiyasu, K.; Shinkai, S.; Hamachi, I. First Thermally Responsive Supramolecular Polymer Based on Glycosylated Amino Acid. *J. Am. Chem. Soc.* **2002**, *124*, 10954−10955.
(227) Jung, J. H.; John, G.; Masuda, M.; Yoshida, K.; Shinkai, S.; Shimizu, T. Self-Assembly of a Sugar-Based Gelator in Water: Its Remarkable Diversity in Gelation Ability and Aggregate Structure. *Langmuir* **2001**, *17*, 7229−7232.
(228) Fuhrhop, J. H.; Spiroski, D.; Boettcher, C. Molecular Monolayer Rods and Tubules Made of Alpha-(L-Lysine),Omega-(Amino) Bolaamphiphiles. *J. Am. Chem. Soc.* **1993**, *115*, 1600−1601.
(229) Suzuki, M.; Nanbu, M.; Yumoto, M.; Shirai, H.; Hanabusa, K. Novel Dumbbell-Form Low-Molecular-Weight Gelators Based on L-Lysine: Their Hydrogelation and Organogelation Properties. *New J. Chem.* **2005**, *29*, 1439−1444.
(230) Suzuki, M.; Yumoto, M.; Kimura, M.; Shirai, H.; Hanabusa, K. New Low-Molecular-Mass Gelators Based on L-Lysine: Amphiphilic Gelators and Water-Soluble Organogelators. *Helv. Chim. Acta* **2004**, *87*, 1−10.
(231) Suzuki, M.; Yumoto, M.; Kimura, M.; Shirai, H.; Hanabusa, K. Hydrogel Formation Using New L-Lysine-Based Low-Molecular-Weight Compounds with Positively Charged Pendant Chains. *Helv. Chim. Acta* **2003**, *86*, 2228−2238.
(232) Suzuki, M.; Owa, S.; Shirai, H.; Hanabusa, K. Supramolecular Hydrogel Formed by Glucoheptonamide of L-Lysine: Simple Preparation and Excellent Hydrogelation Ability. *Tetrahedron* **2007**, *63*, 7302−7308.
(233) Kunitake, T.; Okahata, Y. Totally Synthetic Bilayer Membrane. *J. Am. Chem. Soc.* **1977**, *99*, 3860−3861.
(234) Gore, T.; Dori, Y.; Talmon, Y.; Tirrell, M.; Bianco-Peled, H. Self-Assembly of Model Collagen Peptide Amphiphiles. *Langmuir* **2001**, *17*, 5352−5360.
(235) Bitton, R.; Schmidt, J.; Biesalski, M.; Tu, R.; Tirrell, M.; Bianco-Peled, H. Self-Assembly of Model DNA-Binding Peptide Amphiphiles. *Langmuir* **2005**, *21*, 11888−11895.
(236) Ulijn, R. V.; Smith, A. M. Designing Peptide Based Nanomaterials. *Chem. Soc. Rev.* **2008**, *37*, 664−675.
(237) Zhang, Y.; Yang, Z. M.; Yuan, F.; Gu, H. W.; Gao, P.; Xu, B. Molecular Recognition Remolds the Self-Assembly of Hydrogelators and Increases the Elasticity of the Hydrogel by 10(6)-Fold. *J. Am. Chem. Soc.* **2004**, *126*, 15028−15029.
(238) Zhang, Y.; Li, N.; Delgado, J.; Gao, Y.; Kuang, Y.; Fraden, S.; Epstein, I. R.; Xu, B. Post-Self-Assembly Cross-Linking of Molecular Nanofibers for Oscillatory Hydrogels. *Langmuir* **2012**, *28*, 3063−3066.
(239) Yang, Z. M.; Liang, G. L.; Xu, B. Supramolecular Hydrogels Based on Beta-Amino Acid Derivatives. *Chem. Commun.* **2006**, 738−740.
(240) Lo, M. C.; Men, H.; Branstrom, A.; Helm, J.; Yao, N.; Goldman, R.; Walker, S. A New Mechanism of Action Proposed for Ramoplanin. *J. Am. Chem. Soc.* **2000**, *122*, 3540−3541.
(241) Kumar, D. K.; Jose, D. A.; Das, A.; Dastidar, P. First Snapshot of a Nonpolymeric Hydrogelator Interacting with Its Gelling Solvents. *Chem. Commun.* **2005**, 4059−4061.

DOI: 10.1021/acs.chemrev.5b00299
Chem. Rev. 2015, 115, 13165−13307

(242) Adarsh, N. N.; Kumar, D. K.; Dastidar, P. Composites of N,N'-Bis-(Pyridyl) Urea-Dicarboxylic Acid as New Hydrogelators - a Crystal Engineering Approach. *Tetrahedron* **2007**, *63*, 7386−7396.
(243) Lloyd, G. O.; Steed, J. W. Anion Tuning of the Rheology, Morphology and Gelation of a Low Molecular Weight Salt Hydrogelator. *Soft Matter* **2011**, *7*, 75−84.
(244) Yamamichi, S.; Jinno, Y.; Haraya, N.; Oyoshi, T.; Tomitori, H.; Kashiwagi, K.; Yamanaka, M. Separation of Proteins Using Supramolecular Gel Electrophoresis. *Chem. Commun.* **2011**, *47*, 10344−10346.
(245) Yamanaka, M. Y.; Haraya, M.; Yamamichi, N. S. Chemical Stimuli-Responsive Supramolecular Hydrogel from Amphiphilic Tris-Urea. *Chem. - Asian J.* **2011**, *6*, 1022−1025.
(246) Jinno, Y.; Yamanaka, M. Ionic Surfactants Induce Amphiphilic Tris(Urea) Hydrogel Formation. *Chem. - Asian J.* **2012**, *7*, 1768−1771.
(247) Rodriguez-Llansola, F.; Hermida-Merino, D.; Nieto-Ortega, B.; Ramirez, F. J.; Navarrete, J. T. L.; Casado, J.; Hamley, I. W.; Escuder, B.; Hayes, W.; Miravet, J. F. Self-Assembly Studies of a Chiral Bisurea-Based Superhydrogelator. *Chem. - Eur. J.* **2012**, *18*, 14725−14731.
(248) Wood, D. M.; Greenland, B. W.; Acton, A. L.; Rodriguez-Llansola, F.; Murray, C. A.; Cardin, C. J.; Miravet, J. F.; Escuder, B.; Hamley, I. W.; Hayes, W. Ph-Tunable Hydrogelators for Water Purification: Structural Optimisation and Evaluation. *Chem. - Eur. J.* **2012**, *18*, 2692−2699.
(249) Higashi, D.; Yoshida, M.; Yamanaka, M. Thixotropic Hydrogel Formation in Various Aqueous Solutions through Self-Assembly of an Amphiphilic Tris-Urea. *Chem. - Asian J.* **2013**, *8*, 2584−2587.
(250) Liu, K. Q.; Steed, J. W. Triggered Formation of Thixotropic Hydrogels by Balancing Competitive Supramolecular Synthons. *Soft Matter* **2013**, *9*, 11699−11705.
(251) Meazza, L.; Foster, J. A.; Fucke, K.; Metrangolo, P.; Resnati, G.; Steed, J. W. Halogen-Bonding-Triggered Supramolecular Gel Formation. *Nat. Chem.* **2012**, *5*, 42−47.
(252) Meng, S. C.; Li, W.; Yin, X. L.; Xie, J. M. A Comprehensive Theoretical Study of the Hydrogen Bonding Interactions and Microscopic Solvation Structures of a Pyridyl-Urea-Based Hydrogelator in Aqueous Solution. *Comput. Theor. Chem.* **2013**, *1006*, 76−84.
(253) Pal, A.; Dey, J. L-Cysteine-Derived Ambidextrous Gelators of Aromatic Solvents and Ethanol/Water Mixtures. *Langmuir* **2013**, *29*, 2120−2127.
(254) Baker, B. C.; Acton, A. L.; Stevens, G. C.; Hayes, W. Bis Amide-Aromatic-Ureas-Highly Effective Hydro- and Organogelator Systems. *Tetrahedron* **2014**, *70*, 8303−8311.
(255) James, S. J.; Perrin, A.; Jones, C. D.; Yufit, D. S.; Steed, J. W. Highly Interlocked Anion-Bridged Supramolecular Networks from Interrupted Imidazole-Urea Gels. *Chem. Commun.* **2014**, *50*, 12851−12854.
(256) Kleinsmann, A. J.; Weckenmann, N. M.; Nachtsheim, B. J. Phosphate-Triggered Self-Assembly of N- (Uracil-5-Yl)Methyl Urea: A Minimalistic Urea-Derived Hydrogelator. *Chem. - Eur. J.* **2014**, *20*, 9753−9761.
(257) Vemula, P. K.; John, G. Smart Amphiphiles: Hydro/Organogelators for in Situ Reduction of Gold. *Chem. Commun.* **2006**, 2218−2220.
(258) Piepenbrock, M. O. M.; Lloyd, G. O.; Clarke, N.; Steed, J. W. Gelation Is Crucially Dependent on Functional Group Orientation and May Be Tuned by Anion Binding. *Chem. Commun.* **2008**, 2644−2646.
(259) Yang, J.; Dewal, M. B.; Sobransingh, D.; Smith, M. D.; Xu, Y.; Shimizu, L. S. Examination of the Structural Features That Favor the Columnar Self-Assembly of Bis-Urea Macrocycles. *J. Org. Chem.* **2009**, *74*, 102−110.
(260) de Loos, M.; Friggeri, A.; van Esch, J.; Kellogg, R. M.; Feringa, B. L. Cyclohexane Bis-Urea Compounds for the Gelation of Water and Aqueous Solutions. *Org. Biomol. Chem.* **2005**, *3*, 1631−1639.
(261) Cao, Y.; Tang, L. M. Influence of Ultrasound Treatment on Assembling Structures and Properties of Supramolecular Hydrogels. *Acta Polym. Sin.* **2008**, *8*, 925−928.
(262) Das, U. K.; Dastidar, P. Supramolecular Chirality in Organo-, Hydro-, and Metallogels Derived from Bis-Amides of L-(+)-Tartaric Acid: Formation of Highly Aligned 1d Silica Fibers and Evidence of 5-C Net Sns Topology in a Metallogel Network. *Chem. - Eur. J.* **2012**, *18*, 13079−13090.
(263) Basak, S.; Nandi, N.; Banerjee, A. Selective Binding of Hydrogen Chloride and Its Trapping through Supramolecular Gelation. *Chem. Commun.* **2014**, *50*, 6917−6919.
(264) Wu, J. W.; Tang, L. M.; Chen, K.; Li, F.; Yan, L.; Wang, Y. J. Preparation of a Hydrogen Bonded Supramolecular Hydrogels with Two Dimensional Aggregate Structure. *Acta Polym. Sin.* **2007**, *4*, 397−400.
(265) Sambri, L.; Cucinotta, F.; De Paoli, G.; Stagni, S.; De Cola, L. Ultrasound-Promoted Hydrogelation of Terpyridine Derivatives. *New J. Chem.* **2010**, *34*, 2093−2096.
(266) Bhowmik, S.; Ghosh, B. N.; Rissanen, K. Transition Metal Ion Induced Hydrogelation by Amino-Terpyridine Ligands. *Org. Biomol. Chem.* **2014**, *12*, 8836−8839.
(267) Chen, J.; Kampf, J. W.; McNeil, A. J. Comparing Molecular Gelators and Nongelators Based on Solubilities and Solid-State Interactions. *Langmuir* **2010**, *26*, 13076−13080.
(268) Zurcher, D. M.; Adhia, Y. J.; Romero, J. D.; McNeil, A. J. Modifying a Known Gelator Scaffold for Nitrite Detection. *Chem. Commun.* **2014**, *50*, 7813−7816.
(269) Hong, Y.; Lam, J. W. Y.; Tang, B. Z. Aggregation-Induced Emission. *Chem. Soc. Rev.* **2011**, *40*, 5361−5388.
(270) Luo, J. D.; Xie, Z. L.; Lam, J. W. Y.; Cheng, L.; Chen, H. Y.; Qiu, C. F.; Kwok, H. S.; Zhan, X. W.; Liu, Y. Q.; Zhu, D. B.; et al. Aggregation-Induced Emission of 1-Methyl-1,2,3,4,5-Pentaphenylsilole. *Chem. Commun.* **2001**, 1740−1741.
(271) Kreps, S. I.; Druin, M.; Czorny, B. Fluorescence Analysis for Traces of Naphthacene in Anthracene. *Anal. Chem.* **1965**, *37*, 586−588.
(272) Vodinh, T.; White, D. A. Sensitized Fluorescence Spectrometry Using Solid Organic Substrate. *Anal. Chem.* **1986**, *58*, 1128−1133.
(273) Larison, K. D.; Bremiller, R.; Wells, K. S.; Clements, I.; Haugland, R. P. Use of a New Fluorogenic Phosphatase Substrate in Immunohistochemical Applications. *J. Histochem. Cytochem.* **1995**, *43*, 77−83.
(274) Bhattacharya, S.; Samanta, S. K. Unusual Salt-Induced Color Modulation through Aggregation-Induced Emission Switching of a Bis-Cationic Phenylenedivinylene-Based Pi Hydrogelator. *Chem. - Eur. J.* **2012**, *18*, 16632−16641.
(275) Samanta, S. K.; Bhattacharya, S. Aggregation Induced Emission Switching and Electrical Properties of Chain Length Dependent Pi-Gels Derived from Phenylenedivinylene Bis-Pyridinium Salts in Alcohol-Water Mixtures. *J. Mater. Chem.* **2012**, *22*, 25277−25287.
(276) Bernet, A.; Behr, M.; Schmidt, H. W. Supramolecular Nanotube-Based Fiber Mats by Self-Assembly of a Tailored Amphiphilic Low Molecular Weight Hydrogelator. *Soft Matter* **2011**, *7*, 1058−1065.
(277) Maeda, N.; Masuda, K.; Li, J.; Kabashima, S.; Yoshikawa, I.; Araki, K. Low-Molecular-Mass Gelators: Gelation of Aqueous, Organic, and Aqueous/Organic Biphasic Solutions by Hydrogen Bond-Directed 2-D Amphiphilic Sheet Assemblies. *Soft Matter* **2010**, *6*, 5305−5307.
(278) Kabashima, S.; Kageyama, M.; Okano, T.; Yoshikawa, I.; Araki, K. Amphiphilic Sulfamide as a Low-Molecular-Mass Hydrogelator: A Novel Mode of 3-D Networks Formed by Hydrogen-Bond-Directed 2-D Sheet Assemblies. *J. Colloid Interface Sci.* **2013**, *408*, 107−112.
(279) Ramakanth, I.; Ramesh, N.; Patnaik, A. Fibrous Gels of Cetylpyridinium Chloride in Binary Solvent Mixtures: Structural Characteristics and Phase Behaviour. *J. Mater. Chem.* **2012**, *22*, 17842−17847.
(280) Ramakanth, I.; Patnaik, A. Novel Two-Component Gels of Cetylpyridinium Chloride and the Bola-Amphiphile 6-Amino Caproic Acid: Phase Evolution and Mechanism of Gel Formation. *J. Phys. Chem. B* **2012**, *116*, 2722−2729.

DOI: 10.1021/acs.chemrev.5b00299
Chem. Rev. 2015, 115, 13165−13307

(281) Alanne, A. L.; Lahtinen, M.; Lofman, M.; Turhanen, P.; Kolehmainen, E.; Vepsalainen, J.; Sievanen, E. First Bisphosphonate Hydrogelators: Potential Composers of Biocompatible Gels. *J. Mater. Chem. B* **2013**, *1*, 6201−6212.
(282) Wang, L.; Zhang, M.; Yang, Z.; Xu, B. The First Pamidronate Containing Polymer and Copolymer. *Chem. Commun.* **2006**, 2795−2797.
(283) Yang, Z. M.; Xu, K. M.; Wang, L.; Gu, H. W.; Wei, H.; Zhang, M. J.; Xu, B. Self-Assembly of Small Molecules Affords Multifunctional Supramolecular Hydrogels for Topically Treating Simulated Uranium Wounds. *Chem. Commun.* **2005**, 4414−4416.
(284) Xu, K. M.; Ge, W. W.; Liang, G. L.; Wang, L.; Yang, Z. M.; Wang, Q. G.; Hsing, I. M.; Xu, B. Bisphosphonate-Containing Supramolecular Hydrogels for Topical Decorporation of Uranium-Contaminated Wounds in Mice. *Int. J. Radiat. Biol.* **2008**, *84*, 353−362.
(285) Gaspar, L. J. M.; Baskar, G. Hydrogelation Characteristics of Amphiphilic N-Octadecyl Maleamic Acid Derivative. *J. Mater. Chem.* **2005**, *15*, 5144−5150.
(286) Bieser, A. M.; Tiller, J. C. Surface-Induced Hydrogelation. *Chem. Commun.* **2005**, 3942−3944.
(287) Tiller, J. C. Increasing the Local Concentration of Drugs by Hydrogel Formation. *Angew. Chem., Int. Ed.* **2003**, *42*, 3072−3075.
(288) Kuang, Y.; Shi, J.; Li, J.; Yuan, D.; Alberti, K. A.; Xu, Q.; Xu, B. Pericellular Hydrogel/Nanonets Inhibit Cancer Cells. *Angew. Chem., Int. Ed.* **2014**, *53*, 8104−8107.
(289) Bieser, A. M.; Tiller, J. C. Structure and Properties of an Exceptional Low Molecular Weight Hydrogelator. *J. Phys. Chem. B* **2007**, *111*, 13180−13187.
(290) Morita, C.; Kawai, C.; Kikuchi, A.; Imura, Y.; Kawai, T. Effect of Amide Moieties for Hydrogelators on Gelation Property and Heating-Free Ph Responsive Gel-Sol Phase Transition. *J. Oleo Sci.* **2012**, *61*, 707−713.
(291) Yuan, C.; Guo, J.; Tan, M.; Guo, M.; Qiu, L.; Yan, F. Multistimuli Responsive and Electroactive Supramolecular Gels Based on Ionic Liquid Gemini Guest. *ACS Macro Lett.* **2014**, *3*, 271−275.
(292) Peng, L.; Zhang, H.; Feng, A.; Huo, M.; Wang, Z.; Hu, J.; Gao, W.; Yuan, J. Electrochemical Redox Responsive Supramolecular Self-Healing Hydrogels Based on Host−Guest Interaction. *Polym. Chem.* **2015**, *6*, 3652−3659.
(293) Wang, H.; He, L.; Brycki, B. E.; Kowalczyk, I. H.; Kuliszewska, E.; Yang, Y. J. Electrochemical Characterization of the Hydrophobic Microenvironment within Gemini Surfactant Micellar-Hybridized Supramolecular Gels. *Electrochim. Acta* **2013**, *90*, 326−331.
(294) Li, W.; Kim, Y.; Li, J. F.; Lee, M. Dynamic Self-Assembly of Coordination Polymers in Aqueous Solution. *Soft Matter* **2014**, *10*, 5231−5242.
(295) Moon, K. S.; Kim, H. J.; Lee, E.; Lee, M. Self-Assembly of T-Shaped Aromatic Amphiphiles into Stimulus-Responsive Nanofibers. *Angew. Chem., Int. Ed.* **2007**, *46*, 6807−6810.
(296) Wang, D.; Hao, J. C. Multiple-Stimulus-Responsive Hydrogels of Cationic Surfactants and Azoic Salt Mixtures. *Colloid Polym. Sci.* **2013**, *291*, 2935−2946.
(297) Martin, S. M.; Ward, M. D. Lyotropic Phases Reinforced by Hydrogen Bonding. *Langmuir* **2005**, *21*, 5324−5331.
(298) Lin, Y. Y.; Qiao, Y.; Yan, Y.; Huang, J. B. Thermo-Responsive Viscoelastic Wormlike Micelle to Elastic Hydrogel Transition in Dual-Component Systems. *Soft Matter* **2009**, *5*, 3047−3053.
(299) Graebner, D.; Zhai, L.; Talmon, Y.; Schmidt, J.; Freiberger, N.; Glatter, O.; Herzog, B.; Hoffmann, H. Phase Behavior of Aqueous Mixtures of 2-Phenylbenzimidazole-5-Sulfonic Acid and Cetyltrimethylammonium Bromide: Hydrogels, Vesicles, Tubules, and Ribbons. *J. Phys. Chem. B* **2008**, *112*, 2901−2908.
(300) Sun, S. J.; Song, J.; Shan, Z. Q.; Feng, R. X. Electrochemical Properties of a Low Molecular Weight Gel Electrolyte for Supercapacitor. *J. Electroanal. Chem.* **2012**, *676*, 1−5.
(301) Fan, K. Q.; Song, J.; Li, J. J.; Guan, X. D.; Tao, N. M.; Tong, C. Q.; Shen, H. H.; Niu, L. B. Copper(Ii)-Responsive Gel-Sol Phase Transition in Supramolecular Gel Systems of Salen-Appended Sorbitol. *J. Mater. Chem. C* **2013**, *1*, 7479−7482.
(302) Li, J. J.; Fan, K. Q.; Niu, L. B.; Li, Y. C.; Song, J. Effects of Salt on the Gelation Mechanism of a D-Sorbitol-Based Hydrogelator. *J. Phys. Chem. B* **2013**, *117*, 5989−5995.
(303) Griffiths, P. C.; Knight, D. W.; Morgan, I. R.; Ford, A.; Brown, J.; Davies, B.; Heenan, R. K.; King, S. M.; Dalgliesh, R. M.; Tomkinson, J.; et al. Gelation or Molecular Recognition; Is the Bis-(Alpha,Beta-Dihydroxy Ester)S Motif an Omnigelator? *Beilstein J. Org. Chem.* **2010**, *6*, 1079−1088.
(304) Ohsedo, Y.; Oono, M.; Saruhashi, K.; Watanabe, H. Onset of Mixing-Induced Thixotropy in Hydrogels by Mixing Two Homologues of Low-Molecular-Weight Hydrogelators. *RSC Adv.* **2014**, *4*, 43560−43563.
(305) Ohsedo, Y.; Oono, M.; Saruhashi, K.; Watanabe, H. N-Alkylamido-D-Glucamine-Based Gelators for the Generation of Thixotropic Gels. *RSC Adv.* **2014**, *4*, 48554−48558.
(306) Okesola, B. O.; Smith, D. K. Versatile Supramolecular Ph-Tolerant Hydrogels Which Demonstrate Ph-Dependent Selective Adsorption of Dyes from Aqueous Solution. *Chem. Commun.* **2013**, *49*, 11164−11166.
(307) Patil, S. P.; Jeong, H. S.; Kim, B. H. A Low-Molecular-Weight Supramolecular Hydrogel of Riboflavin Bolaamphiphile for Vegf-Sirna Delivery. *Chem. Commun.* **2012**, *48*, 8901−8903.
(308) Sun, J.; Yu, K. H.; Russo, P. S.; Pople, J.; Henry, A.; Lyles, B.; McCarley, R. S.; Baker, G. R.; Newkome, G. R. In *Polymeric Nanofibers*; Reneker, D. H., Fong, H., Eds.; ACS Symposium Series, Vol. *918*; American Chemical Society: Washington, DC, 2006.
(309) Deng, W.; Yamaguchi, H.; Takashima, Y.; Harada, A. A Chemical-Responsive Supramolecular Hydrogel from Modified Cycloclextrins. *Angew. Chem., Int. Ed.* **2007**, *46*, 5144−5147.
(310) Taira, T.; Suzaki, Y.; Osakada, K. Thermosensitive Hydrogels Composed of Cyclodextrin Pseudorotaxanes. Role of [3]-Pseudorotaxane in the Gel Formation. *Chem. Commun.* **2009**, 7027−7029.
(311) Shi, N.; Yin, G.; Han, M.; Xu, Z. Anions Bonded on the Supramolecular Hydrogel Surface as the Growth Center of Biominerals. *Colloids Surf., B* **2008**, *66*, 84−89.
(312) Kumar, D. K.; Jose, D. A.; Dastidar, P.; Das, A. Nonpolymeric Hydrogelators Derived from Trimesic Amides. *Chem. Mater.* **2004**, *16*, 2332−2335.
(313) Shi, N.; Dong, H.; Yin, G.; Xu, Z.; Li, S. H. A Smart Supramolecular Hydrogel Exhibiting Ph-Modulated Viscoelastic Properties. *Adv. Funct. Mater.* **2007**, *17*, 1837−1843.
(314) Shi, N. E.; Yin, G.; Li, H. B.; Han, M.; Xu, Z. Uncommon Hexagonal Microtubule Based Gel from a Simple Trimesic Amide. *New J. Chem.* **2008**, *32*, 2011−2015.
(315) Leenders, C. M. A.; Mes, T.; Baker, M. B.; Koenigs, M. M. E.; Besenius, P.; Palmans, A. R. A.; Meijer, E. W. From Supramolecular Polymers to Hydrogel Materials. *Mater. Horiz.* **2014**, *1*, 116−120.
(316) Howe, R. C. T.; Smalley, A. P.; Guttenplan, A. P. M.; Doggett, M. W. R.; Eddleston, M. D.; Tan, J. C.; Lloyd, G. O. A Family of Simple Benzene 1,3,5-Tricarboxamide (Bta) Aromatic Carboxylic Acid Hydrogels. *Chem. Commun.* **2013**, *49*, 4268−4270.
(317) Nagarajan, V.; Pedireddi, V. R. Gelation and Structural Transformation Study of Some 1,3,5-Benzenetricarboxamide Derivatives. *Cryst. Growth Des.* **2014**, *14*, 1895−1901.
(318) van Bommel, K. J. C.; van der Pol, C.; Muizebelt, I.; Friggeri, A.; Heeres, A.; Meetsma, A.; Feringa, B. L.; van Esch, J. Responsive Cyclohexane-Based Low-Molecular-Weight Hydrogelators with Modular Architecture. *Angew. Chem., Int. Ed.* **2004**, *43*, 1663−1667.
(319) Friggeri, A.; van der pol, C.; van Bommel, K. J. C.; Heeres, A.; Stuart, M. C. A.; Feringa, B. L.; van Esch, J. Cyclohexane-Based Low Molecular Weight Hydrogelators: A Chirality Investigation. *Chem. - Eur. J.* **2005**, *11*, 5353−5361.
(320) Sardone, L.; Palermo, V.; Devaux, E.; Credgington, D.; De Loos, M.; Marletta, G.; Cacialli, F.; Van Esch, J.; Samori, P. Electric-Field-Assisted Alignment of Supramolecular Fibers. *Adv. Mater.* **2006**, *18*, 1276−1280.
(321) Brizard, A.; Stuart, M.; van Bommel, K.; Friggeri, A.; de Jong, M.; van Esch, J. Preparation of Nanostructures by Orthogonal Self-

DOI: 10.1021/acs.chemrev.5b00299
Chem. Rev. 2015, 115, 13165−13307

Assembly of Hydrogelators and Surfactants. *Angew. Chem., Int. Ed.* **2008**, *47*, 2063−2066.
(322) Herzfeld, J. Crowding-Induced Organization in Cells: Spontaneous Alignment and Sorting of Filaments with Physiological Control Points. *J. Mol. Recognit.* **2004**, *17*, 376−381.
(323) Brizard, A. M.; Stuart, M. C. A.; van Esch, J. H. Self-Assembled Interpenetrating Networks by Orthogonal Self Assembly of Surfactants and Hydrogelators. *Faraday Discuss.* **2009**, *143*, 345−357.
(324) Boekhoven, J.; Brizard, A. M.; van Rijn, P.; Stuart, M. C. A.; Eelkema, R.; van Esch, J. H. Programmed Morphological Transitions of Multisegment Assemblies by Molecular Chaperone Analogues. *Angew. Chem., Int. Ed.* **2011**, *50*, 12285−12289.
(325) Maity, C.; Hendriksen, W. E.; van Esch, J. H.; Eelkema, R. Spatial Structuring of a Supramolecular Hydrogel by Using a Visible-Light Triggered Catalyst. *Angew. Chem., Int. Ed.* **2015**, *54*, 998−1001.
(326) Boekhoven, J.; Hendriksen, W. E.; Koper, G. J. M.; Eelkema, R.; van Esch, J. H. Transient Assembly of Active Materials Fueled by a Chemical Reaction. *Science* **2015**, *349*, 1075−1079.
(327) Sangeetha, N. M.; Bhat, S.; Choudhury, A. R.; Maitra, U.; Terech, P. Properties of Hydrogels Derived from Cationic Analogues of Bile Acid: Remarkably Distinct Flowing Characteristics. *J. Phys. Chem. B* **2004**, *108*, 16056−16063.
(328) Terech, P.; Sangeetha, N. M.; Deme, B.; Maitra, U. Self-Assembled Networks of Ribbons in Molecular Hydrogels of Cationic Deoxycholic Acid Analogues. *J. Phys. Chem. B* **2005**, *109*, 12270−12276.
(329) Terech, P.; Friol, S. Thixotropic Suspensions of Self-Assembled Steroid Nanotubes: Structures, Kinetics and Rheological Specificities. *Macromol. Symp.* **2006**, *241*, 95−102.
(330) Terech, P.; Friol, S.; Sangeetha, N.; Talmon, Y.; Maitra, U. Self-Assembled Nanoribbons and Nanotubes in Water: Energetic Vs Entropic Networks. *Rheol. Acta* **2006**, *45*, 435−443.
(331) Terech, P.; Dourdain, S.; Maitra, U.; Bhat, S. Structure and Rheology of Cationic Molecular Hydrogels of Quinuclidine Grafted Bile Salts. Influence of the Ionic Strength and Counter-Ion Type. *J. Phys. Chem. B* **2009**, *113*, 4619−4630.
(332) Babu, P.; Sangeetha, N. M.; Maitra, U. Supramolecular Chemistry of Bile Acid Derivatives: Formation of Gels. *Macromol. Symp.* **2006**, *241*, 60−67.
(333) Bhat, S.; Maitra, U. Low Molecular Mass Cationic Gelators Derived from Deoxycholic Acid: Remarkable Gelation of Aqueous Solvents. *Tetrahedron* **2007**, *63*, 7309−7320.
(334) Banerjee, S.; Kandanelli, R.; Bhowmik, S.; Maitra, U. Self-Organization of Multiple Components in a Steroidal Hydrogel Matrix: Design, Construction and Studies on Novel Tunable Luminescent Gels and Xerogels. *Soft Matter* **2011**, *7*, 8207−8215.
(335) Banerjee, S.; Vidya, V. M.; Savyasachi, A. J.; Maitra, U. Perfluoroalkyl Bile Esters: A New Class of Efficient Gelators of Organic and Aqueous-Organic Media. *J. Mater. Chem.* **2011**, *21*, 14693−14705.
(336) Maitra, U.; Chakrabarty, A. and Deprotonation Induced Organo/Hydrogelation: Bile Acid Derived Gelators Containing a Basic Side Chain. *Beilstein J. Org. Chem.* **2011**, *7*, 304−309.
(337) Mukhopadhyay, S.; Maitra, U.; Ira; Krishnamoorthy, G.; Schmidt, J.; Talmon, Y. Structure and Dynamics of a Molecular Hydrogel Derived from a Tripodal Cholamide. *J. Am. Chem. Soc.* **2004**, *126*, 15905−15914.
(338) Kalyanikutty, K. P.; Nikhila, M.; Maitra, U.; Rao, C. N. R. Hydrogel-Assisted Synthesis of Nanotubes and Nanorods of CdS, ZnS and CuS, Showing Some Evidence for Oriented Attachment. *Chem. Phys. Lett.* **2006**, *432*, 190−194.
(339) Soto Tellini, V. H.; Jover, A.; Meijide, F.; Vázquez Tato, J.; Galantini, L.; Pavel, N. V. Supramolecular Structures Generated by a p-Tert-Butylphenyl-Amide Derivative of Cholic Acid: From Vesicles to Molecular Tubes. *Adv. Mater.* **2007**, *19*, 1752−1756.
(340) Galantini, L.; Leggio, C.; Jover, A.; Meijide, F.; Pavel, N. V.; Tellini, V. H. S.; Tato, J. V.; Di Leonardo, R.; Ruocco, G. Kinetics of Formation of Supramolecular Tubules of a Sodium Cholate Derivative. *Soft Matter* **2009**, *5*, 3018−3025.
(341) Wang, Y.; Xin, X.; Li, W.; Jia, C.; Wang, L.; Shen, J.; Xu, G. Studies on the Gel Behavior and Luminescence Properties of Biological Surfactant Sodium Deoxycholate/Rare-Earth Salts Mixed Systems. *J. Colloid Interface Sci.* **2014**, *431*, 82−89.
(342) di Gregorio, M. C.; Pavel, N. V.; Miragaya, J.; Jover, A.; Meijide, F.; Tato, J. V.; Tellini, V. H. S.; Galantini, L. Catanionic Gels Based on Cholic Acid Derivatives. *Langmuir* **2013**, *29*, 12342−12351.
(343) Shen, J. S.; Chen, Y. L.; Huang, J. L.; Chen, J. D.; Zhao, C.; Zheng, Y. Q.; Yu, T.; Yang, Y.; Zhang, H. W. Supramolecular Hydrogels for Creating Gold and Silver Nanoparticles in Situ. *Soft Matter* **2013**, *9*, 2017−2023.
(344) Sun, X. F.; Xin, X.; Tang, N.; Guo, L. W.; Wang, L.; Xu, G. Y. Manipulation of the Gel Behavior of Biological Surfactant Sodium Deoxycholate by Amino Acids. *J. Phys. Chem. B* **2014**, *118*, 824−832.
(345) Malik, S.; Kawano, S.; Fujita, N.; Shinkai, S. Pyridine-Containing Versatile Gelators for Post-Modification of Gel Tissues toward Construction of Novel Porphyrin Nanotubes. *Tetrahedron* **2007**, *63*, 7326−7333.
(346) Ramirez-Lopez, P.; de la Torre, M. C.; Asenjo, M.; Ramirez-Castellanos, J.; Gonzalez-Calbet, J. M.; Rodriguez-Gimeno, A.; de Arellano, C. R.; Sierra, M. A. A New Family of "Clicked" Estradiol-Based Low-Molecular-Weight Gelators Having Highly Symmetry-Dependent Gelation Ability. *Chem. Commun.* **2011**, *47*, 10281−10283.
(347) Jing, P.; Yan, J. L.; Cai, X. Q.; Liu, J.; Hu, B. L.; Fang, Y. Solvent-Induced Molecular Gel Formation at Room Temperature and the Preparation of Related Gel-Emulsions. *Sci. China: Chem.* **2013**, *56*, 982−991.
(348) Xu, F. M.; Wang, H. B.; Zhao, J.; Liu, X. S.; Li, D. D.; Chen, C. J.; Ji, J. Chiral Packing of Cholesteryl Group as an Effective Strategy to Get Low Molecular Weight Supramolecular Hydrogels in the Absence of Intermolecular Hydrogen Bond. *Macromolecules* **2013**, *46*, 4235−4246.
(349) Lu, J. R.; Hu, J.; Liu, C. L.; Gao, H. X.; Ju, Y. Water-Induced Gel Formation of an Oleanlic Acid-Adenine Conjugate and the Effects of Uracil Derivative on the Gel Stability. *Soft Matter* **2012**, *8*, 9576−9580.
(350) Geiger, H. C.; Geiger, D. K.; Baldwin, C. Synthesis, Photophysical Characterization, and Gelation Studies of a Stilbene-Cholesterol Derivative - an Advanced Physical Organic Chemistry Laboratory. *J. Chem. Educ.* **2006**, *83*, 106−109.
(351) Wu, J. D.; Lu, J. R.; Hu, J.; Gao, Y. X.; Ma, Q.; Ju, Y. Self-Assembly of Sodium Glycyrrhetinate into a Hydrogel: Characterisation and Properties. *RSC Adv.* **2013**, *3*, 24906−24909.
(352) Li, X.; Wang, Y.; Yang, C.; Shi, S.; Jin, L.; Luo, Z.; Yu, J.; Zhang, Z.; Yang, Z.; Chen, H. Supramolecular Nanofibers of Triamcinolone Acetonide for Uveitis Therapy. *Nanoscale* **2014**, *6*, 14488−14494.
(353) Pal, A.; Basit, H.; Sen, S.; Aswal, V. K.; Bhattacharya, S. Structure and Properties of Two Component Hydrogels Comprising Lithocholic Acid and Organic Amines. *J. Mater. Chem.* **2009**, *19*, 4325−4334.
(354) Song, S. S.; Dong, R. H.; Wang, D.; Song, A. X.; Hao, J. C. Temperature Regulated Supramolecular Structures Via Modifying the Balance of Multiple Non-Covalent Interactions. *Soft Matter* **2013**, *9*, 4209−4218.
(355) Wang, S.; Shen, W.; Feng, Y. L.; Tian, H. A Multiple Switching Bisthienylethene and Its Photochromic Fluorescent Organogelator. *Chem. Commun.* **2006**, 1497−1499.
(356) Kohler, K.; Forster, G.; Hauser, A.; Dobner, B.; Heiser, U. F.; Ziethe, F.; Richter, W.; Steiniger, F.; Drechsler, M.; Stettin, H.; et al. Self-Assembly in a Bipolar Phosphocholine-Water System: The Formation of Nanofibers and Hydrogels. *Angew. Chem., Int. Ed.* **2004**, *43*, 245−247.
(357) Kohler, K.; Forster, G.; Hauser, A.; Dobner, B.; Heiser, U. F.; Ziethe, F.; Richter, W.; Steiniger, F.; Drechsler, M.; Stettin, H.; et al. Temperature-Dependent Behavior of a Symmetric Long-Chain Bolaamphiphile with Phosphocholine Headgroups in Water: From Hydrogel to Nanoparticles. *J. Am. Chem. Soc.* **2004**, *126*, 16804−16813.

DOI: 10.1021/acs.chemrev.5b00299
Chem. Rev. 2015, 115, 13165−13307

(358) Kohler, K.; Meister, A.; Forster, G.; Dobner, B.; Drescher, S.; Ziethe, F.; Richter, W.; Steiniger, F.; Drechsler, M.; Hause, G.; et al. Conformational and Thermal Behavior of a Ph-Sensitive Bolaform Hydrogelator. *Soft Matter* **2006**, *2*, 77−86.
(359) Meister, A.; Drescher, S.; Garamus, V. M.; Karlsson, G.; Graf, G.; Dobner, B.; Blume, A. Temperature-Dependent Self-Assembly and Mixing Behavior of Symmetrical Single-Chain Bolaamphiphiles. *Langmuir* **2008**, *24*, 6238−6246.
(360) Bastrop, M.; Meister, A.; Metz, H.; Drescher, S.; Dobner, B.; Mader, K.; Blume, A. The Motional Dynamics in Bolaamphiphilic Nanofibers and Micellar Aggregates: An Esr Spin Probe Study. *J. Phys. Chem. B* **2009**, *113*, 574−582.
(361) Meister, A.; Drescher, S.; Karlsson, G.; Hause, G.; Baumeister, U.; Hempel, G.; Garamus, V. M.; Dobner, B.; Blume, A. Formation of Square Lamellae by Self-Assembly of Long-Chain Bolaphospholipids in Water. *Soft Matter* **2010**, *6*, 1317−1324.
(362) Graf, G.; Drescher, S.; Meister, A.; Dobner, B.; Blume, A. Self-Assembled Bolaamphiphile Fibers Have Intermediate Properties between Crystalline Nanofibers and Wormlike Micelles: Formation of Viscoelastic Hydrogels Switchable by Changes in Ph and Salinity. *J. Phys. Chem. B* **2011**, *115*, 10478−10487.
(363) Blume, A.; Drescher, S.; Meister, A.; Graf, G.; Dobner, B. Tuning the Aggregation Behaviour of Single-Chain Bolaphospholipids in Aqueous Suspension: From Nanoparticles to Nanofibres to Lamellar Phases. *Faraday Discuss.* **2013**, *161*, 193−213.
(364) Graf, G.; Drescher, S.; Meister, A.; Garamus, V. M.; Dobner, B.; Blume, A. Tuning the Aggregation Behaviour of Single-Chain Bolaamphiphiles in Aqueous Suspension by Changes in Headgroup Asymmetry. *Soft Matter* **2013**, *9*, 9562−9571.
(365) Blume, A.; Drescher, S.; Graf, G.; Köhler, K.; Meister, A. Self-Assembly of Different Single-Chain Bolaphospholipids and Their Miscibility with Phospholipids or Classical Amphiphiles. *Adv. Colloid Interface Sci.* **2014**, *208*, 264−278.
(366) Drescher, S.; Meister, A.; Garamus, V. M.; Hause, G.; Garvey, C. J.; Dobner, B.; Blume, A. Phenylene Bolaamphiphiles: Influence of the Substitution Pattern on the Aggregation Behavior and the Miscibility with Classical Phospholipids. *Eur. J. Lipid Sci. Technol.* **2014**, *116*, 1205−1216.
(367) Drescher, S.; Meister, A.; Graf, G.; Hause, G.; Blume, A.; Dobner, B. General Synthesis and Aggregation Behaviour of New Single-Chain Bolaphospholipids: Variations in Chain and Headgroup Structures. *Chem. - Eur. J.* **2008**, *14*, 6796−6804.
(368) Drescher, S.; Graf, G.; Hause, G.; Dobner, B.; Meister, A. Amino-Functionalized Single-Chain Bolalipids: Synthesis and Aggregation Behavior of New Basic Building Blocks. *Biophys. Chem.* **2010**, *150*, 136−143.
(369) Shinto, K.; Hoffmann, H.; Watanabe, K.; Teshigawara, T. Hydrogels from Diacylphosphatidylcholine. *Colloid Polym. Sci.* **2012**, *290*, 91−95.
(370) Song, B.; Wei, H.; Wang, Z. Q.; Zhang, X.; Smet, M.; Dehaen, W. Supramolecular Nanoribers by Self-Organization of Bola-Amphiphiles through a Combination of Hydrogen Bonding and Pi-Pi Stacking Interactions. *Adv. Mater.* **2007**, *19*, 416−420.
(371) Wu, G. L.; Verwilst, P.; Xu, J.; Xu, H. P.; Wang, R. J.; Smet, M.; Dehaen, W.; Faul, C. F. J.; Wang, Z. Q.; Zhang, X. Bolaamphiphiles Bearing Bipyridine as Mesogenic Core: Rational Exploitation of Molecular Architectures for Controlled Self-Assembly. *Langmuir* **2012**, *28*, 5023−5030.
(372) Berchel, M.; Lemiegre, L.; Trepout, S.; Lambert, O.; Jeftic, J.; Benvegnu, T. Synthesis of Unsymmetrical Saturated or Diacetylenic Cationic Bolaamphiphiles. *Tetrahedron Lett.* **2008**, *49*, 7419−7422.
(373) Voronin, M. A.; Gabdrakhmanov, D. R.; Semenov, V. E.; Valeeva, F. G.; Mikhailov, A. S.; Nizameev, I. R.; Kadirov, M. K.; Zakharova, L. Y.; Reznik, V. S.; Konovalov, A. I. Novel Bolaamphiphilic Pyrimidinophane as Building Block for Design of Nanosized Supramolecular Systems with Concentration-Dependent Structural Behavior. *ACS Appl. Mater. Interfaces* **2011**, *3*, 402−409.
(374) Cai, F.; Shen, J. S.; Wang, J. H.; Zhang, H.; Zhao, J. S.; Zeng, E. M.; Jiang, Y. B. Hydrogelators of Cyclotriveratrylene Derivatives. *Org. Biomol. Chem.* **2012**, *10*, 1418−1423.
(375) Becker, T.; Goh, C. Y.; Jones, F.; McIldowie, M. J.; Mocerino, M.; Ogden, M. I. Proline-Functionalised Calix[4]Arene: An Anion-Triggered Hydrogelator. *Chem. Commun.* **2008**, 3900−3902.
(376) Goh, C. Y.; Becker, T.; Brown, D. H.; Skelton, B. W.; Jones, F.; Mocerino, M.; Ogden, M. I. Self-Inclusion of Proline-Functionalised Calix[4]Arene Leads to Hydrogelation. *Chem. Commun.* **2011**, *47*, 6057−6059.
(377) Verdejo, B.; Rodriguez-Llansola, F.; Escuder, B.; Miravet, J. F.; Ballester, P. Sodium and Ph Responsive Hydrogel Formation by the Supramolecular System Calix[4]Pyrrole Derivative/Tetramethylammonium Cation. *Chem. Commun.* **2011**, *47*, 2017−2019.
(378) Hwang, D.; Lee, E.; Jung, J. H.; Lee, S. S.; Park, K. M. Formation of Calix 4 Arene-Based Supramolecular Gels Triggered by K+ and Rb+: Exemplification of a Structure-Property Relationship. *Cryst. Growth Des.* **2013**, *13*, 4177−4180.
(379) Mecca, T.; Messina, G. M. L.; Marletta, G.; Cunsolo, F. Novel Ph Responsive Calix 8 Arene Hydrogelators: Self-Organization Processes at a Nanometric Scale. *Chem. Commun.* **2013**, *49*, 2530−2532.
(380) Hwang, I.; Jeon, W. S.; Kim, H. J.; Kim, D.; Kim, H.; Selvapalam, N.; Fujita, N.; Shinkai, S.; Kim, K. Cucurbit[7]Uril: A Simple Macrocyclic, Ph-Triggered Hydrogelator Exhibiting Guest-Induced Stimuli-Responsive Behavior. *Angew. Chem., Int. Ed.* **2007**, *46*, 210−213.
(381) Yang, H.; Tan, Y. B.; Wang, Y. X. Fabrication and Properties of Cucurbit[6]Uril Induced Thermo-Responsive Supramolecular Hydrogels. *Soft Matter* **2009**, *5*, 3511−3516.
(382) Kazakova, E. K.; Morozova, Y. E.; Prosvirkin, A. V.; Gubanov, E. F.; Timoshina, T. V.; Muslinkin, A. A.; Habicher, W. D.; Konovalov, A. I. Self-Association of Octaaminoamide Derivatives Calix 4 Resorcinarene in Aqueous Medium and Efficient Gelation of Aqueous Solution. *Colloid J.* **2004**, *66*, 153−159.
(383) Kazakova, E. K.; Morozova, J. E.; Prosvirkin, A. V.; Pich, A. Z.; Gubanov, E. P.; Muslinkin, A. A.; Habicher, W. D.; Konovalov, A. I. Self-Assembly of Octaaminoamido Derivatives of Resorcin[4]Arene in Water a "Cell-Like" Submicron-Scale Hydrogel Structure. *Eur. J. Org. Chem.* **2004**, *2004*, 3323−3329.
(384) Ma, X.; Wang, Q.; Qu, D.; Xu, Y.; Ji, F.; Tian, H. A Light-Driven Pseudo 4 Rotaxane Encoded by Induced Circular Dichroism in a Hydrogel. *Adv. Funct. Mater.* **2007**, *17*, 829−837.
(385) Zhu, L.; Ma, X.; Ji, F.; Wang, Q.; Tian, H. Effective Enhancement of Fluorescence Signals in Rotaxane-Doped Reversible Hydrosol-Gel Systems. *Chem. - Eur. J.* **2007**, *13*, 9216−9222.
(386) Zhang, Q.; Qu, D.-H.; Ma, X.; Tian, H. Sol-Gel Conversion Based on Photoswitching between Noncovalently and Covalently Linked Netlike Supramolecular Polymers. *Chem. Commun.* **2013**, *49*, 9800−9802.
(387) Zhang, Q.; Qu, D.-H.; Wu, J.; Ma, X.; Wang, Q.; Tian, H. A Dual-Modality Photoswitchable Supramolecular Polymer. *Langmuir* **2013**, *29*, 5345−5350.
(388) Chen, H.; Ma, X.; Wu, S.; Tian, H. A Rapidly Self-Healing Supramolecular Polymer Hydrogel with Photostimulated Room-Temperature Phosphorescence Responsiveness. *Angew. Chem., Int. Ed.* **2014**, *53*, 14149−14152.
(389) Roy, S.; Maiti, D. K.; Panigrahi, S.; Basak, D.; Banerjee, A. A New Hydrogel from an Amino Acid-Based Perylene Bisimide and Its Semiconducting, Photo-Switching Behaviour. *RSC Adv.* **2012**, *2*, 11053−11060.
(390) Sukul, P. K.; Asthana, D.; Mukhopadhyay, P.; Summa, D.; Muccioli, L.; Zannoni, C.; Beljonne, D.; Rowan, A. E.; Malik, S. Assemblies of Perylene Diimide Derivatives with Melamine into Luminescent Hydrogels. *Chem. Commun.* **2011**, *47*, 11858−11860.
(391) Roy, S.; Maiti, D. K.; Panigrahi, S.; Basak, D.; Banerjee, A. A Bolaamphiphilic Amino Acid Appended Photo-Switching Supramolecular Gel and Tuning of Photo-Switching Behaviour. *Phys. Chem. Chem. Phys.* **2014**, *16*, 6041−6049.

DOI: 10.1021/acs.chemrev.5b00299
Chem. Rev. 2015, 115, 13165−13307

(392) Datar, A.; Balakrishnan, K.; Zang, L. One-Dimensional Self-Assembly of a Water Soluble Perylene Diimide Molecule by Ph Triggered Hydrogelation. *Chem. Commun.* **2013**, *49*, 6894−6896.
(393) Weingarten, A. S.; Kazantsev, R. V.; Palmer, L. C.; McClendon, M.; Koltonow, A. R.; Samuel, A. P. S.; Kiebala, D. J.; Wasielewski, M. R.; Stupp, S. I. Self-Assembling Hydrogel Scaffolds for Photocatalytic Hydrogen Production. *Nat. Chem.* **2014**, *6*, 964−970.
(394) Rao, K. V.; George, S. J. Synthesis and Controllable Self-Assembly of a Novel Coronene Bisimide Amphiphile. *Org. Lett.* **2010**, *12*, 2656−2659.
(395) Rao, K. V.; Jayaramulu, K.; Maji, T. K.; George, S. J. Supramolecular Hydrogels and High-Aspect-Ratio Nanofibers through Charge-Transfer-Induced Alternate Coassembly. *Angew. Chem., Int. Ed.* **2010**, *49*, 4218−4222.
(396) Molla, M. R.; Ghosh, S. Hydrogen-Bonding-Mediated Vesicular Assembly of Functionalized Naphthalene-Diimide-Based Bolaamphiphile and Guest-Induced Gelation in Water. *Chem. - Eur. J.* **2012**, *18*, 9860−9869.
(397) Rao, K. V.; George, S. J. Supramolecular Alternate Co-Assembly through a Non-Covalent Amphiphilic Design: Conducting Nanotubes with a Mixed D-a Structure. *Chem. - Eur. J.* **2012**, *18*, 14286−14291.
(398) Liu, K.; Yao, Y. X.; Wang, C.; Liu, Y.; Li, Z. B.; Zhang, X. From Bola-Amphiphiles to Supra-Amphiphiles: The Transformation from Two-Dimensional Nanosheets into One-Dimensional Nanofibers with Tunable-Packing Fashion of N-Type Chromophores. *Chem. - Eur. J.* **2012**, *18*, 8622−8628.
(399) Ohsedo, Y.; Miyamoto, M.; Oono, M.; Shikii, K.; Tanaka, A. Hydrogel Formed by a Simple Squaric Acid Derivative. *RSC Adv.* **2013**, *3*, 3844−3847.
(400) Li, H. Y.; Chi, Z. G.; Zheng, B. Y.; Xu, B. J.; Li, X. F.; Zhang, X. Q.; Zhang, Y.; Xu, J. R. In Situ Water Gelation by a Hydrogelator Derived from N-(4-Carboxy Phenyl)Trimellitimide. *J. Controlled Release* **2011**, *152*, E195−E196.
(401) End, N.; Macko, L.; Zehnder, M.; Pfaltz, A. Synthesis of Chiral Bis(Dihydrooxazolylphenyl)Oxalamides, a New Class of Tetradentate Ligands for Asymmetric Catalysis. *Chem. - Eur. J.* **1998**, *4*, 818−824.
(402) Makarevic, J.; Jokic, M.; Raza, Z.; Stefanic, Z.; Kojic-Prodic, B.; Zinic, M. Chiral Bis(Amino Alcohol) Oxalamide Gelators-Gelation Properties and Supramolecular Organization: Racemate Versus Pure Enantiomer Gelation. *Chem. - Eur. J.* **2003**, *9*, 5567−5580.
(403) Makarevic, J.; Jokic, M.; Raza, Z.; Caplar, V.; Katalenic, D.; Stefanic, Z.; Kojic-Prodic, B.; Zinic, M. Chiral Bis(Tyrosinol) and Bis(P-Hydroxyphenylglycinol) Oxalamide Gelators. Influence of Aromatic Groups and Hydrogen Bonding on Gelation Properties. *Croat. Chem. Acta* **2004**, *77*, 403−414.
(404) Dou, X. Q.; Li, P.; Zhang, D.; Feng, C. L. C-2-Symmetric Benzene-Based Hydrogels with Unique Layered Structures for Controllable Organic Dye Adsorption. *Soft Matter* **2012**, *8*, 3231−3238.
(405) Mangunuru, H. P. R.; Yang, H.; Wang, G. J. Synthesis of Peptoid Based Small Molecular Gelators by a Multiple Component Reaction. *Chem. Commun.* **2013**, *49*, 4489−4491.
(406) Yamaguchi, H.; Kobayashi, Y.; Kobayashi, R.; Takashima, Y.; Hashidzume, A.; Harada, A. Photoswitchable Gel Assembly Based on Molecular Recognition. *Nat. Commun.* **2012**, *3*, 603.
(407) Velema, W. A.; Stuart, M. C. A.; Szymanski, W.; Feringa, B. L. Light-Triggered Self-Assembly of a Dichromonyl Compound in Water. *Chem. Commun.* **2013**, *49*, 5001−5003.
(408) Li, J.; Cvrtila, I.; Colomb-Delsuc, M.; Otten, E.; Otto, S. An "Ingredients" Approach to Functional Self-Synthesizing Materials: A Metal-Ion-Selective, Multi-Responsive, Self-Assembled Hydrogel. *Chem. - Eur. J.* **2014**, *20*, 15709−15714.
(409) Yang, R.; Peng, S.; Wan, W.; Hughes, T. C. Azobenzene Based Multistimuli Responsive Supramolecular Hydrogels. *J. Mater. Chem. C* **2014**, *2*, 9122−9131.
(410) Yang, D.; Liu, C.; Zhang, L.; Liu, M. Visualized Discrimination of Atp from Adp and Amp through Collapse of Supramolecular Gels. *Chem. Commun.* **2014**, *50*, 12688−12690.
(411) Wang, Y. J.; Tang, L. M.; Wang, Y. New Hydrogen-Bonded Supramolecular Hydrogels and Fibers Derived from 1,2,4,5-Benzenetetracarboxylic Acid and 4-Hydroxypyridine. *Chem. Lett.* **2006**, *35*, 548−549.
(412) Wang, Y. J.; Tang, L. M.; Yu, J. Investigation of Spontaneous Transition from Low-Molecular-Weight Hydrogel into Macroscopic Crystals. *Cryst. Growth Des.* **2008**, *8*, 884−889.
(413) Tang, L. M.; Wang, Y. J. Highly Stable Supramolecular Hydrogels Formed from 1,3,5-Benzenetricarboxylic Acid and Hydroxyl Pyridines. *Chin. Chem. Lett.* **2009**, *20*, 1259−1262.
(414) Jin, X.; Wang, Y. J.; Tang, L. M. Supramolecular Hydrogels Based on 1,2,4-Benzenetricarboxylic Acid and 4-Hydroxy Pyridine. *Acta Polym. Sin* **2010**, *010*, 462−467.
(415) Wang, Y. J.; Chen, K.; Tang, L. M. From Supramolecular Hydrogel to Macroscopic Spheres: Nucleation-Controlled Polymorphic Transition. *Chem. Lett.* **2009**, *38*, 472−473.
(416) Wang, Y. J.; Tang, L. M.; Wang, L.; Yu, J. Hydrogen-Bonded Supramolecular Hydrogels Derived from 3,3 ',4,4 '-Benzophenonetetracarboxylic Acid and Hydroxylpyridines. *Chin. J. Chem.* **2009**, *27*, 2279−2283.
(417) Kono, S.; Wang, Y. J.; Tang, L. M. Influence of Gelator Structures on Formation and Stability of Supramolecular Hydrogels. *Chin. Chem. Lett.* **2007**, *18*, 1548−1550.
(418) Cao, Y.; Tang, L. M.; Wang, Y. J.; Zhang, B. Y.; Jia, L. K. Influence of Ultrasound Treatment on Assembling Structures and Properties of Supramolecular Hydrogels Formed from 1,3,5-Benzenetricarboxylic Acid and 4-Hydroxypyridine. *Chem. Lett.* **2008**, *37*, 554−555.
(419) Wang, Y. J.; Tang, L. M.; Yu, B. The Fibrous Aggregation Structure-Property Correlation of Supramolecular Hydrogel of Pyromellitic Acid/4-Hydroxypyridine. *Acta Polym. Sin.* **2008**, *8*, 192−196.
(420) Chen, W. Y.; Yang, Y. J.; Rinadi, C.; Zhou, D.; Shen, A. Q. Formation of Supramolecular Hydrogel Microspheres Via Microfluidics. *Lab Chip* **2009**, *9*, 2947−2951.
(421) Dou, X. Q.; Li, P.; Lu, S. Q.; Tian, X. B.; Tang, Y.; Mercer-Chalmers, J. D.; Feng, C. L.; Zhang, D. Highly Directional Co-Assembly of 2,6-Pyridinedicarboxylic Acid and 4-Hydroxypyridine Based on Low Molecular Weight Gelators. *J. Mol. Liq.* **2013**, *180*, 129−134.
(422) Saha, A.; Roy, B.; Garai, A.; Nandi, A. K. Two-Component Thermoreversible Hydrogels of Melamine and Gallic Acid. *Langmuir* **2009**, *25*, 8457−8461.
(423) Manna, S.; Saha, A.; Nandi, A. K. A Two Component Thermoreversible Hydrogel of Riboflavin and Melamine: Enhancement of Photoluminescence in the Gel Form. *Chem. Commun.* **2006**, 4285−4287.
(424) Saha, A.; Manna, S.; Nandi, A. K. Hierarchical Tuning of 1-D Macro Morphology by Changing the Composition of a Binary Hydrogel and Its Influence on the Photoluminescence Property. *Chem. Commun.* **2008**, 3732−3734.
(425) Tantishaiyakul, V.; Dokmaisrijan, S.; Sangfai, T.; Hirun, N.; Li, L.; Juntarapet, S.; Suknuntha, K. Investigation of the Efficiency of Gelation of Melamine with the Positional Isomers of Aminobenzoic Acid. *Colloids Surf., A* **2014**, *446*, 118−126.
(426) Yadav, P.; Ballabh, A. Synthesis, Characterization and Nano-Particles Synthesis Using a Simple Two Component Supramolecular Gelator: A Step Towards Plausible Mechanism of Hydrogelation. *Colloids Surf., A* **2012**, *414*, 333−338.
(427) Fan, K. Q.; Niu, L. B.; Li, J. J.; Feng, R. X.; Qu, R.; Liu, T. Q.; Song, J. Application of Solubility Theory in Bi-Component Hydrogels of Melamine with Di(2-Ethylhexyl) Phosphoric Acid. *Soft Matter* **2013**, *9*, 3057−3062.
(428) Niu, L. B.; Song, J.; Li, J. J.; Tao, N. M.; Lu, M.; Fan, K. Q. Solvent Effects on the Gelation Performance of Melamine and 2-Ethylhexylphosphoric Acid Mono-2-Ethylhexyl Ester in Water-Organic Mixtures. *Soft Matter* **2013**, *9*, 7780−7786.

DOI: 10.1021/acs.chemrev.5b00299
Chem. Rev. 2015, 115, 13165−13307

(429) Shen, Z.; Wang, T.; Liu, M. Tuning the Gelation Ability of Racemic Mixture by Melamine: Enhanced Mechanical Rigidity and Tunable Nanoscale Chirality. *Langmuir* **2014**, *30*, 10772−10778.
(430) Shen, Z. C.; Wang, T. Y.; Liu, M. H. H-Bond and Pi-Pi Stacking Directed Self-Assembly of Two-Component Supramolecular Nanotubes: Tuning Length, Diameter and Wall Thickness. *Chem. Commun.* **2014**, *50*, 2096−2099.
(431) Fameau, A. L.; Houinsou-Houssou, B.; Novales, B.; Navailles, L.; Nallet, F.; Douliez, J. P. 12-Hydroxystearic Acid Lipid Tubes under Various Experimental Conditions. *J. Colloid Interface Sci.* **2010**, *341*, 38−47.
(432) Shen, J. S.; Cai, Q. G.; Jiang, Y. B.; Zhang, H. W. Anion-Triggered Melamine Based Self-Assembly and Hydrogel. *Chem. Commun.* **2010**, *46*, 6786−6788.
(433) Saha, A.; Roy, B.; Esterrani, A.; Nandi, A. K. Effect of Complementary Small Molecules on the Properties of Bicomponent Hydrogel of Riboflavin. *Org. Biomol. Chem.* **2011**, *9*, 770−776.
(434) Bairi, P.; Roy, B.; Chakraborty, P.; Nandi, A. K. Co-Assembled White-Light-Emitting Hydrogel of Melamine. *ACS Appl. Mater. Interfaces* **2013**, *5*, 5478−5485.
(435) Cafferty, B. J.; Gallego, I.; Chen, M. C.; Farley, K. I.; Eritja, R.; Hud, N. V. Efficient Self-Assembly in Water of Long Noncovalent Polymers by Nucleobase Analogues. *J. Am. Chem. Soc.* **2013**, *135*, 2447−2450.
(436) Cafferty, B. J.; Avirah, R. R.; Schuster, G. B.; Hud, N. V. Ultra-Sensitive Ph Control of Supramolecular Polymers and Hydrogels: Pk(a) Matching of Biomimetic Monomers. *Chem. Sci.* **2014**, *5*, 4681−4686.
(437) Krishnan, R.; Gopidas, K. R. Beta-Cyclodextrin as an End-to-End Connector. *J. Phys. Chem. Lett.* **2011**, *2*, 2094−2098.
(438) Kakuta, T.; Takashima, Y.; Nakahata, M.; Otsubo, M.; Yamaguchi, H.; Harada, A. Preorganized Hydrogel: Self-Healing Properties of Supramolecular Hydrogels Formed by Polymerization of Hostguest-Monomers That Contain Cyclodextrins and Hydrophobic Guest Groups. *Adv. Mater.* **2013**, *25*, 2849−2853.
(439) Li, S. Y.; Xing, P. Y.; Hou, Y. H.; Yang, J. S.; Yang, X. Z.; Wang, B.; Hao, A. Y. Formation of a Sheet-Like Hydrogel from Vesicles Via Precipitates Based on an Ionic Liquid-Based Surfactant and Beta-Cyclodextrin. *J. Mol. Liq.* **2013**, *188*, 74−80.
(440) Rizzo, C.; D'Anna, F.; Marullo, S.; Vitale, P.; Noto, R. Two-Component Hydrogels Formed by Cyclodextrins and Dicationic Imidazolium Salts. *Eur. J. Org. Chem.* **2014**, *2014*, 1013−1024.
(441) Xing, B.; Choi, M.-F.; Xu, B. Design of Coordination Polymer Gels as Stable Catalytic Systems. *Chem. - Eur. J.* **2002**, *8*, 5028−5032.
(442) Xing, B.; Choi, M.-F.; Xu, B. A Stable Metal Coordination Polymer Gel Based on a Calix[4]Arene and Its ″Uptake″ of Non-Ionic Organic Molecules from the Aqueous Phase. *Chem. Commun.* **2002**, 362−363.
(443) Tam, A. Y. Y.; Wong, K. M. C.; Yam, V. W. W. Unusual Luminescence Enhancement of Metallogels of Alkynylplatinum(Ii) 2,6-Bis(N-Alkylbenzimidazol-2 '-Yl)Pyridine Complexes Upon a Gel-to-Sol Phase Transition at Elevated Temperatures. *J. Am. Chem. Soc.* **2009**, *131*, 6253−6260.
(444) Kuroiwa, K.; Kimizuka, N. Coordination Structure Changes of Linear Cobalt(Ii) Triazole Complexes Induced by Binding of Long-Chained Alcohols: Adaptive Molecular Clefts. *Chem. Lett.* **2008**, *37*, 192−193.
(445) George, M.; Weiss, R. G. Low Molecular-Mass Gelators with Diyne Functional Groups and Their Unpolymerized and Polymerized Gel Assemblies. *Chem. Mater.* **2003**, *15*, 2879−2888.
(446) Kogiso, M.; Okada, Y.; Yase, K.; Shimizu, T. Metal-Complexed Nanofiber Formation in Water from Dicarboxylic Valylvaline Bolaamphiphiles. *J. Colloid Interface Sci.* **2004**, *273*, 394−399.
(447) Suzuki, M.; Yumoto, M.; Shirai, H.; Hanabusa, K. L-Lysine-Based Supramolecular Hydrogels Containing Various Inorganic Ions. *Org. Biomol. Chem.* **2005**, *3*, 3073−3078.
(448) Shen, J. S.; Mao, G. J.; Zhou, Y. H.; Jiang, Y. B.; Zhang, H. W. A Ligand-Chirality Controlled Supramolecular Hydrogel. *Dalton Trans.* **2010**, *39*, 7054−7058.
(449) Duan, P.; Yanai, N.; Nagatomi, H.; Kimizuka, N. Photon Upconversion in Supramolecular Gel Matrixes: Spontaneous Accumulation of Light-Harvesting Donor−Acceptor Arrays in Nanofibers and Acquired Air Stability. *J. Am. Chem. Soc.* **2015**, *137*, 1887−1894.
(450) Bhowmik, S.; Banerjee, S.; Maitra, U. A Self-Assembled, Luminescent Europium Cholate Hydrogel: A Novel Approach Towards Lanthanide Sensitization. *Chem. Commun.* **2010**, *46*, 8642−8644.
(451) Chakrabarty, A.; Maitra, U.; Das, A. D. Metal Cholate Hydrogels: Versatile Supramolecular Systems for Nanoparticle Embedded Soft Hybrid Materials. *J. Mater. Chem.* **2012**, *22*, 18268−18274.
(452) Qiao, Y.; Lin, Y. Y.; Yang, Z. Y.; Chen, H. F.; Zhang, S. F.; Yan, Y.; Huang, J. B. Unique Temperature-Dependent Supramolecular Self-Assembly: From Hierarchical 1d Nanostructures to Super Hydrogel. *J. Phys. Chem. B* **2010**, *114*, 11725−11730.
(453) Cai, L. C.; Wang, Y. J.; Li, J.; Huang, J. B. Investigation of the Mechanism of Temperature-Responsiveness of Metal-Cholate Supramolecular Hydrogels. *Acta Phys.-chim. Sin.* **2012**, *28*, 2298−2304.
(454) Huang, J. B.; Qiao, Y.; Lin, Y. Y.; Zhang, S. F. Lanthanide-Containing Photoluminescent Materials: From Hybrid Hydrogel to Inorganic Nanotubes. *Chem. - Eur. J.* **2011**, *17*, 5180−5187.
(455) da Silva, F. F.; de Menezes, F. L.; da Luz, L. L.; Alves, S. Supramolecular Luminescent Hydrogels Based on Beta-Amino Acid and Lanthanide Ions Obtained by Self-Assembled Hydrothermal Reactions. *New J. Chem.* **2014**, *38*, 893−896.
(456) Basak, S.; Nanda, J.; Banerjee, A. Multi-Stimuli Responsive Self-Healing Metallo-Hydrogels: Tuning of the Gel Recovery Property. *Chem. Commun.* **2014**, *50*, 2356−2359.
(457) Wang, H.; Li, X.; Fang, F.; Yang, Y. J. Luminescence Enhancement of Europium(Iii) Originating from Self-Assembled Supramolecular Hydrogels. *Dalton Trans.* **2010**, *39*, 7294−7300.
(458) Zheng, Y. H.; Li, Y.; Tan, C. L.; Wang, Q. M. Anion Responsive Dibenzoyl-L-Cystine and Luminescent Lanthanide Soft Material. *Photochem. Photobiol.* **2011**, *87*, 641−645.
(459) Kang, C.; Wang, L.; Bian, Z.; Guo, H.; Ma, X.; Qiu, X.; Gao, L. Supramolecular Hydrogels Derived from Cyclic Amino Acids and Their Applications in the Synthesis of Pt and Ir Nanocrystals. *Chem. Commun.* **2014**, *50*, 13979−13982.
(460) Maity, M.; Maitra, U. An Easily Prepared Palladium-Hydrogel Nanocomposite Catalyst for C-C Coupling Reactions. *J. Mater. Chem. A* **2014**, *2*, 18952−18958.
(461) Ogata, K.; Sasano, D.; Yokoi, T.; Isozaki, K.; Seike, H.; Takaya, H.; Nakamura, M. Pd-Complex-Bound Amino Acid-Based Supramolecular Gel Catalyst for Intramolecular Addition-Cyclization of Alkynoic Acids in Water. *Chem. Lett.* **2012**, *41*, 498−500.
(462) Na, Y. M.; Noh, T. H.; Ha, B. J.; Hong, J.; Jung, O. S. First Hydrogelation of Discrete Metal Complexes. Structures and Fluxional Behavior of Cyclopalladium(Ii) Complexes. *Bull. Korean Chem. Soc.* **2009**, *30*, 573−576.
(463) Andrews, P. C.; Junk, P. C.; Massi, M.; Silberstein, M. Gelation of La(Iii) Cations Promoted by 5-(2-Pyridyl) Tetrazolate and Water. *Chem. Commun.* **2006**, 3317−3319.
(464) King, K. N.; McNeil, A. J. Streamlined Approach to a New Gelator: Inspiration from Solid-State Interactions for a Mercury-Induced Gelation. *Chem. Commun.* **2010**, *46*, 3511−3513.
(465) Carter, K. K.; Rycenga, H. B.; McNeil, A. J. Improving Hg-Triggered Gelation Via Structural Modifications. *Langmuir* **2014**, *30*, 3522−3527.
(466) Ghosh, B. N.; Bhowmik, S.; Mal, P.; Rissanen, K. A Highly Selective, Hg2+ Triggered Hydrogelation: Modulation of Morphology by Chemical Stimuli. *Chem. Commun.* **2014**, *50*, 734−736.
(467) Lesnyak, V.; Voitekhovich, S. V.; Gaponik, P. N.; Gaponik, N.; Eychmuller, A. Cdte Nanocrystals Capped with a Tetrazolyl Analogue of Thioglycolic Acid: Aqueous Synthesis, Characterization, and Metal-Assisted Assembly. *ACS Nano* **2010**, *4*, 4090−4096.
(468) Adarsh, N. N.; Kumar, D. K.; Dastidar, P. Cu^{II} Coordination Polymers Derived from Bis-Pyridyl-Bis-Urea Ligands: Synthesis,

DOI: 10.1021/acs.chemrev.5b00299
Chem. Rev. 2015, 115, 13165−13307

Selective Anion Separation and Metallogelation. *Curr. Sci.* **2011**, *101*, 869−880.
(469) Hamilton, T. D.; Bucar, D. K.; Baltrusaitis, J.; Flanagan, D. R.; Li, Y. J.; Ghorai, S.; Tivanski, A. V.; MacGillivray, L. R. Thixotropic Hydrogel Derived from a Product of an Organic Solid-State Synthesis: Properties and Densities of Metal-Organic Nanoparticles. *J. Am. Chem. Soc.* **2011**, *133*, 3365−3371.
(470) Fang, W. W.; Sun, Z. M.; Tu, T. Novel Supramolecular Thixotropic Metallohydrogels Consisting of Rare Metal-Organic Nanoparticles: Synthesis, Characterization, and Mechanism of Aggregation. *J. Phys. Chem. C* **2013**, *117*, 25185−25194.
(471) Fang, W.; Liu, C.; Lu, Z.; Sun, Z.; Tu, T. Tunable Reversible Metallo-Hydrogels: A New Platform for Visual Discrimination of Biothiols. *Chem. Commun.* **2014**, *50*, 10118−10121.
(472) Fang, W.; Liu, X.; Lu, Z.; Tu, T. Photoresponsive Metallo-Hydrogels Based on Visual Discrimination of the Positional Isomers through Selective Thixotropic Gel Collapse. *Chem. Commun.* **2014**, *50*, 3313−3316.
(473) Bhattacharjee, S.; Bhattacharya, S. Bhattacharya, S. Pyridylenevinylene Based Cu2+-Specific, Injectable Metallo(Hydro) Gel: Thixotropy and Nanoscale Metal-Organic Particles. *Chem. Commun.* **2014**, *50*, 11690−11693.
(474) Wang, J.; Chen, Y.; Law, Y. C.; Li, M. Y.; Zhu, M. X.; Lu, W.; Chui, S. S. Y.; Zhu, N. Y.; Che, C. M. Organo- and Hydrogelators Based on Luminescent Monocationic Terpyridyl Platinum(Ii) Complexes with Biphenylacetylide Ligands. *Chem. - Asian J.* **2011**, *6*, 3011−3019.
(475) Taraban, M. B.; Weerasekare, M.; Trewhella, J.; Shi, X. F.; Jeong, E. K.; Yu, Y. B. Effects of Gadolinium Chelate on the Evolution of the Nanoscale Structure in Peptide Hydrogels. *Biopolymers* **2012**, *98*, 50−58.
(476) Wu, J. J.; Cao, M. L.; Zhang, J. Y.; Ye, B. H. A Nanocomposite Gel Based on 1d Coordination Polymers and Nanoclusters Reversibly Gelate Water Upon Heating. *RSC Adv.* **2012**, *2*, 12718−12723.
(477) Roy, B.; Bairi, P.; Chakraborty, P.; Nandi, A. K. Stimuli-Responsive, Thixotropic Bicomponent Hydrogel of Melamine-Zn(Ii)-Orotate Complex. *Supramol. Chem.* **2013**, *25*, 335−343.
(478) Zhao, G. Z.; Chen, L. J.; Wang, W.; Zhang, J.; Yang, G.; Wang, D. X.; Yu, Y. H.; Yang, H. B. Stimuli-Responsive Supramolecular Gels through Hierarchical Self-Assembly of Discrete Rhomboidal Metallacycles. *Chem. - Eur. J.* **2013**, *19*, 10094−10100.
(479) Taira, T.; Suzaki, Y.; Osakada, K. Metallohydrogel Formed from Amphiphilic Pd Complex and Alpha-Cyclodextrin: Control of Its Sol-Gel Transition. *Chem. Lett.* **2013**, *42*, 1062−1064.
(480) Rest, C.; Mayoral, M. J.; Fucke, K.; Schellheimer, J.; Stepanenko, V.; Fernandez, G. Self-Assembly and (Hydro)Gelation Triggered by Cooperative Pi-Pi and Unconventional C-H Center Dot Center Dot Center Dot X Hydrogen Bonding Interactions. *Angew. Chem., Int. Ed.* **2014**, *53*, 700−705.
(481) Saha, S.; Bachl, J.; Kundu, T.; Diaz, D. D.; Banerjee, R. Amino Acid-Based Multiresponsive Low-Molecular Weight Metallohydrogels with Load-Bearing and Rapid Self-Healing Abilities. *Chem. Commun.* **2014**, *50*, 3004−3006.
(482) Yadav, P.; Ballabh, A. Room Temperature Metallogelation for a Simple Series of Aminothiazole Ligands with Potential Applications in Identifying and Scavenging Mercury Ions. *RSC Adv.* **2014**, *4*, 563−566.
(483) Shen, J. S.; Li, D. H.; Cai, Q. G.; Jiang, Y. B. Highly Selective Iodide-Responsive Gel-Sol State Transition in Supramolecular Hydrogels. *J. Mater. Chem.* **2009**, *19*, 6219−6224.
(484) Casuso, P.; Carrasco, P.; Loinaz, I.; Grande, H. J.; Odriozola, I. Converting Drugs into Gelators: Supramolecular Hydrogels from N-Acetyl-L-Cysteine and Coinage-Metal Salts. *Org. Biomol. Chem.* **2010**, *8*, 5455−5458.
(485) Khizhnyak, S. D.; Ovchinnikov, M. M.; Pakhomov, P. M. Gel Formation in Low-Concentration Aqueous Solutions Containing N-Acetyl-L-Cysteine and Silver Nitrate. *J. Struct. Chem.* **2014**, *55*, 175−179.
(486) Komarov, P. V.; Mikhailov, I. V.; Alekseev, V. G.; Khizhnyak, S. D.; Pakhomov, P. M. Self-Assembly and Gel Formation Processes in an Aqueous Solution of L-Cysteine and Silver Nitrate. *J. Struct. Chem.* **2012**, *53*, 988−1005.
(487) Baranova, O. A.; Khizhnyak, S. D.; Pakhomov, P. M. Supramolecular Hydrogel Based on L-Cysteine and Silver Nanoparticles. *J. Struct. Chem.* **2014**, *55*, 169−174.
(488) Odriozola, I.; Casuso, P.; Loinaz, I.; Cabanero, G.; Grande, H. J. Designing Neutral Metallophilic Hydrogels from Di- and Tripeptides. *Org. Biomol. Chem.* **2011**, *9*, 5059−5061.
(489) Gao, X. N.; Esteves, R. J.; Luong, T. T. H.; Jaini, R.; Arachchige, I. U. Oxidation-Induced Self-Assembly of Ag Nanoshells into Transparent and Opaque Ag Hydrogels and Aerogels. *J. Am. Chem. Soc.* **2014**, *136*, 7993−8002.
(490) Sarkar, S.; Dutta, S.; Chakrabarti, S.; Bairi, P.; Pal, T. Redox-Switchable Copper(I) Metallogel: A Metal-Organic Material for Selective and Naked-Eye Sensing of Picric Acid. *ACS Appl. Mater. Interfaces* **2014**, *6*, 6308−6316.
(491) Sarkar, S.; Dutta, S.; Bairi, P.; Pal, T. Redox-Responsive Copper(I) Metallogel: A Metal-Organic Hybrid Sorbent for Reductive Removal of Chromium(Vi) from Aqueous Solution. *Langmuir* **2014**, *30*, 7833−7841.
(492) Huang, C. C.; Lo, Y. W.; Kuo, W. S.; Hwu, J. R.; Su, W. C.; Shieh, D. B.; Yeh, C. S. Facile Preparation of Self-Assembled Hydrogel-Like Gdpo4 Center Dot H2o Nanorods. *Langmuir* **2008**, *24*, 8309−8313.
(493) Inoue, N.; Otsuka, H.; Wada, S. I.; Takahara, A. Inorganic Nanofiber/Enzyme) Hybrid Hydrogel: Preparation, Characterization, and Enzymatic Activity of Imogolite/Pepsin Conjugate. *Chem. Lett.* **2006**, *35*, 194−195.
(494) Patil, A. J.; Kumar, R. K.; Barron, N. J.; Mann, S. Cerium Oxide Nanoparticle-Mediated Self-Assembly of Hybrid Supramolecular Hydrogels. *Chem. Commun.* **2012**, *48*, 7934−7936.
(495) Daiko, Y.; Akamatsu, T.; Kasuga, T.; Nogami, M. Preparation of Fast Proton-Conducting Zinc Metaphosphate Hydrogel and Its Potential Application to Electric Double-Layer Capacitors. *Chem. Lett.* **2005**, *34*, 24−25.
(496) Akamatsu, T.; Kasuga, T.; Nogami, M. Formation of Metaphosphate Hydrogels and Their Proton Conductivities. *J. Non-Cryst. Solids* **2005**, *351*, 691−696.
(497) Akamatsu, T.; Kasuga, T.; Nogami, M. Electric Double-Layer Capacitor Based on Zinc Metaphosphate Glass-Derived Hydrogel. *Appl. Phys. Lett.* **2006**, *88*, 153501.
(498) Akamatsu, T.; Kasuga, T.; Nogami, M. Formation Mechanism of Zinc Metaphosphate Hydrogels by a Chemicovectorial Method and Their Proton Conductivities. *J. Ceram. Soc. Jpn.* **2006**, *114*, 92−96.
(499) Akamatsu, T.; Kasuga, T. Proton Conductivities of Zinc Phosphate Glass-Derived Hydrogels Controlled by Water Content. *J. Electrochem. Soc.* **2007**, *154*, B258−B262.
(500) Joshi, S. A.; Kulkarni, N. D. A New Trinuclear Cu(Ii) Complex of Inositol as a Hydrogelator. *Chem. Commun.* **2009**, 2341−2343.
(501) Gavara, R.; Llorca, J.; Lima, J. C.; Rodriguez, L. A Luminescent Hydrogel Based on a New Au(I) Complex. *Chem. Commun.* **2013**, *49*, 72−74.
(502) Xiao, X. S.; Lu, W.; Che, C. M. Phosphorescent Nematic Hydrogels and Chromonic Mesophases Driven by Intra- and Intermolecular Interactions of Bridged Dinuclear Cyclometalated Platinum(Ii) Complexes. *Chem. Sci.* **2014**, *5*, 2482−2488.
(503) Ma, X.; Yu, D.; Tang, N.; Wu, J. Tb3+-Containing Supramolecular Hydrogels: Luminescence Properties and Reversible Sol-Gel Transitions Induced by External Stimuli. *Dalton Trans.* **2014**, *43*, 9856−9859.
(504) Moro, A. J.; Rome, B.; Aguilo, E.; Arcau, J.; Puttreddy, R.; Rissanen, K.; Lima, J. C.; Rodriguez, L. A Coumarin Based Gold(I)-Alkynyl Complex: A New Class of Supramolecular Hydrogelators. *Org. Biomol. Chem.* **2015**, *13*, 2026−2033.
(505) Carraro, M.; Sartorel, A.; Scorrano, G.; Maccato, C.; Dickman, M. H.; Kortz, U.; Bonchio, M. Chiral Strandberg-Type Molybdates (Rpo3)(2)Mo5o15 (2-) as Molecular Gelators: Self-Assembled Fibrillar Nanostructures with Enhanced Optical Activity. *Angew. Chem., Int. Ed.* **2008**, *47*, 7275−7279.

DOI: 10.1021/acs.chemrev.5b00299
Chem. Rev. 2015, 115, 13165−13307

(506) He, Z. F.; Ai, H.; Li, B.; Wu, L. X. A Supramolecular Gel Based on an Adenine Symmetrically Grafted Anderson-Type Polyoxometalate Complex. *Chin. Sci. Bull.* **2012**, *57*, 4304−4309.
(507) Fu, I. W.; Markegard, C. B.; Nguyen, H. D. Solvent Effects on Kinetic Mechanisms of Self-Assembly by Peptide Amphiphiles Via Molecular Dynamics Simulations. *Langmuir* **2015**, *31*, 315−324.
(508) Chan, W. C., White, P. D., Eds. *Fmoc Solid Phase Peptide Synthesis: A Practical Approach*; Oxford University Press: New York, 2000.
(509) Jiang, J. A.; Wang, T. Y.; Liu, M. H. Creating Chirality in the Inner Walls of Silica Nanotubes through a Hydrogel Template: Chiral Transcription and Chiroptical Switch. *Chem. Commun.* **2010**, *46*, 7178−7180.
(510) Tirrell, M.; Kokkoli, E.; Biesalski, M. The Role of Surface Science in Bioengineered Materials. *Surf. Sci.* **2002**, *500*, 61−83.
(511) Berndt, P.; Fields, G. B.; Tirrell, M. Synthetic Lipidation of Peptides and Amino-Acids - Monolayer Structure and Properties. *J. Am. Chem. Soc.* **1995**, *117*, 9515−9522.
(512) Yu, Y. C.; Berndt, P.; Tirrell, M.; Fields, G. B. Self-Assembling Amphiphiles for Construction of Protein Molecular Architecture. *J. Am. Chem. Soc.* **1996**, *118*, 12515−12520.
(513) Kunitake, T. Synthetic Bilayer-Membranes - Molecular Design, Self-Organization, and Application. *Angew. Chem., Int. Ed. Engl.* **1992**, *31*, 709−726.
(514) Bhattacharya, S.; Krishnan-Ghosh, Y. First Report of Phase Selective Gelation of Oil from Oil/Water Mixtures. Possible Implications toward Containing Oil Spills. *Chem. Commun.* **2001**, 185−186.
(515) Pal, A.; Dey, J. Water-Induced Physical Gelation of Organic Solvents by N-(N-Alkylcarbamoyl)-L-Alanine Amphiphiles. *Langmuir* **2011**, *27*, 3401−3408.
(516) Patra, T.; Pal, A.; Dey, J. A Smart Supramolecular Hydrogel of N-Alpha-(4-N-Alkyloxybenzoyl)-L-Histidine Exhibiting Ph-Modulated Properties. *Langmuir* **2010**, *26*, 7761−7767.
(517) Gao, P.; Zhan, C. L.; Liu, L. Z.; Zhou, Y. B.; Liu, M. H. Inter- and Intra-Molecular H-Bonds Induced Different Nanostructures from a Multi-H-Bonding (Mhb) Amphiphile: Nanofibers and Nanodisk. *Chem. Commun.* **2004**, 1174−1175.
(518) Minakuchi, N.; Hoe, K.; Yamaki, D.; Ten-no, S.; Nakashima, K.; Goto, M.; Mizuhata, M.; Maruyama, T. Versatile Supramolecular Gelators That Can Harden Water, Organic Solvents and Ionic Liquids. *Langmuir* **2012**, *28*, 9259−9266.
(519) Yu, Q.; Fan, M.; Li, D.; Song, Z.; Cai, M.; Zhou, F.; Liu, W. Thermoreversible Gel Lubricants through Universal Supramolecular Assembly of a Nonionic Surfactant in a Variety of Base Lubricating Liquids. *ACS Appl. Mater. Interfaces* **2014**, *6*, 15783−15794.
(520) Kira, Y.; Okazaki, Y.; Sawada, T.; Takafuji, M.; Ihara, H. Amphiphilic Molecular Gels from Omega-Aminoalkylated L-Glutamic Acid Derivatives with Unique Chiroptical Properties. *Amino Acids* **2010**, *39*, 587−597.
(521) Khatua, D.; Maiti, R.; Dey, J. A Supramolecular Hydrogel That Responds to Biologically Relevant Stimuli. *Chem. Commun.* **2006**, 4903−4905.
(522) Roy, S.; Dasgupta, A.; Das, P. K. Alkyl Chain Length Dependent Hydrogelation of L-Tryptophan-Based Amphiphile. *Langmuir* **2007**, *23*, 11769−11776.
(523) Dutta, S.; Shome, A.; Debnath, S.; Das, P. K. Counterion Dependent Hydrogelation of Amino Acid Based Amphiphiles: Switching from Non-Gelators to Gelators and Facile Synthesis of Silver Nanoparticles. *Soft Matter* **2009**, *5*, 1607−1620.
(524) Suzuki, M.; Owa, S.; Yumoto, M.; Kimura, M.; Shirai, H.; Hanabusa, K. New L-Valine-Based Hydrogelators: Formation of Supramolecular Hydrogels. *Tetrahedron Lett.* **2004**, *45*, 5399−5402.
(525) Suzuki, M.; Yumoto, M.; Kimura, M.; Shirai, H.; Hanabusa, K. Supramolecular Hydrogels Containing Inorganic Salts and Acids. *Tetrahedron Lett.* **2004**, *45*, 2947−2950.
(526) Suzuki, M.; Yumoto, M.; Kimura, M.; Shirai, H.; Hanabusa, K. Supramolecular Hydrogels Formed by L-Lysine Derivatives. *Chem. Lett.* **2004**, *33*, 1496−1497.
(527) Gao, P.; Liu, L. Z.; Zhan, C. L.; Zhou, Y. B.; Liu, M. H. Synthesis and Gelation of N-Stearoyl-L-glutamic Acid and N-Stearoyl-L-glutamic Diethyl Ester. *Acta Chim. Sin.* **2004**, *62*, 895−900.
(528) Fu, X. J.; Wang, N. X.; Zhang, S. Z.; Wang, H.; Yang, Y. J. Formation Mechanism of Supramolecular Hydrogels in the Presence of L-Phenylalanine Derivative as a Hydrogelator. *J. Colloid Interface Sci.* **2007**, *315*, 376−381.
(529) Cao, S. Q.; Fu, X. J.; Wang, N. X.; Wang, H.; Yang, Y. J. Release Behavior of Salicylic Acid in Supramolecular Hydrogels Formed by L-Phenylalanine Derivatives as Hydrogelator. *Int. J. Pharm.* **2008**, *357*, 95−99.
(530) Fu, X. R.; Cao, S. Q.; Wang, N. X.; Zhang, S. Z.; Wang, H.; Yang, Y. J. Effect of Hydrogen Bonding and Hydrophobic Interaction on the Formation of Supramolecular Hydrogels Formed by L-Phenylalanine Derivative Hydrogelator. *Chin. Chem. Lett.* **2007**, *18*, 1001−1004.
(531) Chu, X.; Xing, P.; Li, S.; Ma, M.; Hao, J.; Hao, A. Dual-Tuning Multidimensional Superstructures Based on a T-Shaped Molecule: Vesicle, Helix, Membrane and Nanofiber-Constructed Gel. *RSC Adv.* **2015**, *5*, 1969−1978.
(532) Huang, Z.; Luo, Q.; Guan, S.; Gao, J.; Wang, Y.; Zhang, B.; Wang, L.; Xu, J.; Dong, Z.; Liu, J. Redox Control of Gpx Catalytic Activity through Mediating Self-Assembly of Fmoc-Phenylalanine Selenide into Switchable Supramolecular Architectures. *Soft Matter* **2014**, *10*, 9695−9701.
(533) Amarendar, R. M.; Srivastava, A. Mechano-Responsive Gelation of Water by a Short Alanine-Derivative. *Soft Matter* **2014**, *10*, 4863−4868.
(534) Wang, Y. F.; Huang, R. L.; Qi, W.; Wu, Z. J.; Su, R. X.; He, Z. M. Kinetically Controlled Self-Assembly of Redox-Active Ferrocene-Diphenylalanine: From Nanospheres to Nanofibers. *Nanotechnology* **2013**, *24*, 465603.
(535) Ryan, D. M.; Anderson, S. B.; Senguen, F. T.; Youngman, R. E.; Nilsson, B. L. Self-Assembly and Hydrogelation Promoted by F-5-Phenylalanine. *Soft Matter* **2010**, *6*, 475−479.
(536) Ryan, D. M.; Anderson, S. B.; Nilsson, B. L. The Influence of Side-Chain Halogenation on the Self-Assembly and Hydrogelation of Fmoc-Phenylalanine Derivatives. *Soft Matter* **2010**, *6*, 3220−3231.
(537) Ryan, D. R.; Doran, T. M.; Anderson, S. B.; Nilsson, B. L. Effect of C-Terminal Modification on the Self-Assembly and Hydrogelation of Fluorinated Fmoc-Phe Derivatives. *Langmuir* **2011**, *27*, 4029−4039.
(538) Yang, Z. M.; Wang, L.; Wang, J. Y.; Gao, P.; Xu, B. Phenyl Groups in Supramolecular Nanofibers Confer Hydrogels with High Elasticity and Rapid Recovery. *J. Mater. Chem.* **2010**, *20*, 2128−2132.
(539) Wang, Q. G.; Yang, Z. M.; Ma, M. L.; Chang, C. K.; Xu, B. High Catalytic Activities of Artificial Peroxidases Based on Supramolecular Hydrogels That Contain Heme Models. *Chem. - Eur. J.* **2008**, *14*, 5073−5078.
(540) Wang, Q. G.; Li, L. H.; Xu, B. Bioinspired Supramolecular Confinement of Luminol and Heme Proteins to Enhance the Chemiluminescent Quantum Yield. *Chem. - Eur. J.* **2009**, *15*, 3168−3172.
(541) Adhikari, B.; Nanda, J.; Banerjee, A. Multicomponent Hydrogels from Enantiomeric Amino Acid Derivatives: Helical Nanofibers, Handedness and Self-Sorting. *Soft Matter* **2011**, *7*, 8913−8922.
(542) Graceffa, P.; Lehrer, S. S. The Excimer Fluorescence of Pyrene-Labeled Tropomyosin. A Probe of Conformational Dynamics. *J. Biol. Chem.* **1980**, *255*, 11296−11300.
(543) Martari, M.; Sanderson, R. D. Critical Self-Assembly Concentration of Bolaamphiphilic Peptides and Peptide Hybrids Determined by Fluorescence Measurements. *S. Afr. J. Chem.* **2008**, *61*, 47−52.
(544) Crisp, G. T.; Gore, J. Biotin Derivatives as Gelators of Organic Solvents. *Synth. Commun.* **1997**, *27*, 2203−2215.
(545) Travaglini, L.; Gubitosi, M.; di Gregorio, M. C.; Pavel, N. V.; D'Annibale, A.; Giustini, M.; Soto Tellini, V. H.; Vazquez Tato, J.; Obiols-Rabasa, M.; Bayati, S.; et al. On the Self-Assembly of a

DOI: 10.1021/acs.chemrev.5b00299
Chem. Rev. 2015, 115, 13165−13307

Tryptophan Labeled Deoxycholic Acid. *Phys. Chem. Chem. Phys.* **2014**, *16*, 19492−19504.
(546) Bhuniya, S.; Park, S. M.; Kim, B. H. Biotin-Amino Acid Conjugates: An Approach toward Self-Assembled Hydrogelation. *Org. Lett.* **2005**, *7*, 1741−1744.
(547) Travaglini, L.; D'Annibale, A.; di Gregorio, M. C.; Schillen, K.; Olsson, U.; Sennato, S.; Pavel, N. V.; Galantini, L. Between Peptides and Bile Acids: Self-Assembly of Phenylalanine Substituted Cholic Acids. *J. Phys. Chem. B* **2013**, *117*, 9248−9257.
(548) Rubio, J.; Alfonso, I.; Burguete, M. I.; Luis, S. V. Interplay between Hydrophilic and Hydrophobic Interactions in the Self-Assembly of a Gemini Amphiphilic Pseudopeptide: From Nano-Spheres to Hydrogels. *Chem. Commun.* **2012**, *48*, 2210−2212.
(549) Nebot, V. J.; Escuder, B.; Miravet, J. F.; Smets, J.; Fernandez-Prieto, S. Interplay of Molecular Hydrogelators and Sds Affords Responsive Soft Matter Systems with Tunable Properties. *Langmuir* **2013**, *29*, 9544−9550.
(550) Nebot, V. J.; Diaz-Oltra, S.; Smets, J.; Fernandez Prieto, S.; Miravet, J. F.; Escuder, B. Freezing Capture of Polymorphic Aggregates of Bolaamphiphilic L- Valine- Based Molecular Hydro-gelators. *Chem. - Eur. J.* **2014**, *20*, 5762−5767.
(551) Nieto-Ortega, B.; Nebot, V. J.; Miravet, J. F.; Escuder, B.; Navarrete, J. T. L.; Casado, J.; Ramirez, F. J. Vibrational Circular Dichroism Shows Reversible Helical Handedness Switching in Peptidomimetic L-Valine Fibrils. *J. Phys. Chem. Lett.* **2012**, *3*, 2120−2124.
(552) Wang, T. Y.; Jiang, J. A.; Liu, Y.; Li, Z. B.; Liu, M. Hierarchical Self-Assembly of Bolaamphiphiles with a Hybrid Spacer and L-Glutamic Acid Headgroup: Ph- and Surface-Triggered Hydrogels, Vesicles, Nanofibers, and Nanotubes. *Langmuir* **2010**, *26*, 18694−18700.
(553) Zhang, C.; Xue, X.; Luo, Q.; Li, Y.; Yang, K.; Zhuang, X.; Jiang, Y.; Zhang, J.; Liu, J.; Zou, G.; et al. Self-Assembled Peptide Nanofibers Designed as Biological Enzymes for Catalyzing Ester Hydrolysis. *ACS Nano* **2014**, *8*, 11715−11723.
(554) Mu, Y.; Yu, M. Effects of Hydrophobic Interaction Strength on the Self-Assembled Structures of Model Peptides. *Soft Matter* **2014**, *10*, 4956−4965.
(555) Reches, M.; Gazit, E. Casting Metal Nanowires within Discrete Self-Assembled Peptide Nanotubes. *Science* **2003**, *300*, 625−627.
(556) Holmes, T. C.; de Lacalle, S.; Su, X.; Liu, G. S.; Rich, A.; Zhang, S. G. Extensive Neurite Outgrowth and Active Synapse Formation on Self-Assembling Peptide Scaffolds. *Proc. Natl. Acad. Sci. U. S. A.* **2000**, *97*, 6728−6733.
(557) Silva, G. A.; Czeisler, C.; Niece, K. L.; Beniash, E.; Harrington, D. A.; Kessler, J. A.; Stupp, S. I. Selective Differentiation of Neural Progenitor Cells by High-Epitope Density Nanofibers. *Science* **2004**, *303*, 1352−1355.
(558) Wickremasinghe, N. C.; Kumar, V. A.; Hartgerink, J. D. Two-Step Self-Assembly of Liposome-Multidomain Peptide Nanofiber Hydrogel for Time-Controlled Release. *Biomacromolecules* **2014**, *15*, 3587−3595.
(559) Altunbas, A.; Pochan, D. J. In *Peptide-Based Materials*; Deming, T., Ed.; Topics in Current Chemistry, Vol. *310*; Springer: Heidelberg, Germany, 2012.
(560) Fichman, G.; Gazit, E. Self-Assembly of Short Peptides to Form Hydrogels: Design of Building Blocks, Physical Properties and Technological Applications. *Acta Biomater.* **2014**, *10*, 1671−1682.
(561) Zhao, F.; Li, J.; Zhou, N.; Sakai, J.; Gao, Y.; Shi, J.; Goldman, B.; Browdy, H. M.; Luo, H. R.; Xu, B. De Novo Chemoattractants Form Supramolecular Hydrogels for Immunomodulating Neutrophils in Vivo. *Bioconjugate Chem.* **2014**, *25*, 2116−2122.
(562) Ren, C.; Zhang, J.; Chen, M.; Yang, Z. Self-Assembling Small Molecules for the Detection of Important Analytes. *Chem. Soc. Rev.* **2014**, *43*, 7257−7266.
(563) Liu, L.; Liu, X.; Deng, H.; Wu, Z.; Zhang, J.; Cen, B.; Xu, Q.; Ji, A. Something between the Amazing Functions and Various Morphologies of Self-Assembling Peptides Materials in the Medical Field. *J. Biomater. Sci., Polym. Ed.* **2014**, *25*, 1331−1345.
(564) de Groot, N. S.; Parella, T.; Aviles, F. X.; Vendrell, J.; Ventura, S. Ile-Phe Dipeptide Self-Assembly: Clues to Amyloid Formation. *Biophys. J.* **2007**, *92*, 1732−1741.
(565) Adler-Abramovich, L.; Reches, M.; Sedman, V. L.; Allen, S.; Tendler, S. J. B.; Gazit, E. Thermal and Chemical Stability of Diphenylalanine Peptide Nanotubes: Implications for Nanotechnological Applications. *Langmuir* **2006**, *22*, 1313−1320.
(566) Mahler, A.; Reches, M.; Rechter, M.; Cohen, S.; Gazit, E. Rigid, Self-Assembled Hydrogel Composed of a Modified Aromatic Dipeptide. *Adv. Mater.* **2006**, *18*, 1365−1370.
(567) Reches, M.; Gazit, E. Molecular Self-Assembly of Peptide Nanostructures: Mechanism of Association and Potential Uses. *Curr. Nanosci.* **2006**, *2*, 105−111.
(568) Reches, M.; Gazit, E. Designed Aromatic Homo-Dipeptides: Formation of Ordered Nanostructures and Potential Nanotechnological Applications. *Phys. Biol.* **2006**, *3*, S10−S19.
(569) Ryu, J.; Park, C. B. High Stability of Self-Assembled Peptide Nanowires against Thermal, Chemical, and Proteolytic Attacks. *Biotechnol. Bioeng.* **2010**, *105*, 221−230.
(570) Huang, R. L.; Qi, W.; Su, R. X.; Zhao, J.; He, Z. M. Solvent and Surface Controlled Self-Assembly of Diphenylalanine Peptide: From Microtubes to Nanofibers. *Soft Matter* **2011**, *7*, 6418−6421.
(571) Kumaraswamy, P.; Lakshmanan, R.; Sethuraman, S.; Krishnan, U. M. Self-Assembly of Peptides: Influence of Substrate, Ph and Medium on the Formation of Supramolecular Assemblies. *Soft Matter* **2011**, *7*, 2744−2754.
(572) Zhao, J.; Huang, R.; Qi, W.; Wang, Y.; Su, R.; He, Z. Self-Assembly of Diphenylalanine Based Peptides: Molecular Design, Structural Control and Applications. *Prog. Chem.* **2014**, *26*, 1445−1459.
(573) Kuang, Y.; Du, X.; Zhou, J.; Xu, B. Supramolecular Nanofibrils Inhibit Cancer Progression in Vitro and in Vivo. *Adv. Healthcare Mater.* **2014**, *3*, 1217−1221.
(574) Shi, J.; Du, X.; Huang, Y.; Zhou, J.; Yuan, D.; Wu, D.; Zhang, Y.; Haburcak, R.; Epstein, I. R.; Xu, B. Ligand-Receptor Interaction Catalyzes the Aggregation of Small Molecules to Induce Cell Necroptosis. *J. Am. Chem. Soc.* **2015**, *137*, 26−29.
(575) Chapman, R.; Danial, M.; Koh, M. L.; Jolliffe, K. A.; Perrier, S. Design and Properties of Functional Nanotubes from the Self-Assembly of Cyclic Peptide Templates. *Chem. Soc. Rev.* **2012**, *41*, 6023−6041.
(576) Qin, S. Y.; Jiang, H. F.; Liu, X. J.; Pei, Y.; Cheng, H.; Sun, Y. X.; Zhang, X. Z. High Length-Diameter Ratio Nanotubes Self-Assembled from a Facial Cyclopeptide. *Soft Matter* **2014**, *10*, 947−951.
(577) Leclair, S.; Baillargeon, P.; Skouta, R.; Gauthier, D.; Zhao, Y.; Dory, Y. L. Micrometer-Sized Hexagonal Tubes Self-Assembled by a Cyclic Peptide in a Liquid Crystal. *Angew. Chem., Int. Ed.* **2004**, *43*, 349−353.
(578) Ishihara, Y.; Kimura, S. Nanofiber Formation of Amphiphilic Cyclic Tri-Beta-Peptide. *J. Pept. Sci.* **2010**, *16*, 110−114.
(579) Marchesan, S.; Easton, C. D.; Kushkaki, F.; Waddington, L.; Hartley, P. G. Tripeptide Self-Assembled Hydrogels: Unexpected Twists of Chirality. *Chem. Commun.* **2012**, *48*, 2195−2197.
(580) Tie, Z. X.; Qin, M.; Zou, D. W.; Cao, Y.; Wang, W. Photo-Crosslinking Induced Geometric Restriction Controls the Self-Assembly of Diphenylalanine Based Peptides. *Chin. Phys. Lett.* **2011**, *28*, 028702.
(581) Frederix, P. W. J. M.; Scott, G. G.; Abul-Haija, Y. M.; Kalafatovic, D.; Pappas, C. G.; Javid, N.; Hunt, N. T.; Ulijn, R. V.; Tuttle, T. Exploring the Sequence Space for (Tri-) Peptide Self-Assembly to Design and Discover. *Nat. Chem.* **2015**, *7*, 30−37.
(582) Guilbaud, J. B.; Rochas, C.; Miller, A. F.; Saiani, A. Effect of Enzyme Concentration of the Morphology and Properties of Enzymatically Triggered Peptide Hydrogels. *Biomacromolecules* **2013**, *14*, 1403−1411.
(583) Ghosh, S.; Singh, S. K.; Verma, S. Self-Assembly and Potassium Ion Triggered Disruption of Peptide-Based Soft Structures. *Chem. Commun.* **2007**, 2296−2298.

DOI: 10.1021/acs.chemrev.5b00299
Chem. Rev. 2015, 115, 13165−13307

(584) Tine, M. R.; Alderighi, M.; Duce, C.; Ghezzi, L.; Solaro, R. Effect of Temperature on Self-Assembly of an Ionic Tetrapeptide. *J. Therm. Anal. Calorim.* **2011**, *103*, 75−80.
(585) Hamley, I. W.; Brown, G. D.; Castelletto, V.; Cheng, G.; Venanzi, M.; Caruso, M.; Placidi, E.; Aleman, C.; Revilla-Lopez, G.; Zanuy, D. Self-Assembly of a Designed Amyloid Peptide Containing the Functional Thienylalanine Unit. *J. Phys. Chem. B* **2010**, *114*, 10674−10683.
(586) Crocker, J. C.; Grier, D. G. When Like Charges Attract: The Effects of Geometrical Confinement on Long-Range Colloidal Interactions. *Phys. Rev. Lett.* **1996**, *77*, 1897−1900.
(587) Hermansson, M. The Dlvo Theory in Microbial Adhesion. *Colloids Surf., B* **1999**, *14*, 105−119.
(588) Savin, T.; Doyle, P. S. Electrostatically Tuned Rate of Peptide Self-Assembly Resolved by Multiple Particle Tracking. *Soft Matter* **2007**, *3*, 1194−1202.
(589) Boothroyd, S.; Saiani, A.; Miller, A. F. Controlling Network Topology and Mechanical Properties of Co-Assembling Peptide Hydrogels. *Biopolymers* **2014**, *101*, 669−680.
(590) Boothroyd, S.; Miller, A. F.; Saiani, A. From Fibres to Networks Using Self-Assembling Peptides. *Faraday Discuss.* **2013**, *166*, 195−207.
(591) Saiani, A.; Mohammed, A.; Frielinghaus, H.; Collins, R.; Hodson, N.; Kielty, C. M.; Sherratt, M. J.; Miller, A. F. Self-Assembly and Gelation Properties of Alpha-Helix Versus Beta-Sheet Forming Peptides. *Soft Matter* **2009**, *5*, 193−202.
(592) Hickling, C.; Toogood, H. S.; Saiani, A.; Scrutton, N. S.; Miller, A. F. Nanofi Brillar Peptide Hydrogels for the Immobilization of Biocatalysts for Chemical Transformations. *Macromol. Rapid Commun.* **2014**, *35*, 868−874.
(593) Chan, L.; Cross, H. F.; She, J. K.; Cavalli, G.; Martins, H. F. P.; Neylon, C. *PLoS One* **2007**, *2*, e1164.
(594) Piluso, S.; Cassell, H. C.; Gibbons, J. L.; Waller, T. E.; Plant, N. J.; Miller, A. F.; Cavalli, G. Site-Specific, Covalent Incorporation of Tus, a DNA-Binding Protein, on Ionic-Complementary Self-Assembling Peptide Hydrogels Using Transpeptidase Sortase a as a Conjugation Tool. *Soft Matter* **2013**, *9*, 6752−6756.
(595) Huang, H.; Sun, X. S. Rational Design of Responsive Self-Assembling Peptides from Native Protein Sequences. *Biomacromolecules* **2010**, *11*, 3390−3394.
(596) Riley, J. M.; Aggeli, A.; Koopmans, R. J.; McPherson, M. J. Bioproduction and Characterization of a Ph Responsive Self-Assembling Peptide. *Biotechnol. Bioeng.* **2009**, *103*, 241−251.
(597) Prakash, A.; Parsons, S. J.; Kyle, S.; McPherson, M. J. Recombinant Production of Self-Assembling Beta-Structured Peptides Using Sumo as a Fusion Partner. *Microb. Cell Fact.* **2012**, *11*, 92.
(598) Kyle, S.; Aggeli, A.; Ingham, E.; McPherson, M. J. Production of Self-Assembling Biomaterials for Tissue Engineering. *Trends Biotechnol.* **2009**, *27*, 423−433.
(599) Choi, S. J.; Jeong, W. J.; Kang, S. K.; Lee, M.; Kim, E.; Ryu, D. Y.; Lim, Y. B. Differential Self-Assembly Behaviors of Cyclic and Linear Peptides. *Biomacromolecules* **2012**, *13*, 1991−1995.
(600) Rapaport, H.; Grisaru, H.; Silberstein, T. Hydrogel Scaffolds of Amphiphilic and Acidic Beta-Sheet Peptides. *Adv. Funct. Mater.* **2008**, *18*, 2889−2896.
(601) Dong, H.; Hartgerink, J. D. Short Homodimeric and Heterodimeric Coiled Coils. *Biomacromolecules* **2006**, *7*, 691−695.
(602) Dong, H.; Paramonov, S. E.; Aulisa, L.; Bakota, E. L.; Hartgerink, J. D. Self-Assembly of Multidomain Peptides: Balancing Molecular Frustration Controls Conformation and Nanostructure. *J. Am. Chem. Soc.* **2007**, *129*, 12468−12472.
(603) Bakota, E. L.; Aulisa, L.; Galler, K. M.; Hartgerink, J. D. Enzymatic Cross-Linking of a Nanofibrous Peptide Hydrogel. *Biomacromolecules* **2011**, *12*, 82−87.
(604) Measey, T. J.; Schweitzer-Stenner, R. Aggregation of the Amphipathic Peptides (Aaka)N into Antiparallel Beta-Sheets. *J. Am. Chem. Soc.* **2006**, *128*, 13324−13325.
(605) Jang, S.; Yuan, J. M.; Shin, J.; Measey, T. J.; Schweitzer-Stenner, R.; Li, F. Y. Energy Landscapes Associated with the Self-Aggregation of an Alanine-Based Oligopeptide (Aaka)(4). *J. Phys. Chem. B* **2009**, *113*, 6054−6061.
(606) Kabiri, M.; Bushnak, I.; McDermot, M. T.; Unsworth, L. D. Toward a Mechanistic Understanding of Ionic Self-Complementary Peptide Self-Assembly: Role of Water Molecules and Ions. *Biomacromolecules* **2013**, *14*, 3943−3950.
(607) Wang, K.; Keasling, J. D.; Muller, S. J. Effects of the Sequence and Size of Non-Polar Residues on Self-Assembly of Amphiphilic Peptides. *Int. J. Biol. Macromol.* **2005**, *36*, 232−240.
(608) Pochan, D. J.; Schneider, J. P.; Kretsinger, J.; Ozbas, B.; Rajagopal, K.; Haines, L. Thermally Reversible Hydrogels Via Intramolecular Folding and Consequent Self-Assembly of a De Novo Designed Peptide. *J. Am. Chem. Soc.* **2003**, *125*, 11802−11803.
(609) Sathaye, S.; Zhang, H.; Sonmez, C.; Schneider, J. P.; MacDermaid, C. M.; Von Bargen, C. D.; Saven, J. G.; Pochan, D. J. Engineering Complementary Hydrophobic Interactions to Control Beta-Hairpin Peptide Self-Assembly, Network Branching, and Hydrogel Properties. *Biomacromolecules* **2014**, *15*, 3891−3900.
(610) Ozbas, B.; Rajagopal, K.; Schneider, J. P.; Pochan, D. J. Semiflexible Chain Networks Formed Via Self-Assembly of Beta-Hairpin Molecules. *Phys. Rev. Lett.* **2004**, *93*, 268106.
(611) Veerman, C.; Rajagopal, K.; Palla, C. S.; Pochan, D. J.; Schneider, J. P.; Furst, E. M. Gelation Kinetics of Beta-Hairpin Peptide Hydrogel Networks. *Macromolecules* **2006**, *39*, 6608−6614.
(612) Ozbas, B.; Rajagopal, K.; Haines-Butterick, L.; Schneider, J. P.; Pochan, D. J. Reversible Stiffening Transition in Beta-Hairpin Hydrogels Induced by Ion Complexation. *J. Phys. Chem. B* **2007**, *111*, 13901−13908.
(613) Yucel, T.; Micklitsch, C. M.; Schneider, J. P.; Pochan, D. J. Direct Observation of Early-Time Hydrogelation in Beta-Hairpin Peptide Self-Assembly. *Macromolecules* **2008**, *41*, 5763−5772.
(614) Altunbas, A.; Sharma, N.; Lamm, M. S.; Yan, C. Q.; Nagarkar, R. P.; Schneider, J. P.; Pochan, D. J. Peptide-Silica Hybrid Networks: Biomimetic Control of Network Mechanical Behavior. *ACS Nano* **2010**, *4*, 181−188.
(615) Larsen, T. H.; Branco, M. C.; Rajagopal, K.; Schneider, J. P.; Furst, E. M. Sequence-Dependent Gelation Kinetics of Beta-Hairpin Peptide Hydrogels. *Macromolecules* **2009**, *42*, 8443−8450.
(616) Nagarkar, R. P.; Hule, R. A.; Pochan, D. J.; Schneider, J. P. Strand Swapping Controls the Nanostructure of Beta-Hairpin Peptide Hydrogels. *Biopolymers* **2007**, *88*, 614.
(617) Nagy, K. J.; Giano, M. C.; Jin, A.; Pochan, D. J.; Schneider, J. P. Enhanced Mechanical Rigidity of Hydrogels Formed from Enantiomeric Peptide Assemblies. *J. Am. Chem. Soc.* **2011**, *133*, 14975−14977.
(618) Ozbas, B.; Kretsinger, J.; Rajagopal, K.; Schneider, J. P.; Pochan, D. J. Salt-Triggered Peptide Folding and Consequent Self-Assembly into Hydrogels with Tunable Modulus. *Macromolecules* **2004**, *37*, 7331−7337.
(619) Rajagopal, K.; Lamm, M. S.; Haines-Butterick, L. A.; Pochan, D. J.; Schneider, J. P. Tuning the Ph Responsiveness of Beta-Hairpin Peptide Folding, Self-Assembly, and Hydrogel Material Formation. *Biomacromolecules* **2009**, *10*, 2619−2625.
(620) Rajagopal, K.; Ozbas, B.; Pochan, D. J.; Schneider, J. P. Self-Assembled Hydrogels from Beta-Hairpin Peptides: Tuning Responsiveness and Bulk Material Properties by Peptide Design. *Biopolymers* **2005**, *80*, 487.
(621) Rajagopal, K.; Ozbas, B.; Pochan, D. J.; Schneider, J. P. Probing the Importance of Lateral Hydrophobic Association in Self-Assembling Peptide Hydrogelators. *Eur. Biophys. J.* **2006**, *35*, 162−169.
(622) Rughani, R.; Pochan, D. J.; Schneider, J. P. Self-Assembled Beta-Sheet Hydrogels: Effect of Strand Number on the Folding and Consequent Self-Assembly of Peptides into Hydrogel Material with Tuned Properties. *Biopolymers* **2005**, *80*, 504.
(623) Rughani, R. V.; Lamm, M. S.; Pochan, D. J.; Schneider, J. P. Tuning Hydrogel Properties Via Photo Polymerization of Self-Assembled Beta-Hairpin Peptides. *Biopolymers* **2007**, *88*, 629.
(624) Micklitsch, C. M.; Knerr, P. J.; Branco, M. C.; Nagarkar, R.; Pochan, D. J.; Schneider, J. P. Zinc-Triggered Hydrogelation of a Self-

DOI: 10.1021/acs.chemrev.5b00299
Chem. Rev. 2015, 115, 13165−13307

Assembling Beta-Hairpin Peptide. *Angew. Chem., Int. Ed.* **2011**, *50*, 1577−1579.
(625) Rughani, R. V.; Branco, M. C.; Pochan, D.; Schneider, J. P. De Novo Design of a Shear-Thin Recoverable Peptide-Based Hydrogel Capable of Intrafibrillar Photopolymerization. *Macromolecules* **2010**, *43*, 7924−7930.
(626) Lamm, M. S.; Sharma, N.; Rajagopal, K.; Beyer, F. L.; Schneider, J. P.; Pochan, D. J. Laterally Spaced Linear Nanoparticle Arrays Templated by Laminated Beta-Sheet Fibrils. *Adv. Mater.* **2008**, *20*, 447−451.
(627) Knerr, P. J.; Micklitsch, C. M.; Thorpe, C.; Schneider, J. P. Zinc-Triggered Hydrogelation of Designed Beta-Hairpin Peptides. *Biopolymers* **2007**, *88*, 639.
(628) Branco, M. C.; Sigano, D. M.; Schneider, J. P. Materials from Peptide Assembly: Towards the Treatment of Cancer and Transmittable Disease. *Curr. Opin. Chem. Biol.* **2011**, *15*, 427−434.
(629) Nagarkar, R. P.; Hule, R. A.; Pochan, D. J.; Schneider, J. P. Domain Swapping in Materials Design. *Biopolymers* **2010**, *94*, 141−155.
(630) Rajagopal, K.; Schneider, J. P. Self-Assembling Peptides and Proteins for Nanotechnological Applications. *Curr. Opin. Struct. Biol.* **2004**, *14*, 480−486.
(631) Fletcher, N. L.; Paquet, N.; Dickinson, E. L.; Dexter, A. F. Bioproduction of Highly Charged Designer Peptide Surfactants Via a Chemically Cleavable Coiled-Coil Heteroconcatemer. *Biotechnol. Bioeng.* **2015**, *112*, 242−251.
(632) Banwell, E. F.; Abelardo, E. S.; Adams, D. J.; Birchall, M. A.; Corrigan, A.; Donald, A. M.; Kirkland, M.; Serpell, L. C.; Butler, M. F.; Woolfson, D. N. Rational Design and Application of Responsive Alpha-Helical Peptide Hydrogels. *Nat. Mater.* **2009**, *8*, 596−600.
(633) Sharp, T. H.; Bruning, M.; Mantell, J.; Sessions, R. B.; Thomson, A. R.; Zaccai, N. R.; Brady, R. L.; Verkade, P.; Woolfson, D. N. Cryo-Transmission Electron Microscopy Structure of a Gigadalton Peptide Fiber of De Novo Design. *Proc. Natl. Acad. Sci. U. S. A.* **2012**, *109*, 13266−13271.
(634) Wagner, D. E.; Phillips, C. L.; Ali, W. M.; Nybakken, G. E.; Crawford, E. D.; Schwab, A. D.; Smith, W. F.; Fairman, R. Toward the Development of Peptide Nanofilaments and Nanoropes as Smart Materials. *Proc. Natl. Acad. Sci. U. S. A.* **2005**, *102*, 12656−12661.
(635) Yu, Z. X.; Chen, J.; Luo, Z. L. Designment of a New Self-Assembling Peptide D-Eak16 with D Amino Acid into 3D Nanofiber Scaffold. *Chem. J. Chin. Univ.* **2009**, *30*, 1131−1134.
(636) Lamm, M. S.; Rajagopal, K.; Schneider, J. P.; Pochan, D. J. Laminated Morphology of Nontwisting Beta-Sheet Fibrils Constructed Via Peptide Self-Assembly. *J. Am. Chem. Soc.* **2005**, *127*, 16692−16700.
(637) Leonard, S. R.; Cormier, A. R.; Pang, X. D.; Zimmerman, M. I.; Zhou, H. X.; Paravastu, A. K. Solid-State Nmr Evidence for Beta-Hairpin Structure within Max8 Designer Peptide Nanofibers. *Biophys. J.* **2013**, *105*, 222−230.
(638) Miller, Y.; Ma, B.; Nussinov, R. Polymorphism in Self-Assembly of Peptide-Based Beta-Hairpin Contributes to Network Morphology and Hydrogel Mechanical Rigidity. *J. Phys. Chem. B* **2015**, *119*, 482−490.
(639) Knerr, P. J.; Branco, M. C.; Nagarkar, R.; Pochan, D. J.; Schneider, J. P. Heavy Metal Ion Hydrogelation of a Self-Assembling Peptide Via Cysteinyl Chelation. *J. Mater. Chem.* **2012**, *22*, 1352−1357.
(640) Colherinhas, G.; Fileti, E. Molecular Dynamics Study of Surfactant-Like Peptide Based Nanostructures. *J. Phys. Chem. B* **2014**, *118*, 12215−12222.
(641) Smadbeck, J.; Chan, K. H.; Khoury, G. A.; Xue, B.; Robinson, R. C.; Hauser, C. A.; Floudas, C. A. De Novo Design and Experimental Characterization of Ultrashort Self-Associating Peptides. *PLoS Comput. Biol.* **2014**, *10*, e1003718.
(642) Ruan, L. P.; Luo, H. L.; Zhang, H. Y.; Xing, Z. H. Effect of Sonication on a Novel Designed Peptide. *J. Wuhan Univ. Technol., Mater. Sci. Ed.* **2013**, *28*, 622−626.
(643) Desii, A.; Chiellini, F.; Di Stefano, R.; Tine, M. R.; Solaro, R. Hydrogel Scaffolds by Self-Assembly of a Complementary Ionic Tetrapeptide. *J. Polym. Sci., Part A: Polym. Chem.* **2010**, *48*, 986−990.
(644) Bowerman, C. J.; Liyanage, W.; Federation, A. J.; Nilsson, B. L. Tuning Beta-Sheet Peptide Self-Assembly and Hydrogelation Behavior by Modification of Sequence Hydrophobicity and Aromaticity. *Biomacromolecules* **2011**, *12*, 2735−2745.
(645) Swanekamp, R. J.; Welch, J. J.; Nilsson, B. L. Proteolytic Stability of Amphipathic Peptide Hydrogels Composed of Self-Assembled Pleated Beta-Sheet or Coassembled Rippled Beta-Sheet Fibrils. *Chem. Commun.* **2014**, *50*, 10133−10136.
(646) Bowerman, C. J.; Ryan, D. M.; Nissan, D. A.; Nilsson, B. L. The Effect of Increasing Hydrophobicity on the Self-Assembly of Amphipathic Beta-Sheet Peptides. *Mol. BioSyst.* **2009**, *5*, 1058−1069.
(647) Lee, N. R.; Bowerman, C. J.; Nilsson, B. L. Effects of Varied Sequence Pattern on the Self-Assembly of Amphipathic Peptides. *Biomacromolecules* **2013**, *14*, 3267−3277.
(648) Guy, M. M.; Voyer, N. Structure and Hydrogel Formation Studies on Homologs of a Lactoglobulin-Derived Peptide. *Biophys. Chem.* **2012**, *163-164*, 1−10.
(649) Ruan, L.; Zhang, H.; Luo, H.; Liu, J.; Tang, F.; Shi, Y.-K.; Zhao, X. Designed Amphiphilic Peptide Forms Stable Nanoweb, Slowly Releases Encapsulated Hydrophobic Drug, and Accelerates Animal Hemostasis. *Proc. Natl. Acad. Sci. U. S. A.* **2009**, *106*, 5105−5110.
(650) Ruan, L. P.; Luo, H. L.; Zhang, H. Y.; Zhao, X. J. Investigation on Structure and Properties of a Novel Designed Peptide with Half-Sequence Ionic Complement. *Macromol. Res.* **2009**, *17*, 597−602.
(651) Feng, Y.; Taraban, M.; Yu, Y. B. The Effect of Ionic Strength on the Mechanical, Structural and Transport Properties of Peptide Hydrogels. *Soft Matter* **2012**, *8*, 11723−11731.
(652) Carrick, L.; Tassieri, M.; Waigh, T. A.; Aggeli, A.; Boden, N.; Bell, C.; Fisher, J.; Ingham, E.; Evans, R. M. L. The Internal Dynamic Modes of Charged Self-Assembled Peptide Fibrils. *Langmuir* **2005**, *21*, 3733−3737.
(653) Carrick, L. M.; Aggeli, A.; Boden, N.; Fisher, J.; Ingham, E.; Waigh, T. A. Effect of Ionic Strength on the Self-Assembly, Morphology and Gelation of Ph Responsive Beta-Sheet Tape-Forming Peptides. *Tetrahedron* **2007**, *63*, 7457−7467.
(654) Protopapa, E.; Ringstad, L.; Aggeli, A.; Nelson, A. Interaction of Self-Assembling Beta-Sheet Peptides with Phospholipid Monolayers: The Effect of Serine, Threonine, Glutamine and Asparagine Amino Acid Side Chains. *Electrochim. Acta* **2010**, *55*, 3368−3375.
(655) Li, D. X.; Wang, H. M.; Kong, D. L.; Yang, Z. M. Bsa-Stabilized Molecular Hydrogels of a Hydrophobic Compound. *Nanoscale* **2012**, *4*, 3047−3049.
(656) Jung, J. P.; Jones, J. L.; Cronier, S. A.; Collier, J. H. Modulating the Mechanical Properties of Self-Assembled Peptide Hydrogels Via Native Chemical Ligation. *Biomaterials* **2008**, *29*, 2143−2151.
(657) Measey, T. J.; Schweitzer-Stenner, R.; Sa, V.; Kornev, K. Anomalous Conformational Instability and Hydrogel Formation of a Cationic Class of Self-Assembling Oligopeptides. *Macromolecules* **2010**, *43*, 7800−7806.
(658) Owczarz, M.; Bolisetty, S.; Mezzenga, R.; Arosio, P. Sol-Gel Transition of Charged Fibrils Composed of a Model Amphiphilic Peptide. *J. Colloid Interface Sci.* **2015**, *437*, 244−251.
(659) Ye, Z. Y.; Zhang, H. Y.; Luo, H. L.; Wang, S. K.; Zhou, Q. H.; Du, X. P.; Tang, C. K.; Chen, L. Y.; Liu, J. P.; Shi, Y. K.; et al. Temperature and Ph Effects on Biophysical and Morphological Properties of Self-Assembling Peptide Rada16−1. *J. Pept. Sci.* **2008**, *14*, 152−162.
(660) Yokoi, H.; Kinoshita, T. Strategy for Designing Self-Assembling Peptides to Prepare Transparent Nanofiber Hydrogel at Neutral Ph. *J. Nanomater.* **2012**, *2012*, 1−9.
(661) Aulisa, L.; Dong, H.; Hartgerink, J. D. Self-Assembly of Multidomain Peptides: Sequence Variation Allows Control over Cross-Linking and Viscoelasticity. *Biomacromolecules* **2009**, *10*, 2694−2698.

DOI: 10.1021/acs.chemrev.5b00299
Chem. Rev. 2015, 115, 13165−13307

(662) Bakota, E. L.; Sensoy, O.; Ozgur, B.; Sayar, M.; Hartgerink, J. D. Self-Assembling Multidomain Peptide Fibers with Aromatic Cores. *Biomacromolecules* **2013**, *14*, 1370−1378.
(663) Jun, H. W.; Yuwono, V.; Paramonov, S. E.; Hartgerink, J. D. Enzyme-Mediated Degradation of Peptide-Amphiphile Nanofiber Networks. *Adv. Mater.* **2005**, *17*, 2612−2617.
(664) Ramachandran, S.; Tseng, Y.; Yu, Y. B. Repeated Rapid Shear-Responsiveness of Peptide Hydrogels with Tunable Shear Modulus. *Biomacromolecules* **2005**, *6*, 1316−1321.
(665) Ramachandran, S.; Taraban, M. B.; Trewhella, J.; Gryczynski, I.; Gryczynski, Z.; Yu, Y. B. Effect of Temperature During Assembly on the Structure and Mechanical Properties of Peptide-Based Materials. *Biomacromolecules* **2010**, *11*, 1502−1506.
(666) Taraban, M. B.; Ramachandran, S.; Gryczynski, I.; Gryczynski, Z.; Trewhella, J.; Yu, Y. H. B. Effects of Chain Length on Oligopeptide Hydrogelation. *Soft Matter* **2011**, *7*, 2624−2631.
(667) Cai, R.; Zhao, Y.; Ogura, K.; Tanaka, M.; Kinoshita, T.; Cai, Q. Self-Assembled Gels of Amphiphilic Sequential Peptide in Water and Organic Solvents. *Chem. Lett.* **2011**, *40*, 617−619.
(668) Paramonov, S. E.; Jun, H. W.; Hartgerink, J. D. Modulation of Peptide-Amphiphile Nanofibers Via Phospholipid Inclusions. *Biomacromolecules* **2006**, *7*, 24−26.
(669) Anderson, J. M.; Andukuri, A.; Lim, D. J.; Jun, H. W. Modulating the Gelation Properties of Self-Assembling Peptide Amphiphiles. *ACS Nano* **2009**, *3*, 3447−3454.
(670) Xu, X.-D.; Jin, Y.; Liu, Y.; Zhang, X.-Z.; Zhou, R.-X. Self-Assembly Behavior of Peptide Amphiphiles (Pas) with Different Length of Hydrophobic Alkyl Tails. *Colloids Surf., B* **2010**, *81*, 329−335.
(671) Mitra, R. N.; Das, P. K. In Situ Preparation of Gold Nanoparticles of Varying Shape in Molecular Hydrogel of Peptide Amphiphiles. *J. Phys. Chem. C* **2008**, *112*, 8159−8166.
(672) Li, Y.; Li, B. Z.; Fu, Y. T.; Lin, S. W.; Yang, Y. G. Solvent-Induced Handedness Inversion of Dipeptide Sodium Salts Derived from Alanine. *Langmuir* **2013**, *29*, 9721−9726.
(673) Tang, C. K.; Qiu, F.; Zhao, X. J. Molecular Design and Applications of Self-Assembling Surfactant-Like Peptides. *J. Nanomater.* **2013**, *2013*, 1−9.
(674) Qin, S. Y.; Xu, S. S.; Zhuo, R. X.; Zhang, X. Z. Morphology Transformation Via Ph-Triggered Self-Assembly of Peptides. *Langmuir* **2012**, *28*, 2083−2090.
(675) Yelamaggad, C. V.; Shanker, G.; Rao, R. V. R.; Rao, D. S. S.; Prasad, S. K.; Babu, V. V. S. Supramolecular Helical Fluid Columns from Self-Assembly of Homomeric Dipeptides. *Chem. - Eur. J.* **2008**, *14*, 10462−10471.
(676) Gizzi, P.; Pasc, A.; Dupuy, N.; Parant, S.; Henry, B.; Gerardin, C. Molecular Tailored Histidine-Based Complexing Surfactants: From Micelles to Hydrogels. *Eur. J. Org. Chem.* **2009**, *2009*, 3953−3963.
(677) Pasc, A.; Gizzi, P.; Dupuy, N.; Parant, S.; Ghanbaja, J.; Gerardin, C. Microscopic and Macroscopic Anisotropy in Supramolecular Hydrogels of Histidine-Based Surfactants. *Tetrahedron Lett.* **2009**, *50*, 6183−6186.
(678) Fu, X. J.; Zhang, H.; Zhou, S. K.; Liu, S. B.; Guo, F. Q.; Wang, H.; Yang, Y. J. Supramolecular Hydrogels Based on L-Phenylalanine Derivatives with a Positively Charged Terminal Group. *Helv. Chim. Acta* **2010**, *93*, 158−168.
(679) Mitra, R. N.; Das, D.; Roy, S.; Das, P. K. Structure and Properties of Low Molecular Weight Amphiphilic Peptide Hydrogelators. *J. Phys. Chem. B* **2007**, *111*, 14107−14113.
(680) Otsuka, T.; Maeda, T.; Hotta, A. Effects of Salt Concentrations of the Aqueous Peptide-Amphiphile Solutions on the Sol-Gel Transitions, the Gelation Speed, and the Gel Characteristics. *J. Phys. Chem. B* **2014**, *118*, 11537−11545.
(681) Shundo, A.; Hoshino, Y.; Higuchi, T.; Matsumoto, Y.; Penaloza, D. P., Jr.; Matsumoto, K.; Ohno, M.; Miyaji, K.; Goto, M.; Tanaka, K. Facile Microcapsule Fabrication by Spray Deposition of a Supramolecular Hydrogel. *RSC Adv.* **2014**, *4*, 36097−36100.
(682) Matsumoto, K.; Shundo, A.; Ohno, M.; Fujita, S.; Saruhashi, K.; Miyachi, N.; Miyaji, K.; Tanaka, K. Modulation of Physical Properties of Supramolecular Hydrogels Based on a Hydrophobic Core. *Phys. Chem. Chem. Phys.* **2015**, *17*, 2192−2198.
(683) Rodriguez-Llansola, F.; Miravet, J. F.; Escuder, B. A Supramolecular Hydrogel as a Reusable Heterogeneous Catalyst for the Direct Aldol Reaction. *Chem. Commun.* **2009**, 7303−7305.
(684) Berdugo, C.; Miravet, J. F.; Escuder, B. Substrate Selective Catalytic Molecular Hydrogels: The Role of the Hydrophobic Effect. *Chem. Commun.* **2013**, *49*, 10608−10610.
(685) Pal, A.; Shrivastava, S.; Dey, J. Salt, Ph and Thermoresponsive Supramolecular Hydrogel of N-(4-N-Tetradecyloxybenzoyl)-L-Carnosine. *Chem. Commun.* **2009**, 6997−6999.
(686) Pasc, A.; Akong, F. O.; Cosgun, S.; Gerardin, C. Differences between Beta-Ala and Gly-Gly in the Design of Amino Acids-Based Hydrogels. *Beilstein J. Org. Chem.* **2010**, *6*, 973−977.
(687) Koda, D.; Maruyama, T.; Minakuchi, N.; Nakashima, K.; Goto, M. Proteinase-Mediated Drastic Morphological Change of Peptide-Amphiphile to Induce Supramolecular Hydrogelation. *Chem. Commun.* **2010**, *46*, 979−981.
(688) Dehsorkhi, A.; Hamley, I. W.; Seitsonen, J.; Ruokolainen, J. Tuning Self-Assembled Nanostructures through Enzymatic Degradation of a Peptide Amphiphile. *Langmuir* **2013**, *29*, 6665−6672.
(689) Stendahl, J. C.; Rao, M. S.; Guler, M. O.; Stupp, S. I. Intermolecular Forces in the Self-Assembly of Peptide Amphiphile Nanofibers. *Adv. Funct. Mater.* **2006**, *16*, 499−508.
(690) Tovar, J. D.; Claussen, R. C.; Stupp, S. I. Probing the Interior of Peptide Amphiphile Supramolecular Aggregates. *J. Am. Chem. Soc.* **2005**, *127*, 7337−7345.
(691) Zana, R. Dimeric (Gemini) Surfactants: Effect of the Spacer Group on the Association Behavior in Aqueous Solution. *J. Colloid Interface Sci.* **2002**, *248*, 203−220.
(692) Rico, I.; Lattes, A. Formamide, a Water Substitute. 12. Krafft Temperature and Micelle Formation of Ionic Surfactants in Formamide. *J. Phys. Chem.* **1986**, *90*, 5870−5872.
(693) Brizard, A.; Dolain, C.; Huc, I.; Oda, R. Asp-Gly Based Peptides Confined at the Surface of Cationic Gemini Surfactant Aggregates. *Langmuir* **2006**, *22*, 3591−3600.
(694) Behanna, H. A.; Donners, J.; Gordon, A. C.; Stupp, S. I. Coassembly of Amphiphiles with Opposite Peptide Polarities into Nanofibers. *J. Am. Chem. Soc.* **2005**, *127*, 1193−1200.
(695) Bai, S.; Pappas, C.; Debnath, S.; Frederix, P. W. J. M.; Leckie, J.; Fleming, S.; Ulijn, R. V. Stable Emulsions Formed by Self-Assembly of Interfacial Networks of Dipeptide Derivatives. *ACS Nano* **2014**, *8*, 7005−7013.
(696) Nakayama, T.; Sakuraba, T.; Tomita, S.; Kaneko, A.; Takai, E.; Shiraki, K.; Tashiro, K.; Ishii, N.; Hasegawa, Y.; Yamada, Y.; et al. Charge-Separated Fmoc-Peptide Beta-Sheets: Sequence-Secondary Structure Relationship for Arranging Charged Side Chains on Both Sides. *Asian J. Org. Chem.* **2014**, *3*, 1182−1188.
(697) Chen, L.; McDonald, T. O.; Adams, D. J. Salt-Induced Hydrogels from Functionalised-Dipeptides. *RSC Adv.* **2013**, *3*, 8714−8720.
(698) Wall, B. D.; Tovar, J. D. Synthesis and Characterization of Pi-Conjugated Peptide-Based Supramolecular Materials. *Pure Appl. Chem.* **2012**, *84*, 1039−1045.
(699) Li, R.; Horgan, C. C.; Long, B.; Rodriguez, A. L.; Mather, L.; Barrow, C. J.; Nisbet, D. R.; Williams, R. J. Tuning the Mechanical and Morphological Properties of Self-Assembled Peptide Hydrogels Via Control over the Gelation Mechanism through Regulation of Ionic Strength and the Rate of Ph Change. *RSC Adv.* **2015**, *5*, 301−307.
(700) Shi, Y.; Wang, J.; Wang, H.; Hu, Y.; Chen, X.; Yang, Z. Glutathione-Triggered Formation of a Fmoc-Protected Short Peptide-Based Supramolecular Hydrogel. *PLoS One* **2014**, *9*, e106968.
(701) Zou, Y.; Razmkhah, K.; Chmel, N. P.; Hamley, I. W.; Rodger, A. Spectroscopic Signatures of an Fmoc-Tetrapeptide, Fmoc and Fluorene. *RSC Adv.* **2013**, *3*, 10854−10858.
(702) Du, X. W.; Li, J. F.; Gao, Y.; Kuang, Y.; Xu, B. Catalytic Dephosphorylation of Adenosine Monophosphate (AMP) to Form Supramolecular Nanofibers/hydrogels. *Chem. Commun.* **2012**, *48*, 2098−2100.

DOI: 10.1021/acs.chemrev.5b00299
Chem. Rev. 2015, 115, 13165−13307

(703) Smith, A. M.; Williams, R. J.; Tang, C.; Coppo, P.; Collins, R. F.; Turner, M. L.; Saiani, A.; Ulijn, R. V. Fmoc-Diphenylalanine Self Assembles to a Hydrogel Via a Novel Architecture Based on Pi-Pi Interlocked Beta-Sheets. *Adv. Mater.* **2008**, *20*, 37−41.
(704) Helen, W.; de Leonardis, P.; Ulijn, R. V.; Gough, J.; Tirelli, N. Mechanosensitive Peptide Gelation: Mode of Agitation Controls Mechanical Properties and Nano-Scale Morphology. *Soft Matter* **2011**, *7*, 1732−1740.
(705) Truong, W. T.; Su, Y.; Gloria, D.; Braet, F.; Thordarson, P. Dissolution and Degradation of Fmoc-Diphenylalanine Self-Assembled Gels Results in Necrosis at High Concentrations in Vitro. *Biomater. Sci.* **2015**, *3*, 298−307.
(706) Liu, Y.; Xu, X.-D.; Chen, J.-X.; Cheng, H.; Zhang, X.-Z.; Zhuo, R.-X. Surface Self-Assembly of N-Fluorenyl-9-Methoxycarbonyl Diphenylalanine on Silica Wafer. *Colloids Surf., B* **2011**, *87*, 192−197.
(707) Kim, J. H.; Nam, D. H.; Lee, Y. W.; Nam, Y. S.; Park, C. B. Self-Assembly of Metalloporphyrins into Light-Harvesting Peptide Nanofiber Hydrogels for Solar Water Oxidation. *Small* **2013**, *10*, 1272−1277.
(708) Raeburn, J.; Mendoza-Cuenca, C.; Cattoz, B. N.; Little, M. A.; Terry, A. E.; Cardoso, A. Z.; Griffiths, P. C.; Adams, D. J. The Effect of Solvent Choice on the Gelation and Final Hydrogel Properties of Fmoc-Diphenylalanine. *Soft Matter* **2015**, *11*, 927−935.
(709) Park, S. Y.; Jeong, H.; Kim, H.; Lee, J. Y.; Jang, D. J. Excited-State Proton Transfer and Geminate Recombination in Hydrogels Based on Self-Assembled Peptide Nanotubes. *J. Phys. Chem. C* **2011**, *115*, 24763−24770.
(710) Pont, G.; Chen, L.; Spiller, D. G.; Adams, D. J. The Effect of Polymer Additives on the Rheological Properties of Dipeptide Hydrogelators. *Soft Matter* **2012**, *8*, 7797−7802.
(711) Braun, H. G.; Cardoso, A. Z. Self-Assembly of Fmoc-Diphenylalanine inside Liquid Marbles. *Colloids Surf., B* **2012**, *97*, 43−50.
(712) Orbach, R.; Mironi-Harpaz, I.; Adler-Abramovich, L.; Mossou, E.; Mitchell, E. P.; Forsyth, V. T.; Gazit, E.; Seliktar, D. The Rheological and Structural Properties of Fmoc-Peptide-Based Hydrogels: The Effect of Aromatic Molecular Architecture on Self-Assembly and Physical Characteristics. *Langmuir* **2012**, *28*, 2015−2022.
(713) Berillo, D.; Mattiasson, B.; Galaev, I. Y.; Kirsebom, H. Formation of Macroporous Self-Assembled Hydrogels through Cryogelation of Fmoc-Phe-Phe. *J. Colloid Interface Sci.* **2012**, *368*, 226−230.
(714) Scott, G.; Roy, S.; Abul-Haija, Y. M.; Fleming, S.; Bai, S.; Ulijn, R. V. Pickering Stabilized Peptide Gel Particles as Tunable Microenvironments for Biocatalysis. *Langmuir* **2013**, *29*, 14321−14327.
(715) Dudukovic, N. A.; Zukoski, C. F. Nanoscale Dynamics and Aging of Fibrous Peptide-Based Gels. *J. Chem. Phys.* **2014**, *141*, 164905.
(716) Raeburn, J.; Pont, G.; Chen, L.; Cesbron, Y.; Levy, R.; Adams, D. J. Fmoc-Diphenylalanine Hydrogels: Understanding the Variability in Reported Mechanical Properties. *Soft Matter* **2012**, *8*, 1168−1174.
(717) Tang, C.; Ulijn, R. V.; Saiani, A. Effect of Glycine Substitution on Fmoc-Diphenylalanine Self-Assembly and Gelation Properties. *Langmuir* **2011**, *27*, 14438−14449.
(718) Adams, D. J.; Mullen, L. M.; Berta, M.; Chen, L.; Frith, W. J. Relationship between Molecular Structure, Gelation Behaviour and Gel Properties of Fmoc-Dipeptides. *Soft Matter* **2010**, *6*, 1971−1980.
(719) Roy, S.; Javid, N.; Frederix, P. W. J. M.; Lamprou, D. A.; Urquhart, A. J.; Hunt, N. T.; Halling, P. J.; Ulijn, R. V. Dramatic Specific-Ion Effect in Supramolecular Hydrogels. *Chem. - Eur. J.* **2012**, *18*, 11723−11731.
(720) Mu, X. J.; Eckes, K. M.; Nguyen, M. M.; Suggs, L. J.; Ren, P. Y. Experimental and Computational Studies Reveal an Alternative Supramolecular Structure for Fmoc-Dipeptide Self-Assembly. *Biomacromolecules* **2012**, *13*, 3562−3571.
(721) Fleming, S.; Frederix, P. W. J. M.; Sasselli, I. R.; Hunt, N. T.; Ulijn, R. V.; Tuttle, T. Assessing the Utility of Infrared Spectroscopy as a Structural Diagnostic Tool for Beta-Sheets in Self-Assembling Aromatic Peptide Amphiphiles. *Langmuir* **2013**, *29*, 9510−9515.
(722) Fleming, S.; Debnath, S.; Frederix, P. W. J. M.; Tuttle, T.; Ulijn, R. V. Aromatic Peptide Amphiphiles: Significance of the Fmoc Moiety. *Chem. Commun.* **2013**, *49*, 10587−10589.
(723) Chen, L.; Raeburn, J.; Sutton, S.; Spiller, D. G.; Williams, J.; Sharp, J. S.; Griffiths, P. C.; Heenan, R. K.; King, S. M.; Paul, A.; et al. Tuneable Mechanical Properties in Low Molecular Weight Gels. *Soft Matter* **2011**, *7*, 9721−9727.
(724) Wang, W. P.; Yang, Z. M.; Patanavanich, S.; Xu, B.; Chau, Y. Controlling Self-Assembly within Nanospace for Peptide Nanoparticle Fabrication. *Soft Matter* **2008**, *4*, 1617−1620.
(725) Javid, N.; Roy, S.; Zelzer, M.; Yang, Z. M.; Sefcik, J.; Ulijn, R. V. Cooperative Self-Assembly of Peptide Gelators and Proteins. *Biomacromolecules* **2013**, *14*, 4368−4376.
(726) Johnson, E. K.; Chen, L.; Kubiak, P. S.; McDonald, S. F.; Adams, D. J.; Cameron, P. J. Surface Nucleated Growth of Dipeptide Fibres. *Chem. Commun.* **2013**, *49*, 8698−8700.
(727) Adhikari, B.; Banerjee, A. Short Peptide Based Hydrogels: Incorporation of Graphene into the Hydrogel. *Soft Matter* **2011**, *7*, 9259−9266.
(728) Xie, Z. G.; Zhang, A. Y.; Ye, L.; Feng, Z. G. Synthesis and Gelation of a Series of Low-Molecular-Weight Gelators Based on Fmoc-Dipeptide in Alcoholic Solvents. *Acta Chim. Sin.* **2008**, *66*, 2620−2624.
(729) Pappas, C. G.; Abul-Haija, Y. M.; Flack, A.; Frederix, P. W. J. M.; Ulijn, R. V. Tuneable Fmoc-Phe-(4-X)-Phe-Nh2 Nanostructures by Variable Electronic Substitution. *Chem. Commun.* **2014**, *50*, 10630−10633.
(730) Eckes, K. M.; Mu, X.; Ruehle, M. A.; Ren, P.; Suggs, L. J. Beta Sheets Not Required: Combined Experimental and Computational Studies of Self-Assembly and Gelation of the Ester-Containing Analogue of an Fmoc-Dipeptide Hydrogelator. *Langmuir* **2014**, *30*, 5287−5296.
(731) Dudukovic, N. A.; Zukoski, C. F. Evidence for Equilibrium Gels of Valence-Limited Particles. *Soft Matter* **2014**, *10*, 7849−7856.
(732) Fichman, G.; Adler-Abramovich, L.; Manohar, S.; Mironi-Harpaz, I.; Guterman, T.; Seliktar, D.; Messersmith, P. B.; Gazit, E. Seamless Metallic Coating and Surface Adhesion of Self-Assembled Bioinspired Nanostructures Based on Di-(3,4-Dihydroxy-L-Phenylalanine) Peptide Motif. *ACS Nano* **2014**, *8*, 7220−7228.
(733) Milli, L.; Castellucci, N.; Tomasini, C. Turning around the L-Phe-D-Oxd Moiety for a Versatile Low-Molecularweight Gelator. *Eur. J. Org. Chem.* **2014**, *2014*, 5954−5961.
(734) Lopez-Perez, D. E.; Revilla-Lopez, G.; Hamley, I. W.; Aleman, C. Molecular Insights into Aggregates Made of Amphiphilic Fmoc-Tetrapeptides. *Soft Matter* **2013**, *9*, 11021−11032.
(735) Ou, C. W.; Zhang, J. W.; Zhang, X. L.; Yang, Z. M.; Chen, M. S. Phenothiazine as an Aromatic Capping Group to Construct a Short Peptide-Based 'Super Gelator'. *Chem. Commun.* **2013**, *49*, 1853−1855.
(736) Rodriguez, A. L.; Parish, C. L.; Nisbet, D. R.; Williams, R. J. Tuning the Amino Acid Sequence of Minimalist Peptides to Present Biological Signals Via Charge Neutralised Self Assembly. *Soft Matter* **2013**, *9*, 3915−3919.
(737) Kuang, Y.; Gao, Y.; Shi, J.; Lin, H.-C.; Xu, B. Supramolecular Hydrogels Based on the Epitope of Potassium Ion Channels. *Chem. Commun.* **2011**, *47*, 8772−8774.
(738) Hughes, M.; Frederix, P. W. J. M.; Raeburn, J.; Birchall, L. S.; Sadownik, J.; Coomer, F. C.; Lin, I. H.; Cussen, E. J.; Hunt, N. T.; Tuttle, T.; et al. Sequence/Structure Relationships in Aromatic Dipeptide Hydrogels Formed under Thermodynamic Control by Enzyme-Assisted Self-Assembly. *Soft Matter* **2012**, *8*, 5595−5602.
(739) Sadownik, J. W.; Ulijn, R. V. Locking an Oxidation-Sensitive Dynamic Peptide System in the Gel State. *Chem. Commun.* **2010**, *46*, 3481−3483.
(740) Das, A. K.; Hirst, A. R.; Ulijn, R. V. Evolving Nanomaterials Using Enzyme-Driven Dynamic Peptide Libraries (Edpl). *Faraday Discuss.* **2009**, *143*, 293−303.

DOI: 10.1021/acs.chemrev.5b00299
Chem. Rev. 2015, 115, 13165−13307

(741) Cheng, G.; Castelletto, V.; Moulton, C. M.; Newby, G. E.; Hamley, I. W. Hydrogelation and Self-Assembly of Fmoc-Tripeptides: Unexpected Influence of Sequence on Self-Assembled Fibril Structure, and Hydrogel Modulus and Anisotropy. *Langmuir* **2010**, *26*, 4990−4998.
(742) Shao, H.; Parquette, J. R. A Pi-Conjugated Hydrogel Based on an Fmoc-Dipeptide Naphthalene Diimide Semiconductor. *Chem. Commun.* **2010**, *46*, 4285−4287.
(743) Raeburn, J.; Alston, B.; Kroeger, J.; McDonald, T. O.; Howse, J. R.; Cameron, P. J.; Adams, D. J. Electrochemically-Triggered Spatially and Temporally Resolved Multi-Component Gels. *Mater. Horiz.* **2014**, *1*, 241−246.
(744) Qin, S.-Y.; Jiang, H.-F.; Peng, M.-Y.; Lei, Q.; Zhuo, R.-X.; Zhang, X.-Z. Adjustable Nanofibers Self-Assembled from an Irregular Conformational Peptide Amphiphile. *Polym. Chem.* **2015**, *6*, 519−524.
(745) Rasale, D. B.; Maity, I.; Das, A. K. In Situ Generation of Redox Active Peptides Driven by Selenoester Mediated Native Chemical Ligation. *Chem. Commun.* **2014**, *50*, 11397−11400.
(746) Debnath, S.; Roy, S.; Ulijn, R. V. Peptide Nanofibers with Dynamic Instability through Nonequilibrium Biocatalytic Assembly. *J. Am. Chem. Soc.* **2013**, *135*, 16789−16792.
(747) Muro-Small, M. L.; Chen, J.; McNeil, A. J. Dissolution Parameters Reveal Role of Structure and Solvent in Molecular Gelation. *Langmuir* **2011**, *27*, 13248−13253.
(748) Zhang, Y.; Zhou, R.; Shi, J. F.; Zhou, N.; Epstein, I. R.; Xu, B. Post-Self-Assembly Cross-Linking to Integrate Molecular Nanofibers with Copolymers in Oscillatory Hydrogels. *J. Phys. Chem. B* **2013**, *117*, 6566−6573.
(749) Wang, H.; Wang, Z.; Yi, X.; Long, J.; Liu, J.; Yang, Z. Anti-Degradation of a Recombinant Complex Protein by Incoporation in Small Molecular Hydrogels. *Chem. Commun.* **2011**, *47*, 955−957.
(750) Qin, S. Y.; Pei, Y.; Liu, X. J.; Zhuo, R. X.; Zhang, X. Z. Hierarchical Self-Assembly of a Beta-Amyloid Peptide Derivative. *J. Mater. Chem. B* **2013**, *1*, 668−675.
(751) Li, Y.; Ding, Y.; Qin, M.; Cao, Y.; Wang, W. An Enzyme-Assisted Nanoparticle Crosslinking Approach to Enhance the Mechanical Strength of Peptide-Based Supramolecular Hydrogels. *Chem. Commun.* **2013**, *49*, 8653−8655.
(752) Li, X. M.; Gao, Y. A.; Kuang, Y.; Xu, B. Enzymatic Formation of a Photoresponsive Supramolecular Hydrogel. *Chem. Commun.* **2010**, *46*, 5364−5366.
(753) Li, D. X.; Liu, J. J.; Chu, L. P.; Liu, J. F.; Yang, Z. M. A Novel Mixed-Component Molecular Hydrogel System with Excellent Stabilities. *Chem. Commun.* **2012**, *48*, 6175−6177.
(754) Qin, S. Y.; Chu, Y. F.; Tao, L.; Xu, S. S.; Li, Z. Y.; Zhuo, R. X.; Zhang, X. Z. Controllable Micro/Nanostructures Via Hierarchical Self-Assembly of Cyclopeptides. *Soft Matter* **2011**, *7*, 8635−8641.
(755) Shi, J. F.; Gao, Y.; Zhang, Y.; Pan, Y.; Xu, B. Calcium Ions to Cross-Link Supramolecular Nanofibers to Tune the Elasticity of Hydrogels over Orders of Magnitude. *Langmuir* **2011**, *27*, 14425−14431.
(756) Zhang, X. L.; Chu, X. L.; Wang, L.; Wang, H. M.; Liang, G. L.; Zhang, J. X.; Long, J. F.; Yang, Z. M. Rational Design of a Tetrameric Protein to Enhance Interactions between Self-Assembled Fibers Gives Molecular Hydrogels. *Angew. Chem., Int. Ed.* **2012**, *51*, 4388−4392.
(757) Ren, C. H.; Song, Z. J.; Zheng, W. T.; Chen, X. M.; Wang, L.; Kong, D. L.; Yang, Z. M. Disulfide Bond as a Cleavable Linker for Molecular Self-Assembly and Hydrogelation. *Chem. Commun.* **2011**, *47*, 1619−1621.
(758) Wang, J. Y.; Miao, X. M.; Fengzhao, Q. Q.; Ren, C. H.; Yang, Z. M.; Wang, L. Using a Mild Hydrogelation Process to Confer Stable Hybrid Hydrogels for Enzyme Immobilization. *RSC Adv.* **2013**, *3*, 16739−16746.
(759) Cao, W.; Zhang, X. L.; Miao, X. M.; Yang, Z. M.; Xu, H. P. Gamma-Ray-Responsive Supramolecular Hydrogel Based on a Diselenide-Containing Polymer and a Peptide. *Angew. Chem., Int. Ed.* **2013**, *52*, 6233−6237.
(760) Yang, Z. M.; Gu, H. W.; Du, J.; Gao, J. H.; Zhang, B.; Zhang, X. X.; Xu, B. Self-Assembled Hybrid Nanofibers Confer a Magneto-rheological Supramolecular Hydrogel. *Tetrahedron* **2007**, *63*, 7349−7357.
(761) Zhang, J.; Ou, C.; Shi, Y.; Wang, L.; Chen, M.; Yang, Z. Visualized Detection of Melamine in Milk by Supramolecular Hydrogelations. *Chem. Commun.* **2014**, *50*, 12873−12876.
(762) Mei, J. J.; Zhang, X. L.; Zhu, M. F.; Wang, J. N.; Wang, L.; Wang, L. Y. Barium-Triggered Beta-Sheet Formation and Hydrogelation of a Short Peptide Derivative. *RSC Adv.* **2014**, *4*, 1193−1196.
(763) Kuang, Y.; Gao, Y.; Xu, B. Supramolecular Hydrogelators of N-Terminated Dipeptides Selectively Inhibit Cancer Cells. *Chem. Commun.* **2011**, *47*, 12625−12627.
(764) Wallace, M.; Cardoso, A. Z.; Frith, W. J.; Iggo, J. A.; Adams, D. J. Magnetically Aligned Supramolecular Hydrogels. *Chem. - Eur. J.* **2014**, *20*, 16484−16487.
(765) Colquhoun, C.; Draper, E. R.; Eden, E. G. B.; Cattoz, B. N.; Morris, K. L.; Chen, L.; McDonald, T. O.; Terry, A. E.; Griffiths, P. C.; Serpell, L. C.; et al. The Effect of Self-Sorting and Co-Assembly on the Mechanical Properties of Low Molecular Weight Hydrogels. *Nanoscale* **2014**, *6*, 13719−13725.
(766) Houton, K. A.; Morris, K. L.; Chen, L.; Schmidtmann, M.; Jones, J. T. A.; Serpell, L. C.; Lloyd, G. O.; Adams, D. J. On Crystal Versus Fiber Formation in Dipeptide Hydrogelator Systems. *Langmuir* **2012**, *28*, 9797−9806.
(767) Morris, K. L.; Chen, L.; Raeburn, J.; Sellick, O. R.; Cotanda, P.; Paul, A.; Griffiths, P. C.; King, S. M.; O'Reilly, R. K.; Serpell, L. C.; et al. Chemically Programmed Self-Sorting of Gelator Networks. *Nat. Commun.* **2013**, *4*, 1480.
(768) Cardoso, A. Z.; Alvarez, A. E. A.; Cattoz, B. N.; Griffiths, P. C.; King, S. M.; Frith, W. J.; Adams, D. J. The Influence of the Kinetics of Self-Assembly on the Properties of Dipeptide Hydrogels. *Faraday Discuss.* **2013**, *166*, 101−116.
(769) Chen, L.; Revel, S.; Morris, K.; Serpell, L. C.; Adams, D. J. Effect of Molecular Structure on the Properties of Naphthalene-Dipeptide Hydrogelators. *Langmuir* **2010**, *26*, 13466−13471.
(770) Morris, K. L.; Chen, L.; Rodger, A.; Adams, D. J.; Serpell, L. C. Structural Determinants in a Library of Low Molecular Weight Gelators. *Soft Matter* **2015**, *11*, 1174−1181.
(771) Rasale, D. B.; Maity, I.; Das, A. K. Lipase Catalyzed Inclusion of Gastrodigenin for the Evolution of Blue Light Emitting Peptide Nanofibers. *Chem. Commun.* **2014**, *50*, 8685−8688.
(772) Jones, S. L.; Wong, K. H.; Thordarson, P.; Ladouceur, F. Self-Assembling Electroactive Hydrogels for Flexible Display Technology. *J. Phys-condens. Mater.* **2010**, *22*, 1−7.
(773) Bhattacharjee, S.; Bhattacharya, S. Phthalate Mediated Hydrogelation of a Pyrene Based System: A Novel Scaffold for Shape-Persistent, Self-Healing Luminescent Soft Material. *J. Mater. Chem. A* **2014**, *2*, 17889−17898.
(774) Mahajan, S. S.; Paranji, R.; Mehta, R.; Lyon, R. P.; Atkins, W. M. A Glutathione-Based Hydrogel and Its Site-Selective Interactions with Water. *Bioconjugate Chem.* **2005**, *16*, 1019−1026.
(775) Li, J. W.; Carnall, J. M. A.; Stuart, M. C. A.; Otto, S. Hydrogel Formation Upon Photoinduced Covalent Capture of Macrocycle Stacks from Dynamic Combinatorial Libraries. *Angew. Chem., Int. Ed.* **2011**, *50*, 8384−8386.
(776) Tena-Solsona, M.; Alonso-de Castro, S.; Miravet, J. F.; Escuder, B. Co-Assembly of Tetrapeptides into Complex Ph-Responsive Molecular Hydrogel Networks. *J. Mater. Chem. B* **2014**, *2*, 6192−6197.
(777) Wu, Z. D.; Tan, M.; Chen, X. M.; Yang, Z. M.; Wang, L. Molecular Hydrogelators of Peptoid-Peptide Conjugates with Superior Stability against Enzyme Digestion. *Nanoscale* **2012**, *4*, 3644−3646.
(778) Miao, X. M.; Cao, W.; Zheng, W. T.; Wang, J. Y.; Zhang, X. L.; Gao, J.; Yang, C. B.; Kong, D. L.; Xu, H. P.; Wang, L.; et al. Switchable Catalytic Activity: Selenium-Containing Peptides with Redox-Controllable Self-Assembly Properties. *Angew. Chem., Int. Ed.* **2013**, *52*, 7781−7785.
(779) Ikeda, M.; Tanida, T.; Yoshii, T.; Hamachi, I. Rational Molecular Design of Stimulus-Responsive Supramolecular Hydrogels Based on Dipeptides. *Adv. Mater.* **2011**, *23*, 2819−2822.

DOI: 10.1021/acs.chemrev.5b00299
Chem. Rev. 2015, 115, 13165−13307

(780) Zhang, C.; Liu, C.; Xue, X.; Zhang, X.; Huo, S.; Jiang, Y.; Chen, W.-Q.; Zou, G.; Liang, X.-J. Salt-Responsive Self-Assembly of Luminescent Hydrogel with Intrinsic Gelation-Enhanced Emission. *ACS Appl. Mater. Interfaces* **2014**, *6*, 757−762.
(781) Abul-Haija, Y. M.; Roy, S.; Frederix, P.; Javid, N.; Jayawarna, V.; Ulijn, R. V. Biocatalytically Triggered Co-Assembly of Two-Component Core/Shell Nanofibers. *Small* **2014**, *10*, 973−979.
(782) Bai, S.; Debnath, S.; Gibson, K.; Schlicht, B.; Bayne, L.; Zagnoni, M.; Ulijn, R. V. Biocatalytic Self-Assembly of Nanostructured Peptide Microparticles Using Droplet Microfluidics. *Small* **2014**, *10*, 285−293.
(783) Zhang, J. W.; Gao, J.; Chen, M. S.; Yang, Z. M. Using Phosphatases to Generate Self-Assembled Nanostructures and Their Applications. *Antioxid. Redox Signaling* **2014**, *20*, 2179−2190.
(784) Doran, T. M.; Ryan, D. M.; Nilsson, B. L. Reversible Photocontrol of Self-Assembled Peptide Hydrogel Viscoelasticity. *Polym. Chem.* **2014**, *5*, 241−248.
(785) Qiu, Z. J.; Yu, H. T.; Li, J. B.; Wang, Y.; Zhang, Y. Spiropyran-Linked Dipeptide Forms Supramolecular Hydrogel with Dual Responses to Light and to Ligand-Receptor Interaction. *Chem. Commun.* **2009**, 3342−3344.
(786) Huang, Y. C.; Qiu, Z. J.; Xu, Y. M.; Shi, J. F.; Lin, H. K.; Zhang, Y. Supramolecular Hydrogels Based on Short Peptides Linked with Conformational Switch. *Org. Biomol. Chem.* **2011**, *9*, 2149−2155.
(787) Seliktar, D. Designing Cell-Compatible Hydrogels for Biomedical Applications. *Science* **2012**, *336*, 1124−1128.
(788) Ogawa, Y.; Yoshiyama, C.; Kitaoka, T. Helical Assembly of Azobenzene-Conjugated Carbohydrate Hydrogelators with Specific Affinity for Lectins. *Langmuir* **2012**, *28*, 4404−4412.
(789) Lee, S.; Oh, S.; Lee, J.; Malpani, Y.; Jung, Y. S.; Kang, B.; Lee, J. Y.; Ozasa, K.; Isoshima, T.; Lee, S. Y.; et al. Stimulus-Responsive Azobenzene Supramolecules: Fibers, Gels, and Hollow Spheres. *Langmuir* **2013**, *29*, 5869−5877.
(790) Lin, Y. Y.; Qiao, Y.; Tang, P. F.; Li, Z. B.; Huang, J. B. Controllable Self-Assembled Laminated Nanoribbons from Dipeptide-Amphiphile Bearing Azobenzene Moiety. *Soft Matter* **2011**, *7*, 2762−2769.
(791) Matsuzawa, Y.; Tamaoki, N. Photoisomerization of Azobenzene Units Controls the Reversible Dispersion and Reorganization of Fibrous Self-Assembled Systems. *J. Phys. Chem. B* **2010**, *114*, 1586−1590.
(792) Chen, C. S.; Xu, X. D.; Li, S. Y.; Zhuo, R. X.; Zhang, X. Z. Photo-Switched Self-Assembly of a Gemini Alpha-Helical Peptide into Supramolecular Architectures. *Nanoscale* **2013**, *5*, 6270−6274.
(793) Mukai, M.; Minamikawa, H.; Aoyagi, M.; Asakawa, M.; Shimizu, T.; Kogiso, M. A Hydro/Organo/Hybrid Gelator: A Peptide Lipid with Turning Aspartame Head Groups. *J. Colloid Interface Sci.* **2013**, *395*, 154−160.
(794) Bai, S.; Debnath, S.; Javid, N.; Frederix, P. W. J. M.; Fleming, S.; Pappas, C.; Ulijn, R. V. Differential Self-Assembly and Tunable Emission of Aromatic Peptide Bola-Amphiphiles Containing Perylene Bisimide in Polar Solvents Including Water. *Langmuir* **2014**, *30*, 7576−7584.
(795) Maity, I.; Rasale, D. B.; Das, A. K. Exploiting a Self-Assembly Driven Dynamic Nanostructured Library. *RSC Adv.* **2013**, *3*, 6395−6400.
(796) Makarevic, J.; Jokic, M.; Frkanec, L.; Caplar, V.; Vujicic, N. S.; Zinic, M. Oxalyl Retro-Peptide Gelators. Synthesis, Gelation Properties and Stereochemical Effects. *Beilstein J. Org. Chem.* **2010**, *6*, 945−959.
(797) Deechongkit, S.; Powers, E. T.; You, S. L.; Kelly, J. W. Controlling the Morphology of Cross Beta-Sheet Assemblies by Rational Design. *J. Am. Chem. Soc.* **2005**, *127*, 8562−8570.
(798) Sanders, A. M.; Dawidczyk, T. J.; Katz, H. E.; Tovar, J. D. Peptide-Based Supramolecular Semiconductor Nanomaterials Via Pd-Catalyzed Solid-Phase "Dimerizations". *ACS Macro Lett.* **2012**, *1*, 1326−1329.
(799) Wall, B. D.; Diegelmann, S. R.; Zhang, S. M.; Dawidczyk, T. J.; Wilson, W. L.; Katz, H. E.; Mao, H. Q.; Tovar, J. D. Aligned Macroscopic Domains of Optoelectronic Nanostructures Prepared Via Shear-Flow Assembly of Peptide Hydrogels. *Adv. Mater.* **2011**, *23*, 5009−5014.
(800) Stone, D. A.; Hsu, L.; Stupp, S. I. Self-Assembling Quinquethiophene-Oligopeptide Hydrogelators. *Soft Matter* **2009**, *5*, 1990−1993.
(801) Newkome, G. R.; He, E. F.; Moorefield, C. N. Supra-supermolecules with Novel Properties: Metallodendrimers. *Chem. Rev.* **1999**, *99*, 1689−1746.
(802) Sieminski, A. L.; Semino, C. E.; Gong, H.; Kamm, R. D. Primary Sequence of Ionic Self-assembling Peptide Gels Affects Endothelial Cell Adhesion and Capillary Morphogenesis. *J. Biomed. Mater. Res., Part A* **2008**, *87A*, 494−504.
(803) Ryadnov, M. G.; Woolfson, D. N. Map Peptides: Programming the Self-Assembly of Peptide-Based Mesoscopic Matrices. *J. Am. Chem. Soc.* **2005**, *127*, 12407−12415.
(804) Li, W.; Li, J. F.; Lee, M. Fabrication of Artificial Toroid Nanostructures by Modified Beta-Sheet Peptides. *Chem. Commun.* **2013**, *49*, 8238−8240.
(805) Duan, P. F.; Qin, L.; Zhu, X. F.; Liu, M. H. Hierarchical Self-Assembly of Amphiphilic Peptide Dendrons: Evolution of Diverse Chiral Nanostructures through Hydrogel Formation over a Wide Ph Range. *Chem. - Eur. J.* **2011**, *17*, 6389−6395.
(806) Wang, W. P.; Chau, Y. Efficient and Facile Formation of Two-Component Nanoparticles Via Aromatic Moiety Directed Self-Assembly. *Chem. Commun.* **2011**, *47*, 10224−10226.
(807) Das, A. K.; Banerjee, A. Self-Assembling Synthetic Oligopeptide-Based Gelators. *Macromol. Symp.* **2006**, *241*, 14−22.
(808) Maity, S.; Kumar, P.; Haldar, D. Sonication-Induced Instant Amyloid-Like Fibril Formation and Organogelation by a Tripeptide. *Soft Matter* **2011**, *7*, 5239−5245.
(809) Castellucci, N.; Angelici, G.; Falini, G.; Monari, M.; Tomasini, C. L-Phe-D-Oxd: A Privileged Scaffold for the Formation of Supramolecular Materials. *Eur. J. Org. Chem.* **2011**, *2011*, 3082−3088.
(810) Ke, D. M.; Zhan, C. L.; Li, X.; Wang, X.; Zeng, Y.; Yao, J. N. Ultrasound-Induced Modulations of Tetrapeptide Hierarchical 1-D Self-Assembly and Underlying Molecular Structures Via Sonocrystallization. *J. Colloid Interface Sci.* **2009**, *337*, 54−60.
(811) Konda, M.; Maity, I.; Rasale, D. B.; Das, A. K. A New Class of Phase-Selective Synthetic Beta-Amino Acid Based Peptide Gelator: From Mechanistic Aspects to Oil Spill Recovery. *ChemPlusChem* **2014**, *79*, 1482−1488.
(812) Yuran, S.; Razvag, Y.; Reches, M. Coassembly of Aromatic Dipeptides into Biomolecular Necklaces. *ACS Nano* **2012**, *6*, 9559−9566.
(813) Xie, Z. G.; Zhang, A. Y.; Ye, L.; Wang, X.; Feng, Z. G. Shear-Assisted Hydrogels Based on Self-Assembly of Cyclic Dipeptide Derivatives. *J. Mater. Chem.* **2009**, *19*, 6100−6102.
(814) Hoshizawa, H.; Minemura, Y.; Yoshikawa, K.; Suzuki, M.; Hanabusa, K. Thixotropic Hydrogelators Based on a Cyclo(Dipeptide) Derivative. *Langmuir* **2013**, *29*, 14666−14673.
(815) Qin, S.; Wang, Q.; Pei, Y.; Peng, M.; Zhuo, R.; Zhang, X. Novel Cyclopeptide Bolaamphiphile for Constructing Supramolecular Nanotubes. *Chin. J. Chem.* **2014**, *32*, 22−26.
(816) Elgersma, R. C.; Meijneke, T.; de Jong, R.; Brouwer, A. J.; Posthuma, G.; Rijkers, D. T. S.; Liskamp, R. M. J. Synthesis and Structural Investigations of N-Alkylated Beta-Peptidosulfonamide-Peptide Hybrids of the Amyloidogenic Amylin(20−29) Sequence: Implications of Supramolecular Folding for the Design of Peptide-Based Bionanomaterials. *Org. Biomol. Chem.* **2006**, *4*, 3587−3597.
(817) Mba, M.; Moretto, A.; Armelao, L.; Crisma, M.; Toniolo, C.; Maggini, M. Synthesis and Self-Assembly of Oligo(P-Phenyleneviny-lene) Peptide Conjugates in Water. *Chem. - Eur. J.* **2011**, *17*, 2044−2047.
(818) Zou, R.; Wang, Q.; Wu, J.; Wu, J.; Schmuck, C.; Tian, H. Peptide Self-Assembly Triggered by Metal Ions. *Chem. Soc. Rev.* **2015**, *44*, 5200−5219.
(819) Godeau, G.; Barthelemy, P. Glycosyl-Nucleoside Lipids as Low-Molecular-Weight Gelators. *Langmuir* **2009**, *25*, 8447−8450.

DOI: 10.1021/acs.chemrev.5b00299
Chem. Rev. 2015, 115, 13165−13307

(820) Patwa, A.; Labille, J.; Bottero, J.-Y.; Thiery, A.; Barthelemy, P. Decontamination of Nanoparticles from Aqueous Samples Using Supramolecular Gels. *Chem. Commun.* **2015**, *51*, 2547−2550.
(821) Park, S. M.; Shen, Y.; Kim, B. H. Water Gelation Abilities of Alkylbenzyltriazole-Appended 2 '-Deoxyribonucleoside and Ribonucleoside. *Org. Biomol. Chem.* **2007**, *5*, 610−612.
(822) Park, S. M.; Kim, B. H. Ultrasound-Triggered Water Gelation with a Modified Nucleoside. *Soft Matter* **2008**, *4*, 1995−1997.
(823) Pan, D.; Sun, J.; Jin, H.; Li, Y.; Li, L.; Wu, Y.; Zhang, L.; Yang, Z. Supramolecular Assemblies of Novel Aminonucleoside Phospholipids and Their Bonding to Nucleic Acids. *Chem. Commun.* **2015**, *51*, 469−472.
(824) Skilling, K. J.; Ndungu, A.; Kellam, B.; Ashford, M.; Bradshaw, T. D.; Marlow, M. Gelation Properties of Self-Assembling N-Acyl Modified Cytidine Derivatives. *J. Mater. Chem. B* **2014**, *2*, 8412−8417.
(825) Serpell, C. J.; Barlog, M.; Basu, K.; Fakhoury, J. F.; Bazzi, H. S.; Sleiman, H. F. Nucleobase Peptide Amphiphiles. *Mater. Horiz.* **2014**, *1*, 348−354.
(826) Sreenivasachary, N.; Lehn, J. M. Gelation-Driven Component Selection in the Generation of Constitutional Dynamic Hydrogels Based on Guanine-Quartet Formation. *Proc. Natl. Acad. Sci. U. S. A.* **2005**, *102*, 5938−5943.
(827) Setnicka, V.; Urbanova, M.; Volka, K.; Nampally, S.; Lehn, J. M. Investigation of Guanosine-Quartet Assemblies by Vibrational and Electronic Circular Dichroism Spectroscopy, a Novel Approach for Studying Supramolecular Entities. *Chem. - Eur. J.* **2006**, *12*, 8735−8743.
(828) Buhler, E.; Sreenivasachary, N.; Candau, S. J.; Lehn, J. M. Modulation of the Supramolecular Structure of G-Quartet Assemblies by Dynamic Covalent Decoration. *J. Am. Chem. Soc.* **2007**, *129*, 10058−10059.
(829) Setnicka, V.; Novy, J.; Bohm, S.; Sreenivasachary, N.; Urbanova, M.; Volka, K. Molecular Structure of Guanine-Quartet Supramolecular Assemblies in a Gel-State Based on a Dft Calculation of Infrared and Vibrational Circular Dichroism Spectra. *Langmuir* **2008**, *24*, 7520−7527.
(830) Wang, Y. J.; Desbat, B.; Manet, S.; Aime, C.; Labrot, T.; Oda, R. Aggregation Behaviors of Gemini Nucleotide at the Air-Water Interface and in Solutions Induced by Adenine-Uracil Interaction. *J. Colloid Interface Sci.* **2005**, *283*, 555−564.
(831) Buerkle, L. E.; Li, Z.; Jamieson, A. M.; Rowan, S. J. Tailoring the Properties of Guanosine-Based Supramolecular Hydrogels. *Langmuir* **2009**, *25*, 8833−8840.
(832) Li, Z.; Buerkle, L. E.; Orseno, M. R.; Streletzky, K. A.; Seifert, S.; Jamieson, A. M.; Rowan, S. J. Structure and Gelation Mechanism of Tunable Guanosine-Based Supramolecular Hydrogels. *Langmuir* **2010**, *26*, 10093−10101.
(833) Peters, G. M.; Skala, L. P.; Plank, T. N.; Hyman, B. J.; Reddy, G. N. M.; Marsh, A.; Brown, S. P.; Davis, J. T. A G(4)Center Dot K+ Hydrogel Stabilized by an Anion. *J. Am. Chem. Soc.* **2014**, *136*, 12596−12599.
(834) Dash, J.; Patil, A. J.; Das, R. N.; Dowdall, F. L.; Mann, S. Supramolecular Hydrogels Derived from Silver Ion-Mediated Self-Assembly of 5 '-Guanosine Monophosphate. *Soft Matter* **2011**, *7*, 8120−8126.
(835) Kumar, A.; Gupta, S. K. 5 '-Guanosine Monophosphate Mediated Biocompatible Porous Hydrogel of Beta-Feooh-Viscoelastic Behavior, Loading, and Release Capabilities of Freeze-Dried Gel. *J. Phys. Chem. B* **2014**, *118*, 10543−10551.
(836) Yu, Z. X.; Bai, B. L.; Wang, H. T.; Ran, X.; Jin, G. B.; Sun, J.; Zhao, C. X.; Li, M. Morphology-Tuning by Changing the Composition of a Binary Hydrogel Comprising Thymidine and Melamine. *Mater. Sci. Eng., C* **2011**, *31*, 880−884.
(837) Seela, F.; Pujari, S. S.; Schafer, A. H. Hydrogelation and Spontaneous Fiber Formation of 8-Aza-7-Deazaadenine Nucleoside 'Click' Conjugates. *Tetrahedron* **2011**, *67*, 7418−7425.
(838) Abet, V.; Rodriguez, R. Guanosine and Isoguanosine Derivatives for Supramolecular Devices. *New J. Chem.* **2014**, *38*, 5122−5128.
(839) Adhikari, B.; Shah, A.; Kraatz, H.-B. Self-Assembly of Guanosine and Deoxy-Guanosine into Hydrogels: Monovalent Cation Guided Modulation of Gelation, Morphology and Self-Healing Properties. *J. Mater. Chem. B* **2014**, *2*, 4802−4810.
(840) Yuan, D.; Du, X.; Shi, J.; Zhou, N.; Zhou, J.; Xu, B. Mixing Biomimetic Heterodimers of Nucleopeptides to Generate Biocompatible and Biostable Supramolecular Hydrogels. *Angew. Chem., Int. Ed.* **2015**, *54*, 5705−5708.
(841) Bao, C. Y.; Lu, R.; Jin, M.; Xue, P. C.; Tan, C. H.; Zhao, Y. Y.; Liu, G. F. Synthesis, Self-Assembly and Characterization of a New Glucoside-Type Hydrogel Having a Schiff Base on the Aglycon. *Carbohydr. Res.* **2004**, *339*, 1311−1316.
(842) Bao, C. Y.; Lu, R.; Jin, M.; Xue, P. C.; Tan, C. H.; Zhao, Y. Y.; Liu, G. O. Synthesis and Characterization of Nanostructural Hydrogel and Template for Cds Nanofibers. *J. Nanosci. Nanotechnol.* **2004**, *4*, 1045−1051.
(843) Bao, C. Y.; Lu, R.; Xue, P. C.; Jin, M.; Tan, C. H.; Liu, G. F.; Zhao, Y. Y. Generation of Cds Nano-Necklaces and Nis Nanotubes Templated by Sugar-Appended Hydrogel. *J. Nanosci. Nanotechnol.* **2006**, *6*, 807−812.
(844) John, G.; Jung, J. H.; Masuda, M.; Shimizu, T. Unsaturation Effect on Gelation Behavior of Aryl Glycolipids. *Langmuir* **2004**, *20*, 2060−2065.
(845) Kiyonaka, S.; Sada, K.; Yoshimura, I.; Shinkai, S.; Kato, N.; Hamachi, I. Semi-Wet Peptide/Protein Array Using Supramolecular Hydrogel. *Nat. Mater.* **2004**, *3*, 58−64.
(846) Matsumoto, S.; Yamaguchi, S.; Wada, A.; Matsui, T.; Ikeda, M.; Hamachi, I. Photo-Responsive Gel Droplet as a Nano- or Pico-Litre Container Comprising a Supramolecular Hydrogel. *Chem. Commun.* **2008**, 1545−1547.
(847) Zhou, S. L.; Matsumoto, S.; Tian, H. D.; Yamane, H.; Ojida, A.; Kiyonaka, S.; Hamachi, I. Ph-Responsive Shrinkage/Swelling of a Supramolecular Hydrogel Composed of Two Small Amphiphilic Molecules. *Chem. - Eur. J.* **2005**, *11*, 1130−1136.
(848) Srivastava, A.; Ghorai, S.; Bhattacharjya, A.; Bhattacharya, S. A Tetrameric Sugar-Based Azobenzene That Gels Water at Various Ph Values and in the Presence of Salts. *J. Org. Chem.* **2005**, *70*, 6574−6582.
(849) Jung, J. H.; Rim, J. A.; Han, W. S.; Lee, S. J.; Lee, Y. J.; Cho, E. J.; Kim, J. S.; Ji, Q. M.; Shimizu, T. Hydrogel Behavior of a Sugar-Based Gelator by Introduction of an Unsaturated Moiety as a Hydrophobic Group. *Org. Biomol. Chem.* **2006**, *4*, 2033−2038.
(850) Jung, J. H.; Rim, J. A.; Cho, E. J.; Lee, S. J.; Jeong, I. Y.; Kameda, N.; Masuda, M.; Shimizu, T. Stabilization of an Asymmetric Bolaamphiphilic Sugar-Based Crown Ether Hydrogel by Hydrogen Bonding Interaction and Its Sol-Gel Transcription. *Tetrahedron* **2007**, *63*, 7449−7456.
(851) Jung, S. H.; Kim, E.; Lee, S. J.; Lee, C. G.; Lee, S. S.; Jung, J. H. Morphological Control of Silica Nanomaterials Using Sugar-Based Hydrogel with Different Anions. *Bull. Korean Chem. Soc.* **2008**, *29*, 1630−1632.
(852) Wang, G. J.; Cheuk, S.; Williams, K.; Sharma, V.; Dakessian, L.; Thorton, Z. Synthesis and Characterization of Monosaccharide Lipids as Novel Hydrogelators. *Carbohydr. Res.* **2006**, *341*, 705−716.
(853) Goyal, N.; Mangunuru, H. P. R.; Parikh, B.; Shrestha, S.; Wang, G. Synthesis and Characterization of Ph Responsive D-Glucosamine Based Molecular Gelators. *Beilstein J. Org. Chem.* **2014**, *10*, 3111−3121.
(854) Wang, G. J.; Cheuk, S.; Yang, H.; Goyal, N.; Reddy, P. V. N.; Hopkinson, B. Synthesis and Characterization of Monosaccharide-Derived Carbamates as Low-Molecular-Weight Gelators. *Langmuir* **2009**, *25*, 8696−8705.
(855) Goyal, N.; Cheuk, S.; Wang, G. J. Synthesis and Characterization of D-Glucosamine-Derived Low Molecular Weight Gelators. *Tetrahedron* **2010**, *66*, 5962−5971.
(856) Avalos, M.; Babiano, R.; Cintas, P.; Gomez-Carretero, A.; Jimenez, J. L.; Lozano, M.; Ortiz, A. L.; Palacios, J. C.; Pinazo, A. A Family of Hydrogels Based on Ureido-Linked Aminopolyol-Derived Amphiphiles and Bolaamphiphiles: Synthesis, Gelation under Thermal

DOI: 10.1021/acs.chemrev.5b00299
Chem. Rev. 2015, 115, 13165−13307

and Sonochemical Stimuli, and Mesomorphic Characterization. *Chem. - Eur. J.* **2008**, *14*, 5656−5669.
(857) Cui, J. X.; Zheng, J.; Qiao, W. Q.; Wan, X. H. Solvent-Tuned Multiple Self-Assembly of a New Sugar-Appended Gelator. *J. Colloid Interface Sci.* **2008**, *326*, 267−274.
(858) Munenobu, K.; Hase, T.; Oyoshi, T.; Yamanaka, M. Supramolecular Gel Electrophoresis of Acidic Native Proteins. *Anal. Chem.* **2014**, *86*, 9924−9929.
(859) Sako, Y.; Takaguchi, Y. A Photo-Responsive Hydrogelator Having Gluconamides at Its Peripheral Branches. *Org. Biomol. Chem.* **2008**, *6*, 3843−3847.
(860) Kameta, N.; Yoshida, K.; Masuda, M.; Shimizu, T. Supramolecular Nanotube Hydrogels: Remarkable Resistance Effect of Confined Proteins to Denaturants. *Chem. Mater.* **2009**, *21*, 5892−5898.
(861) Kameta, N.; Masuda, M.; Shimizu, T. Soft Nanotube Hydrogels Functioning as Artificial Chaperones. *ACS Nano* **2012**, *6*, 5249−5258.
(862) Kowalczuk, J.; Jarosz, S.; Tritt-Goc, J. Characterization of Low Molecular-Weight Gelator Methyl-4,6-O-(P-Nitrobenzylidene)-Alpha-D-Glucopyranoside Hydrogels and Water Diffusion in Their Networks. *Tetrahedron* **2009**, *65*, 9801−9806.
(863) Yang, M. N.; Yan, N.; He, G.; Liu, T. H.; Fang, Y. Synthesis and Gelation Behavior of a Pyrene-Containing Glucose Derivative. *Acta Phys.-chim. Sin.* **2009**, *25*, 1040−1046.
(864) Chen, Q.; Lv, Y. X.; Zhang, D. Q.; Zhang, G. X.; Liu, C. Y.; Zhu, D. B. Cysteine and Ph-Responsive Hydrogel Based on a Saccharide Derivative with an Aldehyde Group. *Langmuir* **2010**, *26*, 3165−3168.
(865) Birchall, L. S.; Roy, S.; Jayawarna, V.; Hughes, M.; Irvine, E.; Okorogheye, G. T.; Saudi, N.; De Santis, E.; Tuttle, T.; Edwards, A. A.; et al. Exploiting Ch-Pi Interactions in Supramolecular Hydrogels of Aromatic Carbohydrate Amphiphiles. *Chem. Sci.* **2011**, *2*, 1349−1355.
(866) Pfannemuller, B.; Welte, W. Amphiphilic Properties of Synthetic Glycolipids Based on Amide Linkages 0.1. Electron-Microscopic Studies on Aqueous Gels. *Chem. Phys. Lipids* **1985**, *37*, 227−240.
(867) Buerkle, L. E.; Galleguillos, R.; Rowan, S. J. Nonionic Surfactant-Induced Stabilization and Tailorability of Sugar-Amphiphile Hydrogels. *Soft Matter* **2011**, *7*, 6984−6990.
(868) Capicciotti, C. J.; Leclere, M.; Perras, F. A.; Bryce, D. L.; Paulin, H.; Harden, J.; Liu, Y.; Ben, R. N. Potent Inhibition of Ice Recrystallization by Low Molecular Weight Carbohydrate-Based Surfactants and Hydrogelators. *Chem. Sci.* **2012**, *3*, 1408−1416.
(869) Ochi, R.; Nishida, T.; Ikeda, M.; Hamachi, I. Design of Peptide-Based Bolaamphiphiles Exhibiting Heat-Set Hydrogelation Via Retro-Diels-Alder Reaction. *J. Mater. Chem. B* **2014**, *2*, 1464−1469.
(870) Nandi, S.; Altenbach, H. J.; Jakob, B.; Lange, K.; Ihizane, R.; Schneider, M. P.; Gun, U.; Mayer, A. Amphiphiles Based on D-Glucose: Efficient Low Molecular Weight Gelators. *Org. Lett.* **2012**, *14*, 3826−3829.
(871) Ochi, R.; Kurotani, K.; Ikeda, M.; Kiyonaka, S.; Hamachi, I. Supramolecular Hydrogels Based on Bola-Amphiphilic Glycolipids Showing Color Change in Response to Glycosidases. *Chem. Commun.* **2013**, *49*, 2115−2117.
(872) Rao, H. S. P.; Kamalraj, M.; Swain, J.; Mishra, A. K. Characterization and Phase Transition Study of a Versatile Molecular Gel from a Glucose-Triazole-Hydrogenated Cardanol Conjugate. *RSC Adv.* **2014**, *4*, 12175−12181.
(873) Dhruv, H. D.; Draper, M. A.; Britt, D. W. Role of Lactose in Modifying Gel Transition Temperature and Morphology of Self-Assembled Hydrogels. *Chem. Mater.* **2005**, *17*, 6239−6245.
(874) Acharya, G.; Park, K.; Thompson, D. H. Synthesis and Evaluation of Alpha-Cyclodextrin-Aidonamide Conjugates for D-Glucose Recognition. *J. Drug Delivery Sci. Technol.* **2006**, *16*, 45−48.
(875) Clemente, M. J.; Fitremann, J.; Mauzac, M.; Serrano, J. L.; Oriol, L. Synthesis and Characterization of Maltose-Based Amphiphiles as Supramolecular Hydrogelators. *Langmuir* **2011**, *27*, 15236−15247.
(876) Clemente, M. J.; Romero, P.; Serrano, J. L.; Fitremann, J.; Oriol, L. Supramolecular Hydrogels Based on Glycoamphiphiles: Effect of the Disaccharide Polar Head. *Chem. Mater.* **2012**, *24*, 3847−3858.
(877) Clemente, M. J.; Tejedor, R. M.; Romero, P.; Fitremann, J.; Oriol, L. Maltose-Based Gelators Having Azobenzene as Light-Sensitive Unit. *RSC Adv.* **2012**, *2*, 11419−11431.
(878) Ide, K.; Sato, T.; Aoi, J.; Do, H.; Kobayashi, K.; Honda, Y.; Kirimura, K. L-Menthyl Alpha-Maltoside as a Novel Low-Molecular-Weight Gelator. *Chem. Lett.* **2013**, *42*, 657−659.
(879) Mathiselvam, M.; Loganathan, D.; Varghese, B. Synthesis and Characterization of Thiourea- and Urea-Linked Glycolipids as Low-Molecular-Weight Hydrogelators. *RSC Adv.* **2013**, *3*, 14528−14542.
(880) Hern, D. L.; Hubbell, J. A. Incorporation of Adhesion Peptides into Nonadhesive Hydrogels Useful for Tissue Resurfacing. *J. Biomed. Mater. Res.* **1998**, *39*, 266−276.
(881) Rowley, J. A.; Madlambayan, G.; Mooney, D. J. Alginate Hydrogels as Synthetic Extracellular Matrix Materials. *Biomaterials* **1999**, *20*, 45−53.
(882) Burdick, J. A.; Anseth, K. S. Photoencapsulation of Osteoblasts in Injectable Rgd-Modified Peg Hydrogels for Bone Tissue Engineering. *Biomaterials* **2002**, *23*, 4315−4323.
(883) Gao, Y.; Long, M. J. C.; Shi, J.; Hedstrom, L.; Xu, B. Using Supramolecular Hydrogels to Discover the Interactions between Proteins and Molecular Nanofibers of Small Molecules. *Chem. Commun.* **2012**, *48*, 8404−8406.
(884) Kuang, Y.; Yuan, D.; Zhang, Y.; Kao, A.; Du, X. W.; Xu, B. Interactions between Cellular Proteins and Morphologically Different Nanoscale Aggregates of Small Molecules. *RSC Adv.* **2013**, *3*, 7704−7707.
(885) Ye, E.; Chee, P. L.; Prasad, A.; Fang, X.; Owh, C.; Yeo, V. J. J.; Loh, X. J. Supramolecular Soft Biomaterials for Biomedical Applications. *Mater. Today* **2014**, *17*, 194−202.
(886) Du, X.; Zhou, J.; Wu, L.; Sun, S.; Xu, B. Enzymatic Transformation of Phosphate Decorated Magnetic Nanoparticles for Selectively Sorting and Inhibiting Cancer Cells. *Bioconjugate Chem.* **2014**, *25*, 2129−2133.
(887) Miao, Q.; Wu, Z.; Hai, Z.; Tao, C.; Yuan, Q.; Gong, Y.; Guan, Y.; Jiang, J.; Liang, G. Bipyridine Hydrogel for Selective and Visible Detection and Absorption of Cd(2+). *Nanoscale* **2015**, *7*, 2797−2804.
(888) Du, X.; Zhou, J.; Xu, B. Ectoenzyme Switches the Surface of Magnetic Nanoparticles for Selective Binding of Cancer Cells. *J. Colloid Interface Sci.* **2015**, *447*, 273−277.
(889) Seow, W. Y.; Hauser, C. A. E. Short to Ultrashort Peptide Hydrogels for Biomedical Uses. *Mater. Today* **2014**, *17*, 381−388.
(890) Tian, R.; Chen, J.; Niu, R. F. The Development of Low-Molecular Weight Hydrogels for Applications in Cancer Therapy. *Nanoscale* **2014**, *6*, 3474−3482.
(891) Reithofer, M. R.; Chan, K.-H.; Lakshmanan, A.; Lam, D. H.; Mishra, A.; Gopalan, B.; Joshi, M.; Wang, S.; Hauser, C. A. E. Ligation of Anti-Cancer Drugs to Self-Assembling Ultrashort Peptides by Click Chemistry for Localized Therapy. *Chem. Sci.* **2014**, *5*, 625−630.
(892) Reithofer, M. R.; Lakshmanan, A.; Ping, A. T. K.; Chin, J. M.; Hauser, C. A. E. In Situ Synthesis of Size-Controlled, Stable Silver Nanoparticles within Ultrashort Peptide Hydrogels and Their Anti-Bacterial Properties. *Biomaterials* **2014**, *35*, 7535−7542.
(893) Maity, L.; Parmar, H. S.; Rasale, D. B.; Das, A. K. Self-Programmed Nanovesicle to Nanofiber Transformation of a Dipeptide Appended Bolaamphiphile and Its Dose Dependent Cytotoxic Behaviour. *J. Mater. Chem. B* **2014**, *2*, 5272−5279.
(894) Tanaka, A.; Fukuoka, Y.; Morimoto, Y.; Honjo, T.; Koda, D.; Goto, M.; Maruyama, T. Cancer Cell Death Induced by the Intracellular Self-Assembly of an Enzyme-Responsive Supramolecular Gelator. *J. Am. Chem. Soc.* **2015**, *137*, 770−775.
(895) Jayawarna, V.; Smith, A.; Gough, J. E.; Ulijn, R. V. Three-Dimensional Cell Culture of Chondrocytes on Modified Di-Phenyl-aianine Scaffolds. *Biochem. Soc. Trans.* **2007**, *35*, 535−537.

DOI: 10.1021/acs.chemrev.5b00299
Chem. Rev. 2015, 115, 13165−13307

(896) Liebmann, T.; Rydholm, S.; Akpe, V.; Brismar, H. Self-Assembling Fmoc Dipeptide Hydrogel for in Situ 3d Cell Culturing. *BMC Biotechnol.* **2007**, *7*, 88.
(897) Jayawarna, V.; Richardson, S. M.; Hirst, A. R.; Hodson, N. W.; Saiani, A.; Gough, J. E.; Ulijn, R. V. Introducing Chemical Functionality in Fmoc-Peptide Gels for Cell Culture. *Acta Biomater.* **2009**, *5*, 934−943.
(898) Jayawarna, V.; Richardson, S. M.; Gough, J.; Ulijn, R. Self-Assembling Peptide Hydrogels: Directing Cell Behaviour by Chemical Composition. *Tissue Eng. A* **2008**, *14*, 908.
(899) Zhou, J.; Liao, C.; Zhang, L.; Wang, Q.; Tian, Y. Molecular Hydrogel-Stabilized Enzyme with Facilitated Electron Transfer for Determination of H2o2 Released from Live Cells. *Anal. Chem.* **2014**, *86*, 4395−4401.
(900) Zhou, M.; Smith, A. M.; Das, A. K.; Hodson, N. W.; Collins, R. F.; Ulijn, R. V.; Gough, J. E. Self-Assembled Peptide-Based Hydrogels as Scaffolds for Anchorage-Dependent Cells. *Biomaterials* **2009**, *30*, 2523−2530.
(901) Cheng, G.; Castelletto, V.; Jones, R. R.; Connon, C. J.; Hamley, I. W. Hydrogelation of Self-Assembling Rgd-Based Peptides. *Soft Matter* **2011**, *7*, 1326−1333.
(902) Owczarz, M.; Bolisetty, S.; Mezzenga, R.; Arosio, P. Sol-Gel Transition of Charged Fibrils Composed of a Model Amphiphilic Peptide. *J. Colloid Interface Sci.* **2015**, *437*, 244−251.
(903) Soler-Botija, C.; Bago, J. R.; Llucia-Valldeperas, A.; Valles-Lluch, A.; Castells-Sala, C.; Martinez-Ramos, C.; Fernandez-Muinos, T.; Chachques, J. C.; Monleon Pradas, M.; Semino, C. E.; et al. Engineered 3D Bioimplants Using Elastomeric Scaffold, Self-Assembling Peptide Hydrogel, and Adipose Tissue-Derived Progenitor Cells for Cardiac Regeneration. *Am. J. Transl. Res.* **2014**, *6*, 291−301.
(904) Zou, Z.; Liu, T.; Li, J.; Li, P.; Ding, Q.; Peng, G.; Zheng, Q.; Zeng, X.; Wu, Y.; Guo, X. Biocompatibility of Functionalized Designer Self-Assembling Nanofiber Scaffolds Containing Frm Motif for Neural Stem Cells. *J. Biomed. Mater. Res., Part A* **2014**, *102*, 1286−1293.
(905) Liang, P.; Xiong, J.; Zhao, L.; Xu, Y.; Zhao, J.; Liu, Q. Recombinant Self-Assembling 16-Residue Peptide Nanofiber Scaffolds for Neuronal Axonal Outgrowth. *Eng. Life Sci.* **2015**, *15*, 152−158.
(906) Wang, J.; Zheng, J.; Zheng, Q.; Wu, Y.; Wu, B.; Huang, S.; Fang, W.; Guo, X. Fgl-Functionalized Self-Assembling Nanofiber Hydrogel as a Scaffold for Spinal Cord-Derived Neural Stem Cells. *Mater. Sci. Eng., C* **2015**, *46*, 140−147.
(907) Hamada, K.; Hirose, M.; Yamashita, T.; Ohgushi, H. Spatial Distribution of Mineralized Bone Matrix Produced by Marrow Mesenchymal Stem Cells in Self-Assembling Peptide Hydrogel Scaffold. *J. Biomed. Mater. Res., Part A* **2008**, *84A*, 128−136.
(908) Li, Z.; Hou, T.; Luo, F.; Chang, Z.; Wu, X.; Xing, J.; Deng, M.; Xu, J. Bone Marrow Enriched Graft, Modified by Self-Assembly Peptide, Repairs Critically-Sized Femur Defects in Goats. *Int. Orthop.* **2014**, *38*, 2391−2398.
(909) Kakiuchi, Y.; Hirohashi, N.; Murakami-Murofushi, K. The Macroscopic Structure of Rada16 Peptide Hydrogel Stimulates Monocyte/Macrophage Differentiation in Hl60 Cells Via Cholesterol Synthesis. *Biochem. Biophys. Res. Commun.* **2013**, *433*, 298−304.
(910) Mie, M.; Oomuro, M.; Kobatake, E. Hydrogel Scaffolds Composed of Genetically Synthesized Self-Assembling Peptides for Three-Dimensional Cell Culture. *Polym. J.* **2013**, *45*, 504−508.
(911) Liu, X.; Wang, X. M.; Wang, X. J.; Ren, H.; He, J.; Qiao, L.; Cui, F. Z. Functionalized Self-Assembling Peptide Nanofiber Hydrogels Mimic Stem Cell Niche to Control Human Adipose Stem Cell Behavior in Vitro. *Acta Biomater.* **2013**, *9*, 6798−6805.
(912) Mi, K.; Feng, Z. H.; Liu, Z. J.; Wang, G. X.; Xing, Z. H.; Huang, B.; Zhao, X. J. Self-Assembling Peptide Rada16 Nanofibre Scaffold for a Cancer Cell Three-Dimensional Culture. *Iran. Polym. J.* **2009**, *18*, 801−810.
(913) Zhang, F.; Shi, G. S.; Ren, L. F.; Hu, F. Q.; Li, S. L.; Xie, Z. J. Designer Self-Assembling Peptide Scaffold Stimulates Pre-Osteoblast Attachment, Spreading and Proliferation. *J. Mater. Sci.: Mater. Med.* **2009**, *20*, 1475−1481.
(914) Genove, E.; Schmitmeier, S.; Sala, A.; Borros, S.; Bader, A.; Griffith, L. G.; Semino, C. E. Functionalized Self-Assembling Peptide Hydrogel Enhance Maintenance of Hepatocyte Activity in Vitro. *J. Cell. Mol. Med.* **2009**, *13*, 3387−3397.
(915) Wang, B. C.; Wu, Y. C.; Shao, Z. W.; Yang, S. H.; Che, B.; Sun, C. X.; Ma, Z. L.; Zhang, Y. N. Functionalized Self-Assembling Peptide Nanofiber Hydrogel as a Scaffold for Rabbit Nucleus Pulposus Cells. *J. Biomed. Mater. Res., Part A* **2012**, *100A*, 646−653.
(916) Cho, H.; Balaji, S.; Sheikh, A. Q.; Hurley, J. R.; Tian, Y. F.; Collier, J. H.; Crombleholme, T. M.; Narmoneva, D. A. Regulation of Endothelial Cell Activation and Angiogenesis by Injectable Peptide Nanofibers. *Acta Biomater.* **2012**, *8*, 154−164.
(917) Malinen, M. M.; Palokangas, H.; Yliperttula, M.; Urtti, A. Peptide Nanofiber Hydrogel Induces Formation of Bile Canaliculi Structures in Three-Dimensional Hepatic Cell Culture. *Tissue Eng., Part A* **2012**, *18*, 2418−2425.
(918) Tian, Y. F.; Devgun, J. M.; Collier, J. H. Fibrillized Peptide Microgels for Cell Encapsulation and 3d Cell Culture. *Soft Matter* **2011**, *7*, 6005−6011.
(919) Jung, J. P.; Nagaraj, A. K.; Fox, E. K.; Rudra, J. S.; Devgun, J. M.; Collier, J. H. Co-Assembling Peptides as Defined Matrices for Endothelial Cells. *Biomaterials* **2009**, *30*, 2400−2410.
(920) Beniash, E.; Hartgerink, J. D.; Storrie, H.; Stendahl, J. C.; Stupp, S. I. Self-Assembling Peptide Amphiphile Nanofiber Matrices for Cell Entrapment. *Acta Biomater.* **2005**, *1*, 387−397.
(921) Tysseling-Mattiace, V. M.; Sahni, V.; Niece, K. L.; Birch, D.; Czeisler, C.; Fehlings, M. G.; Stupp, S. I.; Kessler, J. A. Self-Assembling Nanofibers Inhibit Glial Scar Formation and Promote Axon Elongation after Spinal Cord Injury. *J. Neurosci.* **2008**, *28*, 3814−3823.
(922) Matson, J. B.; Stupp, S. I. Self-Assembling Peptide Scaffolds for Regenerative Medicine. *Chem. Commun.* **2012**, *48*, 26−33.
(923) Muraoka, T.; Koh, C. Y.; Cui, H. G.; Stupp, S. I. Light-Triggered Bioactivity in Three Dimensions. *Angew. Chem., Int. Ed.* **2009**, *48*, 5946−5949.
(924) Sur, S.; Matson, J. B.; Webber, M. J.; Newcomb, C. J.; Stupp, S. I. Photodynamic Control of Bioactivity in a Nanofiber Matrix. *ACS Nano* **2012**, *6*, 10776−10785.
(925) Rughani, R. V.; Salick, D. A.; Lamm, M. S.; Yucel, T.; Pochan, D. J.; Schneider, J. P. Folding, Self-Assembly, and Bulk Material Properties of a De Novo Designed Three-Stranded Beta-Sheet Hydrogel. *Biomacromolecules* **2009**, *10*, 1295−1304.
(926) Haines-Butterick, L.; Rajagopal, K.; Branco, M.; Salick, D.; Rughani, R.; Pilarz, M.; Lamm, M. S.; Pochan, D. J.; Schneider, J. P. Controlling Hydrogelation Kinetics by Peptide Design for Three-Dimensional Encapsulation and Injectable Delivery of Cells. *Proc. Natl. Acad. Sci. U. S. A.* **2007**, *104*, 7791−7796.
(927) Yan, C. Q.; Altunbas, A.; Yucel, T.; Nagarkar, R. P.; Schneider, J. P.; Pochan, D. J. Injectable Solid Hydrogel: Mechanism of Shear-Thinning and Immediate Recovery of Injectable Beta-Hairpin Peptide Hydrogels. *Soft Matter* **2010**, *6*, 5143−5156.
(928) Song, Y. L.; Li, Y. X.; Zheng, Q. X.; Wu, K.; Guo, X. D.; Wu, Y. C.; Yin, M.; Wu, Q.; Fu, X. L. Neural Progenitor Cells Survival and Neuronal Differentiation in Peptide-Based Hydrogels. *J. Biomater. Sci., Polym. Ed.* **2011**, *22*, 475−487.
(929) Song, Y. L.; Zheng, Q. X.; Wu, Y. C.; Guo, X. D. Two-Dimensional Effects of Hydrogel Self-Organized from Ikvav-Containing Peptides on Growth and Differentiation of Nscs. *J. Wuhan Univ. Technol., Mater. Sci. Ed.* **2009**, *24*, 186−192.
(930) Song, Y. L.; Zheng, Q. X.; Guo, X. D.; Zheng, J. F. Cytocompatibility of Self-Assembled Hydrogel from Ikvav-Containing Peptide Amphiphile with Neural Stem Cells. *J. Wuhan Univ. Technol., Mater. Sci. Ed.* **2009**, *24*, 753−756.
(931) Sun, J. H.; Zheng, Q. X. Experimental Study on Self-Assembly of Kld-12 Peptide Hydrogel and 3-D Culture of Msc Encapsulated within Hydrogel in Vitro. *J. Huazhong Univ. Sci. Technol., Med. Sci.* **2009**, *29*, 512−516.
(932) Kim, J. E.; Lee, S. M.; Kim, S. H.; Tatman, P.; Gee, A. O.; Kim, D.-H.; Lee, K. E.; Jung, Y.; Kim, S. J. Effect of Self-Assembled Peptide-

DOI: 10.1021/acs.chemrev.5b00299
Chem. Rev. 2015, 115, 13165−13307

Mesenchymal Stem Cell Complex on the Progression of Osteoarthritis in a Rat Model. *Int. J. Nanomed.* **2014**, *9* (Suppl. 1), 141−157.
(933) Raspa, A.; Saracino, G. A. A.; Pugliese, R.; Silva, D.; Cigognini, D.; Vescovi, A.; Gelain, F. Complementary Co-Assembling Peptides: From in Silico Studies to in Vivo Application. *Adv. Funct. Mater.* **2014**, *24*, 6317−6328.
(934) Kang, M. K.; Colombo, J. S.; D'Souza, R. N.; Hartgerink, J. D. Sequence Effects of Self-Assembling Multidomain Peptide Hydrogels on Encapsulated Shed Cells. *Biomacromolecules* **2014**, *15*, 2004−2011.
(935) Galler, K. M.; Aulisa, L.; Regan, K. R.; D'Souza, R. N.; Hartgerink, J. D. Self-Assembling Multidomain Peptide Hydrogels: Designed Susceptibility to Enzymatic Cleavage Allows Enhanced Cell Migration and Spreading. *J. Am. Chem. Soc.* **2010**, *132*, 3217−3223.
(936) Bakota, E. L.; Wang, Y.; Danesh, F. R.; Hartgerink, J. D. Injectable Multidomain Peptide Nanofiber Hydrogel as a Delivery Agent for Stem Cell Secretome. *Biomacromolecules* **2011**, *12*, 1651−1657.
(937) Kumar, V. A.; Taylor, N. L.; Shi, S.; Wang, B. K.; Jalan, A. A.; Kang, M. K.; Wickremasinghe, N. C.; Hartgerink, J. D. Highly Angiogenic Peptide Nanofibers. *ACS Nano* **2015**, *9*, 860−868.
(938) Maude, S.; Miles, D. E.; Felton, S. H.; Ingram, J.; Carrick, L. M.; Wilcox, R. K.; Ingham, E.; Aggeli, A. De Novo Designed Positively Charged Tape-Forming Peptides: Self-Assembly and Gelation in Physiological Solutions and Their Evaluation as 3d Matrices for Cell Growth. *Soft Matter* **2011**, *7*, 8085−8099.
(939) Kyle, S.; Felton, S. H.; McPherson, M. J.; Aggeli, A.; Ingham, E. Rational Molecular Design of Complementary Self-Assembling Peptide Hydrogels. *Adv. Healthcare Mater.* **2012**, *1*, 640−645.
(940) Yang, C. H.; Li, D. X.; Liu, Z.; Hong, G.; Zhang, J.; Kong, D. L.; Yang, Z. M. Responsive Small Molecular Hydrogels Based on Adamantane-Peptides for Cell Culture. *J. Phys. Chem. B* **2012**, *116*, 633−638.
(941) Lv, L. N.; Liu, H. X.; Chen, X. M.; Yang, Z. M. Glutathione-Triggered Formation of Molecular Hydrogels for 3d Cell Culture. *Colloids Surf., B* **2013**, *108*, 352−357.
(942) Yang, C.; Wang, Z.; Ou, C.; Chen, M.; Wang, L.; Yang, Z. A Supramolecular Hydrogelator of Curcumin. *Chem. Commun.* **2014**, *50*, 9413−9415.
(943) Tian, Y.; Wang, H.; Liu, Y.; Mao, L.; Chen, W.; Zhu, Z.; Liu, W.; Zheng, W.; Zhao, Y.; Kong, D.; et al. A Peptide-Based Nanofibrous Hydrogel as a Promising DNA Nanovector for Optimizing the Efficacy of Hiv Vaccine. *Nano Lett.* **2014**, *14*, 1439−1445.
(944) Wang, H.; Wang, Y.; Han, A.; Cai, Y.; Xiao, N.; Wang, L.; Ding, D.; Yang, Z. Cellular Membrane Enrichment of Self-Assembling D-Peptides for Cell Surface Engineering. *ACS Appl. Mater. Interfaces* **2014**, *6*, 9815−9821.
(945) Li, J. B.; Kooger, R.; He, M. T.; Xiao, X.; Zheng, L.; Zhang, Y. A Supramolecular Hydrogel as a Carrier to Deliver Microrna into the Encapsulated Cells. *Chem. Commun.* **2014**, *50*, 3722−3724.
(946) Luo, Z. L.; Yue, Y. Y.; Zhang, Y. F.; Yuan, X.; Gong, J. P.; Wang, L. L.; He, B.; Liu, Z.; Sun, Y. L.; Liu, J.; et al. Designer D-Form Self-Assembling Peptide Nanofiber Scaffolds for 3-Dimensional Cell Cultures. *Biomaterials* **2013**, *34*, 4902−4913.
(947) Wang, W.; Li, G.; Zhang, W.; Gao, J.; Zhang, J.; Li, C.; Ding, D.; Kong, D. Reduction-Triggered Formation of Efk8Molecular Hydrogel for 3d Cell Culture. *RSC Adv.* **2014**, *4*, 30168−30171.
(948) Szkolar, L.; Guilbaud, J. B.; Miller, A. F.; Gough, J. E.; Saiani, A. Enzymatically Triggered Peptide Hydrogels for 3d Cell Encapsulation and Culture. *J. Pept. Sci.* **2014**, *20*, 578−584.
(949) Lu, T. L.; Chen, T.; Zhai, Y. K.; Ma, Y. F.; Xiao, Y. H. Designer Functionalized Self-Assembling Peptide Scaffolds for Adhesion, Proliferation, and Differentiation of Mc3t3-E1. *Soft Mater.* **2014**, *12*, 79−87.
(950) Castillo Diaz, L. A.; Saiani, A.; Gough, J. E.; Miller, A. F. Human Osteoblasts within Soft Peptide Hydrogels Promote Mineralisation in Vitro. *J. Tissue Eng.* **2014**, *5*, 2041731414539344.
(951) Ikeda, M.; Ueno, S.; Matsumoto, S.; Shimizu, Y.; Komatsu, H.; Kusumoto, K. I.; Hamachi, I. Three-Dimensional Encapsulation of Live Cells by Using a Hybrid Matrix of Nanoparticles in a Supramolecular Hydrogel. *Chem. - Eur. J.* **2008**, *14*, 10808−10815.
(952) Yoshii, T.; Ikeda, M.; Hamachi, I. Two-Photon-Responsive Supramolecular Hydrogel for Controlling Materials Motion in Micrometer Space. *Angew. Chem., Int. Ed.* **2014**, *53*, 7264−7267.
(953) Yoshii, T.; Onogi, S.; Shigemitsu, H.; Hamachi, I. Chemically Reactive Supramolecular Hydrogel Coupled with a Signal Amplification System for Enhanced Analyte Sensitivity. *J. Am. Chem. Soc.* **2015**, *137*, 3360−3365.
(954) Chou, T. H.; Chen, C. W.; Liang, C. H.; Yeh, L. H.; Qian, S. Z. Simple Synthesis, Self-Assembly, and Cytotoxicity of Novel Dimeric Cholesterol Derivatives. *Colloids Surf., B* **2014**, *116*, 153−159.
(955) Kretsinger, J. K.; Haines, L. A.; Ozbas, B.; Pochan, D. J.; Schneider, J. P. Cytocompatibility of Self-Assembled Ss-Hairpin Peptide Hydrogel Surfaces. *Biomaterials* **2005**, *26*, 5177−5186.
(956) Chen, C.; Gu, Y.; Deng, L.; Han, S.; Sun, X.; Chen, Y.; Lu, J. R.; Xu, H. Tuning Gelation Kinetics and Mechanical Rigidity of Beta-Hairpin Peptide Hydrogels Via Hydrophobic Amino Acid Substitutions. *ACS Appl. Mater. Interfaces* **2014**, *6*, 14360−14368.
(957) Mehrban, N.; Abelardo, E.; Wasmuth, A.; Hudson, K. L.; Mullen, L. M.; Thomson, A. R.; Birchall, M. A.; Woolfson, D. N. Assessing Cellular Response to Functionalized Alpha-Helical Peptide Hydrogels. *Adv. Healthcare Mater.* **2014**, *3*, 1387−1391.
(958) Orbach, R.; Adler-Abramovich, L.; Zigerson, S.; Mironi-Harpaz, I.; Seliktar, D.; Gazit, E. Self-Assembled Fmoc-Peptides as a Platform for the Formation of Nanostructures and Hydrogels. *Biomacromolecules* **2009**, *10*, 2646−2651.
(959) Chronopoulou, L.; Togna, A. R.; Guarguaglini, G.; Masci, G.; Giammaruco, F.; Togna, G. I.; Palocci, C. Self-Assembling Peptide Hydrogels Promote Microglial Cells Proliferation and Ngf Production. *Soft Matter* **2012**, *8*, 5784−5790.
(960) Huang, Z. P.; Guan, S. W.; Wang, Y. G.; Shi, G. N.; Cao, L. N.; Gao, Y. Z.; Dong, Z. Y.; Xu, J. Y.; Luo, Q.; Liu, J. Q. Self-Assembly of Amphiphilic Peptides into Bio-Functionalized Nanotubes: A Novel Hydrolase Model. *J. Mater. Chem. B* **2013**, *1*, 2297−2304.
(961) Kiss, J. Z.; Muller, D. Contribution of the Neural Cell Adhesion Molecule to Neuronal and Synaptic Plasticity. *Rev. Neurosci.* **2001**, *12*, 297−310.
(962) Welzl, H.; Stork, O. Cell Adhesion Molecules: Key Players in Memory Consolidation? *Physiology* **2003**, *18*, 147−150.
(963) Zhang, Z. X.; Zheng, Q. X.; Wu, Y. C.; Liu, Y. D. Biocompatibility of Fgl Peptide Self-Assembly Nanofibers with Neural Stem Cells in Vitro. *J. Wuhan Univ. Technol., Mater. Sci. Ed.* **2009**, *24*, 992−996.
(964) Yang, Z. M.; Liang, G. L.; Ma, M. L.; Gao, Y.; Xu, B. Conjugates of Naphthalene and Dipeptides Produce Molecular Hydrogelators with High Efficiency of Hydrogelation and Superhelical Nanofibers. *J. Mater. Chem.* **2007**, *17*, 850−854.
(965) Li, X. M.; Kuang, Y.; Lin, H. C.; Gao, Y.; Shi, J. F.; Xu, B. Supramolecular Nanofibers and Hydrogels of Nucleopeptides. *Angew. Chem., Int. Ed.* **2011**, *50*, 9365−9369.
(966) Gao, J.; Shi, Y.; Wang, Y. Z.; Cai, Y. B.; Shen, J.; Kong, D. L.; Yang, Z. M. Enzyme-Controllable F-Nmr Turn on through Disassembly of Peptide-Based Nanospheres for Enzyme Detection. *Org. Biomol. Chem.* **2014**, *12*, 1383−1386.
(967) Marth, J. D. A Unified Vision of the Building Blocks of Life. *Nat. Cell Biol.* **2008**, *10*, 1015−1016.
(968) Li, X. M.; Shi, J. F.; Gao, Y.; Lin, H. C.; Xu, B. Multifunctional, Biocompatible Supramolecular Hydrogelators Consist Only of Nucleobase, Amino Acid, and Glycoside. *J. Am. Chem. Soc.* **2011**, *133*, 17513−17518.
(969) Du, X. W.; Zhou, J.; Guvench, O.; Sangiorgi, F. O.; Li, X. M.; Zhou, N.; Xu, B. Supramolecular Assemblies of a Conjugate of Nucleobase, Amino Acids, and Saccharide Act as Agonists for Proliferation of Embryonic Stem Cells and Development of Zygotes. *Bioconjugate Chem.* **2014**, *25*, 1031−1035.
(970) Li, X. M.; Du, X. W.; Gao, Y.; Shi, J. F.; Kuang, Y.; Xu, B. Supramolecular Hydrogels Formed by the Conjugates of Nucleobases,

DOI: 10.1021/acs.chemrev.5b00299
Chem. Rev. 2015, 115, 13165−13307

Arg-Gly-Asp (Rgd) Peptides, and Glucosamine. *Soft Matter* **2012**, *8*, 7402−7407.
(971) Li, X. M.; Du, X. W.; Li, J. Y.; Gao, Y.; Pan, Y.; Shi, J. F.; Zhou, N.; Xu, B. Introducing D-Amino Acid or Simple Glycoside into Small Peptides to Enable Supramolecular Hydrogelators to Resist Proteolysis. *Langmuir* **2012**, *28*, 13512−13517.
(972) Yuan, D.; Du, X.; Shi, J.; Zhou, N.; Baoum, A. A.; Xu, B. Synthesis of Novel Conjugates of a Saccharide, Amino Acids, Nucleobase and the Evaluation of Their Cell Compatibility. *Beilstein J. Org. Chem.* **2014**, *10*, 2406−2413.
(973) Wu, D. D.; Du, X. W.; Shi, J. F.; Zhou, J.; Xu, B. Supramolecular Nanofibers/Hydrogels of the Conjugates of Nucleobase, Saccharide, and Amino Acids. *Chin. J. Chem.* **2014**, *32*, 313−318.
(974) Wu, D. D.; Zhou, J.; Shi, J. F.; Du, X. W.; Xu, B. A Naphthalene-Containing Amino Acid Enables Hydrogelation of a Conjugate of Nucleobase-Saccharide-Amino Acids. *Chem. Commun.* **2014**, *50*, 1992−1994.
(975) Webber, M. J.; Newcomb, C. J.; Bitton, R.; Stupp, S. I. Switching of Self-Assembly in a Peptide Nanostructure with a Specific Enzyme. *Soft Matter* **2011**, *7*, 9665−9672.
(976) Bella, A.; Ray, S.; Shaw, M.; Ryadnov, M. G. Arbitrary Self-Assembly of Peptide Extracellular Microscopic Matrices. *Angew. Chem., Int. Ed.* **2012**, *51*, 428−431.
(977) Hyland, L. L.; Twomey, J. D.; Vogel, S.; Hsieh, A. H.; Yu, Y. B. Enhancing Biocompatibility of D-Oligopeptide Hydrogels by Negative Charges. *Biomacromolecules* **2013**, *14*, 406−412.
(978) Hsu, S.-M.; Lin, Y.-C.; Chang, J.-W.; Liu, Y.-H.; Lin, H.-C. Intramolecular Interactions of a Phenyl/Perfluorophenyl Pair in the Formation of Supramolecular Nanofibers and Hydrogels. *Angew. Chem., Int. Ed.* **2014**, *53*, 1921−1927.
(979) Hsu, L.-H.; Hsu, S.-M.; Wu, F.-Y.; Liu, Y.-H.; Nelli, S. R.; Yeh, M.-Y.; Lin, H.-C. Nanofibrous Hydrogels Self-Assembled from Naphthalene Diimide (Ndi)/Amino Acid Conjugates. *RSC Adv.* **2015**, *5*, 20410.
(980) Marchesan, S.; Easton, C. D.; Styan, K. E.; Waddington, L. J.; Kushkaki, F.; Goodall, L.; McLean, K. M.; Forsythe, J. S.; Hartley, P. G. Chirality Effects at Each Amino Acid Position on Tripeptide Self-Assembly into Hydrogel Biomaterials. *Nanoscale* **2014**, *6*, 5172−5180.
(981) Godeau, G.; Brun, C.; Arnion, H.; Staedel, C.; Barthelemy, P. Glycosyl-Nucleoside Fluorinated Amphiphiles as Components of Nanostructured Hydrogels. *Tetrahedron Lett.* **2010**, *51*, 1012−1015.
(982) Latxague, L.; Ramin, M. A.; Appavoo, A.; Berto, P.; Maisani, M.; Ehret, C.; Chassande, O.; Barthelemy, P. Control of Stem-Cell Behavior by Fine Tuning the Supramolecular Assemblies of Low-Molecular-Weight Gelators. *Angew. Chem., Int. Ed.* **2015**, *54*, 4517−4521.
(983) Wang, W. J.; Wang, H. M.; Ren, C. H.; Wang, J. Y.; Tan, M.; Shen, J.; Yang, Z. M.; Wang, P. G.; Wang, L. A Saccharide-Based Supramolecular Hydrogel for Cell Culture. *Carbohydr. Res.* **2011**, *346*, 1013−1017.
(984) Martin, A. D.; Robinson, A. B.; Mason, A. F.; Wojciechowski, J. P.; Thordarson, P. Exceptionally Strong Hydrogels through Self-Assembly of an Indole-Capped Dipeptide. *Chem. Commun.* **2014**, *50*, 15541−15544.
(985) Tang, A. M.; Wang, W. J.; Mei, B.; Hu, W. L.; Wu, M.; Liang, G. L. Devd-Based Hydrogelator Minimizes Cellular Apoptosis Induction. *Sci. Rep.* **2013**, *3*, 1848.
(986) Ageitos, J. M.; Baker, P. J.; Sugahara, M.; Numata, K. Proteinase K-Catalyzed Synthesis of Linear and Star Oligo(L-Phenylalanine) Conjugates. *Biomacromolecules* **2013**, *14*, 3635−3642.
(987) Storrie, H.; Guler, M. O.; Abu-Amara, S. N.; Volberg, T.; Rao, M.; Geiger, B.; Stupp, S. I. Supramolecular Crafting of Cell Adhesion. *Biomaterials* **2007**, *28*, 4608−4618.
(988) Yin, W.-N.; Cao, F.-Y.; Han, K.; Zeng, X.; Zhuo, R.-X.; Zhang, X.-Z. The Synergistic Effect of a Bmp-7 Derived Peptide and Cyclic Rgd in Regulating Differentiation Behaviours of Mesenchymal Stem Cells. *J. Mater. Chem. B* **2014**, *2*, 8434−8440.
(989) Castelletto, V.; Moulton, C. M.; Cheng, G.; Hamley, I. W.; Hicks, M. R.; Rodger, A.; Lopez-Perez, D. E.; Revilla-Lopez, G.; Aleman, C. Self-Assembly of Fmoc-Tetrapeptides Based on the Rgds Cell Adhesion Motif. *Soft Matter* **2011**, *7*, 11405−11415.
(990) Zheng, W. T.; Gao, J.; Song, L. J.; Chen, C. Y.; Guan, D.; Wang, Z. H.; Li, Z. B.; Kong, D. L.; Yang, Z. M. Surface-Induced Hydrogelation Inhibits Platelet Aggregation. *J. Am. Chem. Soc.* **2013**, *135*, 266−271.
(991) Hu, Y.; Wang, H.; Wang, J.; Wang, S.; Liao, W.; Yang, Y.; Zhang, Y.; Kong, D.; Yang, Z. Supramolecular Hydrogels Inspired by Collagen for Tissue Engineering. *Org. Biomol. Chem.* **2010**, *8*, 3267−3271.
(992) Liu, H.; Hu, Y.; Wang, H.; Wang, J.; Kong, D.; Wang, L.; Chen, L.; Yang, Z. A Thixotropic Molecular Hydrogel Selectively Enhances Flk1 Expression in Differentiated Murine Embryonic Stem Cells. *Soft Matter* **2011**, *7*, 5430−5436.
(993) Sawada, T.; Tsuchiya, M.; Takahashi, T.; Tsutsumi, H.; Mihara, H. Cell-Adhesive Hydrogels Composed of Peptide Nanofibers Responsive to Biological Ions. *Polym. J.* **2012**, *44*, 651−657.
(994) Dou, X. Q.; Li, P.; Zhang, D.; Feng, C. L. Rgd Anchored C-2-Benzene Based Peg-Like Hydrogels as Scaffolds for Two and Three Dimensional Cell Cultures. *J. Mater. Chem. B* **2013**, *1*, 3562−3568.
(995) Dou, X. Q.; Zhang, D.; Feng, C. L. Wettability of Supramolecular Nanofibers for Controlled Cell Adhesion and Proliferation. *Langmuir* **2013**, *29*, 15359−15366.
(996) Liu, G.-F.; Ji, W.; Wang, W.-L.; Feng, C.-L. Multiresponsive Hydrogel Coassembled from Phenylalanine and Azobenzene Derivatives as 3d Scaffolds for Photoguiding Cell Adhesion and Release. *ACS Appl. Mater. Interfaces* **2015**, *7*, 301−307.
(997) Li, P.; Dou, X. Q.; Feng, C. L.; Zhang, D. Mechanical Reinforcement of C-2-Phenyl-Derived Hydrogels for Controlled Cell Adhesion. *Soft Matter* **2013**, *9*, 3750−3757.
(998) Li, P.; Yin, Z. Q.; Dou, X. Q.; Zhou, G. D.; Feng, C. L. Convenient Three-Dimensional Cell Culture in Supermolecular Hydrogels. *ACS Appl. Mater. Interfaces* **2014**, *6*, 7948−7952.
(999) Liu, G. F.; Zhang, D.; Feng, C. L. Control of Three-Dimensional Cell Adhesion by the Chirality of Nanofibers in Hydrogels. *Angew. Chem., Int. Ed.* **2014**, *53*, 7789−7793.
(1000) He, M.; Li, J.; Tan, S.; Wang, R.; Zhang, Y. Photodegradable Supramolecular Hydrogels with Fluorescence Turn-on Reporter for Photomodulation of Cellular Microenvironments. *J. Am. Chem. Soc.* **2013**, *135*, 18718−18721.
(1001) Xu, J. X.; Zhou, Z.; Wu, B.; He, B. F. Enzymatic Formation of a Novel Cell-Adhesive Hydrogel Based on Small Peptides with a Laterally Grafted L-3,4-Dihydroxyphenylalanine Group. *Nanoscale* **2014**, *6*, 1277−1280.
(1002) Miao, Q. Q.; Bai, X. Y.; Shen, Y. Y.; Mei, B.; Gao, J. H.; Li, L.; Liang, G. L. Intracellular Self-Assembly of Nanoparticles for Enhancing Cell Uptake. *Chem. Commun.* **2012**, *48*, 9738−9740.
(1003) Du, X.; Wu, Z. D.; Long, J. F.; Wang, L. Growth Stimulation of Bacterium Delftia by a Peptide Hydrogel. *RSC Adv.* **2013**, *3*, 18259−18262.
(1004) Ou, C. W.; Zhang, J. W.; Shi, Y.; Wang, Z. Y.; Wang, L.; Yang, Z. M.; Chen, M. S. D-Amino Acid Doping Peptide Hydrogel for the Production of a Cell Colony. *RSC Adv.* **2014**, *4*, 9229−9232.
(1005) Weerasekare, M.; Taraban, M. B.; Shi, X. F.; Jeong, E. K.; Trewhella, J.; Yu, Y. H. B. Sol and Gel States in Peptide Hydrogels Visualized by Gd(Iii)-Enhanced Magnetic Resonance Imaging. *Biopolymers* **2011**, *96*, 734−743.
(1006) Park, M.; Jang, D.; Kim, S. Y.; Hong, J. I. A Chemodosimetric Gelation System Showing Fluorescence and Sol-to-Gel Transition for Fluoride Anions in Aqueous Media. *New J. Chem.* **2012**, *36*, 1145−1148.
(1007) Wang, H.; Fu, C.; Li, X.; He, L.; Yang, Y. J. F– and H +-Triggered Reversible Supramolecular Self-Assembly/Disassembly Probed by a Fluorescent Ru2+ Complex. *Soft Matter* **2011**, *7*, 8892−8897.
(1008) Healey, B. G.; Walt, D. R. Improved Fiber Optic Chemical Sensor for Penicillin. *Anal. Chem.* **1995**, *67*, 4471−4476.

DOI: 10.1021/acs.chemrev.5b00299
Chem. Rev. 2015, 115, 13165−13307

(1009) Belay, A.; Collins, A.; Ruzgas, T.; Kissinger, P. T.; Gorton, L.; Csoregi, E. Redox Hydrogel Based Bienzyme Electrode for L-Glutamate Monitoring. *J. Pharm. Biomed. Anal.* **1999**, *19*, 93−105.
(1010) Cao, C. Y.; Chen, Y.; Wu, F. Z.; Deng, Y.; Liang, G. L. Caspase-3 Controlled Assembly of Nanoparticles for Fluorescence Turn On. *Chem. Commun.* **2011**, *47*, 10320−10322.
(1011) Tamaru, S.; Kiyonaka, S.; Hamachi, I. Three Distinct Readout Modes for Enzyme Activity Can Operate in a Semi-Wet Supramolecular Hydrogel. *Chem. - Eur. J.* **2005**, *11*, 7294−7304.
(1012) Bairi, P.; Roy, B.; Nandi, A. K. Ph and Anion Sensitive Silver(I) Coordinated Melamine Hydrogel with Dye Absorbing Properties: Metastability at Low Melamine Concentration. *J. Mater. Chem.* **2011**, *21*, 11747−11749.
(1013) Zhang, J.; Guo, D. S.; Wang, L. H.; Wang, Z.; Liu, Y. Supramolecular Binary Hydrogels from Calixarenes and Amino Acids and Their Entrapment-Release of Model Dye Molecules. *Soft Matter* **2011**, *7*, 1756−1762.
(1014) Song, S.; Song, A.; Feng, L.; Wei, G.; Dong, S.; Hao, J. Fluorescent Hydrogels with Tunable Nanostructure and Viscoelasticity for Formaldehyde Removal. *ACS Appl. Mater. Interfaces* **2014**, *6*, 18319−18328.
(1015) Song, S.; Wang, H.; Song, A.; Hao, J. Superhydrogels of Nanotubes Capable of Capturing Heavy-Metal Ions. *Chem. - Asian J.* **2014**, *9*, 245−252.
(1016) Sukul, P. K.; Malik, S. Removal of Toxic Dyes from Aqueous Medium Using Adenine Based Bicomponent Hydrogel. *RSC Adv.* **2013**, *3*, 1902−1915.
(1017) Tang, Y. T.; Dou, X. Q.; Ji, Z. A.; Li, P.; Zhu, S. M.; Gu, J. J.; Feng, C. L.; Zhang, D. C-2-Symmetric Cyclohexane-Based Hydrogels: A Rational Designed Lmwg and Its Application in Dye Scavenging. *J. Mol. Liq.* **2013**, *177*, 167−171.
(1018) Sengupta, S.; Goswami, A.; Mondal, R. Silver-Promoted Gelation Studies of an Unorthodox Chelating Tripodal Pyridine-Pyrazole-Based Ligand: Templated Growth of Catalytic Silver Nanoparticles, Gas and Dye Adsorption. *New J. Chem.* **2014**, *38*, 2470−2479.
(1019) Ray, S.; Das, A. K.; Banerjee, A. Ph-Responsive, Bolaamphiphile-Based Smart Metallo-Hydrogels as Potential Dye-Adsorbing Agents, Water Purifier, and Vitamin B-12 Carrier. *Chem. Mater.* **2007**, *19*, 1633−1639.
(1020) Adhikari, B.; Palui, G.; Banerjee, A. Self-Assembling Tripeptide Based Hydrogels and Their Use in Removal of Dyes from Waste-Water. *Soft Matter* **2009**, *5*, 3452−3460.
(1021) Garcia, F.; Sanchez, L. Dendronized Triangular Oligo(Phenylene Ethynylene) Amphiphiles: Nanofibrillar Self-Assembly and Dye Encapsulation. *Chem. - Eur. J.* **2010**, *16*, 3138−3146.
(1022) Reddy, A.; Sharma, A.; Srivastava, A. Optically Transparent Hydrogels from an Auxin-Amino-Acid Conjugate Super Hydrogelator and Its Interactions with an Entrapped Dye. *Chem. - Eur. J.* **2012**, *18*, 7575−7581.
(1023) Wang, H.; Xu, W.; Song, S.; Feng, L.; Song, A.; Hao, J. Hydrogels Facilitated by Monovalent Cations and Their Use as Efficient Dye Adsorbents. *J. Phys. Chem. B* **2014**, *118*, 4693−4701.
(1024) Song, S. S.; Feng, L.; Song, A. X.; Hao, J. C. Room-Temperature Super Hydrogel as Dye Adsorption Agent. *J. Phys. Chem. B* **2012**, *116*, 12850−12856.
(1025) Ghosh, K.; Kar, D.; Bhattacharya, S. Fluoride-Responsive Hydrogel of Cholesterol Appended Pyridinium Urea and Its Metal Detecting Ability and Semi-Conducting Behaviour. *Supramol. Chem.* **2014**, *26*, 313−320.
(1026) Swain, J.; Kamalraj, M.; Rao, H. S. P.; Mishra, A. K. Thermotropic Gelation Induced Changes in Micropolarity and Microviscosity of Hydrogel Derived from Glucose-Triazole-Hydrogenated Cardanol Conjugate: A Study Using Fluorescent Molecular Probe. *RSC Adv.* **2014**, *4*, 55377−55382.
(1027) Yoshimura, I.; Miyahara, Y.; Kasagi, N.; Yamane, H.; Ojida, A.; Hamachi, I. Molecular Recognition in a Supramolecular Hydrogel to Afford a Semi-Wet Sensor Chip. *J. Am. Chem. Soc.* **2004**, *126*, 12204−12205.
(1028) Koshi, Y.; Nakata, E.; Yamane, H.; Hamachi, I. A Fluorescent Lectin Array Using Supramolecular Hydrogel for Simple Detection and Pattern Profiling for Various Glycoconjugates. *J. Am. Chem. Soc.* **2006**, *128*, 10413−10422.
(1029) Wada, A.; Tamaru, S.; Ikeda, M.; Hamachi, I. Mcm-Enzyme-Supramolecular Hydrogel Hybrid as a Fluorescence Sensing Material for Polyanions of Biological Significance. *J. Am. Chem. Soc.* **2009**, *131*, 5321−5330.
(1030) Yamaguchi, S.; Yoshimura, L.; Kohira, T.; Tamaru, S.; Hamachi, I. Cooperation between Artificial Receptors and Supramolecular Hydrogels for Sensing and Discriminating Phosphate Derivatives. *J. Am. Chem. Soc.* **2005**, *127*, 11835−11841.
(1031) Ikeda, M.; Yoshii, T.; Matsui, T.; Tanida, T.; Komatsu, H.; Hamachi, I. Montmorillonite-Supramolecular Hydrogel Hybrid for Fluorocolorimetric Sensing of Polyamines. *J. Am. Chem. Soc.* **2011**, *133*, 1670−1673.
(1032) Ikeda, M.; Fukuda, K.; Tanida, T.; Yoshii, T.; Hamachi, I. A Supramolecular Hydrogel Containing Boronic Acid-Appended Receptor for Fluorocolorimetric Sensing of Polyols with a Paper Platform. *Chem. Commun.* **2012**, *48*, 2716−2718.
(1033) Bhuniya, S.; Kim, B. H. An Insulin-Sensing Sugar-Based Fluorescent Hydrogel. *Chem. Commun.* **2006**, 1842−1844.
(1034) Park, J. S.; Jeong, S.; Ahn, B.; Kim, M.; Oh, W.; Kim, J. Selective Response of Cyclodextrin-Dye Hydrogel to Metal Ions. *J. Inclusion Phenom. Mol. Recognit. Chem.* **2011**, *71*, 79−86.
(1035) Kim, K. Y.; Park, S.; Jung, S. H.; Lee, S. S.; Park, K. M.; Shinkai, S.; Jung, J. H. Geometric Change of a Thiacalix 4 Arene Supramolecular Gel with Volatile Gases and Its Chromogenic Detection for Rapid Analysis. *Inorg. Chem.* **2014**, *53*, 3004−3011.
(1036) Wang, X. Q.; Wang, X. G. Aptamer-Functionalized Hydrogel Diffraction Gratings for the Human Thrombin Detection. *Chem. Commun.* **2013**, *49*, 5957−5959.
(1037) Ivekovic, D.; Milardovic, S.; Grabaric, B. S. Palladium Hexacyanoferrate Hydrogel as a Novel and Simple Enzyme Immobilization Matrix for Amperometric Biosensors. *Biosens. Bioelectron.* **2004**, *20*, 872−878.
(1038) Cusano, A. M.; Causa, F.; Della Moglie, R.; Falco, N.; Scognamiglio, P. L.; Aliberti, A.; Vecchione, R.; Battista, E.; Marasco, D.; Savarese, M.; et al. Integration of Binding Peptide Selection and Multifunctional Particles as Tool-Box for Capture of Soluble Proteins in Serum. *J. R. Soc., Interface* **2014**, *11*, 20140718.
(1039) Murakami, Y.; Maeda, M. Hybrid Hydrogels to Which Single-Stranded (Ss) DNA Probe Is Incorporated Can Recognize Specific Ssdna. *Macromolecules* **2005**, *38*, 1535−1537.
(1040) Xu, X. D.; Lin, B. B.; Feng, J.; Wang, Y.; Cheng, S. X.; Zhang, X. Z.; Zhuo, R. X. Biological Glucose Metabolism Regulated Peptide Self-Assembly as a Simple Visual Biosensor for Glucose Detection. *Macromol. Rapid Commun.* **2012**, *33*, 426−431.
(1041) Liu, H.; Lv, Z. L.; Ding, K. G.; Liu, X. L.; Yuan, L.; Chen, H.; Li, X. M. Incorporation of Tyrosine Phosphate into Tetraphenylethylene Affords an Amphiphilic Molecule for Alkaline Phosphatase Detection, Hydrogelation and Calcium Mineralization. *J. Mater. Chem. B* **2013**, *1*, 5550−5556.
(1042) Kim, J. H.; Lim, S. Y.; Nam, D. H.; Ryu, J.; Ku, S. H.; Park, C. B. Self-Assembled, Photoluminescent Peptide Hydrogel as a Versatile Platform for Enzyme-Based Optical Biosensors. *Biosens. Bioelectron.* **2011**, *26*, 1860−1865.
(1043) Kameta, N.; Masuda, M.; Mizuno, G.; Morii, N.; Shimizu, T. Supramolecular Nanotube Endo Sensing for a Guest Protein. *Small* **2008**, *4*, 561−565.
(1044) Ren, C. H.; Wang, H. M.; Zhang, X. L.; Ding, D.; Wang, L.; Yang, Z. M. Interfacial Self-Assembly Leads to Formation of Fluorescent Nanoparticles for Simultaneous Bacterial Detection and Inhibition. *Chem. Commun.* **2014**, *50*, 3473−3475.
(1045) Vemula, P. K.; Kohler, J. E.; Blass, A.; Williams, M.; Xu, C.; Chen, L.; Jadhav, S. R.; John, G.; Soybel, D. I.; Karp, J. M. Self-Assembled Hydrogel Fibers for Sensing the Multi-Compartment Intracellular Milieu. *Sci. Rep.* **2014**, *4*, 4466.

DOI: 10.1021/acs.chemrev.5b00299
Chem. Rev. 2015, 115, 13165−13307

(1046) Ren, C. H.; Wang, H. M.; Mao, D.; Zhang, X. L.; Fengzhao, Q. Q.; Shi, Y.; Ding, D.; Kong, D. L.; Wang, L.; Yang, Z. M. When Molecular Probes Meet Self-Assembly: An Enhanced Quenching Effect. *Angew. Chem., Int. Ed.* **2015**, *54*, 4823−4827.
(1047) Asai, M.; Sugiyasu, K.; Fujita, N.; Shinkai, S. Facile and Stable Dispersion of Carbon Nanotubes into a Hydrogel Composed of a Low Molecular-Weight Gelator Bearing a Tautomeric Dye Group. *Chem. Lett.* **2004**, *33*, 120−121.
(1048) Griffith, A.; Bandy, T. J.; Light, M.; Stulz, E. Light, M.; Stulz, E. Fluorescent Hydrogel Formation from Carboxyphenyl-Terpyridine. *Chem. Commun.* **2013**, *49*, 731−733.
(1049) Ahn, J.; Park, S.; Lee, J. H.; Jung, S. H.; Moon, S. J.; Jung, J. H. Fluorescent Hydrogels Formed by Ch-Pi and Pi-Pi Interactions as the Main Driving Forces: An Approach toward Understanding the Relationship between Fluorescence and Structure. *Chem. Commun.* **2013**, *49*, 2109−2111.
(1050) Kumar, M.; George, S. J. Green Fluorescent Organic Nanoparticles by Self-Assembly Induced Enhanced Emission of a Naphthalene Diimide Bolaamphiphile. *Nanoscale* **2011**, *3*, 2130−2133.
(1051) Ajayaghosh, A.; George, S. J.; Schenning, A. P. H. J. Hydrogen-Bonded Assemblies of Dyes and Extended Pi-Conjugated Systems. *Supermol. Dye Chem.* **2005**, *258*, 83−118.
(1052) Channon, K. J.; Devlin, G. L.; Magennis, S. W.; Finlayson, C. E.; Tickler, A. K.; Silva, C.; MacPhee, C. E. Modification of Fluorophore Photophysics through Peptide-Driven Self-Assembly. *J. Am. Chem. Soc.* **2008**, *130*, 5487−5491.
(1053) Wu, J. C.; Tian, Q. W.; Hu, H.; Xia, Q.; Zou, Y.; Li, F. Y.; Yi, T.; Huang, C. H. Self-Assembly of Peptide-Based Multi-Colour Gels Triggered by up-Conversion Rare Earth Nanoparticles. *Chem. Commun.* **2009**, 4100−4102.
(1054) Kim, T. H.; Seo, J.; Lee, S. J.; Lee, S. S.; Kim, J.; Jung, J. H. Strongly Fluorescent Hydrogel as a Blue-Emitting Nanomaterial: An Approach toward Understanding Fluorescence-Structure Relationship. *Chem. Mater.* **2007**, *19*, 5815−5817.
(1055) Mukherjee, S.; Kar, T.; Das, P. K. Pyrene-Based Fluorescent Supramolecular Hydrogel: Scaffold for Energy Transfer. *Chem. - Asian J.* **2014**, *9*, 2798−2805.
(1056) Das, S.; Chattopadhyay, A. P.; De, S. Controlling J Aggregation in Fluorescein by Bile Salt Hydrogels. *J. Photochem. Photobiol., A* **2008**, *197*, 402−414.
(1057) Jung, S. H.; Lee, H.; Park, S.; Jung, J. H. A Cyanurate Gel Derived from Two Different Hydrogen-Bonding Interactions in a Binary System: Evidence for the Driving Forces in Gel Formation. *New J. Chem.* **2012**, *36*, 1957−1960.
(1058) Das, R. N.; Kumar, Y. P.; Pagoti, S.; Patil, A. J.; Dash, J. Diffusion and Birefringence of Bioactive Dyes in a Supramolecular Guanosine Hydrogel. *Chem. - Eur. J.* **2012**, *18*, 6008−6014.
(1059) Montalti, M.; Dolci, L. S.; Prodi, L.; Zaccheroni, N.; Stuart, M. C. A.; van Bommel, K. J. C.; Friggeri, A. Energy Transfer from a Fluorescent Hydrogel to a Hosted Fluorophore. *Langmuir* **2006**, *22*, 2299−2303.
(1060) Rao, K. V.; Datta, K. K. R.; Eswaramoorthy, M.; George, S. J. Light-Harvesting Hybrid Hydrogels: Energy-Transfer-Induced Amplified Fluorescence in Noncovalently Assembled Chromophore-Organoclay Composites. *Angew. Chem., Int. Ed.* **2011**, *50*, 1179−1184.
(1061) Park, J. S.; Jeong, S.; Chang, D. W.; Kim, J. P.; Kim, K.; Park, E. K.; Song, K. W. Lithium-Induced Supramolecular Hydrogel. *Chem. Commun.* **2011**, *47*, 4736−4738.
(1062) Wang, H.; Zhang, W. P.; Dong, X. L.; Yang, Y. J. Thermo-Reversibility of the Fluorescence Enhancement of Acridine Orange Induced by Supramolecular Self-Assembly. *Talanta* **2009**, *77*, 1864−1868.
(1063) Gao, Y.; Kuang, Y.; Du, X. W.; Zhou, J.; Chandran, P.; Horkay, F.; Xu, B. Imaging Self-Assembly Dependent Spatial Distribution of Small Molecules in a Cellular Environment. *Langmuir* **2013**, *29*, 15191−15200.
(1064) Castellucci, N.; Sartor, G.; Calonghi, N.; Parolin, C.; Falini, G.; Tomasini, C. A Peptidic Hydrogel That May Behave as a "Trojan Horse". *Beilstein J. Org. Chem.* **2013**, *9*, 417−424.
(1065) Cai, Y. B.; Shi, Y.; Wang, H. M.; Wang, J. Y.; Ding, D.; Wang, L.; Yang, Z. M. Environment-Sensitive Fluorescent Supramolecular Nanofibers for Imaging Applications. *Anal. Chem.* **2014**, *86*, 2193−2199.
(1066) Baranova, O. A.; Kuz'min, N. I.; Samsonova, T. I.; Rebetskaya, I. S.; Petrova, O. P.; Pakhomov, P. M.; Khizhnyak, S. D.; Komarov, P. V.; Ovchinnikov, M. M. Medical Hydrogels Based on Bioactive Compounds. Synthesis, Properties, and Possible Application for Preparing Bactericidal Materials. *Fibre Chem.* **2011**, *43*, 90−103.
(1067) Ng, V. W. L.; Chan, J. M. W.; Sardon, H.; Ono, R. J.; Garcia, J. M.; Yang, Y. Y.; Hedrick, J. L. Antimicrobial Hydrogels: A New Weapon in the Arsenal against Multidrug-Resistant Infections. *Adv. Drug Delivery Rev.* **2014**, *78*, 46−62.
(1068) Salick, D. A.; Kretsinger, J. K.; Pochan, D. J.; Schneider, J. P. Inherent Antibacterial Activity of a Peptide-Based Beta-Hairpin Hydrogel. *J. Am. Chem. Soc.* **2007**, *129*, 14793−14799.
(1069) Sonmez, C.; Nagy, K. J.; Schneider, J. P. Design of Self-Assembling Peptide Hydrogelators Amenable to Bacterial Expression. *Biomaterials* **2015**, *37*, 62−72.
(1070) Salick, D. A.; Pochan, D. J.; Schneider, J. P. Design of an Injectable Beta-Hairpin Peptide Hydrogel That Kills Methicillin-Resistant Staphylococcus Aureus. *Adv. Mater.* **2009**, *21*, 4120−4123.
(1071) Veiga, A. S.; Sinthuvanich, C.; Gaspar, D.; Franquelim, H. G.; Castanho, M. A. R. B.; Schneider, J. P. Arginine-Rich Self-Assembling Peptides as Potent Antibacterial Gels. *Biomaterials* **2012**, *33*, 8907−8916.
(1072) Veiga, A. S.; Sinthuvanich, C.; Gaspar, D.; Franquelim, H. G.; Castanho, M.; Schneider, J. P. Arginine-Rich Self-Assembling Peptides Form Injectable Antibacterial Hydrogels. *J. Pept. Sci.* **2012**, *18*, S112.
(1073) Laverty, G.; McCloskey, A. P.; Gilmore, B. F.; Jones, D. S.; Zhou, J.; Xu, B. Ultrashort Cationic Naphthalene-Derived Self-Assembled Peptides as Antimicrobial Nanomaterials. *Biomacromolecules* **2014**, *15*, 3429−3439.
(1074) Chen, G.; Zhang, J.; Li, D.; Ren, C.; Ou, C.; Wang, L.; Chen, M. Redox-Controllable Self-Assembly and Anti-Bacterial Activity of a Vancomycin Derivative. *RSC Adv.* **2014**, *4*, 61324−61326.
(1075) Mitra, R. N.; Shome, A.; Paul, P.; Das, P. K. Antimicrobial Activity, Biocompatibility and Hydrogelation Ability of Dipeptide-Based Amphiphiles. *Org. Biomol. Chem.* **2009**, *7*, 94−102.
(1076) Debnath, S.; Shome, A.; Das, D.; Das, P. K. Hydrogelation through Self-Assembly of Fmoc-Peptide Functionalized Cationic Amphiphiles: Potent Antibacterial Agent. *J. Phys. Chem. B* **2010**, *114*, 4407−4415.
(1077) Dutta, S.; Kar, T.; Mandal, D.; Das, P. K. Structure and Properties of Cholesterol-Based Hydrogelators with Varying Hydrophilic Terminals: Biocompatibility and Development of Antibacterial Soft Nanocomposites. *Langmuir* **2013**, *29*, 316−327.
(1078) Mahato, M.; Arora, V.; Pathak, R.; Gautam, H. K.; Sharma, A. K. Fabrication of Nanostructures through Molecular Self-Assembly of Small Amphiphilic Glyco-Dehydropeptides. *Mol. BioSyst.* **2012**, *8*, 1742−1749.
(1079) Vudumula, U.; Adhikari, M. D.; Ojha, B.; Goswami, S.; Das, G.; Ramesh, A. Tuning the Bactericidal Repertoire and Potency of Quinoline-Based Amphiphiles for Enhanced Killing of Pathogenic Bacteria. *RSC Adv.* **2012**, *2*, 3864−3871.
(1080) Li, Y.; Zhou, F.; Wen, Y.; Liu, K.; Chen, L.; Mao, Y.; Yang, S.; Yi, T. (−)-Menthol Based Thixotropic Hydrogel and Its Application as a Universal Antibacterial Carrier. *Soft Matter* **2014**, *10*, 3077−3085.
(1081) Liu, S. Q.; Venkataraman, S.; Ong, Z. Y.; Chan, J. M. W.; Yang, C.; Hedrick, J. L.; Yang, Y. Y. Overcoming Multidrug Resistance in Microbials Using Nanostructures Self-Assembled from Cationic Bent-Core Oligomers. *Small* **2014**, *10*, 4130−4135.
(1082) Irwansyah, I.; Li, Y.-Q.; Shi, W.; Qi, D.; Leow, W. R.; Tang, M. B. Y.; Li, S.; Chen, X. Gram-Positive Antimicrobial Activity of Amino Acid-Based Hydrogels. *Adv. Mater.* **2015**, *27*, 648−654.
(1083) Xu, D.; Jiang, L.; Singh, A.; Dustin, D.; Yang, M.; Liu, L.; Lund, R.; Sellati, T. J.; Dong, H. Designed Supramolecular Filamentous Peptides: Balance of Nanostructure, Cytotoxicity and Antimicrobial Activity. *Chem. Commun.* **2015**, *51*, 1289−1292.

DOI: 10.1021/acs.chemrev.5b00299
Chem. Rev. 2015, 115, 13165−13307

(1084) McGovern, S. L.; Caselli, E.; Grigorieff, N.; Shoichet, B. K. A Common Mechanism Underlying Promiscuous Inhibitors from Virtual and High-Throughput Screening. *J. Med. Chem.* **2002**, *45*, 1712−1722.
(1085) McGovern, S. L.; Helfand, B. T.; Feng, B.; Shoichet, B. K. A Specific Mechanism of Nonspecific Inhibition. *J. Med. Chem.* **2003**, *46*, 4265−4272.
(1086) Eidam, O.; Romagnoli, C.; Dalmasso, G.; Barelier, S.; Caselli, E.; Bonnet, R.; Shoichet, B. K.; Prati, F. Fragment-Guided Design of Subnanomolar Beta-Lactamase Inhibitors Active in Vivo. *Proc. Natl. Acad. Sci. U. S. A.* **2012**, *109*, 17448−17453.
(1087) London, N.; Miller, R. M.; Krishnan, S.; Uchida, K.; Irwin, J. J.; Eidam, O.; Gibold, L.; Cimermancic, P.; Bonnet, R.; Shoichet, B. K.; et al. Covalent Docking of Large Libraries for the Discovery of Chemical Probes. *Nat. Chem. Biol.* **2014**, *10*, 1066−1072.
(1088) Owen, S. C.; Doak, A. K.; Ganesh, A. N.; Nedyalkova, L.; McLaughlin, C. K.; Shoichet, B. K.; Shoichet, M. S. Colloidal Drug Formulations Can Explain "Bell-Shaped" Concentration-Response Curves. *ACS Chem. Biol.* **2014**, *9*, 777−784.
(1089) Rahaman, M. N.; Day, D. E.; Bal, B. S.; Fu, Q.; Jung, S. B.; Bonewald, L. F.; Tomsia, A. P. Bioactive Glass in Tissue Engineering. *Acta Biomater.* **2011**, *7*, 2355−2373.
(1090) Ryan, D. M.; Nilsson, B. L. Self-Assembled Amino Acids and Dipeptides as Noncovalent Hydrogels for Tissue Engineering. *Polym. Chem.* **2012**, *3*, 18−33.
(1091) Wang, H. M.; Yang, Z. M. Short-Peptide-Based Molecular Hydrogels: Novel Gelation Strategies and Applications for Tissue Engineering and Drug Delivery. *Nanoscale* **2012**, *4*, 5259−5267.
(1092) He, M.; Zhang, Y. In *Engineering in Translational Medicine*; Cai, W., Ed.;Springer: New York, 2014.
(1093) Skilling, K. J.; Citossi, F.; Bradshaw, T. D.; Ashford, M.; Kellam, B.; Marlow, M. Insights into Low Molecular Mass Organic Gelators: A Focus on Drug Delivery and Tissue Engineering Applications. *Soft Matter* **2014**, *10*, 237−256.
(1094) Arslan, E.; Garip, I. C.; Gulseren, G.; Tekinay, A. B.; Guler, M. O. Bioactive Supramolecular Peptide Nanofibers for Regenerative Medicine. *Adv. Healthcare Mater.* **2014**, *3*, 1357−1376.
(1095) Hunt, J. A.; Chen, R.; van Veen, T.; Bryan, N. Hydrogels for Tissue Engineering and Regenerative Medicine. *J. Mater. Chem. B* **2014**, *2*, 5319−5338.
(1096) Ravichandran, R.; Griffith, M.; Phopase, J. Applications of Self-Assembling Peptide Scaffolds in Regenerative Medicine: The Way to the Clinic. *J. Mater. Chem. B* **2014**, *2*, 8466−8478.
(1097) Teixeira, L. S. M.; Patterson, J.; Luyten, F. P. Skeletal Tissue Regeneration: Where Can Hydrogels Play a Role? *Int. Orthop.* **2014**, *38*, 1861−1876.
(1098) Lu, P.; Takai, K.; Weaver, V. M.; Werb, Z. Extracellular Matrix Degradation and Remodeling in Development and Disease. *Cold Spring Harbor Perspect. Biol.* **2011**, *3*, a005058.
(1099) Lancaster, M. A.; Knoblich, J. A. Organogenesis in a Dish: Modeling Development and Disease Using Organoid Technologies. *Science* **2014**, *345*, 1247125.
(1100) Zimmermann, B. Lung Organoid Culture. *Differentiation* **1987**, *36*, 86−109.
(1101) Helen, W.; Ulijn, R. V.; Gough, J. E. Hydrogels Based on Fmoc-Diphenylalanine and Fmoc-Diglycine for Nucleus Pulposus Disc Tissue Engineering. *Int. J. Exp. Pathol.* **2009**, *90*, A113−A114.
(1102) Buerkle, L. E.; von Recum, H. A.; Rowan, S. J. Toward Potential Supramolecular Tissue Engineering Scaffolds Based on Guanosine Derivatives. *Chem. Sci.* **2012**, *3*, 564−572.
(1103) Wang, Y. Q.; Zhang, Z. L.; Xu, L.; Li, X. Y.; Chen, H. Hydrogels of Halogenated Fmoc-Short Peptides for Potential Application in Tissue Engineering. *Colloids Surf., B* **2013**, *104*, 163−168.
(1104) Rodriguez, A. L.; Wang, T. Y.; Bruggeman, K. F.; Horgan, C. C.; Li, R.; Williams, R. J.; Parish, C. L.; Nisbet, D. R. In Vivo Assessment of Grafted Cortical Neural Progenitor Cells and Host Response to Functionalized Self-Assembling Peptide Hydrogels and the Implications for Tissue Repair. *J. Mater. Chem. B* **2014**, *2*, 7771−7778.
(1105) Aggeli, A.; Bell, M.; Boden, N.; Keen, J. N.; Knowles, P. F.; McLeish, T. C. B.; Pitkeathly, M.; Radford, S. E. Responsive Gels Formed by the Spontaneous Self-Assembly of Peptides into Polymeric Beta-Sheet Tapes. *Nature* **1997**, *386*, 259−262.
(1106) Kyle, S.; Aggeli, A.; Ingham, E.; McPherson, M. J. Recombinant Self-Assembling Peptides as Biomaterials for Tissue Engineering. *Biomaterials* **2010**, *31*, 9395−9405.
(1107) Sun, J. H.; Zheng, Q. X.; Wu, Y. C.; Liu, Y. D.; Guo, X. D.; Wu, W. G. Biocompatibility of Kld-12 Peptide Hydrogel as a Scaffold in Tissue Engineering of Intervertebral Discs in Rabbits. *J. Huazhong Univ. Sci. Technol., Med. Sci.* **2010**, *30*, 173−177.
(1108) Gelain, F.; Cigognini, D.; Caprini, A.; Silva, D.; Colleoni, B.; Donega, M.; Antonini, S.; Cohen, B. E.; Vescovi, A. New Bioactive Motifs and Their Use in Functionalized Self-Assembling Peptides for Nsc Differentiation and Neural Tissue Engineering. *Nanoscale* **2012**, *4*, 2946−2957.
(1109) Caprini, A.; Silva, D.; Zanoni, I.; Cunha, C.; Volonte, C.; Vescovi, A.; Gelain, F. A Novel Bioactive Peptide: Assessing Its Activity over Murine Neural Stem Cells and Its Potential for Neural Tissue Engineering. *New Biotechnol.* **2013**, *30*, 552−562.
(1110) Gelain, F.; Silva, D.; Caprini, A.; Taraballi, F.; Natalello, A.; Villa, O.; Nam, K. T.; Zuckermann, R. N.; Doglia, S. M.; Vescovi, A. Bmhp1-Derived Self-Assembling Peptides: Hierarchically Assembled Structures with Self-Healing Propensity and Potential for Tissue Engineering Applications. *ACS Nano* **2011**, *5*, 1845−1859.
(1111) Amosi, N.; Zarzhitsky, S.; Gilsohn, E.; Salnikov, O.; Monsonego-Ornan, E.; Shahar, R.; Rapaport, H. Acidic Peptide Hydrogel Scaffolds Enhance Calcium Phosphate Mineral Turnover into Bone Tissue. *Acta Biomater.* **2012**, *8*, 2466−2475.
(1112) Dooley, K.; Kim, Y. H.; Lu, H. D.; Tu, R.; Banta, S. Engineering of an Environmentally Responsive Beta Roll Peptide for Use as a Calcium-Dependent Cross-Linking Domain for Peptide Hydrogel Formation. *Biomacromolecules* **2012**, *13*, 1758−1764.
(1113) Angkawidjaja, C.; Paul, A.; Koga, Y.; Takano, K.; Kanaya, S. Importance of a Repetitive Nine-Residue Sequence Motif for Intracellular Stability and Functional Structure of a Family I.3 Lipase. *FEBS Lett.* **2005**, *579*, 4707−4712.
(1114) Dooley, K.; Bulutoglu, B.; Banta, S. Doubling the Cross-Linking Interface of a Rationally Designed Beta Roll Peptide for Calcium-Dependent Proteinaceous Hydrogel Formation. *Biomacromolecules* **2014**, *15*, 3617−3624.
(1115) Huang, C. C.; Ravindran, S.; Yin, Z. Y.; George, A. 3-D Self-Assembling Leucine Zipper Hydrogel with Tunable Properties for Tissue Engineering. *Biomaterials* **2014**, *35*, 5316−5326.
(1116) Galler, K. M.; Hartgerink, J. D.; Cavender, A. C.; Schmalz, G.; D'Souza, R. N. A Customized Self-Assembling Peptide Hydrogel for Dental Pulp Tissue Engineering. *Tissue Eng., Part A* **2012**, *18*, 176−184.
(1117) Lin, B. F.; Megley, K. A.; Viswanathan, N.; Krogstad, D. V.; Drews, L. B.; Kade, M. J.; Qian, Y. C.; Tirrell, M. V. Ph-Responsive Branched Peptide Amphiphile Hydrogel Designed for Applications in Regenerative Medicine with Potential as Injectable Tissue Scaffolds. *J. Mater. Chem.* **2012**, *22*, 19447−19454.
(1118) Zhang, S. G.; Holmes, T. C.; Dipersio, C. M.; Hynes, R. O.; Su, X.; Rich, A. Self-Complementary Oligopeptide Matrices Support Mammalian-Cell Attachment. *Biomaterials* **1995**, *16*, 1385−1393.
(1119) Komatsu, S.; Nagai, Y.; Naruse, K.; Kimata, Y. The Neutral Self-Assembling Peptide Hydrogel Spg-178 as a Topical Hemostatic Agent. *PLoS One* **2014**, *9*, e102778.
(1120) Liu, X.; Wang, X.; Horii, A.; Wang, X.; Qiao, L.; Zhang, S.; Cui, F.-Z. In Vivo Studies on Angiogenic Activity of Two Designer Self-Assembling Peptide Scaffold Hydrogels in the Chicken Embryo Chorioallantoic Membrane. *Nanoscale* **2012**, *4*, 2720−2727.
(1121) Akiyama, N.; Yamamoto-Fukuda, T.; Takahashi, H.; Koji, T. In Situ Tissue Engineering with Synthetic Self-Assembling Peptide Nanofiber Scaffolds, Puramatrix, for Mucosal Regeneration in the Rat Middle-Ear. *Int. J. Nanomed.* **2013**, *8*, 2629−2640.
(1122) Ikeno, M.; Hibi, H.; Kinoshita, K.; Hattori, H.; Ueda, M. Effects of Self-Assembling Peptide Hydrogel Scaffold on Bone

DOI: 10.1021/acs.chemrev.5b00299
Chem. Rev. 2015, 115, 13165−13307

Regeneration with Recombinant Human Bone Morphogenetic Protein-2. *Int. J. Oral Maxillofac. Implants* **2013**, *28*, E283−E289.
(1123) Cheng, T. Y.; Chen, M. H.; Chang, W. H.; Huang, M. Y.; Wang, T. W. Neural Stem Cells Encapsulated in a Functionalized Self-Assembling Peptide Hydrogel for Brain Tissue Engineering. *Biomaterials* **2013**, *34*, 2005−2016.
(1124) Cheng, T. Y.; Wu, H. C.; Huang, M. Y.; Chang, W. H.; Lee, C. H.; Wang, T. W. Self-Assembling Functionalized Nanopeptides for Immediate Hemostasis and Accelerative Liver Tissue Regeneration. *Nanoscale* **2013**, *5*, 2734−2744.
(1125) Mehrban, N.; Mullen, L. M.; Abelardo, E. S.; Branwell, E. L.; Birchall, M. A.; Woolfson, D. N. Alpha-Helical Peptide Hydrogels as Tissue Engineering Scaffolds. *Int. J. Exp. Pathol.* **2011**, *92*, A9.
(1126) Frederix, P.; Kania, R.; Wright, J. A.; Lamprou, D. A.; Ulijn, R. V.; Pickett, C. J.; Hunt, N. T. Encapsulating Fefe -Hydrogenase Model Compounds in Peptide Hydrogels Dramatically Modifies Stability and Photochemistry. *Dalton Trans.* **2012**, *41*, 13112−13119.
(1127) Casolaro, M.; Casolaro, I.; Bottari, S.; Del Bello, B.; Maellaro, E.; Demadis, K. D. Long-Term Doxorubicin Release from Multiple Stimuli-Responsive Hydrogels Based on Alpha-Amino-Acid Residues. *Eur. J. Pharm. Biopharm.* **2014**, *88*, 424−433.
(1128) Liang, L.; Li, Q.-H.; Jin, K.; Luo, T.; Yang, Z.-A.; Xu, X.-D.; Cheng, H. In Vitro and in Vivo Evaluation of Novel Ocular Delivery System of 5-Fluorouracil Peptide Hydrogel. *Asian J. Chem.* **2014**, *26*, 2977−2981.
(1129) Rawat, M.; Singh, D.; Saraf, S.; Saraf, S. Nanocarriers: Promising Vehicle for Bioactive Drugs. *Biol. Pharm. Bull.* **2006**, *29*, 1790−1798.
(1130) Segers, V. F. M.; Lee, R. T. Local Delivery of Proteins and the Use of Self-Assembling Peptides. *Drug Discovery Today* **2007**, *12*, 561−568.
(1131) Prestwich, G. D. Evaluating Drug Efficacy and Toxicology in Three Dimensions: Using Synthetic Extracellular Matrices in Drug Discovery. *Acc. Chem. Res.* **2008**, *41*, 139−148.
(1132) Wang, H. M.; Yang, Z. M. Molecular Hydrogels of Hydrophobic Compounds: A Novel Self-Delivery System for Anti-Cancer Drugs. *Soft Matter* **2012**, *8*, 2344−2347.
(1133) Zhang, J. X.; Ma, P. X. Cyclodextrin-Based Supramolecular Systems for Drug Delivery: Recent Progress and Future Perspective. *Adv. Drug Delivery Rev.* **2013**, *65*, 1215−1233.
(1134) Liu, H. X.; Song, Z. J.; Chen, X. M. Photo-Controllable Molecular Hydrogels for Drug Delivery. *J. Nanosci. Nanotechnol.* **2014**, *14*, 4837−4842.
(1135) Alvarez-Lorenzo, C.; Concheiro, A. Smart Drug Delivery Systems: From Fundamentals to the Clinic. *Chem. Commun.* **2014**, *50*, 7743−7765.
(1136) Chee, P. L.; Prasad, A.; Fang, X.; Owh, C.; Yeo, V. J. J.; Loh, X. J. Supramolecular Cyclodextrin Pseudorotaxane Hydrogels: A Candidate for Sustained Release? *Mater. Sci. Eng., C* **2014**, *39*, 6−12.
(1137) Cheetham, A. G.; Zhang, P.; Lin, Y. A.; Lin, R.; Cui, H. Synthesis and Self-Assembly of a Mikto-Arm Star Dual Drug Amphiphile Containing Both Paclitaxel and Camptothecin. *J. Mater. Chem. B* **2014**, *2*, 7316−7326.
(1138) Mendes, A. C.; Zelikin, A. N. Enzyme Prodrug Therapy Engineered into Biomaterials. *Adv. Funct. Mater.* **2014**, *24*, 5202−5210.
(1139) Sirsi, S. R.; Borden, M. A. State-of-the-Art Materials for Ultrasound-Triggered Drug Delivery. *Adv. Drug Delivery Rev.* **2014**, *72*, 3−14.
(1140) Plourde, F.; Motulsky, A.; Couffin-Hoarau, A. C.; Hoarau, D.; Ong, H.; Leroux, J. C. First Report Implants on the Efficacy of L-Alanine-Based in Situ-Forming for the Long-Term Parenteral Delivery of Drugs. *J. Controlled Release* **2005**, *108*, 433−441.
(1141) Ramachandran, S.; Yu, Y. B. Peptide-Based Viscoelastic Matrices for Drug Delivery and Tissue Repair. *BioDrugs* **2006**, *20*, 263−269.
(1142) Wei, B.; Cheng, I.; Luo, K. Q.; Mi, Y. L. Capture and Release of Protein by a Reversible DNA-Induced Sol-Gel Transition System. *Angew. Chem., Int. Ed.* **2008**, *47*, 331−333.
(1143) Pal, A.; Shrivastava, S.; Dey, J. pH and Thermoresponsive Hydrogels of a Novel Class of N-Acyl Peptides. Characterization, Drug Encapsulation and Release Study. *Amino Acids* **2009**, *37*, 40−41.
(1144) Hulsart-Billstrom, G.; Yuen, P. K.; Hilborn, J.; Larsson, S.; Ossipov, D. The Release of Rhbmp-2 from a Bisphosphonate Hydrogel. *J. Tissue Eng. Regener. Med.* **2012**, *6*, 191.
(1145) Moysan, E.; Gonzalez-Fernandez, Y.; Lautram, N.; Bejaud, J.; Bastiat, G.; Benoit, J.-P. An Innovative Hydrogel of Gemcitabine-Loaded Lipid Nanocapsules: When the Drug Is a Key Player of the Nanomedicine Structure. *Soft Matter* **2014**, *10*, 1767−1777.
(1146) Rodrigues, M.; Calpena, A. C.; Amabilino, D. B.; Garduno-Ramirez, M. L.; Perez-Garcia, L. Supramolecular Gels Based on a Gemini Imidazolium Amphiphile as Molecular Material for Drug Delivery. *J. Mater. Chem. B* **2014**, *2*, 5419−5429.
(1147) Bredikhin, A. A.; Bredikhina, Z. A.; Pashagin, A. V. Liesegang Ring Formation During the Supramolecular Hydrogelation of the Chiral Drug Methocarbamol. *Mendeleev Commun.* **2011**, *21*, 144−145.
(1148) Ou, C. W.; Wang, H. M.; Yang, Z. M.; Chen, M. S. Precursor-Involved and Conversion Rate-Controlled Self-Assembly of a 'Super Gelator' in Thixotropic Hydrogels for Drug Delivery. *Chin. J. Chem.* **2012**, *30*, 1781−1787.
(1149) Cheetham, A. G.; Zhang, P. C.; Lin, Y. A.; Lock, L. L.; Cui, H. G. Supramolecular Nanostructures Formed by Anticancer Drug Assembly. *J. Am. Chem. Soc.* **2013**, *135*, 2907−2910.
(1150) Peresypkin, A. V.; Ellison, M. E.; Panmai, S.; Cheng, Y. U. Effective Gelation of Water by an Amphiphilic Drug. *J. Pharm. Sci.* **2008**, *97*, 2548−2551.
(1151) Roy, R.; Deb, J.; Jana, S. S.; Dastidar, P. Exploiting Supramolecular Synthons in Designing Gelators Derived from Multiple Drugs. *Chem. - Eur. J.* **2014**, *20*, 15320−15324.
(1152) Roy, R.; Deb, J.; Jana, S. S.; Dastidar, P. Peptide Conjugates of a Nonsteroidal Anti-Inflammatory Drug as Supramolecular Gelators: Synthesis, Characterization, and Biological Studies. *Chem. - Asian J.* **2014**, *9*, 3196−3206.
(1153) Su, T.; Tang, Z.; He, H.; Li, W.; Wang, X.; Liao, C.; Sun, Y.; Wang, Q. Glucose Oxidase Triggers Gelation of N-Hydroxyimide-Heparin Conjugates to Form Enzyme-Responsive Hydrogels for Cell-Specific Drug Delivery. *Chem. Sci.* **2014**, *5*, 4204−4209.
(1154) Burch, R. M.; Weitzberg, M.; Blok, N.; Muhlhauser, R.; Martin, D.; Farmer, S. G.; Bator, J. M.; Connor, J. R.; Green, M.; Ko, C.; et al. N-(Fluorenyl-9-Methoxycarbonyl) Amino-Acids, a Class of Antiinflammatory Agents with a Different Mechanism of Action. *Proc. Natl. Acad. Sci. U. S. A.* **1991**, *88*, 355−359.
(1155) Yang, Z. M.; Gu, H. W.; Zhang, Y.; Wang, L.; Xu, B. Small Molecule Hydrogels Based on a Class of Antiinflammatory Agents. *Chem. Commun.* **2004**, 208−209.
(1156) Haldar, D. Two Component Hydrogel with Gamma-Amino Butyric Acid as Potential Receptor and Neurotransmitter Delivery System. *Tetrahedron* **2008**, *64*, 186−190.
(1157) Vemula, P. K.; Li, J.; John, G. Enzyme Catalysis: Tool to Make and Break Amygdalin Hydrogelators from Renewable Resources: A Delivery Model for Hydrophobic Drugs. *J. Am. Chem. Soc.* **2006**, *128*, 8932−8938.
(1158) Parkinson, G. N.; Lee, M. P. H.; Neidle, S. Crystal Structure of Parallel Quadruplexes from Human Telomeric DNA. *Nature* **2002**, *417*, 876−880.
(1159) Davis, J. T. G-Quartets 40 Years Later: From 5 '-Gmp to Molecular Biology and Supramolecular Chemistry. *Angew. Chem., Int. Ed.* **2004**, *43*, 668−698.
(1160) Sreenivasachary, N.; Lehn, J. M. Structural Selection in G-Quartet-Based Hydrogels and Controlled Release of Bioactive Molecules. *Chem. - Asian J.* **2008**, *3*, 134−139.
(1161) Buchs, B.; Fieber, W.; Vigouroux-Elie, F.; Sreenivasachary, N.; Lehn, J.-M.; Hermann, A. Release of Bioactive Volatiles from Supramolecular Hydrogels: Influence of Reversible Acylhydrazone Formation on Gel Stability and Volatile Compound Evaporation. *Org. Biomol. Chem.* **2011**, *9*, 2906−2919.
(1162) Godeau, G.; Bernard, J.; Staedel, C.; Barthelemy, P. Glycosyl-Nucleoside-Lipid Based Supramolecular Assembly as a Nanostructured

DOI: 10.1021/acs.chemrev.5b00299
Chem. Rev. 2015, 115, 13165−13307

Material with Nucleic Acid Delivery Capabilities. *Chem. Commun.* **2009**, 5127−5129.
(1163) Chen, L. Q.; Wu, J. C.; Yuwen, L.; Shu, T. M.; Xu, M.; Zhang, M. M.; Yi, T. Inclusion of Tetracycline Hydrochloride within Supramolecular Gels and Its Controlled Release to Bovine Serum Albumin. *Langmuir* **2009**, *25*, 8434−8438.
(1164) Branco, M. C.; Pochan, D. J.; Wagner, N. J.; Schneider, J. P. The Effect of Protein Structure on Their Controlled Release from An Injectable Peptide Hydrogel. *Biomaterials* **2010**, *31*, 9527−9534.
(1165) Branco, M. C.; Pochan, D. J.; Wagner, N. J.; Schneider, J. P. Macromolecular Diffusion and Release from Self-Assembled Beta-Hairpin Peptide Hydrogels. *Biomaterials* **2009**, *30*, 1339−1347.
(1166) Sinthuvanich, C.; Schneider, J. P. Three-Dimensional Encapsulation and Culturing of Primary Bovine Chondrocytes in Injectable Beta-Hairpin Peptide Hydrogels. *Biopolymers* **2009**, *92*, 318.
(1167) Altunbas, A.; Lee, S. J.; Rajasekaran, S. A.; Schneider, J. P.; Pochan, D. J. Encapsulation of Curcumin in Self-Assembling Peptide Hydrogels as Injectable Drug Delivery Vehicles. *Biomaterials* **2011**, *32*, 5906−5914.
(1168) Komatsu, H.; Matsumoto, S.; Tamaru, S.; Kaneko, K.; Ikeda, M.; Hamachi, I. Supramolecular Hydrogel Exhibiting Four Basic Logic Gate Functions to Fine-Tune Substance Release. *J. Am. Chem. Soc.* **2009**, *131*, 5580−5585.
(1169) Nagai, Y.; Unsworth, L. D.; Koutsopoulos, S.; Zhang, S. G. Slow Release of Molecules in Self-Assembling Peptide Nanofiber Scaffold. *J. Controlled Release* **2006**, *115*, 18−25.
(1170) Briuglia, M.-L.; Urquhart, A. J.; Lamprou, D. A. Sustained and Controlled Release of Lipophilic Drugs from a Self-Assembling Amphiphilic Peptide Hydrogel. *Int. J. Pharm.* **2014**, *474*, 103−111.
(1171) Koutsopoulos, S.; Unsworth, L. D.; Nagai, Y.; Zhang, S. G. Controlled Release of Functional Proteins through Designer Self-Assembling Peptide Nanofiber Hydrogel Scaffold. *Proc. Natl. Acad. Sci. U. S. A.* **2009**, *106*, 4623−4628.
(1172) Gelain, F.; Unsworth, L. D.; Zhang, S. G. Slow and Sustained Release of Active Cytokines from Self-Assembling Peptide Scaffolds. *J. Controlled Release* **2010**, *145*, 231−239.
(1173) Nishimura, A.; Hayakawa, T.; Yamamoto, Y.; Hamori, M.; Tabata, K.; Seto, K.; Shibata, N. Controlled Release of Insulin from Self-Assembling Nanofiber Hydrogel, Puramatrix (Tm): Application for the Subcutaneous Injection in Rats. *Eur. J. Pharm. Sci.* **2012**, *45*, 1−7.
(1174) Zhao, Y.; Tanaka, M.; Kinoshita, T.; Higuchi, M.; Tan, T. W. Controlled Release and Entrapment of Enantiomers in Self-Assembling Scaffolds Composed of Beta-Sheet Peptides. *Biomacromolecules* **2009**, *10*, 3266−3272.
(1175) Zhao, Y.; Tanaka, M.; Kinoshita, T.; Higuchi, M.; Tan, T. W. Self-Assembling Peptide Nanofiber Scaffolds for Controlled Release Governed by Gelator Design and Guest Size. *J. Controlled Release* **2010**, *147*, 392−399.
(1176) Liang, G. L.; Yang, Z. M.; Zhang, R. J.; Li, L. H.; Fan, Y. J.; Kuang, Y.; Gao, Y.; Wang, T.; Lu, W. W.; Xu, B. Supramolecular Hydrogel of a D-Amino Acid Dipeptide for Controlled Drug Release in Vivo. *Langmuir* **2009**, *25*, 8419−8422.
(1177) Naskar, J.; Palui, G.; Banerjee, A. Tetrapeptide-Based Hydrogels: For Encapsulation and Slow Release of an Anticancer Drug at Physiological Ph. *J. Phys. Chem. B* **2009**, *113*, 11787−11792.
(1178) Sutton, S.; Campbell, N. L.; Cooper, A. I.; Kirkland, M.; Frith, W. J.; Adams, D. J. Controlled Release from Modified Amino Acid Hydrogels Governed by Molecular Size or Network Dynamics. *Langmuir* **2009**, *25*, 10285−10291.
(1179) Baral, A.; Roy, S.; Dehsorkhi, A.; Hamley, I. W.; Mohapatra, S.; Ghosh, S.; Banerjee, A. Assembly of an Injectable Noncytotoxic Peptide-Based Hydrogelator for Sustained Release of Drugs. *Langmuir* **2014**, *30*, 929−936.
(1180) Xu, X.-D.; Liang, L.; Chen, C.-S.; Lu, B.; Wang, N.-l.; Jiang, F.-G.; Zhang, X.-Z.; Zhuo, R.-X. Peptide Hydrogel as an Intraocular Drug Delivery System for Inhibition of Postoperative Scarring Formation. *ACS Appl. Mater. Interfaces* **2010**, *2*, 2663−2671.
(1181) Castelletto, V.; Hamley, I. W.; Stain, C.; Connon, C. Slow-Release Rgd-Peptide Hydrogel Monoliths. *Langmuir* **2012**, *28*, 12575−12580.
(1182) Diaz, D. D.; Morin, E.; Schon, E. M.; Budin, G.; Wagner, A.; Remy, J. S. Tailoring Drug Release Profile of Low-Molecular-Weight Hydrogels by Supramolecular Co-Assembly and Thiol-Ene Orthogonal Coupling. *J. Mater. Chem.* **2011**, *21*, 641−644.
(1183) Lee, H.; Lee, J. H.; Kang, S. W.; Lee, J. Y.; John, G.; Jung, J. H. Pyridine-Based Coordination Polymeric Hydrogel with Cu(2+) Ion and Its Encapsulation of a Hydrophobic Molecule. *Chem. Commun.* **2011**, *47*, 2937−2939.
(1184) Kameta, N.; Tanaka, A.; Akiyama, H.; Minamikawa, H.; Masuda, M.; Shimizu, T. Photoresponsive Soft Nanotubes for Controlled Guest Release. *Chem. - Eur. J.* **2011**, *17*, 5251−5255.
(1185) Rodriguez-Llansola, F.; Miravet, J. F.; Escuder, B. Aldehyde Responsive Supramolecular Hydrogels: Towards Biomarker-Specific Delivery Systems. *Chem. Commun.* **2011**, *47*, 4706−4708.
(1186) Zarzhitsky, S.; Rapaport, H. The Interactions between Doxorubicin and Amphiphilic and Acidic Beta-Sheet Peptides Towards Drug Delivery Hydrogels. *J. Colloid Interface Sci.* **2011**, *360*, 525−531.
(1187) Wu, M.; Ye, Z. Y.; Liu, Y. F.; Liu, B.; Zhao, X. Release of Hydrophobic Anticancer Drug from a Newly Designed Self-Assembling Peptide. *Mol. BioSyst.* **2011**, *7*, 2040−2047.
(1188) Roberts, D.; Rochas, C.; Saiani, A.; Miller, A. F. Effect of Peptide and Guest Charge on the Structural, Mechanical and Release Properties of Beta-Sheet Forming Peptides. *Langmuir* **2012**, *28*, 16196−16206.
(1189) Kleinsmann, A. J.; Nachtsheim, B. J. Phenylalanine-Containing Cyclic Dipeptides - the Lowest Molecular Weight Hydrogelators Based on Unmodified Proteinogenic Amino Acids. *Chem. Commun.* **2013**, *49*, 7818−7820.
(1190) Qin, L.; Duan, P. F.; Xie, F.; Zhang, L.; Liu, M. H. A Metal Ion Triggered Shrinkable Supramolecular Hydrogel and Controlled Release by an Amphiphilic Peptide Dendron. *Chem. Commun.* **2013**, *49*, 10823−10825.
(1191) Qin, L.; Xie, F.; Duan, P.; Liu, M. A Peptide Dendron-Based Shrinkable Metallo-Hydrogel for Charged Species Separation and Stepwise Release of Drugs. *Chem. - Eur. J.* **2014**, *20*, 15419−15425.
(1192) Tang, C.; Miller, A. F.; Saiani, A. Peptide Hydrogels as Mucoadhesives for Local Drug Delivery. *Int. J. Pharm.* **2014**, *465*, 427−435.
(1193) Ashwanikumar, N.; Kumar, N. A.; Nair, S. A.; Kumar, G. S. V. Phenylalanine-Containing Self-Assembling Peptide Nanofibrous Hydrogel for the Controlled Release of 5-Fluorouracil and Leucovorin. *RSC Adv.* **2014**, *4*, 29157−29164.
(1194) Fatouros, D. G.; Lamprou, D. A.; Urquhart, A. J.; Yannopoulos, S. N.; Vizirianakis, I. S.; Zhang, S.; Koutsopoulos, S. Lipid-Like Self-Assembling Peptide Nanovesicles for Drug Delivery. *ACS Appl. Mater. Interfaces* **2014**, *6*, 8184−8189.
(1195) Chen, Y.; Tang, C.; Zhang, J.; Gong, M.; Su, B.; Qiu, F. Self-Assembling Surfactant-Like Peptide a(6)K as Potential Delivery System for Hydrophobic Drugs. *Int. J. Nanomed.* **2015**, *10*, 847−858.
(1196) van Bommel, K. J. C.; Friggeri, A.; Stuart, M. C. A.; Feringa, B. L.; van Esch, J. Protecting Substrates from Enzymatic Cleavage: Hydrogels of Low Molecular Weight Gelators Do the Trick. *J. Controlled Release* **2005**, *101*, 287−290.
(1197) van Bommel, K. J. C.; Stuart, M. C. A.; Feringa, B. L.; van Esch, J. Two-Stage Enzyme Mediated Drug Release from Lmwg Hydrogels. *Org. Biomol. Chem.* **2005**, *3*, 2917−2920.
(1198) Bhuniya, S.; Seo, Y. J.; Kim, B. H. (S)-(+)-Ibuprofen-Based Hydrogelators: An Approach toward Anti-Inflammatory Drug Delivery. *Tetrahedron Lett.* **2006**, *47*, 7153−7156.
(1199) Wang, Y. J.; Yan, L.; Tang, L. M.; Yu, R. Assembling and Releasing Performance of Supramolecular Hydrogels Formed from Simple Drug Molecule as the Hydrogelator. *Chin. Chem. Lett.* **2007**, *18*, 1009−1012.
(1200) Pertinhez, T. A.; Conti, S.; Ferrari, E.; Magliani, W.; Spisni, A.; Polonelli, L. Reversible Self-Assembly: A Key Feature for a New

DOI: 10.1021/acs.chemrev.5b00299
Chem. Rev. 2015, 115, 13165−13307

Class of Autodelivering Therapeutic Peptides. *Mol. Pharmaceutics* **2009**, *6*, 1036−1039.
(1201) Vemula, P. K.; Cruikshank, G. A.; Karp, J. M.; John, G. Self-Assembled Prodrugs: An Enzymatically Triggered Drug-Delivery Platform. *Biomaterials* **2009**, *30*, 383−393.
(1202) Yang, Z. M.; Kuang, Y.; Li, X. M.; Zhou, N.; Zhang, Y.; Xu, B. Supramolecular Hydrogel of Kanamycin Selectively Sequesters 16s Rrna. *Chem. Commun.* **2012**, *48*, 9257−9259.
(1203) Li, X.; Li, J.; Gao, Y.; Kuang, Y.; Shi, J.; Xu, B. Molecular Nanofibers of Olsalazine Form Supramolecular Hydrogels for Reductive Release of an Anti-Inflammatory Agent. *J. Am. Chem. Soc.* **2010**, *132*, 17707−17709.
(1204) Saez, J. A.; Escuder, B.; Miravet, J. F. Supramolecular Hydrogels for Enzymatically Triggered Self-Immolative Drug Delivery. *Tetrahedron* **2010**, *66*, 2614−2618.
(1205) Yang, C. B.; Li, D. X.; FengZhao, Q. Q.; Wang, L. Y.; Wang, L.; Yang, Z. M. Disulfide Bond Reduction-Triggered Molecular Hydrogels of Folic Acid Taxol Conjugates. *Org. Biomol. Chem.* **2013**, *11*, 6946−6951.
(1206) Wang, H. M.; Wei, J.; Yang, C. B.; Zhao, H. Y.; Li, D. X.; Yin, Z. N.; Yang, Z. M. The Inhibition of Tumor Growth and Metastasis by Self-Assembled Nanofibers of Taxol. *Biomaterials* **2012**, *33*, 5848−5853.
(1207) Wang, H.; Yang, C.; Wang, L.; Kong, D.; Zhang, Y.; Yang, Z. Self-Assembled Nanospheres as a Novel Delivery System for Taxol: A Molecular Hydrogel with Nanosphere Morphology. *Chem. Commun.* **2011**, *47*, 4439−4441.
(1208) Mao, L. N.; Wang, H. M.; Tan, M.; Ou, L. L.; Kong, D. L.; Yang, Z. M. Conjugation of Two Complementary Anti-Cancer Drugs Confers Molecular Hydrogels as a Co-Delivery System. *Chem. Commun.* **2012**, *48*, 395−397.
(1209) Wang, H. M.; Lv, L. N.; Xu, G. Y.; Yang, C. B.; Sun, J. T.; Yang, Z. M. Molecular Hydrogelators Consist of Taxol and Short Peptides/Amino Acids. *J. Mater. Chem.* **2012**, *22*, 16933−16938.
(1210) Liu, Q. C.; Ou, C. W.; Ren, C. H.; Wang, L.; Yang, Z. M.; Chen, M. S. A Releasable Disulfide Carbonate Linker for Molecular Hydrogelations. *New J. Chem.* **2012**, *36*, 1556−1559.
(1211) Gao, J.; Zheng, W. T.; Zhang, J. M.; Guan, D.; Yang, Z. M.; Kong, D. L.; Zhao, Q. Enzyme-Controllable Delivery of Nitric Oxide from a Molecular Hydrogel. *Chem. Commun.* **2013**, *49*, 9173−9175.
(1212) Liu, J.; Liu, J.; Chu, L.; Zhang, Y.; Xu, H.; Kong, D.; Yang, Z.; Yang, C.; Ding, D. Self-Assembling Peptide of D-Amino Acids Boosts Selectivity and Antitumor Efficacy of 10-Hydroxycamptothecin. *ACS Appl. Mater. Interfaces* **2014**, *6*, 5558−5565.
(1213) Pu, G.; Ren, C.; Li, D.; Wang, L.; Sun, J. A Supramolecular Hydrogel for the Delivery of Bortezomib. *RSC Adv.* **2014**, *4*, 50145−50147.
(1214) Zhang, X.; Zhou, H.; Xie, Y.; Ren, C.; Ding, D.; Long, J.; Yang, Z. Rational Design of Multifunctional Hetero-Hexameric Proteins for Hydrogel Formation and Controlled Delivery of Bioactive Molecules. *Adv. Healthcare Mater.* **2014**, *3*, 1804−1811.
(1215) Patil, S. P.; Kim, S.-H.; Jadhav, J. R.; Lee, J.-h.; Jeon, E. M.; Kim, K.-T.; Kim, B. H. Cancer-Specific Gene Silencing through Therapeutic Sirna Delivery with B Vitamin-Based Nanoassembled Low-Molecular-Weight Hydrogelators. *Bioconjugate Chem.* **2014**, *25*, 1517−1525.
(1216) Li, J. Y.; Li, X. M.; Kuang, Y.; Gao, Y.; Du, X. W.; Shi, J. F.; Xu, B. Self-Delivery Multifunctional Anti-Hiv Hydrogels for Sustained Release. *Adv. Healthcare Mater.* **2013**, *2*, 1586−1590.
(1217) Lin, R.; Cheetham, A. G.; Zhang, P. C.; Lin, Y. A.; Cui, H. G. Supramolecular Filaments Containing a Fixed 41% Paclitaxel Loading. *Chem. Commun.* **2013**, *49*, 4968−4970.
(1218) Huang, H.; Shi, J.; Laskin, J.; Liu, Z.; McVey, D. S.; Sun, X. S. Design of a Shear-Thinning Recoverable Peptide Hydrogel from Native Sequences and Application for Influenza H1n1 Vaccine Adjuvant. *Soft Matter* **2011**, *7*, 8905−8912.
(1219) Li, X. D.; Galliher-Beckley, A.; Huang, H. Z.; Sun, X. Z.; Shi, J. S. Peptide Nanofiber Hydrogel Adjuvanted Live Virus Vaccine Enhances Cross-Protective Immunity to Porcine Reproductive and Respiratory Syndrome Virus. *Vaccine* **2013**, *31*, 4508−4515.
(1220) Hammer, S. M.; Sobieszczyk, M. E.; Janes, H.; Karuna, S. T.; Mulligan, M. J.; Grove, D.; Koblin, B. A.; Buchbinder, S. P.; Keefer, M. C.; Tomaras, G. D.; et al. Efficacy Trial of a DNA/Rad5 Hiv-1 Preventive Vaccine. *N. Engl. J. Med.* **2013**, *369*, 2083−2092.
(1221) Cao, C.; Lin, X.; Wahi, M.; Jackson, E.; Potter, H., Jr. Successful Adjuvant-Free Vaccination of Balb/C Mice with Mutated Amyloid B Peptides. *BMC Neurosci.* **2008**, *9*, 25.
(1222) Huang, Z.-H.; Shi, L.; Ma, J.-W.; Sun, Z.-Y.; Cai, H.; Chen, Y.-X.; Zhao, Y.-F.; Li, Y.-M. A Totally Synthetic, Self-Assembling, Adjuvant-Free Muc1 Glycopeptide Vaccine for Cancer Therapy. *J. Am. Chem. Soc.* **2012**, *134*, 8730−8733.
(1223) Rudra, J. S.; Mishra, S.; Chong, A. S.; Mitchell, R. A.; Nardin, E. H.; Nussenzweig, V.; Collier, J. H. Self-Assembled Peptide Nanofibers Raising Durable Antibody Responses against a Malaria Epitope. *Biomaterials* **2012**, *33*, 6476−6484.
(1224) Rudra, J. S.; Tian, Y. F.; Jung, J. P.; Collier, J. H. A Self-Assembling Peptide Acting as an Immune Adjuvant. *Proc. Natl. Acad. Sci. U. S. A.* **2010**, *107*, 622−627.
(1225) Chesson, C. B.; Huelsmann, E. J.; Lacek, A. T.; Kohlhapp, F. J.; Webb, M. F.; Nabatiyan, A.; Zloza, A.; Rudra, J. S. Antigenic Peptide Nanofibers Elicit Adjuvant-Free Cd8+ T Cell Responses. *Vaccine* **2014**, *32*, 1174−1180.
(1226) Chen, J.; Pompano, R. R.; Santiago, F. W.; Maillat, L.; Sciammas, R.; Sun, T.; Han, H.; Topham, D. J.; Chong, A. S.; Collier, J. H. The Use of Self-Adjuvanting Nanofiber Vaccines to Elicit High-Affinity B Cell Responses to Peptide Antigens without Inflammation. *Biomaterials* **2013**, *34*, 8776−8785.
(1227) Rudra, J. S.; Sun, T.; Bird, K. C.; Daniels, M. D.; Gasiorowski, J. Z.; Chong, A. S.; Collier, J. H. Modulating Adaptive Immune Responses to Peptide Self-Assemblies. *ACS Nano* **2012**, *6*, 1557−1564.
(1228) Hudalla, G. A.; Modica, J. A.; Tian, Y. F.; Rudra, J. S.; Chong, A. S.; Sun, T.; Mrksich, M.; Collier, J. H. A Self-Adjuvanting Supramolecular Vaccine Carrying a Folded Protein Antigen. *Adv. Healthcare Mater.* **2013**, *2*, 1114−1119.
(1229) Zhao, F.; Heesters, B. A.; Chiu, I.; Gao, Y.; Shi, J.; Zhou, N.; Carroll, M. C.; Xu, B. L-Rhamnose-Containing Supramolecular Nanofibrils as Potential Immunosuppressive Materials. *Org. Biomol. Chem.* **2014**, *12*, 6816−6819.
(1230) Li, J. Y.; Kuang, Y.; Gao, Y.; Du, X. W.; Shi, J. F.; Xu, B. D-Amino Acids Boost the Selectivity and Confer Supramolecular Hydrogels of a Nonsteroidal Anti-Inflammatory Drug (Nsaid). *J. Am. Chem. Soc.* **2013**, *135*, 542−545.
(1231) Majumder, J.; Das, M. R.; Deb, J.; Jana, S. S.; Dastidar, P. Beta-Amino Acid and Amino-Alcohol Conjugation of a Nonsteroidal Anti-Inflammatory Drug (Nsaid) Imparts Hydrogelation Displaying Remarkable Biostability, Biocompatibility, and Anti-Inflammatory Properties. *Langmuir* **2013**, *29*, 10254−10263.
(1232) Middelkoop, E.; van den Bogaerdt, A. J.; Lamme, E. N.; Hoekstra, M. J.; Brandsma, K.; Ulrich, M. M. W. Porcine Wound Models for Skin Substitution and Burn Treatment. *Biomaterials* **2004**, *25*, 1559−1567.
(1233) Liang, L. A.; Xu, X. D.; Zhang, X. Z.; Feng, M.; Peng, C.; Jiang, F. G. Prevention of Filtering Surgery Failure by Subconjunctival Injection of a Novel Peptide Hydrogel into Rabbit Eyes. *Biomed. Mater.* **2010**, *5*, 045008.
(1234) Liu, J. P.; Zhao, X. J. Design of Self-Assembling Peptides and Their Biomedical Applications. *Nanomedicine* **2011**, *6*, 1621−1643.
(1235) Yang, Z. M.; Liang, G. L.; Ma, M. L.; Abbah, A. S.; Lu, W. W.; Xu, B. D-Glucosamine-Based Supramolecular Hydrogels to Improve Wound Healing. *Chem. Commun.* **2007**, 843−845.
(1236) Turner, T. D.; Spyratou, O.; Schmidt, R. J. Biocompatibility of Wound Management Products - Standardization of and Determination of Cell-Growth Rate in L929 Fibroblast-Cultures. *J. Pharm. Pharmacol.* **1989**, *41*, 775−780.
(1237) Meng, H.; Chen, L. Y.; Ye, Z. Y.; Wang, S. T.; Zhao, X. J. The Effect of a Self-Assembling Peptide Nanofiber Scaffold (Peptide) When Used as a Wound Dressing for the Treatment of Deep Second

DOI: 10.1021/acs.chemrev.5b00299
Chem. Rev. 2015, 115, 13165−13307

Degree Burns in Rats. *J. Biomed. Mater. Res., Part B* **2009**, *89B*, 379−391.
(1238) Ellis-Behnke, R. G.; Liang, Y.-X.; Tay, D. K. C.; Kau, P. W. F.; Schneider, G. E.; Zhang, S.; Wu, W.; So, K.-F. Nano Hemostat Solution: Immediate Hemostasis at the Nanoscale. *Nanomedicine* **2006**, *2*, 207−215.
(1239) Wang, T.; Zhong, X. Z.; Wang, S. T.; Lv, F.; Zhao, X. J. Molecular Mechanisms of Rada16−1 Peptide on Fast Stop Bleeding in Rat Models. *Int. J. Mol. Sci.* **2012**, *13*, 15279−15290.
(1240) Guo, J. S.; Leung, K. K. G.; Su, H. X.; Yuan, Q. J.; Wang, L.; Chu, T. H.; Zhang, W. M.; Pu, J. K. S.; Ng, G. K. P.; Wong, W. M.; et al. Self-Assembling Peptide Nanofiber Scaffold Promotes the Reconstruction of Acutely Injured Brain. *Nanomedicine* **2009**, *5*, 345−351.
(1241) Luo, Z. L.; Wang, S. K.; Zhang, S. G. Fabrication of Self-Assembling D-Form Peptide Nanofiber Scaffold D-Eak16 for Rapid Hemostasis. *Biomaterials* **2011**, *32*, 2013−2020.
(1242) Patton, M. L.; Mullins, R.; Smith, D.; Korentager, R. An Open, Prospective, Randomized Pilot Investigation Evaluating Pain with the Use of a Soft Silicone Wound Contact Layer Vs Bridal Veil and Staples on Split Thickness Skin Grafts as a Primary Dressing. *J. Burn. Care Res.* **2013**, *34*, 674−681.
(1243) Loo, Y.; Wong, Y. C.; Cai, E. Z.; Ang, C. H.; Raju, A.; Lakshmanan, A.; Koh, A. G.; Zhou, H. J.; Lim, T. C.; Moochhala, S. M.; et al. Ultrashort Peptide Nanofibrous Hydrogels for the Acceleration of Healing of Burn Wounds. *Biomaterials* **2014**, *35*, 4805−4814.
(1244) Ghobril, C.; Charoen, K.; Rodriguez, E. K.; Nazarian, A.; Grinstaff, M. W. A Dendritic Thioester Hydrogel Based on Thiol-Thioester Exchange as a Dissolvable Sealant System for Wound Closure. *Angew. Chem., Int. Ed.* **2013**, *52*, 14070−14074.
(1245) Ishihara, K.; Ueda, T.; Nakabayashi, N. Preparation of Phospholipid Polymers and Their Properties as Polymer Hydrogel Membranes. *Polym. J.* **1990**, *22*, 355−360.
(1246) Lee, J. W.; Kim, S. Y.; Kim, S. S.; Lee, Y. M.; Lee, K. H.; Kim, S. J. Synthesis and Characteristics of Interpenetrating Polymer Network Hydrogel Composed of Chitosan and Poly(Acrylic Acid). *J. Appl. Polym. Sci.* **1999**, *73*, 113−120.
(1247) Fletcher, D. A.; Mullins, D. Cell Mechanics and the Cytoskeleton. *Nature* **2010**, *463*, 485−492.
(1248) Kuang, Y.; Long, M. J. C.; Zhou, J.; Shi, J.; Gao, Y.; Xu, C.; Hedstrom, L.; Xu, B. Prion-Like Nanofibrils of Small Molecules (Prism) Selectively Inhibit Cancer Cells by Impeding Cytoskeleton Dynamics. *J. Biol. Chem.* **2014**, *289*, 29208−29218.
(1249) Jung, J. H.; Ono, Y.; Hanabusa, K.; Shinkai, S. Creation of Both Right-Handed and Left-Handed Silica Structures by Sol-Gel Transcription of Organogel Fibers Comprised of Chiral Diaminocyclohexane Derivatives. *J. Am. Chem. Soc.* **2000**, *122*, 5008−5009.
(1250) Yao, S.; Beginn, U.; Gress, T.; Lysetska, M.; Würthner, F. Supramolecular Polymerization and Gel Formation of Bis(Merocyanine) Dyes Driven by Dipolar Aggregation. *J. Am. Chem. Soc.* **2004**, *126*, 8336−8348.
(1251) Suzuki, M.; Owa, S.; Kimura, M.; Kurose, A.; Shirai, H.; Hanabusa, K. Supramolecular Hydrogels and Organogels Based on Novel L-Valine and L-Isoleucine Amphiphiles. *Tetrahedron Lett.* **2005**, *46*, 303−306.
(1252) Weiss, R. G., Terech, P., Eds. *Molecular Gels: Materials with Self-Assembled Fibrillar Networks*; Springer: Dordrecht, The Netherlands, 2006.
(1253) George, M.; Weiss, R. G. Molecular Organogels. Soft Matter Comprised of Low-Molecular-Mass Organic Gelators and Organic Liquids. *Acc. Chem. Res.* **2006**, *39*, 489−497.
(1254) Yang, Z. M.; Liang, G. L.; Wang, L.; Xu, B. Using a Kinase/Phosphatase Switch to Regulate a Supramolecular Hydrogel and Forming the Supramolecular Hydrogel in Vivo. *J. Am. Chem. Soc.* **2006**, *128*, 3038−3043.
(1255) Yang, Z. M.; Liang, G. L.; Ma, M. L.; Gao, Y.; Xu, B. In Vitro and in Vivo Enzymatic Formation of Supramolecular Hydrogels Based on Self-Assembled Nanofibers of a Beta-Amino Acid Derivative. *Small* **2007**, *3*, 558−562.
(1256) Shi, J.; Du, X.; Yuan, D.; Zhou, J.; Zhou, N.; Huang, Y.; Xu, B. D-Amino Acids Modulate the Cellular Response of Enzymatic-Instructed Supramolecular Nanofibers of Small Peptides. *Biomacromolecules* **2014**, *15*, 3559−3568.
(1257) Yuan, D.; Zhou, R.; Shi, J.; Du, X.; Li, X.; Xu, B. Enzyme-Instructed Self-Assembly of Hydrogelators Consisting of Nucleobases, Amino Acids, and Saccharide. *RSC Adv.* **2014**, *4*, 26487−26490.
(1258) Wu, D.; Du, X.; Shi, J.; Zhou, J.; Zhou, N.; Xu, B. The First Cd73-Instructed Supramolecular Hydrogel. *J. Colloid Interface Sci.* **2015**, *447*, 269−272.
(1259) Yang, Z. M.; Liang, G. L.; Guo, Z. F.; Guo, Z. H.; Xu, B. Intracellular Hydrogelation of Small Molecules Inhibits Bacterial Growth. *Angew. Chem., Int. Ed.* **2007**, *46*, 8216−8219.
(1260) Chen, Y.; Liang, G. L. Enzymatic Self-Assembly of Nanostructures for Theranostics. *Theranostics* **2012**, *2*, 139−147.
(1261) Loo, Y.; Zhang, S. G.; Hauser, C. A. E. From Short Peptides to Nanofibers to Macromolecular Assemblies in Biomedicine. *Biotechnol. Adv.* **2012**, *30*, 593−603.
(1262) Meng, H.; Chen, R. Y.; Xu, L. N.; Li, W. C.; Chen, L. Y.; Zhao, X. J. Peripferal Nerve Regeneration in Response to Synthesized Nanofiber Scaffold Hydrogel. *Life Sci. J.* **2012**, *9*, 42−46.
(1263) Li, Y.; Qin, M.; Cao, Y.; Wang, W. Designing the Mechanical Properties of Peptide-Based Supramolecular Hydrogels for Biomedical Applications. *Sci. China: Phys., Mech. Astron.* **2014**, *57*, 849−858.
(1264) *The Pharmacological Basis of Therapeutics*, 9th ed.; Hardman, J. G., Limbird, L. E., Molinoff, P. B., Ruddon, R. W., Eds.; McGraw-Hill: New York, 1995.
(1265) Walsh, C. *Antibiotics: Actions, Origins, and Resistance*, 1st ed.; ASM Press: Washington, DC, 2003.
(1266) Williams, R. J.; Smith, A. M.; Collins, R.; Hodson, N.; Das, A. K.; Ulijn, R. V. Enzyme-Assisted Self-Assembly under Thermodynamic Control. *Nat. Nanotechnol.* **2009**, *4*, 19−24.
(1267) Williams, R. J.; Mart, R. J.; Ulijn, R. V. Exploiting Biocatalysis in Peptide Self-Assembly. *Biopolymers* **2010**, *94*, 107−117.
(1268) Hughes, M.; Xu, H. X.; Frederix, P. W. J. M.; Smith, A. M.; Hunt, N. T.; Tuttle, T.; Kinloch, I. A.; Ulijn, R. V. Biocatalytic Self-Assembly of 2d Peptide-Based Nanostructures. *Soft Matter* **2011**, *7*, 10032−10038.
(1269) Hirst, A. R.; Roy, S.; Arora, M.; Das, A. K.; Hodson, N.; Murray, P.; Marshall, S.; Javid, N.; Sefcik, J.; Boekhoven, J.; et al. Biocatalytic Induction of Supramolecular Order. *Nat. Chem.* **2010**, *2*, 1089−1094.
(1270) Sadownik, J. W.; Leckie, J.; Ulijn, R. V. Micelle to Fibre Biocatalytic Supramolecular Transformation of an Aromatic Peptide Amphiphile. *Chem. Commun.* **2011**, *47*, 728−730.
(1271) Chau, Y.; Luo, Y.; Cheung, A. C. Y.; Nagai, Y.; Zhang, S. G.; Kobler, J. B.; Zeitels, S. M.; Langer, R. Incorporation of a Matrix Metalloproteinase-Sensitive Substrate into Self-Assembling Peptides - a Model for Biofunctional Scaffolds. *Biomaterials* **2008**, *29*, 1713−1719.
(1272) Giano, M. C.; Pochan, D. J.; Schneider, J. P. Controlled Biodegradation of Self-Assembling β-Hairpin Peptide Hydrogels by Proteolysis with Matrix Metalloproteinase-13. *Biomaterials* **2011**, *32*, 6471−6477.
(1273) Tian, Y. F.; Hudalla, G. A.; Han, H.; Collier, J. H. Controllably Degradable [Small Beta]-Sheet Nanofibers and Gels from Self-Assembling Depsipeptides. *Biomater. Sci.* **2013**, *1*, 1037−1045.
(1274) Williams, R. J.; Hall, T. E.; Glattauer, V.; White, J.; Pasic, P. J.; Sorensen, A. B.; Waddington, L.; McLean, K. M.; Currie, P. D.; Hartley, P. G. The in Vivo Performance of an Enzyme-Assisted Self-Assembled Peptide/Protein Hydrogel. *Biomaterials* **2011**, *32*, 5304−5310.
(1275) Schnepp, Z. A. C.; Gonzalez-McQuire, R.; Mann, S. Hybrid Biocomposites Based on Calcium Phosphate Mineralization of Self-Assembled Supramolecular Hydrogels. *Adv. Mater.* **2006**, *18*, 1869−1872.

DOI: 10.1021/acs.chemrev.5b00299
Chem. Rev. 2015, 115, 13165−13307

(1276) Li, D. X.; Shi, Y.; Wang, L. Mechanical Reinforcement of Molecular Hydrogel by Co-Assembly of Short Peptide-Based Gelators with Different Aromatic Capping Groups. *Chin. J. Chem.* **2014**, *32*, 123−127.
(1277) Wang, H. M.; Yang, C. H.; Tan, M.; Wang, L.; Kong, D. L.; Yang, Z. M. A Structure-Gelation Ability Study in a Short Peptide-Based 'Super Hydrogelator' System. *Soft Matter* **2011**, *7*, 3897−3905.
(1278) Wang, H. M.; Ren, C. H.; Song, Z. J.; Wang, L.; Chen, X. M.; Yang, Z. M. Enzyme-Triggered Self-Assembly of a Small Molecule: A Supramolecular Hydrogel with Leaf-Like Structures and an Ultra-Low Minimum Gelation Concentration. *Nanotechnology* **2010**, *21*, 225606.
(1279) Yang, C. B.; Wang, H. M.; Li, D. X.; Wang, L. Molecular Hydrogels with Esterase-Like Activity. *Chin. J. Chem.* **2013**, *31*, 494−500.
(1280) Hughes, M.; Debnath, S.; Knapp, C. W.; Ulijn, R. V. Antimicrobial Properties of Enzymatically Triggered Self-Assembling Aromatic Peptide Amphiphiles. *Biomater. Sci.* **2013**, *1*, 1138−1142.
(1281) Richardson, P. J.; Brown, S. J.; Bailyes, E. M.; Luzio, J. P. Ectoenzymes Control Adenosine Modulation of Immunoisolated Cholinergic Synapses. *Nature* **1987**, *327*, 232−234.
(1282) Yegutkin, G. G. Nucleotide- and Nucleoside-Converting Ectoenzymes: Important Modulators of Purinergic Signalling Cascade. *Biochim. Biophys. Acta, Mol. Cell Res.* **2008**, *1783*, 673−694.
(1283) Netzel-Arnett, S.; Hooper, J. D.; Szabo, R.; Madison, E. L.; Quigley, J. P.; Bugge, T. H.; Antalis, T. M. Membrane Anchored Serine Proteases: A Rapidly Expanding Group of Cell Surface Proteolytic Enzymes with Potential Roles in Cancer. *Cancer Metastasis Rev.* **2003**, *22*, 237−258.
(1284) Pospisil, P.; Iyer, L. K.; Adelstein, S. J.; Kassis, A. I. A Combined Approach to Data Mining of Textual and Structured Data to Identify Cancer-Related Targets. *BMC Bioinf.* **2006**, *7*, 354.
(1285) Pires, R. A.; Abul-Haija, Y. M.; Costa, D. S.; Novoa-Carballal, R.; Reis, R. L.; Ulijn, R. V.; Pashkuleva, I. Controlling Cancer Cell Fate Using Localized Biocatalytic Self-Assembly of an Aromatic Carbohydrate Amphiphile. *J. Am. Chem. Soc.* **2015**, *137*, 576−579.
(1286) Fishman, W. H.; Inglis, N. R.; Green, S.; Anstiss, C. L.; Gosh, N. K.; Reif, A. E.; Rustigian, R.; Krant, M. J.; Stolbach, L. L. Immunology and Biochemistry of Regan Isoenzyme of Alkaline Phosphatase in Human Cancer. *Nature* **1968**, *219*, 697−699.
(1287) Zhou, R.; Xu, B. Insight of the Cytotoxicity of the Aggregates of Peptides or Aberrant Proteins: A Meta-Analysis. *PLoS One* **2014**, *9*, e95759.
(1288) Zorn, J. A.; Wille, H.; Wolan, D. W.; Wells, J. A. Self-Assembling Small Molecules Form Nanofibrils That Bind Procaspase-3 to Promote Activation. *J. Am. Chem. Soc.* **2011**, *133*, 19630−19633.
(1289) Yang, Z. M.; Xu, K. M.; Guo, Z. F.; Guo, Z. H.; Xu, B. Intracellular Enzymatic Formation of Nanofibers Results in Hydrogelation and Regulated Cell Death. *Adv. Mater.* **2007**, *19*, 3152−3156.
(1290) Kuang, Y.; Xu, B. Disruption of the Dynamics of Microtubules and Selective Inhibition of Glioblastoma Cells by Nanofibers of Small Hydrophobic Molecules. *Angew. Chem., Int. Ed.* **2013**, *52*, 6944−6948.
(1291) Clément, M.-J.; Jourdain, I.; Lachkar, S.; Savarin, P.; Gigant, B.; Knossow, M.; Toma, F.; Sobel, A.; Curmi, P. A. N-Terminal Stathmin-Like Peptides Bind Tubulin and Impede Microtubule Assembly†. *Biochemistry* **2005**, *44*, 14616−14625.
(1292) Budihardjo, I.; Oliver, H.; Lutter, M.; Luo, X.; Wang, X. D. Biochemical Pathways of Caspase Activation During Apoptosis. *Annu. Rev. Cell Dev. Biol.* **1999**, *15*, 269−290.
(1293) Fitzpatrick, A. W. P.; Debelouchina, G. T.; Bayro, M. J.; Clare, D. K.; Caporini, M. A.; Bajaj, V. S.; Jaroniec, C. P.; Wang, L.; Ladizhansky, V.; Mueller, S. A.; et al. Atomic Structure and Hierarchical Assembly of a Cross-Beta Amyloid Fibril. *Proc. Natl. Acad. Sci. U. S. A.* **2013**, *110*, 5468−5473.
(1294) Jaroniec, C. P.; MacPhee, C. E.; Bajaj, V. S.; McMahon, M. T.; Dobson, C. M.; Griffin, R. G. High-Resolution Molecular Structure of a Peptide in an Amyloid Fibril Determined by Magic Angle Spinning Nmr Spectroscopy. *Proc. Natl. Acad. Sci. U. S. A.* **2004**, *101*, 711−716.
(1295) Van Petegem, F. Ryanodine Receptors: Allosteric Ion Channel Giants. *J. Mol. Biol.* **2015**, *427*, 31−53.
(1296) Bai, X.-C.; McMullan, G.; Scheres, S. H. W. How Cryo-Em Is Revolutionizing Structural Biology. *Trends Biochem. Sci.* **2015**, *40*, 49−57.
(1297) Petsko, G. A. 100 Years of X-Ray Crystallography. *Chem. Eng. News* **2014**, *92*, 33−41.
(1298) DiMaio, F.; Song, Y.; Li, X.; Brunner, M. J.; Xu, C.; Conticello, V.; Egelman, E.; Marlovits, T. C.; Cheng, Y.; Baker, D. Atomic-Accuracy Models from 4.5-Angstrom Cryo-Electron Microscopy Data with Density-Guided Iterative Local Refinement. *Nat. Methods* **2015**, *12*, 361−365.
(1299) Ghoussoub, A.; Lehn, J. M. Dynamic Sol-Gel Interconversion by Reversible Cation Binding and Release in G-Quartet-Based Supramolecular Polymers. *Chem. Commun.* **2005**, 5763−5765.
(1300) de Jong, J. J. D.; Hania, P. R.; Pugzlys, A.; Lucas, L. N.; de Loos, M.; Kellogg, R. M.; Feringa, B. L.; Duppen, K.; van Esch, J. H. Light-Driven Dynamic Pattern Formation. *Angew. Chem., Int. Ed.* **2005**, *44*, 2373−2376.
(1301) Brinksma, J.; Feringa, B. L.; Kellogg, R. M.; Vreeker, R.; van Esch, J. Rheology and Thermotropic Properties of Bis-Urea-Based Organogels in Various Primary Alcohols. *Langmuir* **2000**, *16*, 9249−9255.
(1302) Hahne, H.; Maeder, U.; Otto, A.; Bonn, F.; Steil, L.; Bremer, E.; Hecker, M.; Becher, D. A Comprehensive Proteomics and Transcriptomics Analysis of Bacillus Subtilis Salt Stress Adaptation. *J. Bacteriol.* **2010**, *192*, 870−882.
(1303) Zhang, Y.; Zhou, N.; Shi, J.; Pochapsky, S. S.; Pochapsky, T. C.; Zhang, B.; Zhang, X. X.; Xu, B. Unfolding a Molecular Trefoil Derived from a Zwitterionic Metallopeptide to Form Self-Assembled Nanostructures. *Nat. Commun.* **2015**, *6*, 6165.
(1304) Gilbert, W. Origin of Life - the Rna World. *Nature* **1986**, *319*, 618−618.
(1305) Powner, M. W.; Gerland, B.; Sutherland, J. D. Synthesis of Activated Pyrimidine Ribonucleotides in Prebiotically Plausible Conditions. *Nature* **2009**, *459*, 239−242.
(1306) Imai, E.; Honda, H.; Hatori, K.; Matsuno, K. Autocatalytic Synthesis of Oligoglycine in a Simulated Submarine Hydrothermal System. *Origins Life Evol. Biospheres* **1999**, *29*, 249−259.
(1307) Dzieciol, A. J.; Mann, S. Designs for Life: Protocell Models in the Laboratory. *Chem. Soc. Rev.* **2012**, *41*, 79−85.
(1308) Trevors, J. T.; Pollack, G. H. Hypothesis: The Origin of Life in a Hydrogel Environment. *Prog. Biophys. Mol. Biol.* **2005**, *89*, 1−8.
(1309) Yang, D. Y.; Peng, S. M.; Hartman, M. R.; Gupton-Campolongo, T.; Rice, E. J.; Chang, A. K.; Gu, Z.; Lu, G. Q.; Luo, D. Enhanced Transcription and Translation in Clay Hydrogel and Implications for Early Life Evolution. *Sci. Rep.* **2013**, *3*, 3165.
(1310) Pereto, J.; Bada, J. L.; Lazcano, A. Charles Darwin and the Origin of Life. *Origins Life Evol. Biospheres* **2009**, *39*, 395−406.
(1311) Yuan, D.; Shi, J.; Du, X.; Zhou, N.; Xu, B. Supramolecular Glycosylation Accelerates Proteolytic Degradation of Peptide Nanofibrils. *J. Am. Chem. Soc.* **2015**, *137*, 10092−10095.
(1312) Goodsell, D. S.; Olson, A. J. Structural Symmetry and Protein Function. *Annu. Rev. Biophys. Biomol. Struct.* **2000**, *29*, 105−153.
(1313) Caron, P.; Beckers, A.; Cullen, D. R.; Goth, M. I.; Gutt, B.; Laurberg, P.; Pico, A. M.; Valimaki, M.; Zgliczynski, W. Efficacy of the New Long-Acting Formulation of Lanreotide (Lanreotide Autogel) in the Management of Acromegaly. *J. Clin. Endocrinol. Metab.* **2002**, *87*, 99−104.
(1314) Modlin, I. M.; Pavel, M.; Kidd, M.; Gustafsson, B. I. Review Article: Somatostatin Analogues in the Treatment of Gastroenteropancreatic Neuroendocrine (Carcinoid) Tumours. *Aliment. Pharmacol. Ther.* **2010**, *31*, 169−188.
(1315) Farin, H. F.; Van Es, J. H.; Clevers, H. Redundant Sources of Wnt Regulate Intestinal Stem Cells and Promote Formation of Paneth Cells. *Gastroenterology* **2012**, *143*, 1518−1529.
(1316) Sato, T.; van Es, J. H.; Snippert, H. J.; Stange, D. E.; Vries, R. G.; van den Born, M.; Barker, N.; Shroyer, N. F.; van de Wetering, M.;

DOI: 10.1021/acs.chemrev.5b00299
Chem. Rev. 2015, 115, 13165−13307

Clevers, H. Paneth Cells Constitute the Niche for Lgr5 Stem Cells in Intestinal Crypts. *Nature* **2011**, *469*, 415−418.
(1317) Zhou, J.; Du, X.; Li, J.; Yamagata, N.; Xu, B. Taurine Boosts Cellular Uptake of Small D-Peptides for Enzyme-Instructed Intracellular Molecular Self-Assembly. *J. Am. Chem. Soc.* **2015**, *137*, 10040−10043.
(1318) Okita, K.; Ichisaka, T.; Yamanaka, S. Generation of Germline-Competent Induced Pluripotent Stem Cells. *Nature* **2007**, *448*, 313−317.
(1319) Takahashi, K.; Tanabe, K.; Ohnuki, M.; Narita, M.; Ichisaka, T.; Tomoda, K.; Yamanaka, S. Induction of Pluripotent Stem Cells from Adult Human Fibroblasts by Defined Factors. *Cell* **2007**, *131*, 861−872.
(1320) Takahashi, K.; Yamanaka, S. Induction of Pluripotent Stem Cells from Mouse Embryonic and Adult Fibroblast Cultures by Defined Factors. *Cell* **2006**, *126*, 663−676.
(1321) Bauman, J. D.; Patel, D.; Baker, S. F.; Vijayan, R. S. K.; Xiang, A.; Parhi, A. K.; Martinez-Sobrido, L.; LaVoie, E. J.; Das, K.; Arnold, E. Crystallographic Fragment Screening and Structure-Based Optimization Yields a New Class of Influenza Endonuclease Inhibitors. *ACS Chem. Biol.* **2013**, *8*, 2501−2508.
(1322) Markel, H.; Lipman, H. B.; Navarro, J. A.; Sloan, A.; Michalsen, J. R.; Stern, A. M.; Cetron, M. S. Nonpharmaceutical Interventions Implemented by Us Cities During the 1918−1919 Influenza Pandemic. *Jama-j. Am. Med. Assoc.* **2007**, *298*, 644−654.
(1323) Barrientos, S.; Stojadinovic, O.; Golinko, M. S.; Brem, H.; Tomic-Canic, M. Growth Factors and Cytokines in Wound Healing. *Wound. Repair. Regen.* **2008**, *16*, 585−601.
(1324) Vinik, A. I.; Maser, R. E.; Mitchell, B. D.; Freeman, R. Diabetic Autonomic Neuropathy. *Diabetes Care* **2003**, *26*, 1553−1579.
(1325) Whitesides, G. M. Reinventing Chemistry. *Angew. Chem., Int. Ed.* **2015**, *54*, 3196−3209.
(1326) Zhou, J.; Xu, B. Enzyme-Instructed Self-Assembly: A Multistep Process for Potential Cancer Therapy. *Bioconjugate Chem.* **2015**, *26*, 987−999.
(1327) Bansagi, T., Jr.; Vanag, V. K.; Epstein, I. R. Tomography of Reaction-Diffusion Microemulsions Reveals Three-Dimensional Turing Patterns. *Science* **2011**, *331*, 1309−1312.
(1328) Epstein, I. R. The Consequences of Imperfect Mixing in Autocatalytic Chemical and Biological-Systems. *Nature* **1995**, *374*, 321−327.
(1329) Epstein, I. R.; Vanag, V. K.; Balazs, A. C.; Kuksenok, O.; Dayal, P.; Bhattacharya, A. Chemical Oscillators in Structured Media. *Acc. Chem. Res.* **2012**, *45*, 2160−2168.
(1330) Kaur, N.; Kaur, P.; Singh, K. A dioxadithiaazacrown ether−BODIPY dyad Hg^{2+} complex for detection of L-cysteine: fluorescence switching and application to soft material. *RSC Adv.* **2014**, *4*, 29340−29343.

DOI: 10.1021/acs.chemrev.5b00299
Chem. Rev. 2015, 115, 13165−13307